



HAL
open science

Functional analyses of the *Legionella longbeachae* capsule to understand its role in host immune sensing and environmental persistence

Silke Schmidt

► **To cite this version:**

Silke Schmidt. Functional analyses of the *Legionella longbeachae* capsule to understand its role in host immune sensing and environmental persistence. Microbiology and Parasitology. Sorbonne Université, 2023. English. NNT : 2023SORUS480 . tel-04755673

HAL Id: tel-04755673

<https://theses.hal.science/tel-04755673v1>

Submitted on 28 Oct 2024

HAL is a multi-disciplinary open access archive for the deposit and dissemination of scientific research documents, whether they are published or not. The documents may come from teaching and research institutions in France or abroad, or from public or private research centers.

L'archive ouverte pluridisciplinaire **HAL**, est destinée au dépôt et à la diffusion de documents scientifiques de niveau recherche, publiés ou non, émanant des établissements d'enseignement et de recherche français ou étrangers, des laboratoires publics ou privés.

Sorbonne Université

ED515: Complexité du Vivant

Unité de Biologie des Bactéries Intracellulaires, Institut Pasteur

Analyses fonctionnelles de la capsule de *Legionella longbeachae* pour comprendre son rôle dans la détection immunitaire de l'hôte et la persistance environnementale

Thèse de doctorat de Microbiologie

Par **Silke Schmidt**

Dirigée par Carmen Buchrieser

Présentée et soutenue publiquement le 26 octobre 2023

Devant un jury composé de :

Nicolas Biais	Professeur, Sorbonne Université	Président du jury
Géraldine Laloux	Professeure associée, Université catholique de Louvain	Rapportrice
Charles Van der Henst	Professeur associé, Université libre de Bruxelles	Rapporteur
Hubert Hilbi	Professeur, Université de Zurich	Examineur
Jean-Pierre Gorvel	Directeur de Recherche, Université Aix-Marseille	Examineur
Carmen Buchrieser	Professeure, Institut Pasteur	Directrice de thèse

Sorbonne University

ED515: Complexité du Vivant

Laboratory Biology of Intracellular Bacteria, Institut Pasteur

Functional analyses of the *Legionella longbeachae* capsule to understand its role in host immune sensing and environmental persistence

Doctoral thesis in Microbiology

By **Silke Schmidt**

Directed by Carmen Buchrieser

Presented and defended in public on 26 October 2023

Before a jury composed of:

Nicolas Biais	Professor, Sorbonne Université	Jury president
Géraldine Laloux	Associate Professor, Catholic University of Leuven	Reporter
Charles Van der Henst	Associate Professor, Free University of Brussels	Reporter
Hubert Hilbi	Professor, University of Zurich	Examiner
Jean-Pierre Gorvel	Research Director, University Aix-Marseille	Examiner
Carmen Buchrieser	Professor, Institut Pasteur	Thesis supervisor

To Marianne, Burkhard, Katja, and Roswitha.

Reality is not simply there, it does not simply exist: it must be sought out and won.

Paul Celan

Acknowledgments

I want to first and foremost thank my supervisor Carmen for taking me on this journey through the PhD. Thanks to you, I have had the great opportunity to work on this project and I want to especially thank you for your kindness, support, and guidance. My special thanks extend to Sonia, who has taken me under her wing as a master student and without whom we could not have embarked on this journey. I want to further thank all current and past members of the lab for generously sharing their time and expertise, especially Pedro, Tobias, Jessica, Christophe, and Laura. I want to further thank our collaborators in this project: Thierry, Maryse, Martin, Augusto, Danielle, and Dario. Finally, my heartfelt thanks go to my family and friends for their unwavering support and inspiration.

TABLE OF CONTENTS

List of introductory figures	XI
List of introductory tables	XI
List of abbreviations.....	XII
INTRODUCTION.....	1
1. The genus <i>Legionella</i>	1
1.1 Legionellosis	2
1.2 Epidemiology	3
1.3 The <i>Legionella</i> infection cycle	4
1.4 <i>Legionella</i> secretion systems and their role in infection	7
1.5 Molecular mimicry by secreted <i>Legionella</i> effectors	8
1.6 Publication – Legionnaires’ Disease: State of the Art Knowledge of Pathogenesis Mechanisms of <i>Legionella</i>	11
1.7 <i>Legionella longbeachae</i> : discovery and key differences.....	41
1.8 <i>Legionella longbeachae</i> infection and virulence.....	43
1.9 The <i>Legionella longbeachae</i> capsule	44
2. Outer membrane polysaccharides	47
2.1 Bacterial cell wall architectures	47
2.2 Complex polysaccharides in the outer leaflet of diderm bacteria	48
2.3 Biosynthesis pathways of LPS	51
2.3.1 Lipopolysaccharide of <i>Legionella</i>	54
2.4 Regulation of LPS biosynthesis	56
2.5 Role of LPS in infection.....	57
2.5.1 <i>Legionella</i> LPS and its role in infection.....	58
2.6 Capsules in diderm bacteria	59
2.7 Capsule biosynthesis pathways in diderm bacteria	60

2.8 Regulation of bacterial capsule biosynthesis	63
2.9 Roles of capsules in bacterial survival and infection	65
2.9.1 Capsules as barriers against harsh environments	65
2.9.2 Capsules as immune evasion factors	66
3. Aims of the doctoral thesis	69
RESULTS	71
4. Results summary	71
5. Publication – The unique <i>L. longbeachae</i> capsule favors intracellular replication and immune evasion	73
OUTLOOK AND PERSPECTIVES.....	147
REFERENCES.....	155
Annexes	XV
Annex A.....	XVII
Annex B.....	XIX
Annex C.....	XXI

List of introductory figures

Figure 1: <i>Legionella pneumophila</i> colonies on BCYE agar.....	2
Figure 2: Cases of Legionnaires' disease reported to the ECDC Legionnaires' disease surveillance program.	4
Figure 3: The <i>Legionella pneumophila</i> intracellular replication cycle and manipulation of host cell pathways.	6
Figure 4: Detection of <i>Legionella longbeachae</i> by country.....	42
Figure 5: LPS and capsule biosynthesis clusters encoded in the <i>Legionella longbeachae</i> NSW150 genome.	45
Figure 6: Common cell wall architectures in bacteria.....	47
Figure 7: General structure of lipopolysaccharide (LPS).....	49
Figure 8: Biosynthesis pathways of lipopolysaccharide (LPS) in diderm bacteria.....	53
Figure 9: Structure of <i>Legionella pneumophila</i> LPS.	55
Figure 10: Capsules of diderm bacteria imaged by transmission electron microscopy.	60
Figure 11: Capsule biosynthesis pathways in diderm bacteria.....	63

List of introductory tables

Table 1: Monosaccharides and sugar substituents found in bacterial (exo)polysaccharides. ..	50
Table 2: Capsule groups in the model organism <i>E. coli</i>	61
Table 3: Examples of CPS biosynthesis pathways in diderm bacteria.....	62

List of abbreviations

ATP	adenosine triphosphate
BAM	β -barrel assembly machinery
BCYE	buffered charcoal yeast extract
CAMPs	cationic antimicrobial peptides
CD	cluster of differentiation
CDC	Centers for Diseases Control and Prevention
CPS	capsular polysaccharide
CR	complement receptor
DCs	dendritic cells
Dot/Icm	defective organelle trafficking/intracellular multiplication
e.g.	<i>exempli gratia</i> , for example
ECDC	European Centre for Disease Prevention and Control
EEA	European Economic Area
EPS	exopolysaccharide
ER	Endoplasmatic Reticulum
EU	European Union
Glc	glucose
GlcN3N	2,3-diamino-2,3-dideoxyglucose
GlcN-6-P	glucosamine-6-phosphate
GlcNAc	N-acetyl glucosamine
GlcUA	glucuronic acid
GTs	glycosyltransferases
i.e.	<i>id est</i> , that is
IgG	Immunoglobulin G
IgM	Immunoglobulin M
IM	inner membrane
Kdo	α -3-deoxy-D-manno-oct-2-ulopyranosonic acid
LBP	LPS-binding protein
LCV	<i>Legionella</i> -containing vacuole
LD	Legionnaires' disease
Legionaminic acid, Leg	α -(2–4)-linked 5-acetamidino-7-acetamido-8-O-acetyl-3,5,7,9-tetradecoxy-L-glycero-D-galacto-non-2-ulosonic acid
LOS	lipooligosaccharide
LPS	lipopolysaccharide
LTA	lipoteichoic acid
MAIT	mucosal-associated invariant T
Man	mannose
MR	mannose/GlcNAc/fucose receptor
MurNAc	N-acetyl muramine
NBD	nucleotide-binding domain
NDP	nucleoside diphosphate
NMP	nucleoside monophosphate
OM	outer membrane

PAMP	pathogen-associated molecular pattern
PBMCs	peripheral blood mononuclear cells
PG	peptidoglycan
PMNs	polymorphonuclear leukocytes
PO ₄	phosphate
PP	periplasm
PRR	pattern recognition receptor
PS	polysaccharide
QuiNAc	N-acetyl quinovosamine
RBS	ribosome-binding site
Rha	rhamnose
SAH	S-adenosyl homocysteine
SAM	S-adenosyl methionine
sg	serogroup
SP	surfactant protein
T2SS	type 2 secretion system
T4SS	type 4 secretion system
TEM	transmission electron microscopy
TLR	Toll-like receptor
TPR	tetratricopeptide repeat
UDP	uridine diphosphate
Und-P	undecaprenol-phosphate
Und-PP	undecaprenol-pyrophosphate
UTR	untranslated region
WTA	wall teichoic acid

INTRODUCTION

This introduction is organized in three sections. Section 1 gives a short overview of the history of *Legionella*, the epidemiology associated with infections, and the infection cycle of the bacteria.

I co-authored two comprehensive reviews: One that focuses on the pathology and disease mechanisms of *Legionella* entitled “Legionnaires' Disease: State of the Art Knowledge of Pathogenesis Mechanisms of *Legionella*” (presented in section 1.6). This review also includes a detailed introduction of *Legionella longbeachae*. The second review focuses on secreted effector proteins of *Legionella* and microbe-host coevolution, entitled “Molecular Mimicry: a Paradigm of Host-Microbe Coevolution Illustrated by *Legionella*” (presented in Annex A). The first review is followed by a more detailed introduction to *L. longbeachae*, the subject of my PhD thesis (section 1.7).

Section 2 describes bacterial cell wall architectures with a focus on diderm (Gram-negative) bacteria and the two major polysaccharides found in the outer leaflet of the outer membrane: lipopolysaccharide and capsule.

Lastly, section 3 outlines the aims and objectives of this thesis.

1. The genus *Legionella*

Legionella are rod-shaped, facultative intracellular bacteria that can cause a severe pneumonia known as Legionnaires' disease. They are classified as Gram-negative based on Gram staining, inferring that they have a diderm cell wall architecture. The genus *Legionella* belongs to the family Legionellaceae, the order Legionellales and the class Gammaproteobacteria. It received its name after the American Legion (McDade *et al.*, 1977), as *Legionella pneumophila* was identified as the causative agent of a large outbreak of pneumonia at the 58th Annual Convention of the American Legion in Philadelphia, United States. This outbreak counted over 200 infections and 34 deaths (Fraser *et al.*, 1977). Four years later, *Legionella longbeachae* was isolated from patients presenting with pneumonia admitted to the hospital in Long Beach, California (Bibb *et al.*, 1981; McKinney *et al.*, 1981). Today, the genus *Legionella* comprises 65 species (Gomez-Valero *et al.*, 2019), of which about 30 species have been associated with infections in humans (Cunha, Burillo and Bouza, 2016).

Introduction

Legionella are mesophilic and grow optimally at 37°C if nutrients are available, but they tolerate a temperature range from 20-45% degrees for growth in broth culture (Fields, Benson and Besser, 2002; CDC, 2018; Hochstrasser and Hilbi, 2022). They are fastidious to grow in culture as they require a nutrient rich medium. Generally, buffered yeast extract medium supplemented with cysteine and ferric iron is used (Chatfield and Cianciotto, 2013). The bacteria divide by binary fission and have a doubling time of about 2 hours for *Legionella pneumophila* during mid-log phase in an infected host cell at 37°C (Steinert, Hentschel and Hacker, 2002). On buffered charcoal yeast extract (BCYE) plates, *Legionella* form opaque colonies with a smooth colony morphology (Figure 1).



Figure 1: *Legionella pneumophila* colonies on BCYE agar. Single colonies of *L. pneumophila* grown for 5 days at 37°C on buffered charcoal yeast extract (BCYE) agar. From bioMérieux SA, 2023.

1.1 Legionellosis

Legionella can cause legionellosis in humans via inhalation of contaminated aerosols from man-made water sources, moist soils, or potting mixes (Blatt, 1993; Kenagy *et al.*, 2017). Human-to-human transmission has only been reported once, thus human transmission is incidental and generally a dead end for the bacteria (Correia *et al.*, 2016). Two forms of legionellosis are known: Pontiac fever and Legionnaires' disease (LD).

Pontiac fever is a short, self-limiting infection that is marked by fever, headache, and muscle aches. In contrast to LD, it does not lead to pneumonia and patients usually recover from the disease without antibiotic treatment (CDC, 2021a).

On the other hand, LD is a severe form of pneumonia that includes common symptoms such as dry, hacking cough, shortness of breath, fever, and muscle pain. However, it is also often

associated with nausea, diarrhea, and confusion. In rare cases, LD can lead to other extrapulmonary symptoms, such as pericarditis and myocarditis, pancreatitis, renal failure, or arthritis (Roig, Sabria and Castella, 2010). The fatality rate of LD infections ranges from 5% to 40% depending on the clinical setting and reporting region (Bradley and Bryan, 2019). Treatment of LD requires at least 3 weeks of antibiotic intervention, mostly a combination therapy with macrolides such as azithromycin, and fluoroquinolones such as ciprofloxacin (Pedro-Botet and Yu, 2006). While *Legionella* are inherently resistant to β -lactam antibiotics, cases of antibiotic resistance to macrolides/fluoroquinolones have rarely been reported (Bruin *et al.*, 2014; Shadoud *et al.*, 2015; Jia *et al.*, 2019; Natås *et al.*, 2019). Two mechanisms of acquisition of antibiotic resistance were reported to date: one was attributed to point mutations in the *gyrA* gene, which mediates resistance to ciprofloxacin (Bruin *et al.*, 2014). The second one was attributed to the presence of an efflux pump named LpeAB, which mediated lower sensitivity to azithromycin in a sub-population of *L. pneumophila* (Vandewalle-Capo *et al.*, 2017).

1.2 Epidemiology

In Europe and in the United States, *L. pneumophila* is the leading cause of LD responsible for about 80-90% of confirmed cases, followed by other non-*pneumophila* species such as *L. longbeachae*, *L. micdadei*, and *L. bozemanii* (Yu *et al.*, 2002). Among LD cases caused by *L. pneumophila*, strains of serogroup 1 (sg1) make up 90% of cases and only 10% are caused by other serogroups of *L. pneumophila*. In contrast, in Australia and New Zealand, LD is commonly caused by *L. longbeachae* with 39% and 54% of confirmed cases, respectively (Chambers *et al.*, 2021). However, in recent years, sporadic infections caused by *L. longbeachae* have been increasingly reported in Europe and North America, probably partly related to improved detection methods (Health Protection Scotland, 2014; Picard-Masson *et al.*, 2016; de Bruin *et al.*, 2018; Bell *et al.*, 2021). Risk factors for LD include: higher age, pre-existing lung diseases, smoking, immune suppression, and about two thirds of reported cases are male (CDC, 2021b; ECDC, 2023). The case fatality rate of LD infections in the EU/EEA ranged from 7% to 10% between 2013 to 2021 (ECDC, 2023).

In numbers, confirmed cases of LD in the EU/EEA reported by the European Centre for Disease Prevention and Control (ECDC) rose from 4693 cases in 2005 to 10004 cases in 2021 – an increase of 113% (Figure 2) (ECDC, 2023). A decline in cases was reported in 2020, most likely

due to lockdown measures during the Covid-19 pandemic. In France, the numbers of confirmed LD cases rose by 38% overall from 1437 cases in 2005 to 1985 cases in 2021.

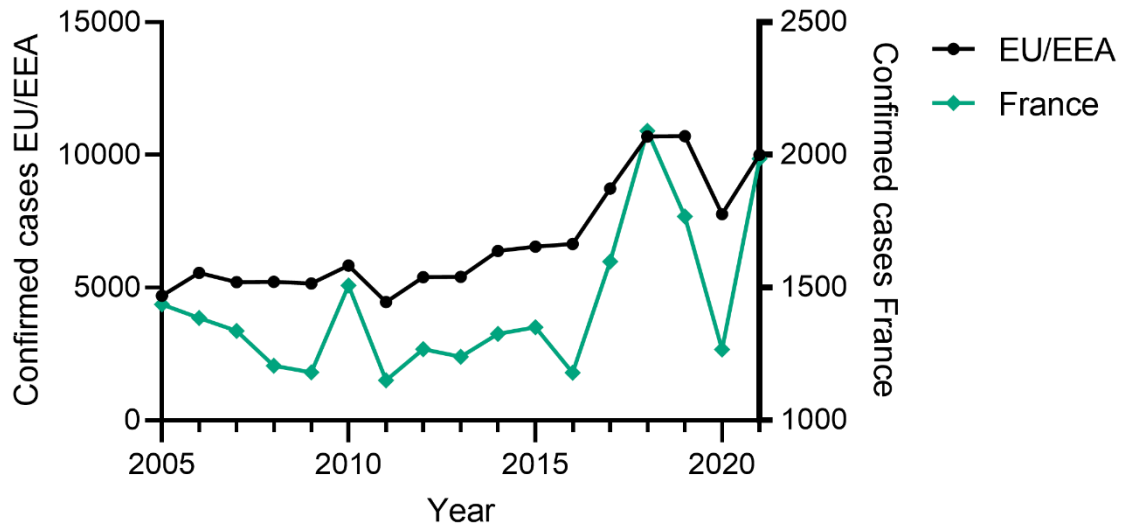


Figure 2: Cases of Legionnaires' disease reported to the ECDC Legionnaires' disease surveillance program. Total number of cases per year and region from 2005-2021. Black line, EU/EEA (left axis); green line, France (right axis). Data retrieved from ECDC Surveillance Atlas of Infectious Diseases (ECDC, 2023).

Infections with *Legionella* are most commonly community-acquired, followed by travel-related and hospital-acquired infections (Cunha, Burillo and Bouza, 2016; Beauté and European Legionnaires' Disease Surveillance Network, 2017; ECDC, 2023). Among the total cases of community-acquired pneumonia in Germany and the United States, an estimated 4-5% are due to infections with *L. pneumophila* (Von Baum *et al.*, 2008; Cunha, Burillo and Bouza, 2016).

1.3 The *Legionella* infection cycle

Legionella spp. replicate intracellularly in susceptible hosts like protozoa or in human lung alveolar macrophages in a membrane-bound compartment, the so-called *Legionella*-containing vacuole (LCV). Indeed, they were the first bacteria to be described to replicate within protozoan hosts, suggesting that this capacity allows them to also infect and replicate in human lung alveolar macrophages (Rowbotham, 1980).

Given the importance of *L. pneumophila* as the leading causative agent of LD, a large body of research has focused on the intracellular life cycle of this species and, thus, most of our knowledge stems from the analyses of *L. pneumophila* host pathogen interactions.

Upon cell contact, *L. pneumophila* enters the cell by receptor-mediated phagocytosis. It was also reported that *L. pneumophila* can be taken up to a lesser extent by so-called coiled phagocytosis, initially described by Horwitz (Horwitz, 1984). The receptors implicated in uptake of *L. pneumophila* are complement receptors 1 (CR1) and 3 (CR3) (Payne and Horwitz, 1987). Upon blocking of these receptors, uptake of the bacteria into human monocytes is strongly reduced (Payne and Horwitz, 1987). It has been shown that complement factors C2 and C3 play a role in opsonization and uptake of *L. pneumophila*, but also antibody-mediated opsonization may be of importance (Horwitz and Silverstein, 1981; Payne and Horwitz, 1987; Bellinger-Kawahara and Horwitz, 1990).

Upon internalization of *L. pneumophila* in host cell phagosomes, the bacteria avoid endocytic maturation and lysosomal fusion with the phagosome and suppress the acidification of the phagosome by inhibiting the host vacuolar ATPase (Horwitz and Maxfield, 1984; Berger and Isberg, 1993). To create a replication-permissive vacuole, *L. pneumophila* secretes a myriad of effectors into the host cell *via* the defective organelle trafficking/intracellular multiplication (Dot/Icm) type 4 secretion system (T4SS). Over 330 putative T4SS effectors have been identified for *L. pneumophila*, which manipulate crucial cellular processes conserved in protozoa and mammalian cells such as vesicle trafficking, protein degradation, apoptosis, or nuclear signaling and gene expression (Figure 3) (Burstein *et al.*, 2016; Mondino *et al.*, 2020).

Early infection is marked by the recruitment and functional modification of the small GTPase Rab1 and Sec22b to facilitate fusion of Endoplasmatic Reticulum (ER)-derived vesicles with the LCV (Machner and Isberg, 2006; Arasaki, Toomre and Roy, 2012). This process is accompanied by manipulation of key components of eukaryotic membrane trafficking pathways to generate a replication-permissive vacuole. By continuously recruiting vesicles to the LCV, *L. pneumophila* expands the LCV and ensures nutrient supply by manipulating host protein ubiquitination and the proteasomal pathways for nutrient supply (Price *et al.*, 2011; Schunder *et al.*, 2014). In addition, it was shown that *L. pneumophila* secretes so-called nucleomodulins that manipulate the host cell transcription machinery directly in the nucleus, including genes associated with innate immune responses (Rolando *et al.*, 2013; Schator *et al.*, 2023), as well as metabolic pathways of the host cell (Rolando *et al.*, 2016; Escoll *et al.*, 2017, 2021). A detailed description of the *L. pneumophila* infection cycle and secreted effectors can be found in two reviews that I co-authored, presented in **section 1.6** and **Annex A**.

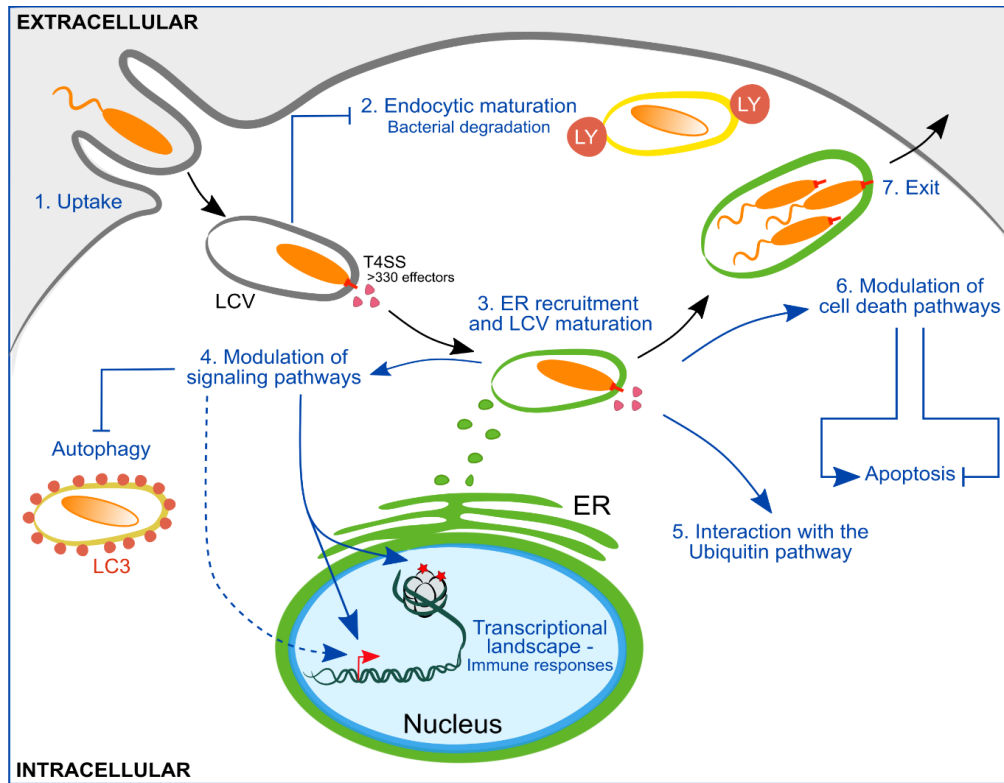


Figure 3: The *Legionella pneumophila* intracellular replication cycle and manipulation of host cell pathways. After uptake, *Legionella* establishes the *Legionella*-containing vacuole (LCV) and suppresses the association with the endolysosomal pathway. The bacteria secrete hundreds of effector proteins into the host cell through a conserved type 4 secretion system (T4SS) to recruit vesicles from the Endoplasmic Reticulum (ER) to the LCV. The bacteria also modulate several pathways in the cell to enable intracellular replication, such as suppression of autophagy, the transcriptional response of the host cell, manipulation of the ubiquitin pathway and cell death pathways. Ultimately, the bacteria switch from a replicative to a virulent phase, marked by the expression of flagella, to egress from the host cell. Adapted from Mondino *et al.*, 2020.

During the final stages of the infection cycle, the continuous depletion of nutrients from the host cell triggers a transcriptional and phenotypic switch in *L. pneumophila* from a replicative phase to a transmissive phase, that is marked by the expression of flagella and motility of the bacteria (Molofsky and Swanson, 2004; Bruggemann *et al.*, 2006). The egress of *L. pneumophila* from host cells seems to be mediated by a pore-forming activity of the bacteria. It was reported that *L. pneumophila* first disrupts the LCV membrane, leading to NLRC4 inflammasome-mediated cell death of the host cell and bacterial release (Alli *et al.*, 2000; Gao and Abu Kwaik, 2000). Moreover, *L. pneumophila* may also be extruded from infected cells in vesicles, as has been shown for infected *Acanthamoeba polyphaga* and *Acanthamoeba castellanii* (Berk *et al.*, 1998).

1.4 *Legionella* secretion systems and their role in infection

Two major secretion systems are encoded by all *Legionella* that are important for virulence and intracellular replication: The Lsp type 2 secretion system (T2SS) and the Dot/Icm T4SS (Marra *et al.*, 1992; Berger and Isberg, 1993; White and Cianciotto, 2019).

The Lsp T2SS system mediates the secretion of 25 known effector proteins into the LCV lumen or the host cell cytoplasm during infection. These effectors are involved in bacterial survival and the modulation of host cell functions, and it has been shown that T2SS mutants are impaired in virulence and infection of host cells both *in vitro* and *in vivo* (Rossier, Starkenburg and Cianciotto, 2004; DebRoy *et al.*, 2006; Rossier, Dao and Cianciotto, 2008; Cianciotto, 2014).

The most important secretion system for infection and intracellular replication is the Dot/Icm T4SS, through which over 330 putative effectors are translocated into the host cell by *L. pneumophila*, and about 220 predicted effectors by *L. longbeachae* (Burstein *et al.*, 2016; Qin *et al.*, 2017; Gomez-Valero *et al.*, 2019). Indeed, mutants with a dysfunctional T4SS fail to establish a replicative vacuole and are impaired in infection of host cells (Marra *et al.*, 1992; Berger and Isberg, 1993; Andrews, Vogel and Isberg, 1998; Segal, Purcell and Shuman, 1998; Vogel *et al.*, 1998; Wood *et al.*, 2015). The Dot/Icm T4SS is encoded by two genetic loci coding together for 27 proteins that make up the T4SS complex, which is further classified as a type 4B secretion system. The T4SS is highly conserved in *L. pneumophila* strains, and it is found in all *Legionella* species (Burstein *et al.*, 2016; Gomez-Valero *et al.*, 2019). Despite the high level of conservation of the T4SS, only 8 effectors constitute the core set of effectors present in all 58 *Legionella* species analyzed, indicating a highly diverse effector repertoire within the genus *Legionella* (Burstein *et al.*, 2016; Gomez-Valero *et al.*, 2019).

The Dot/Icm T4SS is a large protein complex that spans the bacterial inner and outer membrane. It is localized at the cell pole and helps tether the bacteria to the LCV membrane to facilitate effector translocation into the host cell (Jeong *et al.*, 2017; Böck *et al.*, 2021; Costa *et al.*, 2021). A large number of T4SS effectors (about 100) contain a C-terminal secretion signal with polar, negatively charged amino acid residues that are recognized by DotM (Nagai *et al.*, 2005; Burstein *et al.*, 2009; Huang *et al.*, 2011). However, this motif is not present in all translocated effectors, indicating that other recognition signals may be involved (Lifshitz *et al.*, 2013). In addition, structural studies on the formation of the T4SS coupling complex showed the involvement of the chaperones IcmS/IcmW, DotY and DotZ, the ATPase DotL, and LvgA, mediating the recruitment of different sets of effectors to the Dot/Icm T4SS as well as its polarity (Lockwood *et al.*, 2022; Macé *et al.*, 2022). Taken together, these studies suggest that

several pathways for effector recruitment exist in *Legionella* and that the concerted action of many proteins is involved in the complex intracellular life cycle of the bacteria.

In addition, a second T4SS, type 4A, called Lvh system, is randomly distributed among different *Legionella* species (Gomez-Valero *et al.*, 2011, 2019; Qin *et al.*, 2017). This system, named Lvh after the *Legionella* VirB homologues, shows similarity with phage genes suggesting a phage origin, and mobility as it may be excised from the chromosome into a plasmid-like mobile element (Cazalet *et al.*, 2004). The Lvh system was shown to be involved in conjugational DNA transfer, however, it seems to be dispensable for infection of macrophages and protozoa (Segal, Russo and Shuman, 1999; Ridenour *et al.*, 2003).

1.5 Molecular mimicry by secreted *Legionella* effectors

Legionella critically depend on the secretion of effectors into the host cell to establish their replication niche (Segal and Shuman, 1999). Their ability to manipulate diverse host cell pathways stems from both their large effector repertoire and the fact that many effectors harbor eukaryotic-like domains or resemble eukaryotic-like proteins (Cazalet *et al.*, 2004; De Felipe *et al.*, 2005; Burstein *et al.*, 2016; Gomez-Valero *et al.*, 2019).

Our group reported the presence of such effectors in the genome of *L. pneumophila* first (Cazalet *et al.*, 2004). Due to their close homology with amoeba proteins, it was proposed that eukaryotic-like effectors and eukaryotic effector domains were likely acquired by *Legionella* through horizontal gene transfer and co-evolution with their host cells (Cazalet *et al.*, 2004; De Felipe *et al.*, 2005; Lurie-Weinberger *et al.*, 2010; Gomez-Valero *et al.*, 2011). Interestingly, *L. longbeachae* also encodes Rab GTPase-like proteins and SH2-domain containing proteins, which were the first examples of such eukaryotic protein domains found in bacteria (Cazalet *et al.*, 2010; Kaneko *et al.*, 2018). Indeed, it has been recently shown that interactions between *Legionella* and host cells shape the effector repertoire of the bacteria, showing that continuous exposure to different amoeba species impacts the effector repertoire of *L. pneumophila* (Park, Ghosh and O'Connor, 2020).

When analyzing the *Legionella* “genus genome”, our group identified an astonishing 137 different families of eukaryotic protein domains and a total of 18,000 different putative secreted effectors among 58 analyzed *Legionella* species (Gomez-Valero *et al.*, 2019). The capacity of *Legionella* to use molecular mimicry to subvert host cell functions and to establish infection make them a prime example for the study of host-bacteria coevolution. Concepts of host-

microbe coevolution and a detailed description of molecular mimicry by *Legionella* effectors can be found in a review that I co-authored (presented in **Annex A**).

1.6 Publication – Legionnaires’ Disease: State of the Art Knowledge of Pathogenesis Mechanisms of *Legionella*

Bibliographic publication

Published in

Annual Review of Pathology: Mechanisms of Disease

Vol. 15:439-466. Published 24 January 2020.

DOI: 10.1146/annurev-pathmechdis-012419-032742.

Sonia Mondino,¹ Silke Schmidt,^{1,2} Monica Rolando,¹ Pedro Escoll,¹ Laura Gomez-Valero,¹
and Carmen Buchrieser¹

¹Institut Pasteur, Biologie des Bactéries Intracellulaires, CNRS UMR 3525, 75015 Paris, France, ²Sorbonne
Université, Collège doctoral, 75005 Paris, France

For correspondence:

Sonia Mondino	smondino@pasteur.fr
Silke Schmidt	silke.schmidt@pasteur.fr
Monica Rolando	mrolando@pasteur.fr
Pedro Escoll	pedro.escoll-guerrero@pasteur.fr
Laura Gomez-Valero	lgomez@pasteur.fr
Carmen Buchrieser	cbuch@pasteur.fr

Annual Review of Pathology: Mechanisms of Disease
**Legionnaires' Disease: State
of the Art Knowledge of
Pathogenesis Mechanisms
of *Legionella***

Sonia Mondino,¹ Silke Schmidt,^{1,2} Monica Rolando,¹
Pedro Escoll,¹ Laura Gomez-Valero,¹
and Carmen Buchrieser¹

¹Institut Pasteur, Biologie des Bactéries Intracellulaires, CNRS UMR 3525, 75015 Paris, France; email: smondino@pasteur.fr, silke.schmidt@pasteur.fr, mrolando@pasteur.fr, pedro.escoll-guerrero@pasteur.fr, lgomez@pasteur.fr, cbuch@pasteur.fr

²Sorbonne Université, Collège doctoral, 75005 Paris, France

Annu. Rev. Pathol. Mech. Dis. 2020. 15:439–66

First published as a Review in Advance on
October 28, 2019

The *Annual Review of Pathology: Mechanisms of Disease*
is online at pathol.annualreviews.org

<https://doi.org/10.1146/annurev-pathmechdis-012419-032742>

Copyright © 2020 by Annual Reviews.
All rights reserved

Keywords

Legionella, Legionnaires' disease, free-living amoeba, eukaryotic-like proteins

Abstract

Legionella species are environmental gram-negative bacteria able to cause a severe form of pneumonia in humans known as Legionnaires' disease. Since the identification of *Legionella pneumophila* in 1977, four decades of research on *Legionella* biology and Legionnaires' disease have brought important insights into the biology of the bacteria and the molecular mechanisms that these intracellular pathogens use to cause disease in humans. Nowadays, *Legionella* species constitute a remarkable model of bacterial adaptation, with a genus genome shaped by their close coevolution with amoebae and an ability to exploit many hosts and signaling pathways through the secretion of a myriad of effector proteins, many of which have a eukaryotic origin. This review aims to discuss current knowledge of *Legionella* infection mechanisms and future research directions to be taken that might answer the many remaining open questions. This research will without a doubt be a terrific scientific journey worth taking.

**ANNUAL
REVIEWS CONNECT**

www.annualreviews.org

- Download figures
- Navigate cited references
- Keyword search
- Explore related articles
- Share via email or social media

1. INTRODUCTION

1.1. The History of *Legionella* and Legionnaires' Disease

Legionella species are gram-negative bacteria that were unrecognized until the summer of 1976 when an explosive outbreak of pneumonia in Philadelphia, Pennsylvania, United States, caught the attention of the US Centers for Disease Control and Prevention (CDC) and the media. An unusual respiratory disease affected 221 attendees of the 58th annual convention of the American Legion, and 34 fatal cases were reported (1). Due to the importance of the outbreak and the fact that the causative agent was not known, the CDC employed what at that time was the largest team in its history to identify the source of the infection. In December 1976, Joseph E. McDade and Charles C. Shepard identified a bacterium as the causative agent of Legionnaires' disease. They discovered a new rod-shaped gram-negative bacterium, named *Legionella pneumophila* after the American Legion, and the new genus named *Legionella*, which at that time had only one known species (1–3).

Once the organism was identified, further studies revealed that *Legionella* had been already isolated in 1947, but it was not further characterized at that time (4). It was also shown that *Legionella* were the cause of previously unexplained outbreaks of flu-like disease such as the one that occurred in 1968 in Pontiac, Michigan, a clinical condition subsequently named Pontiac fever (5). Today, the genus *Legionella* comprises more than 65 different species, and our understanding of the biology and pathogenicity of the different members of this genus continues to increase.

1.1.1. Ecology and epidemiology. *Legionella* are gram-negative rod-shaped γ -proteobacteria that are ubiquitously found in freshwater environments, as well as in moist soil and composted material (6). *Legionella* were the first bacteria described that multiplied within protozoan hosts, primarily aquatic amoebae, which led to the idea that the capacity of the bacteria to infect protozoa may also allow them to replicate within human lung macrophages (7), a finding that was confirmed later through many different studies (reviewed in Reference 8). Today, it is established that *Legionella* are primarily found in the environment, either associated with their host or as free-living biofilm-associated bacteria (9) (**Figure 1**).

Human infection most commonly occurs as a consequence of inhaling *Legionella*-containing aerosols generated by contaminated manmade water sources, such as showers, hot tubs, plumbing networks, and air-conditioning systems. However, aspiration of contaminated water has been suggested as another route of transmission (10) (**Figure 1**). Although human-to-human transmission was not thought to occur, one case has been reported, suggesting that this form of transmission may exist, but it is rare (11). In general, human infection is incidental and a dead end for the bacteria. Individuals at higher risk for developing Legionnaires' disease are males older than 50 years, smokers, and people with an underlying medical condition such as diabetes, cancer, or immunosuppression; however, anybody can develop Legionnaires' disease (12). Summer and early fall are the most common times of the year for *Legionella* infection to occur.

The burden of Legionnaires' disease in Europe and in the United States is increasing each year, with both regions showing comparable notification rates and similar settings and epidemiology of infections. The increase in reported cases could be due to environmental conditions, such as changes in rainfall, temperature, and climate, that can affect the incidence (13); to the increasing proportion of more susceptible people, such as elderly people and those who are immunocompromised; and partly also to improvements in the surveillance systems in these regions during the past two decades (14).

To put Legionnaires' disease in perspective, from 2011 to 2015, the age-standardized rate of Legionnaires' disease in Europe showed an average annual increase of 0.09 cases per 100,000

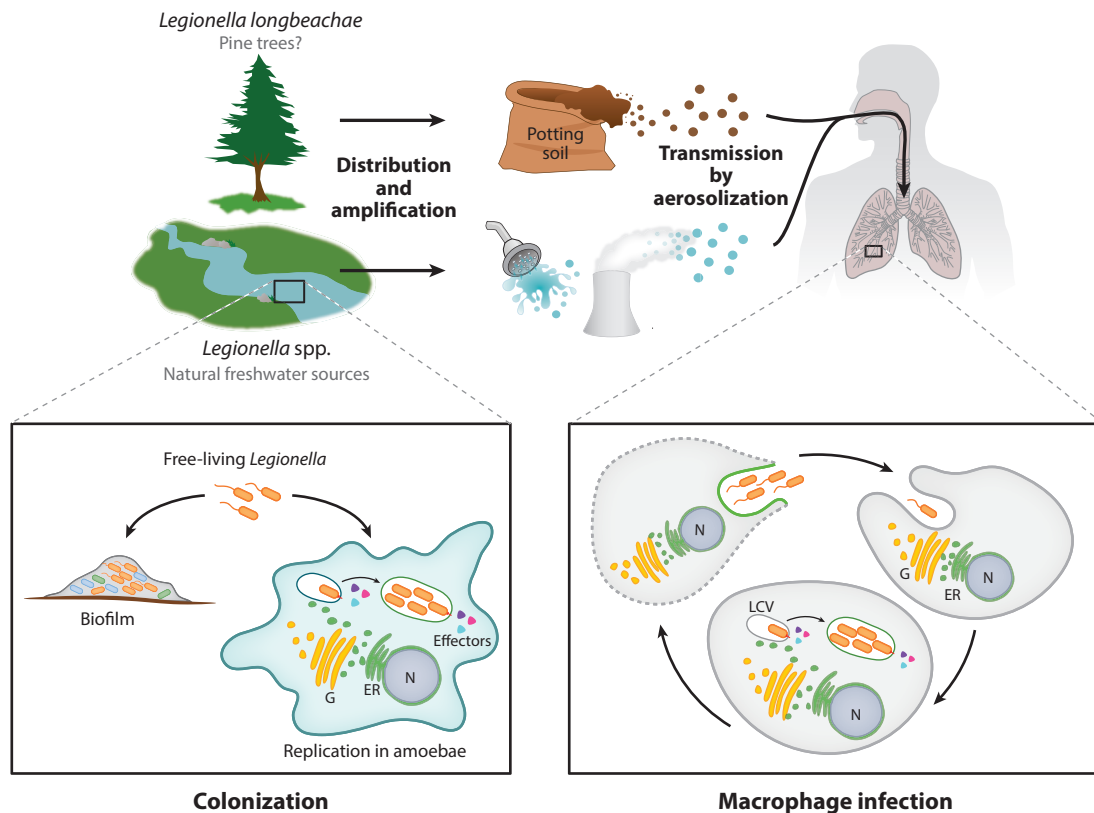


Figure 1

Transmission routes and life cycle of *Legionella pneumophila* and *L. longbeachae*. *Legionella* are commonly found in freshwater environments associated with biofilms or replicating inside amoebae. The development of manmade aquatic environments, such as showers, cooling towers, and fountains, allows for bacterial distribution and amplification in these artificial environments. Subsequent aerosolization from these sources exposes humans to inhalation or aspiration of contaminated water droplets. Through this means, *Legionella* can reach the human lungs, where they can infect alveolar macrophages using the same mechanisms that they utilize to survive within their amoebal hosts. Inside the host cell, *Legionella* reside in a separated compartment, from where they modulate diverse host signaling pathways through the secretion of effector proteins by a dedicated Dot/Icm type 4B secretion system. *L. longbeachae* is found in soil and potting mixes, some of which contain composted pine bark, and, presumably, is also associated with amoebae and biofilm communities. The route of human infection with *L. longbeachae* has not yet been established, but it may involve the inhalation of aerosolized particles generated after the manipulation of contaminated soil-derived products. Abbreviations: ER, endoplasmic reticulum; G, Golgi apparatus; LCV, *Legionella*-containing vacuole; N, nucleus.

individuals, reaching 1.30 cases per 100,000 individuals in 2015. The mortality rate fluctuated between 0.07 and 0.09 deaths per 100,000 individuals, with an overall case–fatality ratio continuously decreasing during the 2011–2015 period. The decreasing case–fatality ratio may be due to improvements in reporting completeness that may be correcting a former bias toward fatal outcomes of the disease (14). During this time, the source of infection was identified for 88% of reported cases. Of these, 70.7% of infections were community acquired; 19.9% were travel associated; and 7.3% were health-care related (14). In addition, a report by the European Centre for Disease Prevention and Control in 2016 showed 1.4 case notifications per 100,000 individuals, the highest ever observed for Europe, with a case–fatality ratio similar to the one observed in 2015 (15). In accordance with reports from Europe, active surveillance in the United States

described an incidence of 1.89 cases of Legionnaires' disease per 100,000 individuals in 2015, with a case-fatality ratio similar to that observed in Europe and with similar epidemiology and sources of infection (16).

To date, the genus *Legionella* comprises 65 species, but, interestingly, not all of them are equally responsible for the laboratory-confirmed cases of Legionnaires' disease worldwide, as *L. pneumophila* accounts for 80–90% of the cases in Europe and the United States (17). Furthermore, even within this species, disease-causing *L. pneumophila* strains are unevenly distributed, as strains of serogroup (Sg) 1 are responsible for approximately 90% of cases. Additionally, within the Sg1 strains, specific clones have recently emerged and already account for more than 50% of the reported cases of Legionnaires' disease in northern Europe, suggesting that these disease-related clones became adapted to manmade aquatic environments (18). *L. longbeachae* accounts for approximately 1% of cases worldwide, but, interestingly, for 50–60% of cases in Australia and New Zealand. However, during the past 10 years, cases caused by *L. longbeachae* infection have also been increasingly reported in Europe (19). Other species and serogroups, such as *L. pneumophila* Sg3 and Sg6, *L. bozemanii*, and *L. micdadei*, may also cause disease in Europe and the United States, but are rare (14, 17, 20).

1.1.2. Detection and treatment. For *Legionella* infection, the time to detection remains critical for the final disease outcome, especially for at-risk populations. A patient with community-acquired Legionnaires' disease generally shows pneumonic as well as extrapulmonary findings, such as gastrointestinal and neurological symptoms, relative bradycardia, hypophosphatemia, or increased serum ferritin levels (21), or some combination of these. In addition to the clinical symptoms, laboratory confirmation is essential for diagnosis; thus, specific detection methods have been developed for assessing *Legionella* infection using sputum or respiratory secretions; tissue, blood, or serum samples; or urine samples (22). These methods include serological and antibody-based assays, bacterial culture, urinary antigen tests, and nucleic acid amplification testing (for detailed reviews see References 22, 23).

Initially, serology was the method of choice to assess infections with *Legionella*, but the use of this technique has dropped significantly because of the development of more user-friendly and rapid methods, such as the urinary antigen test and polymerase chain reaction (PCR)-based detection methods. However, serology remains relevant for retrospective epidemiological investigations and when the infectious agent cannot be isolated despite strong evidence of Legionnaires' disease (22). The urinary antigen test, which detects a component of the *Legionella* cell wall in urine samples, is now widely used as a first-line screening method because it is easy and low cost, and results are rapidly available. However, as it allows only for the detection of *L. pneumophila* Sg1, there is still a need to develop assays that identify different serogroups and *Legionella* species (22, 24). Recently, PCR-based methods, such as the ones developed to detect *L. pneumophila* Sg1 (25) or the emerging *L. pneumophila* ST47 clone (26), have become more commonly used in reference centers, but with the exception of New Zealand, they are still used only rarely for clinical diagnosis (27). The utility of PCR-based assays to complement other diagnostic methods has also been demonstrated by the development of a rapid and reliable multiplexed real-time PCR assay that allows for the detection of four clinically relevant non-*pneumophila* species from mock human sputum specimens (28, 29). Nevertheless, culture on defined growth medium remains the standard reference method for *Legionella* diagnosis and identification, as it allows for identification of different *Legionella* species and serogroups, and subsequent epidemiological studies of their distribution (23).

Fortunately, antibiotic resistance is not yet a problem for *L. pneumophila* infections. To date, one fluoroquinolone (ciprofloxacin)-resistant *L. pneumophila* strain has been isolated from a patient

with Legionnaires' disease in the Netherlands (30), and the in vivo selection of fluoroquinolone resistance mutations in *L. pneumophila* was reported in two infected patients treated with these antibiotics in France (31), suggesting that, overall, antibiotic resistance is rare. Nevertheless, the incidence of fluoroquinolone resistance might be underestimated, supporting the need for prompt identification of *Legionella* infection to ensure the rapid and accurate administration of antibiotic therapy (32). Related to this, a digital PCR assay used to detect fluoroquinolone-resistant mutants of *Legionella* in patients' samples has proven useful as a diagnostic tool to assess the effectiveness of antibiotic therapy (32). Given the rare instances of resistance reported, the recommended antimicrobial therapy still includes fluoroquinolones (ciprofloxacin, levofloxacin, or moxifloxacin) or macrolides (azithromycin) (33).

1.2. *Legionella longbeachae*: Similar but Different

L. longbeachae is a major cause of disease only in Australia and New Zealand (20). However, during the past decade, infections with this bacterium have also been increasingly reported from Europe (19, 34, 35), the United States (36), Canada (37), Thailand (38), and Taiwan (39), a phenomenon that might correlate with increased clinical awareness and the wider use of improved detection methods. A total of 15 serogroups are recognized for *L. pneumophila*, but only 2 are recognized for *L. longbeachae*, with Sg1 being responsible for the majority of reported cases. A comparison of the clinical features and outcomes of disease caused by *L. pneumophila* and *L. longbeachae* showed that both species cause a similar disease pattern, and similar risk factors apply, such as older age, being a smoker, and having immunosuppression or other preexisting medical conditions. However, the main seasons for disease caused by *L. longbeachae* are spring and summer, whereas *L. pneumophila* legionellosis occurs more frequently in late summer and early fall (40).

Legionella species are ubiquitously found in aquatic environments; however, *L. longbeachae* is found in moist soil and potting mixes, presumably also associated with protozoa. Thus, gardening and using potting soil are unique risk factors associated with *L. longbeachae* infections (41). This characteristic might partly explain the differences in the seasons of onset, as gardening activities usually occur more frequently in spring and summer. The route of transmission to humans is still not completely understood, but it may be that infection occurs through the inhalation of aerosolized, contaminated compost particles that are formed when the bags are opened, when the potting mix is handled, or when plants are watered (20, 41) (**Figure 1**). Yet the report of a recent outbreak suggested that waterborne transmission of *L. longbeachae* may also occur, as the bacterium was detected both in the water of a cooling tower and as cause of human infection. However, due to the lack of clinical isolates, the cooling tower could not be confirmed as the source of this infection (42).

L. pneumophila has a pronounced, so-called biphasic life cycle during which it switches between a replicative (avirulent) and a transmissive (virulent) form (43). This differentiation, in which metabolic as well as morphogenetic changes take place, occurs during the transition between intracellular and extracellular environments, and it is accompanied by a specific switch in the gene expression pattern (44). In a simple model, when conditions are favorable for replication (in a nutrient-rich environment), *L. pneumophila* represses the expression of the transmission traits (motility, osmotic- and acid-resistance, cytotoxicity) and expresses the genes necessary to replicate and multiply intracellularly and to use the resources available from the host. Conversely, when the bacteria density increases and nutrients become limited, *L. pneumophila* stops replicating, while inducing the coordinated expression of the transmission traits (45). Thus, the bacteria escape from the cell and spread to new hosts to resume the cycle. During bacterial growth in liquid medium, the replicative and transmissive phases are represented by, respectively, the exponential and

stationary growth phases (43, 46). As a consequence of this biphasic life cycle, the infection of a host cell and survival of *L. pneumophila* inside the cell depend on its metabolic state (47). A key regulator of the switch between these two phases is carbon storage regulator A (CsrA), an RNA-binding protein that is a global repressor of the transmission genes during the replicative phase (47, 48). Its repressive function is relieved under starvation conditions, as limited amino acid availability signals the production of the alarmone guanosine pentaphosphate [(p)ppGpp], which leads to the activation of the two-component system *Legionella* transmission activator and sensor (LetA/LetS) and the alternative sigma factor RNA polymerase sigma factor (RpoS). These regulators activate transcription of the small noncoding RNAs RsmX, -Y, and -Z that sequester CsrA, thereby releasing the repression of the transmissive traits (49, 50). A genome-wide analysis of CsrA targets provided evidence that this protein impacts the central carbon metabolism, motility, and infective capacity of *L. pneumophila* by controlling the expression of at least 40 Dot/Icm type 4B secretion system (T4SS) effector proteins (51). Comparable to *L. pneumophila*, *L. longbeachae* encodes the LetA/LetS two-component system and a CsrA protein that shows 98% amino acid similarity with the *L. pneumophila* CsrA; however, transcriptome analyses have shown that this species does not undergo as dramatic a switch between the two phases as does *L. pneumophila* (50, 52). These findings are in line with the observation that the infective capacity of *L. longbeachae* seems to be independent of its growth phase (53).

Further differences between *L. pneumophila* and *L. longbeachae* were identified when the genome sequence of *L. longbeachae* was analyzed (52, 54). Particularly interesting was the presence of a largely different T4SS effector repertoire, as only about 30% of the effectors present in *L. pneumophila* were also present in *L. longbeachae* (52, 55). Also, while *L. pneumophila* is non-encapsulated and flagellated, *L. longbeachae* encodes for a capsule but not for flagella (52). Actually, the presence of cytosolic flagellin leads to clearance of *L. pneumophila* from mouse macrophages due to the activation of the Naip5–Nlrc4 inflammasome and subsequent cell death by pyroptosis (56). Mice are more susceptible to *L. longbeachae* infection, even when compared with an *L. pneumophila* mutant lacking flagella, suggesting that the high lethality and the poor stimulatory activity of *L. longbeachae* could also be a consequence of the presence of a capsule as well as the different reservoir of effectors (52, 57). Overall, clear phenotypic differences are evident between these two species, and yet little is known about *L. longbeachae*'s biology and infection processes.

2. LEGIONELLA: AN ARMY WITH A LARGE ARSENAL OF WEAPONS

Legionella are able to replicate in a wide variety of phagocytic hosts, ranging from numerous amoeba species to mammalian cells (8), in which they form a distinct membrane-bound replicative niche known as the *Legionella*-containing vacuole (LCV) (**Figure 1**). This sophisticated intracellular compartment allows the bacteria to evade phagolysosomal degradation as well as to shelter from intracellular defenses and to intercept nutrients to support replication. In order to do these things, *Legionella* employ different secretion systems that deliver virulence-associated proteins across one or two cell membranes to the site of action. While the type 2 secretion system (T2SS) and T4SS are encoded by all *Legionella* strains, the type 1 secretion system (T1SS) is restricted to *L. pneumophila*, and the type 4A secretion system (Lvh type) is randomly distributed among different species (58, 59). The T2SS and T4SS have been extensively studied in *L. pneumophila* as they play essential roles during infection.

The delivery of effector proteins via T2SS is a two-step process in which proteins are first transported into the periplasm, where they are recognized by the T2SS apparatus, and then exit through a dedicated pore (60). Subsequently, T2SS effectors may be found associated with the LCV membrane after they escape into the host cytosol (61). This system translocates more than 25 effector proteins (62) that play major roles in intracellular replication in amoebae and also in

L. pneumophila pathogenesis in humans (63). One example is a chitinase that is secreted by T2SS that promotes bacterial persistence in the lungs (64).

The Dot/Icm T4SS is critical for LCV biogenesis and intracellular replication (65, 66). Recently, it was shown that the *L. pneumophila* T4SS is located at the bacterial cell poles, and effector delivery is triggered by phagocytosis (67, 68). Importantly, T4SS governs all steps of the intracellular life of *L. pneumophila* by secreting more than 330 effector proteins that target fundamental cellular processes conserved between protozoa and mammals (Table 1) (Figure 2).

2.1. *Legionella* Successfully Escape Host Cell Degradation

After bacterial uptake, *L. pneumophila* avoids endocytic maturation and phagolysosomal degradation. Instead, the bacterium modulates specific host cell signaling pathways through the secretion of a myriad of T4SS effector proteins, allowing for the formation of a safe niche where *Legionella* can efficiently replicate. During the past two decades, several of these effector proteins have been characterized functionally, leading to a better understanding of the mechanisms employed by *L. pneumophila* to subvert host cell functions. Among these mechanisms, several novel posttranslational modifications of host proteins induced by a bacterial pathogen were reported in *Legionella* for the first time.

2.1.1. *Legionella pneumophila* uptake and evasion of the endocytic maturation pathway.

Although the Dot/Icm T4SS seems to promote bacterial uptake into phagocytic cells (69, 70), the entry mechanism itself depends on the host cell machinery. *L. pneumophila* is engulfed by host cells through a phagocytic and macropinocytic phosphatidylinositol (3,4,5) trisphosphate [PtdIns(3,4,5)P₃]-rich cup (71). Furthermore, it has been shown that a functional T1SS is also required for entry into the host cell (72). Shortly after internalization, phagosomes containing *L. pneumophila* evade endocytic maturation and prevent fusion with lysosomes (73). *L. pneumophila* prevents vacuolar acidification by blocking the host vacuolar ATPase (v-ATPase), a proton pump present throughout the membranes of the endocytic pathway. This process is driven by two secreted effectors: SidK and WipB. SidK binds the v-ATPase regulatory subunit VatA, resulting in the inhibition of ATP hydrolysis and proton translocation (74). WipB is a lysosome-targeted phosphatase that localizes to acidified LAMP1-positive lysosomal compartments where it interacts with the v-ATPase. SidK and WipB may converge to repress the activity of the host v-ATPase (75).

Phagosome maturation is tightly regulated by T4SS, as the Dot/Icm system appears to redirect vacuoles containing *L. pneumophila* away from the canonical endocytic pathway at an extremely early stage of infection. Small GTPases of the Rab family represent an important group of proteins involved in phagosome maturation, and the binding of specific Rab proteins to intracellular organelles enables specific targeting. Proteomic analyses of purified LCVs revealed the presence of several small GTPases anchored to the pathogen vacuole: Rab5, Rab7, Rab14, and Rab21 (76, 77). The GTPase Rab5 is an important regulator of the early endocytic pathway: GTP-bound Rab5 orchestrates the recruitment of several downstream ligands, resulting in PtdIns(3)P-mediated recruitment of early endosomal antigen 1 (EEA1) (78). Interestingly, a secreted effector named VipD has been shown to exhibit phospholipase A1 activity that is activated only upon binding to endosomal Rab5. VipD thus localizes to endosomes and can catalyze the removal of PtdIns(3)P from endosomal membranes. Consequently, EEA1 and other transport and fusion factors are depleted from endosomes, rendering them fusion incompetent (79). PieE, another secreted effector, has been shown to bind both Rab5 and Rab7, but its specific function remains unknown (80). Rab7 is a small GTPase protein that has a crucial role during phagosome maturation, as it gradually replaces Rab5 to induce the fusion between the degradative late endosomes and lysosomes (81). Rab5 and Rab7 also play roles in regulating

Table 1 Selected secreted effectors of *Legionella* with functions discussed in the review

Effector ^a	Gene ^b		Cellular target and function	Reference
	Paris strain	Philadelphia strain		
Bacterial uptake and evasion from the endocytic maturation pathway				
SidK	<i>lpp1030</i>	<i>lpg0968</i>	Blocks the host vacuolar ATPase to restrain vacuolar acidification	74
WipB	<i>lpp2775</i>	<i>lpg2718</i>		75
VipD	<i>lpp2888</i>	<i>lpg2831</i>	Depletes fusion factors from the endosomal membrane	79
PieE	<i>lpp1953</i>	<i>lpg1969</i>	Binds Rab5 and Rab7	80
RidL	<i>lpp2259</i>	<i>lpg2311</i>	Impairs retrograde trafficking	83
Bacterial interaction with the ER and LCV formation				
SidM (DrrA)		<i>lpg2464</i>	Binds the membrane	194
			Recruits Rab1 to the LCV	87, 88
			AMPylates Rab1	89, 90
SidD		<i>lpg2465</i>	DeAMPylates Rab1	91
LepB	<i>lpp2555</i>	<i>lpg2490</i>	Converts Rab1 GTP into Rab1 GDP	92
AnkX	<i>lpp0750</i>	<i>lpg0695</i>	Attaches a phosphocholine moiety to Rab1	93
Lem3	<i>lpp0751</i>	<i>lpg0696</i>	Removes phosphocholination	94
LidA	<i>lpp1002</i>	<i>lpg0940</i>	Enables the tethering of ER-derived vesicles	90
RalF	<i>lpp1932</i>	<i>lpg1950</i>	Recruits Arf1 to the LCV membrane	95
Ceg9	<i>lpp0316</i>	<i>lpg0246</i>	Interacts with Rtn4	97
LseA	Corby strain LPC_2110		Mediates membrane fusion	101
LegC3	<i>lpp1666</i>	<i>lpg1701</i>	Modulates membrane fusion events	102, 103
LegG1 (MitF)		<i>lpg1976</i>	Activates Ran GTPase; implicated in mitochondrial fragmentation	104, 105
Establishing a safe niche: hijacking the host cell response				
Autophagic response				
RavZ		<i>lpg1683</i>	Irreversibly deconjugates LC3	108
	<i>lpp1139</i>	<i>lpg1137</i>	Cleaves syntaxin 17	109
<i>LpSPL</i>	<i>lpp2128</i>	<i>lpg2176</i>	Prevents autophagosome formation	110
Kinase signaling				
LeSHs	11 different effectors		Bind to phosphorylated Tyr	111
LegK7	<i>lpp1899</i>	<i>lpg1924</i>	Targets the Hippo pathway	112
LegK1	<i>lpp1439</i>	<i>lpg1483</i>	Activates NF-κB	114
LnaB	<i>lpp2592</i>	<i>lpg2527</i>	Activates NF-κB	115
MavC	<i>lpp2086</i>	<i>lpg2147</i>	Dampens NF-κB signaling	116
Lgt1	<i>lpp1322</i>	<i>lpg1368</i>	Decrease production of IκB, an inhibitor of the NF-κB pathway	117
Lgt2		<i>lpg2862</i>		
Lgt3	<i>lpp1444</i>	<i>lpg1488</i>		
SidI	<i>lpp2572</i>	<i>lpg2504</i>		
SidL	<i>lpp0504</i>	<i>lpg0437</i>		
Ceg4	<i>lpp0110</i>	<i>lpg0096</i>	Impacts MAPK signaling	121
Epigenetic regulation				
RomA	<i>lpp1683</i>	<i>lpg1718</i>	Changes histone marks	122
mRNA processing				
SnpL	<i>lpp2587</i>	<i>lpg2519</i>	Regulates mRNA processing	123

(Continued)

Table 1 (Continued)

Effector ^a	Gene ^b		Cellular target and function	Reference
	Paris strain	Philadelphia strain		
Ubiquitin pathway				
LubX	<i>lpp2887</i>	<i>lpg2830</i>	E3 ligase; targets Clk1	124
GobX	<i>lpp2521</i>	<i>lpg2455</i>	E3 ligase; locates to Golgi membranes	125
RavN	<i>lpp1112</i>	<i>lpg1111</i>	E3 ligase	126
SidC	<i>lpp2579</i>	<i>lpg2511</i>	E3 ligase; phagosomal remodeling	128
LegU1	<i>lpp0233</i>	<i>lpg0171</i>	F-box domain	129
LicA	<i>lpp1363</i>	<i>lpg1408</i>		
AnkB	<i>lpp2082</i>	<i>lpg2144</i>	F-box domain; ubiquitinates ParvB and supplies nutrients to the vacuole	129–131
SidE	<i>lpp0304</i>	<i>lpg0234</i>	Ubiquitinate ER-associated Rab GTPases and target Rtn4 to control tubular ER dynamics	132, 133, 135
SdeA	<i>lpp2096</i>	<i>lpg2157</i>		
SdeB	<i>lpp2095</i>	<i>lpg2156</i>		
SdeC	<i>lpp2092</i>	<i>lpg2153</i>		
SidJ	<i>lpp2094</i>	<i>lpg2155</i>		
LotA (Lem 21)	<i>lpp2202</i>	<i>lpg2248</i>	Cleaves ubiquitin from the LCV	136
Modulation of cell death				
SidF	<i>lpp2637</i>	<i>lpg2584</i>	Antagonizes proapoptotic Bcl-rambo	138
SdhA	<i>lpp0443</i>	<i>lpg0376</i>	Prevents cell death	139
	<i>lpp0782</i>	<i>lpg0716</i>	Induce proapoptotic caspase-3 activity	
Ceg18	<i>lpp0959</i>	<i>lpg0898</i>		140
Lem12	<i>lpp1595</i>	<i>lpg1625</i>		
LegS2	<i>lpp2128</i>	<i>lpg2176</i>		
VipD	<i>lpp2888</i>	<i>lpg2831</i>		

Abbreviations: ER, endoplasmic reticulum; LCV, *Legionella*-containing vacuole; MAPK, mitogen-activated protein kinase.

^aEmpty cells in the Effector column indicate that no specific name was given to the effector other than the gene name.

^bEmpty cells in the Gene column indicate that there is no orthologous gene in the *Legionella* species.

retrograde trafficking, connecting the endosomal system with the trans-Golgi network (82). *L. pneumophila* affects this trafficking pathway through the secreted effector RidL (83).

2.1.2. *Legionella pneumophila* interaction with the endoplasmic reticulum and formation of *Legionella*-containing vacuoles.

Intercepting vesicular traffic from endoplasmic reticulum (ER) exit sites and vesicle budding from the ER appear to be required for the establishment of the replication vacuole (84). In particular, it has been proposed that the LCV is localized in proximity to the ER exit sites, ideally suited to hijack vesicle trafficking from the retrograde secretory pathway on the route to the Golgi compartment (85). The small GTPases Arf1, Sar1, and Rab1 are important molecules that regulate host vesicular and membrane transport processes; during *L. pneumophila* infection they participate in the recruitment of ER-derived vesicles to the LCV membrane. Rab1 recruitment to the LCV is a well-orchestrated T4SS-dependent process that has been extensively studied. Indeed, Rab1 is a direct target of several different secreted effectors. (a) SidM (DrrA) is a protein containing three functional domains: a C-terminal domain that binds PtdIns(4)P (86), thereby also representing an LCV marker that accumulates on the membrane of the pathogen compartment; a guanine nucleotide exchange factor and a guanine

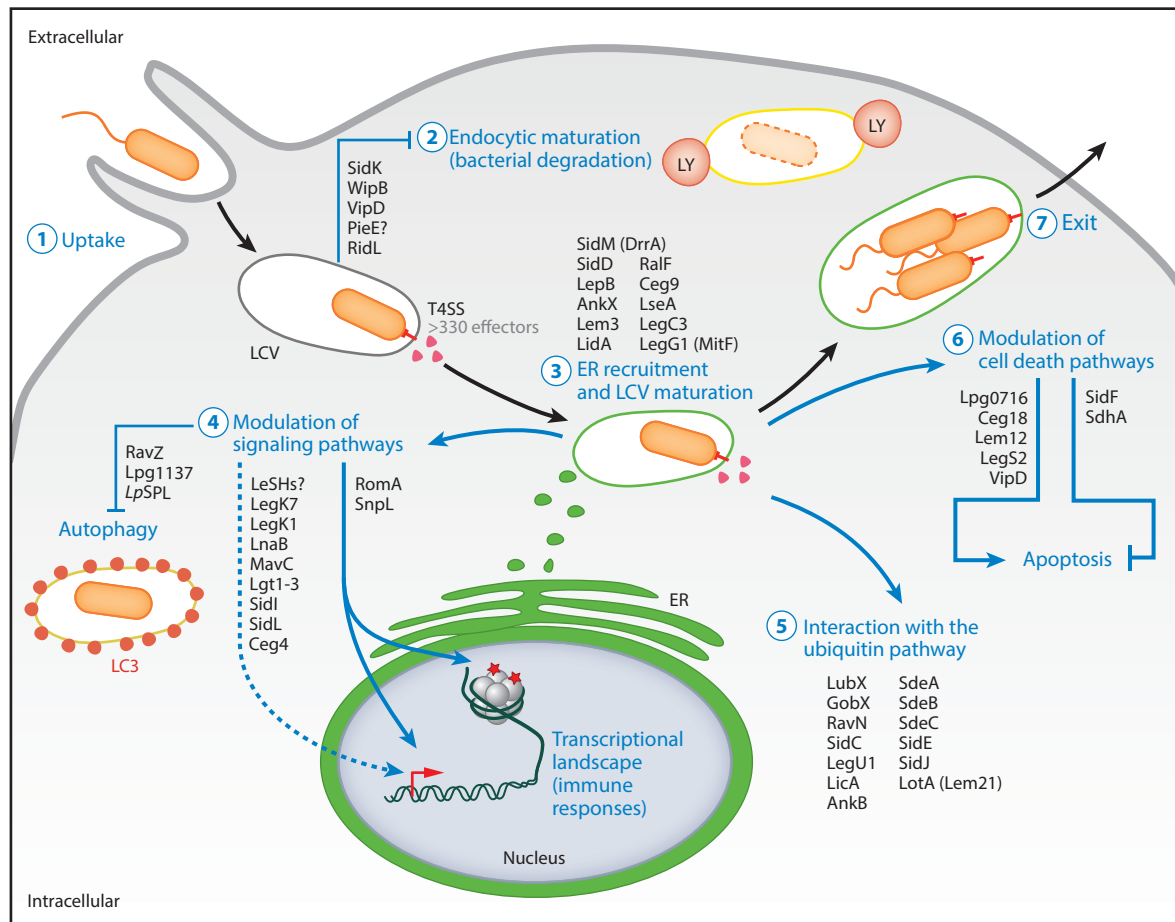


Figure 2

Intracellular pathways regulated by secreted *Legionella pneumophila* effectors: representation of the intracellular cycle of *L. pneumophila* and the effectors secreted by the type 4 secretion system that control the cellular response at each step of the cycle. After bacterial uptake (1), *L. pneumophila* avoids endocytic maturation (2) and instead recruits ER-derived vesicles to the LCV (3), allowing for the formation of a safe niche where (4–6) the bacterium replicates and modulates cell signaling pathways. Once the replication cycle is completed, *L. pneumophila* exits the cell (7) and infects a new host. Abbreviations: ER, endoplasmic reticulum; LCV, *Legionella*-containing vacuole; LY, lysosome.

nucleotide dissociation inhibitor displacement factor that recruit Rab1 to the LCV (87, 88); and an N-terminal enzymatic domain that catalyzes the addition of adenosine monophosphate to Rab1 (AMPylation) (89, 90). (b) SidD has been characterized as a deAMPyase that removes the adenosine monophosphate moiety from Rab1 (91). (c) LepB encodes for a GTPase-activating protein that converts Rab1 GTP into Rab1 GDP (92). (d) The phosphocholinase AnkX attaches a phosphocholine moiety to Rab1, thus disrupting secretory trafficking (93). (e) Lem3 removes this phosphocholination (94). And, finally, (f) LidA has Rab1-binding activity and facilitates the tethering of ER-derived vesicles (90). Thus, the recruitment and functional modifications of Rab1 facilitate the recruitment of ER-derived vesicles to the phagosome membrane.

The function of the small GTPases Arf1 and Sar1 is also important for the recruitment and tethering of ER vesicles to the LCV (84). Arf1 has been shown to play a critical role in coat protein

complex (COP) I-mediated retrograde trafficking in eukaryotic cells, whereas Sar1 is involved in intracellular COPII-mediated protein trafficking from the ER to the Golgi apparatus. The secreted effector RalF is a guanine nucleotide exchange factor that directly activates and recruits Arf1 to the LCV membrane (95). Interestingly, it has been suggested that because the bacteria enter at the cellular periphery, where the ER interacts with the plasma membrane (96), the first microbial encounter would be with the tubular peripheral ER. This was confirmed by the observation that the secreted effector Ceg9 directly associates with Rtn4, a protein that regulates ER tubule formation (97).

The LCV fuses with the ER by a noncanonical pairing of the vesicular membrane SNARE protein Sec22b on ER-derived vesicles with a plasma membrane target SNARE complex containing host syntaxins (98). SNAREs are host proteins that directly facilitate membrane fusion events (99). The SidM (DrrA) effector is sufficient to stimulate SNARE-dependent membrane fusion within Rab1 activation (100). Nonetheless, *L. pneumophila* also encodes for a secreted effector, LseA, that acts as a SNARE protein, which is suggested to mediate membrane fusion events in Golgi-associated pathways (101). Additionally, the LegC3 effector has also been referred to as a SNARE-like protein that can form a SNARE-like hybrid complex with VAMP4 and modulate membrane fusion events (102, 103).

The LCV is also able to move along microtubules, thanks to the activity of the secreted effector LegG1 (MitF), which activates Ran GTPase, thus promoting LCV formation, microtubule stabilization, and LCV motility (104). Interestingly, it has been recently shown that the T4SS effector LegG1 (MitF) is also implicated in mitochondrial fragmentation during infection that depends on the host factors DNMI1L, Ran, and RanBP2 by a mechanism that, although not yet elucidated, has been suggested to involve WASP-Arp2/3-mediated recruitment of DNMI1L to mitochondria. *Legionella*-induced mitochondrial fragmentation leads to a Warburg-like metabolism in the host cell that promotes pathogen replication (105, 106).

2.1.3. *Legionella pneumophila* modulation of host cell signaling pathways. The transformation of the nascent phagosome into a vacuole derived from the ER resembles an immature autophagosome. Indeed, it has been shown that the LCV carries markers associated with autophagosomes (107) and that several T4SS effectors play roles in inhibiting the autophagic response of the host cell to avoid the degradation of the vacuole by the autophagy machinery: (a) RavZ interferes with autophagy by irreversibly deconjugating an autophagy-related ubiquitin-like protein, LC3, from phosphatidylethanolamine (108); (b) Lpg1137 targets the mitochondria-associated ER membranes (MAMs) and cleaves syntaxin 17, a SNARE implicated in autophagy, via its Ser protease activity, thereby blocking the process (109); (c) *LpSPL*, another MAM-located effector, prevents autophagosome formation by disturbing the host's sphingolipid metabolism (110).

During its intracellular replication cycle, *L. pneumophila* continuously interferes with different host cell signaling pathways to hijack the cellular response. An important role in signal transduction in mammalian cells is played by the tyrosine kinase machinery, and Src homology 2 domains, sequence-specific phosphotyrosine-binding modules, which are key actors required for substrate recruitment and catalytic activity. Interestingly, *L. pneumophila* encodes for Src homology 2 domain proteins that can translocate into host cells and bind phosphotyrosine (111). Furthermore, LegK7, a newly described effector kinase, promotes intracellular bacterial growth by targeting the host cell Hippo pathway (112). LegK7, like the Hippo kinase MST1, directly phosphorylates MOB1, thus triggering a signaling cascade that alters the transcriptional landscape of host cells.

Another preferential target of bacterial pathogens is the nuclear factor kappa-light-chain enhancer of activated B cells (NF- κ B) pathway, due to its central role in transcriptional regulation and activation of host innate immune responses. It has been observed that *L. pneumophila* infection

impacts the NF- κ B pathway in a differential way, depending on the stage of infection (113). LegK1 and LnaB are secreted *L. pneumophila* effectors that strongly activate the NF- κ B transcription factor (114, 115). The activity of MavC—a transglutaminase that catalyzes monoubiquitination of the E2 enzyme UBE2N, thus inhibiting the formation of Lys63 polyubiquitinated chains—dampens NF- κ B signaling, probably counteracting the effects of NF- κ B activation at the initial phase of infection (116). Conversely, the Lgt family of cytotoxic glucosyltransferases, Lgt1, -2, and -3, together with SidI, and SidL specifically decrease the production of I κ B, an inhibitor of NF- κ B (117). Thus *L. pneumophila* secretes several different effectors to fine-tune NF- κ B signaling to its advantage.

Similar to the NF- κ B pathway, the mitogen-activated protein kinase (MAPK) pathway is also a central signaling cascade that is essential for the activation of immune responses. Indeed, *L. pneumophila* activates this pathway in a T4SS-dependent manner (118, 119) by secreting five effectors that inhibit host translation and lead to MAPK activation, thus shaping the transcriptional response of the host cell (120). Another secreted effector, Ceg4, can modulate the phosphorylation state of eukaryotic MAPKs through its haloacid dehalogenase–like phosphatase domain (121).

L. pneumophila is also able to directly modulate the host's transcriptional machinery by modifying histone marks. The T4SS-secreted *L. pneumophila* effector RomA methylates Lys14 of histone H3, a key residue usually acetylated at active promoters, to decrease cellular transcription (122). SnpL, another effector, also targets the host cell nucleus, where it binds the eukaryotic transcription elongation factor SUPT5H, which is involved in regulating RNA polymerase II–dependent mRNA processing and elongation (123).

2.1.4. *Legionella pneumophila* and interactions with the ubiquitin and apoptotic pathways.

Ubiquitination is an important posttranslational modification in eukaryotic cells that regulates the activity and cellular localization of proteins and affects essential routes, for example, the immune response. Several T4SS effectors of *L. pneumophila* show similarities to eukaryotic E3 ubiquitin ligases, enzymes that actively participate in protein ubiquitination. LubX and GobX are U-box domain-containing E3 ligases: LubX, structurally similar to the RING E3 ligase domain, directly modifies Cdc2-like kinase 1 (Clk1) (124), whereas the targets of GobX remain to be determined, although its localization to Golgi membranes suggests that it functions at or in close proximity to this compartment (125). RavN encodes an atypical U-box-like motif and possesses E3 ubiquitin ligase activity (126), while SidC, an effector known to enhance ER recruitment to the LCV (127), defines a unique family of E3 ubiquitin ligases. SidC possesses atypical ubiquitin ligase activity as it uses a Cys–His–Asp triad to catalyze the formation of high-molecular-weight polyubiquitin chains through multiple ubiquitin Lys residues (128). LegU1, LegAU13, and LicA are F-box domain-containing proteins, translocated into the cytosol by T4SS, which specifically interact with components of the host ubiquitination machinery. In addition, LegU1 targets and ubiquitinates the host chaperone BAT3, a protein involved in apoptosis and ER stress response (129). AnkB is another F-box-containing secreted effector that interacts with Skp1 to form a Skp–Cullin–F-box complex that ubiquitinates ParvB (130). AnkB has also been suggested to play a role in supplying the replicative vacuole in amino acids through AnkB-dependent degradation of polyubiquitinated proteins that are used by *L. pneumophila* as nutrients (131).

Recently, the members of the SidE effector family (SdeA, SdeB, SdeC, and SidE) were shown to ubiquitinate ER-associated Rab GTPases by a novel ubiquitination mechanism that does not require E1 and E2 enzymes of the host ubiquitination machinery: Ubiquitin is first activated by Arg–ADP ribosylation by the mono-ADP-ribosyltransferase domain of SdeA; the intermediate is then cleaved by the phosphodiesterase domain within the same enzyme; and this occurs concomitantly with the attachment of ubiquitin to Ser residues of substrate proteins via a phosphoribosyl

linker (132, 133). Interestingly, the activity of SidE is affected by SidJ, an effector that reverses the ubiquitination of SidE-modified substrates (134). The members of the SidE family also transfer ubiquitin onto Rtn4 to control tubular ER dynamics (135). LotA (Lem21) is another deubiquitinase that was recently discovered and that possesses a Cys protease activity by which it is able to cleave ubiquitin from the LCV (136).

To preserve its replication niche, *L. pneumophila* modulates host cell-death pathways via the action of several T4SS substrates (137). SidF directly interacts with and neutralizes proapoptotic BNIP3 and Bcl-rambo (138), whereas SdhA contributes to the prevention of cell death by an unknown mechanism (139). Finally, *L. pneumophila* also possesses the ability to promote cell death: Several secreted effectors have been shown to induce proapoptotic caspase-3 activity (140). Therefore, fine-tuned control of the secretion of antiapoptotic and proapoptotic effectors might be necessary to support bacterial replication at the beginning of infection and to promote the release of the pathogen from the host cell at the end of the infection cycle.

2.2. Specific Features of the *Legionella* Dot/Icm T4SS Effector Repertoire

It is well established that *L. pneumophila* delivers more than 330 effector proteins into its host cells (141–144). Interestingly, a lack of phenotypes is often associated with genetic mutations in single effectors, and intracellular growth is completely abolished only when the Dot/Icm T4SS is inactivated. This observation, associated with the presence of multiple paralogs of the same protein, led to the concept of effector redundancy, which suggests there are compensatory roles for two proteins or set of proteins with the same biological activity or different activities that have an impact on the same pathway or cellular process. Transposon site hybridization was used to identify such so-called redundant proteins and allowed for the suggestion that there were several functional groups of effectors that concomitantly act on the same cellular pathway; consequently, their combined deletion altered *L. pneumophila* growth in host cells (145). Some examples are the many effectors that affect Rab1 activity or the Lgt family—Lgt1, Lgt2, and Lgt3—that are differentially regulated during bacterial growth and affect eukaryotic protein synthesis (146).

The *L. pneumophila* effector repertoire contains proteins that regulate the function of other bacterial effectors within the host cell, called metaeffectors. The first metaeffector described was the tandem U-box protein LubX, which ubiquitinates the host kinase Clk1 (124), and also exploits the host proteasome to temporally regulate SidH activity in the host cell (147). Since metaeffectors were first described, several others have been identified, such as SidJ, which modulates the function of SidE family proteins (148), Lpg2505, which inhibits SidI toxicity (149), and Lpg2149, which inhibits both MavC and MvcA (150). Recently, a systematic analysis of effector–effector regulation identified 14 additional metaeffectors whose functions can now be studied in detail (151).

One of the most intriguing features of the *Legionella* T4SS effectors, first identified during *L. pneumophila* genome sequencing analysis, is the presence of a large variety and high number of so-called eukaryotic-like proteins and eukaryotic domain-encoding proteins (152). This finding led to the hypothesis that *L. pneumophila* has acquired these proteins by horizontal gene transfer from its eukaryotic hosts (amoebae) and now uses them to subvert host functions (152). Indeed, further evolutionary analyses supported this hypothesis (153–155). One of the most evident examples is the sphingosine-1-phosphate lyase-encoding gene, which different evolutionary analyses have suggested was acquired from amoebae (156, 157). Furthermore, the protein encoded by this gene was shown to have the same activity as its eukaryotic counterpart, modulating the sphingolipid metabolism, and it is thus an excellent example of molecular mimicry, a main virulence strategy employed by *Legionella* (110, 158).

Interestingly, it is not only *L. pneumophila* but also all *Legionella* species that encode remarkably large effector repertoires, as the genus harbors more than 18,000 effectors that differ surprisingly among species (59, 159). **Figure 3** shows the distribution of the effectors discussed in this review (see also **Table 1**), clearly revealing that many of them are conserved only in *L. pneumophila* and rarely present in other *Legionella* species. All *Legionella* species show evidence of long-lasting coevolution with their protozoan hosts, as the analyses of the genus genome identified effector proteins encoding 137 different eukaryotic-like domains and more than 200 eukaryotic-like proteins (59). An interesting example constitutes the group of Rab-like proteins, which are uniquely present in the effector repertoire of certain *Legionella* species, including *L. longbeachae*, that clearly have been acquired from eukaryotic organisms, probably protists, as seen in the two examples in **Figure 4** (59). Like many bacterial pathogens, *L. pneumophila* also targets host Rab GTPases, for example, by recruiting Rab1 to the LCV to finally control vesicle trafficking from ER exit sites (160). The identification of bacterial Rab-like GTPases in the *Legionella* genome suggests that these bacteria are able to subvert host cell trafficking by secreting their own Rab proteins into the host cell, and these could interact or compete with certain host Rabs during infection.

Despite our increased knowledge about the function of the effectors secreted by *L. pneumophila*, little is known about the effectors of other *Legionella* species. When considering *L. longbeachae*, the second most frequent cause of Legionnaires' disease, more than 66% of the reported *L. pneumophila* Dot/Icm T4SS effectors are missing in this species, while 51 novel substrates have been identified (52). To date, only one *L. longbeachae* effector protein has been characterized. It was shown that SidC, similar to its homolog in *L. pneumophila*, is a PtdIns(4)P-binding protein that resides on the LCV and promotes ER recruitment (161). Previous reports suggested that trafficking of the *L. longbeachae* vacuole might be different from that of *L. pneumophila* because the *L. longbeachae* LCV may acquire early and late endosomal markers (53). However, a recent report suggests that both species may develop similar replicative niches, albeit through different mechanisms, probably correlated with the specific set of effectors each species secretes into the host cell (162). Therefore, gaining better knowledge about the effectors secreted by *L. longbeachae* should enrich our understanding of the diverse mechanisms *Legionella* species utilize to successfully infect their hosts.

3. LEGIONELLA-AMOEBAE INTERACTIONS: A NICHE FOR THE EMERGENCE OF HUMAN PATHOGENS

In the environment, *Legionella* replication within protozoa is likely the most common mechanism of bacterial proliferation (163). Free-living amoebae are a group of protozoa ubiquitously found in soil and natural or man-made aquatic environments. They feed on microorganisms, and interactions over millions of years gave rise to the ability of *Legionella* to overcome intracellular degradation and instead survive or even replicate inside protozoa. Thus, free-living amoebae can act as Trojan horses, delivering microorganisms to new habitats and hosts in the form of intact amoeba or expelled vesicles, while protecting the microorganisms from hostile environmental conditions (164). Indeed, many medically important environmental bacteria, viruses, and fungi are associated with and are able to survive inside amoebae (165). *Legionella*-amoebae interactions were characterized shortly after *Legionella* bacteria were identified (7), and since then, the similarities between the infection of amoebae and of human macrophages have become more evident (8, 166). Indeed, bacterial inactivation mechanisms are the same in amoebae and macrophages, as both consist of lysosomal degradation of the phagocytized material. Additionally, both functional outcomes (digestion and immunity, respectively) are related, as it has been proposed that they share a common evolutionary origin in metazoans (167).

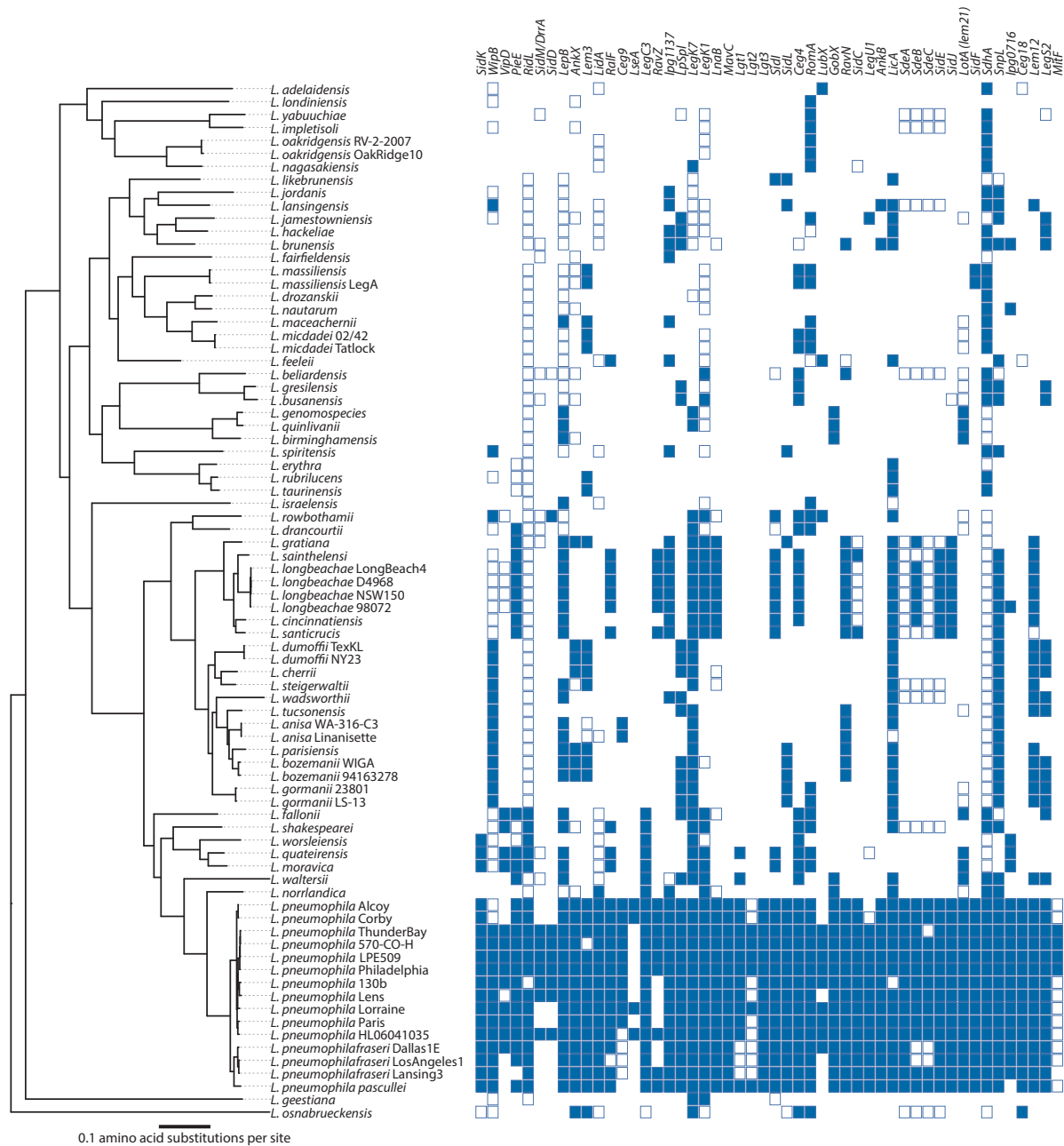


Figure 3

Distribution of 50 selected effectors from *Legionella pneumophila* in 58 different *Legionella* species and 80 *Legionella* strains. The sequence of the effector of *L. pneumophila* strain Philadelphia was used as reference to construct the table of orthologs to define their presence or absence in 80 *Legionella* strains previously analyzed (59). Blue-filled squares indicate the presence of the gene in the corresponding species based on predictions using *PanOCT* (the Pan-genome Ortholog Clustering Tool) with an identity cutoff of 30%, a BLAST (Basic Local Alignment Search Tool) Expect (*E*)-value cutoff of 10^{-5} , and a minimum percentage match length of subject and query of 65%. Blue-outlined squares indicate that an orthologous gene in the corresponding species is present, but the identity and/or the minimum percentage match length is under the cutoff selected for *PanOCT*. Empty spaces indicate that no orthologous gene was identified in the corresponding strain. The scale bar represents 0.1 amino acid substitutions per site.

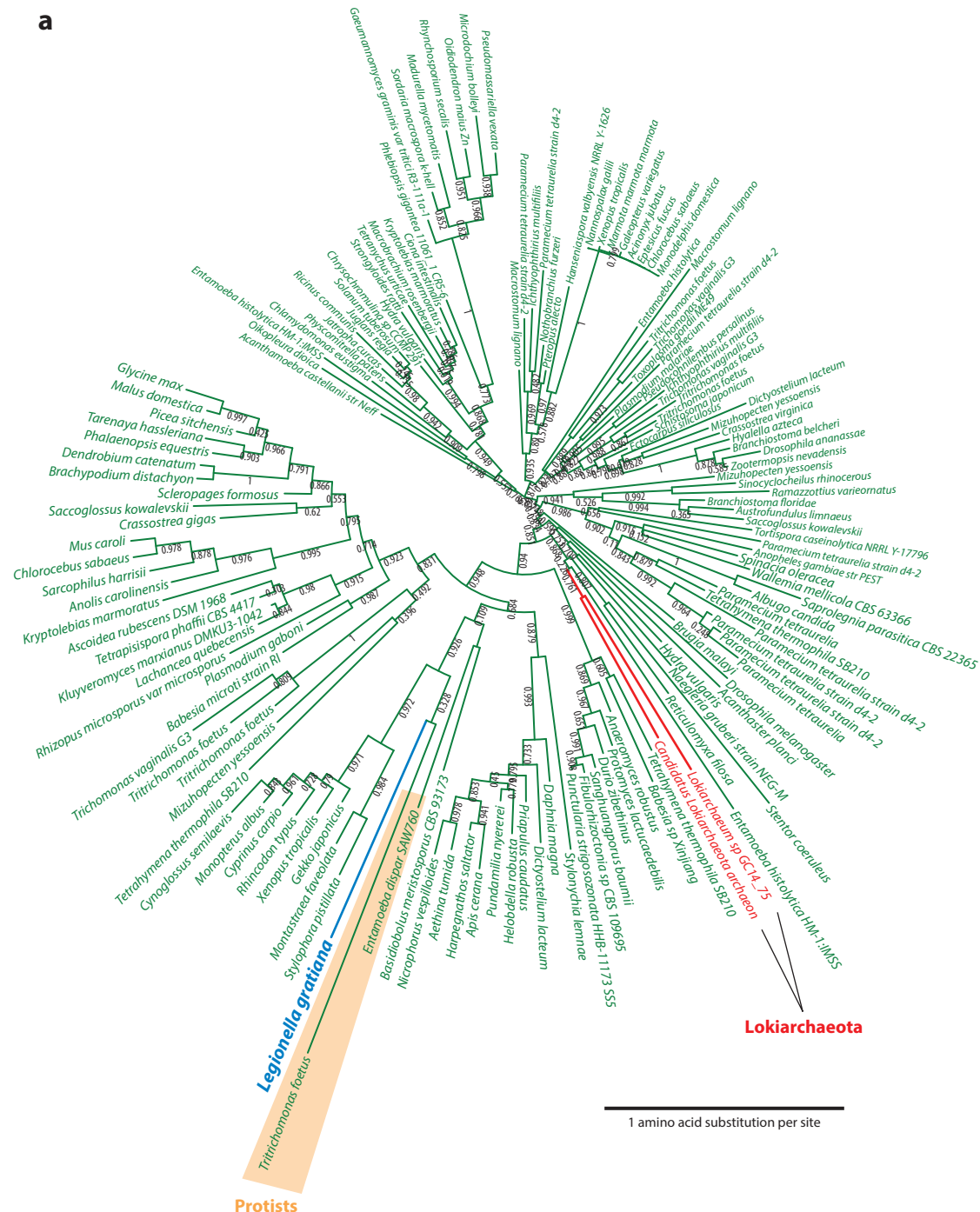


Figure 4

(Continued)

b

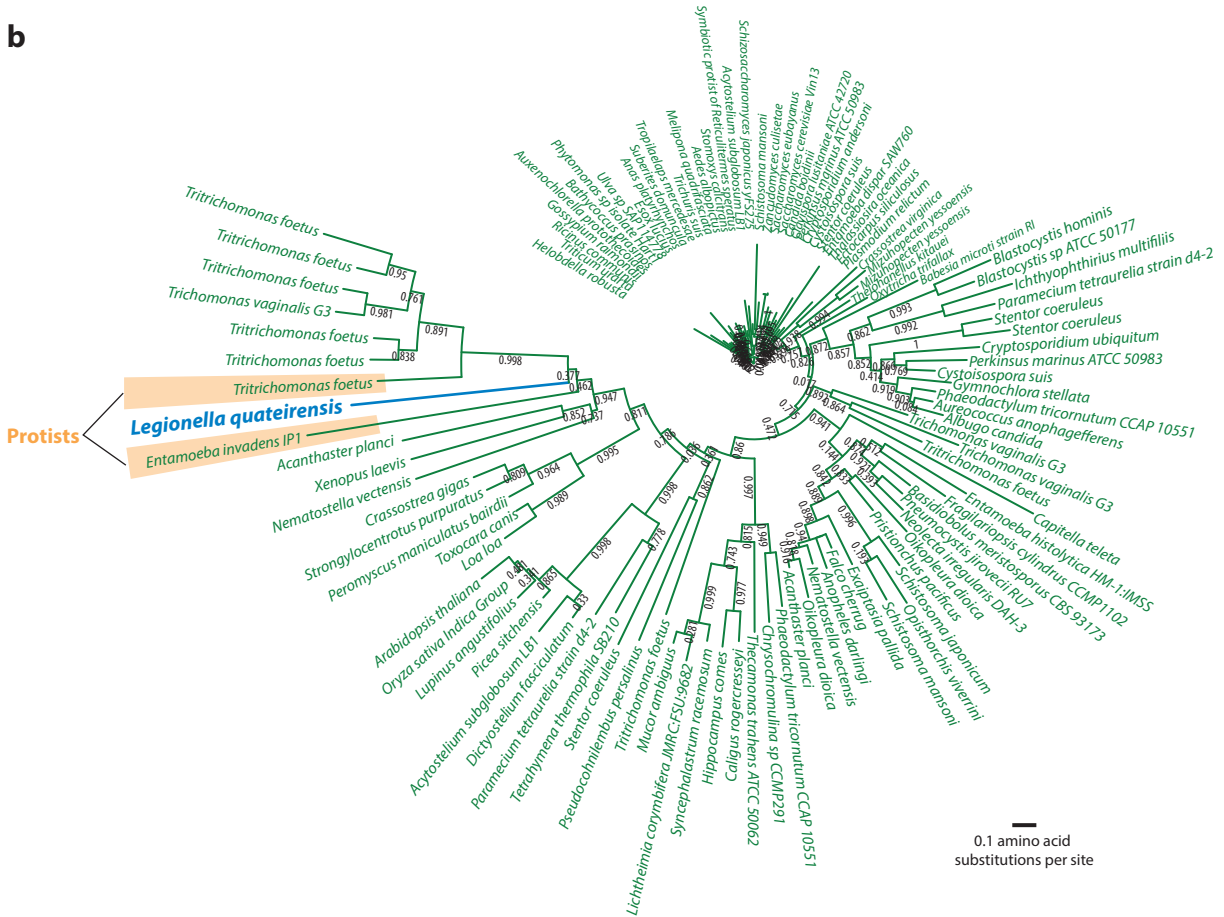


Figure 4

Phylogenetic trees of two Rab domain–containing proteins identified in the genus *Legionella*. (Green indicates eukaryotes; blue indicates *Legionella* species.) Blastp (protein–protein BLAST; Basic Local Alignment Search Tool) was used to search for homologs of these two proteins. Maximum likelihood was used for phylogenetic reconstruction. Local support values are represented by numbers on the corresponding branches. (a) *L. gratiana* protein Lgra3435 was used to recruit homologs. The scale bar represents 1 amino acid substitution per site. (b) *L. quateirensis* protein Lqua0234 was used to recruit homologs. The scale bar represents 0.1 amino acid substitutions per site. Figure adapted from Reference 59.

Among others, amoebae have been shown to be associated with bacteria from the genera *Legionella*, *Mycobacterium*, *Listeria*, and *Chlamydia*; soil fungi such as *Cryptococcus* species; and giant viruses belonging to the families *Mimiviridae* and *Marseilleviridae* (168). Pathogens that become specialized to infect hosts generally undergo genome reduction; however, this phenomenon is not observed in free-living amoebae-resistant bacteria (169). In contrast, it seems that *Legionella* bacteria undergo continuous genome expansion, with more gene gain events than losses, which is a consequence of gene acquisition by horizontal gene transfer, corroborated by the fact that the ancestral genomes were probably smaller (59).

Free-living amoebae seem to be melting pots of evolution in which giant viruses and bacteria can reside simultaneously, leading to gene fluxes in multiple directions and contributing to a so-called global mobilome (157, 169). One example is a protein identified in *L. pneumophila* that

has homologs only in the *Acanthamoeba polyphaga* mimivirus, indicating gene exchange involving eukaryotic viruses (155). Further examples involve other amoeba-associated bacteria, such as *Rickettsia* (170) and *Amoebophilus asiaticus* (171), in which recent genome sequence analyses have identified eukaryotic-like proteins in considerable numbers, similar to the *Legionella* species genomes. However, one of the enigmas of this genetic interchange remains to be resolved: What is the mechanism by which bacteria acquire and integrate the eukaryotic genes into their genome? One plausible explanation could be that the genetic transfer is related to RNA, which is subsequently retrotranscribed with the help of a *Legionella*-encoded reverse transcriptase. This would explain why no introns are present in the *Legionella* genes (157). Once integrated, these genes need to evolve to become specific, secreted effector proteins. Further, it has been proposed that a leaky delivery of these so-called proto-effectors to the host could allow for the selection of mutations to fine-tune protein function and to subsequently allow for the selection of an efficient C-terminal translocation signal (172).

Taken together, amoebae represent a niche allowing for the emergence of human pathogens. Thus, increased knowledge about *Legionella*–amoebae interactions is necessary to enable the development of new mechanisms for disease control and prevention.

4. NEW TECHNOLOGIES AND FUTURE DIRECTIONS

Since the identification of *Legionella* 40 years ago, the study of its biology has uncovered a vast arsenal of molecular tools that these bacteria use to modulate host pathways, and it has also provided insight into previously unknown mechanisms in eukaryotic cells. An example is RomA, a T4SS effector of *L. pneumophila* that methylates Lys14 of histone H3, a modification previously not known in mammalian cells (122). The recent finding that this epigenetic modification also occurs naturally in eukaryotic cells (173) highlights how advances in research achieved by studying mechanisms of bacterial infection can be valuable to further our understanding of basic cellular processes. The development of many new techniques in recent years has allowed for more detailed studies of eukaryotic processes and *Legionella*-induced alterations of host functions. We envisage that future epigenetic research will embrace genome-wide analyses of all known histone modifications during infection, and these will be combined with innovative genome-wide tools to perform precise epigenomic profiling, such as Internal Standard Calibrated Chromatin Immunoprecipitation, or ICeChIP (174). New tools will also ensure that the regulation of host microRNA during infection can be studied (175), as well as nucleosome positioning (176) in *Legionella*-infected cells. Seahorse technology (Agilent) allowed for the simultaneous analysis of oxidative phosphorylation and glycolysis in human primary macrophages infected with *L. pneumophila*, and this showed that specific T4SS-dependent metabolic shifts occur leading to metabolic reprogramming of the host cell (105). Future research using state-of-the-art methods—such as isotopolog profiling (177); integrated, stepwise, mass-isotopomeric flux analyses of the tricarboxylic acid cycle (178); or deep ¹³C labeling (179)—will allow elucidation of detailed reprogramming of metabolic fluxes during infection.

For a long time, the lungs were thought to be sterile organs, but new sequencing technologies have shown that they harbor their own microbiome, like other body sites (180). Thus, next-generation sequencing of bronchoalveolar lavage fluids, sputum, and other clinical lung samples will allow sequencing analyses of the lung microbiome during *Legionella* infection (181). During disease development, *Legionella* might displace lung bacteria, similar to what is observed for the gut mucosa microbiome (180, 182). Notably, the results obtained from such studies will be relevant for the development of new strategies for disease diagnosis, prevention, and control and possibly for the development of new therapeutics.

The expansion of new technologies together with an increased interest in understanding cell biology have contributed to the elucidation of many previously unknown cellular processes, such as exosome production and cargo loading (183), the formation of phase-separated liquid droplets in the nucleus and cytoplasm (184), the formation of membrane nanotubes connecting cells (185, 186), the repertoire of interorganelle communication (187), and the mechanisms of cellular detoxification (188), including those of peroxisomes (189). Following these discoveries, questions arise, such as, what happens with these mechanisms during infection, and is *Legionella* manipulating these cellular processes?

Despite an increasing understanding of the biology and pathogenicity of *L. pneumophila*, there is still a lack of knowledge of the mechanisms of infection of *L. longbeachae*. The prediction of specific effector proteins in this species suggests that *L. longbeachae* is able to manipulate host cell pathways by means different from those used by *L. pneumophila* (52). The high incidence of *L. longbeachae* in Australia and New Zealand has been attributed to the presence of this bacterium in potting soils, which in these areas, in comparison to Europe, are mostly made from composted pine bark or sawdust. This suggests that *L. longbeachae* could be associated with trees and plants and that active multiplication of bacteria occurs during the composting process (190). The analysis of the *L. longbeachae* genome revealed that this species encodes for a set of enzymes probably devoted to the degradation of plant cell-wall components to be used as energy sources (52), thus supporting the hypothesis that *L. longbeachae* may also be associated with or infecting plants (190). This finding raises the question of whether organisms other than protozoa may also be hosts of different *Legionella* species. Indeed, *L. pneumophila* subverts well-established immune pathways in macrophages that are not conserved in amoebae, such as caspase-mediated apoptosis or the NF- κ B pathway; thus, it is tempting to speculate that interactions between *L. pneumophila* and other susceptible hosts closer to higher eukaryotes were also relevant in shaping the repertoire of effectors of this bacterium (8). Some reports support this hypothesis, as it was shown that *L. pneumophila* can colonize and persist within the digestive tract of the nematode *Caenorhabditis elegans* (191); it can cause natural pneumonia in cattle (192); and it was also identified in the microbial community of the gastrointestinal tract in *Panaque nigrolineatus*, a tropical herbivorous freshwater fish (193). The future discovery of *Legionella* hosts other than protozoa will extend our knowledge and will open up new avenues for research into *Legionella*–host interactions.

Taken together, four decades of research on *Legionella* biology and Legionnaires' disease have brought important insights into the infection strategies and the mechanisms that these intracellular pathogens use to infect their hosts and to cause disease in humans. Despite these major advances, many open questions remain. Thus, the study of the intriguing ways that *Legionella* bacteria are exploiting their many hosts and signaling pathways is very exciting. Without doubt, it will teach us not only about the infection strategies of the bacteria but also about eukaryotic biology, thus this will continue to be a terrific scientific journey worth taking.

DISCLOSURE STATEMENT

The authors are not aware of any affiliations, memberships, funding, or financial holdings that might be perceived as affecting the objectivity of this review.

ACKNOWLEDGMENTS

Work in the C.B. laboratory is financed by the Institut Pasteur and funding has been received from the French Government (grants ANR-10-LABX-62-IBEID and ANR-15-CE17-0014-03 to C.B. and grant ANR-18-CE15-0005-01 to M.R.) and the “Fondation de la Recherche Médicale” (grant

EQU201903007847 to C.B.). S.S. is a scholar in the Pasteur-Paris University (PPU) International Ph.D. program and received a stipend from the Institut Pasteur.

LITERATURE CITED

1. Fraser DW, Tsai TR, Orenstein W, Parkin WE, Beecham HJ, et al. 1977. Legionnaires' disease: description of an epidemic of pneumonia. *N. Engl. J. Med.* 297(22):1189–97
2. McDade JE, Shepard CC, Fraser DW, Tsai TR, Redus MA, Dowdle WR. 1977. Legionnaires' disease: isolation of a bacterium and demonstration of its role in other respiratory disease. *N. Engl. J. Med.* 297(22):1197–203
3. Brenner DJ, Steigerwalt AG, McDade JE. 1979. Classification of the Legionnaires' disease bacterium: *Legionella pneumophila*, genus novum, species nova, of the family Legionellaceae, familia nova. *Ann. Intern. Med.* 90(4):656–58
4. McDade JE, Brenner DJ, Bozeman FM. 1979. Legionnaires' disease bacterium isolated in 1947. *Ann. Intern. Med.* 90(4):659–61
5. Glick TH, Gregg MB, Berman B, Mallison G, Rhodes WW, Kassanoff I. 1978. Pontiac fever: an epidemic of unknown etiology in a health department: I. Clinical and epidemiologic aspects. *Am. J. Epidemiol.* 107(2):149–60
6. Newton HJ, Ang DKY, van Driel IR, Hartland EL. 2010. Molecular pathogenesis of infections caused by *Legionella pneumophila*. *Clin. Microbiol. Rev.* 23(2):274–98
7. Rowbotham TJ. 1980. Preliminary report on the pathogenicity of *Legionella pneumophila* for freshwater and soil amoebae. *J. Clin. Pathol.* 33(12):1179–83
8. Escoll P, Rolando M, Gomez-Valero L, Buchrieser C. 2013. From amoeba to macrophages: exploring the molecular mechanisms of *Legionella pneumophila* infection in both hosts. In *Molecular Mechanisms in Legionella Pathogenesis*, ed. H Hilbi, pp. 1–34. Berlin: Springer
9. Taylor M, Ross K, Bentham R. 2009. *Legionella*, protozoa, and biofilms: interactions within complex microbial systems. *Microb. Ecol.* 58(3):538–47
10. Blatt SP, Parkinson MD, Pace E, Hoffman P, Dolan D, et al. 1993. Nosocomial Legionnaires' disease: aspiration as a primary mode of disease acquisition. *Am. J. Med.* 95(1):16–22
11. Correia AM, Ferreira JS, Borges V, Nunes A, Gomes B, et al. 2016. Probable person-to-person transmission of Legionnaires' disease. *N. Engl. J. Med.* 374(5):497–98
12. Cunha CB, Cunha BA. 2017. Legionnaire's disease since Philadelphia: lessons learned and continued progress. *Infect. Dis. Clin. North Am.* 31(1):1–5
13. Walker JT. 2018. The influence of climate change on waterborne disease and *Legionella*: a review. *Perspect. Public Health* 138(5):282–86
14. Beauté J. 2017. Legionnaires' disease in Europe, 2011 to 2015. *Euro Surveill.* 22(27):506
15. ECDC (Eur. Cent. Dis. Prev. Control). 2018. Legionnaires' disease. In *ECDC: Annual Epidemiological Report for 2016*. Stockholm: ECDC
16. Shah P, Barskey A, Binder A, Edens C, Lee S, et al. 2018. *Legionnaires' Disease Surveillance Summary Report, United States: 2014–2015*. Atlanta, GA: CDC (Cent. Dis. Control Prev.)
17. Yu VL, Plouffe JF, Pastoris MC, Stout JE, Schousboe M, et al. 2002. Distribution of *Legionella* species and serogroups isolated by culture in patients with sporadic community-acquired legionellosis: an international collaborative survey. *J. Infect. Dis.* 186(1):127–28
18. David S, Rusniok C, Mentasti M, Gomez-Valero L, Harris SR, et al. 2016. Multiple major disease-associated clones of *Legionella pneumophila* have emerged recently and independently. *Genome Res.* 26(11):1555–64
19. Bacigalupe R, Lindsay D, Edwards G, Fitzgerald JR. 2017. Population genomics of *Legionella longbeachae* and hidden complexities of infection source attribution. *Emerg. Infect. Dis.* 23(5):750–57
20. Currie SL, Beattie TK. 2015. Compost and *Legionella longbeachae*: an emerging infection? *Perspect. Public Health* 135(6):309–15
21. Cunha BA. 2010. Legionnaires' disease: clinical differentiation from typical and other atypical pneumonias. *Infect. Dis. Clin. North Am.* 24(1):73–105

22. Mercante JW, Winchell JM. 2015. Current and emerging *Legionella* diagnostics for laboratory and outbreak investigations. *Clin. Microbiol. Rev.* 28(1):95–133
23. Dunne WM, Picot N, van Belkum A. 2017. Laboratory tests for Legionnaire's disease. *Infect. Dis. Clin. North Am.* 31(1):167–78
24. Fields BS, Benson RF, Besser RE. 2002. *Legionella* and Legionnaires' disease: 25 years of investigation. *Clin. Microbiol. Rev.* 15(3):506–26
25. M  rault N, Rusniok C, Jarraud S, Gomez-Valero L, Cazalet C, et al. 2011. Specific real-time PCR for simultaneous detection and identification of *Legionella pneumophila* serogroup 1 in water and clinical samples. *Appl. Environ. Microbiol.* 77(5):1708–17
26. Mentasti M, Cassier P, David S, Ginevra C, Gomez-Valero L, et al. 2017. Rapid detection and evolutionary analysis of *Legionella pneumophila* serogroup 1 sequence type 47. *Clin. Microbiol. Infect.* 23(4):264.e1–e9
27. Murdoch DR, Podmore RG, Anderson TP, Barratt K, Maze MJ, et al. 2013. Impact of routine systematic polymerase chain reaction testing on case finding for Legionnaires' disease: a pre–post comparison study. *Clin. Infect. Dis.* 57(9):1275–81
28. Cross KE, Mercante JW, Benitez AJ, Brown EW, Diaz MH, Winchell JM. 2016. Simultaneous detection of *Legionella* species and *L. anisa*, *L. bozemanii*, *L. longbeachae* and *L. micdadei* using conserved primers and multiple probes in a multiplex real-time PCR assay. *Diagn. Microbiol. Infect. Dis.* 85(3):295–301
29. Botelho-Nevers E, Grattard F, Viallon A, Allegra S, Jarraud S, et al. 2016. Prospective evaluation of RT-PCR on sputum versus culture, urinary antigens and serology for Legionnaire's disease diagnosis. *J. Infect.* 73(2):123–28
30. Bruin JP, Koshkolda T, IJzerman EPF, L  ck C, Diederer BMW, et al. 2014. Isolation of ciprofloxacin-resistant *Legionella pneumophila* in a patient with severe pneumonia. *J. Antimicrob. Chemother.* 69(10):2869–71
31. Shadoud L, Almahmoud I, Jarraud S, Etienne J, Larrat S, et al. 2015. Hidden selection of bacterial resistance to fluoroquinolones in vivo: the case of *Legionella pneumophila* and humans. *EBioMedicine* 2(9):1179–85
32. Hennebique A, Bidart M, Jarraud S, Beraud L, Schwebel C, et al. 2017. Digital PCR for detection and quantification of fluoroquinolone resistance in *Legionella pneumophila*. *Antimicrob. Agents Chemother.* 61(9):e00628-17
33. Pedro-Botet L, Yu VL. 2006. *Legionella*: macrolides or quinolones? *Clin. Microbiol. Infect.* 12(Suppl. 3):25–30
34. Potts A, Donaghy M, Marley M, Othieno R, Stevenson J, et al. 2013. Cluster of Legionnaires' disease cases caused by *Legionella longbeachae* serogroup 1, Scotland, August to September 2013. *Euro Surveill.* 18(50):20656
35. de Bruin L, Timmerman CP, Huisman PM, Heidt J. 2018. *Legionella longbeachae*: Don't miss it! *Neth. J. Med.* 76(6):294–97
36. MMWR (Morbidity and Mortality Weekly Report). 2000. Legionnaires' disease associated with potting soil—California, Oregon, and Washington, May–June 2000. *MMWR* 49(34):777–78
37. Picard-Masson M, Lajoie   , Lord J, Lalancette C, Marchand G, et al. 2016. Two related occupational cases of *Legionella longbeachae* infection, Quebec, Canada. *Emerg. Infect. Dis.* 22(7):1289–91
38. Phares CR, Wangroongsarb P, Chantira S, Paveenkitiporn W, Tondella M-L, et al. 2007. Epidemiology of severe pneumonia caused by *Legionella longbeachae*, *Mycoplasma pneumoniae*, and *Chlamydia pneumoniae*: 1-year, population-based surveillance for severe pneumonia in Thailand. *Clin. Infect. Dis.* 45(12):e147–55
39. Wei S-H, Tseng L-R, Tan J-K, Cheng C-Y, Hsu Y-T, et al. 2014. Legionnaires' disease caused by *Legionella longbeachae* in Taiwan, 2006–2010. *Int. J. Infect. Dis.* 19:95–97
40. Cameron RL, Pollock KGJ, Lindsay DSJ, Anderson E. 2016. Comparison of *Legionella longbeachae* and *Legionella pneumophila* cases in Scotland; implications for diagnosis, treatment and public health response. *J. Med. Microbiol.* 65(2):142–46
41. Kenagy E, Priest PC, Cameron CM, Smith D, Scott P, et al. 2017. Risk factors for *Legionella longbeachae* Legionnaires' disease, New Zealand. *Emerg. Infect. Dis.* 23(7):1148–54

42. Thornley CN, Harte DJ, Weir RP, Allen LJ, Knightbridge KJ, Wood PRT. 2017. *Legionella longbeachae* detected in an industrial cooling tower linked to a legionellosis outbreak, New Zealand, 2015: possible waterborne transmission? *Epidemiol. Infect.* 145(11):2382–89
43. Molofsky AB, Swanson MS. 2004. Differentiate to thrive: lessons from the *Legionella pneumophila* life cycle. *Mol. Microbiol.* 53(1):29–40
44. Oliva G, Sahr T, Buchrieser C. 2018. The life cycle of *Legionella pneumophila*: Cellular differentiation is linked to virulence and metabolism. *Front. Cell. Infect. Microbiol.* 8:3
45. Brüggemann H, Hagman A, Jules M, Sismeiro O, Dillies M-A, et al. 2006. Virulence strategies for infecting phagocytes deduced from the in vivo transcriptional program of *Legionella pneumophila*. *Cell. Microbiol.* 8(8):1228–40
46. Byrne B, Swanson MS. 1998. Expression of *Legionella pneumophila* virulence traits in response to growth conditions. *Infect. Immun.* 66(7):3029–34
47. Molofsky AB, Swanson MS. 2003. *Legionella pneumophila* CsrA is a pivotal repressor of transmission traits and activator of replication. *Mol. Microbiol.* 50(2):445–61
48. Fettes PS, Forsbach-Birk V, Lynch D, Marre R. 2001. Overexpression of a *Legionella pneumophila* homologue of the *Escherichia coli* regulator *csrA* affects cell size, flagellation, and pigmentation. *Int. J. Med. Microbiol.* 291(5):353–60
49. Rasis M, Segal G. 2009. The LetA–RsmYZ–CsrA regulatory cascade, together with RpoS and PmrA, post-transcriptionally regulates stationary phase activation of *Legionella pneumophila* Icm/Dot effectors. *Mol. Microbiol.* 72(4):995–1010
50. Sahr T, Rusniok C, Dervins-Ravault D, Sismeiro O, Coppée J-Y, Buchrieser C. 2012. Deep sequencing defines the transcriptional map of *Legionella pneumophila* and identifies growth phase-dependent regulated ncRNAs implicated in virulence. *RNA Biol.* 9(4):503–19
51. Sahr T, Rusniok C, Impens F, Oliva G, Sismeiro O, et al. 2017. The *Legionella pneumophila* genome evolved to accommodate multiple regulatory mechanisms controlled by the CsrA-system. *PLOS Genet.* 13(2):e1006629
52. Cazalet C, Gomez-Valero L, Rusniok C, Lomma M, Dervins-Ravault D, et al. 2010. Analysis of the *Legionella longbeachae* genome and transcriptome uncovers unique strategies to cause Legionnaires' disease. *PLOS Genet.* 6(2):e1000851
53. Asare R, Abu Kwaik Y. 2007. Early trafficking and intracellular replication of *Legionella longbeachae* within an ER-derived late endosome-like phagosome. *Cell. Microbiol.* 9(6):1571–87
54. Kozak NA, Buss M, Lucas CE, Frace M, Govil D, et al. 2010. Virulence factors encoded by *Legionella longbeachae* identified on the basis of the genome sequence analysis of clinical isolate D-4968. *J. Bacteriol.* 192(4):1030–44
55. Gomez-Valero L, Rusniok C, Cazalet C, Buchrieser C. 2011. Comparative and functional genomics of *Legionella* identified eukaryotic like proteins as key players in host–pathogen interactions. *Front. Microbiol.* 2:208
56. Ren T, Zamboni DS, Roy CR, Dietrich WF, Vance RE. 2006. Flagellin-deficient *Legionella* mutants evade caspase-1- and *Naip5*-mediated macrophage immunity. *PLOS Pathog.* 2(3):e18
57. Massis LM, Assis-Marques MA, Castanheira FVS, Capobianco YJ, Balestra AC, et al. 2017. *Legionella longbeachae* is immunologically silent and highly virulent in vivo. *J. Infect. Dis.* 215(3):440–51
58. Qin T, Zhou H, Ren H, Liu W. 2017. Distribution of secretion systems in the genus *Legionella* and its correlation with pathogenicity. *Front. Microbiol.* 8:388
59. Gomez-Valero L, Rusniok C, Carson D, Mondino S, Pérez-Cobas AE, et al. 2019. More than 18,000 effectors in the *Legionella* genus genome provide multiple, independent combinations for replication in human cells. *PNAS* 116(6):2265–73
60. Cianciotto NP. 2005. Type II secretion: a protein secretion system for all seasons. *Trends Microbiol.* 13(12):581–88
61. Truchan HK, Christman HD, White RC, Rutledge NS, Cianciotto NP. 2017. Type II secretion substrates of *Legionella pneumophila* translocate out of the pathogen-occupied vacuole via a semipermeable membrane. *mBio* 8(3):e00870-17

62. Cianciotto NP. 2009. Many substrates and functions of type II secretion: lessons learned from *Legionella pneumophila*. *Future Microbiol.* 4(7):797–805
63. Cianciotto NP. 2013. Type II secretion and *Legionella* virulence. In *Molecular Mechanisms in Legionella Pathogenesis*, ed. H Hilbi, pp. 81–102. Berlin: Springer
64. DebRoy S, Dao J, Söderberg M, Rossier O, Cianciotto NP. 2006. *Legionella pneumophila* type II secretome reveals unique exoproteins and a chitinase that promotes bacterial persistence in the lung. *PNAS* 103(50):19146–51
65. Berger KH, Isberg RR. 1993. Two distinct defects in intracellular growth complemented by a single genetic locus in *Legionella pneumophila*. *Mol. Microbiol.* 7(1):7–19
66. Marra A, Blander SJ, Horwitz MA, Shuman HA. 1992. Identification of a *Legionella pneumophila* locus required for intracellular multiplication in human macrophages. *PNAS* 89(20):9607–11
67. Jeong KC, Ghosal D, Chang Y-W, Jensen GJ, Vogel JP. 2017. Polar delivery of *Legionella* type IV secretion system substrates is essential for virulence. *PNAS* 114(30):8077–82
68. Charpentier X, Gabay JE, Reyes M, Zhu JW, Weiss A, Shuman HA. 2009. Chemical genetics reveals bacterial and host cell functions critical for type IV effector translocation by *Legionella pneumophila*. *PLOS Pathog.* 5(7):e1000501
69. Hilbi H, Segal G, Shuman HA. 2001. Icm/Dot-dependent upregulation of phagocytosis by *Legionella pneumophila*. *Mol. Microbiol.* 42(3):603–17
70. Watarai M, Derre I, Kirby J, Growney JD, Dietrich WF, Isberg RR. 2001. *Legionella pneumophila* is internalized by a macropinocytotic uptake pathway controlled by the Dot/Icm system and the mouse *Lgm1* locus. *J. Exp. Med.* 194(8):1081–96
71. Weber S, Wagner M, Hilbi H. 2014. Live-cell imaging of phosphoinositide dynamics and membrane architecture during *Legionella* infection. *mBio* 5(1):e00839–13
72. Fuche F, Vianney A, Andrea C, Doublet P, Gilbert C. 2015. Functional type I secretion system involved in *Legionella pneumophila* virulence. *J. Bacteriol.* 197(3):563–71
73. Horwitz MA. 1983. The Legionnaires' disease bacterium (*Legionella pneumophila*) inhibits phagosome-lysosome fusion in human monocytes. *J. Exp. Med.* 158(6):2108–26
74. Xu L, Shen X, Bryan A, Banga S, Swanson MS, Luo Z-Q. 2010. Inhibition of host vacuolar H⁺-ATPase activity by a *Legionella pneumophila* effector. *PLOS Pathog.* 6(3):e1000822
75. Prevost MS, Pinotsis N, Dumoux M, Hayward RD, Waksman G. 2017. The *Legionella* effector WipB is a translocated Ser/Thr phosphatase that targets the host lysosomal nutrient sensing machinery. *Sci. Rep.* 7(1):9450
76. Urwyler S, Nyfeler Y, Ragaz C, Lee H, Mueller LN, et al. 2009. Proteome analysis of *Legionella* vacuoles purified by magnetic immunoseparation reveals secretory and endosomal GTPases. *Traffic* 10(1):76–87
77. Hoffmann C, Finsel I, Otto A, Pfaffinger G, Rothmeier E, et al. 2014. Functional analysis of novel Rab GTPases identified in the proteome of purified *Legionella*-containing vacuoles from macrophages. *Cell. Microbiol.* 16(7):1034–52
78. Lawe DC, Chawla A, Merithew E, Dumas J, Carrington W, et al. 2002. Sequential roles for phosphatidylinositol 3-phosphate and Rab5 in tethering and fusion of early endosomes via their interaction with EEA1. *J. Biol. Chem.* 277(10):8611–17
79. Gaspar AH, Machner MP. 2014. VipD is a Rab5-activated phospholipase A1 that protects *Legionella pneumophila* from endosomal fusion. *PNAS* 111(12):4560–65
80. Mousnier A, Schroeder GN, Stoneham CA, So EC, Garnett JA, et al. 2014. A new method to determine in vivo interactomes reveals binding of the *Legionella pneumophila* effector PieE to multiple Rab GTPases. *mBio* 5(4):e01148–14
81. Rink J, Ghigo E, Kalaidzidis Y, Zerial M. 2005. Rab conversion as a mechanism of progression from early to late endosomes. *Cell* 122(5):735–49
82. Rojas R, van Vlijmen T, Mardones GA, Prabhu Y, Rojas AL, et al. 2008. Regulation of retromer recruitment to endosomes by sequential action of Rab5 and Rab7. *J. Cell Biol.* 183(3):513–26
83. Finsel I, Ragaz C, Hoffmann C, Harrison CF, Weber S, et al. 2013. The *Legionella* effector RidL inhibits retrograde trafficking to promote intracellular replication. *Cell Host Microbe* 14(1):38–50

84. Robinson CG, Roy CR. 2006. Attachment and fusion of endoplasmic reticulum with vacuoles containing *Legionella pneumophila*. *Cell. Microbiol.* 8(5):793–805
85. Kagan JC, Roy CR. 2002. *Legionella* phagosomes intercept vesicular traffic from endoplasmic reticulum exit sites. *Nat. Cell Biol.* 4(12):945–54
86. Schoebel S, Oesterlin LK, Blankenfeldt W, Goody RS, Itzen A. 2009. RabGDI displacement by DrrA from *Legionella* is a consequence of its guanine nucleotide exchange activity. *Mol. Cell* 36(6):1060–72
87. Murata T, Delprato A, Ingmundson A, Toomre DK, Lambright DG, Roy CR. 2006. The *Legionella pneumophila* effector protein DrrA is a Rab1 guanine nucleotide-exchange factor. *Nat. Cell Biol.* 8(9):971–77
88. Machner MP, Isberg RR. 2007. A bifunctional bacterial protein links GDI displacement to Rab1 activation. *Science* 318(5852):974–77
89. Müller MP, Peters H, Blümer J, Blankenfeldt W, Goody RS, Itzen A. 2010. The *Legionella* effector protein DrrA AMPylates the membrane traffic regulator Rab1b. *Science* 329(5994):946–49
90. Machner MP, Isberg RR. 2006. Targeting of host Rab GTPase function by the intravacuolar pathogen *Legionella pneumophila*. *Dev. Cell* 11(1):47–56
91. Neunuebel MR, Chen Y, Gaspar AH, Backlund PS, Yergey A, Machner MP. 2011. De-AMPylation of the small GTPase Rab1 by the pathogen *Legionella pneumophila*. *Science* 333(6041):453–56
92. Ingmundson A, Delprato A, Lambright DG, Roy CR. 2007. *Legionella pneumophila* proteins that regulate Rab1 membrane cycling. *Nature* 450(7168):365–69
93. Mukherjee S, Liu X, Arasaki K, McDonough J, Galán JE, Roy CR. 2011. Modulation of Rab GTPase function by a protein phosphocholine transferase. *Nature* 477(7362):103–6
94. Tan Y, Arnold RJ, Luo Z-Q. 2011. *Legionella pneumophila* regulates the small GTPase Rab1 activity by reversible phosphorylcholine. *PNAS* 108(52):21212–17
95. Nagai H, Kagan JC, Zhu X, Kahn RA, Roy CR. 2002. A bacterial guanine nucleotide exchange factor activates ARF on *Legionella* phagosomes. *Science* 295(5555):679–82
96. Hubber A, Arasaki K, Nakatsu F, Hardiman C, Lambright D, et al. 2014. The machinery at endoplasmic reticulum–plasma membrane contact sites contributes to spatial regulation of multiple *Legionella* effector proteins. *PLOS Pathog.* 10(7):e1004222
97. Haenssler E, Ramabhadran V, Murphy CS, Heidtman MI, Isberg RR. 2015. Endoplasmic reticulum tubule protein reticulon 4 associates with the *Legionella pneumophila* vacuole and with translocated substrate Ceg9. *Infect. Immun.* 83(9):3479–89
98. Arasaki K, Roy CR. 2010. *Legionella pneumophila* promotes functional interactions between plasma membrane syntaxins and Sec22b. *Traffic* 11(5):587–600
99. Jahn R, Scheller RH. 2006. SNAREs—engines for membrane fusion. *Nat. Rev. Mol. Cell Biol.* 7(9):631–43
100. Arasaki K, Toomre DK, Roy CR. 2012. The *Legionella pneumophila* effector DrrA is sufficient to stimulate SNARE-dependent membrane fusion. *Cell Host Microbe* 11(1):46–57
101. King NP, Newton P, Schuelein R, Brown DL, Petru M, et al. 2015. Soluble NSF attachment protein receptor molecular mimicry by a *Legionella pneumophila* Dot/Icm effector. *Cell. Microbiol.* 17(6):767–84
102. Bennett TL, Kraft SM, Reaves BJ, Mima J, O'Brien KM, Starai VJ. 2013. LegC3, an effector protein from *Legionella pneumophila*, inhibits homotypic yeast vacuole fusion in vivo and in vitro. *PLOS ONE* 8(2):e56798
103. Shi X, Halder P, Yavuz H, Jahn R, Shuman HA. 2016. Direct targeting of membrane fusion by SNARE mimicry: convergent evolution of *Legionella* effectors. *PNAS* 113(31):8807–12
104. Rothmeier E, Pfaffinger G, Hoffmann C, Harrison CF, Grabmayr H, et al. 2013. Activation of Ran GTPase by a *Legionella* effector promotes microtubule polymerization, pathogen vacuole motility and infection. *PLOS Pathog.* 9(9):e1003598
105. Escoll P, Song O-R, Viana F, Steiner B, Lagache T, et al. 2017. *Legionella pneumophila* modulates mitochondrial dynamics to trigger metabolic repurposing of infected macrophages. *Cell Host Microbe* 22(3):302–7
106. Escoll P, Buchrieser C. 2018. Metabolic reprogramming of host cells upon bacterial infection: Why shift to a Warburg-like metabolism? *FEBS J.* 285(12):2146–60

107. Amer AO, Swanson MS. 2005. Autophagy is an immediate macrophage response to *Legionella pneumophila*. *Cell. Microbiol.* 7(6):765–78
108. Choy A, Dancourt J, Mugo B, O'Connor TJ, Isberg RR, et al. 2012. The *Legionella* effector RavZ inhibits host autophagy through irreversible Atg8 deconjugation. *Science* 338(6110):1072–76
109. Arasaki K, Mikami Y, Shames SR, Inoue H, Wakana Y, Tagaya M. 2017. *Legionella* effector Lpg1137 shuts down ER–mitochondria communication through cleavage of syntaxin 17. *Nat. Commun.* 8:15406
110. Rolando M, Escoll P, Nora T, Botti J, Boitez V, et al. 2016. *Legionella pneumophila* S1P-lyase targets host sphingolipid metabolism and restrains autophagy. *PNAS* 113(7):1901–6
111. Kaneko T, Stogios PJ, Ruan X, Voss C, Evdokimova E, et al. 2018. Identification and characterization of a large family of superbinding bacterial SH2 domains. *Nat. Commun.* 9(1):4549
112. Lee P-C, Machner MP. 2018. The *Legionella* effector kinase LegK7 hijacks the host Hippo pathway to promote infection. *Cell Host Microbe* 24(3):429–438.e6
113. Bartfeld S, Engels C, Bauer B, Aurass P, Fliieger A, et al. 2009. Temporal resolution of two-tracked NF- κ B activation by *Legionella pneumophila*. *Cell. Microbiol.* 11(11):1638–51
114. Ge J, Xu H, Li T, Zhou Y, Zhang Z, et al. 2009. A *Legionella* type IV effector activates the NF- κ B pathway by phosphorylating the I κ B family of inhibitors. *PNAS* 106(33):13725–30
115. Losick VP, Haenssler E, Moy M-Y, Isberg RR. 2010. LnaB: a *Legionella pneumophila* activator of NF- κ B. *Cell. Microbiol.* 12(8):1083–97
116. Gan N, Nakayasu ES, Hollenbeck PJ, Luo Z-Q. 2019. *Legionella pneumophila* inhibits immune signalling via MavC-mediated transglutaminase-induced ubiquitination of UBE2N. *Nat. Microbiol.* 4(1):134–43
117. Fontana MF, Banga S, Barry KC, Shen X, Tan Y, et al. 2011. Secreted bacterial effectors that inhibit host protein synthesis are critical for induction of the innate immune response to virulent *Legionella pneumophila*. *PLoS Pathog.* 7(2):e1001289
118. Welsh CT, Summersgill JT, Miller RD. 2004. Increases in c-Jun N-terminal kinase/stress-activated protein kinase and p38 activity in monocyte-derived macrophages following the uptake of *Legionella pneumophila*. *Infect. Immun.* 72(3):1512–18
119. Shin S, Case CL, Archer KA, Nogueira CV, Kobayashi KS, et al. 2008. Type IV secretion-dependent activation of host MAP kinases induces an increased proinflammatory cytokine response to *Legionella pneumophila*. *PLoS Pathog.* 4(11):e1000220
120. Fontana MF, Shin S, Vance RE. 2012. Activation of host mitogen-activated protein kinases by secreted *Legionella pneumophila* effectors that inhibit host protein translation. *Infect. Immun.* 80(10):3570–75
121. Quaile AT, Stogios PJ, Egorova O, Evdokimova E, Valteau D, et al. 2018. The *Legionella pneumophila* effector Ceg4 is a phosphotyrosine phosphatase that attenuates activation of eukaryotic MAPK pathways. *J. Biol. Chem.* 293(9):3307–20
122. Rolando M, Sanulli S, Rusniok C, Gomez-Valero L, Bertholet C, et al. 2013. *Legionella pneumophila* effector RomA uniquely modifies host chromatin to repress gene expression and promote intracellular bacterial replication. *Cell Host Microbe* 13(4):395–405
123. Schuelein R, Spencer H, Dagley LF, Li PF, Luo L, et al. 2018. Targeting of RNA Polymerase II by a nuclear *Legionella pneumophila* Dot/Icm effector SnpL. *Cell. Microbiol.* 20(9):e12852
124. Kubori T, Hyakutake A, Nagai H. 2008. *Legionella* translocates an E3 ubiquitin ligase that has multiple U-boxes with distinct functions. *Mol. Microbiol.* 67(6):1307–19
125. Lin Y-H, Doms AG, Cheng E, Kim B, Evans TR, Machner MP. 2015. Host cell-catalyzed S-palmitoylation mediates Golgi targeting of the *Legionella* ubiquitin ligase GobX. *J. Biol. Chem.* 290(42):25766–81
126. Lin Y-H, Lucas M, Evans TR, Abascal-Palacios G, Doms AG, et al. 2018. RavN is a member of a previously unrecognized group of *Legionella pneumophila* E3 ubiquitin ligases. *PLoS Pathog.* 14(2):e1006897
127. Ragaz C, Pietsch H, Urwyler S, Tiaden A, Weber SS, Hilbi H. 2008. The *Legionella pneumophila* phosphatidylinositol-4 phosphate-binding type IV substrate SidC recruits endoplasmic reticulum vesicles to a replication-permissive vacuole. *Cell. Microbiol.* 10(12):2416–33
128. Hsu F, Luo X, Qiu J, Teng Y-B, Jin J, et al. 2014. The *Legionella* effector SidC defines a unique family of ubiquitin ligases important for bacterial phagosomal remodeling. *PNAS* 111(29):10538–43

129. Ensminger AW, Isberg RR. 2010. E3 ubiquitin ligase activity and targeting of BAT3 by multiple *Legionella pneumophila* translocated substrates. *Infect. Immun.* 78(9):3905–19
130. Lomma M, Dervins-Ravault D, Rolando M, Nora T, Newton HJ, et al. 2010. The *Legionella pneumophila* F-box protein Lpp2082 (AnkB) modulates ubiquitination of the host protein parvin B and promotes intracellular replication. *Cell. Microbiol.* 12(9):1272–91
131. Price CTD, Al-Quadani T, Santic M, Rosenshine I, Abu Kwaik Y. 2011. Host proteasomal degradation generates amino acids essential for intracellular bacterial growth. *Science* 334(6062):1553–57
132. Qiu J, Sheedlo MJ, Yu K, Tan Y, Nakayasu ES, et al. 2016. Ubiquitination independent of E1 and E2 enzymes by bacterial effectors. *Nature* 533(7601):120–24
133. Bhogaraju S, Kalayil S, Liu Y, Bonn F, Colby T, et al. 2016. Phosphoribosylation of ubiquitin promotes serine ubiquitination and impairs conventional ubiquitination. *Cell* 167(6):1636–1649
134. Qiu J, Yu K, Fei X, Liu Y, Nakayasu ES, et al. 2017. A unique deubiquitinase that deconjugates phosphoribosyl-linked protein ubiquitination. *Cell Res.* 27(7):865–81
135. Kotewicz KM, Ramabhadran V, Sjoblom N, Vogel JP, Haenssler E, et al. 2017. A single *Legionella* effector catalyzes a multistep ubiquitination pathway to rearrange tubular endoplasmic reticulum for replication. *Cell Host Microbe* 21(2):169–81
136. Kubori T, Kitao T, Ando H, Nagai H. 2018. LotA, a *Legionella* deubiquitinase, has dual catalytic activity and contributes to intracellular growth. *Cell. Microbiol.* 20(7):e12840
137. Luo Z-Q. 2011. Striking a balance: modulation of host cell death pathways by *Legionella pneumophila*. *Front. Microbiol.* 2:36
138. Banga S, Gao P, Shen X, Fiscus V, Zong W-X, et al. 2007. *Legionella pneumophila* inhibits macrophage apoptosis by targeting pro-death members of the Bcl2 protein family. *PNAS* 104(12):5121–26
139. Laguna RK, Creasey EA, Li Z, Valtz N, Isberg RR. 2006. A *Legionella pneumophila*-translocated substrate that is required for growth within macrophages and protection from host cell death. *PNAS* 103(49):18745–50
140. Zhu W, Hammad LA, Hsu F, Mao Y, Luo Z-Q. 2013. Induction of caspase 3 activation by multiple *Legionella pneumophila* Dot/Icm substrates. *Cell. Microbiol.* 15(11):1783–95
141. Lifshitz Z, Burstein D, Peeri M, Zusman T, Schwartz K, et al. 2013. Computational modeling and experimental validation of the *Legionella* and *Coxiella* virulence-related type-IVB secretion signal. *PNAS* 110(8):E707–15
142. Zhu W, Banga S, Tan Y, Zheng C, Stephenson R, et al. 2011. Comprehensive identification of protein substrates of the Dot/Icm type IV transporter of *Legionella pneumophila*. *PLOS ONE* 6(3):e17638
143. Escoll P, Mondino S, Rolando M, Buchrieser C. 2016. Targeting of host organelles by pathogenic bacteria: a sophisticated subversion strategy. *Nat. Rev. Microbiol.* 14(1):5–19
144. Schroeder GN. 2017. The toolbox for uncovering the functions of *Legionella* Dot/Icm type IVb secretion system effectors: current state and future directions. *Front. Cell. Infect. Microbiol.* 7:528
145. O'Connor TJ, Adepoju Y, Boyd D, Isberg RR. 2011. Minimization of the *Legionella pneumophila* genome reveals chromosomal regions involved in host range expansion. *PNAS* 108(36):14733–40
146. Belyi Y, Jank T, Aktories K. 2013. Cytotoxic glucosyltransferases of *Legionella pneumophila*. In *Molecular Mechanisms in Legionella Pathogenesis*, ed. H Hilbi, pp. 211–26. Berlin: Springer
147. Kubori T, Shinzawa N, Kanuka H, Nagai H. 2010. *Legionella* metaeffector exploits host proteasome to temporally regulate cognate effector. *PLOS Pathog.* 6(12):e1001216
148. Jeong KC, Sexton JA, Vogel JP. 2015. Spatiotemporal regulation of a *Legionella pneumophila* T4SS substrate by the metaeffector SidJ. *PLOS Pathog.* 11(3):e1004695
149. Shames SR, Liu L, Havey JC, Schofield WB, Goodman AL, Roy CR. 2017. Multiple *Legionella pneumophila* effector virulence phenotypes revealed through high-throughput analysis of targeted mutant libraries. *PNAS* 114(48):E10446–54
150. Valteau D, Quaille AT, Cui H, Xu X, Evdokimova E, et al. 2018. Discovery of ubiquitin deamidases in the pathogenic arsenal of *Legionella pneumophila*. *Cell Rep.* 23(2):568–83
151. Urbanus ML, Quaille AT, Stogios PJ, Morar M, Rao C, et al. 2016. Diverse mechanisms of metaeffector activity in an intracellular bacterial pathogen, *Legionella pneumophila*. *Mol. Syst. Biol.* 12(12):893

152. Cazalet C, Rusniok C, Brüggemann H, Zidane N, Magnier A, et al. 2004. Evidence in the *Legionella pneumophila* genome for exploitation of host cell functions and high genome plasticity. *Nat. Genet.* 36(11):1165–73
153. de Felipe KS, Pampou S, Jovanovic OS, Pericone CD, Ye SF, et al. 2005. Evidence for acquisition of *Legionella* type IV secretion substrates via interdomain horizontal gene transfer. *J. Bacteriol.* 187(22):7716–26
154. Gomez-Valero L, Rusniok C, Buchrieser C. 2009. *Legionella pneumophila*: population genetics, phylogeny and genomics. *Infect. Genet. Evol.* 9(5):727–39
155. Lurie-Weinberger MN, Gomez-Valero L, Merault N, Glöckner G, Buchrieser C, Gophna U. 2010. The origins of eukaryotic-like proteins in *Legionella pneumophila*. *Int. J. Med. Microbiol.* 300(7):470–81
156. Degtyar E, Zusman T, Ehrlich M, Segal G. 2009. A *Legionella* effector acquired from protozoa is involved in sphingolipids metabolism and is targeted to the host cell mitochondria. *Cell. Microbiol.* 11(8):1219–35
157. Gomez-Valero L, Buchrieser C. 2013. Genome dynamics in *Legionella*: the basis of versatility and adaptation to intracellular replication. *Cold Spring Harb. Perspect. Med.* 3(6):a009993
158. Nora T, Lomma M, Gomez-Valero L, Buchrieser C. 2009. Molecular mimicry: an important virulence strategy employed by *Legionella pneumophila* to subvert host functions. *Future Microbiol.* 4(6):691–701
159. Burstein D, Amaro F, Zusman T, Lifshitz Z, Cohen O, et al. 2016. Genomic analysis of 38 *Legionella* species identifies large and diverse effector repertoires. *Nat. Genet.* 48(2):167–75
160. Weber MM, Faris R. 2018. Subversion of the endocytic and secretory pathways by bacterial effector proteins. *Front. Cell Dev. Biol.* 6:1
161. Dolinsky S, Haneburger I, Cichy A, Hannemann M, Itzen A, Hilbi H. 2014. The *Legionella longbeachae* Icm/Dot substrate SidC selectively binds phosphatidylinositol 4-phosphate with nanomolar affinity and promotes pathogen vacuole–endoplasmic reticulum interactions. *Infect. Immun.* 82(10):4021–33
162. Wood RE, Newton P, Latomanski EA, Newton HJ. 2015. Dot/Icm effector translocation by *Legionella longbeachae* creates a replicative vacuole similar to that of *Legionella pneumophila* despite translocation of distinct effector repertoires. *Infect. Immun.* 83(10):4081–92
163. Boamah DK, Zhou G, Ensminger AW, O'Connor TJ. 2017. From many hosts, one accidental pathogen: the diverse protozoan hosts of *Legionella*. *Front. Cell. Infect. Microbiol.* 7:477
164. Barker J, Brown MR. 1994. Trojan horses of the microbial world: protozoa and the survival of bacterial pathogens in the environment. *Microbiology* 140(6):1253–59
165. Scheid P. 2014. Relevance of free-living amoebae as hosts for phylogenetically diverse microorganisms. *Parasitol. Res.* 113(7):2407–14
166. Richards AM, Von Dwingelo JE, Price CT, Abu Kwaik Y. 2013. Cellular microbiology and molecular ecology of *Legionella*–amoeba interaction. *Virulence* 4(4):307–14
167. Broderick NA. 2015. A common origin for immunity and digestion. *Front. Immunol.* 6:72
168. Casadevall A, Fu MS, Guimaraes AJ, Albuquerque P. 2019. The ‘amoeboid predator–fungal animal virulence’ hypothesis. *J. Fungi* 5(1):10
169. Moliner C, Fournier P-E, Raoult D. 2010. Genome analysis of microorganisms living in amoebae reveals a melting pot of evolution. *FEMS Microbiol. Rev.* 34(3):281–94
170. Schulz F, Martijn J, Wascher F, Lagkouvardos I, Kostanjšek R, et al. 2016. A Rickettsiales symbiont of amoebae with ancient features. *Environ. Microbiol.* 18(8):2326–42
171. Schmitz-Esser S, Tischler P, Arnold R, Montanaro J, Wagner M, et al. 2010. The genome of the amoeba symbiont “*Candidatus* Amoebohilus asiaticus” reveals common mechanisms for host cell interaction among amoeba-associated bacteria. *J. Bacteriol.* 192(4):1045–57
172. Ensminger AW. 2016. *Legionella pneumophila*, armed to the hilt: justifying the largest arsenal of effectors in the bacterial world. *Curr. Opin. Microbiol.* 29:74–80
173. Zhao B, Xu W, Rong B, Chen G, Ye X, et al. 2018. H3K14me3 genomic distributions and its regulation by KDM4 family demethylases. *Cell Res.* 28(11):1118–20
174. Grzybowski AT, Chen Z, Ruthenburg AJ. 2015. Calibrating ChIP-Seq with nucleosomal internal standards to measure histone modification density genome wide. *Mol. Cell* 58(5):886–99
175. Bansal A, Singh TR, Chauhan RS. 2017. A novel miRNA analysis framework to analyze differential biological networks. *Sci. Rep.* 7(1):14604

176. Schones DE, Cui K, Cuddapah S, Roh T-Y, Barski A, et al. 2008. Dynamic regulation of nucleosome positioning in the human genome. *Cell* 132(5):887–98
177. Eylert E, Herrmann V, Jules M, Gillmaier N, Lautner M, et al. 2010. Isotopologue profiling of *Legionella pneumophila*: role of serine and glucose as carbon substrates. *J. Biol. Chem.* 285(29):22232–43
178. Alves TC, Pongratz RL, Zhao X, Yarborough O, Sereda S, et al. 2015. Integrated, step-wise, mass-isotopomeric flux analysis of the TCA cycle. *Cell Metab.* 22(5):936–47
179. Grankvist N, Watrous JD, Lagerborg KA, Lyutvinskiy Y, Jain M, Nilsson R. 2018. Profiling the metabolism of human cells by deep ¹³C labelling. *Cell Chem. Biol.* 25(11):1419–1427
180. Dickson RP, Erb-Downward JR, Huffnagle GB. 2015. Homeostasis and its disruption in the lung microbiome. *Am. J. Physiol. Lung Cell. Mol. Physiol.* 309(10):L1047–55
181. Pérez-Cobas AE, Buchrieser C. 2019. Analysis of the pulmonary microbiome composition of *Legionella pneumophila*-infected patients. *Methods Mol. Biol.* 1921(4):429–43
182. Pham TAN, Lawley TD. 2014. Emerging insights on intestinal dysbiosis during bacterial infections. *Curr. Opin. Microbiol.* 17:67–74
183. Hadifar S, Fateh A, Yousefi MH, Siadat SD, Vaziri F. 2019. Exosomes in tuberculosis: still terra incognita? *J. Cell. Physiol.* 234(3):2104–11
184. Uversky VN. 2017. Intrinsically disordered proteins in overcrowded milieu: membrane-less organelles, phase separation, and intrinsic disorder. *Curr. Opin. Struct. Biol.* 44:18–30
185. Onfelt B, Nedvetzki S, Benninger RKP, Purbhoo MA, Sowinski S, et al. 2006. Structurally distinct membrane nanotubes between human macrophages support long-distance vesicular traffic or surfing of bacteria. *J. Immunol.* 177(12):8476–83
186. Baidya AK, Bhattacharya S, Dubey GP, Mamou G, Ben-Yehuda S. 2018. Bacterial nanotubes: a conduit for intercellular molecular trade. *Curr. Opin. Microbiol.* 42:1–6
187. Gottschling DE, Nyström T. 2017. The upsides and downsides of organelle interconnectivity. *Cell* 169(1):24–34
188. Staerck C, Gastebois A, Vandeputte P, Calenda A, Larcher G, et al. 2017. Microbial antioxidant defense enzymes. *Microb. Pathog.* 110:56–65
189. Islinger M, Voelkl A, Fahimi HD, Schrader M. 2018. The peroxisome: an update on mysteries 2.0. *Histochem. Cell Biol.* 150(5):443–71
190. Whiley H, Bentham R. 2011. *Legionella longbeachae* and legionellosis. *Emerg. Infect. Dis.* 17(4):579–83
191. Brassinga AKC, Kinchen JM, Cupp ME, Day SR, Hoffman PS, Sifri CD. 2010. *Caenorhabditis* is a metazoan host for *Legionella*. *Cell. Microbiol.* 12(3):343–61
192. Fabbi M, Pastoris MC, Scanziani E, Magnino S, Di Matteo L. 1998. Epidemiological and environmental investigations of *Legionella pneumophila* infection in cattle and case report of fatal pneumonia in a calf. *J. Clin. Microbiol.* 36(7):1942–47
193. McDonald R, Schreier HJ, Watts JEM. 2012. Phylogenetic analysis of microbial communities in different regions of the gastrointestinal tract in *Panaque nigrolineatus*, a wood-eating fish. *PLOS ONE* 7(10):e48018
194. Schoebel S, Blankenfeldt W, Goody RS, Itzen A. 2010. High-affinity binding of phosphatidylinositol 4-phosphate by *Legionella pneumophila* DrrA. *EMBO Rep.* 11(8):598–604

1.7 *Legionella longbeachae*: discovery and key differences

Legionella longbeachae was first isolated in 1980 from four patients presenting with pneumonia admitted to the hospital in Long Beach, California, and a second serogroup was isolated that same year (Bibb *et al.*, 1981; McKinney *et al.*, 1981). While *Legionella* are predominantly found in freshwater environments, this is not the case for *L. longbeachae*, for which studies have shown a link between gardening activities of patients infected with *L. longbeachae* and, ultimately, the bacteria were isolated from potting soil and compost mixes (Steele, Lanser and Sangster, 1990; Steele, Moore and Sangster, 1990; Koide *et al.*, 1999). Though the route of transmission is still not completely understood, it seems that infection with *L. longbeachae* occurs via inhalation of contaminated soil aerosols. Therefore, gardening activities constitute a unique risk factor for infection with *L. longbeachae* (Ruehlemann and Crawford, 1996; Kenagy *et al.*, 2017). It is assumed that *L. longbeachae* – like other *Legionella* species – replicates in protozoan hosts in the environment. However, *L. longbeachae* has also been detected in water samples, that were likely contaminated with soil, raising the possibility that waterborne transmission of *L. longbeachae* may also occur (Ortiz-Roque and Hazen, 1987; Heijnsbergen *et al.*, 2014). To date, no differences in clinical symptoms of LD caused by *L. longbeachae* and *L. pneumophila* have been reported (Amodeo, Murdoch and Pithie, 2010; Chambers *et al.*, 2021).

L. longbeachae infections have been mostly reported in Australia and New Zealand, where they account for 39% and 54% of LD cases, respectively (Chambers *et al.*, 2021). Figure 4 shows the global distribution of *L. longbeachae* either isolated from human and environmental samples or environmental samples only. In recent years, sporadic infections with *L. longbeachae* have also been reported in Japan, Thailand, Europe, and North America, likely due to improved detection methods and raised awareness (Health Protection Scotland, 2014; Chambers *et al.*, 2021; Gonçalves *et al.*, 2021).

Legionella infections are detected by serology, PCR-based methods, bacterial culture, and *via* the urinary antigen test. The latter is widely used as a first line screening tool, but it only provides high accuracy for infections caused by *L. pneumophila* sg 1 and fails to detect other serogroups and non-*pneumophila* species (Mercante and Winchell, 2015). Hence, bacterial culture on defined medium and PCR-based methods need to be used to determine the exact *Legionella* species involved in infection, including *L. longbeachae* (Cross *et al.*, 2016). It is assumed that case numbers reported for *L. longbeachae* are underestimated, as PCR-based methods are not commonly used for clinical diagnosis, with the exception of New Zealand

(Chambers *et al.*, 2021). Indeed, the implementation of almost entirely molecular diagnostic tests in New Zealand showed that the incidence of *L. longbeachae* was higher than previously reported (Graham *et al.*, 2023).

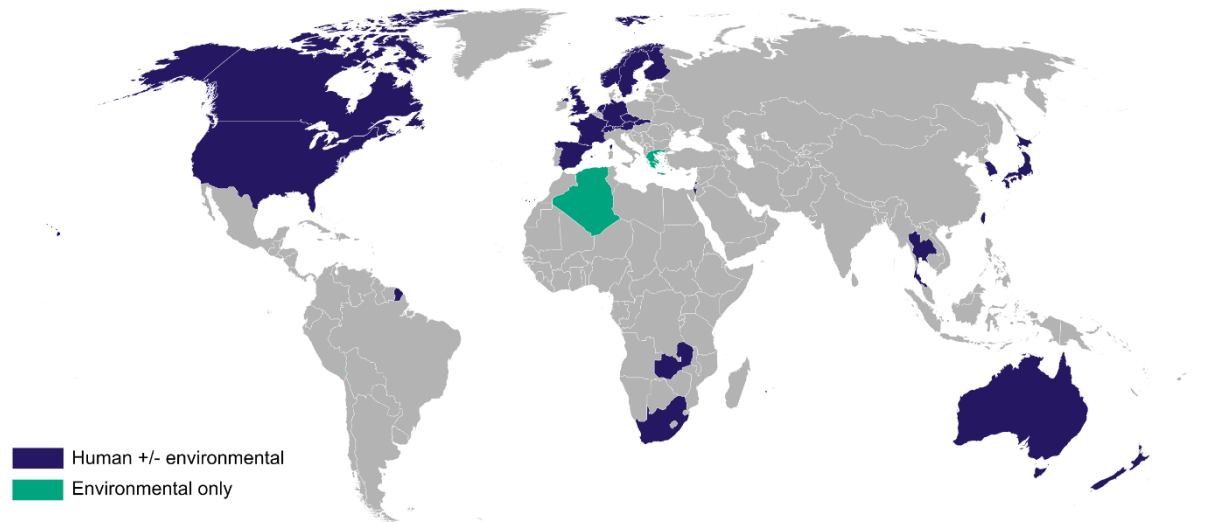


Figure 4: Detection of *Legionella longbeachae* by country. Countries shaded in dark blue have reported *L. longbeachae* both in patient samples and environmental samples. Countries shaded in green reported *L. longbeachae* in environmental samples only. Adapted from Chambers *et al.*, 2021.

At the genome level, *L. longbeachae* has with 4 Mbp a larger genome than *L. pneumophila* that is about 3.5 Mbp in size. Around 34% of the effector repertoire are shared between the two species, but *L. longbeachae* encodes a smaller, predicted repertoire of about 220 putative effectors as compared to over 330 predicted effectors for *L. pneumophila* (Cazalet *et al.*, 2010; Kozak *et al.*, 2010; Burstein *et al.*, 2016). However, this might also be due to the fact that available bioinformatics tools are not entirely able to predict effectors. Thus, the effector repertoire of *L. longbeachae* might be underestimated. Interestingly, *L. longbeachae* encodes a unique set of eukaryotic-like effectors that have homology to Rab GTPases, which are probably implicated in the establishment of the replicative vacuole (Cazalet *et al.*, 2010; Wood *et al.*, 2015). I contributed to a research paper about the role of one of these effectors, named RabL. We showed that it is involved in the modulation of the host immune response during *L. longbeachae* infection (in preparation, see **Annex B**). In addition, *L. longbeachae* encodes proteins with SH2 domains that are known mediators of eukaryotic intracellular phosphotyrosine signaling cascades. Indeed, it was shown that the *L. longbeachae* SH2 domain-containing effectors LeSH and LUSH are phosphotyrosine superbinders as compared to the known eukaryotic Src SH2 domain (Kaneko *et al.*, 2018). Interestingly, *L. longbeachae* also

encodes proteins predicted to be involved in cellulose degradation and pectin degradation, likely reflecting its soil habitat (Cazalet *et al.*, 2010).

Microarray analysis showed that *L. longbeachae* does not have such a distinct switch in gene expression from replicative to virulent phase as *L. pneumophila* (Cazalet *et al.*, 2010). It has been shown that *L. longbeachae* does not express flagella, a hallmark of transmissive phase *L. pneumophila*. It is important to note that although *L. longbeachae* encodes several regulators for flagella expression, it lacks key structural genes for flagella expression (Cazalet *et al.*, 2010; Kozak *et al.*, 2010). Recent studies have shown that the *L. longbeachae* genome is marked by a high degree of DNA methylation and recombination events in the chromosome and in the plasmid, pointing at a high degree of genome plasticity (Slow *et al.*, 2022).

1.8 *Legionella longbeachae* infection and virulence

Early studies of the *L. longbeachae* infection cycle suggested that the bacteria replicate in an LCV that associates with early endosomal and lysosomal markers, in contrast to *L. pneumophila* (Asare and Abu Kwaik, 2007). However, it was later shown in the soil protozoan *Dictyostelium discoideum* that the *L. longbeachae* LCV is decorated with ER markers, similar to *L. pneumophila* (Dolinsky *et al.*, 2014; Hoffmann *et al.*, 2014). Furthermore, *L. longbeachae* wild type bacteria suppress the association of the LCV with the late endosomal marker LAMP-1. Similar to *L. pneumophila*, *L. longbeachae* recruits Rab1 and Sec22b to the LCV (Wood *et al.*, 2015). In addition, the *L. longbeachae* LCV is decorated with polyubiquitinated proteins, as was previously reported for *L. pneumophila* (Shi *et al.*, 2023a, 2023b). Moreover, intracellular replication of *L. longbeachae* critically depends on a functional Dot/Icm T4SS (Wood *et al.*, 2015). Thus, the *L. longbeachae* LCV resembles that of *L. pneumophila*, even though *L. longbeachae* harbors a unique effector repertoire.

In contrast to *L. pneumophila*, *L. longbeachae* can infect common mouse laboratory strains such as C57BL/6, BALBc or A/J mice (Asare *et al.*, 2007; Gobin *et al.*, 2009; Massis *et al.*, 2016). The latter is the only mouse strain that can support replication of *L. pneumophila* due to a point mutation in the *naip5* gene of the NLRC4 inflammasome and a subsequent defect in detection of flagellin in these mice (Molofsky *et al.*, 2006; Pereira *et al.*, 2011). Otherwise, infection of mice leads to a rapid detection of bacterial flagellin, subsequent inflammasome activation as well as caspase activation and clearing of *L. pneumophila* (Ren *et al.*, 2006).

Recently, Wang and collaborators showed that intranasal infection of C57BL/6 mice with *L. longbeachae* leads to an influx and activation of mucosal-associated invariant T cells (MAIT cells) that was associated with immune protection (Wang *et al.*, 2018). Adoptive transfer of MAIT cells to immune-deficient mice protects the animals from lethal infection. By co-culturing peripheral blood mononuclear cells (PBMCs) with infected THP-1 monocytes, the authors show that *L. longbeachae* infection leads to activation of human MAIT cells in PBMCs, suggesting that MAIT cells play a role in protection against *L. longbeachae* infection *in vivo* (Wang *et al.*, 2018).

Massis and collaborators showed that *L. longbeachae* is highly virulent in wild type C57BL/6 mice, causing pulmonary failure and death of the animals (Massis *et al.*, 2016). However, while the bacteria cause severe tissue damage in the lungs and diminished physiological parameters such as reduced O₂ consumption in the animals, *L. longbeachae* fails to induce a strong inflammatory cytokine response *in vitro*. Indeed, compared to a *L. pneumophila* mutant strain lacking flagella, which induces a strong IL-1 β as well as TNF α and IL-8 response *in vitro*, *L. longbeachae* only induces moderate to low expression of these pro-inflammatory cytokines (Massis *et al.*, 2016). The authors therefore termed *L. longbeachae* immunologically silent and concluded that the lack of flagella in *L. longbeachae* cannot be the sole explanation for the observed phenotype in infection. The authors raised the question whether a previously identified capsule cluster in the *L. longbeachae* genome may give rise to a capsule that protects the bacteria from immune recognition (Cazalet *et al.*, 2010; Massis *et al.*, 2016).

1.9 The *Legionella longbeachae* capsule

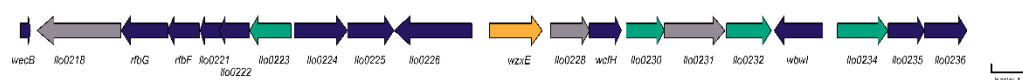
The complete genome of *L. longbeachae* NSW150, a strain of sg 1, was sequenced by our group (Cazalet *et al.*, 2010). Genome analyses revealed two gene clusters that share similarities with lipopolysaccharide (LPS) and capsular polysaccharide (CPS) biosynthesis loci (Cazalet *et al.*, 2010).

The predicted LPS cluster stretches over 24 kb in the genome and comprises several glycosyltransferases and nucleotide sugar precursor genes as well as a translocase of the WzxE type. The putative CPS cluster spans over 48 kb in the genome and comprises several glycosyltransferases and nucleotide sugar precursor genes, similar to the LPS cluster (Figure 5). In addition, the CPS cluster contains an ABC transporter encoded by the *ctrABCD* genes, which share remote similarity to the *Neisseria meningitidis* ABC-type capsule transporter (Cazalet *et al.*, 2010). To better distinguish the LPS and CPS clusters, the genomes of sg 1 and a sg 2 strain

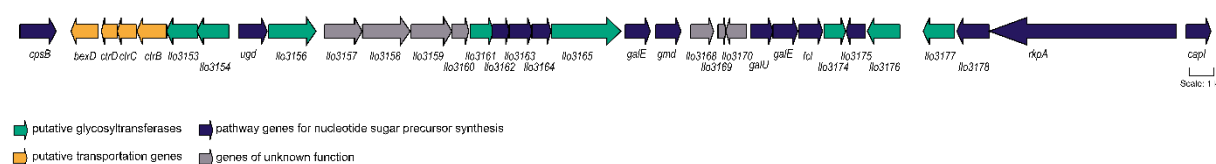
of *L. longbeachae* were compared. While the LPS cluster differed between serogroups, the CPS cluster was conserved among the analyzed genomes, leading to the conclusion that indeed one constitutes the LPS cluster and the other one the CPS cluster (Cazalet *et al.*, 2010).

Based on these findings, we hypothesized that the presence of a capsule may be partly responsible for the high virulence and poor immune stimulation of *L. longbeachae* in mice (Massis *et al.*, 2016) – constituting the premises for this PhD thesis.

A) LPS cluster



B) Capsule cluster



LPS cluster			Capsule cluster (continued)		
Gene	Name	Annotation	Gene	Name	Annotation
<i>llo0217</i>	<i>wecB</i>	UDP-N-acetylglucosamine 2-epimerase	<i>llo3154</i>	-	Glycosyltransferase
<i>llo0218</i>	-	Membrane protein of unknown function	<i>llo3155</i>	<i>ugd</i>	UDP-glucose-6-dehydrogenase
<i>llo0219</i>	<i>rfbG</i>	CDP-glucose 4,6-dehydratase	<i>llo3156</i>	-	Glycosyltransferase
<i>llo0220</i>	<i>rfbF</i>	Glucose-1-phosphate cytidyltransferase	<i>llo3157</i>	-	Protein of unknown function
<i>llo0221</i>	-	Membrane protein, GtrA-like family protein	<i>llo3158</i>	-	Protein of unknown function
<i>llo0222</i>	-	Methyltransferase	<i>llo3159</i>	-	Protein of unknown function
<i>llo0223</i>	-	Glycosyltransferase, family 2	<i>llo3160</i>	-	Protein of unknown function
<i>llo0224</i>	-	Methyltransferase	<i>llo3161</i>	-	Glycosyltransferase, family 2
<i>llo0225</i>	-	Oxidoreductase	<i>llo3162</i>	-	N-acylneuraminate cytidyltransferase
<i>llo0226</i>	-	Putative acyltransferase	<i>llo3163</i>	-	D-isomer specific 2-hydroxyacid dehydrogenase, NAD-binding
<i>llo0227</i>	<i>wzxE</i>	similar to wzxE translocase	<i>llo3164</i>	-	Putative short chain dehydrogenase/reductase
<i>llo0228</i>	-	Protein of unknown function	<i>llo3165</i>	-	Glycosyltransferase
<i>llo0229</i>	<i>wcfH</i>	Putative deacetylase	<i>llo3166</i>	<i>galE2</i>	UDP-galactose-4-epimerase
<i>llo0230</i>	-	Glycosyltransferase, family 2	<i>llo3167</i>	<i>gmd</i>	GDP-D-mannose dehydratase, NAD(P)-binding
<i>llo0231</i>	-	Membrane protein of unknown function	<i>llo3168</i>	-	Protein of unknown function
<i>llo0232</i>	-	Glycosyl transferase, family 1	<i>llo3169</i>	-	Protein of unknown function
<i>llo0233</i>	<i>wbwI</i>	O-acetyltransferase	<i>llo3170</i>	-	Protein of unknown function
<i>llo0234</i>	-	Glycosyltransferase, family 1	<i>llo3171</i>	<i>galU</i>	Glucose-1-phosphate uridylyltransferase
<i>llo0235</i>	-	Putative dTDP-4-dehydrorhamnose reductase	<i>llo3172</i>	<i>galE</i>	UDP-galactose-4-epimerase
<i>llo0236</i>	-	Putative NAD-dependent epimerase/dehydratase	<i>llo3173</i>	<i>fcl</i>	Bifunctional GDP-fucose synthetase
			<i>llo3174</i>	-	Glycosyltransferase (fragment)
			<i>llo3175</i>	-	Oxidoreductase
			<i>llo3176</i>	-	Glycosyltransferase
			<i>llo3177</i>	-	UDP-Glycosyltransferase
			<i>llo3178</i>	-	Putative amidotransferase
			<i>llo3179</i>	<i>rkpA</i>	Putative type I polyketide synthase, wcbR-like
			<i>llo3180</i>	<i>capI</i>	NAD-dependent epimerase/dehydratase
Capsule cluster					
Gene	Name	Annotation			
<i>llo3148</i>	<i>cpsB</i>	Mannose-1-phosphate guanylyltransferase			
<i>llo3149</i>	<i>bexD</i>	CPS export protein, ctrA-like			
<i>llo3150</i>	<i>ctrD</i>	CPS export ATP-binding protein			
<i>llo3151</i>	<i>ctrC</i>	CPS export inner membrane protein			
<i>llo3152</i>	<i>ctrB</i>	CPS export inner membrane protein			
<i>llo3153</i>	-	Mannosyltransferase			

Figure 5: LPS and capsule biosynthesis clusters encoded in the *Legionella longbeachae* NSW150 genome. A) Putative LPS synthesis cluster. B) Putative capsule biosynthesis cluster. Green, putative glycosyltransferase; blue, nucleotide sugar precursor synthesis genes; yellow, putative transportation genes; gray, genes of unknown function. Adapted from Cazalet *et al.*, 2010.

2. Outer membrane polysaccharides

2.1 Bacterial cell wall architectures

Historically, bacteria were divided into two groups based on Gram staining developed by Hans Christian Gram in the 19th century: Gram-negative and Gram-positive bacteria, and many, but not all bacteria fit this binary division. Later, the development of electron microscopy imaging revealed that Gram-negative bacteria contain an inner membrane (IM) and an outer membrane (OM), separated by a thin peptidoglycan layer (PG), and that Gram-positive bacteria contain a single membrane covered by a thick PG layer (Megrian *et al.*, 2020; Tocheva, Ortega and Jensen, 2016). Classic model organisms for each group are the Proteobacterium *Escherichia coli* and the Firmicute *Bacillus subtilis*, respectively. However, the presence of diderm Gram-negative bacteria such as *Veillonella* within the Firmicutes challenges the oversimplification of this phylum as Gram-positive, and advances in phylogenomic analyses have shown a large diversity in bacterial cell wall architectures (Megrian *et al.*, 2020; Sutcliffe, 2010). Recent phylogenomic studies of the Firmicute phylum suggest that the last common bacterial ancestor was a diderm that lost the OM several times during evolution, giving rise to monoderm bacteria (Taib *et al.*, 2020).

In addition to a thick PG layer, the cell wall of monoderms contains membrane-associated proteins and teichoic acid (Figure 6A). A hallmark of the diderm OM is the presence of glycolipids (predominantly lipopolysaccharide, LPS) and outer membrane proteins such as the β -barrel assembly machinery (BAM) complex for OM protein assembly (Figure 6B) (Brown *et al.*, 2015).

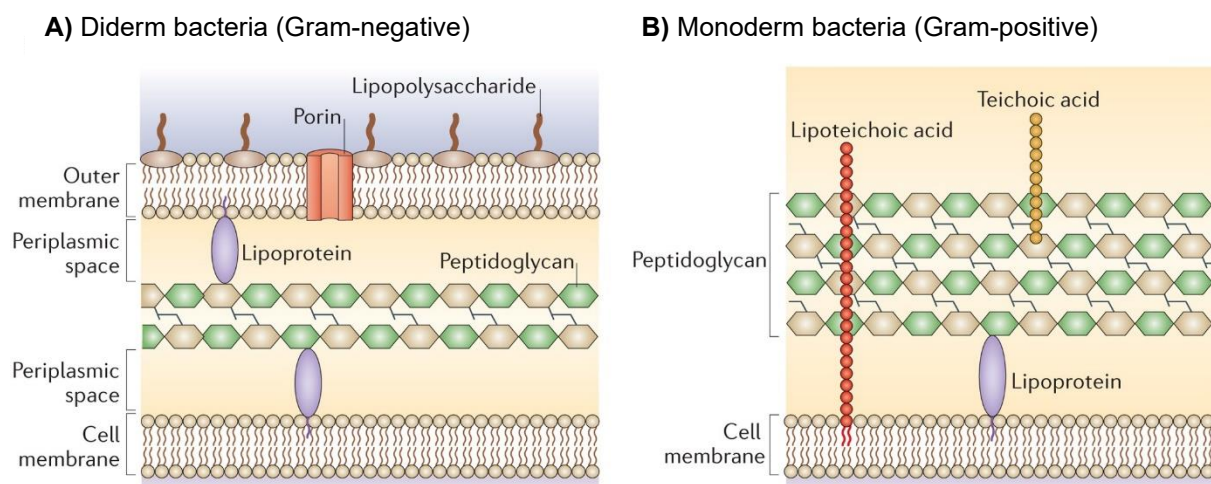


Figure 6: Common cell wall architectures in bacteria. A) Cell wall architecture of diderm bacteria (Gram-negative). The inner membrane is linked to a thin peptidoglycan layer by lipoproteins in the periplasmic space.

The peptidoglycan is linked to the outer membrane by lipoproteins. The outer membrane contains outer membrane proteins such as porins or fimbriae. The inner leaflet of the outer membrane is composed of glycerophospholipids; the outer leaflet is covered with lipopolysaccharide. **B**) Cell wall architecture of monoderm bacteria (Gram-positive). The cell membrane is attached to a thick peptidoglycan layer by lipoproteins, and it contains lipoteichoic acid, which extends beyond the peptidoglycan layer. The peptidoglycan layer also serves as an anchor for (wall) teichoic acid. Adapted from Brown *et al.*, 2015.

Monoderm bacteria do not express LPS but contain teichoic acids in their cell wall, which are either attached to the cell membrane (lipoteichoic acids, LTA) or to the PG layer (wall teichoic acids, WTA). Both WTA and LTA are negatively charged polysaccharides that are important in cell shape maintenance and resistance against antimicrobial compounds (Brown, Santa Maria and Walker, 2013).

The PG sacculus surrounds the inner cell membrane of both monoderm and diderm bacteria, attached by periplasmic lipoproteins. The PG therefore is a key structural determinant of bacterial cell integrity and one of the most important targets of antibiotics (refer to reviews by Bugg and Walsh, 1992; Bush and Bradford, 2019; Vollmer *et al.*, 2008). The PG is composed of linear glycan chains consisting of disaccharides of N-acetylglucosamine (GlcNAc) and N-acetylmuramic acid (MurNAc) subunits, covalently cross-linked by short pentapeptides.

Some bacteria contain an additional outermost layer termed capsule, which shields the bacteria from the environment. Except for the polyglutamate capsule found in *Bacillus*, this layer is typically composed of capsular polysaccharides (CPS), which may cover the OM and OM proteins as well as LPS like a shield.

2.2 Complex polysaccharides in the outer leaflet of diderm bacteria

The OM of diderm bacteria is a complex asymmetric membrane with two different leaflets: an inner leaflet, composed of phospholipids such as phosphatidylethanolamine, phosphatidylglycerol, and cardiolipin (Cronan, 2003); and an outer leaflet, essentially composed of the amphiphilic glycolipid LPS. Seminal studies on the model organisms, *Salmonella enterica* and *Escherichia coli*, have laid the foundation for our understanding of LPS structure (Heinrichs, Yethon and Whitfield, 1998). LPS encompasses a lipid A, which anchors the molecule to the OM, an oligosaccharide core, conserved within a species, and in many bacteria an additional long chain repeat-unit polysaccharide termed O-antigen (Figure 7) (Bertani and Ruiz, 2018). The lipid A is a disaccharide phospholipid, consisting of

phosphorylated GlcNAc and six acyl chains that anchor the molecule in the outer leaflet of the OM. LPS molecules are negatively charged and held together in the OM by divalent cations, such as Mg^{2+} (Silhavy, Kahne and Walker, 2010). The oligosaccharide core can be divided into an inner region which contains Kdo (α -3-deoxy-D-manno-oct-2-ulopyranosonic acid) residues and modified heptose sugars, and an outer region with hexose and heptose sugars. Finally, the O-antigen is extremely variable and composed of species-specific repeating units of oligosaccharides (Alexander and Rietschel, 2001). LPS can also occur without O-antigen and is classified as rough LPS, due to a rough colony morphology of bacteria on agar plates. Pathogenic bacteria, such as *Neisseria*, *Bordetella*, *Campylobacter*, or *Acinetobacter* naturally express rough LPS (Kahler *et al.*, 1998; Caroff *et al.*, 2002; Houlston *et al.*, 2011; Kenyon and Hall, 2013).

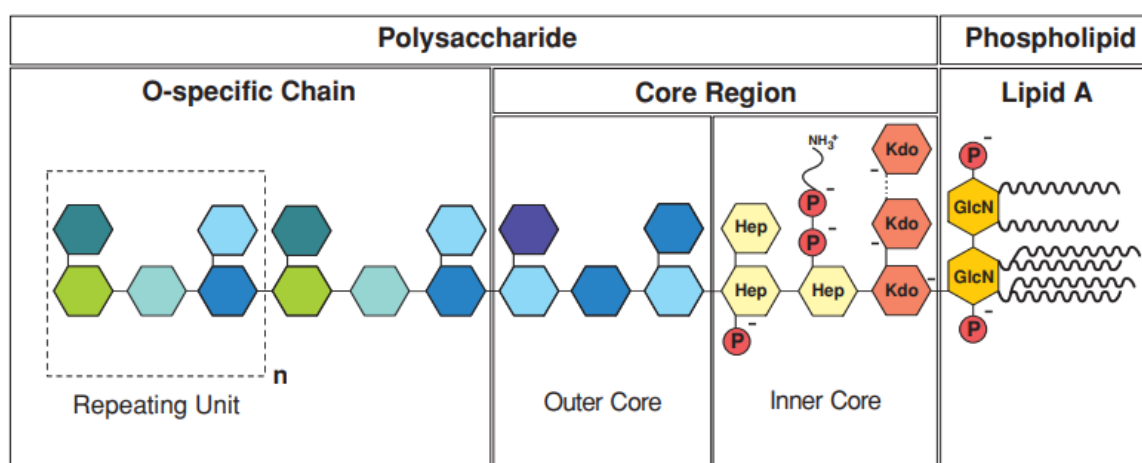


Figure 7: General structure of lipopolysaccharide (LPS). Smooth type LPS contains three domains: a phospholipid fraction, termed the lipid A, core region, and O-antigen chain. Lipid A is commonly hexa-acylated and contains two glucosamine phosphates. The LPS inner core region contains Kdo and heptose sugars, which can further be modified by additional phosphate groups. The outer core contains heptose and hexose sugars. The third domain is the species-specific O-antigen polysaccharide that is composed of repeating units of oligosaccharides. From Alexander and Rietschel 2001.

As mentioned above, some bacteria express a capsule that covers the OM with CPS. Both LPS O-antigen and CPS can be highly diverse among and within a bacterial species and, historically, bacterial species have been distinguished by serotyping of these bacterial surface structures. For example, in *E. coli* there are more than 150 O-serogroups based on 71 O-antigen gene clusters (DebRoy *et al.*, 2016; Liu *et al.*, 2020), and 80 different capsule types that have been described (Mostowy and Holt, 2018). In *Klebsiella* spp., eight different O-antigen gene clusters have been identified and 80 serologically different capsule types (Follador *et al.*, 2016; Mostowy and Holt, 2018).

At the molecular level, LPS and CPS can be very complex structures based on the overall composition: from homopolymers to heteropolymers, differences in chain lengths, branched or unbranched forms through different α - or β -glycosidic linkages, and diverse monosaccharides with substitutions (Liu *et al.*, 2020; Dong *et al.*, 2023). Table 1 gives an overview of common monosaccharides and substitutions found in bacterial (exo)-polysaccharides. Taken together, capsules in combination with different O-antigens in LPS bear an enormous complexity in OM polysaccharides found among diderm bacteria (Mostowy and Holt, 2018). Their roles and biosynthesis pathways are discussed in the following sections.

Table 1: Monosaccharides and sugar substituents found in bacterial (exo)polysaccharides. Table adapted from Sutherland, 2001.

Substituent	Charge	Occurrence
Monosaccharides		
D-Glucose	None	Very common
D-Galactose	None	Very common
D-Mannose	None	Very common
L-Fucose	None	Very common
L-Rhamnose	None	Very common
N-acetyl-D-Glucosamine	None	Very common
N-acetyl-D-Galactosamine	None	Very common
N-acetyl-D-Mannosamine	None	Uncommon
D-Glucosamine	Positive	Rare
D-Glucuronic acid	Negative	Very common
D-Galacturonic acid	Negative	Very common
D-Mannuronic acid	Negative	In alginates, otherwise uncommon
Organic acids		
Acetate	None	Very common - e.g. colanic acid
Glycerate	Negative	<i>Sphingomonas elodea</i>
Propionate	None	Rare - some <i>E. coli</i>
Pyruvate	Negative	Very common - e.g. colanic acid
Succinate	Negative	e.g. <i>Agrobacterium</i> spp.
Inorganic acids		
Phosphate	Negative	Common in some genera, especially Gram-positive spp.
Sulfate	Negative	Cyanobacteria

2.3 Biosynthesis pathways of LPS

LPS biosynthesis is tightly intertwined with cell growth and has been extensively studied in the model organism *E. coli* (Bertani and Ruiz, 2018).

LPS synthesis begins with the Raetz pathway, which involves a series of conserved enzymatic steps to produce lipid A (Figure 8). It is initiated at the inner leaflet of the inner membrane (IM) by acylation of UDP-GlcNAc by LpxA, using an acyl carrier protein. Subsequently, the tetra-acylated precursor molecule lipid IV_A is formed by the consecutive actions of LpxC through LpxK. This is followed by the addition of the Kdo sugars and acyl chains, to complete the Kdo₂-lipid A domain of LPS. Next, core sugars are attached to the Kdo₂-lipid A by several enzymes to form lipooligosaccharide (LOS) (Simpson and Trent, 2019). LOS is then flipped across the IM by MsbA. In the periplasm, the O-antigen is appended to LOS by the O-antigen ligase WaaL and the LPS molecule is transported across the PG layer to the outer leaflet of the OM by the Lpt (LPS transport) complex, where it is inserted (Simpson and Trent, 2019) (Figure 8).

O-antigen precursors are synthesized separately by IM-associated enzyme complexes on the inner leaflet at the IM, attached to a lipid carrier undecaprenyl pyrophosphate (Und-PP). They are subsequently flipped across the IM by an O-antigen flippase, and depending on the biosynthesis pathway, further polymerization can occur either before or after flipping (Simpson and Trent, 2019). One of three possible pathways are involved in O-antigens biosynthesis: **Wzy-dependent, ABC transporter-dependent, or synthase-dependent**. The first two are the most widespread pathways (Greenfield and Whitfield, 2012) (Figure 8), while only one example of synthase-dependent O-antigen synthesis has been identified in *Salmonella enterica* serovar Borreze (Keenleyside and Whitfield, 1996). In the latter, the synthase WbbF, which adds activated NDP-sugars to the nascent O-antigen chain, is also believed to be involved in the O-antigen export across the membrane (Whitfield, Williams and Kelly, 2020).

Regardless of the biosynthetic pathway, all O-antigens share a similar initiation reaction, which involves the formation of sugar-Und-PP, from Und-P and sugar-1-phosphate. This reaction is mediated by WecA in *E. coli* and WbaP in *S. enterica* (Raetz and Whitfield, 2002). In the **Wzy-dependent pathway**, short oligosaccharides are synthesized by glycosyltransferases (GTs) at the inner leaflet of the IM, and then flipped across the membrane by the flippase Wzx. Once in the periplasm, they are assembled into longer O-antigen chains by the polymerase Wzy (Islam and Lam, 2014). The chain length is controlled by Wzz, a polysaccharide co-polymerase in the periplasm (Franco, Liu and Reeves, 1996). This pathway is controlled by Wzx, which exerts substrate specificity for correctly assembled O-antigen units (Liu, Morris and Reeves, 2019).

In the **ABC transporter-dependent pathway**, the O-antigen is synthesized entirely at the inner leaflet of the IM and exported across the membrane by a dedicated ABC transporter/pore complex (Greenfield and Whitfield, 2012). The chain length is regulated by one of two mechanisms: the first one is represented by the polymannose system of *E. coli* O9a. Here, chain extension is terminated by WbdD through the addition of a methyl-phosphate to the terminal sugar of the nascent O-antigen chain, under consumption of S-adenosyl methionine (SAM) (Clarke, Cuthbertson and Whitfield, 2004; Clarke *et al.*, 2011). This terminal modification is recognized by the Wzm/Wzt ABC transporter, which exports the O-antigen across the IM into the periplasmic space (Whitfield, Williams and Kelly, 2020). The prototype for the second mechanism is the polygalactose system of *Klebsiella pneumoniae* O2a. In this case, the O-antigen lacks a non-reducing terminal modification and chain length is controlled stoichiometrically between the ABC transporter and the synthesis machinery (Greenfield and Whitfield, 2012).

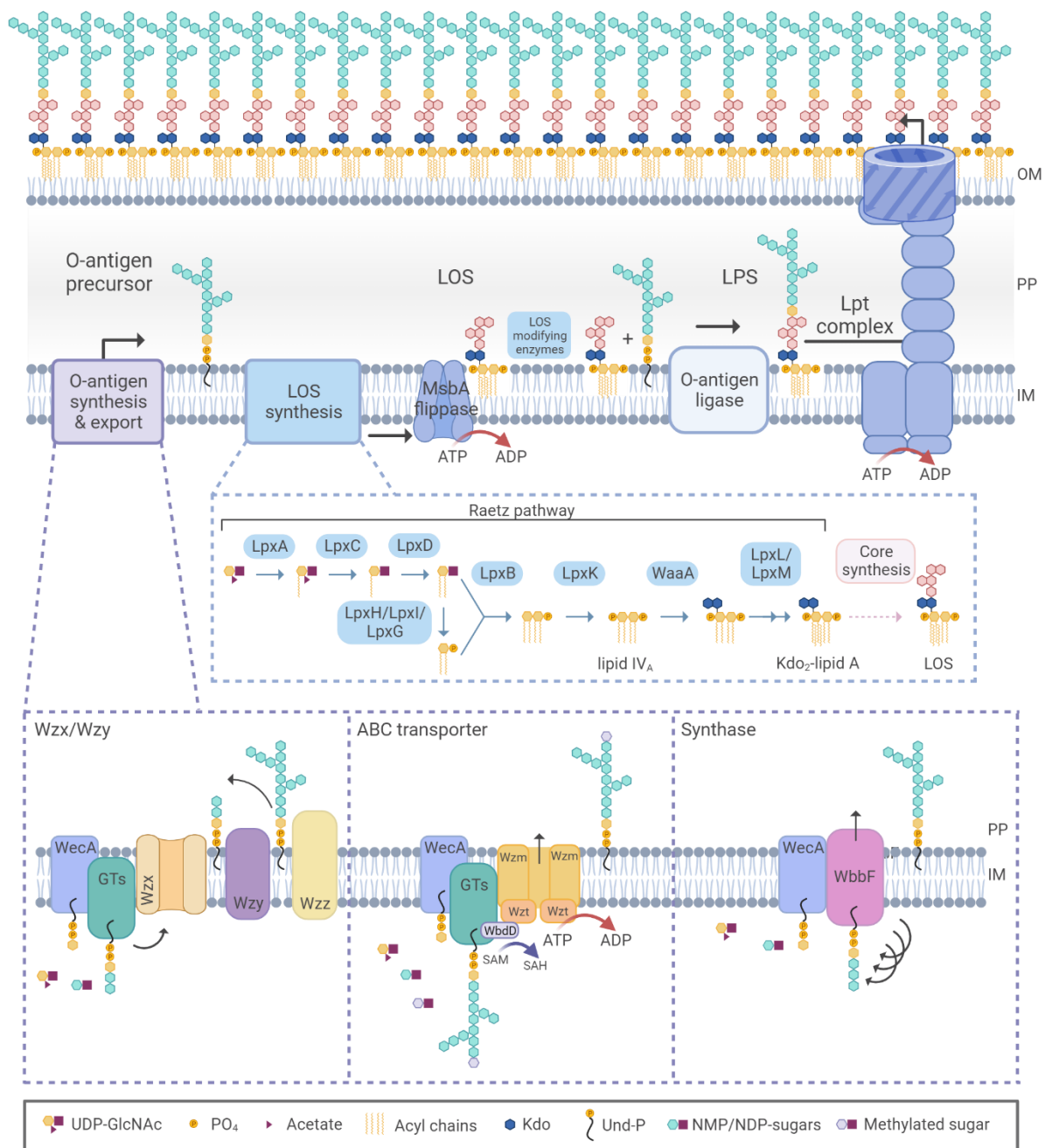


Figure 8: Biosynthesis pathways of lipopolysaccharide (LPS) in diderm bacteria. Kdo₂-lipid A is generated in the Raetz pathway, and after addition of core sugars, lipooligosaccharide (LOS) is flipped to the periplasm (PP) by MsbA. The O-antigen is synthesized and exported by either of three pathways: the Wzx/Wzy pathway, the ABC transporter pathway, or the synthase pathway. In all three pathways, the O-antigen repeat unit is built on the lipid acceptor undecaprenol-pyrophosphate (Und-PP), generated by WecA from undecaprenol-phosphate (Und-P) and UDP-GlcNAc. Subsequently, glycosyltransferases (GTs) add activated sugars to the nascent O-antigen chain. In the Wzx/Wzy pathway, O-antigen repeat units are synthesized in the cytoplasm at the inner membrane (IM), flipped to the PP and concatenated to the full-length O-antigen by Wzy and Wzz. In the ABC transporter pathway, the full O-antigen chain is generated in the cytoplasm at the IM and transported through the ABC transporter/pore complex into the PP. The synthase WbbF concomitantly adds sugars to the O-antigen chain and translocates it into the periplasm. In the periplasm, LOS and O-antigen are attached by an O-antigen ligase and loaded onto the Lpt

complex, which transports the mature LPS to the outer leaflet of the outer membrane (OM). For visualization purposes, outer membrane proteins and capsular polysaccharides were omitted. GlcNAc, N-acetyl glucosamine, PO₄, phosphate; Kdo, 3-deoxy-d-manno-oct-2-ulosonic acid; NMP/NDP, nucleoside monophosphate/nucleoside diphosphate; SAM, S-adenosyl methionine; SAH, S-adenosyl homocysteine; IM, inner membrane; PP, periplasm; Lpt, LPS transport; OM, outer membrane. Adapted from Reeves and Cunneen, 2010; Greenfield and Whitfield, 2012; Simpson and Trent, 2019. Created with BioRender.com.

2.3.1 Lipopolysaccharide of *Legionella*

Different *L. pneumophila* and non-*pneumophila* strains express characteristic LPS profiles that can be used for species typing (Jürgens and Fehrenbach, 1997). Since *L. pneumophila* is the number one cause of LD in the world, studies of the LPS focused mainly on this species, in particular on strains of sg1. *L. pneumophila* lipid A contains 2,3-diamino-2,3-dideoxyglucose (GlcN3N), instead of GlcNAc (Lück and Helbig, 2013), and it is composed of unusual long-chain, branched fatty acids, which may account for its inherently low endotoxicity compared to LPS from enterobacteria (Sonesson *et al.*, 1989; Moll *et al.*, 1992; Neumeister *et al.*, 1998). Lipid A can be modified to alter the physical properties of the OM. In *Legionella*, the *rcp* gene (resistance to cationic antimicrobial peptides, CAMPs), encodes a palmitoyl transferase that transfers palmitate to lipid A, probably promoting bacterial resistance to CAMPs through changes in membrane fluidity, or through avoiding recognition by TLR4 (Shevchuk, Jäger and Steinert, 2011).

The *L. pneumophila* LPS core contains Kdo, mannose, GlcNAc, N-acetyl quinovosamine, and rhamnose, most of which are O-acetylated (Figure 9). Its O-antigen is a homopolymer of legionaminic acid (short for: α -(2–4)-linked 5-acetamidino-7-acetamido-8-O-acetyl-3,5,7,9-tetradecoxy-L-glycero-D-galacto-non-2-ulosonic acid), which lacks free hydroxyl groups, and in some *L. pneumophila* strains, it is also highly O-acetylated (e.g. *L. pneumophila* strain Philadelphia). The lack of free hydroxyl groups or the high degree of O-acetylation renders the *L. pneumophila* LPS highly hydrophobic and it cannot be extracted in the aqueous phase of the classical hot phenol-water isolation method for LPS (Lück and Helbig, 2013). *L. pneumophila* sg1 O-antigen is synthesized and exported by its specific ABC transporter Wzm/Wzt (Cazalet *et al.*, 2008; Shevchuk, Jäger and Steinert, 2011). Importantly, most of the LPS synthesis genes found in *L. pneumophila* sg1 cannot be detected in non-*pneumophila* species, indicating that other biosynthesis clusters exist at the genus level (Cazalet *et al.*, 2008).

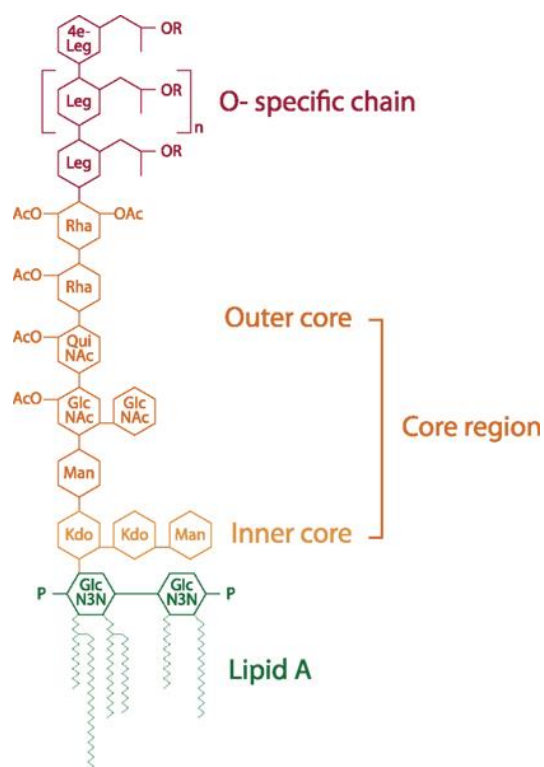


Figure 9: Structure of *Legionella pneumophila* LPS.

The LPS of *L. pneumophila* contains lipid A with unusually long acyl chains and GlcN3N (2,3-diamino-2,3-dideoxy-d-glucopyranose). The LPS core contains Kdo, Man and O-acetylated sugars. The O-antigen contains legionaminic acid. Leg, legionaminic acid; 4e-Leg, 4-epilegionaminic acid; Rha, rhamnose; Man, mannose; QuiNAC, acetylquinosamine; GlcNAC, acetylglucosamine; Kdo, 3-deoxy-d-manno-oct-2-ulosonic acid; P, phosphate; OAc, O-acetyl. From Shevchuk *et al.*, 2011.

O-acetylation of legionaminic acid residues is mediated by the *lag-1* gene, which encodes an LPS O-acetyltransferase. Recent genome-wide association studies revealed that the presence of *lag-1* in *L. pneumophila* sg1 strains is correlated with strains highly prevalent among clinical cases (Wee *et al.*, 2021). The *lag-1* gene product is responsible for 8-O-acetylation of the legionaminic acid residue proximal to the core that is N-methylated. The *lag-1* gene is unstable and only strains that express *lag-1* and have O-acetylated legionaminic acid are recognized by the monoclonal antibody Mab 3/1 (Reichardt *et al.*, 2010). This antibody is part of the so-called Dresden panel that is used to type clinical isolates of *L. pneumophila* sg1 by serological testing. These monoclonal antibodies were generated by hybridoma technology and raised against the LPS of *L. pneumophila* strain Philadelphia and react with the majority of clinical sg1 isolates (Lück *et al.*, 1992). Finally, besides O-acetylated sugars, *L. pneumophila* LPS also contains methylated or N-acetylated sugars (Kooistra *et al.*, 2001, 2002; Shevchuk, Jäger and Steinert, 2011). Moreover, LPS from *L. pneumophila* differs between bacteria grown in BYE medium or grown intracellularly (Barker, Lambert and Brown, 1993). Even in the latter, it has been demonstrated that expression of acetylated and non-acetylated LPS depends on the bacterial location within the LCV in late stages of infection. In this regard, bacteria closer to the phagosome membrane express acetylated LPS, whereas in the center of the vacuole, where close packing of the subpopulation is needed, they express a less hydrophobic non-acetylated LPS (Reichardt *et al.*, 2010). Phase-variation in the *L. pneumophila* LPS was first detected from

bacteria replicating intracellularly in the macrophage-like cell line HL-60 and in bacteria recovered from lungs of infected guinea pigs (Lüneberg *et al.*, 1998). Further analyses of the molecular mechanism underlying LPS phase variation identified a 30 kb plasmid of phage origin that can be inserted in the chromosome or excised and exist as a plasmid. Indeed, excision of the plasmid and presence in high copy numbers in the genome lead to LPS phase variation and loss of virulence (Lüneberg *et al.*, 2004).

Much less is known about *L. longbeachae* LPS, as only one study analyzed its composition (Sonesson *et al.*, 1994). This showed that the *L. longbeachae* lipid A harbors a long-chain fatty acid composition with attached sugars similar to *L. pneumophila* lipid A (Sonesson *et al.*, 1994). The isolated LPS from *L. longbeachae* contained Kdo, GlcN3N, mannose, glucosamine, glucosamine phosphate, and quinovosamine, similar to LPS from *L. pneumophila*. However, the *L. longbeachae* LPS was reported to be of the rough type (i.e. it does not contain O-antigen) (Sonesson *et al.*, 1994).

2.4 Regulation of LPS biosynthesis

In *E. coli*, the first step of lipid A biosynthesis is the acylation of UDP-GlcNAc catalyzed by LpxA. UDP-GlcNAc is an essential metabolite for the synthesis of both PG and LPS, hence this step is an early branch point between both biosynthetic pathways (Anderson, Bulawa and Raetz, 1985; Anderson and Raetz, 1987). UDP-GlcNAc biosynthesis depends on GlmS, which catalyzes the synthesis of the precursor glucosamine-6-phosphate (GlcN-6-P) from glucose-6-phosphate and glutamine. Transcript levels of GlmS are regulated by two small RNAs: GlmY and GlmZ. GlmZ prevents the formation of an inhibitory structure that occludes the ribosome-binding site of *glmS*, facilitating the translation of its mRNA. Under GlcN-6-P limiting conditions, GlmY sequesters the RNase adaptor protein RapZ, which processes and inactivates GlmZ, hence facilitating translation of the *glmS* mRNA (Klein and Raina, 2019).

The acylation of UDP-GlcNAc is followed by an irreversible reaction catalyzed by the deacetylase LpxC. This is the first committed step towards the biosynthesis of lipid A (Young *et al.*, 1995; Klein *et al.*, 2021). LpxC levels and proteolytic turnover are controlled by the protease FtsH, and an IM-anchored protein, LapB. This activity can then be counteracted by LapC (formerly YejM), which senses LPS levels and acts as an antagonist of LapB, dampening LpxC turnover when the demand for LPS is high (Fivenson and Bernhardt, 2020; Shu and Mi, 2022). How LapC and LapB adjust the rate of LpxC degradation is still not fully understood. Moreover, it has been shown that in an FtsH-LapB independent manner, LpxC can also be

degraded by the HslVU protease complex at high temperatures (Biernacka *et al.*, 2020). Adding complexity to the system, LapD (YhcB) has been recently identified as another regulator of LpxC degradation, acting as an antagonist of LapB, which could also aid MsbA-mediated LPS translocation across the IM (Wieczorek *et al.*, 2022). Finally, it has been demonstrated that genes involved in lipid A and LOS biosynthesis are transcriptionally regulated by the RpoE sigma factor and the CpaX/CpaR two-component system (Dartigalongue, Missiakas and Raina, 2001).

A second important checkpoint in LPS biosynthesis exists at the level of the MsbA flippase. Structural analyses revealed that MsbA detects a phosphoglucosamine headgroup and correct hexa-acylation of lipid A by tightly packing the acyl chains in its hydrophobic pocket and preventing or reducing the translocation of under-acylated LPS species (Mi *et al.*, 2017; Ho *et al.*, 2018; Padayatti *et al.*, 2019; Wieczorek *et al.*, 2022). Moreover, it has been proposed that cardiolipin aids in MsbA ATPase activity to transport LPS to the OM, as viability of bacteria with under-acylated LOS can be ensured by the synthesis of cardiolipin (Douglass, Cl  on and Trent, 2021; Gorzelak, Klein and Raina, 2021; Klein *et al.*, 2021).

2.5 Role of LPS in infection

Bacterial LPS is a major pathogen-associated molecular pattern (PAMP), which can be recognized by pattern recognition receptors (PRRs), expressed in innate immune cells, such as macrophages, neutrophils, and dendritic cells. The recognition of LPS by PRRs can trigger rapid inflammatory reactions essential for host innate immunity (Alexander and Rietschel, 2001; Kawai, 2014). The most conserved part of LPS is lipid A, which can be recognized by Toll-like receptor 4 (TLR4) and its coreceptors CD14 and MD2. LPS is first bound by the soluble LPS-binding protein (LBP) and localizes to CD14. The LPS-LBP complex is then transferred by CD14 to the TLR4-MD2 complex, which leads to TLR4 dimerization. The intracellular adaptor molecule MyD88 mediates endocytosis of the TLR4 dimer. Through a cytosolic signaling cascade involving MyD88 and TRIF, transcription of pro-inflammatory cytokines, chemokines, and type I interferons is induced (Ciesielska, Matyjek and Kwiatkowska, 2021). This results in the secretion of pro-inflammatory cytokines such as IL-6, IL-12, or TNF α , and the consequent recruitment and activation of more immune effector cells at the site of infection (Abel *et al.*, 2002; Kawai, 2014).

Bacteria have evolved several strategies to modify their LPS to avoid recognition by TLRs and to dampen TLR-mediated immune responses (Albiger *et al.*, 2007; Simpson and Trent, 2019).

It was shown in *Salmonella enterica* serovar Typhimurium, that O-antigen length relates to evasion of complement-mediated killing and modulation of uptake by macrophages (Murray, Attridge and Morona, 2006). This was also observed in *Pseudomonas aeruginosa*, where long and very-long O-antigen chains were found to protect bacteria from complement-mediated killing by binding complement factors at a distance from the membrane, thus preventing insertion of membrane attack complexes (Kintz *et al.*, 2008). Furthermore, it was described that *Helicobacter pylori* modulates the terminal O-antigen sugars to include L-fucose, generating so-called Lewis antigens that mimic host cell surface molecules and help bacteria in gastric colonization (Maldonado, Sá-Correia and Valvano, 2016). Lipid A modifications have also been found to be associated with bacterial survival in the host. For example, *Yersinia pestis* produces hexa-acylated lipid A at 25°C. However, inside the host, when the temperature rises to 37°C, it produces LPS with tetra-acylated lipid A (Knirel *et al.*, 2005). The latter does not stimulate TLR4 activation because of its poor interaction with TLR4 co-receptors LBP, CD14, and MD2. Moreover, mutant strains that produce hexa-acylated lipid A at 37°C were shown to be avirulent in mice. This indicates a key role for lipid A modifications in virulence (Montminy *et al.*, 2006). A similar role for less acylated lipid A forms in bacterial survival was observed in the human pathogen *Francisella tularensis*, which expresses tetra- or penta-acylated lipid A (Matsuura, 2013).

2.5.1 Legionella LPS and its role in infection

For *L. longbeachae*, only structural and biochemical studies have been performed on isolated LPS, which showed similar fatty acid and sugar compositions as the LPS of *L. pneumophila* sg1 (Sonesson *et al.*, 1994). Thus, the role of *L. longbeachae* LPS in infection is not known to date.

The *L. pneumophila* LPS has inherently low endotoxic activity (Neumeister *et al.*, 1998). Compared to enterobacteria, a 1000-fold higher dose of *Legionella* LPS is necessary to induce cytokine secretion of human monocytes (Neumeister *et al.*, 1998). Early studies on the role of LPS components, pointed out that *Legionella* lipid A contains unusually long fatty acids (Sonesson *et al.*, 1989; Moll *et al.*, 1992), which leads to a low engagement of TLR4 and its co-receptor CD14 (Neumeister *et al.*, 1998). Polymorphisms in TLR4 have been shown to correlate with susceptibility of patients to LD (Hawn *et al.*, 2005), despite the fact that *Legionella* LPS only poorly stimulates TLR4 but rather involves co-engagement of TLR2 and CD14 (Girard *et al.*, 2003). Mice deficient in TLR2 exhibit higher IL-6 and IL-12 cytokine levels as compared to wild type or TLR4-deficient mice (Fuse *et al.*, 2007). Also,

L. pneumophila LPS was shown to induce TNF α production in murine bone marrow-derived macrophages, however this was not found to translate into resistance against infection (Arata *et al.*, 1993). Secreted LPS was shown to inhibit phagosome-lysosome fusion in amoeba and monocytes, leading to *L. pneumophila* evasion of phagosome maturation, altogether suggesting a crucial role of this molecule during bacterial infection (Seeger *et al.*, 2010). Finally, despite its role in O-acetylation, mutations in *lag-1* were not shown to have an adverse effect on bacterial replication in macrophages and amoeba (Lück *et al.*, 2001). However, recent genome-wide association studies demonstrated that *lag-1* confers resistance to complement-mediated killing and put in evidence the existence of a strong correlation between the presence of this gene and *L. pneumophila* clinical isolates (Wee *et al.*, 2021).

2.6 Capsules in diderm bacteria

Capsules are typically the outermost membrane layer found in some bacteria. CPS can be attached to the cell wall or released into the media; in which case they are called exopolysaccharides (EPS). Capsules can be found in many human pathogens such as *Haemophilus influenzae*, *Neisseria meningitidis*, *Klebsiella pneumoniae*, or *E. coli* (Figure 10), and their presence is typically associated with a poor immune response and increased bacterial evasion of innate immune defenses (Wen and Zhang, 2015). In diderm bacteria, CPS are attached to the OM *via* a lipid anchor or a protein anchor, such as the capsule of *E. coli* K30 that is attached to the OM protein Wzi (Rahn *et al.*, 2003; Willis and Whitfield, 2013a). Additionally, CPS may be retained on the OM by ionic interactions with LPS, as shown for *Klebsiella pneumoniae* (Singh *et al.*, 2022).

Biochemically, there is a large diversity of different CPS reported in the literature. They may consist of polysaccharide homopolymers or heteropolymers, linear or extensively branched. Moreover, sugars in the CPS, like in LPS, can be modified, thus affecting its overall charge (refer to Table 1 in section 2.1). It has been described that few bacterial species, such as *Shigella sonnei* and *E. coli* O111, express so-called O-antigen capsules (also referred to as group 4 capsules) (Thomassin *et al.*, 2013; Caboni *et al.*, 2015). These are capsules made of the same building blocks as the O-antigen, yet they do not contain the core Kdo sugars otherwise found in LPS. Moreover, their lipid acceptor may not be lipid A, but a polyprenol-phosphate anchor (Peleg *et al.*, 2005; Snyder *et al.*, 2006; Whitfield, 2006).

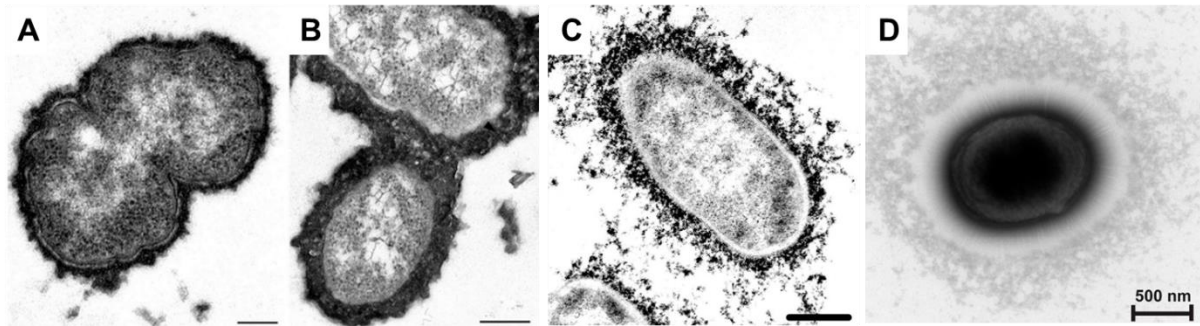


Figure 10: Capsules of diderm bacteria imaged by transmission electron microscopy. **A)** *Neisseria meningitidis* group B capsule stained with ruthenium red. **B)** *Haemophilus influenzae* type b capsule stained with ruthenium red. (A, B) Scale bars = 200 nm. From Birkhead *et al.*, 2017. **C)** *Escherichia coli* K30 capsule stained with cationized ferritin. Scale bar = 500 nm. From Rahn *et al.*, 2003. **D)** *Klebsiella pneumoniae* capsule visualized by negative staining with phosphotungstic acid. The capsule appears as a halo surrounding the bacterial cell. Scale bar = 500 nm. From Fleeman *et al.*, 2020.

2.7 Capsule biosynthesis pathways in diderm bacteria

Historically, four different capsule groups (1 to 4) have been defined in *E. coli* based on biochemical and genetic properties (Whitfield, 2006) (Table 2). Nowadays, most CPS synthesis pathways are divided into three categories based on the mode of chain elongation and translocation, similarly to LPS (see section 2.2): **Wzx/Wzy-dependent, ABC-transporter dependent, or synthase-dependent pathways** (Rendueles *et al.*, 2017) (Figure 11).

The **Wzx/Wzy-dependent pathway** of CPS biosynthesis was extensively characterized in *E. coli*. In this pathway, CPS subunits are synthesized in the cytoplasm, anchored to the IM by undecaprenol-phosphate (Und-P), and translocated across the membrane by the flippase Wzx. Using these lipid-linked repeat units, the full CPS chains are subsequently assembled in the periplasm by Wzy, in coordination with a tyrosine autokinase (Wzc) and its cognate phosphatase (Wzb). The synergistic action of Wzc and Wzb controls the length of the nascent O-antigen chain (Reid and Whitfield, 2005). The assembled CPS is then translocated to the outer leaflet of the OM by Wza, which likely acts as a channel (Whitfield, 2006). This capsule synthesis pathway is found in many enteric pathogens, the prototype of which is the *E. coli* serotype K30 capsular polysaccharide (see Table 2 and Table 3) (Willis and Whitfield, 2013b; Schmid, Sieber and Rehm, 2015).

Table 2: Capsule groups in the model organism *E. coli*. K, capsule; O, O-antigen; PST-1, polysaccharide-specific transport protein-1; MPA-1, membrane-periplasmic auxiliary protein-1; MPA-2, membrane-periplasmic auxiliary protein-2, OMA, outer membrane auxiliary protein. Adapted from Whitfield, 2006.

Characteristics	Group			
	1	2	3	4
Thermostability of K antigen	Yes	No	No	Yes
Coexpressed with O serogroups	Limited range (O8, O9, O20, O101)	Many	Many	Often O8, O9 but occasionally none
Genetic locus	<i>cps</i> near <i>his</i>	<i>kps</i> near <i>ser</i>	<i>kps</i> near <i>ser</i>	Near <i>his</i>
Thermoregulated expression	No	Yes	No	No
Terminal lipid moiety	LPS lipid A core in KLPS, unknown for capsular K antigens	α -glycerophosphate	α -glycerophosphate	LPS lipid A core in KLPS, unknown for capsular K antigens
Polymer chain grows at	Reducing terminus	Nonreducing terminus	Nonreducing terminus	Reducing terminus
Polymerization system	Wzy dependent	Processive glycosyltransferase activity	Processive glycosyltransferase activity	Wzy dependent
PST-1 protein	Wzx	None	None	Wzx
ABC transporter	None	KpsMT	KpsMT	None
MPA-1 protein	Wzc	None	None	Wzc
MPA-2 protein	None	KpsE	KpsE?	None
OMA protein	Wza	KpsD	KpsD?	Wza
Model system(s)	Serotype K30	Serotypes K1, K5	Serotypes K10, K54	Serotypes K40, O111
Similar to capsules in	<i>Klebsiella</i> , <i>Erwinia</i>	<i>Neisseria</i> , <i>Haemophilus</i>	<i>Neisseria</i> , <i>Haemophilus</i>	None known

In the **ABC transporter-dependent pathway**, the CPS chains are fully synthesized in the cytoplasm, anchored to the IM by Und-PP and two units of Kdo, and subsequently translocated across the IM and OM by an ABC transporter/pore complex (Figure 11). This transporter consists of two integral membrane proteins (KpsM in *E. coli*; CtrD in *Neisseria*) inserted in the IM and two nucleotide-binding domain (NBD)-containing polypeptides (KpsT; CtrC). CPS transport to the OM, also requires a polysaccharide co-polymerase (KpsE; CtrB) and an OM polysaccharide protein (KpsD; CtrA). Altogether, these proteins form a continuous channel from the cytoplasm to the OM (Willis and Whitfield, 2013b). Although the interactions between the protein complexes are specific, neither the ABC transporter nor the co-polymerase/pore complexes in *E. coli* have specificity for the CPS produced inside the cell (Willis and Whitfield, 2013b). This capsule synthesis pathway is found in many pathogens infecting mucosa, such as the sialic acid and neuraminic acid capsules found in *E. coli* K1 and *N. meningitidis* group B, respectively (Table 3).

In the **synthase-dependent CPS biosynthesis pathway**, an IM-bound synthase (Alg8 in *Pseudomonas aeruginosa*) concomitantly polymerizes and translocates CPS units across the membrane. The IM-bound synthase activity can be regulated by an IM cyclic di-GMP-dependent co-polymerase (Alg44) (Whitney and Howell, 2013) (Figure 11). In the periplasm, the polysaccharide is bound by a tetratricopeptide repeat domain-containing protein (TPR;

AlgK) and exported across the OM through a β -barrel membrane protein (AlgE). Synthase-dependent polysaccharides can be either linked to the OM by a lipid anchor, be loosely attached to the OM, or be completely dissociated and secreted into the surrounding medium. The latter is known as exopolysaccharide (EPS), and it may form a slime layer around the bacteria. Many polymers generated through the synthase-dependent pathway include polysaccharides with potential biotechnological applications, such as alginate from *P. aeruginosa*, cellulose from *Gluconacetobacter xylinus*, or xanthan gum from *Xanthomonas campestris* (Schmid, Sieber and Rehm, 2015) (Table 3). These exopolysaccharides are also very important in biofilm formation (Di Perri and Ferlazzo, 2022; Balducci *et al.*, 2023).

Table 3: Examples of CPS biosynthesis pathways in diderm bacteria. GlcNAc, N-acetyl glucosamine. Based on reviews by Whitney and Howell, 2013; Schmid, Sieber and Rehm, 2015; Wen and Zhang, 2015; Singh, Adams and Brown, 2019.

Wzx/Wzy-dependent	ABC transporter-dependent	Synthase-dependent
<i>E. coli</i> group 1 capsule (K30)	<i>Campylobacter jejuni</i>	<i>P. aeruginosa</i> (alginate)
<i>E. coli</i> group 4 capsule (O111)	<i>E. coli</i> group 2 capsule (K1)	<i>G. xylinus</i> (cellulose)
<i>S. sonnei</i> O-antigen capsule	<i>E. coli</i> group 3 capsule (K5)	<i>X. campestris</i> (xanthan)
<i>A. baumannii</i>	<i>N. meningitidis</i> group B	<i>Y. pestis</i> (poly-GlcNAc)

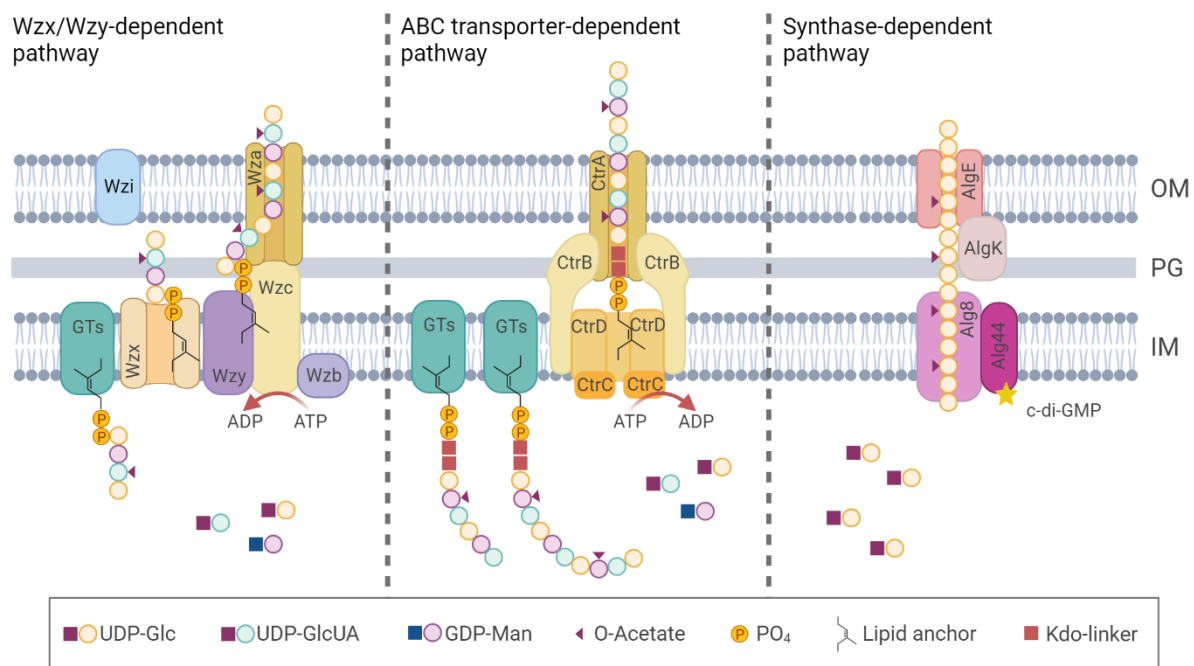


Figure 11: Capsule biosynthesis pathways in diderm bacteria. Three main pathways for capsule biosynthesis have been described for diderm bacteria: Wzx/Wzy-dependent, ABC transporter-dependent, and synthase-dependent. In the first pathway, CPS repeat units are translocated from the inner membrane (IM) to the periplasmic space by Wzx and merged by Wzy and Wzc in the periplasm to the full-length CPS. Wza forms the pore through which the CPS is translocated to the outer membrane (OM). In the second pathway, the full CPS is generated in the cytoplasm and translocated through an ABC transporter/pore complex to the OM. The synthase-dependent CPS is generated and translocated across the IM by the synthase Alg8. The CPS is then translocated across the OM by a β -barrel protein, AlgE. For visualization purposes, LPS and outer membrane proteins were omitted. Nomenclature based on *E. coli*, *N. meningitidis*, and *P. aeruginosa* biosynthesis pathways (left to right). Sugars shown are for visualization only and do not reflect actual compositions of purified capsules from these bacteria. GTs, glycosyltransferases; Glc, glucose; GlcUA, glucuronic acid; Man, mannose; PO₄, phosphate; Kdo, 3-deoxy-d-manno-oct-2-ulosonic acid; IM, inner membrane; PP, periplasm; OM, outer membrane. Adapted from Schmid, Sieber and Rehm, 2015; Willis and Whitfield, 2013b. Created with BioRender.com.

2.8 Regulation of bacterial capsule biosynthesis

Capsule biosynthesis can be regulated at many levels in the cell as well as in response to specific environmental conditions, and several common regulatory mechanisms have been identified in pathogenic bacteria.

At the genomic level, mobilizable insertion sequences in the capsule locus can disrupt capsule production or lead to gene amplification and increased CPS production, as observed in *N. meningitidis* group B and *H. influenzae* type b, or *Acinetobacter baumannii*, respectively (Wen and Zhang, 2015; Whiteway *et al.*, 2022).

At the transcriptional level, one of the best characterized regulatory systems was described for *E. coli* group 1 CPS, which is involved in the temperature-dependent production of colanic acid

in *E. coli* K-12. In this system, RcsF acts as a sensor at the cell surface and relays environmental signals to the two-component system RcsC/RcsB. Upon activation, RcsC in the IM autophosphorylates and phosphorylates RcsD, which in turn phosphorylates and activates RcsB. Phosphorylated RcsB binds to RcsA (a cytoplasmic transcription factor), forming a complex that binds to the promoter upstream of the capsule biosynthesis locus, leading to gene expression (Keenleyside *et al.*, 1992; Jayaratne *et al.*, 1993; Wen and Zhang, 2015).

For *E. coli* K1 and K5 capsules, it was demonstrated that a 39-bp sequence upstream of the CPS biosynthesis genes – the so-called JUMPstart sequence– harbors a specific sequence that can be recognized by RfaH, originally described as LPS anti-terminator. The DNA-RfaH interaction at promoter regions of target genes leads to activation of transcription of capsule biosynthesis genes, together with genes involved in bacterial virulence (Stevens *et al.*, 1994; Stevens, Clarke and Roberts, 1997; Wen and Zhang, 2015). The expression of group 2 capsule genes in *E. coli* is temperature-regulated by BipA and H-NS, predominantly at the level of transcription. BipA (member of the ribosome-binding GTPase superfamily) and H-NS (global transcriptional regulator) activate gene expression at specific CPS promoter regions at 37°C, but act as repressors at 20°C (Rowe *et al.*, 2000; Aldawood and Roberts, 2022). Moreover, group 2 CPS expression in *E. coli* is also growth phase-dependent, modulated by the interplay of three transcriptional regulators: H-NS, SlyA and IHF (Aldawood and Roberts, 2022).

At the translational level, a novel regulatory mechanism was identified in *N. meningitidis* involving an RNA thermosensor. In these structures, the transcript forms a hairpin in the 5' untranslated region (UTR) at lower temperatures, occluding the ribosome-binding site (RBS) and stalling translation. At higher temperatures, the RNA thermosensor destabilizes, revealing the RBS and allowing translation of capsule biosynthesis genes (Loh *et al.*, 2013). In addition, *N. meningitidis* was shown to modulate capsule expression depending on whether they are carrier (non-encapsulated) or invasive (encapsulated) clinical isolates (Merino and Tomás, 2015). Here, capsule phase-variation occurs by a reversible insertion/deletion of one cytidine residue in an oligo-dC stretch within the 5'-UTR of the α -2,8-polysialyltransferase, which leads to a frameshift mutation and expression of a truncated, inactive form of the protein. This modification, which leads to the loss of capsule formation, is present in all unencapsulated *N. meningitidis* strains, indicating a correlation between capsule phase variation and bacterial invasion (Hammerschmidt *et al.*, 1996).

2.9 Roles of capsules in bacterial survival and infection

Bacterial capsules can be expressed constitutively or in response to environmental cues, to facilitate bacterial colonization and persistence. They protect bacteria from phagocytosis, external aggressions, such as desiccation or antibiotics, and play an essential role during infection. Thus, capsules provide an important mechanism of adaptation to different ecological niches (Rendueles *et al.*, 2017).

2.9.1 Capsules as barriers against harsh environments

The capsules of *K. pneumoniae* and *P. aeruginosa* were shown to sequester antimicrobial peptides such as polymyxin B and HNP-1, binding them at a distance from the cell membrane and ensuring bacterial survival (Campos *et al.*, 2004; Llobet, Tomás and Bengoechea, 2008). Similarly, it was shown that the capsule of *N. meningitidis* protects the bacterium from the human cathelicidin antimicrobial peptide LL-37 (Jones *et al.*, 2009). Exposure of *A. baumannii* to sub-minimum inhibitory concentrations of antibiotics, such as erythromycin and colistin, leads to overproduction of the capsule (Geisinger and Isberg, 2015). Likewise, the capsules of *A. baumannii* and *K. pneumoniae* were shown to mediate resistance to desiccation and to provide a fitness advantage in nutrient-poor environments, respectively (Tipton *et al.*, 2018; Buffet, Rocha and Rendueles, 2021).

Capsules are also known to protect bacteria from phage infection, such as the *E. coli* K1 capsule and T7 phage infection (Scholl, Adhya and Merrill, 2005). However, phages have developed mechanisms to overcome this bacterial defense. An example of such interactions is given by *K. pneumoniae* and its infecting phages, which use the capsule for initial adherence but also express serotype-specific capsule depolymerases in their tail proteins to degrade the capsule and allow phage attachment to cell receptors underneath (Dunstan *et al.*, 2021). Hence, instead of being hindered by the capsule, *K. pneumoniae* phages have become dependent on it (Haudiquet *et al.*, 2021). This means that changes in the cell envelope can modulate the interaction between bacteria and phages, affecting the rates of DNA transfer and the bacterial acquisition of virulence factors and antibiotic resistance genes (Rendueles *et al.*, 2018). Indeed, *K. pneumoniae* capsule swap can occur in response to serotype-specific phage predation, leading to inactivation of capsular genes and capsule loss. Non-capsulated strains are more susceptible to acquire genes by conjugation, increasing the likelihood of capsule reacquisition, leading to a new capsule serotype (Haudiquet *et al.*, 2021). This phenomenon does not seem to be limited to *Klebsiella*, as it was shown that bacteria with capsules are more genetically diverse

with fast-evolving gene repertoires, suggesting a positive association between the presence of capsules and the rate of genetic exchanges (Rendueles *et al.*, 2018).

2.9.2 Capsules as immune evasion factors

Capsules protect bacteria from immune recognition and phagocytosis by masking their LPS and/or OM proteins. In particular, they are important for bacterial evasion of complement-mediated opsonophagocytosis and they have been shown to downregulate the expression of pro-inflammatory cytokines (Yoshida *et al.*, 2001; Raffatellu *et al.*, 2005; Wilson *et al.*, 2007; Merino and Tomás, 2015; Wen and Zhang, 2015). An example of this is the Vi capsule of *Salmonella enterica* serotype Typhi, which shields the underlying LPS from TLR4 recognition, consequently leading to lower levels of IL-6 and TNF α release during infection (Wilson *et al.*, 2007). Moreover, some bacteria have evolved capsules that mimic cell surface molecules found in the human body, hence avoiding immune recognition and contributing to infection (Cress *et al.*, 2014). For example, *E. coli* K1 and *N. meningitidis* type B CPS are structurally similar to mammalian polysialic acid, which contributes to the neuroinvasiveness of these pathogens (Kaper, Nataro and Mobley, 2004; Steenbergen and Vimr, 2008; Cress *et al.*, 2014). Similarly, mucosal pathogens often express negatively charged capsules, which simulate the charge of sialic acid residues in the human mucus layer. Consequently, bacteria can escape from entrapment in luminal mucus and mucosal clearance by electrostatic repulsion (Nelson *et al.*, 2007).

The complement-mediated bacterial killing by the host can be blocked at numerous sites by bacterial CPSs, and some capsules protect the bacteria from being attacked by steric mechanisms (Cress *et al.*, 2014). For example, encapsulated bacteria can bind C3b on the bacterial cell surface underneath the capsule, shielding it from recognition by phagocytic cells (Cress *et al.*, 2014). Others can interrupt the binding of C3b to the bacterial surface and consequently disrupt the activation of the complement cascade by affecting regulatory proteins, such as binding of factor H by *E. coli* K1 and *N. meningitidis* group B capsules (Jarva *et al.*, 2005; Merino and Tomás, 2015).

With regards to adaptive immunity, CPSs are considered T-cell independent antigens, as they do not activate T helper cells. Instead, they induce IgM antibodies without Ig-switching to IgG for the generation of immunological memory due to the lack of T helper cell activation (Cress *et al.*, 2014). This results in many encapsulated bacteria being especially dangerous for small children, as their immune system is not yet fully developed. The development of combination

vaccines was a game changer in the fight against the most severe pathogens in children: *Neisseria meningitidis*, *Haemophilus influenzae*, and *Streptococcus pneumoniae*. These vaccines use purified CPS, which has poor T-cell recognition, coupled to a carrier toxin recognized by T-cells (such as diphtheria toxin) to provide long lasting protection against bacterial infection. However, recent studies on the protective mechanism of glycoconjugate vaccines revealed that a subset of carbohydrate-specific T cells may be able to recognize *Streptococcus pneumoniae* CPS, providing new insights into the efficacy of conjugate vaccines against encapsulated bacteria (Sun *et al.*, 2019).

3. Aims of the doctoral thesis

Legionella longbeachae is a human pathogen that can cause Legionnaires' disease, a severe form of pneumonia that can be fatal if left untreated. *In vivo* in the mouse model of infection, *L. pneumophila* is not able to replicate due to the recognition of its flagellin, but *L. longbeachae* is highly virulent, leading to low cytokine induction and mice succumb to the infection. These differences cannot be attributed solely to the lack of flagella in *L. longbeachae* (Massis *et al.*, 2016).

Our group has identified a capsule cluster encoded in the *L. longbeachae* genome, suggesting that the bacteria express a capsule (Cazalet *et al.*, 2010). These findings, together with the observed phenotypes in the mouse model of infection, led to the central hypothesis of this thesis: The *L. longbeachae* capsule favors virulence and infection, and it may help in environmental persistence and host immune evasion. To test this hypothesis, I pursued three main objectives during my PhD work:

- 1- Study the expression and regulation of the capsule in *L. longbeachae*.
- 2- Decipher the role of the capsule in virulence and environmental persistence.
- 3- Identify the capsule composition and purify the capsular polysaccharide.

Moreover, during my PhD, I was involved in the study of the role of a *L. longbeachae* small Rab-like GTPase, and *L. pneumophila* modulation of the reverse mode of action of the F₀F₁ mitochondrial ATPase during infection (presented in **Annex B** and **Annex C**, respectively). Moreover, I co-authored two reviews presented in **section 1.6** of this introduction and in **Annex A**, respectively.

RESULTS

4. Results summary

We first studied the presence of the capsule cluster among different *L. longbeachae* strains, revealing that the locus is highly conserved in this species. Further, we could show that the capsule cluster of *L. longbeachae* is unique in the genus *Legionella*. Next, we aimed at addressing the three main objectives of this thesis:

1- Study the expression and regulation of the capsule in *L. longbeachae*.

To address this objective, we generated a mutant in the capsule transporter and studied the expression of the capsule by transmission electron microscopy (TEM). This revealed that the wild type expresses a capsule in post-exponential growth phase, and we show that the mutant is devoid of the capsule. We complemented the mutant with a plasmid and could show by TEM that capsule expression can be restored. Next, we performed RNAseq analysis to determine the transcriptional profile of the capsule expression in wild type *L. longbeachae* as compared to the capsule mutant. The capsule genes are highly transcribed in exponential phase, and we did not detect significant differences between the wild type and the capsule mutant in their transcriptional profiles. We conclude that the capsule is expressed in a growth phase-dependent manner in the wild type. Further, we generated a dual reporter to follow capsule expression in live infected cells, revealing that the capsule is expressed upon infection of cells.

2- Decipher the role of the capsule in virulence and environmental persistence.

To gain insights into the biological role of the capsule, we infected mice with wild type *L. longbeachae* and the capsule mutant. It has been shown that *L. longbeachae* is highly virulent in mice and the animals succumb to infection within six days (Massis *et al.*, 2016). Surprisingly, the capsule mutant is completely avirulent in mice, and virulence can be partially restored upon complementation of the mutant. We further tested the role of the capsule in the environmental host *Acanthamoeba castellanii*. Our results show that the capsule mutant has a significant growth defect as compared to the wild type. Again, complementation can revert this growth defect. We showed that these phenotypes are not due to a disturbance of the T4SS in the capsule mutant, as the capsule mutant can translocate T4SS effectors at a similar level as the wild type. To test the role of the capsule on cytokine secretion, we infected both human and murine

primary macrophages, as well as murine DCs, and measured the secretion of the known pro-inflammatory cytokines IL-1 β , TNF α , and IL-6. We show that the capsule indeed dampens the secretion of IL-6 in human primary monocyte-derived macrophages, and that in murine cells the capsule mutant also induces higher levels of IL-1 β and IL-6 as compared to the wild type.

Capsules are known to shield bacteria from phagocytosis, and thus we tested the effects of the capsule on phagocytosis and attachment to human monocytes. This revealed that the capsule delays phagocytosis into THP-1 cells, in contrast to the capsule mutant, which is phagocytosed more rapidly. However, attachment to cells seems not be affected by the presence or absence of the capsule. To further test the shielding capacity of the capsule, we used yeast mannan and tested agglutination of the wild type and capsule mutant. This revealed that only the capsule mutant is agglutinated by yeast mannan, and this agglutination is lost in the complemented mutant. To test possible environmental stresses, we exposed the wild type and capsule mutant to detergent and hydrogen peroxide. We did not observe any differences between the two *L. longbeachae* strains, however, *L. longbeachae* seems to be inherently more resistant to such stresses as compared to *L. pneumophila*. In contrast, when exposed to high salt concentrations, the wild type shows a two-log fold growth defect as compared to the capsule mutant.

3- Identify the capsule composition and purify the capsular polysaccharide.

To date, nothing is known about the composition of the capsule of *L. longbeachae* and no capsule-specific antibody is available. To study the chemical composition of the capsule, we investigated different purification methods and analyzed the sugar composition by HPLC. This revealed that both wild type and capsule mutant extracts contained similar sugars. Therefore, we tried to visualize possible structural differences by gel electrophoresis and silver staining, which may allow us to determine the molecular weight of the capsule. Despite testing many different isolation methods, we did not observe a capsular band by gel electrophoresis and silver staining. Finally, we detected a capsular band by staining with Stains-all dye, a dye that can differentially stain highly anionic polysaccharides. This band is absent in extracts from the capsule mutant, and it is present again in the complemented mutant. Thus, we conclude that *L. longbeachae* expresses a highly anionic polysaccharide that cannot be stained by conventional silver staining.

The results of this work are summarized in my main publication below (in submission).

5. Publication – The unique *L. longbeachae* capsule favors intracellular replication and immune evasion

Research article

In submission

Silke SCHMIDT^{1,2}, Sonia MONDINO^{1,&}, Laura GOMEZ-VALERO¹, Pedro ESCOLL¹, Danielle P. A. MASCARENHAS³, Augusto GONÇALVES³, Christophe RUSNIOK¹, Martin SACHSE⁴, Maryse MOYA-NILGES⁴, Thierry FONTAINE⁵, Dario S. ZAMBONI³, Carmen BUCHRIESER^{1,§}

¹Institut Pasteur, Université Paris Cité, Biologie des Bactéries Intracellulaires, CNRS UMR 6047, Paris, France

²Sorbonne Université, Collège Doctoral, Paris, France, ³Department of Cell Biology, Medical School of Ribeirão Preto, FMRP/USP, Ribeirão Preto, Brazil, ⁴UTechS UBI, Centre de Ressources et Recherches Technologiques, Institut Pasteur, Paris, France, ⁵ Biologie et Pathogénicité fongiques, Institut Pasteur, Paris, France

[&] Current address: Laboratory of Molecular and Structural Microbiology, Institut Pasteur de Montevideo, Montevideo, Uruguay.

Contributions:

For my main author research paper, I performed the following experiments: growth and manipulation of *L. longbeachae* bacteria, cloning of complementation and dual reporter plasmids, preparation and staining of bacteria for transmission electron microscopy, capsular polysaccharide extraction, gel electrophoresis and staining, HPLC analysis of monosaccharides, RNA extraction and library preparation for RNA sequencing, live confocal microscopy, imaging of dual reporter and replication assay in *Acanthamoeba castellanii*, beta-lactamase secretion assay for T4SS effectors, phagocytosis and attachment assays in THP-1 cells, isolation of human monocyte-derived macrophages, ELISA measurements of human pro-inflammatory cytokines with SP-X array, bacterial stress assays and agglutination. Finally, I wrote the original draft and performed data analyses as well as revisions of the manuscript.

1 **The unique *Legionella longbeachae* capsule favors intracellular**
2 **replication and immune evasion**

3
4 Silke SCHMIDT^{1,2}, Sonia MONDINO^{1.&}, Laura GOMEZ-VALERO¹, Pedro ESCOLL¹,
5 Danielle P. A. MASCARENHAS³, Augusto GONÇALVES³, Christophe RUSNIOK¹, Martin
6 SACHSE⁴, Maryse MOYA-NILGES⁴, Thierry FONTAINE⁵, Dario S. ZAMBONI³, Carmen
7 BUCHRIESER^{1,§}

8
9 ¹Institut Pasteur, Université Paris Cité, Biologie des Bactéries Intracellulaires, CNRS UMR 6047, Paris, France
10 ²Sorbonne Université, Collège Doctoral, Paris, France, ³Department of Cell Biology, Medical School of Ribeirão
11 Preto, FMRP/USP, Ribeirão Preto, Brazil, ⁴UTechS UBI, Centre de Ressources et Recherches Technologiques,
12 Institut Pasteur, Paris, France, ⁵ Biologie et Pathogénicité fongiques, Institut Pasteur, Paris, France

13
14 & Current address: Laboratory of Molecular and Structural Microbiology, Institut Pasteur de Montevideo,
15 Montevideo, Uruguay.

16
17
18
19
20
21
22 [§] For correspondence:

23 Carmen Buchrieser
24 Institut Pasteur, Biologie des Bactéries Intracellulaires
25 28, rue du Dr. Roux, 75724 Paris Cedex 15, France
26 Tel: (33-1)-44-38-95-40
27 Fax: (33-1)-45-68-87-86
28 E-mail: *cbuch@pasteur.fr*

30 **ABSTRACT**

31 *Legionella longbeachae* and *Legionella pneumophila* are the most common causative agents of
32 Legionnaires' disease. While the clinical manifestations caused by both species are similar,
33 species-specific differences exist in environmental niches, disease epidemiology, and genomic
34 content. One such difference is the presence of a genomic locus predicted to encode a capsule.
35 Here, we show that *L. longbeachae* indeed expresses a capsule in post-exponential growth
36 phase as evidenced by electron microscopy analyses, and that capsule expression is abrogated
37 when deleting a capsule transporter gene. Capsule purification and its analysis *via* HLPC
38 revealed the presence of a highly anionic polysaccharide that is absent in the capsule mutant.
39 The capsule is crucial for replication and virulence *in vivo* in a mouse model of infection and
40 in the natural host *Acanthamoeba castellanii*. It has anti-phagocytic function when
41 encountering innate immune cells such as human macrophages and it is involved in the low
42 cytokine responses in mice and in human monocyte derived macrophages, thus dampening the
43 innate immune response. Thus, the here characterized *L. longbeachae* capsule is a novel
44 virulence factor, unique among the known *Legionella* species, which may aid *L. longbeachae*
45 to survive in its specific niches and which partly confers *L. longbeachae* its unique infection
46 characteristics.

47 INTRODUCTION

48 *Legionella longbeachae* is a rod-shaped Gram-negative bacterium that can cause Legionnaires’
49 disease, a severe form of pneumonia. Like other *Legionella* species, *L. longbeachae* is a
50 facultative intracellular bacterium that causes the disease by inhalation of contaminated
51 aerosols (Mondino *et al.*, 2020). *Legionella* spp. are typically found in aquatic environments,
52 either as free-living bacteria or in biofilm communities (Taylor, Ross and Bentham, 2009;
53 Newton *et al.*, 2010). *Legionella longbeachae*, however, is predominantly isolated from potting
54 soils and infections have been associated with gardening activities (Steele, Lanser and Sangster,
55 1990; Whiley and Bentham, 2011). The clinical symptoms of Legionnaires’ disease caused by
56 *L. longbeachae* are similar to those caused by *L. pneumophila*, the most common causative
57 agent of Legionnaires’ disease (Amodeo, Murdoch and Pithie, 2010). Like *L. pneumophila*,
58 *L. longbeachae* critically depends on a highly conserved type IVB Dot/Icm secretion system
59 (T4SS) to establish an intracellular infection and to build a replication niche, the so-called
60 *Legionella*-containing vacuole (LCV) (Berger and Isberg, 1993; Roy, Berger and Isberg, 1998;
61 Segal, Purcell and Shuman, 1998; Lockwood *et al.*, 2022). Initially it was reported that, in
62 contrast to *L. pneumophila* that recruits ER-vesicles to the LCV upon infection, *L. longbeachae*
63 recruits early and late endosomal vesicles (Asare and Abu Kwaik, 2007). Yet, further studies
64 showed that the *L. longbeachae* LCV is decorated with ER markers such as Rab1 and Sec22b,
65 similar to *L. pneumophila*, and that *L. longbeachae* delays the association of the late endosomal
66 marker LAMP-1 with the LCV (Dolinsky *et al.*, 2014; Wood *et al.*, 2015). Analyses of the
67 genomic content of the *Legionella* genus genome showed that it is highly diverse with an
68 astounding 18,000 predicted T4SS effector proteins (Gomez-Valero *et al.*, 2019). For
69 *L. longbeachae*, about 220 effectors were predicted, but only about 34% are shared with the
70 *L. pneumophila* effector repertoire (Cazalet *et al.*, 2010; Burstein *et al.*, 2016). Furthermore, in-
71 depth analyses of the *L. longbeachae* genome revealed unique sets of genes and extensive
72 genomic recombination events that reflect both an adaptation to its soil environment as well as
73 dynamic genetic exchange with other microorganisms (Cazalet *et al.*, 2010; Bacigalupe *et al.*,
74 2017; Slow *et al.*, 2022).

75 Interestingly, common laboratory mouse strains are resistant to *L. pneumophila*
76 replication, except A/J mice which allow replication of *L. pneumophila* due to Naip5 mutations.
77 In contrast, *L. longbeachae* effectively replicates in the lungs, disseminates, and induces death
78 in mouse strains such as A/J, BALBc, and C57BL/6 mice (Asare *et al.*, 2007; Gobin *et al.*,
79 2009). It was hypothesized that this is due to the lack of flagella in *L. longbeachae*, as the
80 detection of flagella expressed by *L. pneumophila* leads to a rapid activation of the NLRC4

81 inflammasome and clearing of the infection in BALBc or C57BL/6 mice (Molofsky *et al.*, 2006;
82 Ren *et al.*, 2006; Pereira, Marques, *et al.*, 2011). However, a flagellum-deficient
83 *L. pneumophila* strain Paris is not lethal for C57BL/6 mice and it induces a robust pro-
84 inflammatory cytokine response *in vitro* (Pereira, Marques, *et al.*, 2011; Massis *et al.*, 2016).
85 In contrast, mice infected with wild type *L. longbeachae* die within 6 days after infection.
86 *L. longbeachae* spreads from the primary site of infection (the lungs) to the blood and spleens
87 of the animals. In contrast to *L. pneumophila*, *L. longbeachae* only induces a low pro-
88 inflammatory cytokine response *in vitro* (Massis *et al.*, 2016). A unique feature identified in the
89 *L. longbeachae* genome is the presence of a gene cluster of 48 kb predicted to code for a capsule
90 (Cazalet *et al.*, 2010). It comprises 33 genes that are annotated as glycosyltransferases, enzymes
91 for the synthesis of nucleotide sugar precursors, and an ABC transporter, likely for the export
92 of the capsule. The transporter was found to be homologous to the capsule transporter of
93 *Neisseria meningitidis* (Cazalet *et al.*, 2010). We thus hypothesized that the capsule encoded in
94 the *L. longbeachae* genome may be responsible for the enhanced virulence of *L. longbeachae*
95 in mice as compared to *L. pneumophila* (Massis *et al.*, 2016).

96 Many bacterial pathogens such as *Klebsiella pneumoniae* (Opoku-Temeng, Kobayashi
97 and DeLeo, 2019; Patro and Rathinavelan, 2019), *Streptococcus pneumoniae* (Hyams *et al.*,
98 2010; Paton and Trappetti, 2019), *N. meningitidis* (Tzeng *et al.*, 2005; Spinoso *et al.*, 2007;
99 Virji, 2009), or *Acinetobacter baumannii* (Whiteway *et al.*, 2022; Valcek *et al.*, 2023) encode
100 capsules in their genomes and the roles of these capsules in infection have been studied
101 extensively. In diderm bacteria, capsules represent the outermost layer of the bacterial cell wall,
102 extending beyond the lipopolysaccharide (LPS) and membrane proteins in the outer membrane
103 (Whitfield, Wear and Sande, 2020). Capsules are typically composed of polysaccharides
104 attached to the cell surface in linear or branched form. The structural and chemical compositions
105 of capsular polysaccharide (CPS) can be highly diverse and complex (Wen and Zhang, 2015).
106 Capsules can protect bacteria from adverse environmental conditions, or antimicrobial agents
107 such as antibiotics or antimicrobial peptides (Campos *et al.*, 2004; Jones *et al.*, 2009; Geisinger
108 and Isberg, 2015; Tipton *et al.*, 2018; Buffet, Rocha and Rendueles, 2021). Likewise, in
109 pathogenic bacteria, capsules can mimic surface polysaccharides of mammalian cells, thus
110 avoiding recognition by the host immune system (Wen and Zhang, 2015). For example, the
111 capsule of *E. coli* K1 contains polysialic acids that are anti-phagocytic and protect the bacteria
112 from complement-mediated killing (Kaper, Nataro and Mobley, 2004; Steenbergen and Vimr,
113 2008). Before the development of glycoconjugate vaccines, infections with invasive,
114 encapsulated bacteria such as *S. pneumoniae* or *N. meningitidis* were associated with high

115 mortality especially in children due to the poor immunogenicity of CPS (Luck, Tettelin and
116 Orihuela, 2020).

117 In this study, we visualized and characterized the *L. longbeachae* capsule and analyzed
118 its functional role in infection. Comparing a knockout mutant in the capsule transporter and a
119 wild type (WT) strain, we reveal that the capsule plays a key role during infection in mammalian
120 and protozoan hosts. Furthermore, we provide evidence that the capsule is responsible for the
121 low cytokine response in infected macrophages and mice. Thus, we demonstrate that the
122 capsule is a novel virulence feature of *L. longbeachae*, which is unique among the known
123 *Legionella* species.

124

125 RESULTS

126 ***The L. longbeachae capsule cluster is unique among Legionella species.*** We first analyzed
127 the presence of the putative capsule cluster and orthologous genes among 58 different
128 *Legionella* species (Figure 1). This analysis shows that *L. longbeachae* is the only *Legionella*
129 species to encode the entire 48 kb capsule cluster. Two other species, *L. massiliensis* and
130 *L. gormanii*, carry genes similar to the ABC-type transporter genes *ctrBCD* and *bexD*.
131 However, these two species lack most of the glycosyltransferases encoded by *L. longbeachae*.
132 Only *L. massiliensis* encodes an orthologous gene of *llo3174*, a glycosyltransferase of family 2
133 involved in transfer of nucleotide diphospho-sugars to a range of substrates such as dolichol
134 phosphate or teichoic acid. We did not find similar genes in the genomes of *L. pneumophila*,
135 except for an orthologous gene of *llo3163*, a hydroxyacid dehydrogenase similar to *serA*,
136 indicating that the capsule cluster is specific for *L. longbeachae* (see Supplementary Table 1).

137 To deepen these analyses, we selected twelve publicly available *L. longbeachae* strains,
138 comprising nine strains from serogroups 1 (sg1) and three strains from 2 (sg2). All of them
139 contain a similar capsule cluster whose genomic organization and genomic location are
140 conserved (Figure S1). Only a small region in the central part of the capsule cluster shows few
141 differences among the glycosyltransferases and a duplication of *galE* in the NSW150 and
142 B41211CHC genomes (Figure 1 and Figure S1). All twelve strains encode genes for the
143 predicted ABC type transporter *ctrBCD* and *bexD* (*ctrA*-like). Furthermore, they all encode
144 glycosyltransferases and nucleotide sugar precursor genes belonging to the same groups of
145 enzymes (Supplementary Table 2). This extremely high conservation in gene content, sequence
146 similarity, and in the genomic location indicate that the acquisition of the capsule cluster dated
147 back to a common ancestor of *L. longbeachae*.

148

149 ***The L. longbeachae capsule cluster genes share homology to soil-dwelling bacteria.*** The
150 evolutionary history of the capsule cluster in *L. longbeachae* is not known. Thus, we performed
151 BLAST analysis on all its genes using *L. longbeachae* strain NSW150 (sg1) as the reference.
152 Supplementary Table 1 lists the best hits obtained by BLAST search. Across the cluster, we
153 find homologous genes from β -proteobacteria often found in soils, and of γ - and δ -
154 proteobacteria such as the soil-dwelling *Burkholderia* spp., *Geobacter* spp., or *Pseudomonas*
155 spp., but also from *Nitrococcus mobilis* or *Alteromonas* spp., which are present in marine
156 environments. These similarities suggest that the capsule cluster was acquired from soil-
157 dwelling bacteria.

158

159 ***L. longbeachae encodes a specific transporter for O-antigen export.*** To determine if there are
160 distinctive features of the LPS and the capsule biosynthesis pathways in *L. longbeachae*, we
161 also analyzed the *L. longbeachae* LPS cluster genes. The search for orthologous genes of the
162 *L. longbeachae* NSW150 LPS cluster among 58 *Legionella* spp. revealed that, as previously
163 reported by our group, *L. longbeachae* encodes a WzxE like O-antigen flippase and four
164 different glycosyltransferases (Figure S2) (Cazalet *et al.*, 2010). Orthologous genes coding for
165 the WzxE flippase and several glycosyltransferases are present among many *Legionella* spp.,
166 including *L. massiliensis*. However, none of the *L. longbeachae* LPS cluster genes are encoded
167 in *L. pneumophila* (Cazalet *et al.*, 2008), and as shown previously, the Wzm/Wzt ABC
168 transporter is a distinctive marker for *L. pneumophila* sg1 strains (Mérault *et al.*, 2011). LPS
169 biosynthesis involves the ATPase MsbA, a flippase that mediates the translocation of the LPS
170 core across the inner membrane. In the periplasm, the O-antigen is appended to the LPS core
171 to form the mature LPS. To better understand this pathway in *Legionella*, we analyzed the
172 presence of orthologous genes of the LPS core flippase MsbA and the O-antigen exporters
173 Wzm/Wzt (ABC transporter) or Wzx (flippase) among 58 *Legionella* species (Figure S3). This
174 revealed that only *L. pneumophila*, *L. worsleiensis*, *L. likebrunensis*, and *L. quateirensis* encode
175 the Wzm/Wzt type, whereas all other *Legionella* species, including *L. longbeachae*,
176 predominantly encode the Wzx flippase (Figure S3). Thus, our comparative genomics analyses
177 showed that two mechanisms of O-antigen export exist in the genus *Legionella*, with Wzx being
178 the predominant type shared among a large number of species, and that the capsule is exported
179 in a different way *via* an ABC transporter.

180

181 ***Electron microscopy analyses confirms that L. longbeachae expresses a capsule that is absent***
182 ***from L. pneumophila.*** To further analyze the *L. longbeachae* capsule and to study its

183 functional role, we constructed a mutant in the capsule transporter gene *ctrC* (*llo3151*) by
184 replacing it with an apramycin cassette. We chose *ctrC* as a target, since a knockout mutant of
185 a homologous gene in *Campylobacter jejuni* abrogated capsule expression (Bacon *et al.*, 2001).
186 When grown in ACES-buffered yeast extract broth (BYE) medium with or without apramycin,
187 the $\Delta ctrC$ mutant did not display any significant growth differences as compared to the
188 *L. longbeachae* WT (Figure S4). To confirm that *L. longbeachae* indeed expresses a capsule
189 and that the identified gene cluster is responsible for its expression, we used transmission
190 electron microscopy (TEM). The *L. longbeachae* WT and the $\Delta ctrC$ mutant as well as
191 *L. pneumophila* WT (negative control) were grown in BYE until the optical density OD₆₀₀
192 reached mid-log phase and late-log phase, referred to as exponential (E) phase and post-
193 exponential (PE) phase, respectively. Cells were fixed and stained with cationized ferritin. TEM
194 revealed a capsular layer surrounding the *L. longbeachae* WT (Figure 2A). The capsule was
195 observed only in PE phase, indicating a growth phase dependent expression (Figure S5A). Its
196 thickness was estimated to be between 50-100 nm, which is similar to ferritin-stained capsules
197 observed in *E. coli* K30 (Reid and Whitfield, 2005). In contrast, the $\Delta ctrC$ mutant strain was
198 devoid of such a layer (Figure 2A) and *L. pneumophila* WT cells were not stained by the ferritin
199 dye (Figure 2A). Complementation of the $\Delta ctrC$ mutant strain with a plasmid containing *ctrC*
200 as well as the downstream genes *ctrD* and *bexD* under the control of their native promoter
201 restored capsule expression (Figure 2B). We included the downstream genes as macrocolonies
202 of a $\Delta ctrC$ mutant strain complemented with *ctrC* and *ctrD* only barely restored the WT
203 phenotype compared to those complemented with the longer construct (Figure S5B). However,
204 not 100% of the imaged cells expressed a capsular structure indicating that regulation of capsule
205 expression may be more complex (Figure S5C). Taken together, our results confirm that, in
206 contrast to *L. pneumophila*, *L. longbeachae* expresses a capsule on its surface and that *ctrC* is
207 mainly responsible for its expression on the cell surface.

208

209 ***The highly anionic L. longbeachae capsule is resistant to silver staining.*** To isolate the
210 *L. longbeachae* capsule and to characterize its composition, we first used phenol-extraction for
211 polysaccharide (PS) isolation followed by HPLC analyses. This approach allowed the
212 identification of galactosamine, glucosamine, mannose and possibly quinovosamine in both the
213 WT and the capsule mutant extracts (Figure S6A). After elution of the column, we detected
214 high peaks in the WT sample that might correspond to phosphosugars. However, when
215 visualizing these samples by silver or Alcian blue staining, we observed that phenol extraction
216 seems to collapse the LPS structure, similarly to what has been seen for *L. pneumophila* (Lück

217 and Helbig, 2013). Thus, *L. longbeachae* LPS nor CPS can be extracted by phenol (Figure
218 S6B). Using an enzymatic isolation method (McNally *et al.*, 2005) and silver staining revealed
219 that *L. longbeachae* expresses a long O-antigen chain of different lengths between 30-70 kDa.
220 In contrast, a different pattern was present for *L. pneumophila* with two shorter O-antigen
221 fractions as shown previously, confirming that enzymatic PS isolation preserves the LPS
222 structure in both *Legionella* species (Figure 2C) (Lüneberg *et al.*, 1998). However, no
223 differences between the WT and capsule mutant were observed. Therefore, we tested other dyes
224 to visualize CPS. When using Stains-all dye, a carbocyanine dye that stains highly anionic
225 compounds such as glucosaminoglycans (Souza Andrade *et al.*, 2018), the enzymatically
226 prepared *L. longbeachae* PS extracts showed a strong signal in the WT and the complemented
227 strain, but not the capsule mutant or *L. pneumophila* (Figure 2C). When we complemented the
228 capsule mutant, Stains-all reveals that the band observed in WT extracts is restored in the
229 complemented mutant as well (Figure 2D). Again, silver staining did not detect any CPS in the
230 complemented strain (Figure 2D). The presence of a highly anionic PS corroborates our
231 findings from staining with cationized ferritin for TEM and may explain our unique peak seen
232 in HPLC. Taken together, the *L. longbeachae* capsule consists of highly anionic PS that cannot
233 be stained by conventional silver staining methods.

234

235 ***The capsule is expressed in vitro and during infection in a growth phase dependent manner.***

236 *Legionella pneumophila* is known to have distinct gene transcription profiles *in vitro* and during
237 infection depending on the growth phase (Brüggemann *et al.*, 2006). Thus, to learn when the
238 genes encoding the capsule of *L. longbeachae* are expressed and if their expression is growth
239 phase dependent, we performed RNAseq analyses. The *L. longbeachae* WT and the $\Delta ctrC$
240 mutant strain were grown in BYE until the OD₆₀₀ reached E or PE phase. Total RNA was
241 isolated from the bacterial cells, depleted for rRNA, and sequenced to follow their
242 transcriptional profile in both growth phases. This showed that almost all genes of the capsule
243 cluster in the *L. longbeachae* WT strain were significantly downregulated in PE as compared
244 to E phase (Figure 3A). This correlates with the visualization of the capsule in the PE phase
245 (Figure S5A). Thus, expression of the capsule on the cell surface is growth phase dependent.
246 Moreover, when comparing *L. longbeachae* WT and the $\Delta ctrC$ mutant strain, apart from the
247 expression of *ctrC* and the downstream genes of the capsule transporter operon, no significant
248 differences in the transcription of the other capsule genes were observed neither in E phase
249 (Figure S7A) nor in PE phase (Figure S7B, Supplementary Table 3). The transcription of the
250 capsule in E phase and its expression in PE phase suggest that *L. longbeachae* synthesizes its

251 capsule later in infection, probably to be prepared for cell attachment and a new infection of
252 host cells, and/or for survival in the environment.

253 To test this hypothesis, we analyzed the capsule expression during infection, using a
254 dual reporter to follow the transcription of the capsule transporter operon *in cellulosa*. This dual
255 reporter contains a constitutively expressed red fluorescent protein (mKate2) and two copies of
256 superfolder GFP (sfGFP) tagged with a degradation tag (sfGFP_{deg}), each under the control of
257 the native promoter of the capsule transporter. As a negative control we used a plasmid
258 containing constitutively expressed mKate2 and two copies of sfGFP_{deg} without the native
259 capsule promoter. These plasmids were transformed into *L. longbeachae* WT and used to infect
260 THP-1 cells or *Acanthamoeba castellanii* (Figure 3B, Figure S8). We followed the expression
261 of sfGFP and mKate2 expression over time by live confocal imaging on an Opera Phenix
262 system. GFP was detected at 14 hours after infection in the promoter containing constructs but
263 not the negative control. Our results show that the capsule is expressed in both eukaryotic hosts.
264 Thus, the capsule is universally transcribed *in vitro* and upon infection.

265

266 ***The capsule is crucial for virulence in vivo in mice and in the environmental host***
267 ***Acanthamoeba castellanii***. To learn if the *L. longbeachae* capsule plays a role in virulence *in*
268 *vivo*, we infected mice with either the *L. longbeachae* WT or the $\Delta ctrC$ mutant and different
269 bacterial loads and followed their survival over 10-15 days. Upon infection with the WT strain,
270 all animals succumb to the infection within 5 to 6 days, similar to what has been reported
271 previously (Massis *et al.*, 2016). However, all mice infected with the $\Delta ctrC$ mutant survived
272 the infection (Figure 4A, Figure S9A). *L. longbeachae* WT replicates to higher numbers in the
273 murine lungs as compared to the capsule mutant, but both seem to reach the blood stream as we
274 measured comparable levels of CFUs in the spleen (Figures S9B, C). To confirm that the
275 observed phenotype is due to the missing capsule, we infected mice with the *L. longbeachae*
276 $\Delta ctrC$ mutant either complemented or harboring an empty plasmid. All mice infected with the
277 mutant strain carrying the empty plasmid survived the infection. In contrast, 40% of mice
278 infected with the complemented strain died, indicating that the capsule partially restored
279 virulence *in vivo* (Figure 4B). In contrast, when we infected human macrophage-like THP-1
280 cells or murine bone marrow-derived macrophages *in vitro*, we observed only a slight
281 replication defect of the capsule mutant as compared to the WT, indicating that successful
282 infection by *L. longbeachae* depends on the interaction of immune cells with the capsule *in vivo*
283 (Figures S10A, B). Taken together, the lack of the capsule renders the bacteria avirulent in
284 mice.

285 We then infected *A. castellanii* at a low MOI of 0.1 and at an environmental temperature
286 of 20°C with *L. longbeachae* WT, the $\Delta ctrC$ or the $\Delta dotB$ mutant strain. The latter is deficient
287 in the T4SS and was used as a negative control. Replication of the bacteria was monitored by
288 plating the bacteria every 24 hours over seven days. We observed a strong replication defect of
289 the capsule mutant as compared to the WT, which becomes apparent at 72 hours post-infection
290 (Figure 4C). As expected, the $\Delta dotB$ mutant failed to replicate in *A. castellanii* but seems to
291 persist over extended periods of time indicated by the stable CFU counts towards the end of the
292 experiment. Like in mouse infections, *A. castellanii* infected with the complemented strain
293 restored replication of the bacteria to WT levels while the capsule mutant harboring the empty
294 plasmid was impaired in replication (Figure 4D). We further tested the competitive fitness of
295 the capsule mutant by performing a competition assay in *A. castellanii* as described previously
296 (Kessler *et al.*, 2013). This showed that the capsule mutant is completely outcompeted by the
297 *L. longbeachae* WT strain within 48 hours of infection, further underlining the importance of
298 the capsule in virulence of *L. longbeachae* also in its environmental host (Figure 4E).

299 An important question that arose from the *in vivo* infections was whether the strong
300 virulence defect of the capsule mutant may be due to impaired effector secretion through the
301 Dot/Icm T4SS in the $\Delta ctrC$ strain. We thus tested effector translocation using the beta-
302 lactamase (BlaM) secretion assay as described previously (Gomez-Valero *et al.*, 2019). We
303 used a BlaM-fusion to the known T4SS effector RomA (Rolando *et al.*, 2013) and measured
304 BlaM secretion in infected THP-1 cells by flow cytometry after 2 hours of infection. We
305 included the *L. longbeachae* $\Delta dotB$ mutant as negative control and *L. pneumophila* strain Paris
306 as positive control. Both, the *L. longbeachae* WT and the $\Delta ctrC$ mutant translocated RomA
307 successfully into the host cells to similar levels, whereas the $\Delta dotB$ mutant failed to translocate
308 the effector (Figure 4F). Thus, the virulence phenotype of the capsule mutant *in vivo* and in
309 *A. castellanii* is not due to an impaired Dot/Icm T4SS, as this strain maintains the ability to
310 secrete effectors upon infection.

311
312 ***Encapsulated L. longbeachae is more sensitive to salt stress.*** The capsule may protect
313 *L. longbeachae* from adverse environmental conditions. Thus, we grew the bacteria in liquid
314 culture to PE phase and treated the cells with 0.05% Tween-20 with or without added NaCl or
315 sucrose, as described previously (Aurass *et al.*, 2023). After treatment with Tween-20, we did
316 not observe a growth defect neither in the WT nor in the capsule mutant. However, in
317 comparison to *L. pneumophila*, *L. longbeachae* seems inherently more resistant to detergent,
318 independent of the capsule (Figure S11A). Similarly, both the *L. longbeachae* WT and the

319 capsule mutant grew at similar rates after treatment with 2 mM or 10 mM H₂O₂. In comparison
320 to *L. pneumophila*, the two *L. longbeachae* strains were more tolerant to high H₂O₂ present in
321 the medium (Figure S11B). Thus, we conclude that *L. longbeachae* is inherently more resistant
322 to detergent and oxidative stress than *L. pneumophila*.

323 It has been shown that salt stress in *L. pneumophila* is linked to virulence (Hales and
324 Shuman, 1999). Indeed, a *L. pneumophila* mutant in the response regulator LqsR was shown to
325 be less virulent but more resistant to salt stress than WT bacteria (Hales and Shuman, 1999;
326 Tiaden *et al.*, 2007). To test the role of the capsule under salt stress, we grew the *L. longbeachae*
327 WT and capsule mutant as well as *L. pneumophila* WT to PE phase in liquid culture and plated
328 the bacteria on BCYE in the presence or absence of 50 mM or 100 mM NaCl, respectively
329 (Figure S12). At high salt concentrations, both the capsule mutant and *L. pneumophila* exhibit
330 a 3-log-fold growth difference. Surprisingly, however, there is also a 2-log-fold growth
331 difference between the *L. longbeachae* WT, and the capsule mutant grown in the presence of
332 100 mM NaCl. Hence, similar to *L. pneumophila*, the analysis reveals that the less virulent
333 *L. longbeachae* capsule mutant is more resistant to salt stress (Figure S12). This growth
334 difference was not detectable at a lower concentration of 50 mM NaCl, indicating that salt
335 concentration is an important factor for optimal growth of both *Legionella* species.

336
337 ***The L. longbeachae capsule delays phagocytosis in human cells.*** Based on data published for
338 other bacteria, we hypothesized that the capsule of *L. longbeachae* could be implicated in
339 modulating phagocytosis or attachment to eukaryotic cells. To quantify phagocytosis, we
340 incubated the bacteria with THP-1 cells and, after washing off unbound bacteria, we added
341 gentamicin to kill extracellular bacteria and followed the infection by plating bacteria at
342 different timepoints. For attachment studies, we pre-treated half of the cells with 2 μM
343 cytochalasin D (cytoD), a known inhibitor of actin polymerization, and followed the infection
344 by plating the bacteria recovered from the cytoD- as well as the non-treated cells. The overall
345 CFU counts were normalized to the input control. We observed that WT bacteria were
346 phagocytosed more slowly over time than the capsule mutant (Figure 5A). In contrast, both
347 strains attached to THP-1 cells at similar rates, likely due to the synchronization of the infection
348 by centrifugation at the start of each experiment (Figure 5B). This suggests that the capsule is
349 important to delay phagocytosis by host cells.

350 Capsules have been shown to surround the bacterial cell wall and to mask LPS or outer
351 membrane proteins like a shield. To further investigate if this could also be the case for
352 *L. longbeachae*, we tested agglutination by yeast mannan, a complex polysaccharide of the

353 *Saccharomyces cerevisiae* cell wall that can bind bacterial fimbriae (García-Contreras *et al.*,
354 2008; Rollenske *et al.*, 2021). Indeed, the capsule mutant agglutinated, in contrast to the WT
355 and the complemented mutant (Figure S13). These results indicate that the capsule of
356 *L. longbeachae* protects fimbriae and other attachment factors that are exposed on the surface
357 of a capsule mutant.

358

359 ***The L. longbeachae capsule impacts the pro-inflammatory cytokine response in primary***
360 ***innate immune cells.*** Capsules have been shown to mask cell structures like LPS or outer
361 membrane proteins in bacteria. Due to their inherently low immunological recognition, capsules
362 can have detrimental effects in infection settings such as reduced bacterial clearance or failure
363 to mount an effective cytokine response against the pathogen (Wen and Zhang, 2015). Pro-
364 inflammatory cytokines such as IL-6, TNF α , or IL-1 β can be induced upon engagement of
365 pattern-recognition receptors such as Toll-like receptors (TLRs) or C-type lectin receptors
366 (CLRs) by macrophages. To learn whether the *L. longbeachae* capsule plays a role in the
367 cytokine response, we infected primary human monocyte-derived macrophages (hMDMs) with
368 the *L. longbeachae* WT and the capsule mutant strains and measured cytokine levels in cell
369 supernatants at 24 hours post-infection. Based on previous works (Massis *et al.*, 2016), we
370 expected low cytokine levels upon *L. longbeachae* infection. We therefore opted for the high
371 sensitivity SP-X array for human pro-inflammatory cytokines (Simoa). We observed a
372 significant increase in IL-6 levels in the capsule mutant compared to the complemented strain
373 (Figure 6A). Moreover, cytokine levels of the complemented strain were as low as those of the
374 *L. longbeachae* WT strain. In contrast, we did not detect significant differences in TNF α or IL-
375 1 β levels (Figure 6B-C). These cytokines are known mediators of inflammation in the context
376 of *L. pneumophila* infections (Matsiota-Bernard *et al.*, 1993; Liu *et al.*, 2020), and IL-6 and
377 TNF α are highly induced upon infection with the *L. longbeachae* $\Delta dotB$ mutant. However,
378 TNF α and IL-1 β secretion in human macrophages does not seem to be driven by the capsule
379 but are rather dependent on the presence of a functional Dot/Icm T4SS.

380 *L. longbeachae* is lethal for mice and fails to induce a strong cytokine response *in vitro*
381 (Massis *et al.*, 2016). Our results show that the capsule plays a crucial role in virulence, and we
382 therefore tested whether cytokine secretion during infection is also impacted by its presence or
383 absence. We infected murine dendritic cells (DCs) with *L. longbeachae* WT or the capsule
384 mutant. Similar to what was seen in human macrophages, the secretion of IL-6 was highly
385 induced in the capsule mutant and lower in the *L. longbeachae* WT at 24 hours post-infection
386 (Figure 6D). In contrast to human macrophages, secretion of IL-1 β was also induced in murine

387 DCs infected with the capsule mutant as compared to the WT (Figure 6E). Using murine bone
388 marrow derived macrophages (BMDMs), higher IL-6 and IL-1 β were detected at 24 hours in
389 cells infected with the capsule mutant compared to those infected with the WT or the
390 complemented mutant (Figure 6G-H). However, we did not detect a significant difference in
391 TNF α secretion in murine DCs or macrophages (Figure 6F, I). Thus, our results show that in
392 both human and murine infection models the capsule dampens the secretion of pro-
393 inflammatory cytokines.

394

395 **DISCUSSION**

396 In this study, we report that *L. longbeachae* expresses a capsule that is unique within the genus
397 *Legionella* (Figure 1, Figure S1). Its genes seem to have been acquired from bacteria such as
398 *Pseudomonas*, *Klebsiella*, or *Neisseria* which are present in soil environments or the soil-
399 dwelling bacteria *Burkholderia* spp. and *Geobacter* spp., as evidenced by our comparative
400 genomics analyses (Supplementary Table 1). This fits well with the environmental niche of
401 *L. longbeachae*, as this bacterium is mostly isolated from moist soils and potting mixes (Steele,
402 Lanser and Sangster, 1990; Steele, Moore and Sangster, 1990; Koide *et al.*, 1999). Importantly,
403 the genetic organization of the cluster and its position in the genome are conserved among all
404 *L. longbeachae* strains analyzed, suggesting that these genes have been acquired by horizontal
405 gene transfer by a common ancestor of *L. longbeachae* (Figure S1). However, the exact
406 organism from which it has been acquired, probably *en bloc* given the high conservation in all
407 strains, is not known as it has probably not been sequenced yet.

408 Transmission electron microscopy (TEM) confirmed that *L. longbeachae* expresses a
409 capsule, which can be stained by cationized ferritin and that the *ctrC* mutant does not export
410 the capsule (Figure 2A). CtrC is the inner membrane protein component in contact with CtrD,
411 the nucleotide-binding domain containing ATPase of ABC capsule transporters. A deletion of
412 the homologous *kpsM* gene in *Campylobacter jejuni* also abrogated capsule expression and
413 impaired bacterial virulence in a ferret model of infection (Bacon *et al.*, 2001; Karlyshev *et al.*,
414 2002). The thickness of the *L. longbeachae* capsule was estimated to be between 50-100 nm,
415 which is similar to ferritin-stained capsules observed in *E. coli* K30 (Reid and Whitfield, 2005).
416 However, fixation with glutaraldehyde may lead to a collapse of CPS integrity, as seen in
417 *S. pneumoniae* (Hammerschmidt and Rohde, 2019). Thus, the capsule size may be
418 underestimated, and further analyses are necessary to definitely determine its size. Interestingly,
419 RNAseq analyses showed that the capsule cluster is highly transcribed in E phase (Figure 3A),
420 and TEM analyses revealed that the *L. longbeachae* capsule is visible in PE phase (Figure S5).

421 Thus, export of the capsule on the surface happens in later stages of bacterial growth, suggesting
422 that the bacteria prepare themselves for a new infection and/or for survival in the environment
423 (Figure 2A, B). Indeed, using a fluorescence dual reporter to follow capsule transcription in
424 living cells, we showed that the capsule transporter is expressed in both the human macrophage-
425 like cell line THP-1 and in the environmental host *A. castellanii* late in infection (Figure 3B,
426 Figure S8).

427 Using conventional silver staining methods, we did not detect any fraction that
428 corresponded to a possible CPS in the *L. longbeachae* WT, but the pattern looked highly similar
429 to the LPS ladder in both the WT and in the capsule mutant strain (Figure 2C). Hence, depletion
430 of the capsule does not impact bacterial LPS expression, which might have been an explanation
431 for its low virulence. Only when we applied Stains-all dye, we detected a band at around
432 100 kDa in the WT, which is absent in the mutant and in *L. pneumophila* (Figure 2C). Stains-
433 all can be used for differential staining of highly anionic compounds such as
434 glycosaminoglycans like hyaluronic acid, chondroitin sulfate, dermatan sulfate, or heparin
435 (Souza Andrade *et al.*, 2018). Possibly, we cannot detect the capsular polysaccharides by silver
436 staining because it contains highly modified acidic sugars, which are not available for oxidation
437 by periodate in silver staining. Indeed, it has been reported that some *C. jejuni* strains express
438 hyaluronic acid-like and teichoic acid like capsules, which often cannot be stained by silver,
439 due to a high degree of O-methyl phosphoramidate groups in these CPSs (Preston and Penner,
440 1987; McNally *et al.*, 2005, 2006). Overall, bacterial capsules are incredibly diverse, which is
441 exemplified by over 80 different capsule types in *E. coli* and in *K. pneumoniae* (Follador *et al.*,
442 2016; Mostowy and Holt, 2018). In addition, numerous sugar modifications that confer negative
443 charges have been described for bacterial PS (Sutherland, 2001). Our results open new paths
444 for further research into the biochemical composition of the *L. longbeachae* capsule, in order
445 to determine what confers the highly anionic charge and its anti-phagocytic function.

446 Capsules have also been shown to mediate resistance to environmental stresses such as
447 oxidative stress, detergent, or osmotic stress (Campos *et al.*, 2004; Cameron *et al.*, 2012; Da
448 Cruz Nizer *et al.*, 2021). Interestingly, as shown here, *L. longbeachae* is inherently more
449 resistant to oxidative stress and detergents than *L. pneumophila*, independent of the capsule
450 (Figure S11). These differences may be due to different LPS structures of these two *Legionella*
451 species, which confer resistance to oxidative stress or detergents. During our attempts to isolate
452 the CPS, we observed that *L. longbeachae* produces a longer O-antigen than *L. pneumophila*
453 (Figure 2C), which may be an indication as to why this species is more resistant to H₂O₂ and
454 Tween-20. In contrast, when we tested hyperosmotic stress due to NaCl, growth of the WT was

455 highly impaired in the presence of 100 mM NaCl as compared to the capsule mutant and
456 *L. pneumophila*, whose growth was less disturbed (Figure S12). This is similar to what has been
457 shown for the less virulent LsqR mutant of *L. pneumophila*, and our data point to a link between
458 virulence of *L. longbeachae* and osmotic stress (Tiaden *et al.*, 2007). Capsules are hydrated
459 shells surrounding bacteria, which may contain over 95% water (Costerton, Irvin and Cheng,
460 1981) and which can protect them from hyperosmotic stress (Cameron *et al.*, 2012; Kuzhiyil *et*
461 *al.*, 2012; Wang *et al.*, 2023). According to our TEM studies, the capsule is likely negatively
462 charged. Thus, it is plausible that Na⁺ ions present in high salt environments may disrupt the
463 integrity of the capsule, causing membrane stress and leading to a growth defect in the WT.

464 Capsules have been shown to be important virulence factors of many Gram-negative
465 bacteria that are human pathogens, such as *N. meningitidis* group B, *E. coli* K1 and K5,
466 *K. pneumoniae*, or *Haemophilus influenzae* type b (Bortolussi R *et al.*, 1979; Cortés *et al.*, 2002;
467 Lawlor *et al.*, 2005; Sukupolvi-Petty, Grass and StGeme, 2006; Cress *et al.*, 2014; Tzeng,
468 Thomas and Stephens, 2015). Using a mouse model of infection revealed that the capsule is a
469 crucial virulence factor of *L. longbeachae* (Figure 4A). Remarkably, the capsule mutant was
470 even completely avirulent in mice, a phenotype that was partially restored *in vivo* by
471 complementation (Figure 4B). The virulence of *L. longbeachae* is linked to its capacity to
472 replicate better in the lungs of infected mice (Figure S9B). Previous studies have shown that
473 *L. longbeachae* infection is lethal in common laboratory mouse strains (Asare *et al.*, 2007;
474 Gobin *et al.*, 2009; Massis *et al.*, 2016). Here, we provide evidence that the observed high
475 virulence for mice is due to the capsule encoded by *L. longbeachae*. Thus, the *L. longbeachae*
476 capsule is the first virulence factor described for human pathogenetic *Legionella* whose
477 virulence phenotype is comparable with that of the loss of a functional Dot/Icm type IV
478 secretion system.

479 Early studies on the pathogenicity of *L. pneumophila* revealed that the bacteria can
480 replicate inside the amoeba and likely use the same mechanisms for infection of human cells
481 (Rowbotham, 1980). Here, we show that the capsule mutant is impaired in intracellular
482 replication in *A. castellanii*, and upon coinfection the WT rapidly outcompetes the capsule
483 mutant (Figure 4C, E). Thus, the capsule of *L. longbeachae* is important for infection of both
484 mammalian cells and environmental protozoa. Importantly, all *Legionella* species analyzed to
485 date critically depend on the secretion of effector proteins into host cells *via* a highly conserved
486 Dot/Icm type IV secretion system (T4SS), in order to establish infection and their replicative
487 vacuole (Marra *et al.*, 1992; Berger and Isberg, 1993; Andrews, Vogel and Isberg, 1998; Segal,
488 Purcell and Shuman, 1998; Vogel *et al.*, 1998; Wood *et al.*, 2015). A *L. longbeachae* Δ dotB

489 mutant having a nonfunctional T4SS cannot replicate in THP-1 cells, A549 cells and HEK cells
490 *in vitro* (Wood *et al.*, 2015). Here, we show that it also fails to replicate in *A. castellanii* (Figure
491 4C). However, the capsule mutant is not impaired in effector translocation through the T4SS
492 (Figure 4F). Thus, the observed infection phenotypes are not linked to a dysfunctional T4SS
493 but to the lack of a capsule in the mutant strain.

494 Capsules may prevent attachment and agglutination of bacteria (Wen and Zhang, 2015).
495 Similarly, they have been shown to modulate phagocytosis by host cells by masking cellular
496 receptors on the bacterial surface, or by impairing recognition of LPS by TLRs (Evrard *et al.*,
497 2010; Hsieh and Allen, 2020; Merino and Tomás, 2015). Indeed, in *L. longbeachae*, the capsule
498 is involved in delaying bacterial phagocytosis by THP-1 cells (Figure 5A). Moreover, when
499 exposing bacteria to yeast mannan, which can bind proteins on bacterial cell walls leading to
500 agglutination of bacteria (García-Contreras *et al.*, 2008; Rollenske *et al.*, 2021), only the
501 *L. longbeachae* capsule mutant but not the WT or the complemented strain agglutinated (Figure
502 S13). Altogether, this shows that the *L. longbeachae* capsule is an anti-phagocytic factor and it
503 shields bacterial outer membrane components from immune recognition. Further studies will
504 be undertaken to test whether the *L. longbeachae* capsule evades binding of complement
505 factors, which may explain the difference in phagocytosis.

506 By avoiding immune recognition, bacterial capsules have been shown to dampen the
507 host pro-inflammatory cytokine response (Evrard *et al.*, 2010; Cress *et al.*, 2014; Akoolo *et al.*,
508 2022). The *Salmonella enterica* serotype Typhi Vi capsule dampens the expression of pro-
509 inflammatory cytokines IL-6, TNF α , and IL8, and it prevents recognition by TLR4 (Raffatellu
510 *et al.*, 2005; Wilson *et al.*, 2007). A non-encapsulated strain of *K. pneumoniae* induced higher
511 IL-6 levels in bronchoalveolar lavage fluid from infected mice than an encapsulated WT strain
512 (Yoshida *et al.*, 2000). It was shown that the anti-stimulatory CPS1 capsule of the gut symbiont
513 *Bacteroides thetaiotaomicron* dampens pro-inflammatory cytokines IL-6 and TNF α both in
514 bone marrow-derived macrophages and dendritic cells, correlating with higher bacterial loads
515 in the intestine (Hsieh *et al.*, 2020). Furthermore, it has been shown that the lack of capsule in
516 *Campylobacter jejuni* leads to an increased release of IL-6 and TNF α in murine dendritic cells
517 and macrophages (Rose *et al.*, 2012; Kim *et al.*, 2018). The *Acinetobacter baumannii* capsule
518 dampens the secretion of pro-inflammatory cytokines IL-6 and IL-12 in bone marrow-derived
519 dendritic cells (Akoolo *et al.*, 2022). Similarly, the *L. longbeachae* capsule modulates cytokine
520 release in hMDMs, inducing a lower response pro-inflammatory IL-6 in the WT as compared
521 to the capsule mutant (Figure 6A). However, we did not detect any differences in secretion of
522 TNF α or IL-1 β in human cells (Figure 6B, C). In contrast, when we infected murine dendritic

523 cells and murine macrophages, the capsule mutant induced a higher immune response for IL-6
524 and IL-1 β , but not TNF α (Figure 6D-I), suggesting that the absence of capsule permits the
525 liberation of bacterial-derived immunostimulatory components that would be only recognized
526 by murine cells and not by human cells. Such immunostimulatory bacterial-derived components
527 and their receptor counterparts in the host are yet to be identified, however an existing example
528 of such differences between murine and human macrophages is the NAIP5 inflammasome,
529 present in mice and absent in humans, which allows the exclusive recognition of flagellin from
530 *L. pneumophila* by murine macrophages (Zamboni *et al.*, 2006). However, the leaked
531 immunostimulatory component(s) cannot be flagellin as it is absent from *L. longbeachae*. Thus,
532 the *L. longbeachae* capsule dampens the immune response in innate immune cells by a
533 mechanism that might involve the masking of immunostimulatory bacterial-derived
534 components and their release, avoiding their recognition by innate immune pattern-recognition
535 receptors.

536 In conclusion, our study provides evidence for a novel virulence mechanism of
537 *L. longbeachae*, the expression of a capsule. This capsule is important for *L. longbeachae*
538 replication in the environmental host *A. castellanii* and in mice. During infection, the
539 *L. longbeachae* capsule modulates phagocytosis and dampens the innate immune response
540 favoring bacterial replication. Importantly, our findings provide exciting new insights into how
541 *Legionella* escape recognition by host cells and their defenses, and it opens new avenues to
542 explore the architecture of this unique capsular type and to discover its anti-phagocytic
543 molecules.

544

545 **MATERIALS AND METHODS**

546 **Bacterial strains, growth conditions and cell culture**

547 Bacterial strains used in this study are listed in Table 1. *Escherichia coli* DH5 α subcloning
548 efficiency bacteria were grown in Luria-Bertani broth or on LB agar. *Legionella longbeachae*
549 strains and *L. pneumophila* were cultured in N-(2-acetamido)-2-aminoethanesulfonic acid
550 (ACES)-buffered yeast extract broth (BYE) or on ACES-buffered charcoal-yeast (BCYE)
551 extract agar with antibiotics added where appropriate (Feeley *et al.*, 1979). For the
552 *L. longbeachae* $\Delta ctrC$ mutant, 15 μ g/ml apramycin (Sigma) were added to the medium. For
553 plasmid maintenance, 5 μ g/ml of chloramphenicol was added to the medium. For growth in
554 minimal medium, cells were grown in CDM or MDM according to published protocols
555 (Häuslein *et al.*, 2016). *Acanthamoeba castellanii* strain C3 (ATCC 50739) trophozoites were
556 grown in PYG medium according to published protocols (Moffat and Tompkins, 1992; Cazalet

557 *et al.*, 2010). Infection buffer was prepared as PYG 712 medium [2% proteose peptone, 0.1%
558 yeast extract, 0.1 M glucose, 4 mM MgSO₄, 0.4 M CaCl₂, 0.1% sodium citrate dihydrate, 0.05
559 mM Fe(NH₄)₂(SO₄)₂•6H₂O, 2.5 mM NaH₂PO₃, 2.5 mM K₂HPO₃] without proteose peptone,
560 yeast extract, and glucose. The human monocyte cell THP-1 cell line (ATCC TIB-202) was
561 maintained in RPMI GlutaMax supplemented with 10% fetal calf serum (FCS) at 37°C and 5%
562 CO₂. For infections, undifferentiated THP-1 cells were seeded with RPMI and 50 µg/ml of
563 Phorbol 12-myristate 13-acetate (PMA) to start differentiation into adherent cells. Cells were
564 grown in the presence of PMA for three days and recovered overnight in fresh RPMI medium
565 before infection.

566

567 **Construction of *L. longbeachae* Δ *ctrC***

568 The 0.5 kb flanking regions of *L. longbeachae ctrC* (*llo3151*) were amplified using the primer
569 pairs P3/P4 (upstream segment) and P1/P2 (downstream segment) using genomic DNA of
570 *L. longbeachae* NSW150 as a template (see primers listed in Table 2). The apramycin cassette
571 was amplified with primer pair Apra_s/Apra_{as} using pTOPO-ApraR plasmid as template. The
572 three PCR fragments were ligated by PCR using primers P1/P3 and cloned into pGEM®-T easy
573 vector (Promega). Plasmid was then digested with NotI, and the combined *ctrC*::Apramycin
574 fragment was ligated into the suicide plasmid pLAW344 (Wiater, Sadosky and Shuman, 1994)
575 cut with the same restriction enzyme. The resulting plasmid, pLGV012, was introduced into
576 *L. longbeachae* NSW150 as described above, and transformants were plated onto BCYE agar
577 with apramycin. Resulting colonies were grown in BYE with apramycin and plated onto BCYE
578 agar supplemented with apramycin and 5% sucrose. Sucrose-resistant/chloramphenicol-
579 sensitive clones were screened, and successful deletion was verified through PCR and whole
580 genome sequencing.

581

582 **Transformation of *L. longbeachae***

583 *L. longbeachae* was grown on BCYE agar plates at 37°C. Bacteria from a fresh plate were
584 washed three times with ice-cold 10% glycerol, and the final pellet was resuspended in ice-cold
585 10% glycerol. For transformation, a 400 µl aliquot of electrocompetent cells was freshly mixed
586 with 300-600 ng of plasmid DNA and electroporated at 2.5 kV, 1000 µs, and 25 µF. The cultures
587 were recovered in BYE broth at 37°C with shaking for 16 h and then plated onto BCYE agar
588 with the appropriate antibiotic.

589 **Transmission electron microscopy**

590 Bacterial strains were grown overnight in BYE and OD₆₀₀ was followed constantly to determine
591 E phase (OD₆₀₀ 2.0-2.5) or PE phase (OD₆₀₀ 3.7-4.2). Samples of 10 ml were taken at E and PE
592 phase and centrifuged for 15 minutes at 500 g to remove medium. The medium was discarded,
593 and cells were immediately fixed overnight in 0.1 M cacodylate fixation buffer containing 2.5%
594 glutaraldehyde. Subsequently, fixed cells were washed in 0.2 M cacodylate buffer and stained
595 with 1 mg/ml cationized ferritin (Sigma, F7879-2ML) for 30 minutes at room temperature.
596 After another wash, cells were immobilized in 4% agar before osmium fixation. Agar blocks
597 were sequentially dehydrated in increasing volumes of ethanol and embedded in resin and thin
598 sections were sliced on a Leica UC7 ultramicrotome to 70 μm thickness. Resin slices were
599 mounted and imaged on a Tecnai BioTWIN 20-120 kV transmission electron microscope.

600

601 **RNA sequencing and analysis**

602 Bacteria were grown at 37°C in BYE and OD₆₀₀ was measured to follow their growth. When
603 bacteria reached exponential phase (OD₆₀₀ 2.0-2.5), 2x5 ml were pelleted and snap frozen in
604 dry ice and ethanol. Bacterial morphology was checked under a microscope. Similarly, pellets
605 were collected from bacteria grown to post-exponential phase (OD₆₀₀ 3.7-4.2) and stationary
606 phase the following day. Bacterial pellets were resuspended in Qiazol (Qiagen) and RNA was
607 isolated according to the miRNA Mini kit (Qiagen). The samples were Turbo DNase digested
608 (Thermo Scientific) and rRNA was depleted using the RiboCop rRNA Depletion Kit for Gram-
609 negative bacteria (Lexogen). Depleted RNA was metal-catalyzed heat-fragmented using the
610 RNA Fragmentation kit (Ambion). RNA quantity was measured using a Qubit 2.0 (Invitrogen)
611 and size distribution was confirmed between 100-200 nt by BioAnalyzer (Agilent
612 Technologies). Fragmented RNA was subsequently processed according to the TruSeq mRNA
613 sample preparation guide by Illumina. RNAseq was performed using Illumina NextSeq 550
614 multiplex sequencing (Illumina).

615 For analyzing capsule gene expression, we used FASTQ files containing single-end reads
616 generated by Illumina sequencing. Sequencing reads were processed with Cutadapt software
617 (version 1.15) to remove adapters. Trimming was performed with Sickle (version 1.33,
618 <https://github.com/najoshi/sickle>) with a quality threshold (Phred Score) of 20. Reads shorter
619 than 20 nucleotides were discarded. Clean reads were aligned to the *Legionella longbeachae*
620 NSW150 sequence using Bowtie2 (version 2.3.4.3), and only uniquely mapped reads were kept

621 for the read counts. We used Samtools package (<https://github.com/samtools/samtools>) to build
622 indexed BAM files from the mapping results. To count the number of reads overlapping each
623 genomic feature, we used featureCounts from the Subread package (version 1.6.3). Only
624 primary alignments were counted. Differential analysis between the different conditions was
625 performed with the R package Sartools (version 1.3.0) using DESeq2 methods. The “median”
626 option was used to compute size factors.

627

628 **Construction of complementation and dual reporter plasmids**

629 Capsule cluster promoter was amplified using primers SSM_79 and SSM_80, and the region
630 containing *ctrC* (*llo3151*) and *ctrD* (*llo3150*) was amplified using primers SSM_82 and
631 SSM_85. Both PCRs were performed using genomic DNA of *L. longbeachae* NSW150 as a
632 template. Fragments were then ligated by PCR, with primers SSM_86 and SSM_87. The
633 obtained amplicon was cloned into pBCKS (Stratagene) by restriction-free cloning (van den
634 Ent and Löwe, 2006), resulting in plasmid SSM073. To construct plasmid SSM083, *bexD*
635 (*llo3149*) was amplified using primers SSM_113 and SSM_114, and subcloned into SSM073
636 vector by restriction-free cloning (van den Ent and Löwe, 2006)

637 For construction of the reporter plasmid, the capsule transporter promoter (prom_{cap}) was PCR
638 amplified using primers SSO_025 and SSO_049 ($\text{prom}_{\text{cap}1}$) or SSO_050 and SSO_049
639 ($\text{prom}_{\text{cap}2}$) (listed in Table 2). Superfolder GFP (sfGFP, gift from David Bikard) was PCR
640 amplified using primers SSO_051 and SSO_052 (sfGFP1) or SSO_053 and SSO_054
641 (sfGFP2). A C-terminal degradation tag was added to each sfGFP construct by restriction-free
642 cloning (van den Ent and Löwe, 2006) using primers SSO_045 and SSO_046 or SSO_047 and
643 SSO_048. The GFP constructs were fused to the capsule transporter promoter by overlap PCR,
644 one copy with restriction sites for BamHI and HindIII and the second copy with restriction sites
645 HindIII and KpnI. Each copy was first ligated into pBCKS and inserts were confirmed by
646 sequencing. The second copy was subsequently ligated into the first copy pBCKS vector using
647 restriction sites HindIII and KpnI. One copy of mKate2 (Addgene #68441) was fused to a strong
648 promoter from the Anderson collection (Table 2) by overlap PCR using primers SSO_065 and
649 SSO_066 and ligated into the two copy pBCKS vector through restriction sites NotI and
650 BamHI. A control plasmid was constructed by replacing the two promoter regions cap_{prom} with
651 a triple stop codon by restriction-free cloning using primers SSO_621/SSO_622 and
652 SSO_623/SSO_624, respectively. Plasmid DNA was isolated using Nucleospin Plasmid kit
653 (Macherey Nagel) and all plasmids were confirmed by sequencing.

654 **Imaging of dual reporter in THP-1 cells and *A. castellanii***

655 For imaging of THP-1 cells, bacteria expressing the dual reporter constructs (pSS016 or
656 pSS017) were grown to post-exponential phase in BYE medium with 5 µg/ml chloramphenicol.
657 Differentiated THP-1 cells were infected at an MOI of 10 in a µClear 96-well plate (Greiner)
658 for 1 hour. Cells were washed three times in PBS and supplemented with fresh RPMI medium.
659 Subsequently, cells were stained with CellMask™ Deep Red Plasma Membrane Stain
660 (Invitrogen, C10046) at 5 µg/ml for 20 minutes and washed once. Nuclei were stained with
661 Hoechst dye (Invitrogen, H3570) at 1 µg/ml. Live imaging was performed at 40x magnification
662 using the Opera Phenix confocal microscope (PerkinElmer). Images were obtained every hour
663 and analyzed using the Harmony® high-content analysis software (PerkinElmer). *A. castellanii*
664 were infected in infection buffer at an MOI of 10 for 1 hour at 37°C. After one hour, cells were
665 extensively washed in PBS to remove extracellular bacteria and maintained in infection buffer
666 at 37°C. Cells were imaged at 40x magnification using the EVOS inverted digital microscope
667 (Thermo Fisher).

668

669 **Animals and *in vivo* infections**

670 Mice used in this study were bred and maintained in institutional animal facilities of University
671 of São Paulo – School of Medicine of Ribeirão Preto/SP. All mice were at least 8 weeks old at
672 the time of infection and were in a C57BL/6 (Jax 000664) genetic background. For the survival
673 and CFU experiments, approximately 10 and 7 mice per group were used, as indicated in the
674 figures. For *in vivo* experiments, the mice were anesthetized with ketamine and xylazine
675 (300 mg/kg and 30 mg/kg, respectively) by intraperitoneal injection followed by intranasal
676 inoculation with 40 µl of RPMI 1640 containing bacteria. For CFU determination, the lungs
677 were harvested and homogenized in 5 ml of RPMI 1640 in a tissue homogenizer (Power Gen
678 125; Thermo Scientific) (Pereira, Morgantetti, *et al.*, 2011; Mascarenhas *et al.*, 2015). Lung
679 homogenates were diluted in RPMI and plated on BCYE agar plates containing streptomycin
680 for CFU determination as previously described. For survival determination, mice were observed
681 once a day with the measurement of their weight (Massis *et al.*, 2016). The care of the mice
682 followed the institutional guidelines on ethics in animal experiments.

683

684 **Bone marrow-derived dendritic cells and macrophages**

685 Bone marrow-derived dendritic cells (BMDCs) and bone marrow-derived macrophages
686 (BMDMs) were generated from C57BL/6 mice as previously described (Lutz *et al.*, 1999;

687 Marim *et al.*, 2010). Mice were euthanized and bone marrow cells were obtained from femurs
688 and tibias. BMDCs were harvested from femurs and differentiated with RPMI 1640 (Gibco,
689 Thermo Fisher) containing 20% Fetal Bovine Serum (FBS, Gibco) and 20 ng/ml of recombinant
690 GM-CSF (eBioscience), 2 mM L-glutamine (Sigma-Aldrich), 15 mM HEPES (Gibco) and 100
691 U/ml penicillin-streptomycin (Sigma-Aldrich) at 37°C with 5% CO₂ for 7 days. The non-
692 adherent/loosely adherent fraction was harvested by collecting the culture supernatant and
693 carefully washing the plate with PBS. After centrifugation of the total volume collected,
694 BMDCs were resuspended in RPMI 1640 supplemented with 10% FBS and plated as indicated.
695 BMDMs were harvested from femurs and differentiated with RPMI 1640 (Gibco, Thermo
696 Fisher) containing 20% FBS and 30% L929-Cell Conditioned Medium (LCCM), 2 mM L-
697 glutamine (Sigma-Aldrich), 15 mM HEPES (Gibco) and 100 U/ml penicillin-streptomycin
698 (Sigma-Aldrich) at 37°C with 5% CO₂ for 7 days. Of note, in some experiments LCCM was
699 replaced for 10% of a conditional medium from 3T3 cells stably expressing mouse MCSF. Cells
700 were detached with cold PBS, resuspended in RPMI 1640 supplemented with 10% FBS and
701 plated as indicated for each method.

702

703 **Replication and competition assays in *Acanthamoeba castellanii***

704 Amoeba trophozoites grown at 20°C were washed in infection buffer, seeded at 1x10⁶/ml and
705 left to adhere for one hour prior to infection. Bacteria were resuspended in infection buffer to
706 an MOI of 0.1 and left to infect for 1 hour. Dilutions of an aliquot of input bacteria was plated
707 on BCYE to determine CFUs used for infection (t₀). After one hour of infection, amoeba were
708 washed three times in PBS to remove extracellular bacteria and resuspended in infection buffer.
709 Samples of 500 µl were taken at this timepoint (t₁), centrifuged at 14000 rpm for 3 minutes and
710 vortexed for one minute to break up amoebae. Samples were subsequently taken every 24 hours
711 for seven days. Experiments were carried out in triplicates and CFUs were counted after three
712 to four days of growth on BCYE at 37°C.

713 Competition assay was carried out as previously described (Finsel *et al.*, 2013). Briefly,
714 *A. castellanii* (5 × 10⁶ per flask) in infection buffer was infected at an MOI of 0.1 with a 1:1
715 mix of wild type *L. longbeachae* and Δ *ctrC* mutant bacteria. The infected amoebae were grown
716 for seven days at 37°C. Every two days, a sample of lysed amoebae was diluted 1:100 and used
717 to infect a fresh flask of amoebae (100 µl homogenate per flask). Dilutions were plated on
718 BCYE agar plates containing apramycin or not, to determine CFUs.

719

720 **Replication assays in THP-1 cells**

721 Infection assays of THP-1 cells (ATTC™: TIB-202) were done as previously described
722 (Lomma *et al.*, 2010). Briefly, cells were seeded and differentiated into macrophage-like
723 adherent cells in 12-well tissue culture trays (Falcon, BD lab ware) at a density of 2×10^5
724 cells/well. Stationary phase *L. longbeachae* were resuspended in serum free medium and added
725 to cells at an MOI of 10. After 2 h of incubation, cells were treated with 100 µg/ml gentamycin
726 for 30 minutes to kill extracellular bacteria. Infected cells were then washed before incubation
727 with serum-free medium. At 2, 24, 48, and 72 h, THP-1 cells were lysed with 0.1% Triton X-
728 100. The infection efficiency of the different *L. longbeachae* strains was monitored by
729 determining the number of CFUs after plating on BCYE agar.

730

731 **Bacterial replication in BMDMs**

732 For CFU determination, macrophages were seeded at 2×10^5 cells/well in 24-well plates and
733 cultivated in RPMI 1640 with 10% FBS. Cultures were infected at a multiplicity of infection
734 (MOI) of 10, centrifuged for 5 minutes at $200 \times g$ at room temperature. After 1 hour of infection,
735 BMDMs were washed twice with PBS, and 1 ml of medium was added to each well. For CFU
736 determination, the cultures were lysed in sterile water, and the cell lysates were combined with
737 the cell culture supernatant from the respective wells. Lysates plus supernatants from each well
738 were diluted in water, plated on BCYE agar plates, and incubated for 4 days at 37°C for CFU
739 determination (Pereira, Morgantetti, *et al.*, 2011; Mascarenhas *et al.*, 2015).

740

741 **Beta-lactamase translocation assay**

742 Translocation of T4SS effectors was performed as previously described (Charpentier *et al.*,
743 2009). Plasmids pXDC61 or SSM012 were electroporated into *L. longbeachae* strains or
744 *L. pneumophila* strain Paris as a positive control. Triplicate wells of THP-1 cells were seeded
745 in 96- well plates at 10^5 cells/well and differentiated into adherent cells with 50 µg/ml PMA for
746 three days. Cells were recovered in RPMI without PMA for another night. Freshly transformed
747 bacteria were induced by addition of 1 mM IPTG and THP-1 cells were infected at MOI 50
748 with stationary phase bacteria. Cells were subsequently centrifuged to synchronize the
749 infection. At 1h30 after infection cell were incubated with CCF4-AM (Life Technologies) and
750 0.1 M probenecid at room temperature in the dark. After another 1.5 hours, cells were detached
751 with non-enzymatic cell dissociation solution (Sigma). Flow cytometry was performed using a

752 MACSQuant VYB system (Miltenyi Biotec), with excitation at 405 nm (violet) and emission
753 collection with filters at 525/50 nm (Green) and 450/50 nm (Blue). Flow data were analyzed by
754 FlowJo 10 software (LLC). Gates for green and blue fluorescence were set based on uninfected
755 cells without any treatment. Western blots were performed on protein lysates from induced
756 bacteria to confirm expression of blaM.

757

758 **Attachment and phagocytosis assays**

759 THP-1 cells (ATTC™: TIB-202) were seeded at 4×10^5 cells/well in 12 well plates in RPMI-
760 10% FCS and differentiated for three days with 50 nM PMA. After 96 hours of differentiation,
761 RPMI without PMA was used to recover the cells overnight. For attachment assays, cells were
762 treated with 2 μ M cytochalasin D (Sigma) for two hours prior to infection. Bacterial strains
763 were grown in BYE overnight and bacterial growth was monitored until the bacteria reached
764 post-exponential growth phase (OD_{600} 3.7-4.2). The bacteria were diluted to reach an MOI of
765 10 in RPMI with or without 2 μ M cytochalasin D for attachment assays. At the indicated
766 timepoints, cells were washed three times with PBS to remove non-adhered bacteria and half
767 of the wells were treated with 100 μ g/ml gentamicin for one hour to kill extracellular bacteria
768 (control for internalized bacteria). Cells were lysed by addition of ddH₂O for 15' at 37°C.
769 Dilutions of CFUs were plated for both the gentamicin-treated and untreated wells to determine
770 total CFUs vs. adhered CFUs, respectively. For phagocytosis assays, cells were washed at the
771 indicated timepoints and treated with 100 μ g/ml gentamicin for one hour to kill extracellular
772 bacteria. Cells were lysed in ddH₂O for 15 minutes at 37°C and dilutions were plated to
773 determine CFUs. An aliquot of bacteria used for infections was plated for each strain to
774 determine CFUs at t0.

775

776 **Detergent, oxidative, and osmotic stress assays**

777 To test the resistance of the capsule mutant to salt stress, bacteria were grown in BYE to PE
778 phase (OD_{600} 3.7-4.2) and diluted to 2×10^9 /ml. Ten-fold dilutions were spotted in triplicates
779 onto BCYE plates supplemented with 100 mM NaCl or plain BCYE plates and bacteria were
780 grown at 37°C for 6 days. Tween-20 was tested as previously described (Aurass *et al.*, 2023).
781 Briefly, bacteria were grown in BYE medium to post-exponential growth phase (OD_{600} 3.7-
782 4.2), washed in ultrapure water and adjusted to an OD_{600} of 2.5. Subsequently, cells were treated
783 with 0.05% Tween-20 \pm 300 mM of either NaCl or sucrose for 30 minutes at 37°C with

784 moderate shaking. Ten-fold dilutions were spotted in duplicates on BCYE plates and bacteria
785 were grown at 37°C for 6 days. Similarly, for oxidative stress, post-exponential bacteria were
786 washed once, adjusted to OD₆₀₀ of 2.5, and incubated in the presence of 2 mM or 10 mM H₂O₂
787 for 30 minutes at 37°C with moderate shaking. Ten-fold dilutions were spotted onto BCYE agar
788 plates in duplicates and bacteria were grown at 37°C for 6 days.

789

790 **Agglutination assay**

791 Bacteria were grown to post-exponential phase (OD₆₀₀ 3.7-4.2), washed in PBS adjusted to an
792 OD₆₀₀ of 2.5. Subsequently, agglutination was tested by adding 1 mg/ml yeast mannan (Sigma)
793 to the bacterial solutions and incubation at 37°C for 15 minutes. Cells were subsequently
794 observed at 100x magnification on an EVOS inverted digital microscope (Thermo Fisher).

795

796 **Polysaccharide extractions, gel electrophoresis, and HPLC analysis**

797 Bacteria were grown to post-exponential growth phase in BYE medium and washed in PBS.
798 For phenol extraction, cells were treated with 45% hot phenol for 30 minutes according to
799 previous protocols (Westphal, Lüderitz and Bister, 1952). The aqueous phase was
800 subsequently extracted and extensively dialyzed against water to remove residual phenol. To
801 remove nucleic acids and proteins, extracts were treated with DNase, RNase, and proteinase K,
802 each overnight. After dialysis, extracts were ultracentrifuged using a Beckman Coulter Optima
803 ultracentrifuge at 100 000 rpm for two hours. Samples were freeze-dried and resuspended in
804 ultrapure water for analysis by Dionex and SDS gel electrophoresis. For enzymatic extractions
805 of polysaccharides, bacterial cell pellets were treated with mutanolysin (Sigma) and lysozyme
806 (Sigma) according to published protocols (McNally *et al.*, 2005). Cell debris was removed by
807 centrifugation and extracts were treated with DNase, RNase, and proteinase K, and
808 subsequently dialyzed against water. Following ultracentrifugation, extracts were resuspended
809 in ultrapure water.

810 SDS gel electrophoresis was performed using pre-cast mPAGE™ 4-20% bis-tris gels (Merck)
811 and 20 µl of PS extracts were mixed in Laemmli buffer and boiled at 95°C for 10 minutes. For
812 silver staining, SDS gels were fixed in 45% ethanol solution containing 0.5% periodic acid
813 (Sigma). After extensive washes in water, gels were submerged in 0.1% silver nitrate solution
814 in water for 15 minutes. Gels were rinsed in water and developed in 3% sodium carbonate
815 solution with added formaldehyde to fix the silver dye. Developer was neutralized by addition

816 of citric acid (Sigma). For Alcian blue staining, gels were stained in 0.1% Alcian blue solution
817 in 40% ethanol/5% acetic acid for 1 hour and destained in acetic acid solution (Karlyshev *et al.*,
818 2002). For Stains-all staining, gels were fixed in 50% ethanol/10% acetic acid solution for 1
819 hour and extensively washed in water. A 0.1% Stains-all solution was prepared in water and
820 gels were stained in the dark for 30 minutes. Gels were subsequently destained in water.

821 For analysis of monosaccharides. monosaccharides were first released by acid hydrolysis (TFA
822 4 N, 4 hours at 100°C or HCl 6 N, 6 hours at 100°C). After vacuum drying of the hydrolysate,
823 monosaccharides were identified and quantified by high performance anion exchange
824 chromatography (HPAEC) with a pulsed electrochemical detector and an anion exchange
825 column (CarboPAC PA-1, 4.6 x 250 mm, Dionex) using 18 mM NaOH as mobile phase at a
826 flow rate of 1 mL/min; glucosamine and galactosamine were used as standards (Talaga, Vialle
827 and Moreau, 2002).

828

829 **Isolation of human monocyte-derived macrophages**

830 Ficoll gradient centrifugation (Lympholyte®, Cedarlane) was performed to isolate human
831 peripheral blood mononuclear cells (PMBCs) from freshly extracted blood from healthy
832 donors. To isolate CD14+ cells, anti-hCD14 magnetic beads were used and isolated cells were
833 differentiated to human monocyte-derived macrophages (hMDMs) by addition of 50 ng/ml
834 rhM-CSF (R&D Systems) to XVivo medium (Lonza). After 3 days, medium was exchanged,
835 and cells were differentiated for another 3 days in fresh XVivo supplemented with rhM-CSF.
836 All donors gave written consent under the agreement C- CPSL UNT –No. 15/EFS/023 between
837 the Institut Pasteur and EFS (L'Établissement français du sang), in accordance with articles
838 L1243-4 and R1243-61 of the French Public Health Code and approved by the French Ministry
839 of Science and Technology. Supply and handling of human blood cells followed official
840 guidelines of the agreement between the Institut Pasteur, EFS, and the regulation of blood
841 donation in France.

842

843 **ELISA of human pro-inflammatory cytokines**

844 Differentiated hMDMs were seeded at 3×10^4 cells per well in XVivo (Lonza) and infected with
845 different bacterial strains at an MOI of 10. Cell supernatants were collected at 24 hours post-
846 infection and centrifuged to remove cell debris and extracellular bacteria. The cleared cellular
847 supernatants were rapidly frozen on dry ice and stored at -80 °C until cytokine measurements

848 were performed. ELISA was performed using the SP-X CorPlex™ Human Cytokine Panel 1
849 (Quanterix), a sandwich-based multiplex ELISA with higher sensitivity and broad range of
850 detection of 10 human pro-inflammatory cytokines. The SP-X array was performed from 6
851 independent experiments according to the manufacturer's instructions, including triplicate
852 standard wells and duplicate wells for each sample. The data was analyzed using the proprietary
853 SP-X analysis software.

854

855 **ELISA of murine pro-inflammatory cytokines**

856 For ELISA experiments, BMDMs and BMDCs were seeded in 24-well plates (5×10^5
857 cells/well). Infections were performed in RPMI 1640 supplemented with 10% FBS. After the
858 indicate time points, the supernatants were collected for cytokine determination using ELISA
859 kits according to the manufacturer's recommendations (R&D and BD Bioscience).

860 **Table 1: Bacteria and plasmids used in this study.**

Bacteria		
Name	Source	Additional information
<i>E. coli</i> DH5 α	Invitrogen	Ref. 18265017
<i>L. longbeachae</i> strain NSW150	(Cazalet <i>et al.</i> , 2010)	Wild type strain, serogroup 1
<i>L. longbeachae</i> $\Delta ctrC$	This study	KO of <i>ctrC</i> in NSW150 background
<i>L. longbeachae</i> $\Delta dotB$	(Wood <i>et al.</i> , 2015)	Genomic deletion of <i>dotB</i>
<i>L. pneumophila</i> strain Paris	(Cazalet <i>et al.</i> , 2004)	Wild type strain, serogroup 1
Plasmids		
Name	Source	Additional information
pGEM [®] -T easy vector	Promega	Cloning vector, Amp ^R
pBCKS+	Stratagene	lacZ, Cm ^R
TOPO-mKate2	Addgene	Ref. 68441, mKate2, Kan ^R
pLAW344	(Wiater, Sadosky and Shuman, 1994)	Suicide plasmid incl. <i>sacB</i> cassette, Cm ^R
pLGV012	This study	pLAW344- <i>ctrC</i> ::Apramycin
pXDC61	(De Felipe <i>et al.</i> , 2008)	N-terminal blaM, Cm ^R
pSSM012	(Rolando <i>et al.</i> , 2013)	pXDC61-blaM-RomA
pSSM073	This study	Complementation of <i>ctrC</i> , including <i>ctrD</i> , under the control of the native capsule promoter prom _{cap} , Cm ^R
pSSM083	This study	Complementation of <i>ctrC</i> , including <i>ctrD</i> and <i>bexD</i> , native capsule promoter prom _{cap} , Cm ^R
pSS016	This study	Dual reporter without prom _{cap} , Cm ^R
pSS017	This study	Dual reporter incl. prom _{cap} , Cm ^R

861

862

863 **Table 2: Primers used in this study.**

Oligo name	Sequence	Direction
Apra_as	CCCTCCAACGTCATCTCGTTCTC	reverse
Apra_s	CATCAGCAAAAGGGGATGATAAGTTT	forward
P1	TCCCGAGCTCAGTGAAGTCT	forward
P2	AAACTTATCATCCCCTTTTGCTGATGACGCACCCATTACTCCATTC	reverse
P3	TTGGGAAAACGCTCAGAAAC	forward
P4	GAGAACGAGATGACGTTGGAGGGGGCTCAAGAGCAAACCATA	reverse
SSM_79	GGATCCCTCTCTCCCTTTACGGCGGTAT	forward
SSM_80	TTGTTAGGAAATGCACATTTTGCATCGACACCAATCCTTAATGTCAAAA	reverse
SSM_82	GGTACCTTAAGTTTGCTTGTGTGAAAATTCG	forward
SSM_85	ATGCAAAATGTGCATTTTCCTAAC	reverse
SSM_86	GGCCGCTCTAGAAGTGTGGATCCCTCTCTCCCTTTACGGCG	forward
SSM_087	ACTAAAGGGAACAAAAGCTGGGTACCTTAAGTTTGCTTGTGTTGAAAATTCG	reverse
SSM_113	GGAAGCTTACGAATTTTACAACAAGCAAACCTTAAATAAGTTTTTACAGGAGTTAATTTTT AAAGTGATAAAG	forward
SSM_114	ACTAAAGGGAACAAAAGCTGGGTACCTAAGCCCTTATAACCTGTGTTGC	reverse
SSO_025	GGCCGCTCTAGAAGTGTGGATCCACTCTCTCCCTTTACGGCG	forward
SSO_049	CAGTTCTCACCTTTACTCATCGACACCAATCCTTAATGTCAAAAATTC	reverse
SSO_050	CTACAAACCAGGCATCAAATAGTAAAAGCTTACTCTCTCCCTTTACGGCG	forward
SSO_049	CAGTTCTCACCTTTACTCATCGACACCAATCCTTAATGTCAAAAATTC	reverse
SSO_051	ATGAGTAAAGGTGAAGAAGTTCAC	forward
SSO_052	CGCCGTAAAGGGAGAGAGTAAGCTTTTACTATTTGATGCCTGGTTGTAG	reverse
SSO_053	GAACAAAAGCTGGGTACCTTACTATTTGATGCCTGGTTGTAG	reverse
SSO_045	TGGATGAACTCTACAAACCAGGCATCAAAGCTGCTAATGATGAAAATTATGCTGATGCT	forward
SSO_046	GAGGTGACGGTATCGATAAGCTTTTACTAAGAAGCATCAGCATAATTTTCATCATTAG C	reverse
SSO_047	CATTTTTATCTATAATATTGGCAAATCTGCTACAGCGCTGCTAATGATGAAAATTATGCT G	forward
SSO_048	CATTATTATTTATCCTGATTGATTCAGGTTATTTACTAAGAAGCATCAGCATAATTTTCA TCA	reverse
SSO_065	GCGGTGGCGGCCGCTTTACAGCTAGCTCAGTCCTAGGTATTATGCTAGCGAATTCGCTA GATTTAAGAAGGAGATATACATATGGTGAGCGAGCTGATTAAG	forward
SSO_066	GGAGAGAGTGGATCCTCATCTGTGCCCCAGTTTGC	reverse
SSO_621	GATGATGGATCCTGACTAAGTACAGTAAAGGTGAAGAAGTTCACC	forward
SSO_622	GATGATAAGCTTTTAAAGAAGCATCAGCATAATTTTCATC	reverse
SSO_623	GATGATAAGCTTTGACTAAGTACAGTAAAGGTGAAGAAGTTCACC	forward
SSO_624	GATGATGGTACCTTAAAGAAGCATCAGCATAATTTTCATC	reverse

864

865

866 **Conflict of Interest Statement**

867 The authors declare that the research was conducted in the absence of any commercial or
868 financial relationships that could be construed as a potential conflict of interest.

869

870 **Acknowledgements**

871 Work in the C.B. laboratory is financed by the Institut Pasteur and funding has been received
872 from the French Government (grants ANR-10-LABX-62-IBEID and ANR-15-CE17-0014-03
873 to C.B.) and the “Fondation pour la Recherche Médicale” (grant EQU201903007847 to C.B.).
874 S.S. is a scholar in the Pasteur-Paris University (PPU) International Ph.D. program and received
875 stipends from the Institut Pasteur and the “Fondation pour la Recherche Médicale”
876 (FDT202204015116). We thank the Institut Pasteur UTechs CB platform for cytometry and
877 biomarkers for assistance with SP-X ELISA measurements. We gratefully acknowledge the
878 kind financial support of the Institut Pasteur (Paris) and the Région Ile-de-France (program
879 DIM1Health). Further, we want to thank Hayley Newton for kindly gifting us the *Llo ΔdotB*
880 mutant and David Bikard for sfGFP. Work in the D.S.Z. laboratory is financed by The São
881 Paulo Research Foundation (FAPESP grant 2019/11342-6).

882

883 **REFERENCES**

- 884 Akoolo, L., Pires, S., Kim, J., Parker, D., 2022. The Capsule of *Acinetobacter baumannii* Protects against the
885 Innate Immune Response. *J. Innate Immun.* 14, 543–554. <https://doi.org/10.1159/000522232>
- 886 Amodeo, M.R., Murdoch, D.R., Pithie, A.D., 2010. Legionnaires’ disease caused by *Legionella longbeachae* and
887 *Legionella pneumophila*: comparison of clinical features, host-related risk factors, and outcomes. *Clin. Microbiol.*
888 *Infect.* 16, 1405–1407. <https://doi.org/10.1111/j.1469-0691.2009.03125.x>
- 889 Andrews, H.L., Vogel, J.P., Isberg, R.R., 1998. Identification of Linked *Legionella pneumophila* Genes Essential
890 for Intracellular Growth and Evasion of the Endocytic Pathway. *Infect. Immun.* 66, 950–958.
891 <https://doi.org/10.1128/IAI.66.3.950-958.1998>
- 892 Asare, R., Abu Kwaik, Y., 2007. Early trafficking and intracellular replication of *Legionella longbeachaea* within
893 an ER-derived late endosome-like phagosome. *Cell. Microbiol.* 9, 1571–1587. <https://doi.org/10.1111/j.1462-5822.2007.00894.x>
- 895 Asare, R., Santic, M., Gobin, I., Doric, M., Suttles, J., Graham, J.E., Price, C.D., Abu Kwaik, Y., 2007. Genetic
896 Susceptibility and Caspase Activation in Mouse and Human Macrophages Are Distinct for *Legionella*
897 *longbeachae* and *L. pneumophila*. *Infect. Immun.* 75, 1933–1945. <https://doi.org/10.1128/IAI.00025-07>
- 898 Aurass, P., Kim, S., Pinedo, V., Cava, F., Isberg, R.R., 2023. Identification of Genes Required for Long-Term
899 Survival of *Legionella pneumophila* in Water. *mSphere* 8, e00454-22. <https://doi.org/10.1128/msphere.00454-22>

- 900 Bacigalupe, R., Lindsay, D., Edwards, G., Fitzgerald, J.R., 2017. Population Genomics of *Legionella longbeachae*
901 and Hidden Complexities of Infection Source Attribution. *Emerg. Infect. Dis.* 23, 750–757.
902 <https://doi.org/10.3201/eid2305.161165>
- 903 Bacon, D.J., Szymanski, C.M., Burr, D.H., Silver, R.P., Alm, R.A., Guerry, P., 2001. A phase-variable capsule is
904 involved in virulence of *Campylobacter jejuni* 81-176. *Mol. Microbiol.* 40, 769–777.
- 905 Berger, K.H., Isberg, R.R., 1993. Two distinct defects in intracellular growth complemented by a single genetic
906 locus in *Legionella pneumophila*. *Mol. Microbiol.* 7, 7–19. <https://doi.org/10.1111/j.1365-2958.1993.tb01092.x>
- 907 Bortolussi R, Ferrieri P, Björkstén B, Quie P G, 1979. Capsular K1 polysaccharide of *Escherichia coli*: relationship
908 to virulence in newborn rats and resistance to phagocytosis. *Infect. Immun.* 25, 293–298.
909 <https://doi.org/10.1128/iai.25.1.293-298.1979>
- 910 Brüggemann, H., Hagman, A., Jules, M., Sismeiro, O., Dillies, M.-A., Gouyette, C., Kunst, F., Steinert, M.,
911 Heuner, K., Coppee, J.-Y., Buchrieser, C., 2006. Virulence strategies for infecting phagocytes deduced from the
912 *in vivo* transcriptional program of *Legionella pneumophila*. *Cell. Microbiol.* 8, 1228–1240.
913 <https://doi.org/10.1111/j.1462-5822.2006.00703.x>
- 914 Buffet, A., Rocha, E.P.C., Rendueles, O., 2021. Nutrient conditions are primary drivers of bacterial capsule
915 maintenance in *Klebsiella*. *Proc R Soc B* 288. <https://doi.org/10.1098/rspb.2020.2876>
- 916 Burstein, D., Amaro, F., Zusman, T., Lifshitz, Z., Cohen, O., Gilbert, J.A., Pupko, T., Shuman, H.A., Segal, G.,
917 2016. Genomic analysis of 38 *Legionella* species identifies large and diverse effector repertoires. *Nat. Genet.* 48,
918 167–175. <https://doi.org/10.1038/ng.3481>
- 919 Cameron, A., Frirdich, E., Huynh, S., Parker, C.T., Gaynor, E.C., 2012. Hyperosmotic Stress Response of
920 *Campylobacter jejuni*. *J. Bacteriol.* 194, 6116–6130. <https://doi.org/10.1128/JB.01409-12>
- 921 Campos, M.A., Vargas, M.A., Regueiro, V., Llompарт, C.M., Albertí, S., Bengoechea, J.A., 2004. Capsule
922 Polysaccharide Mediates Bacterial Resistance to Antimicrobial Peptides. *Infect. Immun.* 72, 7107–7114.
923 <https://doi.org/10.1128/IAI.72.12.7107-7114.2004>
- 924 Cazalet, C., Gomez-Valero, L., Rusniok, C., Lomma, M., Dervins-Ravault, D., Newton, H.J., Sansom, F.M.,
925 Jarraud, S., Zidane, N., Ma, L., Bouchier, C., Etienne, J., Hartland, E.L., Buchrieser, C., 2010. Analysis of the
926 *Legionella longbeachae* Genome and Transcriptome Uncovers Unique Strategies to Cause Legionnaires' Disease.
927 *PLoS Genet.* 6, e1000851. <https://doi.org/10.1371/journal.pgen.1000851>
- 928 Cazalet, C., Jarraud, S., Ghavi-Helm, Y., Kunst, F., Glaser, P., Etienne, J., Buchrieser, C., 2008. Multigenome
929 analysis identifies a worldwide distributed epidemic *Legionella pneumophila* clone that emerged within a highly
930 diverse species. *Genome Res.* 18, 431–441. <https://doi.org/10.1101/gr.7229808>
- 931 Cazalet, C., Rusniok, C., Brüggemann, H., Zidane, N., Magnier, A., Ma, L., Tichit, M., Jarraud, S., Bouchier, C.,
932 Vandenesch, F., Kunst, F., Etienne, J., Glaser, P., Buchrieser, C., 2004. Evidence in the *Legionella pneumophila*
933 genome for exploitation of host cell functions and high genome plasticity. *Nat. Genet.* 36, 1165–1173.
934 <https://doi.org/10.1038/ng1447>
- 935 Charpentier, X., Gabay, J.E., Reyes, M., Zhu, J.W., Weiss, A., Shuman, H.A., 2009. Chemical Genetics Reveals
936 Bacterial and Host Cell Functions Critical for Type IV Effector Translocation by *Legionella pneumophila*. *PLoS*
937 *Pathog.* 5, e1000501. <https://doi.org/10.1371/journal.ppat.1000501>
- 938 Cortés, G., Borrell, N., De Astorza, B., Gómez, C., Sauleda, J., Albertí, S., 2002. Molecular Analysis of the
939 Contribution of the Capsular Polysaccharide and the Lipopolysaccharide O Side Chain to the Virulence of
940 *Klebsiella pneumoniae* in a Murine Model of Pneumonia. *Infect. Immun.* 70, 2583–2590.
941 <https://doi.org/10.1128/IAI.70.5.2583-2590.2002>
- 942 Costerton, J.W., Irvin, R.T., Cheng, K.J., 1981. The Bacterial Glycocalyx in Nature and Disease. *Annu. Rev.*
943 *Microbiol.* 35, 299–324. <https://doi.org/10.1146/annurev.mi.35.100181.001503>

- 944 Cress, B.F., Englaender, J.A., He, W., Kasper, D., Linhardt, R.J., Koffas, M.A.G., 2014. Masquerading microbial
945 pathogens: capsular polysaccharides mimic host-tissue molecules. *FEMS Microbiol. Rev.* 38, 660–697.
946 <https://doi.org/10.1111/1574-6976.12056>
- 947 Da Cruz Nizer, W.S., Inkovskiy, V., Versey, Z., Stempel, N., Cassol, E., Overhage, J., 2021. Oxidative Stress
948 Response in *Pseudomonas aeruginosa*. *Pathogens* 10, 1187. <https://doi.org/10.3390/pathogens10091187>
- 949 De Felipe, K.S., Glover, R.T., Charpentier, X., Anderson, O.R., Reyes, M., Pericone, C.D., Shuman, H.A., 2008.
950 *Legionella* Eukaryotic-Like Type IV Substrates Interfere with Organelle Trafficking. *PLoS Pathog.* 4, e1000117.
951 <https://doi.org/10.1371/journal.ppat.1000117>
- 952 Dolinsky, S., Haneburger, I., Cichy, A., Hannemann, M., Itzen, A., Hilbi, H., 2014. The *Legionella longbeachae*
953 Icm/Dot Substrate SidC Selectively Binds Phosphatidylinositol 4-Phosphate with Nanomolar Affinity and
954 Promotes Pathogen Vacuole-Endoplasmic Reticulum Interactions. *Infect. Immun.* 82, 4021–4033.
955 <https://doi.org/10.1128/IAI.01685-14>
- 956 Evrard, B., Balestrino, D., Dosgilbert, A., Bouya-Gachancard, J.-L.J., Charbonnel, N., Forestier, C., Tridon, A.,
957 2010. Roles of Capsule and Lipopolysaccharide O Antigen in Interactions of Human Monocyte-Derived Dendritic
958 Cells and *Klebsiella pneumoniae*. *Infect. Immun.* 78, 210–219. <https://doi.org/10.1128/IAI.00864-09>
- 959 Feeley, J.C., Gibson, R.J., Gorman, G.W., Langford, N.C., Rasheed, J.K., Mackel, D.C., Baine, W.B., 1979.
960 Charcoal-yeast extract agar: primary isolation medium for *Legionella pneumophila*. *J. Clin. Microbiol.* 10, 437–
961 441. <https://doi.org/10.1128/jcm.10.4.437-441.1979>
- 962 Finsel, I., Ragaz, C., Hoffmann, C., Harrison, C.F., Weber, S., van Rahden, V.A., Johannes, L., Hilbi, H., 2013.
963 The *Legionella* Effector RidL Inhibits Retrograde Trafficking to Promote Intracellular Replication. *Cell Host*
964 *Microbe* 14, 38–50. <https://doi.org/10.1016/j.chom.2013.06.001>
- 965 Follador, R., Heinz, E., Wyres, K.L., Ellington, M.J., Kowarik, M., Holt, K.E., Thomson, N.R., 2016. The diversity
966 of *Klebsiella pneumoniae* surface polysaccharides. *Microb. Genomics* 2. <https://doi.org/10.1099/mgen.0.000073>
- 967 García-Contreras, R., Zhang, X.-S., Kim, Y., Wood, T.K., 2008. Protein Translation and Cell Death: The Role of
968 Rare tRNAs in Biofilm Formation and in Activating Dormant Phage Killer Genes. *PLoS ONE* 3, e2394.
969 <https://doi.org/10.1371/journal.pone.0002394>
- 970 Geisinger, E., Isberg, R.R., 2015. Antibiotic Modulation of Capsular Exopolysaccharide and Virulence in
971 *Acinetobacter baumannii*. *PLOS Pathog.* 11, e1004691. <https://doi.org/10.1371/journal.ppat.1004691>
- 972 Gobin, I., Susa, M., Begic, G., Hartland, E.L., Doric, M., 2009. Experimental *Legionella longbeachae* infection in
973 intratracheally inoculated mice. *J. Med. Microbiol.* 58, 723–730. <https://doi.org/10.1099/jmm.0.007476-0>
- 974 Gomez-Valero, L., Rusniok, C., Carson, D., Mondino, S., Pérez-Cobas, A.E., Rolando, M., Pasricha, S., Reuter,
975 S., Demirtas, J., Crumbach, J., Descorps-Declere, S., Hartland, E.L., Jarraud, S., Dougan, G., Schroeder, G.N.,
976 Frankel, G., Buchrieser, C., 2019. More than 18,000 effectors in the *Legionella* genus genome provide multiple,
977 independent combinations for replication in human cells. *Proc. Natl. Acad. Sci.* 116, 2265–2273.
978 <https://doi.org/10.1073/pnas.1808016116>
- 979 Hales, L.M., Shuman, H.A., 1999. The *Legionella pneumophila* rpoS Gene Is Required for Growth within
980 *Acanthamoeba castellanii*. *J. Bacteriol.* 181, 4879–4889. <https://doi.org/10.1128/JB.181.16.4879-4889.1999>
- 981 Hammerschmidt, S., Rohde, M., 2019. Electron Microscopy to Study the Fine Structure of the Pneumococcal Cell,
982 in: Iovino, F. (Ed.), *Streptococcus Pneumoniae: Methods and Protocols*. Springer New York, New York, NY, pp.
983 13–33. https://doi.org/10.1007/978-1-4939-9199-0_2
- 984 Hammerschmidt, S., Wolff, S., Hocke, A., Rosseau, S., Müller, E., Rohde, M., 2005. Illustration of Pneumococcal
985 Polysaccharide Capsule during Adherence and Invasion of Epithelial Cells. *Infect. Immun.* 73, 4653–4667.
986 <https://doi.org/10.1128/IAI.73.8.4653-4667.2005>
- 987 Häuslein, I., Manske, C., Goebel, W., Eisenreich, W., Hilbi, H., 2016. Pathway analysis using ¹³C-glycerol and
988 other carbon tracers reveals a bipartite metabolism of *Legionella pneumophila*. *Mol. Microbiol.* 100, 229–246.

- 989 Hsieh, S., Porter, N.T., Donermeyer, D.L., Horvath, S., Strout, G., Saunders, B.T., Zhang, N., Zinselmeyer, B.,
990 Martens, E.C., Stappenbeck, T.S., Allen, P.M., 2020. Polysaccharide Capsules Equip the Human Symbiont
991 *Bacteroides thetaiotaomicron* to Modulate Immune Responses to a Dominant Antigen in the Intestine. *J. Immunol.*
992 204, 1035–1046. <https://doi.org/10.4049/jimmunol.1901206>
- 993 Hsieh, S.A., Allen, P.M., 2020. Immunomodulatory Roles of Polysaccharide Capsules in the Intestine. *Front.*
994 *Immunol.* 11, 690. <https://doi.org/10.3389/fimmu.2020.00690>
- 995 Hyams, C., Camberlein, E., Cohen, J.M., Bax, K., Brown, J.S., 2010. The *Streptococcus pneumoniae* Capsule
996 Inhibits Complement Activity and Neutrophil Phagocytosis by Multiple Mechanisms. *Infect. Immun.* 78, 704–
997 715. <https://doi.org/10.1128/IAI.00881-09>
- 998 Jones, A., Geörg, M., Maudsdotter, L., Jonsson, A.-B., 2009. Endotoxin, Capsule, and Bacterial Attachment
999 Contribute to *Neisseria meningitidis* Resistance to the Human Antimicrobial Peptide LL-37. *J. Bacteriol.* 191,
1000 3861–3868. <https://doi.org/10.1128/JB.01313-08>
- 1001 Kaper, J.B., Nataro, J.P., Mobley, H.L.T., 2004. Pathogenic *Escherichia coli*. *Nat. Rev. Microbiol.* 2, 123–140.
1002 <https://doi.org/10.1038/nrmicro818>
- 1003 Karlyshev, A.V., Linton, D., Gregson, N.A., Lastovica, A.J., Wren, B.W., 2002. Genetic and biochemical evidence
1004 of a *Campylobacter jejuni* capsular polysaccharide that accounts for Penner serotype specificity: Genetics and
1005 biochemistry of *C. jejuni* LPS biosynthesis. *Mol. Microbiol.* 35, 529–541. <https://doi.org/10.1046/j.1365-2958.2000.01717.x>
- 1007 Kessler, A., Schell, U., Sahr, T., Tiaden, A., Harrison, C., Buchrieser, C., Hilbi, H., 2013. The *Legionella*
1008 *pneumophila* orphan sensor kinase LqsT regulates competence and pathogen-host interactions as a component of
1009 the LAI-1 circuit: *Legionella* sensor kinase LqsT. *Environ. Microbiol.* 15, 646–662.
1010 <https://doi.org/10.1111/j.1462-2920.2012.02889.x>
- 1011 Kim, S., Vela, A., Clohisey, S.M., Athanasiadou, S., Kaiser, P., Stevens, M.P., Vervelde, L., 2018. Host-specific
1012 differences in the response of cultured macrophages to *Campylobacter jejuni* capsule and O-methyl
1013 phosphoramidate mutants. *Vet. Res.* 49, 3. <https://doi.org/10.1186/s13567-017-0501-y>
- 1014 Koide, M., Saito, A., Okazaki, M., Umeda, B., Benson, R.F., 1999. Isolation of *Legionella longbeachae* Serogroup
1015 1 from Potting Soils in Japan. *Clin. Infect. Dis.* 29, 943–944. <https://doi.org/10.1086/520470>
- 1016 Kuzhiyil, A., Lee, Y., Shim, A., Xiong, A., 2012. Osmotic Stress Induces Kanamycin Resistance in *Escherichia*
1017 *coli* B23 through Increased Capsule Formation 16.
- 1018 Lawlor, M.S., Hsu, J., Rick, P.D., Miller, V.L., 2005. Identification of *Klebsiella pneumoniae* virulence
1019 determinants using an intranasal infection model: *Klebsiella pneumoniae* intranasal STM. *Mol. Microbiol.* 58,
1020 1054–1073. <https://doi.org/10.1111/j.1365-2958.2005.04918.x>
- 1021 Liu, X., Boyer, M.A., Holmgren, A.M., Shin, S., 2020. *Legionella*-Infected Macrophages Engage the Alveolar
1022 Epithelium to Metabolically Reprogram Myeloid Cells and Promote Antibacterial Inflammation. *Cell Host*
1023 *Microbe* 28, 683-698.e6. <https://doi.org/10.1016/j.chom.2020.07.019>
- 1024 Lockwood, D.C., Amin, H., Costa, T.R.D., Schroeder, G.N., 2022. The *Legionella pneumophila* Dot/Icm type IV
1025 secretion system and its effectors: This article is part of the Bacterial Cell Envelopes collection. *Microbiology* 168.
1026 <https://doi.org/10.1099/mic.0.001187>
- 1027 Lomma, M., Dervins-Ravault, D., Rolando, M., Nora, T., Newton, H.J., Sansom, F.M., Sahr, T., Gomez-Valero,
1028 L., Jules, M., Hartland, E.L., Buchrieser, C., 2010. The *Legionella pneumophila* F-box protein Lpp2082 (AnkB)
1029 modulates ubiquitination of the host protein parvin B and promotes intracellular replication. *Cell. Microbiol.* 12,
1030 1272–1291. <https://doi.org/10.1111/j.1462-5822.2010.01467.x>
- 1031 Lück, C., Helbig, J.H., 2013. Characterization of *Legionella* Lipopolysaccharide, in: Buchrieser, C., Hilbi, H.
1032 (Eds.), *Legionella: Methods and Protocols*. Humana Press, Totowa, NJ, pp. 381–390. https://doi.org/10.1007/978-1-62703-161-5_24

- 1034 Luck, J.N., Tettelin, H., Orihuela, C.J., 2020. Sugar-Coated Killer: Serotype 3 Pneumococcal Disease. *Front. Cell.*
1035 *Infect. Microbiol.* 10, 613287. <https://doi.org/10.3389/fcimb.2020.613287>
- 1036 Lüneberg, E., Zähringer, U., Knirel, Y.A., Steinmann, D., Hartmann, M., Steinmetz, I., Rohde, M., Köhl, J.,
1037 Frosch, M., 1998. Phase-variable Expression of Lipopolysaccharide Contributes to the Virulence of *Legionella*
1038 *pneumophila*. *J. Exp. Med.* 188, 49–60. <https://doi.org/10.1084/jem.188.1.49>
- 1039 Lutz, M.B., Kukutsch, N., Ogilvie, A.L.J., Rößner, S., Koch, F., Romani, N., Schuler, G., 1999. An advanced
1040 culture method for generating large quantities of highly pure dendritic cells from mouse bone marrow. *J. Immunol.*
1041 *Methods* 223, 77–92. [https://doi.org/10.1016/S0022-1759\(98\)00204-X](https://doi.org/10.1016/S0022-1759(98)00204-X)
- 1042 Marim, F.M., Silveira, T.N., Lima, D.S., Zamboni, D.S., 2010. A Method for Generation of Bone Marrow-Derived
1043 Macrophages from Cryopreserved Mouse Bone Marrow Cells. *PLoS ONE* 5, e15263.
1044 <https://doi.org/10.1371/journal.pone.0015263>
- 1045 Marra, A., Blander, S.J., Horwitz, M.A., Shuman, H.A., 1992. Identification of a *Legionella pneumophila* locus
1046 required for intracellular multiplication in human macrophages. *Proc. Natl. Acad. Sci.* 89, 9607–9611.
1047 <https://doi.org/10.1073/pnas.89.20.9607>
- 1048 Mascarenhas, D.P.A., Pereira, M.S.F., Manin, G.Z., Hori, J.I., Zamboni, D.S., 2015. Interleukin 1 Receptor–
1049 Driven Neutrophil Recruitment Accounts to MyD88–Dependent Pulmonary Clearance of *Legionella pneumophila*
1050 Infection *In Vivo*. *J. Infect. Dis.* 211, 322–330. <https://doi.org/10.1093/infdis/jiu430>
- 1051 Massis, L.M., Assis-Marques, M.A., Castanheira, F.V.S., Capobianco, Y.J., Balestra, A.C., Escoll, P., Wood, R.E.,
1052 Manin, G.Z., Correa, V.M.A., Alves-Filho, J.C., Cunha, F.Q., Buchrieser, C., Borges, M.C., Newton, H.J.,
1053 Zamboni, D.S., 2016. *Legionella longbeachae* is immunologically silent and highly virulent *in vivo*. *J. Infect. Dis.*
1054 *jiw560*. <https://doi.org/10.1093/infdis/jiw560>
- 1055 Matsiota-Bernard, P., Léfèbre, C., Sedqui, M., Cornillet, P., Guenounou, M., 1993. Involvement of tumor necrosis
1056 factor alpha in intracellular multiplication of *Legionella pneumophila* in human monocytes. *Infect. Immun.* 61,
1057 4980–4983. <https://doi.org/10.1128/iai.61.12.4980-4983.1993>
- 1058 McNally, D.J., Jarrell, H.C., Khieu, N.H., Li, J., Vinogradov, E., Whitfield, D.M., Szymanski, C.M., Brisson, J.-
1059 R., 2006. The HS:19 serostrain of *Campylobacter jejuni* has a hyaluronic acid-type capsular polysaccharide with
1060 a nonstoichiometric sorbose branch and O-methyl phosphoramidate group. *FEBS J* 273, 3975–89.
- 1061 McNally, D.J., Jarrell, H.C., Khieu, N.H., Vinogradov, E., Szymanski, C.M., Brisson, J.-R., 2005. The HS:1
1062 serostrain of *Campylobacter jejuni* has a complex teichoic acid-like capsular polysaccharide with
1063 nonstoichiometric fructofuranose branches and O-methyl phosphoramidate groups. *FEBS J* 272, 4407–22.
- 1064 Mérault, N., Rusniok, C., Jarraud, S., Gomez-Valero, L., Cazalet, C., Marin, M., Brachet, E., Aegerter, P., Gaillard,
1065 J.L., Etienne, J., Herrmann, J.L., Lawrence, C., Buchrieser, C., 2011. Specific Real-Time PCR for Simultaneous
1066 Detection and Identification of *Legionella pneumophila* Serogroup 1 in Water and Clinical Samples. *Appl.*
1067 *Environ. Microbiol.* 77, 1708–1717. <https://doi.org/10.1128/AEM.02261-10>
- 1068 Merino, S., Tomás, J.M., 2015. Bacterial Capsules and Evasion of Immune Responses, in: John Wiley & Sons,
1069 Ltd (Ed.), *ELS*. Wiley, pp. 1–10. <https://doi.org/10.1002/9780470015902.a0000957.pub4>
- 1070 Moffat, J.F., Tompkins, L.S., 1992. A quantitative model of intracellular growth of *Legionella pneumophila* in
1071 *Acanthamoeba castellanii*. *Infect. Immun.* 60, 296–301. <https://doi.org/10.1128/iai.60.1.296-301.1992>
- 1072 Molofsky, A.B., Byrne, B.G., Whitfield, N.N., Madigan, C.A., Fuse, E.T., Tateda, K., Swanson, M.S., 2006.
1073 Cytosolic recognition of flagellin by mouse macrophages restricts *Legionella pneumophila* infection. *J. Exp. Med.*
1074 203, 1093–1104. <https://doi.org/10.1084/jem.20051659>
- 1075 Mondino, S., Schmidt, S., Rolando, M., Escoll, P., Gomez-Valero, L., Buchrieser, C., 2020. Legionnaires' Disease:
1076 State of the Art Knowledge of Pathogenesis Mechanisms of *Legionella*. *Annu. Rev. Pathol. Mech. Dis.* 15, 439–
1077 466. <https://doi.org/10.1146/annurev-pathmechdis-012419-032742>
- 1078 Mostowy, R.J., Holt, K.E., 2018. Diversity-Generating Machines: Genetics of Bacterial Sugar-Coating. *Trends*
1079 *Microbiol.* 26, 1008–1021. <https://doi.org/10.1016/j.tim.2018.06.006>

- 1080 Newton, H.J., Ang, D.K.Y., van Driel, I.R., Hartland, E.L., 2010. Molecular Pathogenesis of Infections Caused by
1081 *Legionella pneumophila*. Clin. Microbiol. Rev. 23, 274–298. <https://doi.org/10.1128/CMR.00052-09>
- 1082 Opoku-Temeng, C., Kobayashi, S.D., DeLeo, F.R., 2019. *Klebsiella pneumoniae* capsule polysaccharide as a
1083 target for therapeutics and vaccines. Comput. Struct. Biotechnol. J. 17, 1360–1366.
1084 <https://doi.org/10.1016/j.csbj.2019.09.011>
- 1085 Paton, J.C., Trappetti, C., 2019. *Streptococcus pneumoniae* Capsular Polysaccharide. Microbiol. Spectr. 7, 7.2.33.
1086 <https://doi.org/10.1128/microbiolspec.GPP3-0019-2018>
- 1087 Patro, L.P.P., Rathinavelan, T., 2019. Targeting the Sugary Armor of *Klebsiella* Species. Front. Cell. Infect.
1088 Microbiol. 9, 367. <https://doi.org/10.3389/fcimb.2019.00367>
- 1089 Pereira, M.S.F., Marques, G.G., DeLama, J.E., Zamboni, D.S., 2011a. The Nlrc4 Inflammasome contributes to
1090 restriction of pulmonary infection by flagellated *Legionella* spp. that trigger pyroptosis. Front. Microbiol. 2.
1091 <https://doi.org/10.3389/fmicb.2011.00033>
- 1092 Pereira, M.S.F., Morgantetti, G.F., Massis, L.M., Horta, C.V., Hori, J.I., Zamboni, D.S., 2011b. Activation of
1093 NLRC4 by Flagellated Bacteria Triggers Caspase-1-Dependent and -Independent Responses To Restrict
1094 *Legionella pneumophila* Replication in Macrophages and *In Vivo*. J. Immunol. 187, 6447–6455.
1095 <https://doi.org/10.4049/jimmunol.1003784>
- 1096 Preston, M.A., Penner, J.L., 1987. Structural and antigenic properties of lipopolysaccharides from serotype
1097 reference strains of *Campylobacter jejuni*. Infect. Immun. 55, 1806–1812. <https://doi.org/10.1128/iai.55.8.1806-1812.1987>
- 1099 Raffatellu, M., Chessa, D., Wilson, R.P., Dusold, R., Rubino, S., Bäumler, A.J., 2005. The Vi Capsular Antigen
1100 of *Salmonella enterica* Serotype Typhi Reduces Toll-Like Receptor-Dependent Interleukin-8 Expression in the
1101 Intestinal Mucosa. Infect. Immun. 73, 3367–3374. <https://doi.org/10.1128/IAI.73.6.3367-3374.2005>
- 1102 Reid, A.N., Whitfield, C., 2005. Functional Analysis of Conserved Gene Products Involved in Assembly of
1103 *Escherichia coli* Capsules and Exopolysaccharides: Evidence for Molecular Recognition between Wza and Wzc
1104 for Colanic Acid Biosynthesis. J. Bacteriol. 187, 5470–5481. <https://doi.org/10.1128/JB.187.15.5470-5481.2005>
- 1105 Ren, T., Zamboni, D.S., Roy, C.R., Dietrich, W.F., Vance, R.E., 2006. Flagellin-Deficient *Legionella* Mutants
1106 Evade Caspase-1- and Naip5-Mediated Macrophage Immunity. PLoS Pathog. 2, e18.
1107 <https://doi.org/10.1371/journal.ppat.0020018>
- 1108 Rolando, M., Sanulli, S., Rusniok, C., Gomez-Valero, L., Bertholet, C., Sahr, T., Margueron, R., Buchrieser, C.,
1109 2013. *Legionella pneumophila* Effector RomA Uniquely Modifies Host Chromatin to Repress Gene Expression
1110 and Promote Intracellular Bacterial Replication. Cell Host Microbe 13, 395–405.
1111 <https://doi.org/10.1016/j.chom.2013.03.004>
- 1112 Rollenske, T., Burkhalter, S., Muerner, L., von Gunten, S., Lukasiewicz, J., Wardemann, H., Macpherson, A.J.,
1113 2021. Parallelism of intestinal secretory IgA shapes functional microbial fitness. Nature 598, 657–661.
1114 <https://doi.org/10.1038/s41586-021-03973-7>
- 1115 Rose, A., Kay, E., Wren, B.W., Dallman, M.J., 2012. The *Campylobacter jejuni* NCTC11168 capsule prevents
1116 excessive cytokine production by dendritic cells. Med. Microbiol. Immunol. (Berl.) 201, 137–144.
1117 <https://doi.org/10.1007/s00430-011-0214-1>
- 1118 Rowbotham, T.J., 1980. Preliminary report on the pathogenicity of *Legionella pneumophila* for freshwater and
1119 soil amoebae. J. Clin. Pathol. 33, 1179–1183. <https://doi.org/10.1136/jcp.33.12.1179>
- 1120 Roy, C.R., Berger, K.H., Isberg, R.R., 1998. *Legionella pneumophila* DotA protein is required for early phagosome
1121 trafficking decisions that occur within minutes of bacterial uptake. Mol. Microbiol. 28, 663–674.
1122 <https://doi.org/10.1046/j.1365-2958.1998.00841.x>
- 1123 Segal, G., Purcell, M., Shuman, H.A., 1998. Host cell killing and bacterial conjugation require overlapping sets of
1124 genes within a 22-kb region of the *Legionella pneumophila* genome. Proc. Natl. Acad. Sci. 95, 1669–1674.
1125 <https://doi.org/10.1073/pnas.95.4.1669>

- 1126 Slow, S., Anderson, T., Murdoch, D.R., Bloomfield, S., Winter, D., Biggs, P.J., 2022. Extensive epigenetic
1127 modification with large-scale chromosomal and plasmid recombination characterise the *Legionella longbeachae*
1128 serogroup 1 genome. *Sci. Rep.* 12, 5810. <https://doi.org/10.1038/s41598-022-09721-9>
- 1129 Souza Andrade, J.P., Pacheco Oliveira, C., Freire Tovar, A.M., de Souza Mourao, P.A., Vilanova, E., 2018. A
1130 color-code for glycosaminoglycans identification by means of polyacrylamidegel electrophoresis stained with the
1131 cationic carbocyanine dye Stains-all. *Electrophoresis* 39, 666–669.
- 1132 Spinosa, M.R., Progida, C., Talà, A., Cogli, L., Alifano, P., Bucci, C., 2007. The *Neisseria meningitidis* Capsule
1133 Is Important for Intracellular Survival in Human Cells. *Infect. Immun.* 75, 3594–3603.
1134 <https://doi.org/10.1128/IAI.01945-06>
- 1135 Steele, T.W., Lanser, J., Sangster, N., 1990a. Isolation of *Legionella longbeachae* serogroup 1 from potting mixes.
1136 *Appl. Environ. Microbiol.* 56, 49–53. <https://doi.org/10.1128/aem.56.1.49-53.1990>
- 1137 Steele, T.W., Moore, C.V., Sangster, N., 1990b. Distribution of *Legionella longbeachae* serogroup 1 and other
1138 Legionellae in potting soils in Australia. *Appl. Environ. Microbiol.* 56, 2984–2988.
1139 <https://doi.org/10.1128/aem.56.10.2984-2988.1990>
- 1140 Steenbergen, S.M., Vimr, E.R., 2008. Biosynthesis of the *Escherichia coli* K1 group 2 polysialic acid capsule
1141 occurs within a protected cytoplasmic compartment. *Mol. Microbiol.* 68, 1252–1267.
1142 <https://doi.org/10.1111/j.1365-2958.2008.06231.x>
- 1143 Sukupolvi-Petty, S., Grass, S., StGeme, J.W., 2006. The *Haemophilus influenzae* Type b *hcsA* and *hcsB* Gene
1144 Products Facilitate Transport of Capsular Polysaccharide across the Outer Membrane and Are Essential for
1145 Virulence. *J. Bacteriol.* 188, 3870–3877. <https://doi.org/10.1128/JB.01968-05>
- 1146 Sutherland, I.W., 2001. Polysaccharides: Bacterial and Fungal, in: John Wiley & Sons, Ltd (Ed.), ELS. Wiley.
1147 <https://doi.org/10.1038/npg.els.0000699>
- 1148 Talaga, P., Vialle, S., Moreau, M., 2002. Development of a high-performance anion-exchange chromatography
1149 with pulsed-amperometric detection based quantification assay for pneumococcal polysaccharides and conjugates.
1150 *Vaccine* 20, 2474–2484. [https://doi.org/10.1016/S0264-410X\(02\)00183-4](https://doi.org/10.1016/S0264-410X(02)00183-4)
- 1151 Taylor, M., Ross, K., Bentham, R., 2009. *Legionella*, Protozoa, and Biofilms: Interactions Within Complex
1152 Microbial Systems. *Microb. Ecol.* 58, 538–547. <https://doi.org/10.1007/s00248-009-9514-z>
- 1153 Tiaden, A., Spirig, T., Weber, S.S., Brüggemann, H., Bosshard, R., Buchrieser, C., Hilbi, H., 2007. The *Legionella*
1154 *pneumophila* response regulator LqsR promotes host cell interactions as an element of the virulence regulatory
1155 network controlled by RpoS and LetA. *Cell. Microbiol.* 9, 2903–2920. <https://doi.org/10.1111/j.1462-5822.2007.01005.x>
- 1157 Tipton, K.A., Chin, C.-Y., Farokhyfar, M., Weiss, D.S., Rather, P.N., 2018. Role of Capsule in Resistance to
1158 Disinfectants, Host Antimicrobials, and Desiccation in *Acinetobacter baumannii*. *Antimicrob. Agents Chemother.*
1159 62, e01188-18. <https://doi.org/10.1128/AAC.01188-18>
- 1160 Tzeng, Y.-L., Datta, A.K., Strole, C.A., Lobritz, M.A., Carlson, R.W., Stephens, D.S., 2005. Translocation and
1161 Surface Expression of Lipidated Serogroup B Capsular Polysaccharide in *Neisseria meningitidis*. *Infect. Immun.*
1162 73, 1491–1505. <https://doi.org/10.1128/IAI.73.3.1491-1505.2005>
- 1163 Tzeng, Y.-L., Thomas, J., Stephens, D.S., 2015. Regulation of capsule in *Neisseria meningitidis*. *Crit. Rev.*
1164 *Microbiol.* 1–14. <https://doi.org/10.3109/1040841X.2015.1022507>
- 1165 Valcek, A., Philippe, C., Whiteway, C., Robino, E., Nesporova, K., Bové, M., Coenye, T., De Pooter, T., De
1166 Coster, W., Strazisar, M., Van der Henst, C., 2023. Phenotypic Characterization and Heterogeneity among Modern
1167 Clinical Isolates of *Acinetobacter baumannii*. *Microbiol. Spectr.* 11, e03061-22.
1168 <https://doi.org/10.1128/spectrum.03061-22>
- 1169 van den Ent, F., Löwe, J., 2006. RF cloning: A restriction-free method for inserting target genes into plasmids. *J.*
1170 *Biochem. Biophys. Methods* 67, 67–74. <https://doi.org/10.1016/j.jbbm.2005.12.008>

- 1171 Virji, M., 2009. Pathogenic neisseriae: surface modulation, pathogenesis and infection control. *Nat. Rev.*
 1172 *Microbiol.* 7, 274–286. <https://doi.org/10.1038/nrmicro2097>
- 1173 Vogel, Joseph.P., Andrews, H.L., Wong, S.K., Isberg, R.R., 1998. Conjugative Transfer by the Virulence System
 1174 of *Legionella pneumophila*. *Science* 279, 873–876. <https://doi.org/10.1126/science.279.5352.873>
- 1175 Wang, W., Cao, Y., Li, J., Lu, S., Ge, H., Pan, S., Pan, X., Wang, L., 2023. The impact of osmotic stresses on the
 1176 biofilm formation, immunodetection, and morphology of *Aeromonas hydrophila*. *Microbiol. Res.* 269, 127301.
 1177 <https://doi.org/10.1016/j.micres.2023.127301>
- 1178 Wen, Z., Zhang, J.-R., 2015. Bacterial Capsules, in: *Molecular Medical Microbiology*. Elsevier, pp. 33–53.
 1179 <https://doi.org/10.1016/B978-0-12-397169-2.00003-2>
- 1180 Westphal, O., Lüderitz, O., Bister, F., 1952. Über die Extraktion von Bakterien mit Phenol/Wasser. *Z. Für*
 1181 *Naturforschung B* 7, 148–155. <https://doi.org/10.1515/znb-1952-0303>
- 1182 Whiley, H., Bentham, R., 2011. *Legionella longbeachae* and Legionellosis. *Emerg. Infect. Dis.* 17, 579–583.
 1183 <https://doi.org/10.3201/eid1704.100446>
- 1184 Whiteway, C., Valcek, A., Philippe, C., Strazisar, M., De Pooter, T., Mateus, I., Breine, A., Van der Henst, C.,
 1185 2022. Scarless excision of an insertion sequence restores capsule production and virulence in *Acinetobacter*
 1186 *baumannii*. *ISME J.* 16, 1473–1477. <https://doi.org/10.1038/s41396-021-01179-3>
- 1187 Whitfield, C., Wear, S.S., Sande, C., 2020. Assembly of Bacterial Capsular Polysaccharides and
 1188 Exopolysaccharides. *Annu. Rev. Microbiol.* 74, 521–543. <https://doi.org/10.1146/annurev-micro-011420-075607>
- 1189 Wiater, L.A., Sadosky, A.B., Shuman, H.A., 1994. Mutagenesis of *Legionella pneumophila* using Jn903 dIIIacZ:
 1190 identification of a growth-phase-regulated pigmentation gene. *Mol. Microbiol.* 11, 641–653.
 1191 <https://doi.org/10.1111/j.1365-2958.1994.tb00343.x>
- 1192 Wilson, R.P., Raffatellu, M., Chessa, D., Winter, S.E., Tükel, C., Bäumlner, A.J., 2007. The Vi-capsule prevents
 1193 Toll-like receptor 4 recognition of *Salmonella*. *Cell. Microbiol.* 10, 876–890.
- 1194 Wood, R.E., Newton, P., Latomanski, E.A., Newton, H.J., 2015. Dot/Icm Effector Translocation by *Legionella*
 1195 *longbeachae* Creates a Replicative Vacuole Similar to That of *Legionella pneumophila* despite Translocation of
 1196 Distinct Effector Repertoires. *Infect. Immun.* 83, 4081–4092. <https://doi.org/10.1128/IAI.00461-15>
- 1197 Yoshida, K., Matsumoto, T., Tateda, K., Uchida, K., Tsujimoto, S., Yamaguchi, K., 2000. Role of bacterial capsule
 1198 in local and systemic inflammatory responses of mice during pulmonary infection with *Klebsiella pneumoniae*. *J*
 1199 *Med Microbiol* 49, 1003–1010.
- 1200 Zamboni, D.S., Kobayashi, K.S., Kohlsdorf, T., Ogura, Y., Long, E.M., Vance, R.E., Kuida, K., Mariathasan, S.,
 1201 Dixit, V.M., Flavell, R.A., Dietrich, W.F., Roy, C.R., 2006. The Bir1e cytosolic pattern-recognition receptor
 1202 contributes to the detection and control of *Legionella pneumophila* infection. *Nat. Immunol.* 7, 318–325.
 1203 <https://doi.org/10.1038/ni1305>
- 1204

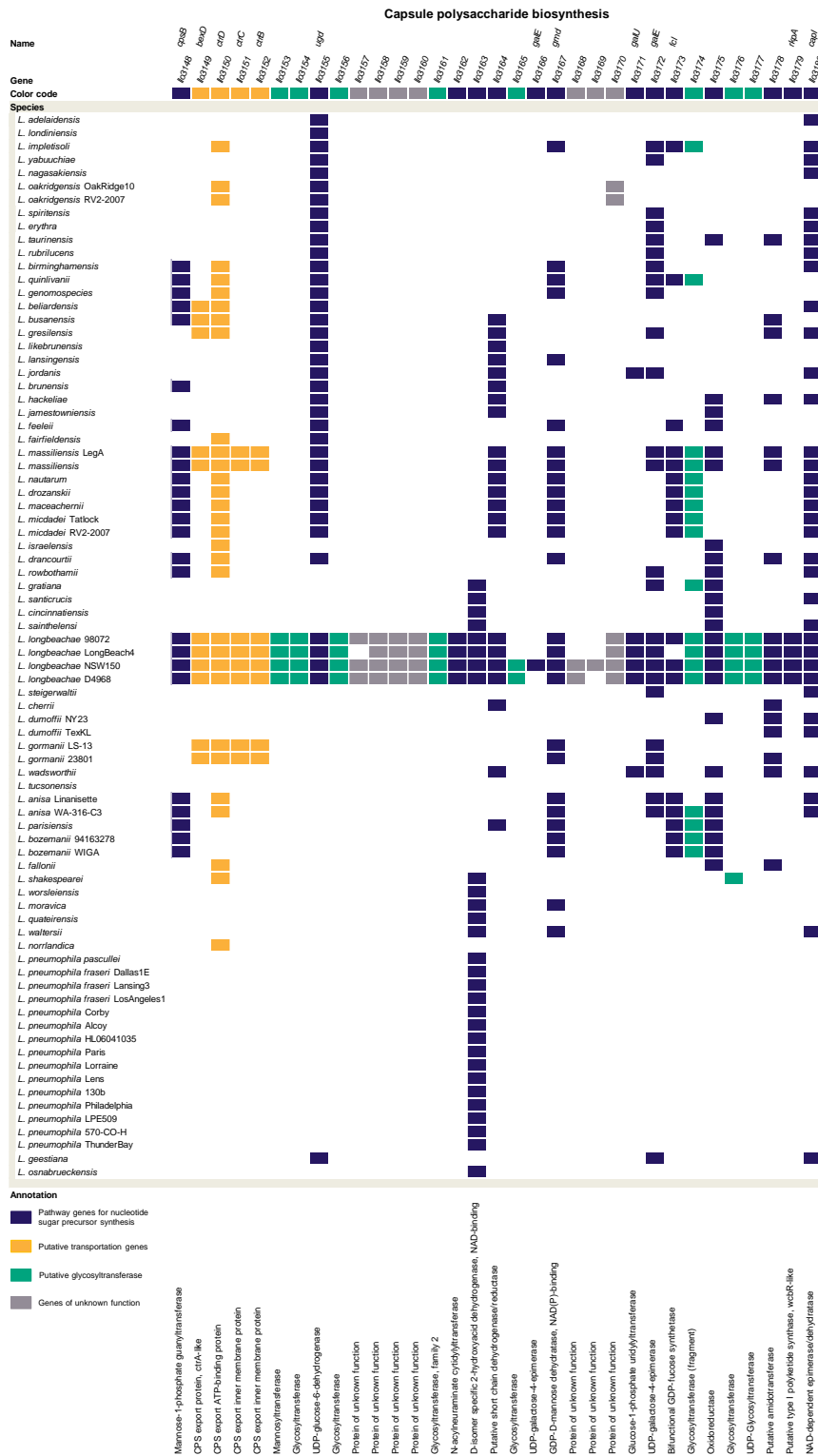
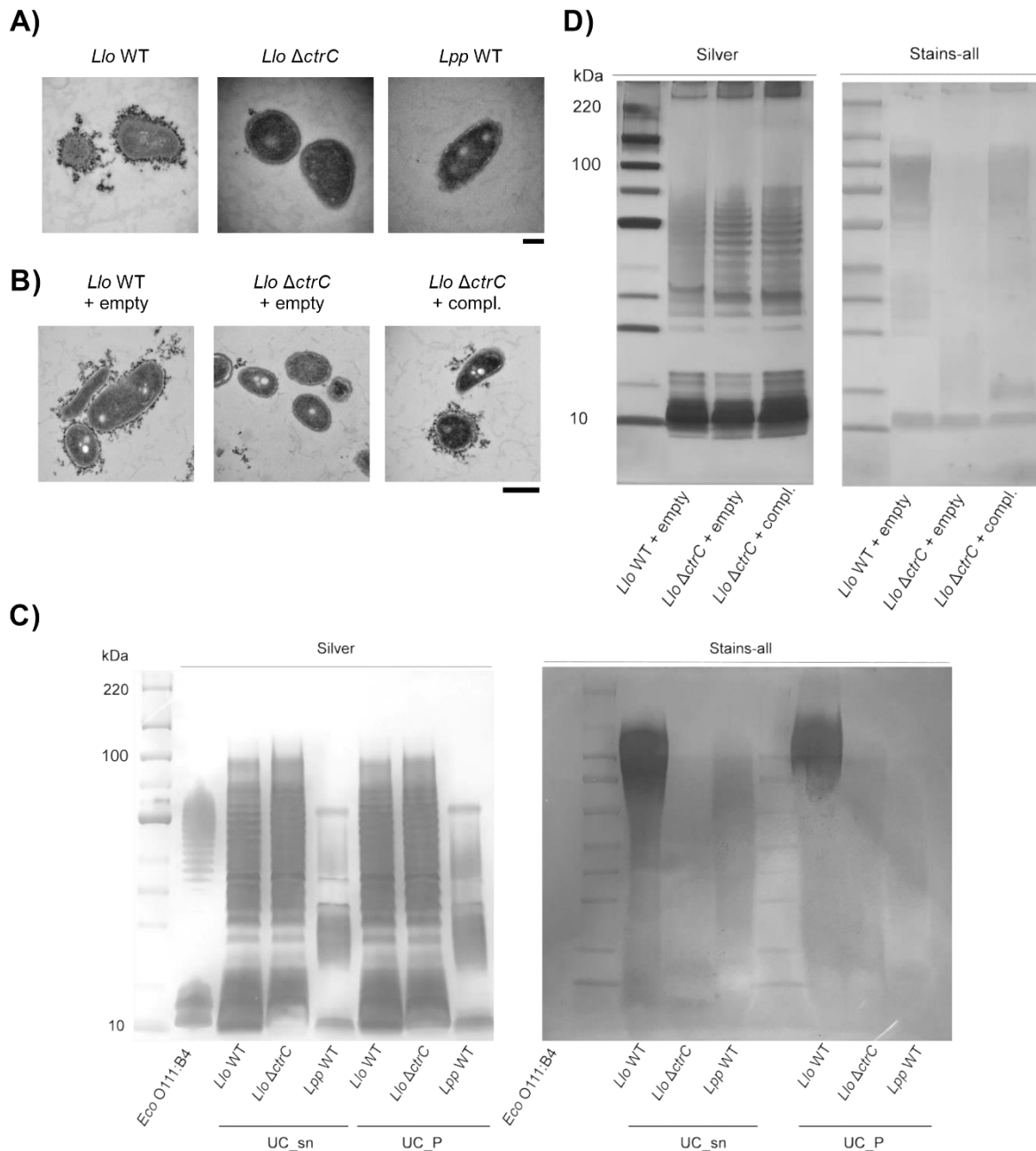


Figure 1: Presence or absence of orthologous genes coding for the capsule in 80 *Legionella* species/strains. Colored squares represent orthologous genes. Orthologous gene reconstruction was done with PanOCT: amino acid percentage identity cutoff was 30%, BLAST e-value cutoff 10^{-5} , and minimum percentage match length of subject and query was 65%.



1225

1226 **Figure 2: The *L. longbeachae* capsule is expressed in exponential growth phase and**

1227 **contains a highly anionic polysaccharide that cannot be stained by silver staining. A)**

1228 *L. longbeachae* WT, Δ *ctrC* and *L. pneumophila* WT (negative control) were grown in BYE

1229 medium to post-exponential phase. Fixed cells were stained with cationized ferritin. TEM

1230 images are representative of n=3 independent experiments. Scale bar = 200 nm. **B)**

1231 *L. longbeachae* WT or Δ *ctrC* harboring an empty plasmid (pBCKS) or the complementation

1232 plasmid (SSM083) were fixed in post-exponential phase and processed like samples in A).

1233 Representative images of n=3 independent experiments. Scale bar = 500 nm. **C)**

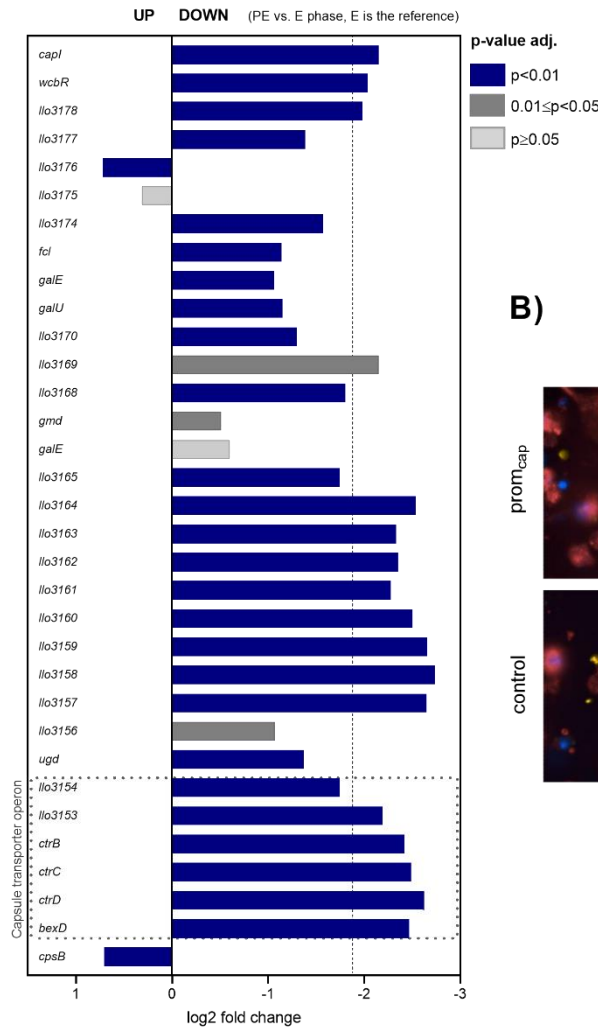
1234 Polysaccharides were extracted from *Llo* WT, Δ *ctrC* or *Lpp* WT by enzymatic isolation and

1235 subjected to ultracentrifugation. SDS gels were stained with silver nitrate or Stains-all dye.

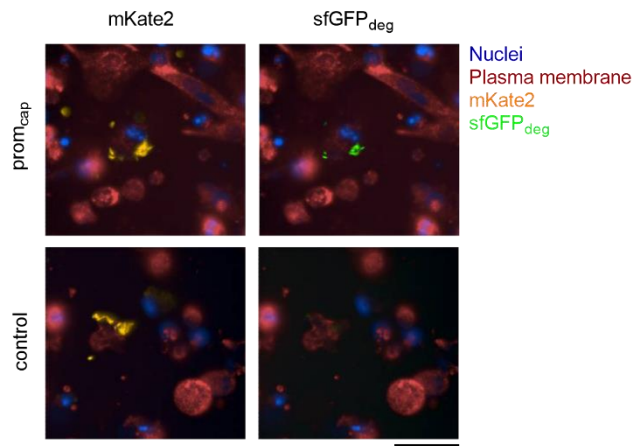
1236 Purified LPS from *E. coli* O111:B4 (Sigma) was used as a control for silver staining. **D)** Extracts
 1237 from *Llo* WT or $\Delta ctrC$ harboring the empty plasmid (pBCKS) or the complemented mutant
 1238 were stained by silver nitrate or Stains-all.

1239

A)

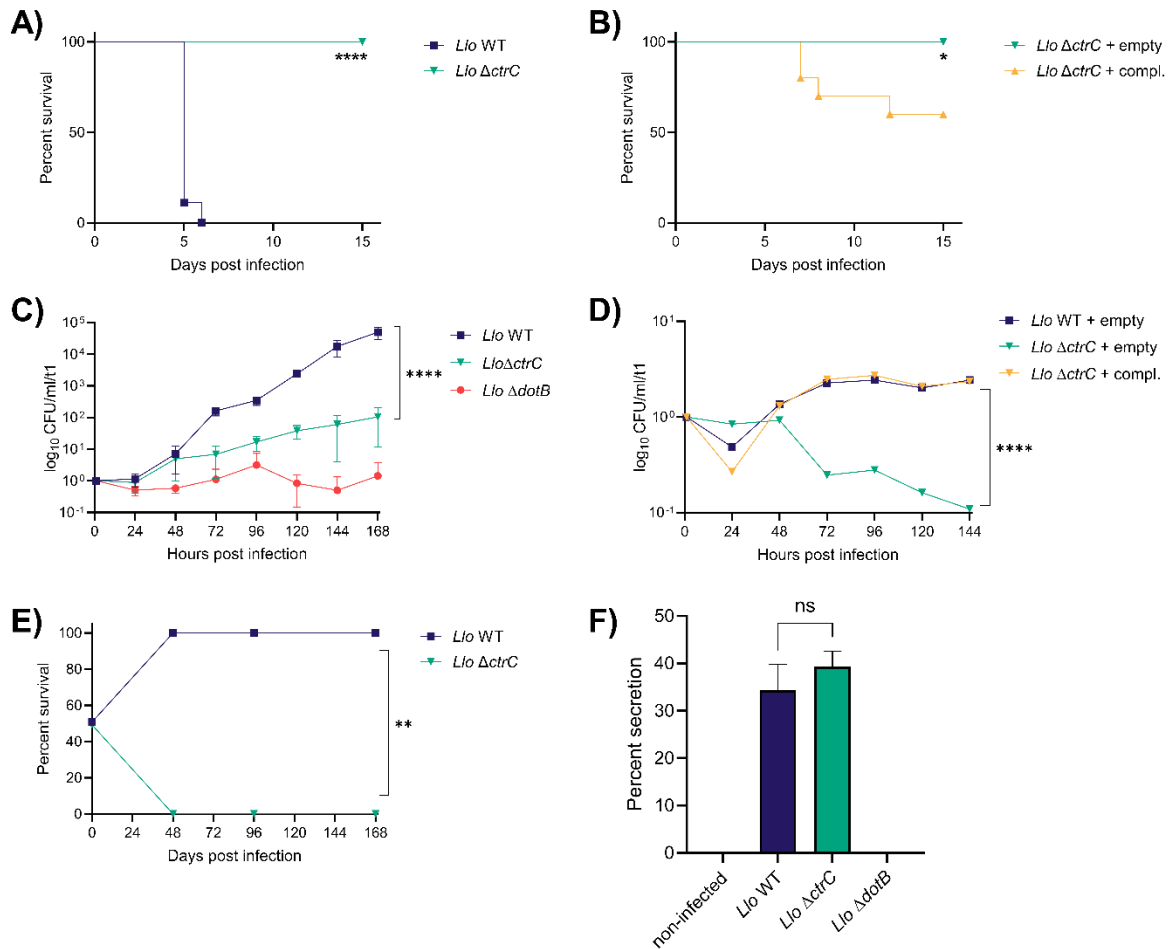


B)



1240

1241 **Figure 3: The *L. longbeachae* capsule is transcribed in liquid medium and *in cellulo*, but**
 1242 **it is not expressed in a $\Delta ctrC$ mutant.** **A)** RNAseq of WT transcripts (n=4); E vs. PE (E is the
 1243 reference); consider relevant genes with log2 fold change of ± 2 and adjusted p value ≤ 0.05 . **B)**
 1244 THP-1 cells were infected with wild type *L. longbeachae* expressing constitutive mKate2 and
 1245 inducible sfGFPdeg under the control of the capsule promoter (prom_{cap}). A control plasmid
 1246 containing constitutive mKate2 and two copies of sfGFPdeg without the capsule promoter was
 1247 included. Cells were imaged at 22 hours post infection. Scale bar = 50 μ m.

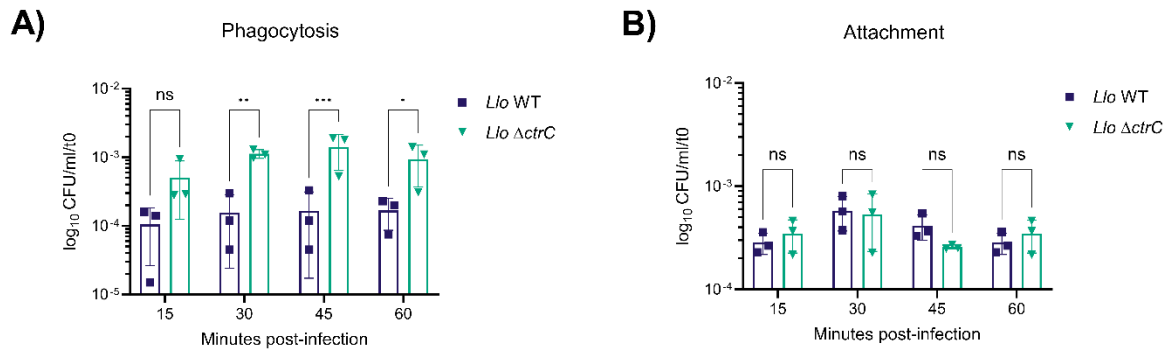


1248

1249 **Figure 4: The capsule mutant is impaired in replication and avirulent *in vivo*, despite a**
 1250 **functional Dot/Icm type IV secretion system. A)** Female C57BL/6 mice were infected with
 1251 10^7 CFU of *Llo* WT or Δ *ctrC* via the nasal route. Survival was monitored over 15 days. Each
 1252 group contained 9 mice. **B)** Infection of female C57BL/6 mice with the capsule mutant
 1253 harboring an empty plasmid (pBCKS) or the complementation plasmid (SSM083) with 10^7
 1254 CFUs. 10 mice per group. Statistical significance was determined by Log-rank (Mantel-Cox)
 1255 test. *, $p \leq 0.05$; ****, $p \leq 0.0001$. **C)** *Acanthamoeba castellanii* trophozoites were infected at
 1256 MOI 0.1 at 20°C over 7 days. Samples were taken every 24 hours and CFUs are normalized to
 1257 the input control. Data show means \pm SD for n=3 independent experiments. **D)** *A. castellanii*
 1258 trophozoites were infected with *Llo* WT or Δ *ctrC* harboring an empty control plasmid (pBCKS)
 1259 or the complementation plasmid (SSM083) at an MOI of 1. Samples were taken every 24 hours
 1260 and CFUs normalized to t=1. Data show means \pm SD for n=3 independent experiments. **E)**
 1261 *A. castellanii* trophozoites were infected at MOI XYZ with equal amounts of *Llo* WT or Δ *ctrC*.
 1262 Samples were taken every 24 hours and normalized to the input control. Data show % survival
 1263 for n=2 independent experiments. Statistical significance was tested by non-linear regression
 1264 analysis using a straight-line model. **F)** Translocation of the known T4SS effector RomA was

1265 tested in THP-1 cells infected with *Llo* WT, $\Delta ctrC$, or a T4SS mutant, $\Delta dotB$. Data represent
1266 means \pm SD of n=2 experiments. Statistical significance was tested by two-tailed t-test. ns, non-
1267 significant; *, $p \leq 0.05$, **, $p \leq 0.01$, ***, $p \leq 0.001$, ****, $p \leq 0.0001$.

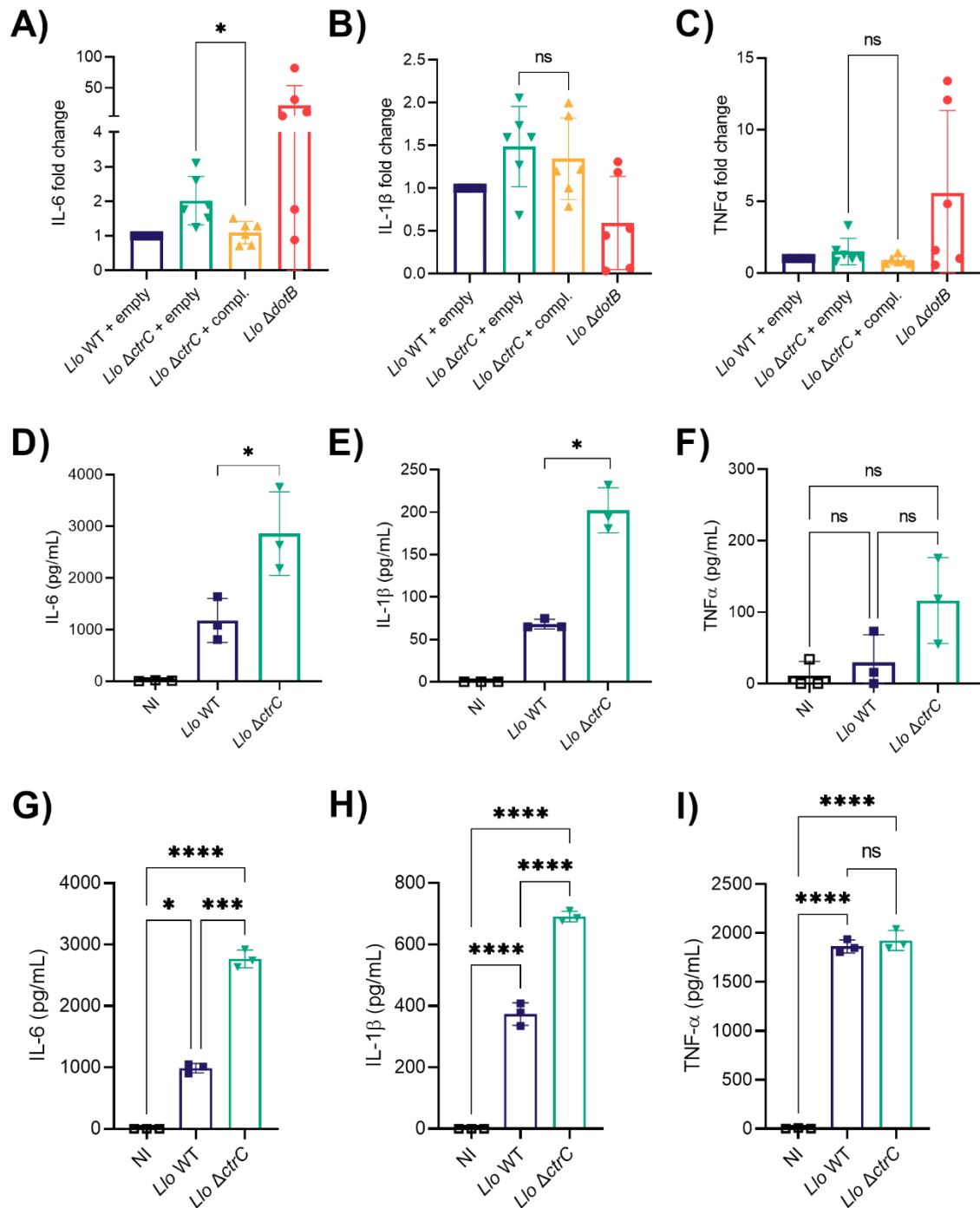
1268



1269

1270 **Figure 5: The capsule delays phagocytosis of host cells.** **A)** For phagocytosis, differentiated
1271 THP-1 cells were infected with *Llo* WT or the *ctrC* mutant at MOI 10. Gentamycin was added
1272 at the indicated timepoints for 1 hour to kill extracellular bacteria and cells were lysed in water
1273 for CFU plating. Data show means \pm SD of n=3 independent experiments normalized to the
1274 input control at t=0. **B)** For attachment, THP-1 cells were pre-treated with 2 μ M cytochalasin
1275 D for two hours before infection with *Llo* WT or *ctrC* at MOI 10. At the indicated timepoints,
1276 gentamycin was added to half of the wells to kill extracellular bacteria. Cells were lysed in
1277 water and CFUs of gentamycin-treated cells (intracellular bacteria) and non-treated cells (total
1278 bacteria) were plated. Intracellular bacteria were deducted from total CFUs, normalized to the
1279 input control at t=0 and data plotted as means \pm SD of n=3 independent experiments. Statistical
1280 significance was tested by two-way ANOVA with Tukey's post-test. ns, non-significant; *,
1281 $p \leq 0.05$, **, $p \leq 0.01$, ***, $p \leq 0.001$.

1282



1283

1284 **Figure 6: The capsule influences the cytokine response of primary macrophages and**

1285 **dendritic cells. A-D) Human monocyte derived macrophages (hMDMs) were infected at MOI**

1286 **10 and cell supernatants were collected at 24 hours post-infection. High-sensitivity SP-X array**

1287 **was performed on cell supernatants. Data show means ± SD of fold change over *L. longbeachae***

1288 **WT of n=6 independent experiments. Statistical significance was tested by pairwise t-tests; ns,**

1289 **non-significant; *, p≤0.05. D-F) Murine bone-marrow derived DCs were infected at MOI 10**

1290 **and cell supernatants collected at 24 hours post-infection. Data show means ± SD of n=3**

1291 independent experiments. **G-I** Murine bone-marrow derived macrophages were infected at
1292 MOI 10 and cell supernatants collected at 24 hours post-infection. Data show means \pm SD of
1293 n=3 independent experiments. Statistical significance was tested by one-way ANOVA with
1294 Tukey's post-test. ns, non-significant; *, $p \leq 0.05$; **, $p \leq 0.01$; ***, $p \leq 0.001$; ****, $p \leq 0.0001$.

1295

1296

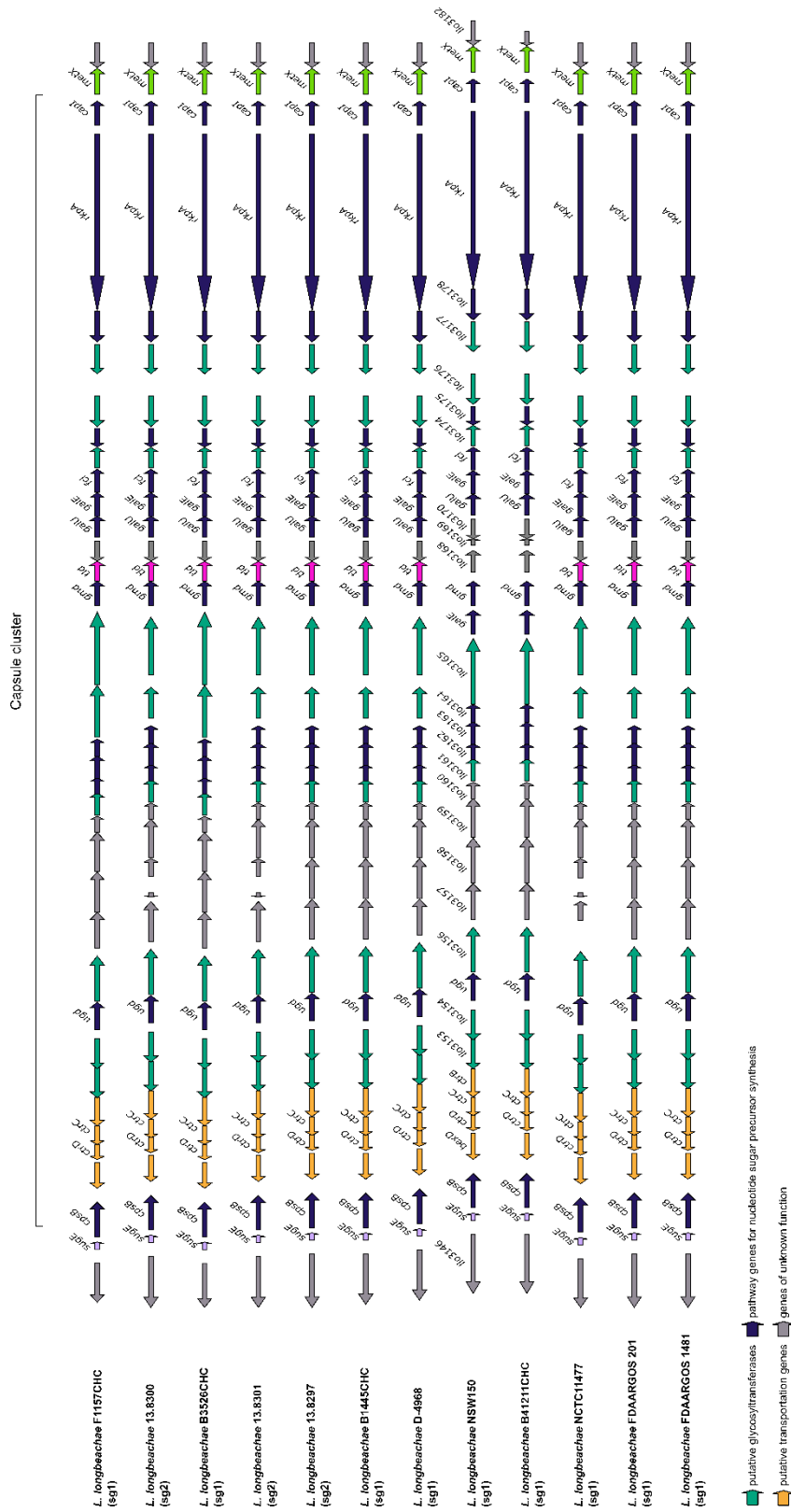


Figure S1: The capsule cluster is conserved among different *L. longbeachae* strains. Visualization of the gene content of the cluster capsule in serogroup 1 and serogroup 2 *Legionella longbeachae* strains using GeneSpy (Garcia *et al.*, 2019). Genes coding for the capsule plus two flanking genes on either side are represented. To obtain homogeneous and comparable annotations, all the genome sequences were reannotated using PROKKA. Based on the new annotation files, gene names and biochemical functions are used to infer families, and a color is attributed for each one.

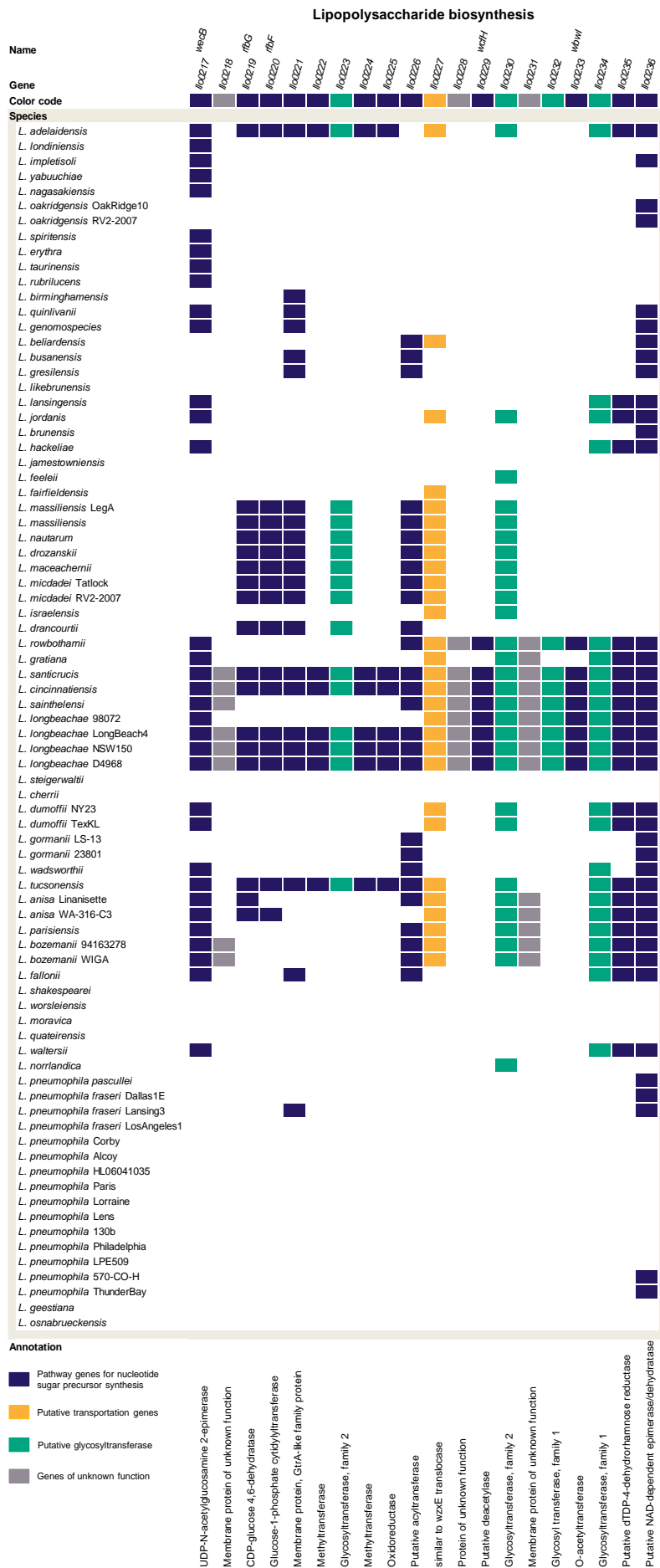


Figure S2: Orthologous genes of the *L. longbeachae* NSW150 LPS cluster among *Legionella* species. Colored squares represent orthologous genes. Orthologous gene reconstruction was done with PanOCT: amino acid percentage identity cutoff 30%, BLAST e-value cutoff 10^{-5} , and minimum percentage match length of subject and query 65%.

Tree scale: 0.1



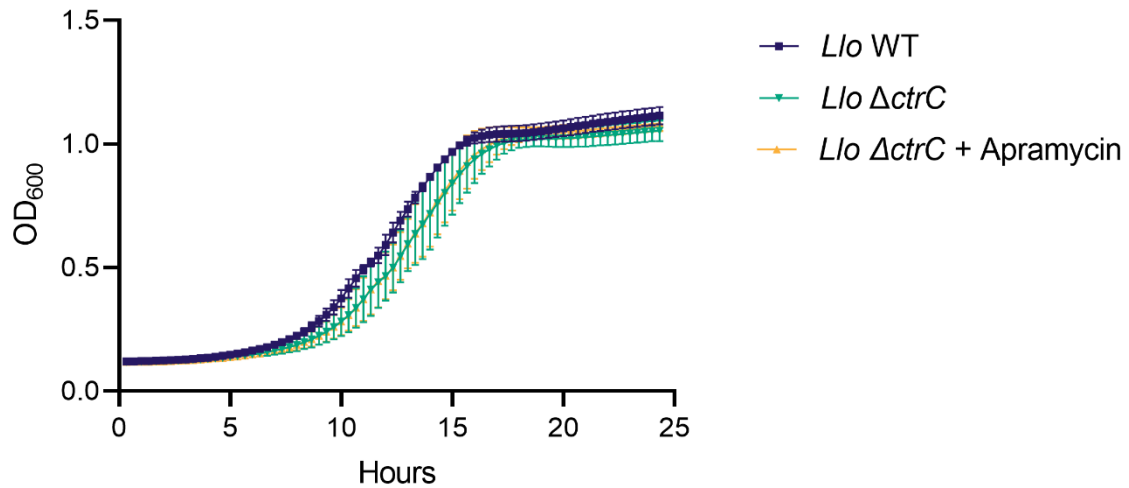
1315

1316 **Figure S3: Legionella harbor two different mechanisms for O-antigen export.** Colored

1317 squares represent orthologous genes. Orthologous gene reconstruction was done with PanOCT:

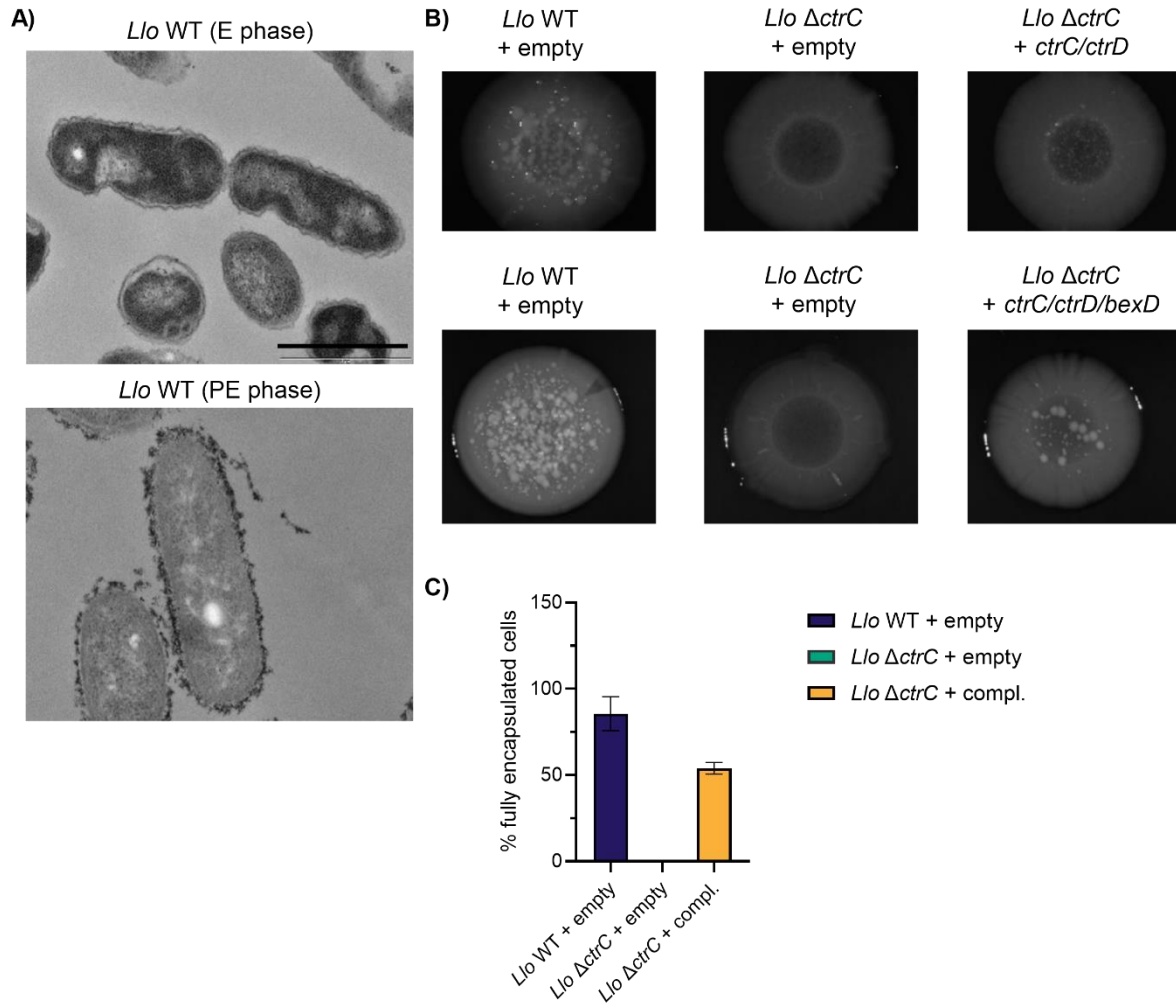
1318 amino acid percentage identity cutoff 30%, BLAST e-value cutoff 10^{-5} , and minimum
1319 percentage match length of subject and query 65%.

1320



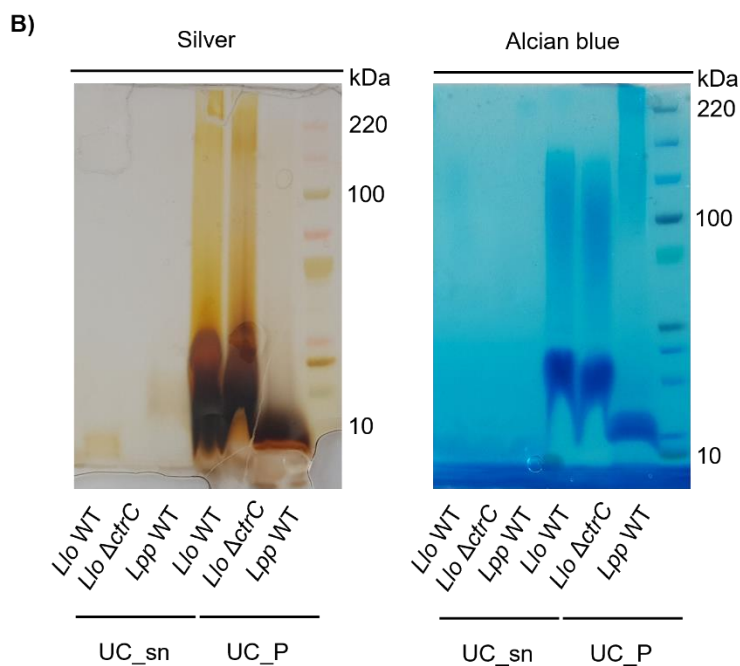
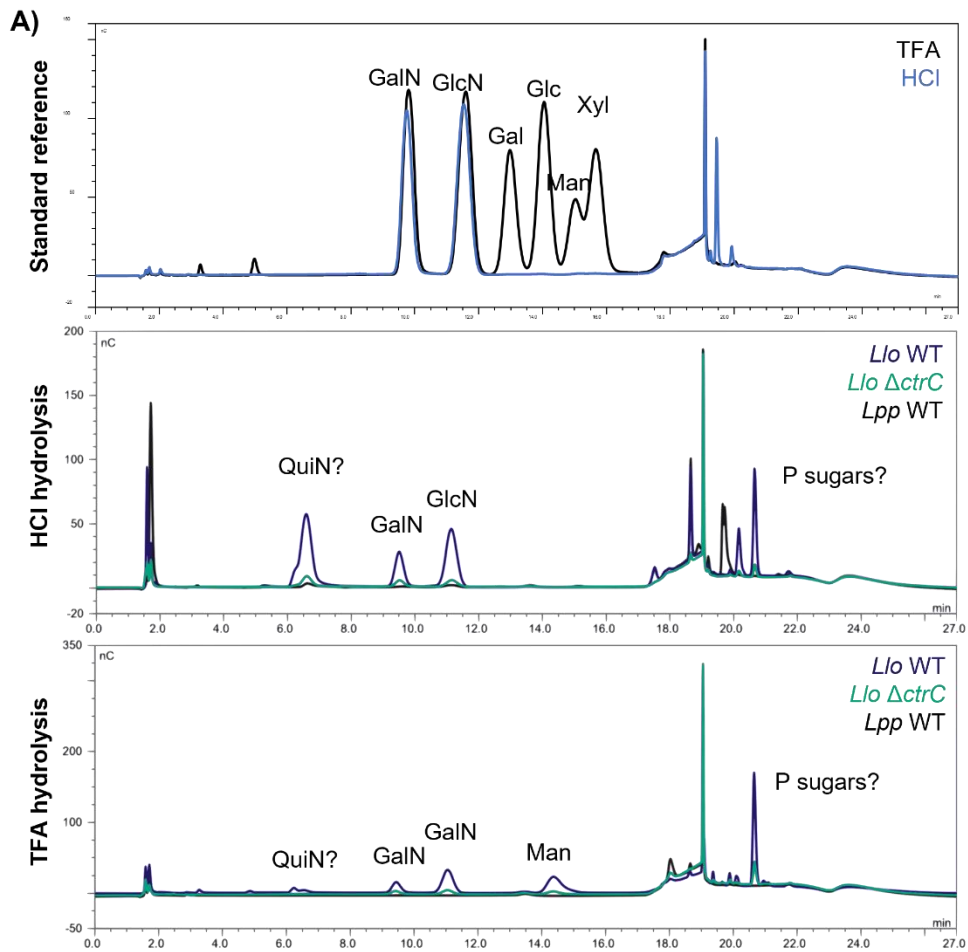
1321

1322 **Figure S4: The *L. longbeachae* WT and capsule mutant grow at similar rates in BYE**
1323 **medium.** *Llo* WT or Δ ctrC \pm apramycin were grown in BYE medium at 37°C and OD₆₀₀ was
1324 followed using a BioTek™ Synergy Plate Reader 2. Data show means \pm SD of n=3 independent
1325 experiments.



1326

1327 **Figure S5: Quantification of capsule complementation by TEM and growth phase**
 1328 **dependent expression of the capsule in the *L. longbeachae* WT.** **A)** *Llo* WT bacteria were
 1329 grown to E phase (OD₆₀₀ 2.0-2.5) or PE phase (OD₆₀₀ 3.7-4.2), fixed and stained with cationized
 1330 ferritin for TEM imaging. Scale bar = 1 μ m. **B)** Quantification of encapsulated bacteria from
 1331 TEM images presented in Figure 2B. **C)** Macrocolonies of *Llo* WT or Δ *ctrC* harboring an empty
 1332 control plasmid (pBCKS) or the complementation plasmids (SSM073 or SSM083). Cells were
 1333 grown to PE phase and 10 μ l were spotted onto BCYE plates for 6 days. Colonies were imaged
 1334 using a Leica M80 Stereo Microscope with top light and 1x magnification.



1335

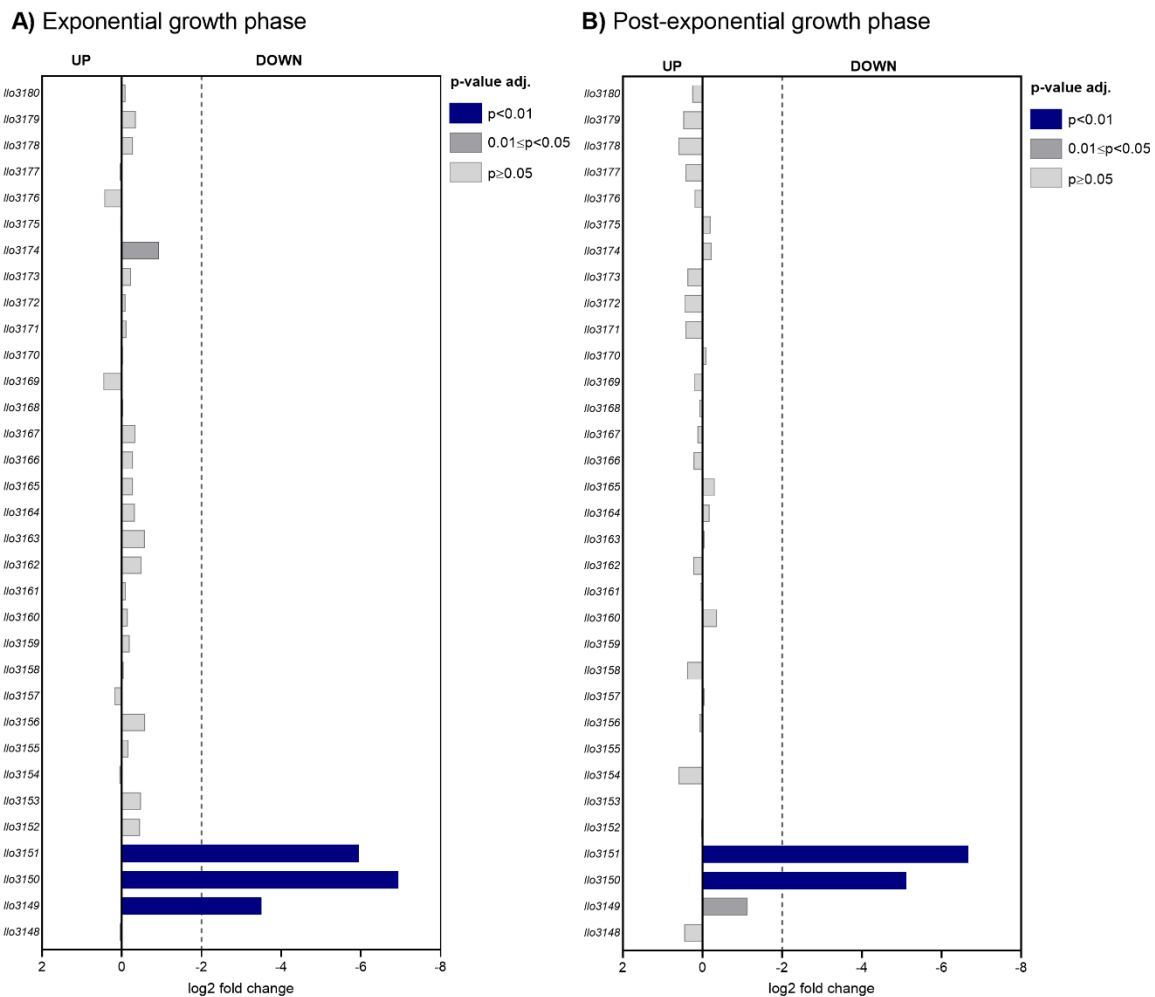
1336 **Figure S6: Characterization and visualization of *L. longbeachae* cell wall polysaccharides.**

1337 **A)** Elution profiles of High-Performance Anion Exchange Chromatography. Top graph,

1338 standard reference hydrolyzed with TFA. Middle and bottom panel, bacterial phenol extracts

1339 after 30 kDa cut-off spin column, hydrolyzed with HCl and TFA. Blue line, *Llo* WT; green line,
 1340 *Llo* $\Delta ctrC$; black line, *Lpp* WT. **B)** SDS gel electrophoresis of phenol extracts stained with
 1341 silver nitrate or Alcian blue. QuiN, quinovosamine; GalN, galactosamine; GlcN, glucosamine;
 1342 Gal, galactose; Glc, glucose; Man, mannose; Xyl, xylose; UC_sn, supernatants after
 1343 ultracentrifugation; UC_P, pellets after ultracentrifugation.

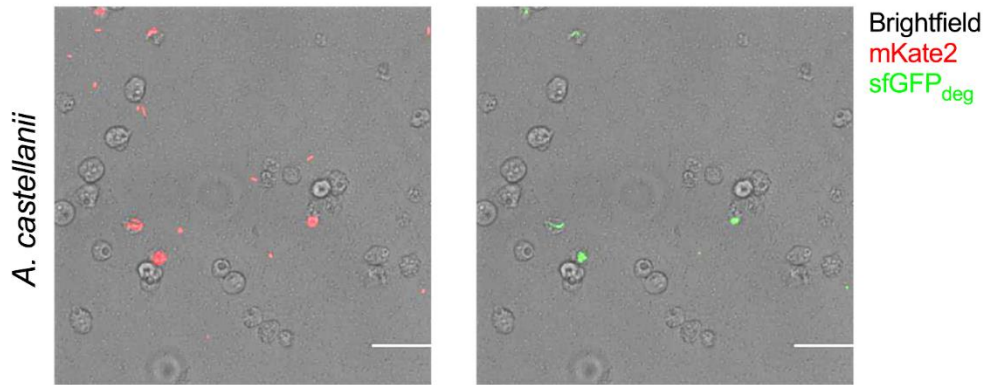
1344



1345

1346 **Figure S7: RNAseq data of *L. longbeachae* WT vs. capsule mutant in E and PE phase (WT**
 1347 **is the reference). A) Comparison of E phase bacteria. B) Comparison of PE phase bacteria.**
 1348 WT vs. $\Delta ctrC$ (WT is the reference); consider relevant genes with log₂ fold change of ± 2 and
 1349 adjusted p value ≤ 0.05 . n=4 independent experiments.

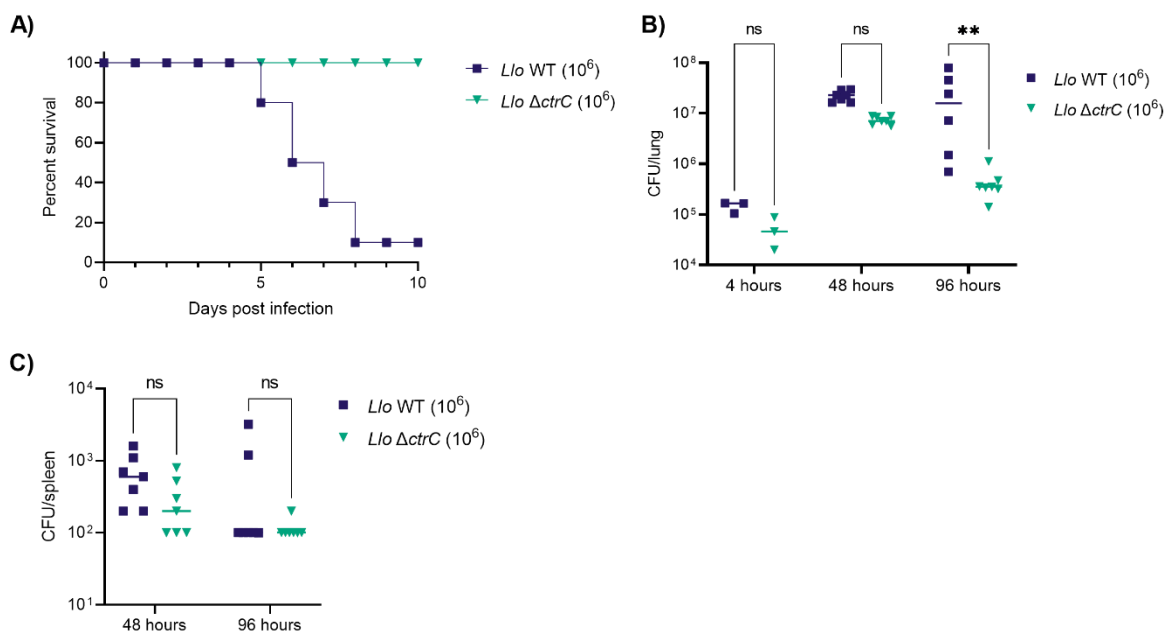
1350



1351

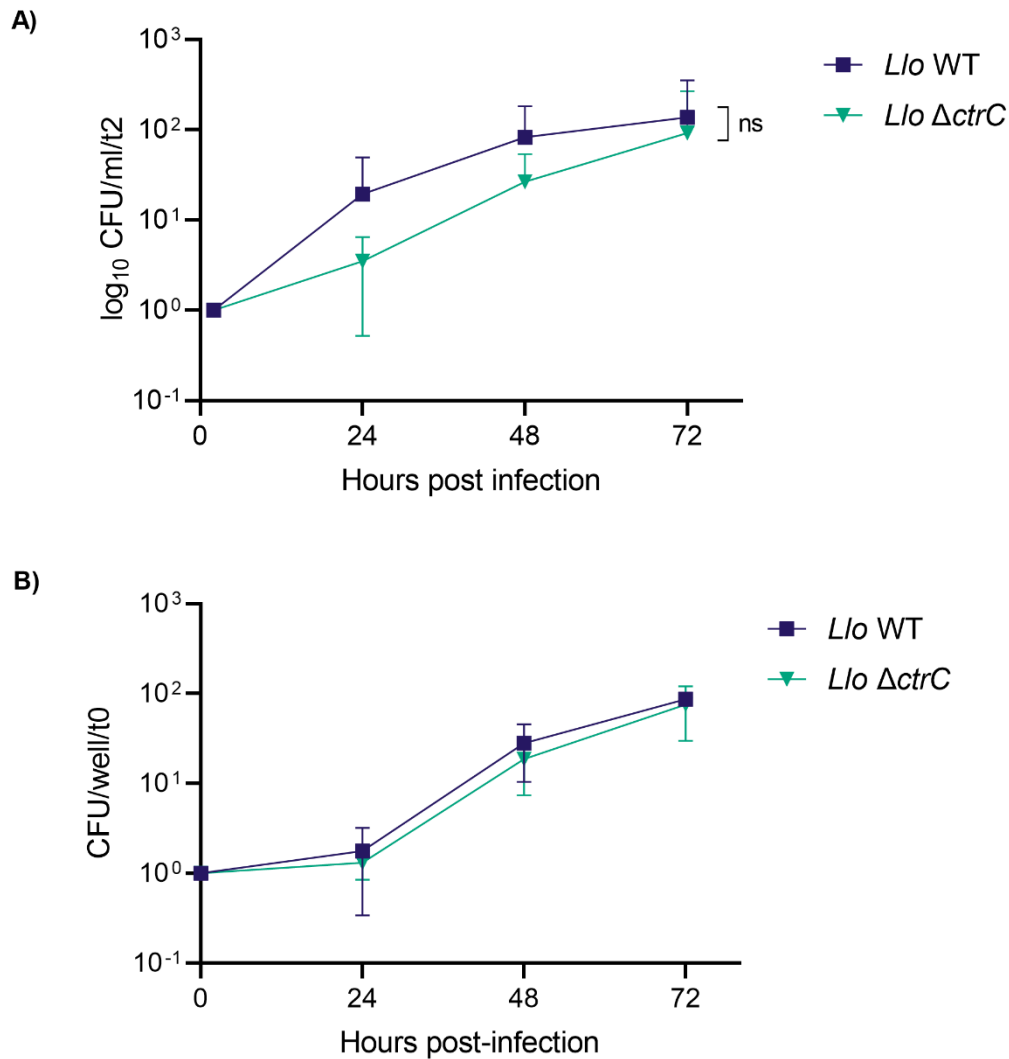
1352 **Figure S8: The *L. longbeachae* capsule is transcribed upon infection of *Acanthamoeba***
 1353 ***castellanii*.** *A. castellanii* was infected with *Llo* WT bacteria harboring the dual reporter plasmid
 1354 (pSS017) at MOI 10 and 37°C for 1 hour. Cells were imaged 24 hours post-infection using an
 1355 EVOS inverted digital microscope. Scale bar = 100 μm.

1356



1357

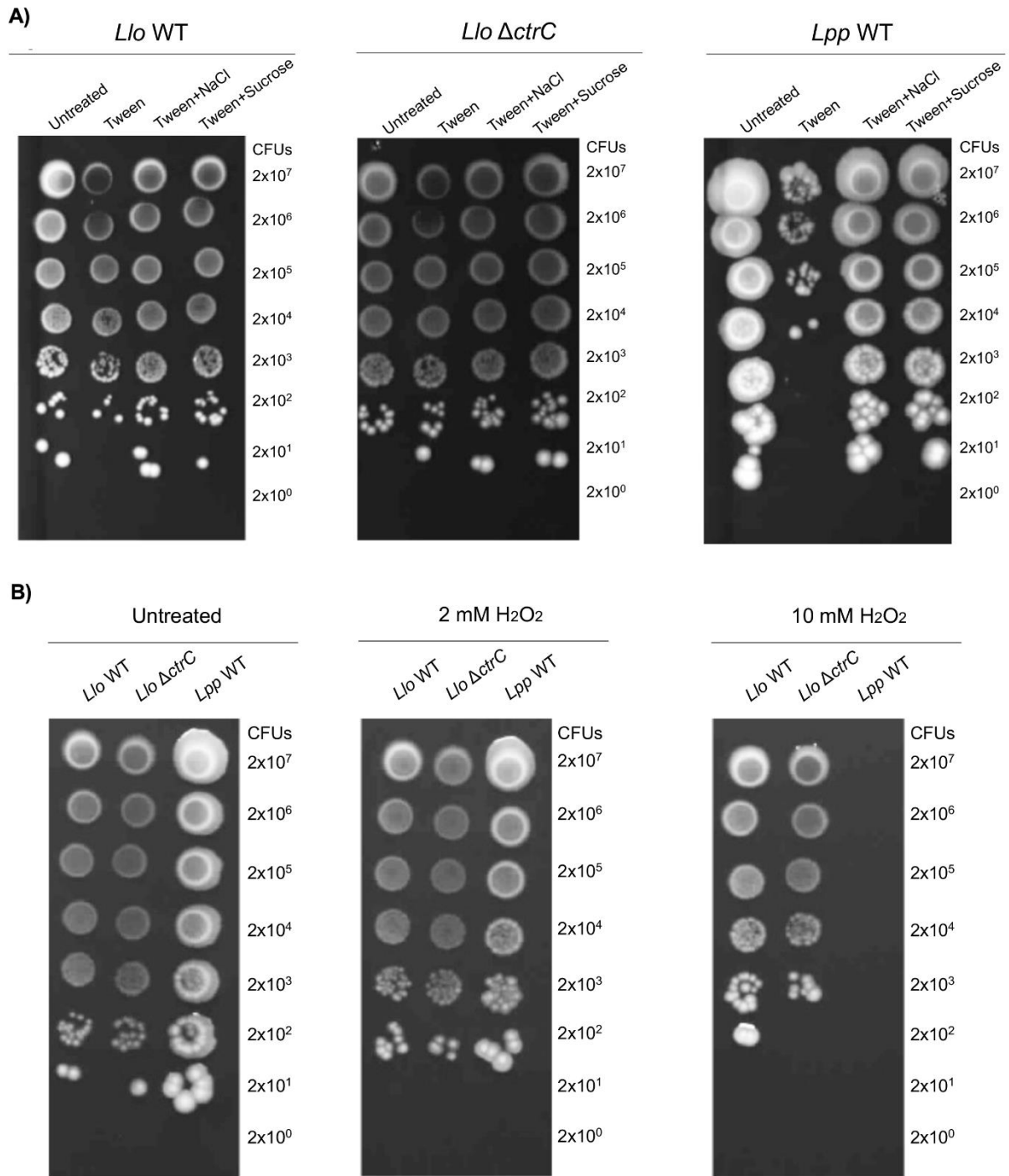
1358 **Figure S9: The *L. longbeachae* capsule mutant replicates less in lungs of infected mice. A)**
 1359 Female C57BL/6 mice were infected with 10⁶ bacteria and survival was monitored over ten
 1360 days. 9 mice per group. **B)** CFUs from lungs of infected mice were plated at 4, 48, and 96 hours
 1361 post-infection. Dots represent number of animals per group. **C)** CFUs from spleens of infected
 1362 mice were plated at 48 and 96 hours post-infection. Dots represent number of animals per group.
 1363 Statistical analysis was performed by two-way ANOVA with Šídák's multiple comparisons test.
 1364 ns, non-significant; **, p < 0.01.



1365

1366 **Figure S10: The *L. longbeachae* WT and capsule mutant replicate to similar levels in THP-**
 1367 **1 cells and murine BMDMs. A)** Differentiated THP-1 cells were infected at MOI 10 for 1
 1368 hour and treated with gentamycin to kill extracellular bacteria. CFUs were plated every 24 hours
 1369 and normalized to the input control. Data show means ± SD of n=6 independent experiments
 1370 **B)** Bone marrow-derived macrophages (BMDMs) were infected at MOI 10 and CFUs plated
 1371 every 24 hours normalized to the input control. Data show means ± SD of n=3 independent
 1372 experiments.

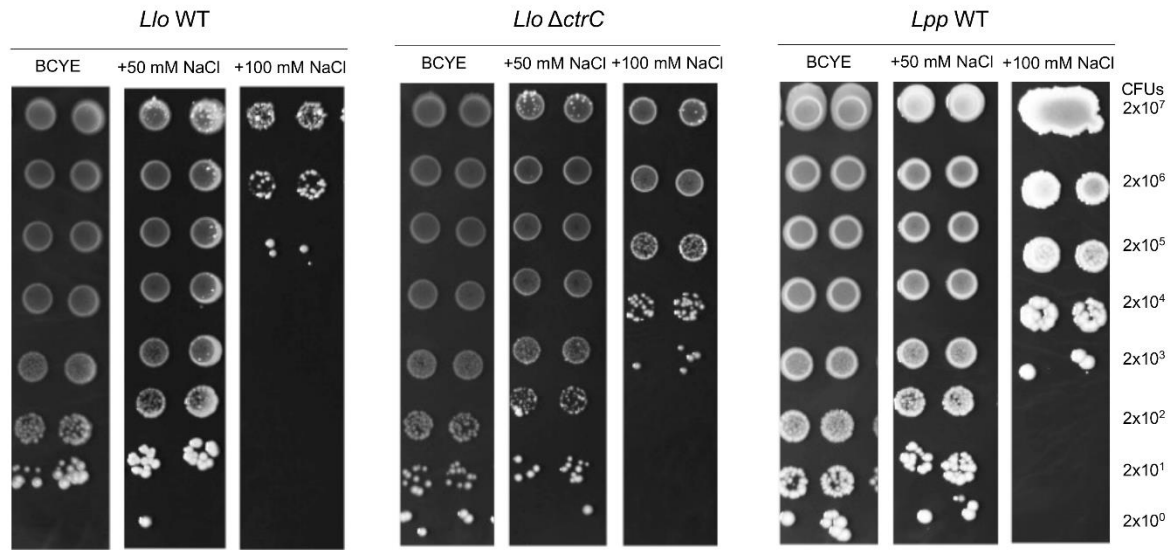
1373



1374

1375 **Figure S11: *L. longbeachae* is inherently more resistant to detergent and oxidative stress**
 1376 **than *L. pneumophila*.** Bacteria were grown to PE phase (OD₆₀₀ 3.7-4.2) in BYE medium for
 1377 each experiment. **A)** Treatment with Tween-20 ± 300 mM NaCl or 300 mM sucrose. **B)**
 1378 Treatment with 2 mM or 10 mM H₂O₂. Representative images of n=2 independent experiments.

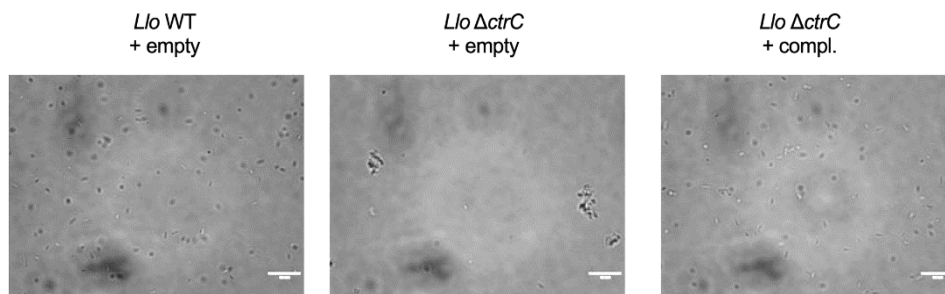
1379



1380

1381 **Figure S12: Growth of *L. longbeachae* WT and capsule mutant strains under salt stress,**
 1382 **compared to *L. pneumophila*.** Cells were grown to PE phase (OD₆₀₀ 3.7-4.2) in BYE medium
 1383 and spotted onto BCYE plates \pm NaCl. Representative images of n=3 independent experiments.

1384



1385

1386 **Figure S13: The capsule mutant agglutinates in the presence of yeast mannan.** Bacteria
 1387 were grown to PE phase (OD₆₀₀ 3.7-4.2), washed, and treated with 1 mg/ml yeast mannan for
 1388 15 minutes. Scale bar = 10 μ m.

Genomic Object Editor: Ilo3148							
PB id	Ident %	Eval	Gene	Description	EC number	Keywords	Organism
Q48462	56.81		0 manC	Mannose-1-phosphate guanylyltransferase	2.7.7.13	Capsule biogenesis/degradation, GTP-binding, Lipopolysaccharide biosynthesis, Nucleotide-binding, Nucleotidyltransferase, Transferase	Klebsiella pneumoniae
Q01410	57.08		0 manC	Mannose-1-phosphate guanylyltransferase	2.7.7.13	GTP-binding, Lipopolysaccharide biosynthesis, Nucleotide-binding, Nucleotidyltransferase, Transferase	Salmonella montevideo
P37753	56.38		0 manC	Mannose-1-phosphate guanylyltransferase	2.7.7.13	GTP-binding, Lipopolysaccharide biosynthesis, Nucleotide-binding, Nucleotidyltransferase, Transferase	Escherichia coli
P26404	56.13		0 rfbM	Mannose-1-phosphate guanylyltransferase RfbM	2.7.7.13	Direct protein sequencing, GTP-binding, Lipopolysaccharide biosynthesis, Nucleotide-binding, Nucleotidyltransferase, Reference proteome, Transferase	Salmonella typhimurium (strain LT2 / SGSC1412 / ATCC 700720)
Q8X7P1	56.14		0 manC1	Mannose-1-phosphate guanylyltransferase 1	2.7.7.13	GTP-binding, Nucleotide-binding, Nucleotidyltransferase, Reference proteome, Transferase	Escherichia coli O157:H7
P07874	55.25		0 algA	Mannose-6-phosphate isomerase / Mannose-1-phosphate guanylyltransferase	5.3.1.8, 2.7.7.13	Alginate biosynthesis, Cobalt, Direct protein sequencing, GTP-binding, Isomerase, Multifunctional enzyme, Nucleotide-binding, Nucleotidyltransferase, Reference proteome, Transferase	Pseudomonas aeruginosa (strain ATCC 15692 / DSM 22644 / CIP 104116 / JCM 14847 / LMG 12228 / 1C / PRS 101 / PAO1)
P24174	55.93		0 manC	Mannose-1-phosphate guanylyltransferase	2.7.7.13	Capsule biogenesis/degradation, GTP-binding, Lipopolysaccharide biosynthesis, Nucleotide-binding, Nucleotidyltransferase, Reference proteome, Transferase	Escherichia coli (strain K12)
P26340	55.93		0 manC	Mannose-1-phosphate guanylyltransferase ManC	2.7.7.13	Capsule biogenesis/degradation, GTP-binding, Lipopolysaccharide biosynthesis, Nucleotide-binding, Nucleotidyltransferase, Reference proteome, Transferase	Salmonella typhimurium (strain LT2 / SGSC1412 / ATCC 700720)
B0RVK6	56.68		0 xanB	Mannose-6-phosphate isomerase / Mannose-1-phosphate guanylyltransferase	5.3.1.8, 2.7.7.13	Exopolysaccharide synthesis, GTP-binding, Isomerase, Lipopolysaccharide biosynthesis, Multifunctional enzyme, Nucleotide-binding, Nucleotidyltransferase, Transferase	Xanthomonas campestris pv. campestris (strain B100)
O85342	56.03		0 manC2	Mannose-1-phosphate guanylyltransferase 2	2.7.7.13	GTP-binding, Lipopolysaccharide biosynthesis, Nucleotide-binding, Nucleotidyltransferase, Reference proteome, Transferase	Escherichia coli O157:H7
P0C7J3	56.47		0 xanB	Mannose-6-phosphate isomerase / Mannose-1-phosphate guanylyltransferase	5.3.1.8, 2.7.7.13	Exopolysaccharide synthesis, GTP-binding, Isomerase, Lipopolysaccharide biosynthesis, Multifunctional enzyme, Nucleotide-binding, Nucleotidyltransferase, Reference proteome, Transferase	Xanthomonas campestris pv. campestris (strain ATCC 33913 / DSM 3586 / NCPPB 528 / LMG 568 / P 25)
Q07024	56.01		0 rfbA	Putative mannose-1-phosphate guanylyltransferase	2.7.7.13	GTP-binding, Lipopolysaccharide biosynthesis, Nucleotide-binding, Nucleotidyltransferase, Reference proteome, Transferase	Vibrio cholerae serotype O1 (strain ATCC 39315 / El Tor Inaba N16961)
Genomic Object Editor: Ilo3149							
PB id	Ident %	Eval	Gene	Description	EC number	Keywords	Organism
D3HMB3	100		0 bexD	Capsule polysaccharide export protein bexD	—	Reference proteome, Signal	Legionella longbeachae serogroup 1 (strain NSW150)
A0A1P8FL76	52.28	2E-127	—	Capsular biosynthesis protein	—	Reference proteome, Signal, Transport	Betaproteobacteria bacterium GR16-43
A0A1I3G2S8	54.64	1E-126	—	Polysaccharide export outer membrane protein	—	Signal	Collimonas sp. OK307
A0A1T4QGS8	51.37	5E-123	—	Polysaccharide export outer membrane protein	—	Signal	Geobacter thiogenes
B3E8Y1	52.47	7E-123	—	Polysaccharide export protein	—	Reference proteome, Signal, Transport	Geobacter lovleyi (strain ATCC BAA-1151 / DSM 17278 / SZ)
Q39JA8	51.61	7E-123	—	Polysaccharide export protein	—	Membrane, Signal, Transmembrane, Transmembrane helix	Burkholderia lata (strain ATCC 17760 / DSM 23089 / LMG 22485 / NCIMB 9086 / R18194 / 383)
A0A1I9YRW4	51.76	6E-122	—	Capsular biosynthesis protein	—	Signal, Transport	Paraburkholderia sprentiae WSM5005
A0A2S5SX59	51.32	1E-121	—	Capsular biosynthesis protein	—	Reference proteome, Signal, Transport	Zhizhongheella caldifontis
A0A0J9DW18	51.1	1E-121	—	Capsular biosynthesis protein	—	Signal	Ralstonia sp. MD27
Q7BMG8	50.68	4E-120	wcbC	Capsular biosynthesis protein	—	Signal	Burkholderia pseudomallei
A0A0F7R2Q8	42.63	1E-98	cpx15D	Capsular polysaccharide export protein D	—	Signal	Actinobacillus pleuropneumoniae
Q44132	42.74	5E-98	cpxD	CpxD	—	Signal	Actinobacillus pleuropneumoniae
A0A059WCS1	42.74	2E-97	cpxD	Sugar ABC transporter substrate-binding protein CpxD	—	Signal	Actinobacillus pleuropneumoniae serovar 8 str. 405
A0A059WNF9	41.84	3E-97	cpxD	Sugar ABC transporter substrate-binding protein CpxD	—	Signal	Actinobacillus pleuropneumoniae
Q9RP76	42.63	1E-95	cpxD	CpxD	—	Signal	Mannheimia haemolytica
Q7WS64	40.53	3E-93	bexD	BexD	—	Signal	Haemophilus influenzae
Q714V0	40.79	2E-92	bexD	BexD	—	Signal	Haemophilus influenzae
Q9L9L6	41.42	3E-87	cexD	CexD	—	Signal	Pasteurella multocida
Q8KS22	39.94	1E-86	ctrA	Capsular transport protein	—	Signal	Neisseria meningitidis
Genomic Object Editor: Ilo3150							
PB id	Ident %	Eval	Gene	Description	EC number	Keywords	Organism
D3HMB4	100	1.00E-153	ctrD	Capsule polysaccharide export ATP-binding protein ctrD (Capsular-polysaccharide-transporting ATPase)	3.6.3.38	ATP-binding, Hydrolase, Nucleotide-binding, Reference proteome	Legionella longbeachae serogroup 1 (strain NSW150)
A0A1I9YRU6	67.59	7.00E-108	—	ATP-binding protein	—	ATP-binding, Cell inner membrane, Cell membrane, Membrane, Nucleotide-binding, Translocase	Paraburkholderia sprentiae WSM5005
A0A1V2XQM1	68.52	3.00E-107	—	ATP-binding protein	—	ATP-binding, Cell inner membrane, Cell membrane, Membrane, Nucleotide-binding, Translocase, Transport	Burkholderia cenocepacia

Supplementary Table 1

Highest hits of the *L. longbeachae* capsule cluster genes against the NCBI database (Trembl).

A0A2U9SFH7	68.06	2.00E-106	_	ABC transporter ATP-binding protein	_	ATP-binding, Cell inner membrane, Cell membrane, Membrane, Nucleotide-binding, Translocase, Transport	Burkholderia sp. JP2-270
B2UAD6	68.22	1.00E-105	_	ABC transporter related	_	ATP-binding, Cell inner membrane, Cell membrane, Membrane, Nucleotide-binding, Reference proteome, Translocase	Ralstonia pickettii (strain 12J)
U3GDS8	68.22	1.00E-105	_	ABC transporter domain-containing protein	_	ATP-binding, Cell inner membrane, Cell membrane, Membrane, Nucleotide-binding, Translocase	Ralstonia sp. 5_2_56FAA
A0A117DUD2	68.69	8.00E-105	_	ABC transporter-like protein	_	ATP-binding, Cell inner membrane, Cell membrane, Membrane, Nucleotide-binding, Translocase	Ralstonia sp. NT80
S9RTK8	68.69	8.00E-105	_	ATP-binding protein	_	ATP-binding, Cell inner membrane, Cell membrane, Membrane, Nucleotide-binding, Translocase	Ralstonia sp. AU12-08
A0A1G8E0F9	67.76	4.00E-104	_	Capsular polysaccharide transport system ATP-binding protein	_	ATP-binding, Cell inner membrane, Cell membrane, Membrane, Nucleotide-binding, Translocase	Paraburkholderia phenazinium
U2FWZ6	67.45	9.00E-104	_	Capsular polysaccharide ABC transporter, ATP-binding protein KpsT	_	ATP-binding, Cell inner membrane, Cell membrane, Membrane, Nucleotide-binding, Translocase, Transport	Burkholderia sp. AU4i
A0A1N6LM37	67.29	4.00E-103	_	Capsular polysaccharide transport system ATP-binding protein	_	ATP-binding, Cell inner membrane, Cell membrane, Membrane, Nucleotide-binding, Translocase, Transport	Burkholderia sp. GAS332
K7QQ86	63.85	6.00E-97	ctrD	CtrD	_	ATP-binding, Nucleotide-binding	Kingella kingae
B3FHD0	63.85	1.00E-94	ctrD	ATP-binding cassette domain-containing protein	_	ATP-binding, Nucleotide-binding	Neisseria meningitidis
B3FHE0	63.38	9.00E-94	ctrD	ATP-binding protein	3.6.3.38	ATP-binding, Hydrolase, Nucleotide-binding	Neisseria meningitidis
Q9S6K7	61.5	6.00E-92	cpxA	Capsule polysaccharide export transport system ATP-binding	_	ATP-binding, Nucleotide-binding	Actinobacillus pleuropneumoniae
Q7B3Y6	60.28	9.00E-91	bexA	BexA	_	ATP-binding, Nucleotide-binding	Haemophilus influenzae
Q44135	61.03	9.00E-91	cpxA	CpxA	_	ATP-binding, Nucleotide-binding	Actinobacillus pleuropneumoniae
O85464	60.09	1.00E-90	hexA	ABC transporter ATP-binding protein	_	ATP-binding, Nucleotide-binding	Pasteurella multocida
Q9L9L9	60.56	3.00E-90	cexA	CexA	_	ATP-binding, Nucleotide-binding	Pasteurella multocida
Q93UJ9	62.25	2.00E-89	wzt2	Wzt2	_	ATP-binding, Cell inner membrane, Cell membrane, Membrane, Nucleotide-binding, Translocase, Transport	Burkholderia pseudomallei
Q9RP79	60.28	2.00E-89	cpxA	Leukotoxin translocation ATP-binding protein LktB	7.4.2.5	ATP-binding, Nucleotide-binding	Mannheimia haemolytica

Genomic Object Editor: Ilo3151

PB id	Ident %	Eval	Gene	Description	EC number	Keywords	Organism
P32015	45.82	9.00E-74	ctrC	Capsule polysaccharide export inner-membrane protein CtrC	_	Capsule biogenesis/degradation, Cell inner membrane, Polysaccharide transport, Transmembrane	Neisseria meningitidis serogroup B (strain MC58)
P57012	45.82	4.00E-71	ctrC	Capsule polysaccharide export inner-membrane protein CtrC	_	Capsule biogenesis/degradation, Cell inner membrane, Polysaccharide transport, Transmembrane	Neisseria meningitidis serogroup A / serotype 4A (strain DSM 15465 / Z2491)
P19391	40.89	1.00E-66	bexB	Capsule polysaccharide export inner-membrane protein BexB	_	Capsule biogenesis/degradation, Cell inner membrane, Polysaccharide transport, Transmembrane	Haemophilus influenzae
P19390	40.4	8.00E-66	bexB	Capsule polysaccharide export inner-membrane protein BexB	_	Capsule biogenesis/degradation, Cell inner membrane, Polysaccharide transport, Transmembrane	Haemophilus influenzae
P22235	40	6.00E-65	bexB	Capsule polysaccharide export inner-membrane protein BexB	_	Capsule biogenesis/degradation, Cell inner membrane, Polysaccharide transport, Transmembrane	Haemophilus influenzae
P24584	26.64	5.00E-23	kpsM	Polysialic acid transport protein KpsM	_	Cell inner membrane, Cell membrane, Membrane, Transmembrane, Transmembrane helix, Transport	Escherichia coli
P23889	26.23	8.00E-22	kpsM	Polysialic acid transport protein KpsM	_	Cell inner membrane, Cell membrane, Membrane, Transmembrane, Transmembrane helix, Transport	Escherichia coli

Genomic Object Editor: Ilo3152

PB id	Ident %	Eval	Gene	Description	EC number	Keywords	Organism
P57034	41	5.00E-90	ctrB	Capsule polysaccharide export inner-membrane protein CtrB	_	Capsule biogenesis/degradation, Cell inner membrane, Polysaccharide transport, Transmembrane	Neisseria meningitidis serogroup A / serotype 4A (strain DSM 15465 / Z2491)
P22930	39.72	2.00E-85	bexC	Capsule polysaccharide export inner-membrane protein BexC	_	Capsule biogenesis/degradation, Cell inner membrane, Polysaccharide transport, Transmembrane	Haemophilus influenzae
P32014	38.78	2.00E-83	ctrB	Capsule polysaccharide export inner-membrane protein CtrB	_	Capsule biogenesis/degradation, Cell inner membrane, Polysaccharide transport, Transmembrane	Neisseria meningitidis serogroup B (strain MC58)
P62586	25.07	7.00E-35	kpsE	Capsule polysaccharide export inner-membrane protein KpsE	_	Capsule biogenesis/degradation, Cell inner membrane, Polysaccharide transport, Transmembrane	Escherichia coli
P42501	25.07	2.00E-34	kpsE	Capsule polysaccharide export inner-membrane protein KpsE	_	Capsule biogenesis/degradation, Cell inner membrane, Polysaccharide transport, Transmembrane	Escherichia coli
P43111	23.98	2.00E-18	vexD	Vi polysaccharide export inner-membrane protein VexD	_	Capsule biogenesis/degradation, Cell inner membrane, Polysaccharide transport, Transmembrane	Salmonella typhi
Q48452	20.75	0.063	_	Putative tyrosine-protein kinase in cps region	2.7.10.-	ATP-binding, Cell inner membrane, Exopolysaccharide synthesis, Nucleotide-binding, Phosphoprotein, Transferase Transmembrane	Klebsiella pneumoniae
Q9F7B1	21.72	0.25	wzc	Tyrosine-protein kinase wzc	2.7.10.-	ATP-binding, Cell inner membrane, Exopolysaccharide synthesis, Nucleotide-binding, Phosphoprotein, Transferase Transmembrane	Salmonella typhimurium (strain LT2 / SGSC1412 / ATCC 700720)

Genomic Object Editor: Ilo3153

PB id	Ident %	Eval	Gene	Description	EC number	Keywords	Organism
-------	---------	------	------	-------------	-----------	----------	----------

Supplementary Table 1

Highest hits of the *L. longbeachae* capsule cluster genes against the NCBI database (Trembl).

D3HMB7	100	0	_	Putative glycosyl transferase group 1	_	Reference proteome, Transferase	Legionella longbeachae serogroup 1 (strain NSW150)
F5YH16	25.36	2.00E-30	_	Glycosyltransferase, family 1	_	Coiled coil, Reference proteome, Transferase	Treponema primitia (strain ATCC BAA-887 / DSM 12427 / ZAS-2)
A0A2P6CAZ8	26.72	3.00E-30	_	Glycos_transf_1 domain-containing protein	_	-	Polaribacter butkevichii
A0A193SEV6	28.15	3.00E-29	_	Putative mannosyltransferase B	_	Glycosyltransferase, Transferase	Klebsiella pneumoniae
I9BN45	27.16	5.00E-29	_	Glycos_transf_1 domain-containing protein	_	Coiled coil	Bacteroides fragilis CL05T12C13
E4VU69	26.98	3.00E-28	_	Glycosyltransferase, group 1 family protein	2.4.-.-	Coiled coil, Glycosyltransferase, Transferase	Bacteroides fragilis 3_1_12
O84909	30.59	7E-14	wbpY	Glycosyltransferase WbpY	_	Transferase	Pseudomonas aeruginosa
Q47594	25.25	7E-12	mtfB	Mannosyltransferase	_	Glycosyltransferase, Transferase	Escherichia coli
Q9RMT9	25.25	7E-12	wbdB	WbdB	_	-	Klebsiella pneumoniae
C8YZ35	27.32	9E-09	wejJ	WejJ	_	-	Escherichia coli
M4QPQ6	31.2	3.00E-08	wbdA	Mannosyltransferase	_	Glycosyltransferase, Transferase	Escherichia coli
Q9RMU0	34.02	2.00E-07	wbdA	WbdA	_	-	Klebsiella pneumoniae
C8YZ32	29.1	2.00E-07	wejI	WejI	_	-	Escherichia coli
Q00481	25.59	2.00E-07	_	Glycosyltransferase	_	Transferase	Salmonella enterica
Q93CS4	41.54	1.00E-06	wbxA	Putative glycosyl transferase	_	Transferase	Shigella boydii
Q9LC66	31.53	2.00E-06	wbdA	Mannosyltransferase	_	Glycosyltransferase, Transferase	Klebsiella pneumoniae
Q47593	31.53	2.00E-06	mtfA	Mannosyltransferase A	_	Glycosyltransferase, Transferase	Escherichia coli
M4QN28	31.53	2.00E-06	wbdA	Mannosyltransferase	_	Glycosyltransferase, Transferase	Escherichia coli

Genomic Object Editor: Ilo3154

PB id	Ident %	Eval	Gene	Description	EC number	Keywords	Organism
D3HMB8	100	0	_	Putative glycosyl transferase, group 1	_	Coiled coil, Reference proteome, Transferase	Legionella longbeachae serogroup 1 (strain NSW150)
A0A254RBS0	36.96	2.00E-76	_	Uncharacterized protein	_	Membrane, Transmembrane, Transmembrane helix	Fibrobacter sp. UWR2
A0A1V4R768	32.1	1.00E-64	_	Glycos_transf_1 domain-containing protein	_	-	Candidatus Cloacimonas sp. 4484_140
A0A2E0ZAU5	34.06	3.00E-56	_	Colanic acid biosynthesis glycosyltransferase WcaL	_	Transferase	Anaerolineaceae bacterium
A0A0P9DL51	31.5	6.00E-52	_	Colanic acid biosynthesis glycosyl transferase	_	Reference proteome, Transferase	Kouleothrix aurantiaca
F2NHK4	32.51	6.00E-51	_	Glycosyl transferase group 1	_	Reference proteome, Transferase	Desulfobacca acetoxidans (strain ATCC 700848 / DSM 11109 / ASRB2)
A0A2V2RIU7	31.47	2.00E-50	_	Colanic acid biosynthesis glycosyltransferase WcaL	_	Transferase	Acidobacteria bacterium
A0A193SBW5	28.34	9.00E-27	wclQ	Glycosyltransferase protein	2.4.1.57	Glycosyltransferase, Transferase	Klebsiella pneumoniae
A4F3K9	26.62	6E-13	aerI	Putative glycosyltransferase	_	Transferase	Planktothrix agardhii NIVA-CYA 126
Q204F0	24.43	6E-11	cps2G	Cps1/2G	_	Glycosyltransferase, Transferase	Streptococcus suis
Q9RHD0	25.96	7E-11	wbpU	Glycosyl transferase-like protein	2.4.1.21	Glycosyltransferase, Transferase	Pseudomonas aeruginosa
Q6L735	26.35	4E-10	_	Glycosyltransferase	_	Glycosyltransferase, Transferase	Streptomyces kanamyceticus
Q8KWP7	29.7	1E-09	cps9vG	Capsular polysaccharide biosynthesis protein Cps4H	2.4.1.21	Glycosyltransferase, Transferase	Streptococcus pneumoniae
D2KXE7	22.45	3E-09	epsG	Putative glycosyltransferase	_	Transferase	Lactobacillus fermentum
Q8GJ89	25.38	4E-09	wbyC	Putative glycosyltransferase	_	Transferase	Yersinia pseudotuberculosis
Q9EVX4	25.2	7E-09	cpsG	Putative hexose transferase	_	Transferase	Streptococcus salivarius
Q00481	27.03	1.00E-08	_	Glycosyltransferase	_	Transferase	Salmonella enterica

Genomic Object Editor: Ilo3155

PB id	Ident %	Eval	Gene	Description	EC number	Keywords	Organism
D3HMB9	100	0	ugd	UDP-glucose 6-dehydrogenase	1.1.1.22	NAD, Oxidoreductase, Reference proteome	Legionella longbeachae serogroup 1 (strain NSW150)
A0A088U1Y7	65.98	0	_	UDP-glucose 6-dehydrogenase	1.1.1.22	NAD, Oxidoreductase	Burkholderia cenocepacia
B3QQB3	65.46	0	_	UDP-glucose 6-dehydrogenase	1.1.1.22	NAD, Oxidoreductase	Chlorobaculum parvum (strain NCIB 8327)
A0A0B0YZU4	64.95	0	ugd	UDP-glucose 6-dehydrogenase	1.1.1.22	NAD, Oxidoreductase	Escherichia coli
D2ZEC2	65.21	0	_	UDP-glucose 6-dehydrogenase	1.1.1.22	NAD, Oxidoreductase	Enterobacter cancerogenus ATCC 35316
A0A132F643	65.72	0	_	UDP-glucose 6-dehydrogenase	1.1.1.22	NAD, Oxidoreductase	Burkholderia pseudomultivorans
A0A2J0NPG5	64.95	0	_	UDP-glucose 6-dehydrogenase	1.1.1.22	NAD, Oxidoreductase	Enterobacter mori
V3QX60	64.95	0	_	UDP-glucose 6-dehydrogenase	1.1.1.22	NAD, Oxidoreductase	Enterobacter sp. MGH 24
A0A0D7LW76	64.69	0	_	UDP-glucose 6-dehydrogenase	1.1.1.22	NAD, Oxidoreductase	Citrobacter freundii
A0A0M7DFE8	64.69	0	ugd	UDP-glucose 6-dehydrogenase	1.1.1.22	NAD, Oxidoreductase	Enterobacter cloacae
A0A0H3CLX6	64.69	0	_	UDP-glucose 6-dehydrogenase	1.1.1.22	NAD, Oxidoreductase	Enterobacter cloacae subsp. cloacae (strain ATCC 13047 / DSM 30054 / NBRC 13355 / NCDC 279-56)
A0A0J9WZA6	64.18	9.00E-178	ugd	UDP-glucose 6-dehydrogenase	1.1.1.22	3D-structure, NAD, Nucleotide-binding, Oxidoreductase	Klebsiella pneumoniae subsp. pneumoniae NTUH-K2044
O06519	63.92	5.00E-177	ugd	UDP-glucose 6-dehydrogenase	1.1.1.22	NAD, Oxidoreductase	Escherichia coli
Q6U8B9	63.66	5.00E-177	ugd	UDP-glucose 6-dehydrogenase	1.1.1.22	NAD, Oxidoreductase	Raoultella terrigena
Q56625	62.11	6.00E-176	_	UDP-glucose 6-dehydrogenase	1.1.1.22	NAD, Oxidoreductase	Vibrio cholerae O139
Q9RP54	63.14	1.00E-174	ugd	UDP-glucose 6-dehydrogenase	1.1.1.22	NAD, Oxidoreductase	Escherichia coli
M9P0X4	60.31	1.00E-169	ugd	UDP-glucose 6-dehydrogenase	1.1.1.22	NAD, Oxidoreductase	Providencia alcalifaciens

Genomic Object Editor: Ilo3156

PB id	Ident %	Eval	Gene	Description	EC number	Keywords	Organism
D3HMC0	100	0	_	Putative glycosyl transferase group 1	_	Reference proteome, Transferase	Legionella longbeachae serogroup 1 (strain NSW150)
H2FUE7	47.1	0	_	Glycosyl transferase group 1	_	Reference proteome, Transferase	Oceanimonas sp. (strain GK1)
A4BRU1	46.78	0	_	Glycosyltransferase	_	Reference proteome, Transferase	Nitrococcus mobilis Nb-231
A0A113JCB7	36.83	2.00E-114	_	Glycosyl transferases group 1	_	Transferase	Nitrosomonas sp. Nm34
A0A0P9U3K9	36.88	6.00E-113	_	Glycos_transf_1 domain-containing protein	_	-	Pseudomonas syringae pv. helianthi
A0A101D0Z2	35.6	1.00E-110	_	Glycos_transf_1 domain-containing protein	_	-	Halomonas sp. 54_146
A0A1H2QA17	35.97	1.00E-107	_	Glycosyltransferase involved in cell wall biosynthesis	_	Transferase	Nitrosomonas communis
A0A114MRS6	36.35	1.00E-106	_	Glycosyl transferases group 1	_	Transferase	Nitrosomonas communis

Supplementary Table 1

Highest hits of the *L. longbeachae* capsule cluster genes against the NCBI database (Trembl).

K9E0G4	35.75	2.00E-105	_	Glycos_transf_1 domain-containing protein	_	Reference proteome	Massilia timonae CCUG 45783
Q9RQU9	29.38	1.00E-31	wbqA	Putative perosamine transferase	_	Transferase	Caulobacter vibrioides
L7S459	34.65	4.00E-08	gwEuk	Glycose transferase group 1 domain protein	_	Transferase	Phytophthora hibernalis
M4QPQ6	28.67	6.00E-08	wbdA	Mannosyltransferase	_	Glycosyltransferase, Transferase	Escherichia coli
L7S4R0	34.65	1.00E-07	gwEuk	Glycose transferase group 1 domain protein	_	Transferase	Phytophthora ramorum
L7SZH1	33.66	3.00E-07	gwEuk 30.30.1	Glycosyltransferase group 1 domain	_	Transferase	Phytophthora lateralis
Q9RMU0	23.38	2.00E-06	wbdA	WbdA	_	_	Klebsiella pneumoniae

Genomic Object Editor: Ilo3157

PB id	Ident %	Eval	Gene	Description	EC number	Keywords	Organism
D3HMC1	100	0	_	Uncharacterized protein	_	Coiled coil, Reference proteome	Legionella longbeachae serogroup 1 (strain NSW150)
A0A2S4KG72	25.84	1.00E-33	_	Uncharacterized protein	_	Coiled coil	Diaphorobacter sp. LR2014-1
A0A2D4Y0U4	22.8	3.00E-24	_	Uncharacterized protein	_	Coiled coil	Sphingomonadaceae bacterium
A0A011N114	28.01	1.00E-21	_	Uncharacterized protein	_	Coiled coil	Candidatus Accumulibacter sp. BA-92
A0A2T7UAV0	23.98	2.00E-21	_	Uncharacterized protein	_	Coiled coil	Limnohabitans planktonicus II-D5
A0A1H8X4C5	34.33	1.00E-17	_	Uncharacterized protein	_	_	Pseudomonas sp. Snoq117.2
A0A0K8NZ38	26.47	3.00E-17	_	Uncharacterized protein	_	Coiled coil, Reference proteome	Ideonella sakaiensis (strain NBRC 110686 / TISTR 2288 / 201-F6)
D0QYN0	23.73	1E-12	ccbE	CcbE	_	Coiled coil	Avibacterium paragallinarum
D0QYN6	22.59	3E-12	ccbE	CcbE	_	Coiled coil	Avibacterium paragallinarum
Q9DUN0	31.97	1.00E-08	_	Orf73	_	3D-structure	Human herpesvirus 8
Q91LX9	31.97	1.00E-08	_	ORF73	_	_	Human herpesvirus 8
W5U981	24.81	1.00E-08	_	Htt	_	_	Homo sapiens
Q76SB0	29.41	2.00E-08	_	ORF 73	_	3D-structure	Human herpesvirus 8 type M
Q98148	29.41	2.00E-08	_	Kaposi's sarcoma-associated herpes-like virus ORF73 homolog	_	3D-structure	Human herpesvirus 8
E5LC01	31.15	2.00E-08	ORF73	LANA	_	_	Human herpesvirus 8
Q9DUM3	31.97	2.00E-08	_	Latent nuclear antigen	_	3D-structure	Human herpesvirus 8
Q2KPA5	27.05	4.00E-08	_	Clock	_	Coiled coil, DNA-binding, Repeat	Macrobrachium rosenbergii
D0QYL8	22.3	1.00E-07	acbE	AcbE	_	Coiled coil	Avibacterium paragallinarum
B5SUM8	23.18	4.00E-07	MED15	Mediator of RNA polymerase II transcription subunit 15	_	Activator, Coiled coil, Nucleus, Transcription, Transcription regulation	Hyla arborea

Genomic Object Editor: Ilo3158

PB id	Ident %	Eval	Gene	Description	EC number	Keywords	Organism
D3HMC2	100	0	_	Uncharacterized protein	_	Coiled coil, Reference proteome	Legionella longbeachae serogroup 1 (strain NSW150)
A0A1R4GY81	23.72	9.00E-54	_	Uncharacterized protein	_	Coiled coil, Reference proteome	Crenothrix polyspora
A0A1Y11YW1	25.57	4.00E-50	_	Signal recognition particle receptor protein FlsY	_	Coiled coil, Receptor	Comamonas testosteroni
A0A114MS07	24.75	1.00E-49	_	Uncharacterized protein	_	Coiled coil	Nitrosomonas communis
A0A096GZV8	23.08	3.00E-45	_	Methyltransf_21 domain-containing protein	_	Coiled coil	Comamonas testosteroni
A0A113JE51	24.08	4.00E-41	_	Uncharacterized protein	_	Coiled coil	Nitrosomonas sp. Nm34
D6Z4R0	24.66	6.00E-41	_	Chromosome segregation ATPase-like protein	_	Coiled coil, Reference proteome	Desulfurivibrio alkaliphilus (strain DSM 19089 / UNIQEM U267 / AHT2)
A0A0W7Z290	25.41	8.00E-41	_	Uncharacterized protein	_	Coiled coil, Reference proteome	Comamonas kerstersii
A0A0F7KD18	25.04	1.00E-39	_	Uncharacterized protein	_	Coiled coil, Reference proteome	Nitrosomonas communis
A0A1F9IRE7	26.98	2.00E-38	_	Uncharacterized protein	_	Coiled coil	Deltaproteobacteria bacterium RIFCSLOWO2_02_FULL_53_8
Q6X1Y7	22.33	4.00E-24	lepB	Effector protein B	_	Coiled coil, Transmembrane	Legionella pneumophila
Q5ZSM7	22.33	4.00E-24	lepB	LepB	_	Coiled coil, Transmembrane	Legionella pneumophila subsp. pneumophila (strain Philadelphia 1 / ATCC 33152 / DSM 7513)
Q7K5Q6	26.48	4.00E-23	maebl	Erythrocyte binding protein 3	_	Coiled coil, Signal	Plasmodium falciparum
Q8T5C7	26.48	4.00E-23	maebl	Chimeric erythrocyte-binding protein MAEBL	_	Coiled coil, Signal, Transmembrane	Plasmodium falciparum
Q7K5Q5	26.48	4.00E-23	maebl	Erythrocyte binding protein 2	_	Coiled coil, Signal	Plasmodium falciparum
E5LC01	20.78	1.00E-22	ORF73	LANA	_	_	Human herpesvirus 8
Q6A178	26.8	2.00E-22	mt1	Myosin tail 1 protein	_	Coiled coil	Cryptosporidium parvum
Q91LX9	21.05	3.00E-22	_	ORF73	_	_	Human herpesvirus 8
Q25893	26.88	5.00E-22	LSA-1	Liver stage antigen	_	Membrane, Transmembrane, Transmembrane helix	Plasmodium falciparum
O44934	23.21	9.00E-22	_	Myosin heavy chain isoform A	_	Actin-binding, ATP-binding, Coiled coil, Myosin, Nucleotide-binding	Doryteuthis pealeii
G1EIL6	20.49	1.00E-21	tnks1bp1	Tankyrase 1 binding protein 1	_	_	Danio rerio
Q9U0S6	23.82	1.00E-20	prm MHC	Pedal retractor muscle myosin heavy chain	_	Actin-binding, ATP-binding, Coiled coil, Myosin, Nucleotide-binding	Mytilus galloprovincialis
A0A140UGH3	23.68	1.00E-20	_	Myosin 2 heavy chain striated muscle	_	Actin-binding, ATP-binding, Coiled coil, Myosin, Nucleotide-binding	Aphonopelma

Genomic Object Editor: Ilo3159

PB id	Ident %	Eval	Gene	Description	EC number	Keywords	Organism
D3HMC3	100	0	_	Uncharacterized protein	_	Reference proteome	Legionella longbeachae serogroup 1 (strain NSW150)
A4BRT8	41.15	5.00E-131	_	Uncharacterized protein	_	Reference proteome	Nitrococcus mobilis Nb-231
A0A1H3CQ84	58.71	1.00E-69	_	Uncharacterized protein	_	Reference proteome	Roseicetrum antarcticum
A0A1X7A7H2	42.42	6.00E-66	_	Uncharacterized protein	_	Coiled coil, Reference proteome	Limimariicola soesokkakensis
A0A1Q4CSG6	55.22	1.00E-64	_	Uncharacterized protein	_	_	Rhodobacterales bacterium 65-51
A0A2E9GVE9	42.72	4.00E-48	_	Uncharacterized protein	_	_	Deltaproteobacteria bacterium
A0A2E6LM58	35.68	2.00E-30	_	Methyltransf_21 domain-containing protein	_	Coiled coil	Gammmaproteobacteria bacterium
A0A0F7KKU9	35.58	2.00E-29	_	Methyltransf_21 domain-containing protein	_	Coiled coil, Reference proteome	Nitrosomonas communis
A0A113JDG0	35.58	2.00E-29	_	Methyltransferase, FkbM family	_	Coiled coil, Methyltransferase, Transferase	Nitrosomonas sp. Nm34
A0A1H2Q970	42.41	2.00E-27	_	Methyltransferase, FkbM family	_	Methyltransferase, Transferase	Nitrosomonas communis

Genomic Object Editor: Ilo3160

PB id	Ident %	Eval	Gene	Description	EC number	Keywords	Organism
D3HMC4	100	4.00E-170	_	Putative lipopolysaccharide core biosynthesis protein	_	Reference proteome	Legionella longbeachae serogroup 1 (strain NSW150)
A0A0P7WRL6	64.44	4.00E-105	_	Uncharacterized protein	_	_	Idiomarinaceae bacterium HL-53
A0A1Q4CSD3	53.78	2.00E-81	_	Uncharacterized protein	_	_	Rhodobacteriales bacterium 65-51
A4BRT7	58.29	6.00E-81	_	Uncharacterized protein	_	Reference proteome	Nitrococcus mobilis Nb-231
A0A1H9L2A0	52.73	1.00E-79	_	Uncharacterized protein	_	Reference proteome	Litorimicrobium taeanense
A0A254QKC4	52.65	2.00E-79	_	Uncharacterized protein	_	Reference proteome	Phaeobacter sp. 22111-1F12B
A0A1V0RJS1	54.13	5.00E-78	_	Uncharacterized protein	_	_	Roseovarius mucosus
K1XV28	52.27	6.00E-73	_	Uncharacterized protein	_	_	uncultured bacterium
A0YTV4	51.83	1.00E-72	_	TPR_REGION domain-containing	_	Coiled coil, Reference proteome, TPR repeat	Lyngbya sp. (strain PCC 8106)
Q9XC98	26.44	0.003	_	Lipopolysaccharide core biosynthesis protein RfaZ	_	Membrane, Transferase, Transmembrane, Transmembrane helix	Klebsiella pneumoniae
I7AU32	27.78	0.62	waaZ	3-deoxy-D-manno-oct-2-ulosonate III transferase WaaZ	2.4.99.15	Glycosyltransferase, Transferase	Escherichia coli

Genomic Object Editor: Ilo3161

PB id	Ident %	Eval	Gene	Description	EC number	Keywords	Organism
D3HMC5	100	0	_	Putative glycosyl transferase family 2	_	Reference proteome, Transferase	Legionella longbeachae serogroup 1 (strain NSW150)
Q07Z86	59.24	9.00E-140	_	Glycosyl transferase, family 2	_	Reference proteome, Transferase	Shewanella frigidimarina (strain NCIMB 400)
A0A0P8B481	60.88	1.00E-130	_	Family 2 glycosyltransferase	_	Transferase	Idiomarinaceae bacterium HL-53
A0A0F7M0S2	54.78	2.00E-122	_	Glycosyl transferase	_	Reference proteome, Transferase	Spongiibacter sp. IMCC21906
A0A1B7WX93	57	3.00E-119	_	Glycosyl transferase family 2	_	Transferase	Anabaena sp. MDT14b
A0A1G1H1U7	58.36	2.00E-117	_	Glycosyl transferase family 2	_	Transferase	Nitrospirae bacterium GWC2_57_9
A0A1X7A7Q4	51.1	7.00E-113	_	N-glycosyltransferase	_	Reference proteome, Transferase	Limimariicola soesokkakensis
A0A090SRU4	54.79	3.00E-112	_	Glyco_trans_2-like domain-containing protein	_	_	Vibrio maritimus
A0A1W9GAI3	54.61	1.00E-110	_	Glycosyl transferase family 2	_	Transferase	Nitrospira sp. SG-bin2
A0A1V0RJU4	50.47	3.00E-109	_	Putative glycosyl transferase	_	Transferase	Roseovarius mucosus
Q3ZK45	41.07	2.00E-20	epsG	EpsG	_	_	Lactococcus lactis
O66259	30.32	2E-14	_	Glycosyltransferase	_	Transferase	Aggregatibacter actinomycetemcomitans
Q9XDQ0	30.67	1E-13	ORF14	Putative glycosyltransferase	_	Transferase	Aggregatibacter actinomycetemcomitans
Q54129	31.22	2E-11	wbaN	Rhamnosyl transferase	_	Transferase	Salmonella enterica
Q9AQA9	30	5E-11	_	Putative rhamnosyltransferase	_	Transferase	Aggregatibacter actinomycetemcomitans
K4P2X6	33.33	3.00E-07	wbyL	WbyL	_	_	Yersinia similis
Q8GNC0	30.56	2.00E-06	lgtA	N-acetylglucosamine glycosyltransferase	_	Transferase	Haemophilus ducreyi

Genomic Object Editor: Ilo3162

PB id	Ident %	Eval	Gene	Description	EC number	Keywords	Organism
D3HMC6	100	3.00E-161	_	Putative acylneuraminatase cytidylyltransferase	_	Nucleotidyltransferase, Reference proteome, Transferase	Legionella longbeachae serogroup 1 (strain NSW150)
K2JYG6	70.45	2.00E-106	_	Acylneuraminatase cytidylyltransferase	_	Nucleotidyltransferase, Reference proteome, Transferase	Gallaecimonas xiamenensis 3-C-1
A0A0F7M0J7	68.66	6.00E-104	_	CMP-N-acetylneuraminic acid synthetase	_	Reference proteome	Spongiibacter sp. IMCC21906
A0A0M1JD43	68.42	8.00E-101	_	Acylneuraminatase cytidylyltransferase	_	Nucleotidyltransferase, Reference proteome, Transferase	Achromatium sp. WMS3
A0A0M1J3Y3	67.94	1.00E-99	_	Acylneuraminatase cytidylyltransferase	_	Nucleotidyltransferase, Reference proteome, Transferase	Achromatium sp. WMS3
A0A011NPN0	65.9	1.00E-97	_	3-deoxy-manno-octulosonate cytidylyltransferase	_	Nucleotidyltransferase, Reference proteome, Transferase	Candidatus Accumulibacter sp. SK-11
A0A250KNV9	66.21	2.00E-97	_	Acylneuraminatase cytidylyltransferase	_	Nucleotidyltransferase, Reference proteome, Transferase	Methylocaldum marinum
A0A1H9KWA5	63.27	2.00E-96	_	CMP-N-acetylneuraminic acid synthetase	_	Reference proteome	Litorimicrobium taeanense
A0A0N8KBF2	66.51	4.00E-96	neuA	N-acetylneuraminatase cytidylyltransferase NeuA	_	Nucleotidyltransferase, Transferase	Idiomarinaceae bacterium HL-53
A0A254QKC9	65.75	2.00E-95	_	Acylneuraminatase cytidylyltransferase	_	Nucleotidyltransferase, Reference proteome, Transferase	Phaeobacter sp. 22111-1F12B
Q933W2	23.64	1.00E-07	neuA1	Acylneuraminatase cytidylyltransferase	_	Nucleotidyltransferase, Transferase	Campylobacter jejuni
Q077S2	21.98	2.00E-07	naaC	Acylneuraminatase cytidylyltransferase	2.7.7.43	Nucleotidyltransferase, Transferase	Escherichia coli

Genomic Object Editor: Ilo3163

PB id	Ident %	Eval	Gene	Description	EC number	Keywords	Organism
D3HMC7	100	0	_	Putative D-isomer specific 2-hydroxyacid dehydrogenase	_	NAD, Oxidoreductase, Reference proteome	Legionella longbeachae serogroup 1 (strain NSW150)
B8CL20	68.06	8.00E-152	_	D-isomer specific 2-hydroxyacid dehydrogenase, catalytic region, D-isomer specific 2-hydroxyacid dehydrogenase, NAD-binding	_	NAD, Oxidoreductase	Shewanella piezotolerans (strain WP3 / JCM 13877)
Q07Z88	67.2	1.00E-150	_	D-isomer specific 2-hydroxyacid dehydrogenase, NAD-binding	_	NAD, Oxidoreductase, Reference proteome	Shewanella frigidimarina (strain NCIMB 400)
A0A0P7ZKZ6	66.56	8.00E-147	serA	D-3-phosphoglycerate dehydrogenase	1.1.1.95	NAD, Oxidoreductase	Idiomarinaceae bacterium HL-53
A0A0C3MQY8	65.05	2.00E-143	_	Phosphoglycerate dehydrogenase	_	NAD, Oxidoreductase	Shewanella sp. cp20
A4BRT3	60.91	3.00E-133	_	Phosphoglycerate dehydrogenase	_	NAD, Oxidoreductase, Reference proteome	Nitrococcus mobilis Nb-231
A0A254QKD0	60.33	3.00E-126	_	Phosphoglycerate dehydrogenase	_	Oxidoreductase, Reference proteome	Phaeobacter sp. 22111-1F12B
A0A0P1EMI7	58.55	1.00E-124	serA_2	D-3-phosphoglycerate dehydrogenase	1.1.1.95	Oxidoreductase, Reference proteome	Shimia marina
A0A1Q4CSG3	59.22	3.00E-124	_	Phosphoglycerate dehydrogenase	_	Oxidoreductase	Rhodobacteriales bacterium 65-51
A0A1X7A7P1	58.17	1.00E-123	tkrA_2	Glyoxylate/hydroxypyruvate reductase B	1.1.1.79	Oxidoreductase, Pyruvate, Reference proteome	Limimariicola soesokkakensis
F8AEA4	35.64	8.00E-37	gyaR	Glyoxylate reductase	1.1.1.26	3D-structure, Cytoplasm, NAD, Oxidoreductase	Pyrococcus yayanosii (strain CH1 / JCM 16557)
Q2TL63	32.23	2.00E-32	_	D-3-phosphoglycerate dehydrogenase	1.1.1.95	Amino-acid biosynthesis, NAD, Oxidoreductase, Serine biosynthesis	Mesorhizobium ciceri
A8RON0	30.55	1.00E-31	ApPGDH	D-3-phosphoglycerate dehydrogenase	1.1.1.95	Amino-acid biosynthesis, NAD, Oxidoreductase, Serine biosynthesis	Aphanethece halophytica

Supplementary Table 1

Highest hits of the *L. longbeachae* capsule cluster genes against the NCBI database (Trembl).

U5TVU1	32.22	4.00E-27	mcyI	McyI	—	Oxidoreductase	Nostoc sp. 152
G4XDR8	32.37	2.00E-26	ptxD	Phosphite dehydrogenase	—	3D-structure, Oxidoreductase	Ralstonia sp. 4506

Genomic Object Editor: Ilo3164

PB id	Ident %	Eval	Gene	Description	EC number	Keywords	Organism
Q8KWT4	31.47	5.00E-25	bacC	Dihydroantocapsin 7-dehydrogenase	1.1.1.385	Antibiotic biosynthesis, NAD, Oxidoreductase	Bacillus subtilis
Q9WYG0	32.51	1.00E-24	—	Uncharacterized oxidoreductase TM_0325	1.-.-.-	Oxidoreductase, Reference proteome	Thermotoga maritima (strain ATCC 43589 / MSB8 / DSM 3109 / JCM 10099)
P39640	30	2.00E-23	bacC	Dihydroantocapsin 7-dehydrogenase	1.1.1.385	3D-structure, Antibiotic biosynthesis, NAD, Oxidoreductase, Reference proteome	Bacillus subtilis (strain 168)
P50199	28.81	2.00E-23	gno	Gluconate 5-dehydrogenase	1.1.1.-	Carbohydrate metabolism, Cytoplasm, Direct protein sequencing, NADP, Oxidoreductase, Reference proteome	Gluconobacter oxydans (strain 621H)
Q56318	29.27	9.00E-23	—	Uncharacterized oxidoreductase TM_0019	1.-.-.-	NADP, Oxidoreductase, Reference proteome	Thermotoga maritima (strain ATCC 43589 / MSB8 / DSM 3109 / JCM 10099)
P40288	28.23	1.00E-21	—	Glucose 1-dehydrogenase	1.1.1.47	3D-structure, Direct protein sequencing, NADP, Oxidoreductase, Sporulation	Bacillus megaterium
Q51576	29.64	1.00E-21	—	Uncharacterized oxidoreductase PA3106	1.-.-.-	NADP, Oxidoreductase, Reference proteome	Pseudomonas aeruginosa (strain ATCC 15692 / DSM 22644 / CIP 104116 / JCM 14847 / LMG 12228 / 1C / PRS 101 / PAO1)
P39482	27.35	1.00E-21	gdhI	Glucose 1-dehydrogenase 1	1.1.1.47	Germination, NADP, Oxidoreductase, Sporulation	Bacillus megaterium
P46331	30.08	2.00E-21	yxbG	Uncharacterized oxidoreductase YxbG	1.-.-.-	NAD, Oxidoreductase, Reference proteome	Bacillus subtilis (strain 168)
Q92RN6	34.74	4.00E-21	galD	Probable galactose dehydrogenase GalD	1.1.1.-	NADP, Oxidoreductase, Reference proteome	Rhizobium meliloti (strain 1021)
P08074	30.36	6.00E-21	Cbr2	Carbonyl reductase	NADPH 2	1.1.1.184	2455724, 7705352, 15489334, 8040004, 8999926, 21183079, 8805511
P05406	31.64	8.00E-21	fixR	Protein FixR	—	Nitrogen fixation, Oxidoreductase, Reference proteome	Bradyrhizobium diazoefficiens (strain JCM 10833 / BCRC 13528 / IAM 13628 / NBRC 14792 / USDA 110)
Q53882	28.96	8.00E-21	dauE	Aklaviketone reductase DauE	1.1.1.362	Antibiotic biosynthesis, NADP, Oxidoreductase	Streptomyces sp. (strain C5)

Genomic Object Editor: Ilo3165

PB id	Ident %	Eval	Gene	Description	EC number	Keywords	Organism
D3HMC9	100	0	—	Putative glycosyl transferase family 2	—	Reference proteome, Transferase	Legionella longbeachae serogroup 1 (strain NSW150)
A4BRT1	62.34	0	—	Uncharacterized protein	—	Reference proteome	Nitrococcus mobilis Nb-231
A0A1X7A785	58.81	0	—	Uncharacterized protein	—	Coiled coil, Reference proteome	Limimariicola soesokkakensis
A0A239Q0E7	54.37	0	—	Methyltransferase domain-containing protein	—	Coiled coil, Membrane, Methyltransferase, Reference proteome, Transferase, Transmembrane, Transmembrane helix	Amphiplicatus metritiotherophilus
A0A2E7LM08	49.77	0	—	Glycosyl transferase family 2	—	Transferase	Dehalococcoidia bacterium
A0A1Q4CSM0	47.31	0	—	Uncharacterized protein	—	—	Rhodobacterales bacterium 65-51
A0A2M7GNM0	70.08	8.00E-129	—	Uncharacterized protein	—	Coiled coil, Membrane, Transmembrane, Transmembrane helix	Rhodobacterales bacterium CG15_BIG_FIL_POST_REV_8_21_14_020_59_13
K2KDH9	58.53	4.00E-99	—	Uncharacterized protein	—	Reference proteome	Gallaecimonas xiamenensis 3-C-1
B8CL24	59.92	1.00E-96	—	Uncharacterized protein	—	—	Shewanella piezotolerans (strain WP3 / JCM 13877)

Genomic Object Editor: Ilo3166

PB id	Ident %	Eval	Gene	Description	EC number	Keywords	Organism
D3HMD0	100	0	galE	UDP-glucose 4-epimerase	5.1.3.2	Carbohydrate metabolism, Isomerase, NAD, Reference proteome	Legionella longbeachae serogroup 1 (strain NSW150)
D3HMD6	63.44	1.00E-160	galE	UDP-glucose 4-epimerase	5.1.3.2	Carbohydrate metabolism, Isomerase, NAD, Reference proteome	Legionella longbeachae serogroup 1 (strain NSW150)
R4YS92	56.36	1.00E-131	galE	UDP-glucose 4-epimerase	5.1.3.2	Carbohydrate metabolism, Isomerase, NAD, Reference proteome	Oleispira antarctica RB-8
A0A2C4RG95	55.49	6.00E-129	galE	UDP-glucose 4-epimerase	5.1.3.2	Carbohydrate metabolism, Isomerase, NAD	Bacillus sp. AFS043905
A0A1H9KXM1	56.36	6.00E-127	—	UDP-glucose 4-epimerase	5.1.3.2	Carbohydrate metabolism, Isomerase, NAD	Butyrivibrio fibrisolvens
A0A1M6BZ40	56.06	1.00E-126	—	UDP-glucose 4-epimerase	5.1.3.2	Carbohydrate metabolism, Isomerase, NAD	Butyrivibrio fibrisolvens DSM 3071
A0A1H9ELV8	55.76	5.00E-126	—	UDP-glucose 4-epimerase	5.1.3.2	Carbohydrate metabolism, Isomerase, NAD, Reference proteome	Butyrivibrio sp. TB
A0A098L0R3	55.79	1.00E-124	—	UDP-glucose 4-epimerase	5.1.3.2	Carbohydrate metabolism, Coiled coil, Isomerase, NAD	Geobacillus thermoleovorans B23
A0A1G8VHA8	54.55	1.00E-124	—	UDP-glucose 4-epimerase	5.1.3.2	Carbohydrate metabolism, Coiled coil, Isomerase, NAD, Reference proteome	Lachnospiraceae bacterium G41
M5WMM1	53.5	1.00E-114	UGE	UDP-glucose 4-epimerase	5.1.3.-	Carbohydrate metabolism, Isomerase, NAD, Reference proteome	Prunus persica
Q58IJ6	53.33	3.00E-113	UGE1	UDP-glucose 4-epimerase	5.1.3.-	Carbohydrate metabolism, Coiled coil, Isomerase, NAD	Hordeum vulgare
Q9RP56	50.3	7.00E-113	galE	UDP-glucose 4-epimerase	5.1.3.2	Carbohydrate metabolism, Isomerase, NAD	Escherichia coli
Q58IJ5	50.45	4.00E-110	UGE2	UDP-glucose 4-epimerase	5.1.3.-	Carbohydrate metabolism, Isomerase, NAD	Hordeum vulgare
A0A2D0W0L9	49.24	1.00E-109	gne	UDP-glucose 4-epimerase	5.1.3.2	Carbohydrate metabolism, Isomerase, NAD	Escherichia fergusonii
Q2QD27	50	2.00E-109	gne	UDP-glucose 4-epimerase	5.1.3.2	Carbohydrate metabolism, Isomerase, NAD	Aeromonas hydrophila
M9VRS7	48.77	2.00E-109	galE2	UDP-glucose 4-epimerase	5.1.3.2	Carbohydrate metabolism, Isomerase, NAD	Streptococcus oralis

Genomic Object Editor: Ilo3167

PB id	Ident %	Eval	Gene	Description	EC number	Keywords	Organism
D3HMD1	100	0	gmd	GDP-mannose 4,6-dehydratase	4.2.1.47	Lyase, NADP, Reference proteome	Legionella longbeachae serogroup 1 (strain NSW150)
A0A024HQL7	76.09	0	bre-1	GDP-mannose 4,6-dehydratase	4.2.1.47	Lyase, NADP, Reference proteome	Pseudomonas knackmussii (strain DSM 6978 / LMG 23759 / B13)
A0A0A7EDA1	75.66	0	gmd	GDP-mannose 4,6-dehydratase	4.2.1.47	Lyase, NADP, Reference proteome	Pseudoalteromonas piratica
A0A0Q5FPZ0	75.22	0	gmd	GDP-mannose 4,6-dehydratase	4.2.1.47	Lyase, NADP	Pseudomonas sp. Leaf127
V9UXM5	74.34	0	gmd	GDP-mannose 4,6-dehydratase	4.2.1.47	Lyase, NADP	Pseudomonas montelii SB3101
A0A177YY40	74.93	0	gmd_1	GDP-mannose 4,6-dehydratase	4.2.1.47	Lyase, NADP	Pseudomonas putida
A0A2J81D5	75.66	0	gmd	GDP-mannose 4,6-dehydratase	4.2.1.47	Lyase, NADP	Vibrio diazotrophicus
A0A2S5IDD8	74.93	0	gmd	GDP-mannose 4,6-dehydratase	4.2.1.47	Lyase, NADP	Pseudomonas aeruginosa

Supplementary Table 1

Highest hits of the *L. longbeachae* capsule cluster genes against the NCBI database (Trembl).

R1XR6	75.37	0	gmd	GDP-mannose 4,6-dehydratase	4.2.1.47	Lyase, NADP	Grimontia indica
A0A2V4KC88	74.93	0	gmd	GDP-mannose 4,6-dehydratase	4.2.1.47	Lyase, NADP	Pseudomonas sp. MB-090624
A0A147GBA3	74.64	0	gmd	GDP-mannose 4,6-dehydratase	4.2.1.47	Lyase, NADP	Pseudomonas parafulva
F3KBD8	75.07	0	gmd	GDP-mannose 4,6-dehydratase	4.2.1.47	Lyase, NADP, Reference proteome	gamma proteobacterium IMCC2047
C8YZ33	74.49	0	gmd	GDP-mannose 4,6-dehydratase	4.2.1.47	Lyase, NADP	Escherichia coli
D2KWB3	73.47	0	gmd	GDP-mannose 4,6-dehydratase	4.2.1.47	Lyase, NADP	Pseudomonas savastanoi pv. glycinea
M4HNX2	71.51	6.00E-179	boeN	GDP-mannose 4,6-dehydratase	4.2.1.47	Lyase, NADP	Burkholderia cepacia
K4NNR8	53.26	8.00E-121	gmd	GDP-mannose 4,6-dehydratase	4.2.1.47	Lyase, NADP	Yersinia similis
Q9R966	51.63	4.00E-120	gmd	GDP-mannose 4,6-dehydratase	4.2.1.47	Lyase, NADP	Brucella melitensis
O85352	53.1	4.00E-120	gmd	GDP-mannose 4,6-dehydratase	4.2.1.47	Lyase, NADP	Caulobacter vibrioides
Q5ND85	52.26	8.00E-116	gmd	GDP-mannose 4,6-dehydratase	4.2.1.47	Lyase, NADP	Yersinia sp. A125 KOH2
A0A1B1R128	52.68	9.00E-116	GMD2	GDP-mannose 4,6-dehydratase	4.2.1.47	Lyase	Mortierella alpina
F1CLL6	51.15	1.00E-115	gmd	GDP-mannose 4,6-dehydratase	4.2.1.47	Lyase, NADP	Yersinia pseudotuberculosis
Q6T1X7	53.89	1.00E-115	gmd	GDP-mannose 4,6-dehydratase	4.2.1.47	Lyase, NADP	Aneurinibacillus thermoaerophilus

Genomic Object Editor: Ilo3168

PB id	Ident %	Eval	Gene	Description	EC number	Keywords	Organism
D3HMD2	100	0	_	Putative capsular polysaccharide biosynthesis protein	_	Coiled coil, Reference proteome	Legionella longbeachae serogroup 1 (strain NSW150)
A0A1Q4CWN3	47.39	6.00E-88	_	Wcbl domain-containing protein	_	Coiled coil	Rhodobacteriales bacterium 65-51
A0A2H4UTY7	28.2	5.00E-24	_	Wcbl domain-containing protein	_	Reference proteome	Bodo saltans virus
A0A2N1DBJ2	26.25	7E-10	_	Wcbl domain-containing protein	_	Reference proteome	Paraglaciocola sp. MB-3u-78
U7Q8X3	22.59	7E-09	_	Nucleotide-diphospho-sugar	_	Transferase	Lyngbya aestuarii BL J
A0A1M7TIW0	28.49	9.00E-07	_	Wcbl domain-containing protein	_	Reference proteome	Desulfovibrio litoralis DSM 11393
Q93UJ4	25.22	1.00E-04	wcbl	Wcbl	_	_	Burkholderia pseudomallei
Q63R74	24.78	3.00E-04	wcbl	Putative capsular polysaccharide biosynthesis protein	_	3D-structure, Reference proteome	Burkholderia pseudomallei (strain K96243)

Genomic Object Editor: Ilo3169

PB id	Ident %	Eval	Gene	Description	EC number	Keywords	Organism
D3HMD3	99.03	1.00E-66	_	Uncharacterized protein	_	Membrane, Reference proteome, Transmembrane, Transmembrane helix	Legionella longbeachae serogroup 1 (strain NSW150)
NO MORE HITS!							

Genomic Object Editor: Ilo3170

PB id	Ident %	Eval	Gene	Description	EC number	Keywords	Organism
D3HMD4	100	0	_	SGL domain-containing protein	_	Reference proteome	Legionella longbeachae serogroup 1 (strain NSW150)
A0A1J8P5Y9	40.71	8.00E-59	_	Gluconolactonase	_	_	Candidatus Rickettsiella isopodorum
K2D0F4	38.67	4.00E-58	_	SMP-30/Gluconolactonase/LRE protein	_	_	uncultured bacterium
A0A1G0G7G2	38.67	4.00E-58	_	SGL domain-containing protein	_	_	Gammaproteobacteria bacterium RIFCSPHIGHO2_02_FULL_39_13
A8PKQ3	38.43	9.00E-58	_	SMP-30/Gluconolactonase/LRE protein	_	Reference proteome	Rickettsiella grylli
A0A1Y5DM83	34.91	9.00E-53	_	SGL domain-containing protein	_	_	Arcobacter sp. 31_11_sub10_T18
A9KEW0	34.96	1.00E-52	_	Gluconolactonase	3.1.1.17	Hydrolase	Coxiella burnetii (strain Dugway 5J108-111)
A0A2E5LWQ5	40.32	2.00E-52	_	Gluconolactonase	_	_	Dehalococcoidia bacterium
A0A1G0GPR6	37.8	2.00E-52	_	SGL domain-containing protein	_	_	Gammaproteobacteria bacterium RIFCSPHIGHO2_12_FULL_36_30
Q83AU0	34.59	2.00E-51	_	Gluconolactonase	3.1.1.17	Hydrolase, Reference proteome	Coxiella burnetii (strain RSA 493 / Nine Mile phase I)
A9CPS8	26.84	9.00E-19	GNL	Lactonase	_	_	Euglena gracilis
E7BDE8	26.95	2.00E-17	Dca	DCA protein	_	_	Drosophila guanche
Q8TA68	26.92	2.00E-17	H-LRE	Luciferin-regenerating enzyme	_	_	Aquatica lateralis
Q86DU5	24.53	6.00E-17	LRE	Luciferin-regenerating enzyme	_	_	Photinus pyralis

Genomic Object Editor: Ilo3171

PB id	Ident %	Eval	Gene	Description	EC number	Keywords	Organism
D3HMD5	100	0	galU	UTP--glucose-1-phosphate uridylyltransferase	2.7.7.9	Nucleotidyltransferase, Reference proteome, Transferase	Legionella longbeachae serogroup 1 (strain NSW150)
A0A1J4QD25	66.43	7.00E-133	_	UTP--glucose-1-phosphate uridylyltransferase	2.7.7.9	Nucleotidyltransferase, Reference proteome, Transferase	Oceanisphaera psychrotolerans
K6YSZ7	62.85	1.00E-132	galU	UTP--glucose-1-phosphate uridylyltransferase	2.7.7.9	Nucleotidyltransferase, Reference proteome, Transferase	Paraglaciocola arctica BSs20135
A0A233RFF0	66.55	2.00E-132	galU	UTP--glucose-1-phosphate uridylyltransferase	2.7.7.9	Nucleotidyltransferase, Reference proteome, Transferase	Oceanimonas doudoroffii
A0A135ZYV6	64.44	4.00E-132	_	UTP--glucose-1-phosphate uridylyltransferase	2.7.7.9	Nucleotidyltransferase, Reference proteome, Transferase	Paraglaciocola hydrolytica
R4YTW2	63.79	5.00E-132	galU	UTP--glucose-1-phosphate uridylyltransferase	2.7.7.9	Nucleotidyltransferase, Reference proteome, Transferase	Oleispira antarctica RB-8
A0A2S9VBQ5	65.23	6.00E-132	galU	UTP--glucose-1-phosphate uridylyltransferase	2.7.7.9	Nucleotidyltransferase, Transferase	Alteromonas alba
A0A2D5LH48	65.23	6.00E-132	galU	UTP--glucose-1-phosphate uridylyltransferase	2.7.7.9	Nucleotidyltransferase, Transferase	Alteromonas sp
A0A1E8FAQ7	65.34	9.00E-132	_	UTP--glucose-1-phosphate uridylyltransferase	2.7.7.9	Nucleotidyltransferase, Reference proteome, Transferase	Alteromonas lipolytica
A0A2D9S173	65.7	1.00E-131	galU	UTP--glucose-1-phosphate uridylyltransferase	2.7.7.9	Nucleotidyltransferase, Transferase	Alteromonadaceae bacterium
E1SP06	63.7	2.00E-131	_	UTP--glucose-1-phosphate uridylyltransferase	2.7.7.9	Nucleotidyltransferase, Reference proteome, Transferase	Ferrimonas balearica (strain DSM 9799 / CCM 4581 / KCTC 23876 / PAT)
C7FFE7	65.47	3.00E-128	_	UTP--glucose-1-phosphate uridylyltransferase	2.7.7.9	Nucleotidyltransferase, Transferase	Proteus mirabilis
A7KAV1	65	4.00E-127	_	UTP--glucose-1-phosphate uridylyltransferase	2.7.7.9	Nucleotidyltransferase, Transferase	Aeromonas hydrophila
O85215	62.37	2.00E-126	galU	UTP--glucose-1-phosphate uridylyltransferase	2.7.7.9	Nucleotidyltransferase, Transferase	Actinobacillus pleuropneumoniae
D4I3X5	63.7	6.00E-121	galU	UTP--glucose-1-phosphate uridylyltransferase	2.7.7.9	3D-structure, Nucleotidyltransferase, Transferase	Erwinia amylovora (strain CFBP1430)
Q70AL9	62.45	2.00E-120	galU	UTP--glucose-1-phosphate uridylyltransferase	2.7.7.9	Nucleotidyltransferase, Transferase	Yersinia enterocolitica
Q84BL0	60.07	8.00E-120	galU	UTP--glucose-1-phosphate uridylyltransferase	2.7.7.9	Nucleotidyltransferase, Transferase	Aeromonas hydrophila
Q848R8	59.04	1.00E-118	galU	UTP--glucose-1-phosphate uridylyltransferase	2.7.7.9	Nucleotidyltransferase, Transferase	Aeromonas hydrophila

Supplementary Table 1

Highest hits of the *L. longbeachae* capsule cluster genes against the NCBI database (Trembl).

Q70AL8	59.29	2.00E-111	galF	UTP--glucose-1-phosphate uridylyltransferase	2.7.7.9	Nucleotidyltransferase, Transferase	Yersinia enterocolitica
Q937X5	54.58	4.00E-97	galF	Alpha-D-glucosyl-1-phosphate uridylyltransferase	2.7.7.9	Nucleotidyltransferase, Transferase	Edwardsiella ictaluri
Q8GNG1	53.98	2.00E-96	galF	Alpha-D-glucosyl-1-phosphate uridylyltransferase	2.7.7.9	Lipopolysaccharide biosynthesis, Nucleotidyltransferase, Transferase	Escherichia coli
Genomic Object Editor: Ilo3172							
PB id	Ident %	Eval	Gene	Description	EC number	Keywords	Organism
D3HMD6	100		0 galE	UDP-glucose 4-epimerase	5.1.3.2	Carbohydrate metabolism, Isomerase, NAD, Reference proteome	Legionella longbeachae serogroup 1 (strain NSW150)
D3HMD0	63.44	1.00E-160	galE	UDP-glucose 4-epimerase	5.1.3.2	Carbohydrate metabolism, Isomerase, NAD, Reference proteome	Legionella longbeachae serogroup 1 (strain NSW150)
R4YS92	60.42	6.00E-147	galE	UDP-glucose 4-epimerase	5.1.3.2	Carbohydrate metabolism, Isomerase, NAD, Reference proteome	Oleispira antarctica RB-8
A0A2E7E932	57.75	1.00E-131	galE	UDP-glucose 4-epimerase	5.1.3.2	Carbohydrate metabolism, Isomerase, NAD	Oceanospirillaceae bacterium
I0JQM5	53.89	2.00E-129	galE2	UDP-glucose 4-epimerase	5.1.3.2	Carbohydrate metabolism, Isomerase, NAD, Reference proteome	Halobacillus halophilus (strain ATCC 35676 / DSM 2266 / JCM 20832 / NBRC 102448/ NCIMB 2269)
A0A173Z112	55.45	4.00E-129	galE_1	UDP-glucose 4-epimerase	5.1.3.2	Carbohydrate metabolism, Isomerase, NAD, Reference proteome	Clostridium ventriculi
A0A1H8C287	55.32	2.00E-127	_	UDP-glucose 4-epimerase	5.1.3.2	Carbohydrate metabolism, Isomerase, NAD	Paenispodosarcina quisquiliarum
A0A1I2KKT0	53.59	3.00E-127	_	UDP-glucose 4-epimerase	5.1.3.2	Carbohydrate metabolism, Isomerase, NAD	Halobacillus alkaliphilus
Q2QD27	54.27	1.00E-120	gne	UDP-glucose 4-epimerase	5.1.3.2	Carbohydrate metabolism, Isomerase, NAD	Aeromonas hydrophila
Q5JBH4	53.64	2.00E-116	galE	UDP-glucose 4-epimerase	5.1.3.2	Carbohydrate metabolism, Isomerase, NAD	Escherichia coli
Q4KXC7	53.03	3.00E-115	galE	UDP-glucose 4-epimerase	5.1.3.2	Carbohydrate metabolism, Isomerase, NAD	Escherichia coli
Q937X4	50.76	3.00E-114	galE	UDP-glucose 4-epimerase	5.1.3.2	Carbohydrate metabolism, Isomerase, NAD	Edwardsiella ictaluri
M9VRS7	49.25	6.00E-114	galE2	UDP-glucose 4-epimerase	5.1.3.2	Carbohydrate metabolism, Isomerase, NAD	Streptococcus oralis
A0A0F7YYT2	51.83	8.00E-114	gne1	UDP-glucose 4-epimerase	5.1.3.2	Carbohydrate metabolism, Isomerase, NAD	Acinetobacter baumannii AB5075
M9POX5	52.44	2.00E-113	galE	UDP-glucose 4-epimerase	5.1.3.2	Carbohydrate metabolism, Isomerase, NAD	Providencia alcalifaciens
Q9X3S6	50.91	2.00E-113	galE	UDP-glucose 4-epimerase	5.1.3.2	Carbohydrate metabolism, Isomerase, NAD	Neisseria meningitidis
O54385	53.05	3.00E-113	galE	UDP-glucose 4-epimerase	5.1.3.2	Carbohydrate metabolism, Isomerase, NAD	Brucella abortus
Q9F8B2	51.66	4.00E-113	galE	UDP-glucose 4-epimerase	5.1.3.2	Carbohydrate metabolism, Isomerase, NAD	Moraxella catarrhalis
Genomic Object Editor: Ilo3173							
PB id	Ident %	Eval	Gene	Description	EC number	Keywords	Organism
D3HMD7	99.69		0 fcl	GDP-L-fucose synthase	1.1.1.271	Isomerase, Multifunctional enzyme, NADP, Oxidoreductase, Reference proteome	Legionella longbeachae serogroup 1 (strain NSW150)
W8R8L8	69.62	3.00E-167	fcl	GDP-L-fucose synthase	1.1.1.271	Isomerase, Multifunctional enzyme, NADP, Oxidoreductase	Pseudomonas stutzeri
A0A2N8SP15	69.3	3.00E-167	fcl	GDP-L-fucose synthase	1.1.1.271	Isomerase, Multifunctional enzyme, NADP, Oxidoreductase	Pseudomonas stutzeri
A0A0D9AQH8	68.97	1.00E-166	fcl	GDP-L-fucose synthase	1.1.1.271	Isomerase, Multifunctional enzyme, NADP, Oxidoreductase	Pseudomonas stutzeri
A0A2E2GGE9	69.28	4.00E-166	fcl	GDP-L-fucose synthase	1.1.1.271	Isomerase, Multifunctional enzyme, NADP, Oxidoreductase	Pseudomonas sp
A0A2N1CMA6	68.97	4.00E-166	fcl	GDP-L-fucose synthase	1.1.1.271	Isomerase, Multifunctional enzyme, NADP, Oxidoreductase	Pseudomonas sp. Choline-3u-10
A0A172WSZ4	68.97	6.00E-166	fcl	GDP-L-fucose synthase	1.1.1.271	Isomerase, Multifunctional enzyme, NADP, Oxidoreductase	Pseudomonas stutzeri
A0A1M5PMK2	68.97	2.00E-165	fcl	GDP-L-fucose synthase	1.1.1.271	Isomerase, Multifunctional enzyme, NADP, Oxidoreductase	Pseudomonas xanthomarina DSM 18231
A0A2W5D1Z8	69.09	5.00E-165	fcl	GDP-L-fucose synthase	1.1.1.271	Isomerase, Multifunctional enzyme, NADP, Oxidoreductase	Pseudomonas kuykendallii
A0A078LSR6	68.44	7.00E-165	fcl	GDP-L-fucose synthase	1.1.1.271	Isomerase, Multifunctional enzyme, NADP, Oxidoreductase, Reference proteome	Pseudomonas sauidiphocaensis
K4NRM2	66.98	1.00E-161	fcl	GDP-L-fucose synthase	1.1.1.271	Isomerase, Multifunctional enzyme, NADP, Oxidoreductase	Yersinia similis
Q56873	67.61	1.00E-158	fcl	GDP-L-fucose synthase	1.1.1.271	Isomerase, Multifunctional enzyme, NADP, Oxidoreductase	Yersinia enterocolitica
Q5ND84	64.89	1.00E-152	fcl	GDP-L-fucose synthase	1.1.1.271	Isomerase, Multifunctional enzyme, NADP, Oxidoreductase	Yersinia sp. A125 KOH2
Q4KXD6	64.38	2.00E-151	fcl	GDP-L-fucose synthase	1.1.1.271	Isomerase, Multifunctional enzyme, NADP, Oxidoreductase	Escherichia coli
Q5XL46	63.21	1.00E-150	wcaG	GDP-L-fucose synthase	1.1.1.271	Isomerase, Multifunctional enzyme, NADP, Oxidoreductase	Klebsiella pneumoniae
A5Y7V9	63.44	1.00E-149	fcl	GDP-L-fucose synthase	1.1.1.271	Isomerase, Multifunctional enzyme, NADP, Oxidoreductase, Reference proteome	Salmonella enterica subsp. enterica serovar Poona
Q9FTA3	62.81	8.00E-147	fcl	GDP-L-fucose synthase	1.1.1.271	Isomerase, Multifunctional enzyme, NADP, Oxidoreductase	Salmonella typhimurium
Genomic Object Editor: Ilo3174							
PB id	Ident %	Eval	Gene	Description	EC number	Keywords	Organism
D3HMD8	100		0 _	Putative glycosyltransferase	_	Reference proteome, Transferase	Legionella longbeachae serogroup 1 (strain NSW150)
A0A011PZP5	50.53	1.00E-98	kfoC_1	Chondroitin polymerase	_	Transferase	Candidatus Accumulibacter sp. BA-92
A0A011PC78	53.31	9.00E-81	kfoC_1	Chondroitin polymerase	_	Reference proteome, Transferase	Candidatus Accumulibacter sp. SK-11
A0A011PMS9	51.82	3.00E-78	kfoC_1	Chondroitin polymerase	_	Reference proteome, Transferase	Candidatus Accumulibacter sp. SK-12
A4BRS0	48.95	5.00E-71	_	Glycosyltransferase	_	Reference proteome, Transferase	Nitrococcus mobilis Nb-231
A4CTD8	45.56	8.00E-67	_	Glycosyltransferase	_	Transferase	Synechococcus sp. (strain WH7805)
A0A1R4GZF7	54.37	1.00E-66	_	Glyco_trans_2-like domain- containing protein	_	Reference proteome	Crenothrix polyspora
L8BAN0	45.45	2.00E-66	_	Putative Glycosyltransferase	_	Transferase	Rubrivivax gelatinosus S1
D9PNG8	46.79	1.00E-61	_	Glycosyltransferase	_	Transferase	sediment metagenome
A0A2V6Q4G8	45.12	8.00E-60	_	Glycosyltransferase	_	Transferase	Candidatus Rokubacteria bacterium
Q6XQ52	29.11	2.00E-16	wbsK	Glycosyl transferase family 2	_	Transferase	Escherichia coli
D0QYM5	30.39	4.00E-16	acbD	AcbD	_	_	Avibacterium paragallinarum
D0QYL9	30.39	4.00E-16	acbD	AcbD	_	_	Avibacterium paragallinarum
Q9RFX0	36.43	5.00E-16	cps7H	Putative glycosyltransferase Cps7H	_	Transferase	Streptococcus suis
K4P2X6	29.74	2E-15	wbyL	WbyL	_	_	Yersinia similis
F8RC13	34.13	5E-15	wpaD	WpaD	_	_	Providencia alcalifaciens
Q8GMK1	32.17	1E-14	wbsA	Glycosyl transferase family 2	_	Transferase	Escherichia coli
Q56869	28.95	1E-13	wbcG	WbcG	_	_	Yersinia enterocolitica
A3F4D9	31.48	4E-13	epsM	EpsM	_	Membrane, Plasmid, Transmembrane, Transmembrane helix	Lactococcus lactis subsp. cremoris

F1CLM1	33.06	8E-13	wbZE	Putative glycosyl transferase	–	Transferase	Yersinia pseudotuberculosis
Genomic Object Editor: Ilo3175							
PB id	Ident %	Eval	Gene	Description	EC number	Keywords	Organism
D3HMD9	100	0	–	Putative polysaccharide biosynthesis dehydrogenase/reductase protein	–	Membrane, Reference proteome, Transmembrane, Transmembrane helix	Legionella longbeachae serogroup 1 (strain NSW150)
A0A1G0WY14	53.36	8.00E-88	–	Short-chain dehydrogenase	–	–	Legionellales bacterium RIFCSPHIGHO2_12_FULL_37_14
A0A1G0GZU1	53.91	5.00E-86	–	Short-chain dehydrogenase	–	Membrane, Transmembrane, Transmembrane helix	Gammaproteobacteria bacterium RIFCSPHIGHO2_12_FULL_40_19
A0A1G0G9X5	50.4	7.00E-77	–	Uncharacterized protein	–	Membrane, Transmembrane, Transmembrane helix	RIFCSPHIGHO2_02_FULL_39_13 uncultured bacterium
K2BBG0	50.4	7.00E-77	–	Polysaccharide biosynthesis dehydrogenase/reductase protein	–	Membrane, Transmembrane, Transmembrane helix	uncultured bacterium
A0A2G6HQW6	48.21	1.00E-74	–	Short-chain dehydrogenase	–	Membrane, Transmembrane, Transmembrane helix	Thiothrix nivea
A0A2G6DK36	47.81	4.00E-72	–	Short-chain dehydrogenase	–	Membrane, Transmembrane, Transmembrane helix	Proteobacteria bacterium
A0A228K644	46.48	3.00E-71	–	SDR family oxidoreductase	–	–	Burkholderia sp. AU27893
A0A2S5DYT0	46.48	3.00E-71	–	KR domain-containing protein	–	–	Burkholderia contaminans
A0A103ZCF2	44.92	2.00E-70	–	Capsular biosynthesis protein	–	–	Burkholderia cepacia
A0A1V6KJP8	45.31	3.00E-70	–	Capsular biosynthesis protein	–	–	Burkholderia cenocepacia
Q9KHD1	31.87	2.00E-19	–	Putative beta-ketoacyl reductase	–	–	Streptomyces griseus subsp. griseus
C6ZD46	30.89	9.00E-19	ydfG	NADP-dependent L-serine/L-allo-threonine dehydrogenase ydfG	1.1.1.-	Oxidoreductase	Legionella jamestowniensis
Q5EGQ6	32.02	5.00E-18	rkpH	RkpH	1.1.1.56	Oxidoreductase	Rhizobium fredii
B8XU9	28.72	9.00E-17	–	Ketoacyl-reductase like protein	–	–	Karodinium veneficum
K7ZSN0	29.79	1.00E-16	lgnI	Gluconate 5-dehydrogenase	–	Reference proteome	Paracoccus laeviglucoovorans
Q8RR58	25.53	3.00E-16	acrM	Acyl coenzyme A reductase	–	Coiled coil	Acinetobacter sp. M-1
Q7LZT0	27.92	6.00E-16	–	3(or 17)beta-hydroxysteroid dehydrogenase I	1.1.1.51	Oxidoreductase	Anguilla japonica
Q9API9	29.69	6.00E-16	phaB	Acetoacetyl-CoA reductase	1.1.1.36	Oxidoreductase	Methylorubrum extorquens
Q6RH38	27.92	1E-15	–	17b-hydroxysteroid dehydrogenase	–	Oxidoreductase	Anguilla japonica
Genomic Object Editor: Ilo3176							
PB id	Ident %	Eval	Gene	Description	EC number	Keywords	Organism
D3HME0	100	0	–	Putative glycosyltransferase	2.4.1.-	Glycosyltransferase, Reference proteome, Transferase	Legionella longbeachae serogroup 1 (strain NSW150)
A0A2S5SX42	46.4	1.00E-100	–	Glycosyltransferase family 1 protein	–	Reference proteome, Transferase	Zhizhongheella caldifontis
H8FUS8	43.8	2.00E-94	–	Putative glycosyltransferase	2.4.-.-	Glycosyltransferase, Reference proteome, Transferase	Phaeosporillum molischianum DSM 120
A0A259BE26	43.86	1.00E-93	–	Glycos_transf_1 domain-containing protein	–	–	Halothiobacillus sp. 24-54-40
A0A0W0Z520	41.88	1.00E-91	–	Glycosyltransferase	2.4.1.-	Glycosyltransferase, Reference proteome, Transferase	Legionella shakespearei DSM 23087
A0A2N3B0J3	45.1	1.00E-85	–	Glycosyltransferase family 1 protein	–	Transferase	Alphaproteobacteria bacterium HGW-Alphaproteobacteria-7
A0A255Y7H4	38.96	8.00E-84	–	Glycos_transf_1 domain-containing protein	–	Reference proteome	Sandarakinorhabdus cyanobacterium
A0A1X1PB15	43.84	9.00E-81	–	Glycos_transf_1 domain-containing protein	–	Coiled coil	Burkholderia puraquae
T2N217	40.21	1.00E-80	–	Glycos_transf_1 domain-containing protein	–	–	Ralstonia sp. 5_2_56FAA
M4QN28	35.29	2.00E-64	wbdA	Mannosyltransferase	–	Glycosyltransferase, Transferase	Escherichia coli
Q47593	35.04	7.00E-64	mtfA	Mannosyltransferase A	–	Glycosyltransferase, Transferase	Escherichia coli
Q9LC66	35.04	7.00E-64	wbdA	Mannosyltransferase	–	Glycosyltransferase, Transferase	Klebsiella pneumoniae
Q9LC67	35.58	1.00E-62	wbdA	Mannosyltransferase	–	Glycosyltransferase, Transferase	Escherichia coli
C8YZ32	35.34	1.00E-60	wejl	Wejl	–	–	Escherichia coli
O84908	32.57	1.00E-33	wbpX	Glycosyltransferase Gtf1	–	Transferase	Pseudomonas aeruginosa
Q93UK1	26.73	1E-13	wcbB	WcbB	–	–	Burkholderia pseudomallei
M4M6T9	29.17	6E-10	–	Glycosyl transferase group 1	–	Transferase	Acidiphilium sp. PM
O84909	31.76	2.00E-07	wbpY	Glycosyltransferase WbpY	–	Transferase	Pseudomonas aeruginosa
Q93UJ8	35.65	5.00E-06	wcbE	WcbE	–	–	Burkholderia pseudomallei
Q9RMT9	31.97	5.00E-06	wbdB	WbdB	–	–	Klebsiella pneumoniae
Genomic Object Editor: Ilo3177							
PB id	Ident %	Eval	Gene	Description	EC number	Keywords	Organism
D3HME3	100	0	–	Uncharacterized protein	–	Membrane, Reference proteome, Transmembrane, Transmembrane helix	Legionella longbeachae serogroup 1 (strain NSW150)
A0A1G0GZV7	49.04	5.00E-130	–	Uncharacterized protein	–	–	Gammaproteobacteria bacterium RIFCSPHIGHO2_12_FULL_40_19
A0A1T4X2W9	36.1	5.00E-73	–	Glycosyltransferase family 28 C-terminal domain-containing protein	–	Coiled coil, Reference proteome, Transferase	Clostridium sp. USBA 49
U2CYI4	34	2.00E-68	–	Glycosyltransferase family 28 protein	–	Coiled coil, Reference proteome, Transferase	Clostridiales bacterium oral taxon 876 str. F0540
A0A1T4Y1N0	32.46	2.00E-60	–	Glycosyltransferase family 28 C-terminal domain-containing protein	–	Coiled coil, Reference proteome, Transferase	Caloramator quimbayensis
A0A2C6TA21	30.79	2.00E-51	–	Uncharacterized protein	–	Coiled coil	Nostoc linckia z16
A0A0C2V1S8	30.18	3.00E-49	–	Glyco_tran_28_C domain-containing protein	–	Reference proteome	Paenibacillus sp. VKM B-2647
A0A111D9I8	22.14	4E-09	–	UDP-N-acetylglucosamine:LPS N-acetylglucosamine transferase	–	Glycosyltransferase, Reference proteome, Transferase	Brevinema andersonii
A0A1J4VM15	21.36	5.00E-08	–	Uncharacterized protein	–	Glycosyltransferase, Membrane, Transferase, Transmembrane, Transmembrane helix	Candidatus Omniphica bacterium CG1_02_46_14
A0A1V4IVN9	20.83	1.00E-07	ugtP	Processive diacylglycerol beta-glycosyltransferase	2.4.1.-	Glycosyltransferase, Reference proteome, Transferase	Clostridium chromiireducens
Genomic Object Editor: Ilo3178							
PB id	Ident %	Eval	Gene	Description	EC number	Keywords	Organism
D3HME4	100	0	–	Putative aminotransferase	2.3.1.47	Acyltransferase, Aminotransferase, Pyridoxal phosphate	Legionella longbeachae serogroup 1 (strain NSW150)
A0A1G0WY90	63.45	0	–	8-amino-7-oxononanoate synthase	–	Pyridoxal phosphate	Legionellales bacterium RIFCSPHIGHO2_12_FULL_37_14

Supplementary Table 1

Highest hits of the *L. longbeachae* capsule cluster genes against the NCBI database (Trembl).

A0A157QUK5	61.34	0	wcbT	Polyketide synthase	2.3.1.-	Acyltransferase, Transferase	Bordetella trematum
A0A157SWX8	58.8	2.00E-180	wcbT	Polyketide synthase	2.3.1.-	Acyltransferase, Pyridoxal phosphate, Transferase	Bordetella ansorpii
A0A132F5H0	60.84	2.00E-179	_	8-amino-7-oxononanoate synthase	_	Pyridoxal phosphate	Burkholderia pseudomultivorans
A0A113G3G2	59.77	2.00E-179	_	8-amino-7-oxononanoate synthase	_	Pyridoxal phosphate	Collimonas sp. OK307
A0A1B4F580	61.07	3.00E-179	_	8-amino-7-oxononanoate synthase	_	Pyridoxal phosphate	Burkholderia sp. LA-2-3-30-S1-D2
A0A088UAL4	60.84	4.00E-179	_	Beta-eliminating lyase family protein	_	Lyase, Pyridoxal phosphate	Burkholderia cenocepacia
A0A2A4CCM4	60.61	1.00E-178	_	8-amino-7-oxononanoate synthase	_	Pyridoxal phosphate	Burkholderia sp. IDO3
Q5EGQ7	48.95	3.00E-134	rkpG	RkpG	2.3.1.29	Acyltransferase, Transferase	Rhizobium fredii
Q52936	51.62	3.00E-123	rkpG	Acyl-transferase	_	Transferase	Rhizobium meliloti
A7BFV7	33.33	6.00E-66	spt	Serine palmitoyltransferase	2.3.1.50	Acyltransferase, Pyridoxal phosphate, Transferase	Sphingobacterium spiritovorum
Q9AJN1	34.38	1.00E-65	bioF	8-amino-7-ketopelargonate synthase	2.3.1.47	Biotin biosynthesis, Pyridoxal phosphate, Transferase	Kurthia sp. 538-KA26
Q9AJM7	34.82	2.00E-65	bioFII	8-amino-7-ketopelargonate synthase	2.3.1.47	Biotin biosynthesis, Pyridoxal phosphate, Transferase	Kurthia sp. 538-KA26
A7BFV6	35.39	9.00E-65	spt	8-amino-7-oxononanoate synthase	2.3.1.47, 2.3.1.50	Acyltransferase, Pyridoxal phosphate, Transferase	Sphingobacterium multivorum
A7BFV8	32.14	2.00E-57	spt	Serine palmitoyltransferase	2.3.1.50	Acyltransferase, Pyridoxal phosphate, Transferase	Bacteriovorax stolpii
B2XR73	32.03	2.00E-56	LCB2	Serine C-palmitoyltransferase	2.3.1.50	Endoplasmic reticulum, Lipid metabolism, Membrane, Pyridoxal phosphate, Sphingolipid metabolism, Transferase, Transmembrane	Nicotiana benthamiana

Genomic Object Editor: llo3179

PB id	Ident %	Eval	Gene	Description	EC number	Keywords	Organism
D3HME5	100	0	rkpA	Malonyl CoA-acyl carrier protein transacylase	-	Multifunctional enzyme, NADP, Phosphopantetheine, Phosphoprotein, Reference proteome, Transferase	Legionella longbeachae serogroup 1 (strain NSW150)
A0A1G0H3Y5	48.92	0	_	Malonyl CoA-acyl carrier protein transacylase	-	Multifunctional enzyme, NADP, Phosphopantetheine, Phosphoprotein, Transferase	Gammaproteobacteria bacterium RIFCSPHIGHO2_12_FULL_38_11
A0A1G0GZW1	49.27	0	_	Malonyl CoA-acyl carrier protein transacylase	-	Multifunctional enzyme, NADP, Phosphopantetheine, Phosphoprotein, Transferase	Gammaproteobacteria bacterium RIFCSPHIGHO2_12_FULL_40_19
A0A1G0G9V3	47.94	0	_	Malonyl CoA-acyl carrier protein transacylase	-	Multifunctional enzyme, NADP, Phosphopantetheine, Phosphoprotein, Transferase	Gammaproteobacteria bacterium RIFCSPHIGHO2_02_FULL_39_13
K2C9B0	47.94	0	_	Carrier domain-containing protein	-	Multifunctional enzyme, NADP, Phosphopantetheine, Phosphoprotein, Transferase	uncultured bacterium
A0A1G0WYA8	46.27	0	_	Malonyl CoA-acyl carrier protein transacylase	-	Coiled coil, Multifunctional enzyme, NADP, Phosphopantetheine, Phosphoprotein, Transferase	Legionellales bacterium RIFCSPHIGHO2_12_FULL_37_14
A0A1T4X2T5	41.79	0	_	Malonyl CoA-acyl carrier protein transacylase	-	Coiled coil, Multifunctional enzyme, NADP, Phosphopantetheine, Phosphoprotein, Reference proteome, Transferase	Thiothrix eikelboomii
A0A2G6HQX1	41.42	0	_	Malonyl CoA-acyl carrier protein transacylase	-	Multifunctional enzyme, NADP, Phosphopantetheine, Phosphoprotein, Transferase	Thiothrix nivea
A0A2G6DKI5	41.28	0	_	Malonyl CoA-acyl carrier protein transacylase	-	Multifunctional enzyme, NADP, Phosphopantetheine, Phosphoprotein, Transferase	Proteobacteria bacterium
A0A1H9YTQ4	40.46	0	_	Malonyl CoA-acyl carrier protein transacylase	-	Multifunctional enzyme, NADP, Phosphopantetheine, Phosphoprotein, Transferase	Nitrosomonas europaea
Q82UT4	40.46	0	rkpA	Malonyl CoA-acyl carrier protein transacylase	-	Multifunctional enzyme, NADP, Phosphopantetheine, Phosphoprotein, Reference proteome, Transferase	Nitrosomonas europaea (strain ATCC 19718 / CIP 103999 / KCTC 2705 / NBRC 14298)
A0A238XMI4	40.34	0	_	Malonyl CoA-acyl carrier protein transacylase	-	Multifunctional enzyme, NADP, Phosphopantetheine, Phosphoprotein, Transferase	Methylobacillus rhizosphaerae
Q6E7K0	30.12	0	_	3-hydroxyacyl-CoA dehydrogenase	1.1.1.35	3D-structure, Coiled coil, Multifunctional enzyme, NADP, Nucleotide-binding, Phosphopantetheine, Phosphoprotein, Transferase	Lynngbya majuscula
A0A0A0WDX2	31.31	0	puwB	PuwB	-	Coiled coil, Multifunctional enzyme, NADP, Phosphopantetheine, Phosphoprotein, Transferase	Cylindrosporum alatosporum CCALA 988
F4Y426	28.41	0	_	CurJ	-	3D-structure, Phosphopantetheine, Phosphoprotein, Reference proteome, Transferase	Moorea producens 3L
Q6DNE3	28.41	0	curJ	CurJ	-	3D-structure, Phosphopantetheine, Phosphoprotein, Transferase	Lynngbya majuscula
Q5EGQ8	31.94	0	rkpA	Malonyl CoA-acyl carrier protein transacylase	-	Multifunctional enzyme, Phosphopantetheine, Phosphoprotein, Transferase	Rhizobium fredii
Q6ZY03	44.68	0	pkS4	Polyketide synthase I	-	Phosphopantetheine, Phosphoprotein, Transferase	uncultured bacterium
A0A1B3TNB2	35.66	0	hapB	Malonyl CoA-acyl carrier protein transacylase	-	Coiled coil, Multifunctional enzyme, NADP, Phosphopantetheine, Phosphoprotein, Transferase	Byssovorax cruenta
Q9KIZ7	34.07	0	epoD	Malonyl CoA-acyl carrier protein transacylase	-	Coiled coil, Multifunctional enzyme, Phosphopantetheine, Phosphoprotein, Transferase	Sorangium cellulosum
Q3KRU5	25.72	0	pkSx1	PKSx1	-	Acyltransferase, Coiled coil, Methyltransferase, Multifunctional enzyme, NADP, Oxidoreductase, Phosphopantetheine, Phosphoprotein, Transferase	Xylaria sp. BCC 1067
Q8RJY0	34.6	0	stiG	Malonyl CoA-acyl carrier protein transacylase	-	Coiled coil, Phosphopantetheine, Phosphoprotein, Transferase	Stigmatella aurantiaca
Q93TW8	34.15	0	mxuD	Malonyl CoA-acyl carrier protein transacylase	-	Coiled coil, Phosphopantetheine, Phosphoprotein, Transferase	Stigmatella aurantiaca

Genomic Object Editor: llo3180

PB id	Ident %	Eval	Gene	Description	EC number	Keywords	Organism
-------	---------	------	------	-------------	-----------	----------	----------

Supplementary Table 1

Highest hits of the *L. longbeachae* capsule cluster genes against the NCBI database (Trembl).

D3HME6	100	0 capI	Protein capI	–	Reference proteome	Legionella longbeachae serogroup 1 (strain NSW150)
D5BMZ1	63.17	3.00E-152	Putative nucleotide sugar epimerase	5.1.3.-	Isomerase, Reference proteome	Puniceispirillum marinum (strain IMCC1322)
A0A149VYE0	65.06	4.00E-152	dTDP-glucose 4,6-dehydratase	4.2.1.46	Lyase, Reference proteome	Ferrovum sp. Z-31
A0A1Q8YJ37	63.64	2.00E-151	NAD-dependent epimerase/dehydratase	–	Reference proteome	Rhodoferrax antarcticus ANT.BR
A0A1F4K1Q8	61.76	4.00E-150	Protein CapI	–	–	Burkholderiales bacterium RIFCSPLOWO2_12_FULL_61_40
A0A2E1QD17	60.66	4.00E-148	Epimerase domain-containing protein	–	–	Euryarchaeota archaeon
A0A1F9MKL1	62.54	2.00E-146	Capsular biosynthesis protein CpsI	–	–	Deltaproteobacteria bacterium RIFOXYD12_FULL_53_23
A0A1H7HPY1	60.36	2.00E-146	UDP-glucuronate 4-epimerase	–	–	Roseateles sp. YR242
A0A1F9KZI9	62.84	1.00E-145	Epimerase domain-containing protein	–	–	Deltaproteobacteria bacterium RIFOXYD12_FULL_56_24
Q6U8B8	59.16	1.00E-138	Putative nucleotide sugar epimerase	–	–	Raoultella terrigena
Q9RP53	57.66	6.00E-134	NAD-dependent epimerase	4.2.1.46	Lyase	Escherichia coli
Q4GY28	55.52	5.00E-127	UDP-sugar epimerase	–	–	Erwinia amylovora
Q6URR1	54.63	9.00E-127	Putative epimerase	–	–	Xenorhabdus nematophila
Q68979	55.22	3.00E-121	Nucleotide sugar epimerase	–	–	Vibrio vulnificus
Q56626	53.45	1.00E-116	Nucleotide sugar epimerase	–	–	Vibrio cholerae O139
P96481	48.18	5.00E-100	Putative epimerase	–	–	Streptococcus pneumoniae
Q70PA0	44.11	3.00E-90	Epimerase domain-containing protein	–	–	Melittangium lichenicola
I1VCA9	45.24	6.00E-90	UDP-D-glucuronate 4-epimerase 1	–	–	Arabidopsis thaliana
Q6K9M5	44.97	1.00E-88	Os02g0791500 protein	–	Membrane, Reference proteome, Transmembrane, Transmembrane helix	Oryza sativa subsp. japonica

Percent identity compared to NSW150																		
Strain	serogroup	Ilo3148	Ilo3149	Ilo3150	Ilo3151	Ilo3152	Ilo3153	Ilo3154	Ilo3155	Ilo3156	Ilo3157	Ilo3158	Ilo3159	Ilo3160	Ilo3161	Ilo3162	Ilo3163	Ilo3164
<i>L. longbeachae</i> F1157CHC	sg1	98.306	97.658	98.003	91.154	97.442	99.365	99.768	99.743	99.896	99.608	96.319	99.940	99.855	99.054	98.238	99.786	97.002
<i>L. longbeachae</i> 13.8300	sg2	98.238	97.387	98.157	91.282	96.617	98.571	99.227	99.829	99.637	98.529	--	100.000	100.000	100.000	100.000	100.000	97.002
<i>L. longbeachae</i> B3526CHC	sg1	98.238	97.387	98.157	91.282	96.617	98.571	99.149	99.829	98.445	99.477	96.185	99.819	99.565	98.318	97.504	99.359	97.002
<i>L. longbeachae</i> 13.8301	sg2	98.238	97.387	98.157	91.282	96.617	98.571	99.227	99.829	99.637	98.529	--	100.000	100.000	100.000	100.000	100.000	97.002
<i>L. longbeachae</i> 13.8297	sg2	98.238	97.387	98.157	91.282	96.617	98.571	99.227	99.829	99.637	98.529	96.319	100.000	100.000	100.000	100.000	100.000	97.002
<i>L. longbeachae</i> B1445CHC	sg1	98.306	97.658	98.003	91.154	97.442	99.286	99.845	100.000	99.948	98.529	96.319	100.000	100.000	99.895	100.000	100.000	97.002
<i>L. longbeachae</i> D-4968	sg1	98.306	97.658	98.003	91.154	97.442	99.286	99.845	100.000	99.948	99.869	96.319	100.000	100.000	99.895	100.000	100.000	97.002
<i>L. longbeachae</i> NSW150	sg1	100.000	100.000	100.000	100.000	100.000	100.000	100.000	100.000	100.000	100.000	100.000	100.000	100.000	100.000	100.000	100.000	100.000
<i>L. longbeachae</i> B41211CHC	sg1	100.000	100.000	100.000	100.000	100.000	100.000	99.923	100.000	100.000	100.000	100.000	100.000	100.000	100.000	100.000	100.000	100.000
<i>L. longbeachae</i> NCTC11477	sg1	98.374	97.477	98.003	91.282	97.442	99.524	99.923	100.000	99.948	--	--	100.000	100.000	99.895	100.000	100.000	97.002
<i>L. longbeachae</i> FDAARGOS 201	sg1	98.374	97.477	98.003	91.282	97.442	99.524	99.923	100.000	99.948	98.529	96.319	100.000	100.000	99.895	100.000	100.000	97.002
<i>L. longbeachae</i> FDAARGOS 1481	sg1	98.374	97.477	98.003	91.282	97.442	99.524	99.923	100.000	99.948	98.529	96.319	100.000	100.000	99.895	100.000	100.000	97.002
Percent identity compared to NSW150																		
Strain	serogroup	Ilo3165	Ilo3166	Ilo3167	Ilo3168	Ilo3169	Ilo3170	Ilo3171	Ilo3172	Ilo3173	Ilo3174	Ilo3175	Ilo3176	Ilo3177	Ilo3178	Ilo3179	Ilo3180	
<i>L. longbeachae</i> F1157CHC	sg1	--	--	85.659	--	--	99.880	99.336	100.000	100.000	100.000	99.872	100.000	100.000	100.000	100.000	100.000	
<i>L. longbeachae</i> 13.8300	sg2	--	--	85.756	--	--	99.640	99.225	99.604	99.689	99.431	99.489	98.115	98.424	98.712	99.224	99.705	
<i>L. longbeachae</i> B3526CHC	sg1	--	--	85.756	--	--	99.520	99.225	99.604	99.689	99.431	99.489	98.115	98.424	98.712	99.224	99.705	
<i>L. longbeachae</i> 13.8301	sg2	--	--	85.756	--	--	99.640	99.225	99.604	99.689	99.431	99.489	98.115	98.424	98.712	99.224	99.705	
<i>L. longbeachae</i> 13.8297	sg2	--	--	85.756	--	--	99.640	99.225	99.604	99.689	99.431	99.489	98.115	98.424	98.712	99.224	99.705	
<i>L. longbeachae</i> B1445CHC	sg1	--	--	85.756	--	--	99.880	99.779	99.901	100.000	100.000	100.000	100.000	100.000	99.924	100.000	100.000	
<i>L. longbeachae</i> D-4968	sg1	--	--	85.756	--	--	99.880	99.779	99.901	100.000	100.000	100.000	100.000	100.000	100.000	100.000	100.000	
<i>L. longbeachae</i> NSW150	sg1	100.000	100.000	100.000	100.000	100.000	100.000	100.000	100.000	100.000	100.000	100.000	100.000	100.000	100.000	100.000	100.000	
<i>L. longbeachae</i> B41211CHC	sg1	100.000	100.000	100.000	100.000	100.000	100.000	100.000	100.000	100.000	100.000	100.000	100.000	100.000	100.000	100.000	100.000	
<i>L. longbeachae</i> NCTC11477	sg1	--	--	85.756	--	--	99.880	99.779	99.901	100.000	100.000	100.000	100.000	100.000	100.000	100.000	100.000	
<i>L. longbeachae</i> FDAARGOS 201	sg1	--	--	85.756	--	--	99.880	99.779	99.901	100.000	100.000	100.000	100.000	100.000	100.000	100.000	100.000	
<i>L. longbeachae</i> FDAARGOS 1481	sg1	--	--	85.756	--	--	99.880	99.779	99.901	100.000	100.000	100.000	100.000	100.000	100.000	100.000	100.000	

Genes up- or downregulated in E Phase (WT is the reference)				
Gene	Gene name	log2 FC	padj	Putative function
<i>llo0333</i>	--	2.036	3.32E-07	Glycine transporter
<i>llo0471</i>	--	-2.248	2.00E-02	Unknown protein
<i>llo0616</i>	<i>groES</i>	-2.105	2.16E-03	Co-chaperonin with GroEL
<i>llo0666</i>	--	-2.053	1.17E-02	Uroporphyrin-III C-methyltransferase
<i>llo0686</i>	<i>asnA</i>	-2.958	2.46E-04	Asparagine synthetase A
<i>llo1148</i>	--	-2.196	1.92E-05	Secreted endonuclease
<i>llo1188</i>	--	2.392	3.11E-08	Unknown protein
<i>llo1391</i>	--	-2.093	3.07E-10	Putative Thiol:disulfide interchange protein
<i>llo1421</i>	--	-2.626	1.87E-03	Putative fatty acid desaturase
<i>llo1641</i>	--	-2.307	2.32E-05	Unknown protein, weakly similar to eukyotic proteins
<i>llo2353b</i>	--	3.107	2.08E-05	Arginine ABC transporter
<i>llo2487</i>	--	2.008	4.21E-07	Unknown protein
<i>llo2505</i>	<i>dnaK</i>	-2.18	1.35E-03	Chaperone protein
<i>llo2810</i>	--	2.142	1.84E-03	Truncated transposase
<i>llo2873</i>	--	-2.26	6.98E-03	LvrB homolog
<i>llo2874</i>	<i>csrA</i>	-2.808	7.46E-05	Translational regulator
<i>llo3149</i>	<i>bexD</i>	-3.508	1.96E-51	CPS export protein
<i>llo3150</i>	<i>ctrD</i>	-6.947	2.97E-95	CPS export, ATP-binding protein
<i>llo3151</i>	<i>ctrC</i>	-5.952	3.50E-50	CPS export, IM binding protein
<i>llo3266</i>	--	2.141	1.79E-09	Unknown protein
<i>llo3308</i>	--	2.221	1.89E-05	Putative endoglucanase
<i>llo3444</i>	--	2.546	1.83E-08	Coiled-coil protein
<i>LEGLO_2011</i>	<i>llo4038</i>	-2.036	1.68E-03	Unknown protein
<i>LEGLO_2385</i>	<i>llo4052</i>	2.797	7.12E-02	Unknown protein
<i>LEGLO_2621</i>	<i>llo4063</i>	2.709	2.23E-11	Unknown protein
<i>LEGLO_2873</i>	<i>llo4071</i>	-3.731	7.79E-07	Transposase
<i>LEGLO_5S_1</i>	<i>rRNA 5S</i>	-5.284	7.37E-09	--
<i>LEGLO_5S_2</i>	<i>rRNA 5S</i>	-5.259	7.76E-09	--
<i>LEGLO_5S_3</i>	<i>rRNA 5S</i>	-5.21	6.16E-09	--
<i>LEGLO_5S_4</i>	<i>rRNA 5S</i>	-5.279	7.37E-09	--
<i>LEGLO_tRNA19</i>	<i>tRNA-Glu</i>	-2.508	2.62E-08	--
<i>LEGLO_tRNA24</i>	<i>tRNA-Val</i>	-2.13	2.21E-03	--
<i>LEGLO_tRNA27</i>	<i>tRNA-Asp</i>	-2.753	1.55E-07	--
<i>LEGLO_tRNA28</i>	<i>tRNA-Ser</i>	-2.744	1.00E-11	--
<i>LEGLO_tRNA32</i>	<i>tRNA-Lys</i>	-2.073	2.39E-03	--
<i>LEGLO_tRNA36</i>	<i>tRNA-Ser</i>	-3.552	4.97E-10	--
<i>LEGLO_tRNA44</i>	<i>tRNA-Arg</i>	-2.288	4.97E-10	--
Genes up- or downregulated in PE Phase (WT is the reference)				
Gene	Gene name	log2 FC	padj	Putative function
<i>llo0455</i>	--	-2.46	1.87E-02	Unknown protein
<i>llo0591</i>	--	-2.346	9.07E-03	Hypothetical protein
<i>llo1676b</i>	--	-2.423	3.93E-02	Transposase
<i>llo2373</i>	--	2.687	1.87E-02	Putative periplasmic binding protein
<i>llo2945</i>	--	-2.181	2.12E-02	Unknown protein
<i>llo3150</i>	<i>ctrD</i>	-5.117	9.28E-26	CPS export, ATP-binding protein
<i>llo3151</i>	<i>ctrC</i>	-6.678	6.71E-23	CPS export, IM binding protein
<i>LEGLO_2219</i>	<i>llo4044</i>	-2.108	4.31E-03	Unknown protein
<i>LEGLO_2873</i>	<i>llo4071</i>	-3.678	1.97E-05	Transposase
<i>LEGLO_tRNA11</i>	<i>tRNA-Gly</i>	-3.076	6.26E-06	--
<i>LEGLO_tRNA13</i>	<i>tRNA-Leu</i>	-2.084	3.41E-02	--
<i>LEGLO_tRNA19</i>	<i>tRNA-Glu</i>	-2.234	4.05E-02	--
<i>LEGLO_tRNA20</i>	<i>tRNA-Pro</i>	-4.088	6.26E-06	--
<i>LEGLO_tRNA21</i>	<i>tRNA-Arg</i>	-2.533	7.24E-05	--
<i>LEGLO_tRNA22</i>	<i>tRNA-His</i>	-2.848	1.20E-03	--
<i>LEGLO_tRNA24</i>	<i>tRNA-Val</i>	-3.081	5.33E-05	--
<i>LEGLO_tRNA25</i>	<i>tRNA-Asp</i>	-2.985	5.70E-04	--
<i>LEGLO_tRNA26</i>	<i>tRNA-Val</i>	-2.966	7.93E-06	--
<i>LEGLO_tRNA27</i>	<i>tRNA-Asp</i>	-3.278	4.92E-04	--
<i>LEGLO_tRNA28</i>	<i>tRNA-Ser</i>	-2.703	5.70E-04	--
<i>LEGLO_tRNA29</i>	<i>tRNA-Arg</i>	-2.53	1.86E-03	--
<i>LEGLO_tRNA32</i>	<i>tRNA-Lys</i>	-2.997	3.08E-06	--
<i>LEGLO_tRNA36</i>	<i>tRNA-Ser</i>	-5.31	2.47E-05	--
<i>LEGLO_tRNA40</i>	<i>tRNA-Asn</i>	-4.144	1.62E-07	--
<i>LEGLO_tRNA44</i>	<i>tRNA-Arg</i>	-3.541	9.34E-06	--
<i>LEGLO_tRNA6</i>	<i>tRNA-Thr</i>	-2.396	2.12E-02	--

Color code p-value adj.
 p>0,01
 0,01≤p<0,05

Color code p-value adj.
 p>0,01
 0,01≤p<0,05

OUTLOOK AND PERSPECTIVES

L. longbeachae is a human pathogen that can cause a severe form of pneumonia, called Legionnaires' disease (LD). In contrast to many other *Legionella* species that were isolated from aquatic environments, this species was isolated from soil environments, and it displays distinct genomic features that may reflect this habitat (Steele, Lanser and Sangster, 1990; Steele, Moore and Sangster, 1990; Koide *et al.*, 1999; Cazalet *et al.*, 2010). For example, the *L. longbeachae* NSW150 genome encodes genes for pectin and cellulose degradation. In addition, it encodes Rab-like GTPases, and it lacks flagella, despite encoding several regulatory genes for flagella expression (Cazalet *et al.*, 2010). Despite a similar intracellular life cycle and LCV decoration as compared to *L. pneumophila* (Wood *et al.*, 2015), *L. longbeachae* encodes a unique effector repertoire and shares only 65% of orthologous genes with *L. pneumophila* (Cazalet *et al.*, 2010). Interestingly, our group identified a gene cluster in the genome of *L. longbeachae* that was predicted to code for a capsule (Cazalet *et al.*, 2010). The non-flagellated *L. longbeachae* is highly virulent in wild type mice, in contrast to the flagellated *L. pneumophila*. The latter can only establish infection in A/J mice, as these mice do not recognize the bacterial flagellin and cannot clear the infection (Molofsky *et al.*, 2006; Ren *et al.*, 2006; Asare *et al.*, 2007; Gobin *et al.*, 2009; Pereira *et al.*, 2011; Massis *et al.*, 2016). On the other hand, *L. longbeachae* causes lung damage in infected mice and leads to death of the animals. At the same time, it fails to induce a strong pro-inflammatory cytokine response, in contrast to a non-flagellated mutant of *L. pneumophila* (Massis *et al.*, 2016). Thus, *L. longbeachae* seems to establish infection in an immunologically silent manner (Massis *et al.*, 2016).

The highly virulent phenotype in mice cannot be solely attributed to the lack of flagella and we thus hypothesized that the capsule encoded in the *L. longbeachae* genome may be responsible for this phenotype. Capsules are known virulence factors of many pathogenic bacteria and they can shield the bacteria from immune responses in the host or protect them from environmental stresses. Therefore, during my PhD thesis, I studied the role of the *L. longbeachae* capsule in infection and in environmental persistence. This work has provided new insights into the unique virulence features of *L. longbeachae*, and now opens many questions for further research.

Which genes are responsible for capsule biosynthesis in *L. longbeachae*?

We show that the capsule locus is unique within the genus *Legionella*, as only *L. longbeachae* strains encode the full 48 kb cluster in their genomes. This capsule locus is highly conserved in all analyzed strains of *L. longbeachae* sg1 and sg2, and it shares homologous genes with soil-dwelling bacteria, such as *Pseudomonas* and *Burkholderia*, among others. The genomic localization of the cluster is conserved in all analyzed strains, indicating that the acquisition of the cluster may have occurred by a common ancestor of *L. longbeachae*.

The capsule locus contains an ABC transporter homologous to the *ctrABCD* capsule transporter locus found in *Neisseria* spp (Cazalet *et al.*, 2010). ABC transporter-dependent capsule loci display different genetic organizations, as exemplified by the model organisms *E. coli* and *N. meningitidis*. In *E. coli*, the K1 and K5 capsule loci consist of three main regions: region 1 contains genes involved in CPS export and translocation, region 3 encodes the KpsM/KpsT ABC transporter and region 2 encodes the serotype-specific CPS biosynthesis cluster (Whitfield, 2006). In *N. meningitidis*, the capsule locus is interspersed with genes involved in LPS synthesis (Harrison *et al.*, 2013). All capsule-encoding serogroups of *N. meningitidis* encode the central ABC transporter and export genes *ctrABCD*, adjacent to a region that encodes serogroup-specific CPS biosynthesis genes. A third region contains a transcription factor *tex* and methyltransferases. These capsule-specific genes are flanked by two LPS synthesis regions. Lastly, *N. meningitidis* encodes *ctrE* and *ctrF*, which are β -Kdo transferases involved in the attachment of the CPS to a lipid anchor (Tzeng *et al.*, 2002, 2005; Tzeng, Thomas and Stephens, 2015).

Our analyses show that the *L. longbeachae* capsule cluster also contains genes that may be involved in LPS biosynthesis, such as *ugd*, *galE1* and *galE2*. In addition, *llo3160* and *llo3165* encode putative Kdo III transferases similar to *waaZ*. Kdo III transferases have been shown to add a third Kdo to the LPS core in *E. coli* (Klein *et al.*, 2011). Further, the *llo3168* gene encodes a putative WcbI-domain containing protein. In *Burkholderia pseudomallei*, deletion of *wcbI* leads to a loss of reactivity to a CPS-specific antibody, as well as attenuated virulence, and structural analyses suggest that WcbI functions as a CPS acetyltransferase (Cuccui *et al.*, 2012; Vivoli *et al.*, 2014). Of note, deletion of the *rkpA* homolog *wcbR* in *B. pseudomallei* leads to a loss of CPS-specific antibody reactivity (Cuccui *et al.*, 2012). The role of the *rkpA* homolog *llo3179* is unknown in *L. longbeachae*, and it may present a target for future studies on the lipid biosynthesis required for CPS expression. Targeted deletions of these genes may advance our understanding as to whether they are involved in LPS or CPS synthesis.

Our comparative genome analyses revealed that two other *Legionella* species (*L. massiliensis* and *L. gormanii*) encode orthologous genes of the *ctrBCD/bexD* ABC transporter. However, they do not encode orthologs of the glycosyltransferases found in the *L. longbeachae* capsule cluster. *L. gormanii* (previously known as *Fluoribacter gormanii*) was first isolated from wet soil (Cordes *et al.*, 1979; Morris *et al.*, 1980), but has since also been found in man-made water environments (Svetlicic *et al.*, 2023). *L. massiliensis* was isolated from a cooling tower in the South of France (Campocasso *et al.*, 2012). Capsule clusters can be acquired by horizontal gene transfer and recombination (Manson, Hancock and Gilmore, 2010; Lãm *et al.*, 2011; Putonti *et al.*, 2013; Mostowy *et al.*, 2017). Thus, given the diverse ecological niches, it can be speculated that *L. longbeachae*, *L. gormanii*, and *L. massiliensis* acquired the *ctrBCD/bexD* genes from interactions with other environmental bacteria. In addition, we detected orthologous genes of *ctrD* and *bexD* in *L. oakridgensis*, *L. micdadei*, and *L. anisa*. However, these species also do not encode most of the glycosyltransferases found in *L. longbeachae*. Possibly, we do not detect other orthologs because they are below the similarity cutoff of 30% identity, or because other genes of the ABC transporter complex have been lost in these species. Domain-guided predictions may further help in detecting putative export related genes or glycosyltransferases in these other *Legionella* spp.

By generating a knockout mutant in the *ctrC* gene of *L. longbeachae*, we could show by electron microscopy that the capsule is no longer produced. We can partially complement this mutant and restore capsule production. However, we do not know which genes exactly are involved in the biosynthesis of the capsule. Sugar precursors that can be used for bacterial capsules may be generated in many metabolic pathways in the cell, and those genes need not be confined to the capsule locus only (e.g. *L. longbeachae* encodes three copies of *galE*, and two copies of *galU*). However, our study of the biosynthesis of the capsule was limited by the lack of other mutants in *L. longbeachae*, as it is very challenging and time consuming to create knockout mutants in this species. Ideally, to further identify capsule-specific biosynthesis genes, mutants in both the LPS and the capsule loci need to be obtained. In addition to the afore-mentioned genes in the capsule cluster, these mutants may involve the LPS flippase WzxE (*llo0227*), the O-antigen ligase encoded in a different locus (*llo2039*), or the WecA starter enzyme for LPS O-antigen biosynthesis (*llo2072*). We tried to obtain these different mutants but, unfortunately, we did not succeed. Mutants in the LPS biosynthesis pathway may in addition help us to separate the O-antigen from CPS.

What are the regulatory circuits governing capsule expression in *L. longbeachae*?

Using RNAseq, we show that the capsule cluster is transcribed in exponential growth phase and downregulated in post-exponential growth phase. Thus, transcription of the capsule occurs during exponential growth, but the capsule is expressed later during post-exponential phase, as seen by TEM imaging. When we analyzed the transcriptional profiles of the capsule mutant, with the exception of the capsule transporter, we did not detect significantly different transcription profiles between wild type and mutant *L. longbeachae* across the capsule locus. The biosynthesis pathways of LPS and CPS can be intertwined, as both may incorporate common nucleotide sugar precursors. For example, transcription of the *E. coli* K5 capsule is coregulated by the LPS anti-terminator RfaH (Stevens *et al.*, 1994; Stevens, Clarke and Roberts, 1997; Rahn, Drummelsmith and Whitfield, 1999). We can speculate that sugar biosynthesis may be unaltered in the capsule mutant and that sugars, which would otherwise be integrated in the capsule, might be used in other anabolic processes in the cell, such as LPS biosynthesis. However, the dissection of these two different biosynthesis pathways and their regulation in *L. longbeachae* requires the generation of several mutant strains, as mentioned before.

Capsule biosynthesis can be regulated in a temperature-dependent manner, as exemplified by group 2 capsules in *E. coli*. This regulation happens *via* the transcriptional regulators, BipA and H-NS, which activate gene expression at specific CPS promoter regions at 37°C, but act as repressors at 20°C (Rowe *et al.*, 2000; Aldawood and Roberts, 2022). Moreover, group 2 CPS expression in *E. coli* was shown to be growth phase dependent (Aldawood and Roberts, 2022). Knockout mutants of the transcriptional regulators H-NS, SlyA, and IHF, may aid us in understanding the regulatory network governing capsule expression in *L. longbeachae*. A detailed study of promoter sequences and potential transcription factor consensus sequences may further help us in identifying transcriptional regulators of the capsule.

What is the capsule composed of and what might be the receptor(s) on host cells?

Unfortunately, *L. longbeachae* cannot be grown in published minimal media that are known to support growth of *L. pneumophila* (Häuslein *et al.*, 2016; Hochstrasser and Hilbi, 2022) – which would allow us to purify the CPS from liquid growth media. In our capsule purifications, we detected similar monosaccharides in phenol extracts from both the *L. longbeachae* wild type and the capsule mutant. However, the structural integrity of these extracts was highly compromised. Due to the high hydrophobicity of the *L. pneumophila* LPS, it is known that hot

phenol extraction is not suitable to isolate LPS from this species (Lück and Helbig, 2013). In contrast, when we used an enzymatic isolation method, we could show a ladder like pattern in the PS extracts from both *L. longbeachae* strains as well as *L. pneumophila*. The bimodal distribution that we see in the *L. pneumophila* O-antigen has been shown previously (Lüneberg *et al.*, 1998), thus confirming that enzymatic isolation is also a suitable method for *L. longbeachae* PS extraction. The *L. longbeachae* extracts clearly show an extended O-antigen ladder. This contrasts with previous studies by Sonesson and collaborators, who reported that *L. longbeachae* expressed a rough type LPS (Sonesson *et al.*, 1994). It must be noted that this study based its findings on phenol extracts, which is most likely why they did not detect O-antigen in *L. longbeachae*. However, using conventional silver staining methods, we did not detect any fraction that would correspond to CPS in the *L. longbeachae* wild type. Only when we applied Stains-all dye, we detected a band at around 100 kDa, which was absent in the capsule mutant and in *L. pneumophila* as control. Thus, for further experiments, anion exchange purification may aid in isolation of the highly anionic fraction in the *L. longbeachae* wild type. With a purified CPS, we may generate a capsule-specific antibody and identify possible cellular receptors.

Capsules and O-antigen play an important role in avoiding complement-mediated killing. The length of O-antigen was reported to mediate escape from complement-mediated killing in *Salmonella enterica* and *Pseudomonas aeruginosa* (Murray, Attridge and Morona, 2006; Kintz *et al.*, 2008). Capsules, on the other hand, can bind complement factors and shield them from recognition by innate immune cells (Cress *et al.*, 2014). It has also been described that capsules mediate the binding of complement regulatory proteins, which aid in avoiding complement deposition and formation of the membrane attack complex on bacteria (Jarva *et al.*, 2005; Merino and Tomás, 2015). This opens interesting questions to be addressed for the interaction of the *L. longbeachae* CPS with complement. We may further test the binding of complement factors, such as C3b, as well as the binding of serum antibodies, such as IgG and IgM, to *L. longbeachae* wild type as compared to the capsule mutant. This may aid in understanding how the wild type delays phagocytosis into host cells.

Capsules can be detected by carbohydrate-binding proteins, so-called lectins. Pulmonary cell-associated lectins, which are expressed by macrophages and dendritic cells, include the mannose/GlcNAc/fucose receptor (MR), DC-SIGN, and Dectin-1 (Sahly *et al.*, 2008). The latter detects β -glucan on fungi, and DC-SIGN recognizes mannose-rich glycans (Sahly *et al.*, 2008). DC-SIGN is involved in the uptake of bacteria, and it has been shown to enhance production of IL-10 and to decrease T helper 1 cell polarization in a capsule-dependent manner

in *K. pneumoniae* (Evrard *et al.*, 2010). Secreted lectins in the lung include surfactant protein A and D (SP-A; SP-D). Both secreted and cell-bound lectins have been shown to recognize LPS and capsule of pathogens, such as *E. coli*, *K. pneumoniae*, or *P. aeruginosa* (Sahly *et al.*, 2008). Nothing is known about the direct interaction of *L. longbeachae* with lectin receptors and other PRRs. Thus, testing the role of the capsule may provide better insights into how cellular uptake and/or immune evasion are mediated by wild type bacteria.

What roles do specific immune cell subsets play in the host response to the *L. longbeachae* capsule?

Capsules have been shown to be important virulence factors in many diderm bacteria, such as *N. meningitidis* group B, *E. coli* K1 and K5, *K. pneumoniae*, or *Haemophilus influenzae* type b (Bortolussi R *et al.*, 1979; Cortés *et al.*, 2002; Lawlor *et al.*, 2005; Sukupolvi-Petty, Grass and StGeme, 2006; Cress *et al.*, 2014; Tzeng, Thomas and Stephens, 2015). Our data show that the capsule is a crucial virulence factor for *L. longbeachae* in the mouse model of infection, and that the capsule mutant is completely avirulent. We can partially restore virulence *in vivo* by complementation. We further show that wild type *L. longbeachae* can replicate better in murine lungs than the capsule mutant. Neutrophils are among the first line defense to counteract pathogenic bacteria and they play a crucial role in limiting infection (Balamayooran *et al.*, 2010). It has been shown that *L. pneumophila* can infect neutrophils, if the *lag-1* gene coding for an LPS O-acetylase is absent (Wee *et al.*, 2021). Previous studies also reported that polymorphonuclear leukocytes (PMNs), which include neutrophils, can phagocytose *L. pneumophila* (Horwitz and Silverstein, 1981; Verbrugh *et al.*, 1985). Thus, testing the interaction of *L. longbeachae* with neutrophils and their response to the capsule may provide more insight into the early immune response to the bacteria. It must be noted that when we infected THP-1 cells and BMDMs *in vitro*, we did not observe a replication defect of the capsule mutant as compared to the wild type. Therefore, we can ask the questions which other immune cells may play a role in response to the *L. longbeachae* capsule. Dendritic cells (DCs) are important mediators between innate and adaptive immune responses, and we detected a stronger pro-inflammatory cytokine secretion when we infected murine DCs with the capsule mutant than with the wild type. In addition, DCs express PRRs that include lectin receptors, which may recognize the capsule and modulate the immune response, as shown for *K. pneumoniae* (Evrard *et al.*, 2010).

Does the capsule protect *L. longbeachae* from antimicrobial peptides and antibiotics?

Capsules have been shown to mediate resistance to cationic antimicrobial peptides (CAMPs) (Campos *et al.*, 2004; Llobet, Tomás and Bengoechea, 2008; Jones *et al.*, 2009). Likewise, capsules can mediate protection from antibiotics and the presence of capsule coding genes correlates with the presence of antibiotic resistance genes in diderm bacteria (Geisinger and Isberg, 2015; Rendueles *et al.*, 2018). In our study, we did not address the questions of whether the capsule protects *L. longbeachae* from these antimicrobial compounds. Testing whether the capsule mediates resistance to CAMPs or antibiotics may provide us with valuable information on the importance of the capsule in the life cycle of *L. longbeachae* in the environment and in the eukaryotic host.

REFERENCES

- Abel, B., Thieblemont, N., Quesniaux, V.J.F., Brown, N., Mpagi, J., Miyake, K., Bihl, F., Ryffel, B., 2002. Toll-Like Receptor 4 Expression Is Required to Control Chronic *Mycobacterium tuberculosis* Infection in Mice. *J. Immunol.* 169, 3155–3162. <https://doi.org/10.4049/jimmunol.169.6.3155>
- Albiger, B., Dahlberg, S., Henriques-Normark, B., Normark, S., 2007. Role of the innate immune system in host defence against bacterial infections: focus on the Toll-like receptors. *J. Intern. Med.* 261, 511–528. <https://doi.org/10.1111/j.1365-2796.2007.01821.x>
- Aldawood, E., Roberts, I.S., 2022. Regulation of *Escherichia coli* Group 2 Capsule Gene Expression: A Mini Review and Update. *Front. Microbiol.* 13, 858767. <https://doi.org/10.3389/fmicb.2022.858767>
- Alexander, C., Rietschel, E.Th., 2001. Invited review: Bacterial lipopolysaccharides and innate immunity. *J. Endotoxin Res.* 7, 167–202. <https://doi.org/10.1177/09680519010070030101>
- Alli, O.A.T., Gao, L.-Y., Pedersen, L.L., Zink, S., Radulic, M., Doric, M., Kwaik, Y.A., 2000. Temporal Pore Formation-Mediated Egress from Macrophages and Alveolar Epithelial Cells by *Legionella pneumophila*. *INFECT IMMUN* 68.
- Amodeo, M.R., Murdoch, D.R., Pithie, A.D., 2010. Legionnaires' disease caused by *Legionella longbeachae* and *Legionella pneumophila*: comparison of clinical features, host-related risk factors, and outcomes. *Clin. Microbiol. Infect.* 16, 1405–1407. <https://doi.org/10.1111/j.1469-0691.2009.03125.x>
- Anderson, M.S., Bulawa, C.E., Raetz, C.R., 1985. The biosynthesis of gram-negative endotoxin. Formation of lipid A precursors from UDP-GlcNAc in extracts of *Escherichia coli*. *J. Biol. Chem.* 260, 15536–15541. [https://doi.org/10.1016/S0021-9258\(17\)36289-0](https://doi.org/10.1016/S0021-9258(17)36289-0)
- Anderson, M.S., Raetz, C.R., 1987. Biosynthesis of lipid A precursors in *Escherichia coli*. A cytoplasmic acyltransferase that converts UDP-N-acetylglucosamine to UDP-3-O-(R-3-hydroxymyristoyl)-N-acetylglucosamine. *J. Biol. Chem.* 262, 5159–5169. [https://doi.org/10.1016/S0021-9258\(18\)61169-X](https://doi.org/10.1016/S0021-9258(18)61169-X)
- Andrews, H.L., Vogel, J.P., Isberg, R.R., 1998. Identification of Linked *Legionella pneumophila* Genes Essential for Intracellular Growth and Evasion of the Endocytic Pathway. *Infect. Immun.* 66, 950–958. <https://doi.org/10.1128/IAI.66.3.950-958.1998>
- Arasaki, K., Toomre, D.K., Roy, C.R., 2012. The *Legionella pneumophila* Effector DrrA Is Sufficient to Stimulate SNARE-Dependent Membrane Fusion. *Cell Host Microbe* 11, 46–57. <https://doi.org/10.1016/j.chom.2011.11.009>
- Arata, S., Newton, C., Klein, T.W., Yamamoto, Y., Friedman, H., 1993. *Legionella pneumophila* Induced Tumor Necrosis Factor Production in Permissive versus Nonpermissive Macrophages. *Exp. Biol. Med.* 203, 26–29. <https://doi.org/10.3181/00379727-203-43568>
- Asare, R., Abu Kwaik, Y., 2007. Early trafficking and intracellular replication of *Legionella longbeachaea* within an ER-derived late endosome-like phagosome. *Cell. Microbiol.* 9, 1571–1587. <https://doi.org/10.1111/j.1462-5822.2007.00894.x>
- Asare, R., Santic, M., Gobin, I., Doric, M., Suttles, J., Graham, J.E., Price, C.D., Abu Kwaik, Y., 2007. Genetic Susceptibility and Caspase Activation in Mouse and Human Macrophages Are Distinct for *Legionella longbeachae* and *L. pneumophila*. *Infect. Immun.* 75, 1933–1945. <https://doi.org/10.1128/IAI.00025-07>
- Balamayooran, G., Batra, S., Fessler, M.B., Happel, K.I., Jeyaseelan, S., 2010. Mechanisms of Neutrophil Accumulation in the Lungs Against Bacteria. *Am. J. Respir. Cell Mol. Biol.* 43, 5–16. <https://doi.org/10.1165/rcmb.2009-0047TR>
- Balducci, E., Papi, F., Capialdi, D.E., Del Bino, L., 2023. Polysaccharides' Structures and Functions in Biofilm Architecture of Antimicrobial-Resistant (AMR) Pathogens. *Int. J. Mol. Sci.* 24, 4030. <https://doi.org/10.3390/ijms24044030>

References

- Barker, J., Lambert, P.A., Brown, M.R., 1993. Influence of intra-amoebic and other growth conditions on the surface properties of *Legionella pneumophila*. *Infect. Immun.* 61, 3503–3510. <https://doi.org/10.1128/iai.61.8.3503-3510.1993>
- Beauté, J., European Legionnaires' Disease Surveillance Network, 2017. Legionnaires' disease in Europe, 2011 to 2015. *Eurosurveillance* 22. <https://doi.org/10.2807/1560-7917.ES.2017.22.27.30566>
- Bell, H., Chintalapati, S., Patel, P., Halim, A., Kithas, A., Schmalzle, S.A., 2021. *Legionella longbeachae* pneumonia: Case report and review of reported cases in non-endemic countries. *IDCases* 23, e01050. <https://doi.org/10.1016/j.idcr.2021.e01050>
- Bellinger-Kawahara, C., Horwitz, M.A., 1990. Complement Component C3 Fixes Selectively to the Major Outer Membrane Protein (MOMP) of *Legionella pneumophila* and Mediates Phagocytosis of Liposome-MOMP Complexes by Human Monocytes. *J Exp Med* 1201–1210.
- Berger, K.H., Isberg, R.R., 1993. Two distinct defects in intracellular growth complemented by a single genetic locus in *Legionella pneumophila*. *Mol. Microbiol.* 7, 7–19. <https://doi.org/10.1111/j.1365-2958.1993.tb01092.x>
- Berk, S.G., Ting, R.S., Turner, G.W., Ashburn, R.J., 1998. Production of Respirable Vesicles Containing Live *Legionella pneumophila* Cells by Two *Acanthamoeba* spp. *Appl. Environ. Microbiol.* 64, 279–286. <https://doi.org/10.1128/AEM.64.1.279-286.1998>
- Bertani, B., Ruiz, N., 2018. Function and Biogenesis of Lipopolysaccharides. *EcoSal Plus* 8, ecosalplus.ESP-0001-2018. <https://doi.org/10.1128/ecosalplus.ESP-0001-2018>
- Bibb, W.F., Sorg, R.J., Thomason, B.M., Hicklin, M.D., Steigerwalt, A.G., Brenner, D.J., Wulf, M.R., 1981. Recognition of a second serogroup of *Legionella longbeachae*. *J. Clin. Microbiol.* 14, 674–677. <https://doi.org/10.1128/jcm.14.6.674-677.1981>
- Biernacka, D., Gorzelak, P., Klein, G., Raina, S., 2020. Regulation of the First Committed Step in Lipopolysaccharide Biosynthesis Catalyzed by LpxC Requires the Essential Protein LapC (YejM) and HslVU Protease. *Int. J. Mol. Sci.* 21, 9088. <https://doi.org/10.3390/ijms21239088>
- bioMérieux SA, 2023. Legionella Agar with L-cysteine (BCYE) [WWW Document]. URL <https://www.biomerieux-culturemedia.com/product/95-legionella-agar-with-l-cysteine--bcye--and-without-l-cysteine--bcy-> (accessed 8.20.23).
- Birkhead, M., Ganesh, K., Ndlangisa, K.M., Koornhof, H., 2017. Transmission electron microscopy protocols for capsule visualisation in pathogenic respiratory and meningeal bacteria.
- Blatt, S., 1993. Nosocomial, Legionnaires' Disease: Aspiration as a Primary Mode of Disease Acquisition. *Am. J. Med.* 95, 16–22.
- Böck, D., Hüsler, D., Steiner, B., Medeiros, J.M., Welin, A., Radomska, K.A., Hardt, W.-D., Pilhofer, M., Hilbi, H., 2021. The Polar *Legionella* Icm/Dot T4SS Establishes Distinct Contact Sites with the Pathogen Vacuole Membrane. *mBio* 12, e02180-21. <https://doi.org/10.1128/mBio.02180-21>
- Bortolussi R, Ferrieri P, Björkstén B, Quie P G, 1979. Capsular K1 polysaccharide of *Escherichia coli*: relationship to virulence in newborn rats and resistance to phagocytosis. *Infect. Immun.* 25, 293–298. <https://doi.org/10.1128/iai.25.1.293-298.1979>
- Bradley, B.T., Bryan, A., 2019. Emerging respiratory infections: The infectious disease pathology of SARS, MERS, pandemic influenza, and *Legionella*. *Semin. Diagn. Pathol.* 36, 152–159. <https://doi.org/10.1053/j.semdp.2019.04.006>
- Brown, L., Wolf, J.M., Prados-Rosales, R., Casadevall, A., 2015. Through the wall: extracellular vesicles in Gram-positive bacteria, mycobacteria and fungi. *Nat. Rev. Microbiol.* 13, 620–630. <https://doi.org/10.1038/nrmicro3480>
- Brown, S., Santa Maria, J.P., Walker, S., 2013. Wall Teichoic Acids of Gram-Positive Bacteria. *Annu. Rev. Microbiol.* 67, 313–336. <https://doi.org/10.1146/annurev-micro-092412-155620>

- Bruggemann, H., Hagman, A., Jules, M., Sismeiro, O., Dillies, M.-A., Gouyette, C., Kunst, F., Steinert, M., Heuner, K., Coppee, J.-Y., Buchrieser, C., 2006. Virulence strategies for infecting phagocytes deduced from the *in vivo* transcriptional program of *Legionella pneumophila*. *Cell. Microbiol.* 8, 1228–1240. <https://doi.org/10.1111/j.1462-5822.2006.00703.x>
- Bruin, J.P., Koshkolda, T., IJzerman, E.P.F., Luck, C., Diederer, B.M.W., Den Boer, J.W., Mouton, J.W., 2014. Isolation of ciprofloxacin-resistant *Legionella pneumophila* in a patient with severe pneumonia. *J. Antimicrob. Chemother.* 69, 2869–2871. <https://doi.org/10.1093/jac/dku196>
- Buffet, A., Rocha, E.P.C., Rendueles, O., 2021. Nutrient conditions are primary drivers of bacterial capsule maintenance in *Klebsiella*. *Proc R Soc B* 288. <https://doi.org/10.1098/rspb.2020.2876>
- Bugg, T.D.H., Walsh, C.T., 1992. Intracellular Steps of Bacterial Cell Wall Peptidoglycan Biosynthesis: Enzymology, Antibiotics, and Antibiotic Resistance. *Nat Prod Rep* 9, 199–215.
- Burstein, D., Amaro, F., Zusman, T., Lifshitz, Z., Cohen, O., Gilbert, J.A., Pupko, T., Shuman, H.A., Segal, G., 2016. Genomic analysis of 38 *Legionella* species identifies large and diverse effector repertoires. *Nat. Genet.* 48, 167–175. <https://doi.org/10.1038/ng.3481>
- Burstein, D., Zusman, T., Degtyar, E., Viner, R., Segal, G., Pupko, T., 2009. Genome-Scale Identification of *Legionella pneumophila* Effectors Using a Machine Learning Approach. *PLoS Pathog.* 5, e1000508. <https://doi.org/10.1371/journal.ppat.1000508>
- Bush, K., Bradford, P.A., 2019. Interplay between β -lactamases and new β -lactamase inhibitors. *Nat. Rev. Microbiol.* 17, 295–306. <https://doi.org/10.1038/s41579-019-0159-8>
- Caboni, M., Pédrón, T., Rossi, O., Goulding, D., Pickard, D., Citiulo, F., MacLennan, C.A., Dougan, G., Thomson, N.R., Saul, A., Sansonetti, P.J., Gerke, C., 2015. An O Antigen Capsule Modulates Bacterial Pathogenesis in *Shigella sonnei*. *PLOS Pathog.* 11, e1004749. <https://doi.org/10.1371/journal.ppat.1004749>
- Campocasso, A., Boughalmi, M., Fournous, G., Raoult, D., La Scola, B., 2012. *Legionella tunisiensis* sp. nov. and *Legionella massiliensis* sp. nov., isolated from environmental water samples. *Int. J. Syst. Evol. Microbiol.* 62, 3003–3006. <https://doi.org/10.1099/ijs.0.037853-0>
- Campos, M.A., Vargas, M.A., Regueiro, V., Llompарт, C.M., Albertí, S., Bengoechea, J.A., 2004. Capsule Polysaccharide Mediates Bacterial Resistance to Antimicrobial Peptides. *Infect. Immun.* 72, 7107–7114. <https://doi.org/10.1128/IAI.72.12.7107-7114.2004>
- Caroff, M., Karibian, D., Cavaillon, J.-M., Haeffner-Cavaillon, N., 2002. Structural and functional analyses of bacterial lipopolysaccharides. *Microbes Infect.* 4, 915–926. [https://doi.org/10.1016/S1286-4579\(02\)01612-X](https://doi.org/10.1016/S1286-4579(02)01612-X)
- Cazalet, C., Gomez-Valero, L., Rusniok, C., Lomma, M., Dervins-Ravault, D., Newton, H.J., Sansom, F.M., Jarraud, S., Zidane, N., Ma, L., Bouchier, C., Etienne, J., Hartland, E.L., Buchrieser, C., 2010. Analysis of the *Legionella longbeachae* Genome and Transcriptome Uncovers Unique Strategies to Cause Legionnaires' Disease. *PLoS Genet.* 6, e1000851. <https://doi.org/10.1371/journal.pgen.1000851>
- Cazalet, C., Jarraud, S., Ghavi-Helm, Y., Kunst, F., Glaser, P., Etienne, J., Buchrieser, C., 2008. Multigenome analysis identifies a worldwide distributed epidemic *Legionella pneumophila* clone that emerged within a highly diverse species. *Genome Res.* 18, 431–441. <https://doi.org/10.1101/gr.7229808>
- Cazalet, C., Rusniok, C., Brüggemann, H., Zidane, N., Magnier, A., Ma, L., Tichit, M., Jarraud, S., Bouchier, C., Vandenesch, F., Kunst, F., Etienne, J., Glaser, P., Buchrieser, C., 2004. Evidence in the *Legionella pneumophila* genome for exploitation of host cell functions and high genome plasticity. *Nat. Genet.* 36, 1165–1173. <https://doi.org/10.1038/ng1447>
- CDC, 2021a. *Legionella* (Legionnaires' Disease and Pontiac Fever); Diagnosis, Treatment, and Complications [WWW Document]. URL <https://www.cdc.gov/legionella/about/diagnosis.html> (accessed 7.4.23).
- CDC, 2021b. *Legionella* (Legionnaires' Disease and Pontiac Fever); Disease Specifics [WWW Document]. URL <https://www.cdc.gov/legionella/clinicians/disease-specifics.html> (accessed 7.4.23).

References

- CDC, 2018. *Legionella* (Legionnaires' Disease and Pontiac Fever); What Owners and Managers of Buildings and Healthcare Facilities Need to Know about the Growth and Spread of *Legionella* [WWW Document]. URL <https://www.cdc.gov/legionella/wmp/overview/growth-and-spread.html#:~:text=Legionella%20grows%20best%20within%20a,and%20keep%20hot%20water%20hot>. (accessed 7.4.23).
- Chambers, S.T., Slow, S., Scott-Thomas, A., Murdoch, D.R., 2021. Legionellosis Caused by Non-*Legionella pneumophila* Species, with a Focus on *Legionella longbeachae*. *Microorganisms* 9, 291. <https://doi.org/10.3390/microorganisms9020291>
- Chatfield, C.H., Cianciotto, N.P., 2013. Culturing, Media, and Handling of *Legionella*, in: Buchrieser, C., Hilbi, H. (Eds.), *Legionella: Methods and Protocols*. Humana Press, Totowa, NJ, pp. 151–162. https://doi.org/10.1007/978-1-62703-161-5_7
- Cianciotto, N.P., 2014. Type II Secretion and *Legionella* Virulence, in: Hilbi, H. (Ed.), *Molecular Mechanisms in Legionella Pathogenesis*. Springer Berlin Heidelberg, Berlin, Heidelberg, pp. 81–102. https://doi.org/10.1007/82_2013_339
- Ciesielska, A., Matyjek, M., Kwiatkowska, K., 2021. TLR4 and CD14 trafficking and its influence on LPS-induced pro-inflammatory signaling. *Cell. Mol. Life Sci.* 78, 1233–1261. <https://doi.org/10.1007/s00018-020-03656-y>
- Clarke, B.R., Cuthbertson, L., Whitfield, C., 2004. Nonreducing Terminal Modifications Determine the Chain Length of Polymannose O Antigens of *Escherichia coli* and Couple Chain Termination to Polymer Export via an ATP-binding Cassette Transporter. *J. Biol. Chem.* 279, 35709–35718. <https://doi.org/10.1074/jbc.M404738200>
- Clarke, B.R., Richards, M.R., Greenfield, L.K., Hou, D., Lowary, T.L., Whitfield, C., 2011. *In Vitro* Reconstruction of the Chain Termination Reaction in Biosynthesis of the *Escherichia coli* O9a O-Polysaccharide. *J. Biol. Chem.* 286, 41391–41401. <https://doi.org/10.1074/jbc.M111.295857>
- Cordes, L.G., Wilkinson, H.W., Gorman, G.W., Fikes, B., Fraser, D.W., 1979. ATYPICAL *LEGIONELLA*-LIKE ORGANISMS: FASTIDIOUS WATER-ASSOCIATED BACTERIA PATHOGENIC FOR MAN. *Lancet*.
- Correia, A.M., Ferreira, J.S., Borges, V., Nunes, A., Gomes, B., Capucho, R., Gonçalves, J., Antunes, D.M., Almeida, S., Mendes, A., Guerreiro, M., Sampaio, D.A., Vieira, L., Machado, J., Simões, M.J., Gonçalves, P., Gomes, J.P., 2016. Probable Person-to-Person Transmission of Legionnaires' Disease. *N. Engl. J. Med.* 374, 497–498. <https://doi.org/10.1056/NEJMc1505356>
- Cortés, G., Borrell, N., De Astorza, B., Gómez, C., Sauleda, J., Albertí, S., 2002. Molecular Analysis of the Contribution of the Capsular Polysaccharide and the Lipopolysaccharide O Side Chain to the Virulence of *Klebsiella pneumoniae* in a Murine Model of Pneumonia. *Infect. Immun.* 70, 2583–2590. <https://doi.org/10.1128/IAI.70.5.2583-2590.2002>
- Costa, T.R.D., Harb, L., Khara, P., Zeng, L., Hu, B., Christie, P.J., 2021. Type IV secretion systems: Advances in structure, function, and activation. *Mol. Microbiol.* 115, 436–452. <https://doi.org/10.1111/mmi.14670>
- Cress, B.F., Englaender, J.A., He, W., Kasper, D., Linhardt, R.J., Koffas, M.A.G., 2014. Masquerading microbial pathogens: capsular polysaccharides mimic host-tissue molecules. *FEMS Microbiol. Rev.* 38, 660–697. <https://doi.org/10.1111/1574-6976.12056>
- Cronan, J.E., 2003. Bacterial Membrane Lipids: Where Do We Stand? *Annu. Rev. Microbiol.* 57, 203–224. <https://doi.org/10.1146/annurev.micro.57.030502.090851>
- Cross, K.E., Mercante, J.W., Benitez, A.J., Brown, E.W., Diaz, M.H., Winchell, J.M., 2016. Simultaneous detection of *Legionella* species and *L. anisa*, *L. bozemanii*, *L. longbeachae* and *L. micdadei* using conserved primers and multiple probes in a multiplex real-time PCR assay. *Diagn. Microbiol. Infect. Dis.* 85, 295–301. <https://doi.org/10.1016/j.diagmicrobio.2016.03.022>
- Cuccui, J., Milne, T.S., Harmer, N., George, A.J., Harding, S.V., Dean, R.E., Scott, A.E., Sarkar-Tyson, M., Wren, B.W., Titball, R.W., Prior, J.L., 2012. Characterization of the *Burkholderia pseudomallei* K96243 Capsular Polysaccharide I Coding Region. *Infect. Immun.* 80, 1209–1221. <https://doi.org/10.1128/IAI.05805-11>

- Cunha, B.A., Burillo, A., Bouza, E., 2016. Legionnaires' disease. *The Lancet* 387, 376–385. [https://doi.org/10.1016/S0140-6736\(15\)60078-2](https://doi.org/10.1016/S0140-6736(15)60078-2)
- Dartigalongue, C., Missiakas, D., Raina, S., 2001. Characterization of the *Escherichia coli* σ^E Regulon. *J. Biol. Chem.* 276, 20866–20875. <https://doi.org/10.1074/jbc.M100464200>
- de Bruin, L., Timmerman, C.P., Huisman, P.M., Heidt, J., 2018. *Legionella longbeachae*; don't miss it! *Neth. J. Med.* 76.
- De Felipe, K.S., Pampou, S., Jovanovic, O.S., Pericone, C.D., Ye, S.F., Kalachikov, S., Shuman, H.A., 2005. Evidence for Acquisition of *Legionella* Type IV Secretion Substrates via Interdomain Horizontal Gene Transfer. *J. Bacteriol.* 187, 7716–7726. <https://doi.org/10.1128/JB.187.22.7716-7726.2005>
- DeRoy, C., Fratamico, P.M., Yan, X., Baranzoni, G., Liu, Y., Needleman, D.S., Tebbs, R., O'Connell, C.D., Allred, A., Swimley, M., Mwangi, M., Kapur, V., Raygoza Garay, J.A., Roberts, E.L., Katani, R., 2016. Comparison of O-Antigen Gene Clusters of All O-Serogroups of *Escherichia coli* and Proposal for Adopting a New Nomenclature for O-Typing. *PLOS ONE* 11, e0147434. <https://doi.org/10.1371/journal.pone.0147434>
- DeRoy, S., Dao, J., Söderberg, M., Rossier, O., Cianciotto, N.P., 2006. *Legionella pneumophila* type II secretome reveals unique exoproteins and a chitinase that promotes bacterial persistence in the lung. *Proc. Natl. Acad. Sci.* 103, 19146–19151. <https://doi.org/10.1073/pnas.0608279103>
- Di Perri, G.D., Ferlazzo, G., 2022. Biofilm Development and Approaches to Biofilm Inhibition by Exopolysaccharides. *New Microbiol.* 45, 227–236.
- Dolinsky, S., Haneburger, I., Cichy, A., Hannemann, M., Itzen, A., Hilbi, H., 2014. The *Legionella longbeachae* Icm/Dot Substrate SidC Selectively Binds Phosphatidylinositol 4-Phosphate with Nanomolar Affinity and Promotes Pathogen Vacuole-Endoplasmic Reticulum Interactions. *Infect. Immun.* 82, 4021–4033. <https://doi.org/10.1128/IAI.01685-14>
- Dong, A., Liu, C., Hua, X., Yu, Y., Guo, Y., Wang, D., Liu, X., Chen, H., Wang, H., Zhu, L., 2023. Bioinformatic analysis of structures and encoding genes of *Escherichia coli* surface polysaccharides sheds light on the heterologous biosynthesis of glycans. *BMC Genomics* 24, 168. <https://doi.org/10.1186/s12864-023-09269-6>
- Douglass, M.V., Cléon, F., Trent, M.S., 2021. Cardiolipin aids in lipopolysaccharide transport to the gram-negative outer membrane. *Proc. Natl. Acad. Sci.* 118, e2018329118. <https://doi.org/10.1073/pnas.2018329118>
- Dunstan, R.A., Bamert, R.S., Belousoff, M.J., Short, F.L., Barlow, C.K., Pickard, D.J., Wilksch, J.J., Schittenhelm, R.B., Strugnell, R.A., Dougan, G., Lithgow, T., 2021. Mechanistic Insights into the Capsule-Targeting Depolymerase from a *Klebsiella pneumoniae* Bacteriophage. *Microbiol. Spectr.* 9, e01023-21. <https://doi.org/10.1128/Spectrum.01023-21>
- ECDC, 2023. Surveillance Atlas of Infectious Diseases [WWW Document]. URL <http://atlas.ecdc.europa.eu/public/index.aspx> (accessed 6.4.23).
- Escoll, P., Platon, L., Dramé, M., Sahr, T., Schmidt, S., Rusniok, C., Buchrieser, C., 2021. Reverting the mode of action of the mitochondrial FOF1-ATPase by *Legionella pneumophila* preserves its replication niche. *eLife* 10, e71978. <https://doi.org/10.7554/eLife.71978>
- Escoll, P., Song, O.-R., Viana, F., Steiner, B., Lagache, T., Olivo-Marin, J.-C., Impens, F., Brodin, P., Hilbi, H., Buchrieser, C., 2017. *Legionella pneumophila* Modulates Mitochondrial Dynamics to Trigger Metabolic Repurposing of Infected Macrophages. *Cell Host Microbe* 22, 302-316.e7. <https://doi.org/10.1016/j.chom.2017.07.020>
- Evrard, B., Balestrino, D., Dosgilbert, A., Bouya-Gachancard, J.-L.J., Charbonnel, N., Forestier, C., Tridon, A., 2010. Roles of Capsule and Lipopolysaccharide O Antigen in Interactions of Human Monocyte-Derived Dendritic Cells and *Klebsiella pneumoniae*. *Infect. Immun.* 78, 210–219. <https://doi.org/10.1128/IAI.00864-09>
- Fields, B.S., Benson, R.F., Besser, R.E., 2002. *Legionella* and Legionnaires' Disease: 25 Years of Investigation. *Clin. Microbiol. Rev.* 15, 506–526. <https://doi.org/10.1128/CMR.15.3.506-526.2002>

References

- Fivenson, E.M., Bernhardt, T.G., 2020. An Essential Membrane Protein Modulates the Proteolysis of LpxC to Control Lipopolysaccharide Synthesis in *Escherichia coli*. *mBio* 11, e00939-20. <https://doi.org/10.1128/mBio.00939-20>
- Fleeman, R.M., Macias, L.A., Brodbelt, J.S., Davies, B.W., 2020. Defining principles that influence antimicrobial peptide activity against capsulated *Klebsiella pneumoniae*. *Proc. Natl. Acad. Sci.* 117, 27620–27626. <https://doi.org/10.1073/pnas.2007036117>
- Follador, R., Heinz, E., Wyres, K.L., Ellington, M.J., Kowarik, M., Holt, K.E., Thomson, N.R., 2016. The diversity of *Klebsiella pneumoniae* surface polysaccharides. *Microb. Genomics* 2. <https://doi.org/10.1099/mgen.0.000073>
- Franco, A.V., Liu, D., Reeves, P.R., 1996. A Wzz (Cld) protein determines the chain length of K lipopolysaccharide in *Escherichia coli* O8 and O9 strains. *J. Bacteriol.* 178, 1903–1907. <https://doi.org/10.1128/jb.178.7.1903-1907.1996>
- Fraser, D.W., Tsai, T.R., Orenstein, W., Parkin, W.E., Beecham, H.J., Sharrar, R.G., Harris, J., Mallison, G.F., Martin, S.M., McDade, J.E., Shepard, C.C., Brachman, P.S., The Field Investigation Team, 1977. LEGIONNAIRES' DISEASE. Description of an Epidemic Pneumonia. *N. Engl. J. Med.* 297.
- Fuse, E.T., Tateda, K., Kikuchi, Y., Matsumoto, T., Gondaira, F., Azuma, A., Kudoh, S., Standiford, T.J., Yamaguchi, K., 2007. Role of Toll-like receptor 2 in recognition of *Legionella pneumophila* in a murine pneumonia model. *J. Med. Microbiol.* 56, 305–312. <https://doi.org/10.1099/jmm.0.46913-0>
- Gao, L.-Y., Abu Kwaik, Y., 2000. The mechanism of killing and exiting the protozoan host *Acanthamoeba polyphaga* by *Legionella pneumophila*. *Environ. Microbiol.* 2, 79–90. <https://doi.org/10.1046/j.1462-2920.2000.00076.x>
- Geisinger, E., Isberg, R.R., 2015. Antibiotic Modulation of Capsular Exopolysaccharide and Virulence in *Acinetobacter baumannii*. *PLOS Pathog.* 11, e1004691. <https://doi.org/10.1371/journal.ppat.1004691>
- Girard, R., Pedron, T., Uematsu, S., Balloy, V., Chignard, M., Akira, S., Chaby, R., 2003. Lipopolysaccharides from *Legionella* and *Rhizobium* stimulate mouse bone marrow granulocytes via Toll-like receptor 2. *J. Cell Sci.* 116, 293–302. <https://doi.org/10.1242/jcs.00212>
- Gobin, I., Susa, M., Begic, G., Hartland, E.L., Doric, M., 2009. Experimental *Legionella longbeachae* infection in intratracheally inoculated mice. *J. Med. Microbiol.* 58, 723–730. <https://doi.org/10.1099/jmm.0.007476-0>
- Gomez-Valero, L., Rusniok, C., Carson, D., Mondino, S., Pérez-Cobas, A.E., Rolando, M., Pasricha, S., Reuter, S., Demirtas, J., Crumbach, J., Descorps-Declere, S., Hartland, E.L., Jarraud, S., Dougan, G., Schroeder, G.N., Frankel, G., Buchrieser, C., 2019. More than 18,000 effectors in the *Legionella* genus genome provide multiple, independent combinations for replication in human cells. *Proc. Natl. Acad. Sci.* 116, 2265–2273. <https://doi.org/10.1073/pnas.1808016116>
- Gomez-Valero, L., Rusniok, C., Jarraud, S., Vacherie, B., Rouy, Z., Barbe, V., Medigue, C., Etienne, J., Buchrieser, C., 2011. Extensive recombination events and horizontal gene transfer shaped the *Legionella pneumophila* genomes. *BMC Genomics* 12, 536. <https://doi.org/10.1186/1471-2164-12-536>
- Gonçalves, I.G., Fernandes, H.S., Melo, A., Sousa, S.F., Simões, L.C., Simões, M., 2021. LegionellaDB – A Database on *Legionella* Outbreaks. *Trends Microbiol.* 29, 863–866. <https://doi.org/10.1016/j.tim.2021.01.015>
- Gorzela, P., Klein, G., Raina, S., 2021. Molecular Basis of Essentiality of Early Critical Steps in the Lipopolysaccharide Biogenesis in *Escherichia coli* K-12: Requirement of MsbA, Cardiolipin, LpxL, LpxM and GcvB. *Int. J. Mol. Sci.* 22, 5099. <https://doi.org/10.3390/ijms22105099>
- Graham, F.F., Harte, D., Zhang, J., Fyfe, C., Baker, Michael.G., 2023. Increased Incidence of Legionellosis after Improved Diagnostic Methods, New Zealand, 2000–2020. *Emerg. Infect. Dis.* 29. <https://doi.org/10.3201/eid2906.221598>
- Greenfield, L.K., Whitfield, C., 2012. Synthesis of lipopolysaccharide O-antigens by ABC transporter-dependent pathways. *Carbohydr. Res.* 356, 12–24. <https://doi.org/10.1016/j.carres.2012.02.027>

- Hammerschmidt, S., Müller, A., Sillmann, H., Miühlenhoff, M., Borrow, R., Fox, A., Putten, J., Zollinger, W.D., Gerardy-Schahn, R., Frosch, M., 1996. Capsule phase variation in *Neisseria meningitidis* serogroup B by slipped-strand mispairing in the polysialyltransferase gene (*siaD*): correlation with bacterial invasion and the outbreak of meningococcal disease. *Mol. Microbiol.* 20, 1211–1220. <https://doi.org/10.1111/j.1365-2958.1996.tb02641.x>
- Harrison, O.B., Claus, H., Jiang, Y., Bennett, J.S., Bratcher, H.B., Jolley, K.A., Corton, C., Care, R., Poolman, J.T., Zollinger, W.D., Frasc, C.E., Stephens, D.S., Feavers, I., Frosch, M., Parkhill, J., Vogel, U., Quail, M.A., Bentley, S.D., Maiden, M.C.J., 2013. Description and Nomenclature of *Neisseria meningitidis* Capsule Locus. *Emerg. Infect. Dis.* 19, 566–573. <https://doi.org/10.3201/eid1904.111799>
- Haudiquet, M., Buffet, A., Rendueles, O., Rocha, E.P.C., 2021. Interplay between the cell envelope and mobile genetic elements shapes gene flow in populations of the nosocomial pathogen *Klebsiella pneumoniae*. *PLOS Biol.* 19, e3001276. <https://doi.org/10.1371/journal.pbio.3001276>
- Häuslein, I., Manske, C., Goebel, W., Eisenreich, W., Hilbi, H., 2016. Pathway analysis using ¹³C-glycerol and other carbon tracers reveals a bipartite metabolism of *Legionella pneumophila*. *Mol. Microbiol.* 100, 229–246.
- Hawn, T.R., Verbon, A., Janer, M., Zhao, L.P., Beutler, B., Aderem, A., 2005. Toll-like receptor 4 polymorphisms are associated with resistance to Legionnaires' disease. *Proc. Natl. Acad. Sci.* 102, 2487–2489. <https://doi.org/10.1073/pnas.0409831102>
- Health Protection Scotland, 2014. Cluster of *Legionella longbeachae* cases in Scotland in September/October 2013. Health Protection Scotland.
- Heijnsbergen, E., Roda Husman, A.M., Lodder, W.J., Bouwknecht, M., Docters Van Leeuwen, A.E., Bruin, J.P., Euser, S.M., Boer, J.W., Schalk, J.A.C., 2014. Viable *Legionella pneumophila* bacteria in natural soil and rainwater puddles. *J. Appl. Microbiol.* 117, 882–890. <https://doi.org/10.1111/jam.12559>
- Heinrichs, D.E., Yethon, J.A., Whitfield, C., 1998. Molecular basis for structural diversity in the core regions of the lipopolysaccharides of *Escherichia coli* and *Salmonella enterica*. *Mol. Microbiol.* 30, 221–232. <https://doi.org/10.1046/j.1365-2958.1998.01063.x>
- Ho, H., Miu, A., Alexander, M.K., Garcia, N.K., Oh, A., Zilberleyb, I., Reichelt, M., Austin, C.D., Tam, C., Shriver, S., Hu, H., Labadie, S.S., Liang, J., Wang, L., Wang, J., Lu, Y., Purkey, H.E., Quinn, J., Franke, Y., Clark, K., Beresini, M.H., Tan, M.-W., Sellers, B.D., Maurer, T., Koehler, M.F.T., Weckler, A.T., Kiefer, J.R., Verma, V., Xu, Y., Nishiyama, M., Payandeh, J., Koth, C.M., 2018. Structural basis for dual-mode inhibition of the ABC transporter MsbA. *Nature* 557, 196–201. <https://doi.org/10.1038/s41586-018-0083-5>
- Hochstrasser, R., Hilbi, H., 2022. The *Legionella* Lqs-LvbR Regulatory Network Controls Temperature-Dependent Growth Onset and Bacterial Cell Density. *Appl. Environ. Microbiol.* 88.
- Hoffmann, C., Finsel, I., Otto, A., Pfaffinger, G., Rothmeier, E., Hecker, M., Becher, D., Hilbi, H., 2014. Functional analysis of novel Rab GTPases identified in the proteome of purified *Legionella*-containing vacuoles from macrophages: Macrophage LCV proteome. *Cell. Microbiol.* n/a-n/a. <https://doi.org/10.1111/cmi.12256>
- Horwitz, M., 1984. Phagocytosis of the legionnaires' disease bacterium (*Legionella pneumophila*) occurs by a novel mechanism: Engulfment within a Pseudopod coil. *Cell* 36, 27–33. [https://doi.org/10.1016/0092-8674\(84\)90070-9](https://doi.org/10.1016/0092-8674(84)90070-9)
- Horwitz, M.A., Maxfield, F.R., 1984. *Legionella pneumophila* inhibits acidification of its phagosome in human monocytes. *J. Cell Biol.* 99, 1936–1943. <https://doi.org/10.1083/jcb.99.6.1936>
- Horwitz, M.A., Silverstein, S.C., 1981. Interaction of the legionnaires' disease bacterium (*Legionella pneumophila*) with human phagocytes. II. Antibody promotes binding of *L. pneumophila* to monocytes but does not inhibit intracellular multiplication. *J. Exp. Med.* 153, 398–406. <https://doi.org/10.1084/jem.153.2.398>
- Houliston, R.S., Vinogradov, E., Dzieciatkowska, M., Li, J., St. Michael, F., Karwaski, M.-F., Brochu, D., Jarrell, H.C., Parker, C.T., Yuki, N., Mandrell, R.E., Gilbert, M., 2011. Lipooligosaccharide of *Campylobacter jejuni*. *J. Biol. Chem.* 286, 12361–12370. <https://doi.org/10.1074/jbc.M110.181750>

References

- Huang, L., Boyd, D., Amyot, W.M., Hempstead, A.D., Luo, Z., O'Connor, T.J., Chen, C., Machner, M., Montminy, T., Isberg, R.R., 2011. The E Block motif is associated with *Legionella pneumophila* translocated substrates. *Cell. Microbiol.* 13, 227–245. <https://doi.org/10.1111/j.1462-5822.2010.01531.x>
- Islam, S.T., Lam, J.S., 2014. Synthesis of bacterial polysaccharides via the Wzx/Wzy-dependent pathway. *Can. J. Microbiol.* 60, 697–716. <https://doi.org/10.1139/cjm-2014-0595>
- Jarva, H., Ram, S., Vogel, U., Blom, A.M., Meri, S., 2005. Binding of the Complement Inhibitor C4bp to Serogroup B *Neisseria meningitidis*. *J. Immunol.* 174, 6299–6307. <https://doi.org/10.4049/jimmunol.174.10.6299>
- Jayaratne, P., Keenleyside, W.J., MacLachlan, P.R., Dodgson, C., Whitfield, C., 1993. Characterization of rcsB and rcsC from *Escherichia coli* O9:K30:H12 and examination of the role of the rcs regulatory system in expression of group I capsular polysaccharides. *J. Bacteriol.* 175, 5384–5394. <https://doi.org/10.1128/jb.175.17.5384-5394.1993>
- Jeong, K.C., Ghosal, D., Chang, Y.-W., Jensen, G.J., Vogel, J.P., 2017. Polar delivery of *Legionella* type IV secretion system substrates is essential for virulence. *Proc. Natl. Acad. Sci.* 114, 8077–8082. <https://doi.org/10.1073/pnas.1621438114>
- Jia, X., Ren, H., Nie, X., Li, Y., Li, J., Qin, T., 2019. Antibiotic Resistance and Azithromycin Resistance Mechanism of *Legionella pneumophila* Serogroup 1 in China. *Antimicrob. Agents Chemother.* 63, e00768-19. <https://doi.org/10.1128/AAC.00768-19>
- Jones, A., Geörg, M., Maudsdotter, L., Jonsson, A.-B., 2009. Endotoxin, Capsule, and Bacterial Attachment Contribute to *Neisseria meningitidis* Resistance to the Human Antimicrobial Peptide LL-37. *J. Bacteriol.* 191, 3861–3868. <https://doi.org/10.1128/JB.01313-08>
- Jürgens, D., Fehrenbach, F.J., 1997. Identification of *Legionella* species by lipopolysaccharide antigen pattern. *J. Clin. Microbiol.* 35, 3054–3057. <https://doi.org/10.1128/jcm.35.12.3054-3057.1997>
- Kahler, C.M., Martin, L.E., Shih, G.C., Rahman, M.M., Carlson, R.W., Stephens, D.S., 1998. The (α →8)-Linked Polysialic Acid Capsule and Lipooligosaccharide Structure Both Contribute to the Ability of Serogroup B *Neisseria meningitidis* To Resist the Bactericidal Activity of Normal Human Serum. *Infect. Immun.* 66, 5939–5947. <https://doi.org/10.1128/IAI.66.12.5939-5947.1998>
- Kaneko, T., Stogios, P.J., Ruan, X., Voss, C., Evdokimova, E., Skarina, T., Chung, A., Liu, X., Li, L., Savchenko, A., Ensminger, A.W., Li, S.S.-C., 2018. Identification and characterization of a large family of superbinding bacterial SH2 domains. *Nat. Commun.* 9, 4549. <https://doi.org/10.1038/s41467-018-06943-2>
- Kaper, J.B., Nataro, J.P., Mobley, H.L.T., 2004. Pathogenic *Escherichia coli*. *Nat. Rev. Microbiol.* 2, 123–140. <https://doi.org/10.1038/nrmicro818>
- Kawai, T., 2014. Toll-like receptor signaling pathways. *Front. Immunol.*
- Keenleyside, W.J., Jayaratne, P., MacLACHLAN, P.R., Whitfield, C., 1992. The rcsA Gene of *Escherichia coli* O9:K30:H12 Is Involved in the Expression of the Serotype-Specific Group I K (Capsular) Antigen. *J BACTERIOL.*
- Keenleyside, W.J., Whitfield, C., 1996. A Novel Pathway for O-Polysaccharide Biosynthesis in *Salmonella enterica* Serovar Borreze. *J. Biol. Chem.* 271, 28581–28592. <https://doi.org/10.1074/jbc.271.45.28581>
- Kenagy, E., Priest, P.C., Cameron, C.M., Smith, D., Scott, P., Cho, V., Mitchell, P., Murdoch, D.R., 2017. Risk Factors for *Legionella longbeachae* Legionnaires' Disease, New Zealand. *Emerg. Infect. Dis.* 23. <https://doi.org/10.3201/eid2307.161429>
- Kenyon, J.J., Hall, R.M., 2013. Variation in the Complex Carbohydrate Biosynthesis Loci of *Acinetobacter baumannii* Genomes. *PLoS ONE* 8, e62160. <https://doi.org/10.1371/journal.pone.0062160>
- Kintz, E., Scarff, J.M., DiGiandomenico, A., Goldberg, J.B., 2008. Lipopolysaccharide O-Antigen Chain Length Regulation in *Pseudomonas aeruginosa* Serogroup O11 Strain PA103. *J. Bacteriol.* 190, 2709–2716. <https://doi.org/10.1128/JB.01646-07>

- Klein, G., Lindner, B., Brade, H., Raina, S., 2011. Molecular Basis of Lipopolysaccharide Heterogeneity in *Escherichia coli*. *J. Biol. Chem.* 286, 42787–42807. <https://doi.org/10.1074/jbc.M111.291799>
- Klein, G., Raina, S., 2019. Regulated Assembly of LPS, Its Structural Alterations and Cellular Response to LPS Defects. *Int. J. Mol. Sci.* 20, 356. <https://doi.org/10.3390/ijms20020356>
- Klein, G., Wieczorek, A., Szuster, M., Raina, S., 2021. Checkpoints That Regulate Balanced Biosynthesis of Lipopolysaccharide and Its Essentiality in *Escherichia coli*. *Int. J. Mol. Sci.* 23, 189. <https://doi.org/10.3390/ijms23010189>
- Knirel, Y.A., Lindner, B., Vinogradov, E.V., Kocharova, N.A., Senchenkova, S.N., Shaikhutdinova, R.Z., Dentovskaya, S.V., Fursova, N.K., Bakhteeva, I.V., Titareva, G.M., Balakhonov, S.V., Holst, O., Gremyakova, T.A., Pier, G.B., Anisimov, A.P., 2005. Temperature-Dependent Variations and Intraspecies Diversity of the Structure of the Lipopolysaccharide of *Yersinia pestis*. *Biochemistry* 44, 1731–1743. <https://doi.org/10.1021/bi048430f>
- Koide, M., Saito, A., Okazaki, M., Umeda, B., Benson, R.F., 1999. Isolation of *Legionella longbeachae* Serogroup 1 from Potting Soils in Japan. *Clin. Infect. Dis.* 29, 943–944. <https://doi.org/10.1086/520470>
- Kooistra, O., Lüneberg, E., Knirel, Y.A., Frosch, M., Zähringer, U., 2002. N-Methylation in polylegionaminic acid is associated with the phase-variable epitope of *Legionella pneumophila* serogroup 1 lipopolysaccharide. *Eur. J. Biochem.* 269, 560–572. <https://doi.org/10.1046/j.0014-2956.2001.02683.x>
- Kooistra, O., Lüneberg, E., Lindner, B., Knirel, Y.A., Frosch, M., Zähringer, U., 2001. Complex O -Acetylation in *Legionella pneumophila* Serogroup 1 Lipopolysaccharide. Evidence for Two Genes Involved in 8- O -Acetylation of Legionaminic Acid. *Biochemistry* 40, 7630–7640. <https://doi.org/10.1021/bi002946r>
- Kozak, N.A., Buss, M., Lucas, C.E., Frace, M., Govil, D., Travis, T., Olsen-Rasmussen, M., Benson, R.F., Fields, B.S., 2010. Virulence Factors Encoded by *Legionella longbeachae* Identified on the Basis of the Genome Sequence Analysis of Clinical Isolate D-4968. *J. Bacteriol.* 192, 1030–1044. <https://doi.org/10.1128/JB.01272-09>
- Lâm, T.-T., Claus, H., Frosch, M., Vogel, U., 2011. Sequence analysis of serotype-specific synthesis regions II of *Haemophilus influenzae* serotypes c and d: evidence for common ancestry of capsule synthesis in Pasteurellaceae and *Neisseria meningitidis*. *Res. Microbiol.* 162, 483–487. <https://doi.org/10.1016/j.resmic.2011.04.002>
- Lawlor, M.S., Hsu, J., Rick, P.D., Miller, V.L., 2005. Identification of *Klebsiella pneumoniae* virulence determinants using an intranasal infection model: *Klebsiella pneumoniae* intranasal STM. *Mol. Microbiol.* 58, 1054–1073. <https://doi.org/10.1111/j.1365-2958.2005.04918.x>
- Lifshitz, Z., Burstein, D., Peeri, M., Zusman, T., Schwartz, K., Shuman, H.A., Pupko, T., Segal, G., 2013. Computational modeling and experimental validation of the *Legionella* and *Coxiella* virulence-related type-IVB secretion signal. *Proc. Natl. Acad. Sci.* 110. <https://doi.org/10.1073/pnas.1215278110>
- Liu, B., Furevi, A., Perepelov, A.V., Guo, X., Cao, H., Wang, Q., Reeves, P.R., Knirel, Y.A., Wang, L., Widmalm, G., 2020. Structure and genetics of *Escherichia coli* O antigens. *FEMS Microbiol. Rev.* 44, 655–683. <https://doi.org/10.1093/femsre/fuz028>
- Liu, M.A., Morris, P., Reeves, P.R., 2019. Wzx flippases exhibiting complex O-unit preferences require a new model for Wzx–substrate interactions. *MicrobiologyOpen* 8, e00655. <https://doi.org/10.1002/mbo3.655>
- Llobet, E., Tomás, J.M., Bengoechea, J.A., 2008. Capsule polysaccharide is a bacterial decoy for antimicrobial peptides. *Microbiology* 154, 3877–3886. <https://doi.org/10.1099/mic.0.2008/022301-0>
- Lockwood, D.C., Amin, H., Costa, T.R.D., Schroeder, G.N., 2022. The *Legionella pneumophila* Dot/Icm type IV secretion system and its effectors. *Microbiology* 168. <https://doi.org/10.1099/mic.0.001187>
- Loh, E., Kugelberg, E., Tracy, A., Zhang, Q., Gollan, B., Ewles, H., Chalmers, R., Pelicic, V., Tang, C.M., 2013. Temperature triggers immune evasion by *Neisseria meningitidis*. *Nature* 502, 237–240. <https://doi.org/10.1038/nature12616>

References

- Lück, C., Helbig, J.H., 2013. Characterization of *Legionella* Lipopolysaccharide, in: Buchrieser, C., Hilbi, H. (Eds.), *Legionella: Methods and Protocols*. Humana Press, Totowa, NJ, pp. 381–390. https://doi.org/10.1007/978-1-62703-161-5_24
- Lück, P.C., Freier, T., Steudel, C., Knirel, Y.A., Lüneberg, E., Zähringer, U., Helbig, J.H., 2001. A point mutation in the active site of *Legionella pneumophila* O-acetyltransferase results in modified lipopolysaccharide but does not influence virulence.
- Lück, P.C., Helbig, J.H., Ehret, W., Marre, R., Witzleb, W., 1992. Subtyping of *Legionella pneumophila* serogroup 1 strains isolated in Germany using monoclonal antibodies. *Zentralblatt Für Bakteriologie* 277, 179–187. [https://doi.org/10.1016/S0934-8840\(11\)80611-0](https://doi.org/10.1016/S0934-8840(11)80611-0)
- Lüneberg, E., Mayer, B., Daryab, N., Kooistra, O., Zähringer, U., Rohde, M., Swanson, J., Frosch, M., 2004. Chromosomal insertion and excision of a 30 kb unstable genetic element is responsible for phase variation of lipopolysaccharide and other virulence determinants in *Legionella pneumophila*. *Mol. Microbiol.* 39, 1259–1271. <https://doi.org/10.1111/j.1365-2958.2001.02314.x>
- Lüneberg, E., Zähringer, U., Knirel, Y.A., Steinmann, D., Hartmann, M., Steinmetz, I., Rohde, M., Köhl, J., Frosch, M., 1998. Phase-variable Expression of Lipopolysaccharide Contributes to the Virulence of *Legionella pneumophila*. *J. Exp. Med.* 188, 49–60. <https://doi.org/10.1084/jem.188.1.49>
- Lurie-Weinberger, M.N., Gomez-Valero, L., Merault, N., Glöckner, G., Buchrieser, C., Gophna, U., 2010. The origins of eukaryotic-like proteins in *Legionella pneumophila*. *Int. J. Med. Microbiol.* 300, 470–481. <https://doi.org/10.1016/j.ijmm.2010.04.016>
- Macé, K., Meir, A., Lukoyanova, N., Liu, L., Chetrit, D., Hospenthal, M.K., Roy, C.R., Waksman, G., 2022. Proteins DotY and DotZ modulate the dynamics and localization of the type IVB coupling complex of *Legionella pneumophila*. *Mol. Microbiol.* 117, 307–319. <https://doi.org/10.1111/mmi.14847>
- Machner, M.P., Isberg, R.R., 2006. Targeting of Host Rab GTPase Function by the Intravacuolar Pathogen *Legionella pneumophila*. *Dev. Cell* 11, 47–56. <https://doi.org/10.1016/j.devcel.2006.05.013>
- Maldonado, R.F., Sá-Correia, I., Valvano, M.A., 2016. Lipopolysaccharide modification in Gram-negative bacteria during chronic infection. *FEMS Microbiol. Rev.* 40, 480–493. <https://doi.org/10.1093/femsre/fuw007>
- Manson, J.M., Hancock, L.E., Gilmore, M.S., 2010. Mechanism of chromosomal transfer of *Enterococcus faecalis* pathogenicity island, capsule, antimicrobial resistance, and other traits. *Proc. Natl. Acad. Sci.* 107, 12269–12274. <https://doi.org/10.1073/pnas.1000139107>
- Marra, A., Blander, S.J., Horwitz, M.A., Shuman, H.A., 1992. Identification of a *Legionella pneumophila* locus required for intracellular multiplication in human macrophages. *Proc. Natl. Acad. Sci.* 89, 9607–9611. <https://doi.org/10.1073/pnas.89.20.9607>
- Massis, L.M., Assis-Marques, M.A., Castanheira, F.V.S., Capobianco, Y.J., Balestra, A.C., Escoll, P., Wood, R.E., Manin, G.Z., Correa, V.M.A., Alves-Filho, J.C., Cunha, F.Q., Buchrieser, C., Borges, M.C., Newton, H.J., Zamboni, D.S., 2016. *Legionella longbeachae* is immunologically silent and highly virulent *in vivo*. *J. Infect. Dis.* jiw560. <https://doi.org/10.1093/infdis/jiw560>
- Matsuura, M., 2013. Structural Modifications of Bacterial Lipopolysaccharide that Facilitate Gram-Negative Bacteria Evasion of Host Innate Immunity. *Front. Immunol.* 4. <https://doi.org/10.3389/fimmu.2013.00109>
- McDade, J.E., Shepard, C.C., Fraser, D.W., Tsai, T.R., Redus, M.A., Dowdle, W.R., The Laboratory Investigation Team, 1977. LEGIONNAIRES' DISEASE. Isolation of a Bacterium and Demonstration of Its Role in Other Respiratory Disease. *N. Engl. J. Med.* 297.
- McKinney, R.M. et al., 1981. *Legionella longbeachae* Species Nova, Another Etiologic Agent of Human Pneumonia. *Ann. Intern. Med.* 94, 739. <https://doi.org/10.7326/0003-4819-94-6-739>
- Megrian, D., Taib, N., Witwinowski, J., Beloin, C., Gribaldo, S., 2020. One or two membranes? Diderm Firmicutes challenge the Gram-positive/Gram-negative divide. *Mol. Microbiol.* 113, 659–671. <https://doi.org/10.1111/mmi.14469>

- Mercante, J.W., Winchell, J.M., 2015. Current and Emerging *Legionella* Diagnostics for Laboratory and Outbreak Investigations. *Clin. Microbiol. Rev.* 28, 95–133. <https://doi.org/10.1128/CMR.00029-14>
- Merino, S., Tomás, J.M., 2015. Bacterial Capsules and Evasion of Immune Responses, in: John Wiley & Sons, Ltd (Ed.), *ELS*. Wiley, pp. 1–10. <https://doi.org/10.1002/9780470015902.a0000957.pub4>
- Mi, W., Li, Y., Yoon, S.H., Ernst, R.K., Walz, T., Liao, M., 2017. Structural basis of MsbA-mediated lipopolysaccharide transport. *Nature* 549, 233–237. <https://doi.org/10.1038/nature23649>
- Moll, H., Sonesson, A., Jantzen, E., Marre, R., Zähringer, U., 1992. Identification of 27-oxo-octacosanoic acid and heptacosane-1,27-dioic acid in *Legionella pneumophila*. *FEMS Microbiol. Lett.* 97, 1–6. <https://doi.org/10.1111/j.1574-6968.1992.tb05430.x>
- Molofsky, A.B., Byrne, B.G., Whitfield, N.N., Madigan, C.A., Fuse, E.T., Tateda, K., Swanson, M.S., 2006. Cytosolic recognition of flagellin by mouse macrophages restricts *Legionella pneumophila* infection. *J. Exp. Med.* 203, 1093–1104. <https://doi.org/10.1084/jem.20051659>
- Molofsky, A.B., Swanson, M.S., 2004. Differentiate to thrive: lessons from the *Legionella pneumophila* life cycle. *Mol. Microbiol.* 53, 29–40. <https://doi.org/10.1111/j.1365-2958.2004.04129.x>
- Mondino, S., Schmidt, S., Rolando, M., Escoll, P., Gomez-Valero, L., Buchrieser, C., 2020. Legionnaires' Disease: State of the Art Knowledge of Pathogenesis Mechanisms of *Legionella*. *Annu. Rev. Pathol. Mech. Dis.* 15, 439–466. <https://doi.org/10.1146/annurev-pathmechdis-012419-032742>
- Montminy, S.W., Khan, N., McGrath, S., Walkowicz, M.J., Sharp, F., Conlon, J.E., Fukase, K., Kusumoto, S., Sweet, C., Miyake, K., Akira, S., Cotter, R.J., Goguen, J.D., Lien, E., 2006. Virulence factors of *Yersinia pestis* are overcome by a strong lipopolysaccharide response. *Nat. Immunol.* 7, 1066–1073. <https://doi.org/10.1038/ni1386>
- Morris, G.K., Steigerwalt, A., Feeley, J.C., Wong, E.S., Martin, W.T., Patton, C.M., Brenner, D.J., 1980. *Legionella gormanii* sp. nov. *J. Clin. Microbiol.* 12, 718–721. <https://doi.org/10.1128/jcm.12.5.718-721.1980>
- Mostowy, R.J., Croucher, N.J., De Maio, N., Chewapreecha, C., Salter, S.J., Turner, P., Aanensen, D.M., Bentley, S.D., Didelot, X., Fraser, C., 2017. Pneumococcal Capsule Synthesis Locus cps as Evolutionary Hotspot with Potential to Generate Novel Serotypes by Recombination. *Mol. Biol. Evol.* 34, 2537–2554. <https://doi.org/10.1093/molbev/msx173>
- Mostowy, R.J., Holt, K.E., 2018. Diversity-Generating Machines: Genetics of Bacterial Sugar-Coating. *Trends Microbiol.* 26, 1008–1021. <https://doi.org/10.1016/j.tim.2018.06.006>
- Murray, G.L., Attridge, S.R., Morona, R., 2006. Altering the Length of the Lipopolysaccharide O Antigen Has an Impact on the Interaction of *Salmonella enterica* Serovar Typhimurium with Macrophages and Complement. *J. Bacteriol.* 188, 2735–2739. <https://doi.org/10.1128/JB.188.7.2735-2739.2006>
- Nagai, H., Cambronne, E.D., Kagan, J.C., Amor, J.C., Kahn, R.A., Roy, C.R., 2005. A C-terminal translocation signal required for Dot/Icm-dependent delivery of the *Legionella* RalF protein to host cells. *Proc. Natl. Acad. Sci.* 102, 826–831. <https://doi.org/10.1073/pnas.0406239101>
- Natås, O.B., Brekken, A.L., Bernhoff, E., Hetland, M.A.K., Löhr, I.H., Lindemann, P.C., 2019. Susceptibility of *Legionella pneumophila* to antimicrobial agents and the presence of the efflux pump LpeAB. *J. Antimicrob. Chemother.* 74, 1545–1550. <https://doi.org/10.1093/jac/dkz081>
- Nelson, A.L., Roche, A.M., Gould, J.M., Chim, K., Ratner, A.J., Weiser, J.N., 2007. Capsule Enhances Pneumococcal Colonization by Limiting Mucus-Mediated Clearance. *Infect. Immun.* 75, 83–90. <https://doi.org/10.1128/IAI.01475-06>
- Neumeister, B., Faigle, M., Sommer, M., Zähringer, U., Stelter, F., Menzel, R., Schütt, C., Northoff, H., 1998. Low Endotoxic Potential of *Legionella pneumophila* Lipopolysaccharide due to Failure of Interaction with the Monocyte Lipopolysaccharide Receptor CD14. *INFECT IMMUN* 66.
- Ortiz-Roque, C.M., Hazen, T.C., 1987. Abundance and distribution of Legionellaceae in Puerto Rican waters. *Appl. Environ. Microbiol.* 53, 2231–2236. <https://doi.org/10.1128/aem.53.9.2231-2236.1987>

References

- Padayatti, P.S., Lee, S.C., Stanfield, R.L., Wen, P.-C., Tajkhorshid, E., Wilson, I.A., Zhang, Q., 2019. Structural Insights into the Lipid A Transport Pathway in MsbA. *Structure* 27, 1114–1123.e3. <https://doi.org/10.1016/j.str.2019.04.007>
- Park, J.M., Ghosh, S., O'Connor, T.J., 2020. Combinatorial selection in amoebal hosts drives the evolution of the human pathogen *Legionella pneumophila*. *Nat. Microbiol.* 5, 599–609. <https://doi.org/10.1038/s41564-019-0663-7>
- Payne, N.R., Horwitz, M., 1987. PHAGOCYTOSIS OF *LEGIONELLA PNEUMOPHILA* IS MEDIATED BY HUMAN MONOCYTE COMPLEMENT RECEPTORS. *J. Exp. Med.* 166, 1377–1389. <https://doi.org/10.1084/jem.166.5.1377>
- Pedro-Botet, L., Yu, V.L., 2006. Legionella: macrolides or quinolones? *Clin. Microbiol. Infect.* 12, 25–30. <https://doi.org/10.1111/j.1469-0691.2006.01394.x>
- Peleg, A., Shifrin, Y., Ilan, O., Nadler-Yona, C., Nov, S., Koby, S., Baruch, K., Altuvia, S., Elgrably-Weiss, M., Abe, C.M., Knutton, S., Saper, M.A., Rosenshine, I., 2005. Identification of an *Escherichia coli* Operon Required for Formation of the O-Antigen Capsule. *J. Bacteriol.* 187, 5259–5266. <https://doi.org/10.1128/JB.187.15.5259-5266.2005>
- Pereira, M.S.F., Marques, G.G., Del Lama, J.E., Zamboni, D.S., 2011. The Nlrc4 Inflammasome contributes to restriction of pulmonary infection by flagellated *Legionella* spp. that trigger pyroptosis. *Front. Microbiol.* 2. <https://doi.org/10.3389/fmicb.2011.00033>
- Picard-Masson, M., Lajoie, É., Lord, J., Lalancette, C., Marchand, G., Levac, É., Lemieux, M.-A., Hudson, P., Lajoie, L., 2016. Two Related Occupational Cases of *Legionella longbeachae* Infection, Quebec, Canada. *Emerg. Infect. Dis.* 22, 1289–1291. <https://doi.org/10.3201/eid2207.160184>
- Price, C.T.D., Al-Quadani, T., Santic, M., Rosenshine, I., Abu Kwaik, Y., 2011. Host Proteasomal Degradation Generates Amino Acids Essential for Intracellular Bacterial Growth. *Science* 334, 1553–1557. <https://doi.org/10.1126/science.1212868>
- Putonti, C., Nowicki, B., Shaffer, M., Fofanov, Y., Nowicki, S., 2013. Where does *Neisseria* acquire foreign DNA from: an examination of the source of genomic and pathogenic islands and the evolution of the *Neisseria* genus. *BMC Evol. Biol.* 13, 184. <https://doi.org/10.1186/1471-2148-13-184>
- Qin, T., Zhou, H., Ren, H., Liu, W., 2017. Distribution of Secretion Systems in the Genus *Legionella* and Its Correlation with Pathogenicity. *Front. Microbiol.* 08. <https://doi.org/10.3389/fmicb.2017.00388>
- Raetz, C.R.H., Whitfield, C., 2002. Lipopolysaccharide Endotoxins. *Annu. Rev. Biochem.* 71, 635–700. <https://doi.org/10.1146/annurev.biochem.71.110601.135414>
- Raffatellu, M., Chessa, D., Wilson, R.P., Dusold, R., Rubino, S., Bäumlner, A.J., 2005. The Vi Capsular Antigen of *Salmonella enterica* Serotype Typhi Reduces Toll-Like Receptor-Dependent Interleukin-8 Expression in the Intestinal Mucosa. *Infect. Immun.* 73, 3367–3374. <https://doi.org/10.1128/IAI.73.6.3367-3374.2005>
- Rahn, A., Beis, K., Naismith, J.H., Whitfield, C., 2003. A Novel Outer Membrane Protein, Wzi, Is Involved in Surface Assembly of the *Escherichia coli* K30 Group 1 Capsule. *J. Bacteriol.* 185, 5882–5890. <https://doi.org/10.1128/JB.185.19.5882-5890.2003>
- Rahn, A., Drummelsmith, J., Whitfield, C., 1999. Conserved Organization in the *cps* Gene Clusters for Expression of *Escherichia coli* Group 1 K Antigens: Relationship to the Colanic Acid Biosynthesis Locus and the *cps* Genes from *Klebsiella pneumoniae*. *J. Bacteriol.* 181, 2307–2313. <https://doi.org/10.1128/JB.181.7.2307-2313.1999>
- Reeves, P.R., Cunneen, M.M., 2010. Biosynthesis of O-antigen chains and assembly, in: *Microbial Glycobiology*. Elsevier, pp. 319–335. <https://doi.org/10.1016/B978-0-12-374546-0.00018-3>
- Reichardt, K., Jacobs, E., Röske, I., Helbig, J.H., 2010. *Legionella pneumophila* carrying the virulence-associated lipopolysaccharide epitope possesses two functionally different LPS components. *Microbiology* 156, 2953–2961. <https://doi.org/10.1099/mic.0.039933-0>

- Reid, A.N., Whitfield, C., 2005. Functional Analysis of Conserved Gene Products Involved in Assembly of *Escherichia coli* Capsules and Exopolysaccharides: Evidence for Molecular Recognition between Wza and Wzc for Colanic Acid Biosynthesis. *J. Bacteriol.* 187, 5470–5481. <https://doi.org/10.1128/JB.187.15.5470-5481.2005>
- Ren, T., Zamboni, D.S., Roy, C.R., Dietrich, W.F., Vance, R.E., 2006. Flagellin-Deficient *Legionella* Mutants Evade Caspase-1- and Naip5-Mediated Macrophage Immunity. *PLoS Pathog.* 2, e18. <https://doi.org/10.1371/journal.ppat.0020018>
- Rendueles, O., De Sousa, J.A.M., Bernheim, A., Touchon, M., Rocha, E.P.C., 2018. Genetic exchanges are more frequent in bacteria encoding capsules. *PLOS Genet.* 14, e1007862. <https://doi.org/10.1371/journal.pgen.1007862>
- Rendueles, O., Garcia-Garcerà, M., Néron, B., Touchon, M., Rocha, E.P.C., 2017. Abundance and co-occurrence of extracellular capsules increase environmental breadth: Implications for the emergence of pathogens. *PLOS Pathog.* 13, e1006525. <https://doi.org/10.1371/journal.ppat.1006525>
- Ridenour, D.A., Cirillo, S.L.G., Feng, S., Samrakandi, M.M., Cirillo, J.D., 2003. Identification of a Gene That Affects the Efficiency of Host Cell Infection by *Legionella pneumophila* in a Temperature-Dependent Fashion. *Infect. Immun.* 71, 6256–6263. <https://doi.org/10.1128/IAI.71.11.6256-6263.2003>
- Roig, J., Sabria, M., Castella, X., 2010. Legionnaires' Disease, in: *Infectious Diseases in Critical Care*. Springer Verlag Berlin Heidelberg, pp. 404–412.
- Rolando, M., Escoll, P., Nora, T., Botti, J., Boitez, V., Bedia, C., Daniels, C., Abraham, G., Stogios, P.J., Skarina, T., Christophe, C., Dervins-Ravault, D., Cazalet, C., Hilbi, H., Rupasinghe, T.W.T., Tull, D., McConville, M.J., Ong, S.Y., Hartland, E.L., Codogno, P., Levade, T., Naderer, T., Savchenko, A., Buchrieser, C., 2016. *Legionella pneumophila* S1P-lyase targets host sphingolipid metabolism and restrains autophagy. *Proc. Natl. Acad. Sci.* 113, 1901–1906. <https://doi.org/10.1073/pnas.1522067113>
- Rolando, M., Sanulli, S., Rusniok, C., Gomez-Valero, L., Bertholet, C., Sahr, T., Margueron, R., Buchrieser, C., 2013. *Legionella pneumophila* Effector RomA Uniquely Modifies Host Chromatin to Repress Gene Expression and Promote Intracellular Bacterial Replication. *Cell Host Microbe* 13, 395–405. <https://doi.org/10.1016/j.chom.2013.03.004>
- Rossier, O., Dao, J., Cianciotto, N.P., 2008. The Type II Secretion System of *Legionella pneumophila* Elaborates Two Aminopeptidases, as Well as a Metalloprotease That Contributes to Differential Infection among Protozoan Hosts. *Appl. Environ. Microbiol.* 74, 753–761. <https://doi.org/10.1128/AEM.01944-07>
- Rossier, O., Starkenburg, S.R., Cianciotto, N.P., 2004. *Legionella pneumophila* Type II Protein Secretion Promotes Virulence in the A/J Mouse Model of Legionnaires' Disease Pneumonia. *Infect. Immun.* 72, 310–321. <https://doi.org/10.1128/IAI.72.1.310-321.2004>
- Rowbotham, T.J., 1980. Preliminary report on the pathogenicity of *Legionella pneumophila* for freshwater and soil amoebae. *J. Clin. Pathol.* 33, 1179–1183. <https://doi.org/10.1136/jcp.33.12.1179>
- Rowe, S., Hodson, N., Griffiths, G., Roberts, I.S., 2000. Regulation of the *Escherichia coli* K5 Capsule Gene Cluster: Evidence for the Roles of H-NS, BipA, and Integration Host Factor in Regulation of Group 2 Capsule Gene Clusters in Pathogenic *E. coli*. *J. Bacteriol.* 182, 2741–2745. <https://doi.org/10.1128/JB.182.10.2741-2745.2000>
- Ruehleemann, S.A., Crawford, G.R., 1996. Panic in the potting shed: The association between *Legionella longbeachae* serogroup 1 and potting soils in Australia. *Med. J. Aust.* 164, 36–38. <https://doi.org/10.5694/j.1326-5377.1996.tb94110.x>
- Sahly, H., Keisari, Y., Crouch, E., Sharon, N., Ofek, I., 2008. Recognition of Bacterial Surface Polysaccharides by Lectins of the Innate Immune System and Its Contribution to Defense against Infection: the Case of Pulmonary Pathogens. *Infect. Immun.* 76, 1322–1332. <https://doi.org/10.1128/IAI.00910-07>
- Schator, D., Mondino, S., Berthelet, J., Di Silvestre, C., Ben Assaya, M., Rusniok, C., Rodrigues-Lima, F., Wehenkel, A., Buchrieser, C., Rolando, M., 2023. *Legionella* para-effectors target chromatin and promote bacterial replication. *Nat. Commun.* 14, 2154. <https://doi.org/10.1038/s41467-023-37885-z>

References

- Schmid, J., Sieber, V., Rehm, B., 2015. Bacterial exopolysaccharides: biosynthesis pathways and engineering strategies. *Front. Microbiol.* 6. <https://doi.org/10.3389/fmicb.2015.00496>
- Scholl, D., Adhya, S., Merrill, C., 2005. *Escherichia coli* K1's Capsule Is a Barrier to Bacteriophage T7. *Appl. Environ. Microbiol.* 71, 4872–4874. <https://doi.org/10.1128/AEM.71.8.4872-4874.2005>
- Schunder, E., Gillmaier, N., Kutzner, E., Herrmann, V., Lautner, M., Heuner, K., Eisenreich, W., 2014. Amino Acid Uptake and Metabolism of *Legionella pneumophila* Hosted by *Acanthamoeba castellanii*. *J. Biol. Chem.* 289, 21040–21054. <https://doi.org/10.1074/jbc.M114.570085>
- Seeger, E.M., Thuma, M., Fernandez-Moreira, E., Jacobs, E., Schmitz, M., Helbig, J.H., 2010. Lipopolysaccharide of *Legionella pneumophila* shed in a liquid culture as a nonvesicular fraction arrests phagosome maturation in amoeba and monocytic host cells. *FEMS Microbiol. Lett.* 307, 113–119. <https://doi.org/10.1111/j.1574-6968.2010.01976.x>
- Segal, G., Purcell, M., Shuman, H.A., 1998. Host cell killing and bacterial conjugation require overlapping sets of genes within a 22-kb region of the *Legionella pneumophila* genome. *Proc. Natl. Acad. Sci.* 95, 1669–1674. <https://doi.org/10.1073/pnas.95.4.1669>
- Segal, G., Russo, J.J., Shuman, H.A., 1999. Relationships between a new type IV secretion system and the icm/dot virulence system of *Legionella pneumophila*. *Mol. Microbiol.* 34, 799–809. <https://doi.org/10.1046/j.1365-2958.1999.01642.x>
- Segal, G., Shuman, H.A., 1999. *Legionella pneumophila* Utilizes the Same Genes To Multiply within *Acanthamoeba castellanii* and Human Macrophages. *Infect. Immun.* 67, 2117–2124. <https://doi.org/10.1128/IAI.67.5.2117-2124.1999>
- Shadoud, L., Almahmoud, I., Jarraud, S., Etienne, J., Larrat, S., Schwebel, C., Timsit, J.-F., Schneider, D., Maurin, M., 2015. Hidden Selection of Bacterial Resistance to Fluoroquinolones *In Vivo*: The Case of *Legionella pneumophila* and Humans. *EBioMedicine* 2, 1179–1185. <https://doi.org/10.1016/j.ebiom.2015.07.018>
- Shevchuk, O., Jäger, J., Steinert, M., 2011. Virulence Properties of the *Legionella Pneumophila* Cell Envelope. *Front. Microbiol.* 2. <https://doi.org/10.3389/fmicb.2011.00074>
- Shi, Y., Liu, H., Ma, K., Luo, Z.-Q., Qiu, J., 2023a. *Legionella longbeachae* effector protein RavZ inhibits autophagy and regulates phagosome ubiquitination during infection. *PLOS ONE* 18, e0281587. <https://doi.org/10.1371/journal.pone.0281587>
- Shi, Y., Liu, H., Ma, K., Luo, Z.-Q., Qiu, J., 2023b. *Legionella longbeachae* Regulates the Association of Polyubiquitinated Proteins on Bacterial Phagosome with Multiple Deubiquitinases. *Microbiol. Spectr.* 11, e04179-22. <https://doi.org/10.1128/spectrum.04179-22>
- Shu, S., Mi, W., 2022. Regulatory mechanisms of lipopolysaccharide synthesis in *Escherichia coli*. *Nat. Commun.* 13, 4576. <https://doi.org/10.1038/s41467-022-32277-1>
- Silhavy, T.J., Kahne, D., Walker, S., 2010. The Bacterial Cell Envelope. *Cold Spring Harb. Perspect. Biol.* 2, a000414–a000414. <https://doi.org/10.1101/cshperspect.a000414>
- Simpson, B.W., Trent, M.S., 2019. Pushing the envelope: LPS modifications and their consequences. *Nat. Rev. Microbiol.* 17, 403–416. <https://doi.org/10.1038/s41579-019-0201-x>
- Singh, J.K., Adams, F.G., Brown, M.H., 2019. Diversity and Function of Capsular Polysaccharide in *Acinetobacter baumannii*. *Front. Microbiol.* 9, 3301. <https://doi.org/10.3389/fmicb.2018.03301>
- Singh, S., Wilksch, J.J., Dunstan, R.A., Mularski, A., Wang, N., Hocking, D., Jebeli, L., Cao, H., Clements, A., Jenney, A.W.J., Lithgow, T., Strugnell, R.A., 2022. LPS O Antigen Plays a Key Role in *Klebsiella pneumoniae* Capsule Retention. *Microbiol. Spectr.* 10, e01517-21. <https://doi.org/10.1128/spectrum.01517-21>
- Slow, S., Anderson, T., Murdoch, D.R., Bloomfield, S., Winter, D., Biggs, P.J., 2022. Extensive epigenetic modification with large-scale chromosomal and plasmid recombination characterise the *Legionella longbeachae* serogroup 1 genome. *Sci. Rep.* 12, 5810. <https://doi.org/10.1038/s41598-022-09721-9>

- Snyder, D.S., Gibson, D., Heiss, C., Kay, W., Azadi, P., 2006. Structure of a capsular polysaccharide isolated from *Salmonella enteritidis*. *Carbohydr. Res.* 341, 2388–2397. <https://doi.org/10.1016/j.carres.2006.06.010>
- Sonesson, A., Jantzen, E., Bryn, K., Larsson, L., Eng, J., 1989. Chemical composition of a lipopolysaccharide from *Legionella pneumophila*. *Arch Microbiol* 153, 72–78. <https://doi.org/10.1007/BF00277544>
- Sonesson, A., Jantzen, E., Tangen, T., Zähringer, U., 1994. Chemical composition of lipopolysaccharides from *Legionella bozemanii* and *Legionella longbeachae*. *Arch Microbiol* 162, 215–21.
- Steele, T.W., Lanser, J., Sangster, N., 1990a. Isolation of *Legionella longbeachae* serogroup 1 from potting mixes. *Appl. Environ. Microbiol.* 56, 49–53. <https://doi.org/10.1128/aem.56.1.49-53.1990>
- Steele, T.W., Moore, C.V., Sangster, N., 1990b. Distribution of *Legionella longbeachae* serogroup 1 and other Legionellae in potting soils in Australia. *Appl. Environ. Microbiol.* 56, 2984–2988. <https://doi.org/10.1128/aem.56.10.2984-2988.1990>
- Steenbergen, S.M., Vimr, E.R., 2008. Biosynthesis of the *Escherichia coli* K1 group 2 polysialic acid capsule occurs within a protected cytoplasmic compartment. *Mol. Microbiol.* 68, 1252–1267. <https://doi.org/10.1111/j.1365-2958.2008.06231.x>
- Steinert, M., Hentschel, U., Hacker, J., 2002. *Legionella pneumophila*: an aquatic microbe goes astray. *FEMS Microbiol. Rev.* 26, 149–162. <https://doi.org/10.1111/j.1574-6976.2002.tb00607.x>
- Stevens, M.P., Clarke, B.R., Roberts, I.S., 1997. Regulation of the *Escherichia coli* K5 capsule gene cluster by transcription antitermination. *Mol. Microbiol.* 24, 1001–1012. <https://doi.org/10.1046/j.1365-2958.1997.4241780.x>
- Stevens, M.P., HÄ¶nfling, P., Jann, B., Jann, K., Roberts, I.S., 1994. Regulation of *Escherichia coli* K5 capsular polysaccharide expression: Evidence for involvement of RfaH in the expression of group II capsules. *FEMS Microbiol. Lett.* 124, 93–98. <https://doi.org/10.1111/j.1574-6968.1994.tb07267.x>
- Sukupolvi-Petty, S., Grass, S., StGeme, J.W., 2006. The *Haemophilus influenzae* Type b *hcsA* and *hcsB* Gene Products Facilitate Transport of Capsular Polysaccharide across the Outer Membrane and Are Essential for Virulence. *J. Bacteriol.* 188, 3870–3877. <https://doi.org/10.1128/JB.01968-05>
- Sun, X., Stefanetti, G., Berti, F., Kasper, D.L., 2019. Polysaccharide structure dictates mechanism of adaptive immune response to glycoconjugate vaccines. *Proc. Natl. Acad. Sci.* 116, 193–198. <https://doi.org/10.1073/pnas.1816401115>
- Sutcliffe, I.C., 2010. A phylum level perspective on bacterial cell envelope architecture. *Trends Microbiol.* 18, 464–470. <https://doi.org/10.1016/j.tim.2010.06.005>
- Sutherland, I.W., 2001. Polysaccharides: Bacterial and Fungal, in: John Wiley & Sons, Ltd (Ed.), ELS. Wiley. <https://doi.org/10.1038/npg.els.0000699>
- Svetlicic, E., Jaén-Luchoro, D., Klobucar, R.S., Jers, C., Kazazic, S., Franjevic, D., Klobucar, G., Shelton, B.G., Mijakovic, I., 2023. Genomic characterization and assessment of pathogenic potential of *Legionella* spp. isolates from environmental monitoring. *Front. Microbiol.* 13, 1091964. <https://doi.org/10.3389/fmicb.2022.1091964>
- Taib, N., Megrian, D., Witwinowski, J., Adam, P., Poppleton, D., Borrel, G., Beloin, C., Gribaldo, S., 2020. Genome-wide analysis of the Firmicutes illuminates the diderm/monoderm transition. *Nat. Ecol. Evol.* 4, 1661–1672. <https://doi.org/10.1038/s41559-020-01299-7>
- Thomassin, J.-L., Lee, M.J., Brannon, J.R., Sheppard, D.C., Gruenheid, S., Le Moual, H., 2013. Both Group 4 Capsule and Lipopolysaccharide O-Antigen Contribute to Enteropathogenic *Escherichia coli* Resistance to Human α -Defensin 5. *PLoS ONE* 8, e82475. <https://doi.org/10.1371/journal.pone.0082475>
- Tipton, K.A., Chin, C.-Y., Farokhyfar, M., Weiss, D.S., Rather, P.N., 2018. Role of Capsule in Resistance to Disinfectants, Host Antimicrobials, and Desiccation in *Acinetobacter baumannii*. *Antimicrob. Agents Chemother.* 62, e01188-18. <https://doi.org/10.1128/AAC.01188-18>

References

- Tocheva, E.I., Ortega, D.R., Jensen, G.J., 2016. Sporulation, bacterial cell envelopes and the origin of life. *Nat. Rev. Microbiol.* 14, 535–542. <https://doi.org/10.1038/nrmicro.2016.85>
- Tzeng, Y.-L., Datta, A., Kolli, V.K., Carlson, R.W., Stephens, D.S., 2002. Endotoxin of *Neisseria meningitidis* Composed Only of Intact Lipid A: Inactivation of the Meningococcal 3-Deoxy- D -Manno-Octulosonic Acid Transferase. *J. Bacteriol.* 184, 2379–2388. <https://doi.org/10.1128/JB.184.9.2379-2388.2002>
- Tzeng, Y.-L., Datta, A.K., Strole, C.A., Lobritz, M.A., Carlson, R.W., Stephens, D.S., 2005. Translocation and Surface Expression of Lipidated Serogroup B Capsular Polysaccharide in *Neisseria meningitidis*. *Infect. Immun.* 73, 1491–1505. <https://doi.org/10.1128/IAI.73.3.1491-1505.2005>
- Tzeng, Y.-L., Thomas, J., Stephens, D.S., 2015. Regulation of capsule in *Neisseria meningitidis*. *Crit. Rev. Microbiol.* 1–14. <https://doi.org/10.3109/1040841X.2015.1022507>
- Vandewalle-Capo, M., Massip, C., Descours, G., Charavit, J., Chastang, J., Billy, P.A., Boisset, S., Lina, G., Gilbert, C., Maurin, M., Jarraud, S., Ginevra, C., 2017. Minimum inhibitory concentration (MIC) distribution among wild-type strains of *Legionella pneumophila* identifies a subpopulation with reduced susceptibility to macrolides owing to efflux pump genes. *Int. J. Antimicrob. Agents* 50, 684–689. <https://doi.org/10.1016/j.ijantimicag.2017.08.001>
- Verbrugh, H.A., Lee, D.A., Elliott, G.R., Keane, W.F., 1985. Opsonization of *Legionella pneumophila* in human serum: key roles for specific antibodies and the classical complement pathway.
- Vivoli, M., Ayres, E., Beaumont, E., Isupov, M.N., Harmer, N.J., 2014. Structural insights into WcbI, a novel polysaccharide-biosynthesis enzyme. *IUCrJ* 1, 28–38. <https://doi.org/10.1107/S205225251302695X>
- Vogel, Joseph.P., Andrews, H.L., Wong, S.K., Isberg, R.R., 1998. Conjugative Transfer by the Virulence System of *Legionella pneumophila*. *Science* 279, 873–876. <https://doi.org/10.1126/science.279.5352.873>
- Vollmer, W., Blanot, D., De Pedro, M.A., 2008. Peptidoglycan structure and architecture. *FEMS Microbiol. Rev.* 32, 149–167. <https://doi.org/10.1111/j.1574-6976.2007.00094.x>
- Von Baum, H., Ewig, S., Marre, R., Suttrop, N., Gonschior, S., Welte, T., Lück, C., Competence Network for Community Acquired Pneumonia Study Group, 2008. Community-Acquired *Legionella* Pneumonia: New Insights from the German Competence Network for Community Acquired Pneumonia. *Clin. Infect. Dis.* 46, 1356–1364. <https://doi.org/10.1086/586741>
- Wang, H., D’Souza, C., Lim, X.Y., Kostenko, L., Pediongco, T.J., Eckle, S.B.G., Meehan, B.S., Shi, M., Wang, N., Li, S., Liu, L., Mak, J.Y.W., Fairlie, D.P., Iwakura, Y., Gunnarsen, J.M., Stent, A.W., Godfrey, D.I., Rossjohn, J., Westall, G.P., Kjer-Nielsen, L., Strugnell, R.A., McCluskey, J., Corbett, A.J., Hinks, T.S.C., Chen, Z., 2018. MAIT cells protect against pulmonary *Legionella longbeachae* infection. *Nat. Commun.* 9, 3350. <https://doi.org/10.1038/s41467-018-05202-8>
- Wee, B.A., Alves, J., Lindsay, D.S.J., Klatt, A.-B., Sargison, F.A., Cameron, R.L., Pickering, A., Gorzynski, J., Corander, J., Marttinen, P., Opitz, B., Smith, A.J., Fitzgerald, J.R., 2021. Population analysis of *Legionella pneumophila* reveals a basis for resistance to complement-mediated killing. *Nat. Commun.* 12, 7165. <https://doi.org/10.1038/s41467-021-27478-z>
- Wen, Z., Zhang, J.-R., 2015. Bacterial Capsules, in: *Molecular Medical Microbiology*. Elsevier, pp. 33–53. <https://doi.org/10.1016/B978-0-12-397169-2.00003-2>
- White, R.C., Cianciotto, N.P., 2019. Assessing the impact, genomics and evolution of type II secretion across a large, medically important genus: the *Legionella* type II secretion paradigm. *Microb. Genomics* 5. <https://doi.org/10.1099/mgen.0.000273>
- Whiteway, C., Valcek, A., Philippe, C., Strazisar, M., De Pooter, T., Mateus, I., Breine, A., Van der Henst, C., 2022. Scarless excision of an insertion sequence restores capsule production and virulence in *Acinetobacter baumannii*. *ISME J.* 16, 1473–1477. <https://doi.org/10.1038/s41396-021-01179-3>
- Whitfield, C., 2006. Biosynthesis and Assembly of Capsular Polysaccharides in *Escherichia coli*. *Annu. Rev. Biochem.* 75, 39–68. <https://doi.org/10.1146/annurev.biochem.75.103004.142545>

- Whitfield, C., Williams, D.M., Kelly, S.D., 2020. Lipopolysaccharide O-antigens—bacterial glycans made to measure. *J. Biol. Chem.* 295, 10593–10609. <https://doi.org/10.1074/jbc.REV120.009402>
- Whitney, J.C., Howell, P.L., 2013. Synthase-dependent exopolysaccharide secretion in Gram-negative bacteria. *Trends Microbiol.* 21, 63–72. <https://doi.org/10.1016/j.tim.2012.10.001>
- Wieczorek, A., Sendobra, A., Maniyeri, A., Sugalska, M., Klein, G., Raina, S., 2022. A New Factor LapD Is Required for the Regulation of LpxC Amounts and Lipopolysaccharide Trafficking. *Int. J. Mol. Sci.* 23, 9706. <https://doi.org/10.3390/ijms23179706>
- Willis, L.M., Whitfield, C., 2013a. KpsC and KpsS are retaining 3-deoxy- D -manno -oct-2-ulosonic acid (Kdo) transferases involved in synthesis of bacterial capsules. *Proc. Natl. Acad. Sci.* 110, 20753–20758. <https://doi.org/10.1073/pnas.1312637110>
- Willis, L.M., Whitfield, C., 2013b. Structure, biosynthesis, and function of bacterial capsular polysaccharides synthesized by ABC transporter-dependent pathways. *Carbohydr. Res.* 378, 35–44. <https://doi.org/10.1016/j.carres.2013.05.007>
- Wilson, R.P., Raffatellu, M., Chessa, D., Winter, S.E., Tükel, C., Bäuml, A.J., 2007. The Vi-capsule prevents Toll-like receptor 4 recognition of *Salmonella*. *Cell. Microbiol.* 10, 876–890.
- Wood, R.E., Newton, P., Latomanski, E.A., Newton, H.J., 2015. Dot/Icm Effector Translocation by *Legionella longbeachae* Creates a Replicative Vacuole Similar to That of *Legionella pneumophila* despite Translocation of Distinct Effector Repertoires. *Infect. Immun.* 83, 4081–4092. <https://doi.org/10.1128/IAI.00461-15>
- Yoshida, K., Matsumoto, T., Tateda, K., Uchida, K., Tsujimoto, S., Yamaguchi, K., 2001. Induction of interleukin-10 and down-regulation of cytokine production by *Klebsiella pneumoniae* capsule in mice with pulmonary infection. *J. Med. Microbiol.* 50, 456–461. <https://doi.org/10.1099/0022-1317-50-5-456>
- Young, K., Silver, L.L., Bramhill, D., Cameron, P., Eveland, S.S., Raetz, C.R.H., Hyland, S.A., Anderson, M.S., 1995. The envA Permeability/Cell Division Gene of *Escherichia coli* Encodes the Second Enzyme of Lipid A Biosynthesis. *J. Biol. Chem.* 270, 30384–30391. <https://doi.org/10.1074/jbc.270.51.30384>
- Yu, V.L., Plouffe, J.F., Pastoris, M.C., Stout, J.E., Schousboe, M., Widmer, A., Summersgill, J., File, T., Heath, C.M., Paterson, D.L., Cheresky, A., 2002. Distribution of *Legionella* Species and Serogroups Isolated by Culture in Patients with Sporadic Community-Acquired Legionellosis: An International Collaborative Survey. *J Infect Dis* 186, 127–8.

References

Annexes

Annex A

**Molecular Mimicry: a Paradigm of Host-Microbe Coevolution Illustrated
by *Legionella***

Bibliographic publication

Published in

mBio

Vol. 11:e01201-10. Published 06 October 2020.

DOI: <https://doi.org/10.1128/mbio.01201-20>

Sonia Mondino,^{a,b} Silke Schmidt,^{a,b,c} and Carmen Buchrieser^{a,b}

^aInstitut Pasteur, Biologie des Bactéries Intracellulaires, Paris, France ^bCNRS UMR 3525, Paris, France,
^cSorbonne Université, Collège doctoral, Paris, France

For correspondence:

Carmen Buchrieser cbuch@pasteur.fr



Molecular Mimicry: a Paradigm of Host-Microbe Coevolution Illustrated by *Legionella*

Sonia Mondino,^{a,b} Silke Schmidt,^{a,b,c}  Carmen Buchrieser^{a,b}

^aInstitut Pasteur, Biologie des Bactéries Intracellulaires, Paris, France

^bCNRS UMR 3525, Paris, France

^cSorbonne Université, Collège Doctoral, Paris, France

ABSTRACT Through coevolution with host cells, microorganisms have acquired mechanisms to avoid the detection by the host surveillance system and to use the cell's supplies to establish themselves. Indeed, certain pathogens have evolved proteins that imitate specific eukaryotic cell proteins, allowing them to manipulate host pathways, a phenomenon termed molecular mimicry. Bacterial "eukaryotic-like proteins" are a remarkable example of molecular mimicry. They are defined as proteins that strongly resemble eukaryotic proteins or that carry domains that are predominantly present in eukaryotes and that are generally absent from prokaryotes. The widest diversity of eukaryotic-like proteins known to date can be found in members of the bacterial genus *Legionella*, some of which cause a severe pneumonia in humans. The characterization of a number of these proteins shed light on their importance during infection. The subsequent identification of eukaryotic-like genes in the genomes of other amoeba-associated bacteria and bacterial symbionts suggested that eukaryotic-like proteins are a common means of bacterial evasion and communication, shaped by the continuous interactions between bacteria and their protozoan hosts. In this review, we discuss the concept of molecular mimicry using *Legionella* as an example and show that eukaryotic-like proteins effectively manipulate host cell pathways. The study of the function and evolution of such proteins is an exciting field of research that is leading us toward a better understanding of the complex world of bacterium-host interactions. Ultimately, this knowledge will teach us how host pathways are manipulated and how infections may possibly be tackled.

KEYWORDS molecular mimicry, eukaryotic-like proteins, *Legionella*, amoeba-resistant bacteria, host-pathogen interactions, *Legionella pneumophila*

During host-pathogen interactions, a continuous coevolution of the host defenses and the microbes' mechanisms of evasion take place. In some pathogens, this process led to the evolution of secreted effector proteins that imitate eukaryotic functions, so-called molecular mimics. The concept of molecular mimicry was initially described by Raymond T. Damian in 1964, and it referred to the sharing of antigenic determinants between parasite and host (1). He discussed the origin and consequences of molecular mimicry, showing that it allows the parasite to avoid recognition by the host immune system and thus to survive. However, due to the resemblance between epitopes from the microorganisms and the antigens present in the host, infections can initiate or stimulate a strong autoimmune response. Hence, it was suggested that molecular mimicry may also be involved in the development of human autoimmune diseases (2; reviewed in reference 3).

Later, the concept of molecular mimicry was expanded, referring to the display of pathogen-encoded factors that resemble structures of the host at the molecular level and that benefit the pathogen due to this resemblance. These mimics can be perfect

Citation Mondino S, Schmidt S, Buchrieser C. 2020. Molecular mimicry: a paradigm of host-microbe coevolution illustrated by *Legionella*. mBio 11:e01201-20. <https://doi.org/10.1128/mBio.01201-20>.

Editor Danielle A. Garsin, University of Texas Health Science Center at Houston

Copyright © 2020 Mondino et al. This is an open-access article distributed under the terms of the [Creative Commons Attribution 4.0 International license](https://creativecommons.org/licenses/by/4.0/).

Address correspondence to Carmen Buchrieser, cbuch@pasteur.fr.

Published 6 October 2020

mimics when they co-opt host factors or imperfect when they resemble host components and yet perform distinct functions which confer an advantage to the pathogen (4, 5). Four different types of mimicry exist: (i) similarity in the sequences and structures of full-length proteins or domains, (ii) structural similarity without sequence homology, (iii) similarity in protein short linear motifs (SLiMs), also known as motif mimicry, and (iv) similarity of binding surface architectures even without sequence homology, known as interface mimicry (6, 7).

Molecular mimics can emerge by two main mechanisms. The first one is convergent evolution, in which nonhomologous proteins encoded by microorganisms evolve features of host proteins mainly through mutations (5, 8). These microbial proteins then mimic specific chemical groups or biophysical properties of host proteins that are relevant for protein function. However, such mimics are difficult to detect, as detailed functional and structural analyses are necessary (5, 8). Alternatively, mimics can arise from the acquisition of host cell genes through horizontal gene transfer, which can be evidenced by sequence similarity with host proteins and by phylogenetic analyses. After horizontal acquisition, genes are generally sculpted and evolve further to be efficiently processed by the bacterial transcriptional/translational machinery. This may involve the loss of introns, the acquisition of regulatory elements necessary for correct gene expression, and the acquisition of a secretion signal that will allow recognition of the acquired protein by bacterial secretion systems. As a consequence, the divergent evolution of the mimic may obscure the common origins of these genes (5). Convergent evolution and vertical acquisition of eukaryotic-like functions are not exclusive processes but can be observed even in a single bacterial protein. An interesting example is SptP, a type III secreted effector of *Salmonella enterica* serovar Typhimurium with N-terminal GTPase-activating protein (GAP) activity for Rac1 and Cdc42 (9). The crystal structure of the SptP-Rac1 complex revealed that the GAP domain functionally mimics host GAPs through a combination of specific structural elements, suggesting that the GAP activity has evolved convergently from the selective pressures of host-pathogen coevolution (10). In contrast, the carboxyl-terminal part of SptP, with tyrosine-phosphatase activity, harbors sequence and structure similarity to those of their eukaryotic counterparts, suggesting that this function was acquired by horizontal gene transfer (8). Thus, horizontal gene transfer followed by fusion to a bacterial protein might be an important mechanism for the emergence of bacterial proteins with eukaryotic-like domains (11).

The increasing availability of bacterial genome data improved our knowledge of the diversity of bacterial mimics that resemble eukaryotic proteins or that harbor eukaryotic-like domains. The latter can be defined according to their distribution within the bacterial or eukaryotic genomes. In a recent study, our group has defined a eukaryotic domain as one that is found in more than 75% of eukaryotic genomes and less than 25% of prokaryotic genomes (12). While these domains tend to be widespread in eukaryotes, they are generally absent or rarely present in bacteria, except in those that closely interact with a eukaryotic host (13). Furthermore, eukaryotic-like proteins, which are bacterial proteins that are similar to eukaryotic proteins (e.g., they have at least 20% amino acid identity over more than a third of the protein length), have been identified in some bacterial genomes (12). The presence of bacterial eukaryotic-like proteins is a strong indicator that such proteins are effectors, which are generally secreted by dedicated secretion systems during infection (14, 15). Indeed, eukaryotic-like proteins and their role in infection have been described in several intracellular pathogens, such as *Legionella*, *Coxiella*, *Mycobacterium*, *Chlamydia*, and *Bacillus* (16–20). However, to our knowledge, the highest number and widest variety of eukaryotic-like proteins have been found in bacteria belonging to the genus *Legionella* (12, 21). Analyses of the *Legionella* genus genome identified proteins encoding 137 different eukaryotic-like domains and more than 200 eukaryotic-like proteins, constituting a remarkable example of molecular mimicry of host proteins by an opportunistic human pathogen (12). In this review, we take *Legionella* as a model and we discuss examples of molecular mimicry of eukaryotic domains and eukaryotic proteins in the context of

pathogenesis and symbiosis, with an emphasis on effectors for which a function has been described.

LEGIONELLA, A BLIND COPYCAT

When our group sequenced and analyzed the *Legionella pneumophila* strain Paris genome, it was surprising to find a high number of genes coding for eukaryotic-like proteins or proteins with eukaryotic-like motifs (15). We thus hypothesized that these proteins may help the bacterium to hijack the host cell (15). *Legionella* spp. are Gram-negative, facultative, intracellular bacteria that are ubiquitously present in aquatic environments. An exception is *Legionella longbeachae*, which is isolated mainly from moist soil and potting mixes (22, 23). The bacteria are found either free-living, associated with biofilms, or parasitizing protozoan hosts, such as amoebae (24). Apart from its natural protozoan hosts, *Legionella* is also able to infect human alveolar lung macrophages. This infection can lead to a severe pneumonia called Legionnaires' disease, which can be fatal if not treated promptly (23, 25).

Infection of humans occurs through inhalation of aerosolized, contaminated water droplets generated by artificial water systems, such as air-conditioning units, shower heads, or cooling towers. The number one causative agent of Legionnaires' disease worldwide is *L. pneumophila*, causing 80 to 90% of the confirmed cases, followed by *L. longbeachae*, which is particularly prevalent in Southeast Asia, Australia, and New Zealand (23). Nearly everything that we know today about the intracellular lifestyle of *Legionella* was obtained by studying *L. pneumophila*. Starting with cell contact, *L. pneumophila* secretes into the host cytoplasm effectors that help (i) to avoid phagolysosomal degradation and (ii) to establish a dedicated replicative niche, named the *Legionella*-containing vacuole (LCV). These effectors have been shown to manipulate diverse cellular signaling and vesicular trafficking pathways to recruit endoplasmic reticulum (ER)-derived vesicles to the LCV, to redirect cellular proteins to the LCV for nutrient supply, to subvert the host cell immune response, or to suppress autophagy and apoptosis of the infected cell (26).

An astonishing number (18,000) of different effectors have recently been predicted in the genus *Legionella*, but only 8 of them are conserved in the 58 species analyzed (12). To date, *L. pneumophila* is the uncontested champion in the bacterial kingdom, with over 330 translocated effectors (representing 10% of its genome) that are delivered to the host cell cytosol through the Dot/Icm type 4B secretion system (T4SS) (27). A large body of research that sheds light on the functional roles of specific effectors encoded by *L. pneumophila* has been collected in the last several years. These studies have substantially contributed to our understanding of molecular mimicry of eukaryotic protein domains/motifs as a central survival mechanism of *Legionella* (Table 1; Fig. 1).

Intracellular lifestyle: *Legionella* effectors that manipulate small GTPases and membrane trafficking. *Legionella* critically depends on the establishment of the LCV and the hijacking of cellular pathways to efficiently replicate inside the host cell. Small GTPases of the Arf, Rho, Ras, and Rab families play a central role in eukaryotic intracellular trafficking, cell motility, and intracellular signaling events, among others (28). A hallmark of small GTPases is the switch between an active GTP-bound state and an inactive GDP-bound state. The switch between these states is mediated by guanine nucleotide exchange factors (GEFs), which induce the exchange of GDP for GTP, leading to GTPase activation, and GTPase-activating proteins (GAPs), which accelerate the hydrolysis of GTP, leading to the inactive state. Small GTPases can be activated only by GEFs when they are bound to membranes, which requires the constant cycling of small GTPases between endomembranes and the cytosol, which is regulated by solubilizing guanine dissociation inhibitors (GDIs) (28). These eukaryotic/endogenous regulators of small GTPases interact with the proteins via a shared conserved domain. Arf GEFs contain Sec7 domains and regulate protein and lipid trafficking in eukaryotic cells (29). Human regulator of chromatin condensation 1 (RCC1) contains signature RCC1 repeats and functions as a GEF for the small GTPase Ran (30).

TABLE 1 Eukaryotic-like effectors of *Legionella* with functions discussed herein

Effector(s)	Domain(s)	Function(s)	Identified target(s)	Reference(s)
Legionella proteins with eukaryotic domains				
Manipulation of small GTPases and membrane trafficking				
RalF	Sec7	Acts as an Arf1 GEF	Arf1	31, 32
<i>Legionella</i> Rab GTPases	Rab GTPase-like	Unknown	Unknown	12, 85
MitF (LegG1)	RCC1	Activates Ran, promotes LCV and host cell motility; implicated in mitochondrial fragmentation	RanBP10	36, 37, 38, 40
PieG	RCC1	Activates Ran, promotes LCV and host cell motility	Ran, RanGAP1	40
PpgA	RCC1	Activates Ran, promotes LCV and host cell motility	RanGAP1	40
LseA	Qc-SNARE	Probably mediates membrane fusion events	Qa-, Qb- and R-type SNAREs	43
Ylfb (LegC2), LegC3, Ylfa (LegC7)	Coiled-coil motifs reminiscent of Q-SNARE	Modulate membrane fusion events	VAMP4	48, 49, 50, 51
Manipulation of host cell transcription				
Roma	Ankyrin repeat, SET	Changes histone marks; methylates nonhistone proteins	H3K14, AROS	56, 57
LegAS4	Ankyrin repeat, SET	Changes histone marks	H3K4	58
AnkH	Ankyrin repeat	Interferes with transcriptional elongation by RNA polymerase II	LARP7 of the 7SK snRNP complex	61
Manipulation of the ubiquitination pathway				
LubX	U-box	E3 ligase	Clk1, SidH	66, 67, 69
AnkB	Ankyrin repeat, F-box	Interacts with the ubiquitination machinery, supplies amino acids to the <i>Legionella</i> vacuole	Skp1, ParvB	72, 73, 75
RavN	U-box-like motif	E3 ligase	Unknown	70
Lpg2370	RING-type E3 ligase	E3 ligase	Unknown	70
MavM	RING-type E3 ligase	E3 ligase	Unknown	70
MavJ	HECT-type E3 ligase	E3 ligase	Unknown	70
LotA	Ovarian tumor (OTU) superfamily of cysteine proteases	Deubiquitinase	Ubiquitin moieties on the LCV	82
Ceg23	Ovarian tumor (OTU) superfamily of cysteine proteases	Deubiquitinase	K63-linked polyubiquitin on the LCV	83
RavD	OTULIN-like interaction surface, papain fold	Deubiquitinase	M1-linked linear ubiquitin on the LCV	84
Manipulation of protein phosphorylation				
LegK1	STPK	Mimics I κ B kinases, activates NF- κ B signaling	I κ B family of inhibitors	88
LegK4	STPK	Inhibits host translation	Hsp70 chaperone family	89, 90
LegK2	STPK	Inhibits actin polymerization on the <i>Legionella</i> vacuole	ARPC1B and ARP3 subunits of the ARP2/3 complex	87, 91
LegK7	Structural homology to STPK	Mimics MST1, hijacks the Hippo signaling pathway	MOB1A	92, 93
SidJ	Structural homology to STPK	Pseudokinase that mediates protein polyglutamylation, activated by host calmodulin	SidE family of effectors	94, 95, 96, 97
Lpg2603	Atypical protein kinase structure	Active kinase <i>in vitro</i> , activated by host inositol hexakisphosphate	Unknown	98
Ceg4	HAD	Phosphotyrosine phosphatase, putative regulator of MAPK signaling	p38 MAPK	101
Lem4	HAD	Phosphotyrosine phosphatase	Unknown	102

(Continued on following page)

TABLE 1 (Continued)

Effector(s)	Domain(s)	Function(s)	Identified target(s)	Reference(s)
<i>Legionella</i> SH2 domain-containing proteins	SH2	Bind to phosphotyrosines	Unknown	104
<i>Legionella</i> proteins that resemble eukaryotic-like proteins				
LpSpl	Sphingosine 1-phosphate lyase	Restrains autophagy	Intracellular sphingosine	105, 106
LpdA	Phospholipase D	Modulates phosphatidic acid cellular levels	Lipid substrates	107, 108
LncP	Mitochondrial carrier family of proteins	Mediates the unidirectional transport of ATP	ATP	109
Lpg1905, Lpg0971	ecto-NTPDase	Unknown	Unknown	110, 112, 113
GamA	Amylase	Unknown	Unknown	115
LamB	Amylase	Unknown	Unknown	116
LamA	Amylase	Blocks amoeba encystation	Intracellular glycogen	117

L. pneumophila uses the molecular mimicry of all of the above-mentioned eukaryotic protein domains, resulting in the bacterial manipulation of membrane trafficking. The translocated effector RalF contains a Sec7 domain and acts as an Arf GEF in the host cell, directly activating and recruiting Arf1 to the LCV membrane (31). Indeed, structural analysis confirmed that the Sec7 domain of RalF has the same overall structure as its eukaryotic counterparts, demonstrating that the bacterial and eukaryotic proteins are structurally highly conserved (32).

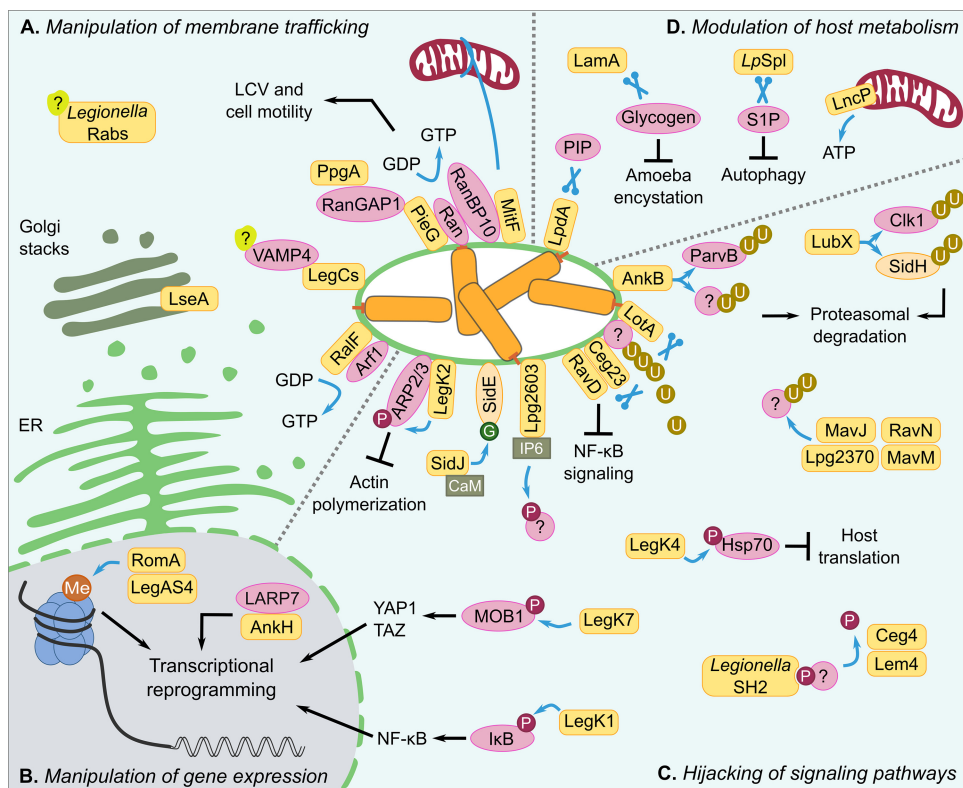


FIG 1 Selected *Legionella* eukaryotic-like T4SS-dependent effectors as discussed herein. *Legionella* spp. translocate eukaryotic-like proteins to manipulate specific host cell processes, like membrane trafficking (A), gene expression (B), signaling pathways (C), and host metabolism (D). While many of these translocated effectors harbor eukaryotic-like domains, others resemble eukaryotic proteins themselves. The functions of the different *Legionella* effectors implicated in the depicted processes are further discussed in the text. Orange box, *Legionella* effector; pink oval, host target protein/molecule; orange oval, *Legionella* target protein; Me, methylation; U, ubiquitination; P, phosphorylation; G, glutamylation, CaM, calmodulin; IP6, inositol hexakisphosphate; ER, endoplasmic reticulum.

Furthermore, *L. pneumophila* uses at least six secreted effectors (SidM [DrrA], SidD, AnkX, Lem3, LepB, and LidA), which mediate the recruitment of Rab1 and its functional modification to facilitate the fusion of ER-derived vesicles with the LCV membrane (for reviews on this topic, see references 33 and 34). Surprisingly, most of these Rab1-modulating effectors are absent in *L. longbeachae* and several other *Legionella* species (12). Notably, genome analyses identified genes encoding eukaryotic Rab GTPase domain-containing proteins in some *Legionella* species, including *L. longbeachae*, suggesting that these bacterial Rab-like proteins are able to subvert host cell trafficking (12). Although there is no evidence to date that these effectors functionally replace the Rab1-modulating proteins of *L. pneumophila* or that they use the canonical GTP/GDP cycle, they are an intriguing example of molecular mimicry in the genus *Legionella*, and further research will shed light on the specific roles of these unique bacterial Rab-like proteins in infection.

Another eukaryotic-like domain used by *L. pneumophila* is the RCC1 domain, a seven-beta-propeller fold specific for Ran GEFs, which was first identified in the secreted effector MitF (LegG1) (35). In fact, MitF (LegG1) has been shown to function as a bacterial Ran activator, promoting microtubule stabilization, LCV motility, and cell migration during infection (36, 37). In addition, it was recently shown that MitF (LegG1) is implicated in mitochondrial fragmentation, probably through WASP-Arp2/3-mediated recruitment of DNM1L. This modulation of mitochondrial dynamics by *L. pneumophila* induces a Warburg-like metabolism in the host cell that promotes bacterial replication (38). Several intracellular pathogens induce a shift in the host cell metabolism, probably supporting the bacterium's specific nutritional needs during infection (39). A recent study highlights an interesting history of divergent evolution of RCC1-containing effectors among different *L. pneumophila* strains, ultimately leading to changes of their specific cellular targets but not their Ran GEF function. The RCC1 repeat-containing proteins MitF (LegG1) and PpgA of *L. pneumophila* strain Philadelphia-1 target RanBP10 and RanGAP1, while PieG from *L. pneumophila* strain Paris activates Ran by binding to Ran itself and RanGAP1 (40). Despite their different cellular targets, all three effectors lead to Ran activation as well as increased LCV and host cell motility (40).

In addition, *L. pneumophila* secretes effectors that mimic eukaryotic soluble N-ethylmaleimide-sensitive factor attachment protein receptors (SNAREs). SNAREs contain coiled-coil domains that consist of amphipathic alpha-helices that can wrap around each other to form helical bundles. These proteins tether membranes together to mediate membrane fusion events in the eukaryotic cell, for example in vesicular trafficking (41, 42). SNAREs are broadly classified into R- and Q-SNAREs based on the interaction of an arginine residue with three glutamine residues in the SNARE core complex. The analysis of LseA in *L. pneumophila* revealed strong sequence homology to the fungal SNARE protein syntaxin-6 (43). LseA resembles a Qc-SNARE protein by its coiled-coil domain, and it contains a C-terminal eukaryotic CAAX motif predicted to be necessary for binding to host organelles. C-terminal prenylation motifs, or CAAX boxes, harbor a conserved cysteine residue that is lipidated by host prenylation enzymes during infection (44–46). Indeed, it was shown that LseA localizes to Golgi membranes and binds multiple host SNAREs of the Qa, Qb, and R types, thus probably mediating membrane fusion events in Golgi membrane-associated pathways (43). The C-terminal CAAX prenylation motif, like nuclear localization signals (NLS) or ER retention motifs, are defined as SLiM mimicry, which allows to position effectors to specific host organelles. SLiM mimicry has recently been reviewed extensively (47).

The putative Q-SNAREs LegC3 and Ylfa (LegC7) were identified by sequence-based structure prediction to contain coiled-coil domains and were shown to disrupt yeast endosomal trafficking (48, 49). Moreover, these two proteins together with Ylfb (LegC2), another SNARE-like protein, were shown to mediate membrane fusion events by binding to the eukaryotic R-SNARE vesicle-associated membrane protein 4 (VAMP4), possibly promoting LCV expansion (50, 51).

Taken together, molecular mimicry of Sec7, Rab GTPase, coiled-coil, or RCC1 eukaryotic domains facilitates *L. pneumophila* intracellular replication through the modulation of proteins that are key components of eukaryotic membrane trafficking pathways.

Targeting the control center: *Legionella* effectors that manipulate host cell transcription. During infection, some of the secreted bacterial proteins, so-called nucleomodulins, ultimately hijack the cell nucleus (52, 53). Examples of eukaryotic mimics that modulate the transcriptional machinery of the host cell include bacterial proteins containing ankyrin motifs and SET [eukaryotic su(var)3-9, enhancer-of-zeste and trithorax] domains. Ankyrin repeats mediate protein-protein binding, while SET domains mediate methylation of lysine residues of histones and modify chromatin condensation as well as transcriptional activity at specific sites (54, 55). The T4SS-dependent effector RomA of the *L. pneumophila* strain Paris contains two eukaryotic-like domains: a C-terminal ankyrin repeat domain and an N-terminal SET domain. RomA methylates lysine 14 of histone H3 (H3K14), a residue usually acetylated at active promoters, to downregulate gene transcription in infected cells, including genes associated with innate immunity (56). In addition, it was recently shown that RomA also methylates nonhistone proteins in human cells, suggesting a multifaceted role for this effector during infection. RomA also targets AROS, a regulator of the human deacetylase SIRT1, although the specific role of this modification during *Legionella* infection remains to be investigated (57). LegAS4, the homolog of RomA in *L. pneumophila* strain Philadelphia-1, was reported to localize to the cell nucleolus, where it methylates H3K4, probably leading to increased transcription of host cell ribosomal DNA (58). However, as with infection of alveolar epithelial cells with *L. pneumophila* strain Paris, infection with *L. pneumophila* strain Philadelphia-1 leads to strong methylation of the H3K14 histone mark (59). Further structural analysis revealed that the LegAS4 SET domain is structurally similar to the eukaryotic SET domain, suggesting that this protein may have evolved from a common eukaryotic ancestor by horizontal gene transfer (60).

AnkH, an ankyrin repeat-containing protein, is the only effector known thus far for which a direct role of the ankyrin repeat has been described in *Legionella* infection. It is also one of eight core effectors common to all *Legionella* species sequenced to date (12, 21). *L. pneumophila* AnkH directly interacts with the nuclear protein La-related protein (LARP7), which is a component of the 7SK small nuclear ribonucleoprotein (snRNP) complex in human cells. The AnkH-LARP7 interaction partially impedes interaction of LARP7 with the 7SK snRNP complex components, thus interfering with transcriptional elongation by RNA polymerase II. As a consequence, AnkH-dependent global transcriptional reprogramming of the host cell promotes intracellular bacterial growth (61). The N-terminal domain of AnkH contains four ankyrin repeats with a typical structural fold of two alpha-helices, forming a helix-turn-helix motif, joined by a beta-hairpin loop. It was observed that a mutation of the third beta-hairpin loop in the ankyrin repeat domain abrogates binding of AnkH to LARP7 and leads to an intracellular growth defect of *L. pneumophila*. Taken together, these findings suggest that AnkH-mediated transcriptional reprogramming is essential for infection (61).

There is an increasing number of bacteria for which molecular mimicry of eukaryotic proteins that target the host cell nucleus has been described. Like *Legionella*, *Chlamydia trachomatis*, *Bacillus anthracis*, and *Burkholderia thailandensis* secrete SET domain-containing proteins that target host cell histones. Furthermore, *Anaplasma phagocytophilum* secretes an ankyrin repeat-containing protein (AnkA) that directly binds to host DNA, leading to decreased transcription, as reviewed in reference 52. Genome analyses might identify new eukaryotic mimics targeting the host nucleus among *Legionella* effectors, as well as in other bacterial pathogens.

Forging ubiquitin signaling: *Legionella* effectors that target the cellular ubiquitination pathway. Ubiquitination is a key posttranslational modification with functions in the degradation of proteins, vesicular trafficking, innate immune response, autophagy, and apoptosis. Protein ubiquitination involves the covalent attachment of ubiquitin to the epsilon amino group of lysine as singular chains or branched chains.

Three enzymes mediate this reaction in an ATP-dependent manner: a ubiquitin-activating enzyme (E1), a ubiquitin-conjugating enzyme (E2), and a ubiquitin ligase (E3) that confers target protein specificity (62). Eukaryotic E3 enzymes are broadly classified into two classes: HECT and RING-type E3 ligases. The RING E3 enzymes are characterized by their RING or U-box fold catalytic domain, and some multicomponent RING E3 complexes also include F-box domain-containing proteins (63). RING and U-box domains share overall structural similarity; however, U-box domains do not contain central Zinc-binding residues found in RING domain proteins (64). RING/U-box E3 ligases function as scaffolds for transfer of ubiquitin to target proteins without the attachment of ubiquitin to the E3 ligase itself, whereas HECT-like E3 ligases form a covalent thioester E3-ubiquitin intermediate via a conserved cysteine in their active site before transfer of ubiquitin to the target protein (64, 65).

Many bacterial pathogens, including *Legionella*, *Salmonella*, and *Shigella*, target the cellular ubiquitination machinery (65). Interestingly, particular amoeba-associated bacteria encode a large number of proteins that most likely interfere with the host's ubiquitination signaling, suggesting that it is crucial for bacterial replication in protozoan hosts (13). Indeed, nearly all *Legionella* genomes analyzed to date contain F-box (1 to 18 per genome)- and/or U-box (1 to 3 per genome)-encoding genes (12). The T4SS effector LubX contains two U-box domains, and it was shown to mediate polyubiquitination of the host Cdc2-like kinase 1 (Clk1); however, the consequence of this modification needs to be further elucidated (15, 66). In addition, LubX was shown to target the *Legionella* effector SidH for proteasomal degradation at late stages of infection, thus functioning as a key regulator to temporally coordinate the activity of a cognate effector (67). Thus, LubX was the first identified metaeffector, meaning effectors that target another effector during infection. Subsequently, it was found that putative metaeffectors are present in considerable numbers in the *Legionella* genomes (68). Interestingly, functional and structural analyses revealed that only the N-terminal U-box domain of LubX has E3 ligase activity and that it is the exclusive E2-interacting module within the protein (69). The second C-terminal U-box, however, seems to be necessary for the interaction of LubX with the target proteins, although the single residue that appears to be critical for binding of LubX to the cognate effector SidH was found to be located outside the U-box fold (66, 69).

Despite a lack of sequence homology to known eukaryotic E3 ligases, the crystal structure of the N-terminal region of RavN revealed a U-box-like motif with a surface area analogous to those of the E2 binding regions of other eukaryotic E3 ligases (70). This suggests that RavN has been acquired by *Legionella* through horizontal gene transfer early during evolution and structurally altered over time in order to best fulfil its current function. Indeed, RavN was shown to function as an E3 ubiquitin ligase in eukaryotic cells (70). Using pairwise comparison of profile hidden Markov models, three other *Legionella* E3 ligase effectors with homology to RING-type E3 (Lpg2370 and MavM) or to HECT-type E3 ligases (MavJ) were identified, all of which exerted ubiquitinase activity in transfected cells (70).

The *L. pneumophila* genomes sequenced to date encode one to four F-box domains each (12, 15). The functionally best-described F-box protein is AnkB, which also contains a eukaryotic ankyrin domain and, in certain strains, also a CAAX motif (71). AnkB interacts with Skp1 and the host ubiquitination machinery to modulate the ubiquitination status of ParvB, a linker of cytoskeletal dynamics and cell survival (72, 73). In addition, AnkB of *L. pneumophila* strain Philadelphia-1 was shown to be prenylated by the host prenyltransferase machinery at the CAAX motif to anchor the protein in the LCV membrane (44). It was recently proposed that AnkB of *L. pneumophila* strain Paris, which does not contain a CAAX box, harbors an ER retention motif instead. This motif may allow this protein to be anchored in the LCV membrane (74). It has been suggested that AnkB mediates degradation of polyubiquitinated proteins on the LCV that are further used by *L. pneumophila* as nutrients (75).

In addition to having proteins with the eukaryotic U-box and F-box domains, *Legionella* translocates proteins that manipulate ubiquitination signaling through non-

canonical mechanisms of ubiquitination. Members of the SidE family of effectors attach phosphoribosylated ubiquitin to a serine residue of host Rab GTPases in an NAD⁺-dependent manner. This previously unknown protein ubiquitination is mediated solely by the *Legionella* effector, independently of host E1 and E2 enzymes (76, 77). It was also shown that SidE family effectors are able to cleave the most common ubiquitin chains found in eukaryotic cells through an N-terminal deubiquitinase domain *in vitro* (78). Based on these novel functions, other deubiquitinases specific for phosphoribosylated ubiquitin were recently identified in *L. pneumophila* (79). However, as several of these proteins do not encode known eukaryotic domains, we will not discuss them in more detail here (for reviews, see references 80 and 81).

In contrast, *Legionella* encodes other proteins with distant homology to the eukaryotic ovarian tumor (OTU) superfamily of cysteine proteases that function as deubiquitinases. An example is LotA, a T4SS-dependent effector that uniquely harbors two catalytic pockets and localizes to the LCV, where it removes ubiquitin moieties. However, its specific function during infection needs to be further elucidated (82). Furthermore, the effector Ceg23 adopts an OTU-like fold despite limited sequence similarity, as revealed by structural analysis of the N-terminal region (83). Ceg23 specifically cleaves Lys63-linked ubiquitin through a Cys-His-Asp catalytic triad and prevents the accumulation of Lys63-polyubiquitin on the LCV. Interestingly, RavD adopts an interaction surface similar to that of the eukaryotic OTU deubiquitinase with linear specificity (OTULIN) when in complex with linear di-ubiquitin. RavD is a cysteine-dependent deubiquitinase with a unique papain-like fold, which uses an unusual Cys-His-Ser catalytic triad to specifically cleave Met1-linked linear ubiquitin chains. In infection, RavD prevents the accumulation of linear ubiquitin chains on the LCV, leading to a downregulation of the host proinflammatory nuclear factor kappa-light-chain enhancer of activated B cell (NF- κ B) signaling (84). Taken together, *Legionella* encodes a remarkable diversity of effectors that help to modulate ubiquitin signaling in host cells.

Rewriting and exploiting of protein phosphorylation: *Legionella* effectors mimicking eukaryotic kinases and phosphatases. Protein kinases and phosphatases are key players in signal transduction in mammalian cells. Hence, their function is often hijacked by bacterial effectors during infection. While some effectors described for *Legionella* mimic serine/threonine protein kinases (STPK), others contain haloacid dehalogenase (HAD)-like domains or Src homology 2 (SH2) domains (15, 85, 86). Five different proteins in *L. pneumophila* that show primary amino acid sequence homology to eukaryotic protein kinases have been identified to date, four of which are secreted effectors that have been characterized in more detail (87).

The *L. pneumophila* eukaryotic-like STPK LegK1 impacts the host NF- κ B pathway through functionally mimicking host inhibitor of nuclear factor kappa B ($\text{I}\kappa\text{B}$) kinases (88). The activity of LegK1 might be independent of signaling components upstream of host $\text{I}\kappa\text{B}$ kinases, as it does not require the canonical activation of its kinase domain, indicating that LegK1 might be constitutively active or regulated by means other than phosphorylation of its activation loop (88). Like LegK1, LegK4 is a constitutively active eukaryotic-like STPK that does not depend on phosphorylation of its activation loop but probably on the stabilizing effect of its kinase domain dimerization (89). LegK4 phosphorylates a conserved threonine in the substrate-binding domain of the host Hsp70 chaperone family (90). Due to LegK4-mediated phosphorylation, Hsp70 has reduced ATPase activity and is impeded in its protein refolding capacity, which ultimately leads to a global translation inhibition of the host cell. Altogether, this suggests that LegK4 impacts host translation and the unfolded protein response, which might be beneficial for bacterial replication (90).

The protein kinase LegK2 was initially reported to be involved in the recruitment of ER vesicles to the LCV and in bacterial replication during infection (87). However, it was shown later that LegK2 phosphorylates the ARPC1B and ARP3 subunits of the actin nucleator ARP2/3 complex to inhibit actin polymerization on the LCV. Thereby, it hinders late endosome/lysosome association with the *Legionella* phagosome, contributing to the bacterial escape from the endocytic pathway (91).

LegK7 was recently identified as a bacterial protein kinase with folding homology to eukaryotic protein kinases such as PKA α , based on profile hidden Markov model structure prediction (92). LegK7 was shown to hijack the conserved Hippo signaling pathway by functionally mimicking the host Hippo kinase MST1. Indeed, LegK7 phosphorylates MOB1A, which in turn leads to the degradation of the cotranscriptional regulators YAP1 and TAZ, thus triggering a signaling cascade that alters the transcriptional landscape of the host cell to promote *L. pneumophila* replication (92). A recent crystallographic study of the LegK7-MOB1A complex revealed that the N-terminal half of LegK7 is structurally similar to eukaryotic protein kinases and that MOB1A directly binds to the LegK7 kinase domain. LegK7 uses MOB1A as an allosteric activator and as a scaffold for the recruitment and phosphorylation of the downstream substrates (93).

Additionally, *L. pneumophila* encodes atypical protein kinases that are activated by host cofactors. One such example is SidJ (Lpg2155), a pseudokinase that contains a eukaryotic Ser/Thr protein kinase-like fold but which mediates polyglutamylation of translocated effectors of the SidE family (94, 95). Interestingly, SidJ function is dependent on the host cofactor calmodulin (94–97). Structural analysis of the translocated effector Lpg2603 revealed atypical kinase features. Lpg2603 is an active kinase *in vitro* that is allosterically activated by the host cofactor inositol hexakisphosphate (98). Another effector that is activated by host cofactors is LtpM, a glycosyltransferase that is activated by host phosphoinositides (99). Importantly, *Legionella* spp. also encode a large variety of kinases and phosphatases that target host phosphoinositide (PI) lipids. The roles of these PI kinases and PI phosphatases, including PI binding effectors and PI lipases, have recently been reviewed in detail and will thus not be further discussed in this review (100).

Recently, two *Legionella* effectors harboring HAD-like domains have been identified as eukaryotic-like protein phosphatases. Ceg4 is an atypical HAD-like phosphotyrosine phosphatase implicated in the regulation of host mitogen-activated protein kinase (MAPK)-signaling pathways (101). Similarly, Lem4 was described as a protein tyrosine phosphatase with structural similarity to the murine phosphatase MDP-1 (102). However, the roles of Ceg4 and Lem4 during *Legionella* infection are open questions for future research.

Besides protein kinases and phosphatases, SH2 domains are important phosphotyrosine-binding modules that function as scaffolds for intracellular kinase signaling cascades. SH2 domains are structurally conserved and consist of an antiparallel beta-sheet surrounded by two alpha-helices (103). *L. longbeachae* was the first prokaryote reported to encode eukaryotic SH2 domains (85). Recently, using a structure-guided sequence alignment, 93 putative SH2 domains were identified in 84 *Legionella* proteins (104). SH2 domains in *Legionella* are distinct in amino acid sequence but share both the SH2 domain fold and a conserved phosphotyrosine-binding pocket with their eukaryotic counterparts (104). Interestingly, some *Legionella* SH2 domains bind to phosphotyrosine peptides with greater affinities than known mammalian SH2 domains and thus were termed phosphotyrosine superbinders by the authors of this study. Moreover, the presence of additional eukaryotic-like domains in some *Legionella* SH2-containing proteins suggests that they may be enzymes that modulate specific pathways during infection (104). Further studies are needed to unveil the functions of this diverse set of *Legionella* proteins in the modulation of host cell phosphotyrosine signaling during infection.

AS CLOSE AS IT GETS: *LEGIONELLA* EFFECTORS THAT RESEMBLE EUKARYOTIC PROTEINS

In addition to revealing modular effectors with eukaryotic domains, genomic analyses of the *Legionella* genus genome revealed the presence of putative bacterial effectors that resemble eukaryotic proteins over more than a third of the protein length (12). The characterization of many of these mimics showed that these proteins encode the same enzymatic activities as their eukaryotic counterparts. Some of these enzymes

target specific metabolic pathways in the host cell, conferring an advantage to the bacteria that allows them to use the resources of their host cell to thrive during infection.

Legionella eukaryotic-like proteins that target the host cell metabolism. Several of the *Legionella* eukaryotic-like proteins identified to date are predicted to function in metabolic pathways of the host cell, probably to scavenge nutrients from the cell to ensure intracellular replication of the bacteria. One example is the *L. pneumophila* sphingosine 1-phosphate lyase (*LpSpl/LegS2*). This protein structurally and functionally mimics eukaryotic sphingosine 1-phosphate lyases (105, 106). Recently, it was shown that *LpSpl* reduces intracellular sphingosine levels of host cells during infection. The manipulation of the host sphingolipid metabolism restrains the autophagic response and promotes the intracellular survival of *L. pneumophila* (105). Another effector, *LpdA*, shows homology with eukaryotic phospholipase D enzymes (107). *LpdA* hydrolyses several lipid substrates, leading to a modulation of the cellular levels of phosphatidic acid and contributing to the virulence of *L. pneumophila* in mice (108). A protein shown to interfere with ATP transport is *LncP*. It shows high sequence homology to eukaryotic proteins of the mitochondrial carrier family (MCF) (109). *LncP* localizes to the mitochondrial inner membrane, from where it mediates the unidirectional transport of ATP. However, the contribution of *LncP* activity to *L. pneumophila* intracellular replication and survival remains to be determined (109).

Furthermore, the *L. pneumophila* genome encodes two ectonucleoside triphosphate diphosphohydrolases (ecto-NTPDases) (15). These enzymes harbor five conserved apyrase regions and catalyze the hydrolysis of nucleoside triphosphates and diphosphates to the monophosphate form (110, 111). *L. pneumophila* *Lpg1905* and *Lpg0971* are eukaryotic-like ecto-NTPDases required for optimal intracellular replication and virulence in a mouse model of infection, although the specific functions of these proteins have yet to be elucidated (110, 112, 113). Unlike many other *Legionella* eukaryotic-like proteins, neither of the ecto-NTPDases are translocated into the host cell by the T4SS (113). However, the presence of a putative N-terminal secretion signal and the detection of protein secretion from bacterial cells suggest that they might be localized in the LCV lumen during infection (112, 114).

Amylases are enzymes that catalyze the hydrolysis of starch and glycogen into glucose. The identification of putative amylases in *L. pneumophila*, together with the fact that these bacteria do not synthesize starch or glycogen themselves, suggests that these proteins might be relevant for infection. *L. pneumophila* *GamA* is a eukaryotic-like glucoamylase secreted by the T2SS, although the importance of this protein during infection needs to be further elucidated (115). In contrast, *LamB* is a *Legionella* amylase required for intracellular replication and virulence in a mouse model of infection (116). However, it is not yet clear if this protein is a secreted effector, as *LamB* does not contain a T2SS secretion signal and experimental validation of secretion by the T4SS was unsuccessful (116). Finally, *LamA* was recently described as a T4SS-dependent amylase that catalyzes rapid glycogenolysis in amoebae, blocking amoeba encystation and promoting *L. pneumophila* proliferation (117).

These effectors highlight the breadth of molecular mimicry exerted by several *Legionella* effectors which skew host cell pathways and facilitate bacterial infection (Table 1; Fig. 1). Given the diversity and the large number of effectors in the genus *Legionella*, exciting discoveries are ahead of us that may identify further mechanisms of host cell modulation *via* bacterial mimicry of eukaryotic cell processes.

EUKARYOTIC-LIKE PROTEINS SHAPED BY BACTERIUM-PROTOZOAN INTERACTIONS

In the environment, *Legionella* are able to survive and replicate in a wide variety of protozoa, showcasing the most common mechanism of bacterial proliferation (118). The long-lasting coevolution of *Legionella* with its protozoan hosts has distinctly shaped the bacterial genome (12, 21). Many intracellular bacteria undergo genome reduction as a consequence of specialization to the intracellular lifestyle. However, this

phenomenon is not observed in amoeba-resistant bacteria like *Legionella* (119). In contrast, it seems that *Legionella* spp. undergo continuous genome expansion as a consequence of gene acquisition by horizontal gene transfer from their protozoan hosts, a phenomenon that was also corroborated by the finding that the ancestral genomes were probably smaller than they are today (12).

Comparative genomics and evolutionary analyses of nearly the entire *Legionella* genus genome revealed that all *Legionella* species have highly dynamic genomes with a diverse effector repertoire of 18,000 predicted proteins, encompassing at least 137 different eukaryotic domains and over 200 different eukaryotic proteins (12). It has already been shown that many of these predicted effectors have a modular structure and encode a combination of different eukaryotic domains (21). Furthermore, a recent study provided insightful evidence that the combined selective pressures of different amoebal hosts drive the evolution of *Legionella* species. These selective pressures ultimately shape the individual diversity of effector repertoires, which are probably related to the type of amoebae that *Legionella* organisms encounter and the frequency of the encounter (120). The origins of several of the eukaryotic-like proteins in the *Legionella* genome were corroborated by several phylogenetic analyses, which demonstrated that these proteins were acquired through horizontal gene transfer from a protist host (11, 12, 15, 85, 86, 121, 122). Thus, *Legionella* constitute one of the best-described examples of eukaryote-to-prokaryote gene transfer. A classic case constitutes the gene encoding the sphingosine 1-phosphate lyase (*spl*) of *L. pneumophila* (105). Different evolutionary analyses showed that the *spl* gene was acquired by horizontal gene transfer from a protist host, as the closest homologs are those from *Entamoeba* spp., *Tetrahymena thermophila*, and *Paramecium tetraurelia* (106, 122). Further homologs of this gene were found in 16 of the 58 *Legionella* species/subspecies analyzed. The phylogenetic analysis of these different *spl* genes showed that they have been acquired and lost several times during the evolution of the genus (122). Interestingly, *Legionella* spp. seem to acquire genes not only from their protozoan hosts but also from plants or fungi, as evidenced by the identification of eukaryotic-like proteins with pentatricopeptide repeats, alliinase, or caleosin domains in some *Legionella* species (12, 85). Thus, genomic exchange between *Legionella* and higher-order organisms also seems to occur (12).

These findings led to the suggestion that amoebae constitute melting pots of evolution, where gene fluxes in multiple directions may happen among amoebae, intracellular bacteria, fungi, and giant viruses, ultimately contributing to the evolution of these different organisms (119, 123). As an example, the ankyrin-containing protein Lpg2416 from *L. pneumophila* has its only homolog in the *Acanthamoeba polyphaga* mimivirus, a giant virus infecting *Acanthamoeba*, suggesting that *Legionella* may have acquired this eukaryotic-like protein from giant viruses (11). Additionally, genes can also be exchanged among different amoeba-related bacteria, as it was shown for bacteria of the orders *Legionellales*, *Chlamydiales*, and *Rickettsiales*, adding complexity to the possible evolutionary scenarios (124–126).

During the last two decades, genome analyses of different bacterium-associated amoebae showed that despite their different lifestyles and phylogenies, they share a set of eukaryotic protein domains necessary for bacterium-host interactions. Indeed, it has been shown that functional domains predominantly found in eukaryotes, such as ankyrin repeats, SEL1 repeats, leucine-rich repeats, and F-box and U-box domains were significantly enriched in the proteomes of amoeba-associated bacteria, like "*Candidatus* Amoebophilus asiaticus" (an obligate intracellular amoeba parasite), *Chlamydiae*, *Rickettsia bellii*, *Francisella tularensis*, and *Mycobacterium avium* (127). Furthermore, phylogenetic analyses were undertaken for some of the identified eukaryotic-like proteins in "*Candidatus* Amoebophilus asiaticus", suggesting that they had been acquired by horizontal gene transfer from a protozoan host (127). Taken together, these observations suggest that amoebae provide a specific environment for gene exchange between microorganisms invading them as pathogens

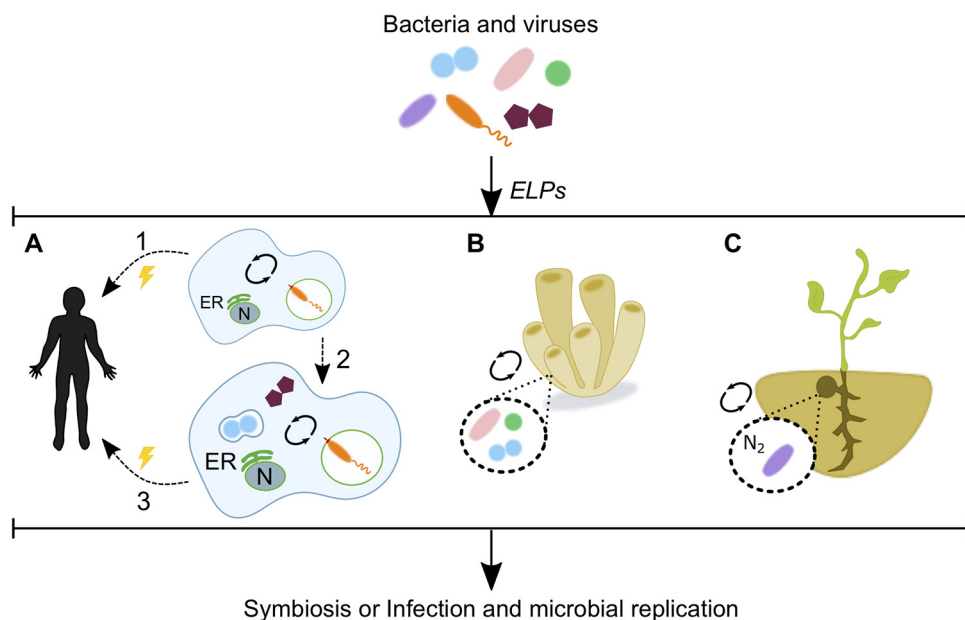


FIG 2 Eukaryotic-like proteins as mediators of pathogenesis and symbiosis. Microorganisms use eukaryotic-like proteins (ELPs) to communicate with their hosts. (A) *Legionella* spp. translocate eukaryotic-like proteins to multiply within protozoa, and this capacity enabled the bacterial transition to humans (arrow 1). The simultaneous occurrence of *Legionella* with other bacteria and giant viruses inside amoebae allows for the genetic interchange between these microorganisms and the host (arrow 2) and the acquisition of diverse functions which might confer an advantage during human infection (arrow 3). (B, C) Despite their role in pathogenicity, eukaryotic-like proteins are also used by cooperative bacterial communities to interact with their hosts. Eukaryotic-like proteins are used by prokaryotes to establish a symbiosis with marine sponges (B) and by rhizobia to form nitrogen-fixing symbioses with legumes (C). N, nucleus; ER, endoplasmic reticulum.

or symbionts, but also that amoebae might be “active players” in these events as donors of their own DNA (Fig. 2).

It is still unknown how the eukaryotic genes are taken up and how the DNA is subsequently integrated in the bacterial genome. *Legionella* spp., for example, are able to develop competence for natural transformation, which may facilitate the genetic exchange inside amoebae (128). However, other mechanisms, like the transfer of mRNA, may be imagined, in particular as certain *Legionella* genomes contain a gene predicted to encode a group II intron reverse transcriptase (122). Despite the current lack of experimental evidence to corroborate this hypothesis, the nature of this exchange may explain the lack of introns and regulatory elements in the bacterial genes. Once integrated into the bacterial genome, these genes need to evolve to be specifically recognized by the secretion machinery and become secreted proteins. Thus, it has been proposed that a low-level, leaky delivery of these so-called proto-effectors to the host may allow for the selection of mutations to fine-tune the protein’s translocation levels, in order to finally select for an efficient C-terminal translocation signal (27). Recently, it was shown that LvgA of *L. pneumophila* is an adaptor protein that recognizes effectors for secretion by the T4SS. However, not all effectors were recognized by LvgA, suggesting that the Dot/Icm-type 4B coupling protein (T4CP) complex is likely to be heterogeneous in terms of the adaptors displayed and that additional, yet to be identified adaptor proteins might exist (129).

Taken together, amoebae are key players in the evolution of amoeba-resistant bacteria like *Legionella*. Large-scale genome sequencing of different aquatic amoebae, a field only poorly studied to date, is greatly needed to improve our knowledge of the extent of interkingdom gene transfer and may provide evidence of currently unknown gene fluxes between different species of amoebae and bacteria. This knowledge will further advance our understanding of the origins of bacterial eukaryotic-like proteins and may allow us to elucidate the mechanisms by which they were acquired.

EUKARYOTIC-LIKE PROTEINS IN THE CONTEXT OF PATHOGENESIS AND SYMBIOSIS

The observation that *Legionella* species are able to multiply within protozoan hosts, primarily aquatic amoebae, led to the idea that the capacity of the bacteria to replicate within human phagocytic cells may have evolved from their ability to survive within protozoa (130), a hypothesis which was later confirmed by different studies (as reviewed in reference 131). Amoebae and macrophages have similar mechanisms of phagocytosis and bacterial inactivation; both consist of degradation of the phagocytized material, further supporting the idea that resistance to amoeba is an important driving force in the evolution of human pathogens. Indeed, pathogenicity might have been an ancient microbial mechanism of defense against predators, which evolved through time to allow microbes to survive within higher organisms (132). Then, amoeba-bacterium interactions drove the selection of bacterial features necessary for life within a eukaryotic host, including the evolution of specific eukaryotic-like proteins (133–135). *Legionella* certainly constitute an example of such adaptations, as it has recently been shown that *L. pneumophila* growth in macrophages results from the cumulative selective pressures of multiple amoeba hosts, which in some cases lead to redundancy among effectors (120). This observation suggests that different *Legionella* species have evolved distinct virulence mechanisms, including the use of specific eukaryotic-like proteins, as a consequence of their differential adaptations to amoeba predation, which finally enabled the transition from environmental reservoirs to humans (120). However, it is important to point out that eukaryotic-like effectors or effectors with eukaryotic domains might lead to different outcomes in infections of amoeba and human alveolar macrophages. While some effectors may facilitate survival in the environmental host, they may not be beneficial for infection of human cells because they may trigger immune surveillance pathways. One such example is LamA, a translocated amylase, which degrades glycogen in the host cytosol and prevents amoeba encystation. In contrast, the activity of LamA in human macrophages induces an M1-like proinflammatory phenotype of the cells, leading to a growth restriction of the bacteria (117).

Conversely, microbes typically considered beneficial and nonpathogenic can also display features that are typically considered hallmarks of pathogens, suggesting that these gene products may also be mutualistic factors, depending on the context (136). To date, eukaryotic-like proteins have been identified in the genomes of symbiotic bacteria associated with amoebae, fungi, sponges, and plants, suggesting that disease is not the only outcome of microbial molecular mimicry. In contrast, manipulation through molecular mimicry is also beneficial for the establishment of cooperative interactions between bacterial communities and their eukaryotic hosts (13) (Fig. 2). For example, root nodule bacteria (also known as rhizobia) are free-living soil bacteria that have the ability to form nitrogen-fixing symbioses with legumes (137). A multistep analysis of 163 rhizobial genomes identified five domains of eukaryotic origin that were overrepresented in these bacteria, compared to their presence in a negative-control genome set from phylogenetically related organisms not known to be associated with plants. Within these five putative eukaryotic-like proteins, only three were predicted to be secreted, overall suggesting that these rhizobial eukaryotic-like proteins may contribute to the modulation of the plant host responses during the symbiosis establishment (137).

Over the last decade, eukaryotic-like proteins have also been identified in the symbionts of marine sponges. Metatranscriptomic analyses of the microbiomes of three different sponges, namely, *Cymbastella concentrica*, *Scopalina* sp., and *Tedania anhelens*, identified eukaryotic-like proteins in 2.3%, 1.4%, and 1.3% of all prokaryotic transcripts, respectively, demonstrating constituent expression of eukaryotic-like proteins in the sponge symbionts (138). Particular classes of eukaryotic-like proteins and domains, such as cadherin, tetratricopeptide repeats, and ankyrin repeats, were expressed differently between the microbiomes of the different sponge species. Moreover, some of them were associated or cotranscribed with translocation systems, suggesting their involve-

ment in bacterium-host interactions (138). Indeed, it has been observed that the heterologous expression of four eukaryotic-like, ankyrin-repeat proteins from a sponge symbiont allowed *Escherichia coli* to modulate phagocytosis by amoebae (139). Hence, the functions of these eukaryotic-like proteins might facilitate bacterial survival and subsequent establishment within the sponge cells. A recent metagenomic analysis showed a high number of genes encoding eukaryotic-like proteins in the microbiomes of two of the most abundant Antarctic sponges, *Myxilla* sp. and *Leucetta antarctica*, thus pointing to common molecular mechanisms mediating symbiosis with sponges across different environments, including Antarctica (140).

In summary, there is increasing evidence suggesting that modulation of host pathways by eukaryotic-like proteins may constitute a common mechanism associated with bacterial survival within protozoan, fungal, plant, and metazoan hosts. The final outcomes of these interactions are not uniform; instead, bacterial clearance, symbiosis, or disease can occur (Fig. 2).

FINAL REMARKS

Mimicry constitutes one of the most common adaptive mechanisms in nature, and bacteria do not fall short, since this tool at the molecular level (known as molecular mimicry) represents a key element of bacterium-host interactions. *Legionella* adaptation to protozoan hosts makes these bacteria a remarkable model for the study of molecular mimicry. Indeed, the increasing characterization of *Legionella* proteins that mimic specific eukaryotic functions gives an idea of the multiplicity of host pathways that are targeted during infection. Moreover, the recent identification of eukaryotic-like proteins encoded in the genomes of other amoeba-resistant and -symbiotic bacteria highlights the importance of these eukaryotic-like mimics both in the context of infection and as a means of bacterial communication. In this regard, the identification of bacterial eukaryotic-like proteins in microbiomes is particularly exciting. Overall, eukaryotic-like proteins are powerful tools that allow bacteria to communicate with their hosts and to thrive in the environment. The study of molecular mimics highlights the complexity of bacterium-host interactions and bacterium-host coevolution, particularly important in the context of human health and disease.

ACKNOWLEDGMENTS

S.M., S.S., and C.B. contributed to the conception and the design of the minireview. S.M. and S.S. researched and wrote the paper. C.B. directed and contributed to the writing of the manuscript.

Work in the C.B. laboratory is financed by the Institut Pasteur, and funding has been received from the French Government (grants ANR-10-LABX-62-IBEID and ANR-15-CE17-0014-03 to C.B.) and the Fondation de la Recherche Médicale (grant EQU201903007847 to C.B.). S.S. is a scholar in the Pasteur-Paris University (PPU) international Ph.D. program and received a stipend from the Institut Pasteur.

We declare that the research was conducted in the absence of any commercial or financial relationships that could be construed as a potential conflict of interest.

REFERENCES

- Damian RT. 1964. Molecular mimicry: antigen sharing by parasite and host and its consequences. *Am Nat* 98:129–149. <https://doi.org/10.1086/282313>.
- Zabriskie JB, Freimer EH. 1966. An immunological relationship between the group. A streptococcus and mammalian muscle. *J Exp Med* 124: 661–678. <https://doi.org/10.1084/jem.124.4.661>.
- Cusick MF, Libbey JE, Fujinami RS. 2012. Molecular mimicry as a mechanism of autoimmune disease. *Clin Rev Allergy Immunol* 42:102–111. <https://doi.org/10.1007/s12016-011-8294-7>.
- Ludin P, Nilsson D, Mäser P. 2011. Genome-wide identification of molecular mimicry candidates in parasites. *PLoS One* 6:e17546. <https://doi.org/10.1371/journal.pone.0017546>.
- Elde NC, Malik HS. 2009. The evolutionary conundrum of pathogen mimicry. *Nat Rev Microbiol* 7:787–797. <https://doi.org/10.1038/nrmicro2222>.
- Guyen-Maiorov E, Tsai C-J, Nussinov R. 2016. Pathogen mimicry of host protein-protein interfaces modulates immunity. *Semin Cell Dev Biol* 58:136–145. <https://doi.org/10.1016/j.semcdb.2016.06.004>.
- Via A, Uyar B, Brun C, Zanzoni A. 2015. How pathogens use linear motifs to perturb host cell networks. *Trends Biochem Sci* 40:36–48. <https://doi.org/10.1016/j.tibs.2014.11.001>.
- Stebbins CE, Galan JE. 2001. Structural mimicry in bacterial virulence. *Nature* 412:701–705. <https://doi.org/10.1038/35089000>.
- Fu Y, Galan JE. 1999. A *Salmonella* protein antagonizes Rac-1 and Cdc42 to mediate host-cell recovery after bacterial invasion. *Nature* 401: 293–297. <https://doi.org/10.1038/45829>.
- Stebbins CE, Galan JE. 2000. Modulation of host signaling by a bacterial mimic: structure of the *Salmonella* effector SptP bound to Rac1. *Mol Cell* 6:1449–1460. [https://doi.org/10.1016/s1097-2765\(00\)00141-6](https://doi.org/10.1016/s1097-2765(00)00141-6).

11. Lurie-Weinberger MN, Gomez-Valero L, Meraut N, Glöckner G, Buchrieser C, Gophna U. 2010. The origins of eukaryotic-like proteins in *Legionella pneumophila*. *Int J Med Microbiol* 300:470–481. <https://doi.org/10.1016/j.ijmm.2010.04.016>.
12. Gomez-Valero L, Rusniok C, Carson D, Mondino S, Pérez-Cobas AE, Rolando M, Pasricha S, Reuter S, Demirtas J, Crumbach J, Descorps-Declere S, Hartland EL, Jarraud S, Dougan G, Schroeder GN, Frankel G, Buchrieser C. 2019. More than 18,000 effectors in the *Legionella* genus genome provide multiple, independent combinations for replication in human cells. *Proc Natl Acad Sci U S A* 116:2265–2273. <https://doi.org/10.1073/pnas.1808016116>.
13. Frank AC. 2019. Molecular host mimicry and manipulation in bacterial symbionts. *FEMS Microbiol Lett* 366:fnz038. <https://doi.org/10.1093/femsle/fnz038>.
14. Jehl M-A, Arnold R, Rattei T. 2011. Effective—a database of predicted secreted bacterial proteins. *Nucleic Acids Res* 39:D591–D595. <https://doi.org/10.1093/nar/gkq1154>.
15. Cazalet C, Rusniok C, Brüggemann H, Zidane N, Magnier A, Ma L, Tichit M, Jarraud S, Bouchier C, Vandenesch F, Kunst F, Etienne J, Glaser P, Buchrieser C. 2004. Evidence in the *Legionella pneumophila* genome for exploitation of host cell functions and high genome plasticity. *Nat Genet* 36:1165–1173. <https://doi.org/10.1038/ng1447>.
16. Gomez-Valero L, Rusniok C, Cazalet C, Buchrieser C. 2011. Comparative and functional genomics of *Legionella* identified eukaryotic like proteins as key players in host-pathogen interactions. *Front Microbiol* 2:208. <https://doi.org/10.3389/fmicb.2011.00208>.
17. Voth DE, Beare PA, Howe D, Sharma UM, Samoilis G, Cockrell DC, Omsland A, Heinzen RA. 2011. The *Coxiella burnetii* cryptic plasmid is enriched in genes encoding type IV secretion system substrates. *J Bacteriol* 193:1493–1503. <https://doi.org/10.1128/JB.01359-10>.
18. Av-Gay Y, Everett M. 2000. The eukaryotic-like Ser/Thr protein kinases of *Mycobacterium tuberculosis*. *Trends Microbiol* 8:238–244. [https://doi.org/10.1016/s0966-842x\(00\)01734-0](https://doi.org/10.1016/s0966-842x(00)01734-0).
19. Pennini ME, Perrinet S, Dautry-Varsat A, Subtil A. 2010. Histone methylation by NUE, a novel nuclear effector of the intracellular pathogen *Chlamydia trachomatis*. *PLoS Pathog* 6:e1000995. <https://doi.org/10.1371/journal.ppat.1000995>.
20. Mujtaba S, Winer BY, Jaganathan A, Patel J, Sgobba M, Schuch R, Gupta YK, Haider S, Wang R, Fischetti VA. 2013. Anthrax SET protein: a potential virulence determinant that epigenetically represses NF- κ B activation in infected macrophages. *J Biol Chem* 288:23458–23472. <https://doi.org/10.1074/jbc.M113.467696>.
21. Burstein D, Amaro F, Zusman T, Lifshitz Z, Cohen O, Gilbert JA, Pupko T, Shuman HA, Segal G. 2016. Genomic analysis of 38 *Legionella* species identifies large and diverse effector repertoires. *Nat Genet* 48:167–175. <https://doi.org/10.1038/ng.3481>.
22. Newton HJ, Ang DKY, van Driel IR, Hartland EL. 2010. Molecular pathogenesis of infections caused by *Legionella pneumophila*. *Clin Microbiol Rev* 23:274–298. <https://doi.org/10.1128/CMR.00052-09>.
23. Mondino S, Schmidt S, Rolando M, Escoll P, Gomez-Valero L, Buchrieser C. 2020. Legionnaires' disease: state of the art knowledge of pathogenesis mechanisms of *Legionella*. *Annu Rev Pathol* 15:439–466. <https://doi.org/10.1146/annurev-pathmechdis-012419-032742>.
24. Taylor M, Ross K, Bentham R. 2009. *Legionella*, protozoa, and biofilms: interactions within complex microbial systems. *Microb Ecol* 58:538–547. <https://doi.org/10.1007/s00248-009-9514-z>.
25. McDade JE, Shepard CC, Fraser DW, Tsai TR, Redus MA, Dowdle WR. 1977. Legionnaires' disease: isolation of a bacterium and demonstration of its role in other respiratory disease. *N Engl J Med* 297:1197–1203. <https://doi.org/10.1056/NEJM197712012972202>.
26. Isberg RR, O'Connor TJ, Heidtman M. 2009. The *Legionella pneumophila* replication vacuole: making a cosy niche inside host cells. *Nat Rev Microbiol* 7:13–24. <https://doi.org/10.1038/nrmicro1967>.
27. Ensminger AW. 2016. *Legionella pneumophila*, armed to the hilt: justifying the largest arsenal of effectors in the bacterial world. *Curr Opin Microbiol* 29:74–80. <https://doi.org/10.1016/j.mib.2015.11.002>.
28. Cherfilis J, Zeghouf M. 2013. Regulation of small GTPases by GEFs, GAPs, and GDIs. *Physiol Rev* 93:269–309. <https://doi.org/10.1152/physrev.00003.2012>.
29. Jackson CL, Bouvet S. 2014. Arfs at a glance. *J Cell Sci* 127:4103–4109. <https://doi.org/10.1242/jcs.144899>.
30. Bischoff FR, Ponstingl H. 1991. Catalysis of guanine nucleotide exchange on Ran by the mitotic regulator RCC1. *Nature* 354:80–82. <https://doi.org/10.1038/354080a0>.
31. Nagai H, Kagan JC, Zhu X, Kahn RA, Roy CR. 2002. A bacterial guanine nucleotide exchange factor activates ARF on *Legionella* phagosomes. *Science* 295:679–682. <https://doi.org/10.1126/science.1067025>.
32. Amor JC, Swails J, Zhu X, Roy CR, Nagai H, Ingmundson A, Cheng X, Kahn RA. 2005. The structure of RalF, an ADP-ribosylation factor guanine nucleotide exchange factor from *Legionella pneumophila*, reveals the presence of a cap over the active site. *J Biol Chem* 280:1392–1400. <https://doi.org/10.1074/jbc.M410820200>.
33. Neunuebel MR, Machner MP. 2012. The taming of a Rab GTPase by *Legionella pneumophila*. *Small GTPases* 3:28–33. <https://doi.org/10.4161/sgtp.18704>.
34. So EC, Mattheis C, Tate EW, Frankel G, Schroeder GN. 2015. Creating a customized intracellular niche: subversion of host cell signaling by *Legionella* type IV secretion system effectors. *Can J Microbiol* 61:617–635. <https://doi.org/10.1139/cjm-2015-0166>.
35. Hadjebi O, Casas-Terradellas E, Garcia-Gonzalo FR, Rosa JL. 2008. The RCC1 superfamily: from genes, to function, to disease. *Biochim Biophys Acta* 1783:1467–1479. <https://doi.org/10.1016/j.bbamcr.2008.03.015>.
36. Rothmeier E, Pfaffinger G, Hoffmann C, Harrison CF, Grabmayr H, Repnik U, Hannemann M, Wölke S, Bausch A, Griffiths G, Müller-Taubenberger A, Itzen A, Hilbi H. 2013. Activation of Ran GTPase by a *Legionella* effector promotes microtubule polymerization, pathogen vacuole motility and infection. *PLoS Pathog* 9:e1003598. <https://doi.org/10.1371/journal.ppat.1003598>.
37. Simon S, Wagner MA, Rothmeier E, Müller-Taubenberger A, Hilbi H. 2014. Icm/Dot-dependent inhibition of phagocyte migration by *Legionella* is antagonized by a translocated Ran GTPase activator. *Cell Microbiol* 16:977–992. <https://doi.org/10.1111/cmi.12258>.
38. Escoll P, Song O-R, Viana F, Steiner B, Lagache T, Olivo-Marín J-C, Impens F, Brodin P, Hilbi H, Buchrieser C. 2017. *Legionella pneumophila* modulates mitochondrial dynamics to trigger metabolic repurposing of infected macrophages. *Cell Host Microbe* 22:302–316.e7. <https://doi.org/10.1016/j.chom.2017.07.020>.
39. Escoll P, Buchrieser C. 2018. Metabolic reprogramming of host cells upon bacterial infection: why shift to a Warburg-like metabolism? *FEBS J* 285:2146–2160. <https://doi.org/10.1111/febs.14446>.
40. Swart AL, Steiner B, Gomez-Valero L, Schütz S, Hannemann M, Janning P, Irminger M, Rothmeier E, Buchrieser C, Itzen A, Panse VG, Hilbi H. 2020. Divergent evolution of *Legionella* RCC1 repeat effectors defines the range of Ran GTPase cycle targets. *mBio* 11:e00405-20. <https://doi.org/10.1128/mBio.00405-20>.
41. Burkhard P, Stetefeld J, Strelkov SV. 2001. Coiled coils: a highly versatile protein folding motif. *Trends Cell Biol* 11:82–88. [https://doi.org/10.1016/s0962-8924\(00\)01898-5](https://doi.org/10.1016/s0962-8924(00)01898-5).
42. Han J, Pluhackova K, Böckmann RA. 2017. The multifaceted role of SNARE proteins in membrane fusion. *Front Physiol* 8:5. <https://doi.org/10.3389/fphys.2017.00005>.
43. King NP, Newton P, Schuelein R, Brown DL, Petru M, Zarsky V, Dolezal P, Luo L, Bugarcic A, Stanley AC, Murray RZ, Collins BM, Teasdale RD, Hartland EL, Stow JL. 2015. Soluble NSF attachment protein receptor molecular mimicry by a *Legionella pneumophila* Dot/Icm effector. *Cell Microbiol* 17:767–784. <https://doi.org/10.1111/cmi.12405>.
44. Ivanov SS, Charron G, Hang HC, Roy CR. 2010. Lipidation by the host prenyltransferase machinery facilitates membrane localization of *Legionella pneumophila* effector proteins. *J Biol Chem* 285:34686–34698. <https://doi.org/10.1074/jbc.M110.170746>.
45. Ivanov SS, Roy C. 2013. Host lipidation: a mechanism for spatial regulation of *Legionella* effectors. *Curr Top Microbiol Immunol* 376:135–154. https://doi.org/10.1007/82_2013_344.
46. Price CTD, Al-Quadani T, Santic M, Jones SC, Abu Kwaik Y. 2010. Exploitation of conserved eukaryotic host cell farnesylation machinery by an F-box effector of *Legionella pneumophila*. *J Exp Med* 207:1713–1726. <https://doi.org/10.1084/jem.20100771>.
47. Sámano-Sánchez H, Gibson TJ. 2020. Mimicry of short linear motifs by bacterial pathogens: a drugging opportunity. *Trends Biochem Sci* 45:526–544. <https://doi.org/10.1016/j.tibs.2020.03.003>.
48. Bennett TL, Kraft SM, Reaves BJ, Mima J, O'Brien KM, Starai VJ. 2013. LegC3, an effector protein from *Legionella pneumophila*, inhibits homotypic yeast vacuole fusion in vivo and in vitro. *PLoS One* 8:e56798. <https://doi.org/10.1371/journal.pone.0056798>.
49. O'Brien KM, Lindsay EL, Starai VJ. 2015. The *Legionella pneumophila* effector protein, LegC7, alters yeast endosomal trafficking. *PLoS One* 10:e0116824. <https://doi.org/10.1371/journal.pone.0116824>.
50. Campodonico EM, Roy CR, Ninio S. 2016. *Legionella pneumophila* type

- IV effectors Ylfa and Ylfb are SNARE-like proteins that form homo- and heteromeric complexes and enhance the efficiency of vacuole remodeling. *PLoS One* 11:e0159698. <https://doi.org/10.1371/journal.pone.0159698>.
51. Shi X, Halder P, Yavuz H, Jahn R, Shuman HA. 2016. Direct targeting of membrane fusion by SNARE mimicry: convergent evolution of *Legionella* effectors. *Proc Natl Acad Sci U S A* 113:8807–8812. <https://doi.org/10.1073/pnas.1608755113>.
 52. Escoll P, Mondino S, Rolando M, Buchrieser C. 2016. Targeting of host organelles by pathogenic bacteria: a sophisticated subversion strategy. *Nat Rev Microbiol* 14:5–19. <https://doi.org/10.1038/nrmicro.2015.1>.
 53. Biernie H, Cossart P. 2012. When bacteria target the nucleus: the emerging family of nucleomodulins. *Cell Microbiol* 14:622–633. <https://doi.org/10.1111/j.1462-5822.2012.01758.x>.
 54. Alvarez-Venegas R. 2014. Bacterial SET domain proteins and their role in eukaryotic chromatin modification. *Front Genet* 5:65. <https://doi.org/10.3389/fgene.2014.00065>.
 55. Dillon SC, Zhang X, Trievel RC, Cheng X. 2005. The SET-domain protein superfamily: protein lysine methyltransferases. *Genome Biol* 6:227–210. <https://doi.org/10.1186/gb-2005-6-8-227>.
 56. Rolando M, Sanulli S, Rusniok C, Gomez-Valero L, Bertholet C, Sahr T, Margueron R, Buchrieser C. 2013. *Legionella pneumophila* effector RomA uniquely modifies host chromatin to repress gene expression and promote intracellular bacterial replication. *Cell Host Microbe* 13:395–405. <https://doi.org/10.1016/j.chom.2013.03.004>.
 57. Schuhmacher MK, Rolando M, Bröhm A, Weirich S, Kudithipudi S, Buchrieser C, Jeltsch A. 2018. The *Legionella pneumophila* methyltransferase RomA methylates also non-histone proteins during infection. *J Mol Biol* 430:1912–1925. <https://doi.org/10.1016/j.jmb.2018.04.032>.
 58. Li T, Lu Q, Wang G, Xu H, Huang H, Cai T, Kan B, Ge J, Shao F. 2013. SET-domain bacterial effectors target heterochromatin protein 1 to activate host rDNA transcription. *EMBO Rep* 14:733–740. <https://doi.org/10.1038/embor.2013.86>.
 59. Rolando M, Buchrieser C. 2014. *Legionella pneumophila* type IV effectors hijack the transcription and translation machinery of the host cell. *Trends Cell Biol* 24:771–778. <https://doi.org/10.1016/j.tcb.2014.06.002>.
 60. Son J, Jo CH, Murugan RN, Bang JK, Hwang KY, Lee WC. 2015. Crystal structure of *Legionella pneumophila* type IV secretion system effector LegAS4. *Biochem Biophys Res Commun* 465:817–824. <https://doi.org/10.1016/j.bbrc.2015.08.094>.
 61. Dwingelo Von J, Chung IYW, Price CT, Li L, Jones S, Cygler M, Abu Kwaik Y. 2019. Interaction of the ankyrin H core effector of *Legionella* with the host LARP7 component of the 75K snRNP complex. *mBio* 10:e01942-19. <https://doi.org/10.1128/mBio.01942-19>.
 62. Varshavsky A. 2012. The ubiquitin system, an immense realm. *Annu Rev Biochem* 81:167–176. <https://doi.org/10.1146/annurev-biochem-051910-094049>.
 63. Zheng N, Shabek N. 2017. Ubiquitin ligases: structure, function, and regulation. *Annu Rev Biochem* 86:129–157. <https://doi.org/10.1146/annurev-biochem-060815-014922>.
 64. Hatakeyama S, Nakayama K-II. 2003. U-box proteins as a new family of ubiquitin ligases. *Biochem Biophys Res Commun* 302:635–645. [https://doi.org/10.1016/S0006-291X\(03\)00245-6](https://doi.org/10.1016/S0006-291X(03)00245-6).
 65. Pisano A, Albano F, Vecchio E, Renna M, Scala G, Quinto I, Fiume G. 2018. Revisiting bacterial ubiquitin ligase effectors: weapons for host exploitation. *Int J Mol Sci* 19:3576. <https://doi.org/10.3390/ijms19113576>.
 66. Kubori T, Hyakutake A, Nagai H. 2008. *Legionella* translocates an E3 ubiquitin ligase that has multiple U-boxes with distinct functions. *Mol Microbiol* 67:1307–1319. <https://doi.org/10.1111/j.1365-2958.2008.06124.x>.
 67. Kubori T, Shinzawa N, Kanuka H, Nagai H. 2010. *Legionella* metaeffector exploits host proteasome to temporally regulate cognate effector. *PLoS Pathog* 6:e1001216. <https://doi.org/10.1371/journal.ppat.1001216>.
 68. Urbanus ML, Quaille AT, Stogios PJ, Morar M, Rao C, Di Leo R, Evdokimova E, Lam M, Oatway C, Cuff ME, Osipiuk J, Michalska K, Nocek BP, Taipale M, Savchenko A, Ensminger AW. 2016. Diverse mechanisms of metaeffector activity in an intracellular bacterial pathogen, *Legionella pneumophila*. *Mol Syst Biol* 12:893. <https://doi.org/10.15252/msb.20167381>.
 69. Quaille AT, Urbanus ML, Stogios PJ, Nocek B, Skarina T, Ensminger AW, Savchenko A. 2015. Molecular characterization of LubX: functional divergence of the U-box fold by *Legionella pneumophila*. *Structure* 23:1459–1469. <https://doi.org/10.1016/j.str.2015.05.020>.
 70. Lin Y-H, Lucas M, Evans TR, Abascal-Palacios G, Doms AG, Beauchene NA, Rojas AL, Hierro A, Machner MP. 2018. RavN is a member of a previously unrecognized group of *Legionella pneumophila* E3 ubiquitin ligases. *PLoS Pathog* 14:e1006897. <https://doi.org/10.1371/journal.ppat.1006897>.
 71. Al-Khodor S, Price CT, Habyarimana F, Kalia A, Abu Kwaik Y. 2008. A Dot/Icm-translocated ankyrin protein of *Legionella pneumophila* is required for intracellular proliferation within human macrophages and protozoa. *Mol Microbiol* 70:908–923. <https://doi.org/10.1111/j.1365-2958.2008.06453.x>.
 72. Price CT, Al-Khodor S, Al-Quadani T, Santic M, Habyarimana F, Kalia A, Kwaik YA. 2009. Molecular mimicry by an F-box effector of *Legionella pneumophila* hijacks a conserved polyubiquitination machinery within macrophages and protozoa. *PLoS Pathog* 5:e1000704. <https://doi.org/10.1371/journal.ppat.1000704>.
 73. Lomma M, Dervins-Ravault D, Rolando M, Nora T, Newton HJ, Sansom FM, Sahr T, Gomez-Valero L, Jules M, Hartland EL, Buchrieser C. 2010. The *Legionella pneumophila* F-box protein Lpp2082 (AnkB) modulates ubiquitination of the host protein parvin B and promotes intracellular replication. *Cell Microbiol* 12:1272–1291. <https://doi.org/10.1111/j.1462-5822.2010.01467.x>.
 74. Perpich JD, Kalia A, Price CTD, Jones SC, Wong K, Gehring K, Kwaik YA. 2017. Divergent evolution of di-lysine ER retention vs. farnesylation motif-mediated anchoring of the AnkB virulence effector to the *Legionella*-containing vacuolar membrane. *Sci Rep* 7:5123–5113. <https://doi.org/10.1038/s41598-017-05211-5>.
 75. Price CTD, Al-Quadani T, Santic M, Rosenshine I, Abu Kwaik Y. 2011. Host proteasomal degradation generates amino acids essential for intracellular bacterial growth. *Science* 334:1553–1557. <https://doi.org/10.1126/science.1212868>.
 76. Bhogaraju S, Kalayil S, Liu Y, Bonn F, Colby T, Matic I, Dikic I. 2016. Phosphoribosylation of ubiquitin promotes serine ubiquitination and impairs conventional ubiquitination. *Cell* 167:1636–1649.e13. <https://doi.org/10.1016/j.cell.2016.11.019>.
 77. Qiu J, Sheedlo MJ, Yu K, Tan Y, Nakayasu ES, Das C, Liu X, Luo Z-Q. 2016. Ubiquitination independent of E1 and E2 enzymes by bacterial effectors. *Nature* 533:120–124. <https://doi.org/10.1038/nature17657>.
 78. Sheedlo MJ, Qiu J, Tan Y, Paul LN, Luo Z-Q, Das C. 2015. Structural basis of substrate recognition by a bacterial deubiquitinase important for dynamics of phagosome ubiquitination. *Proc Natl Acad Sci U S A* 112:15090–15095. <https://doi.org/10.1073/pnas.1514568112>.
 79. Shin D, Mukherjee R, Liu Y, Gonzalez A, Bonn F, Liu Y, Rogov VV, Heinz M, Stolz A, Hummer G, Dötsch V, Luo Z-Q, Bhogaraju S, Dikic I. 2020. Regulation of phosphoribosyl-linked serine ubiquitination by deubiquitinases DupA and DupB. *Mol Cell* 77:164–179.e6. <https://doi.org/10.1016/j.molcel.2019.10.019>.
 80. Qiu J, Luo Z-Q. 2017. Hijacking of the host ubiquitin network by *Legionella pneumophila*. *Front Cell Infect Microbiol* 7:487. <https://doi.org/10.3389/fcimb.2017.00487>.
 81. Puvar K, Luo Z-Q, Das C. 2019. Uncovering the structural basis of a new twist in protein ubiquitination. *Trends Biochem Sci* 44:467–477. <https://doi.org/10.1016/j.tibs.2018.11.006>.
 82. Kubori T, Kitao T, Ando H, Nagai H. 2018. LotA, a *Legionella* deubiquitinase, has dual catalytic activity and contributes to intracellular growth. *Cell Microbiol* 20:e12840. <https://doi.org/10.1111/cmi.12840>.
 83. Ma K, Zhen X, Zhou B, Gan N, Cao Y, Fan C, Ouyang S, Luo Z-Q, Qiu J. 2020. The bacterial deubiquitinase Ceg23 regulates the association of Lys-63-linked polyubiquitin molecules on the *Legionella* phagosome. *J Biol Chem* 295:1646–1657. <https://doi.org/10.1074/jbc.RA119.011758>.
 84. Wan M, Wang X, Huang C, Xu D, Wang Z, Zhou Y, Zhu Y. 2019. A bacterial effector deubiquitinase specifically hydrolyses linear ubiquitin chains to inhibit host inflammatory signalling. *Nat Microbiol* 4:1282–1293. <https://doi.org/10.1038/s41564-019-0454-1>.
 85. Cazalet C, Gomez-Valero L, Rusniok C, Lomma M, Dervins-Ravault D, Newton HJ, Sansom FM, Jarraud S, Zidane N, Ma L, Bouchier C, Etienne J, Hartland EL, Buchrieser C. 2010. Analysis of the *Legionella longbeachae* genome and transcriptome uncovers unique strategies to cause Legionnaires' disease. *PLoS Genet* 6:e1000851. <https://doi.org/10.1371/journal.pgen.1000851>.
 86. de Felipe KS, Pampou S, Jovanovic OS, Pericone CD, Ye SF, Kalachikov S, Shuman HA. 2005. Evidence for acquisition of *Legionella* type IV secretion substrates via interdomain horizontal gene transfer. *J Bacteriol* 187:7716–7726. <https://doi.org/10.1128/JB.187.22.7716-7726.2005>.
 87. Hervet E, Charpentier X, Vianney A, Lazzaroni J-C, Gilbert C, Atlan D, Doublet P. 2011. Protein kinase LegK2 is a type IV secretion system effector involved in endoplasmic reticulum recruitment and intracellu-

- lar replication of *Legionella pneumophila*. *Infect Immun* 79:1936–1950. <https://doi.org/10.1128/IAI.00805-10>.
88. Ge J, Xu H, Li T, Zhou Y, Zhang Z, Li S, Liu L, Shao F. 2009. A *Legionella* type IV effector activates the NF- κ B pathway by phosphorylating the I κ B family of inhibitors. *Proc Natl Acad Sci U S A* 106:13725–13730. <https://doi.org/10.1073/pnas.0907200106>.
 89. Flayhan A, Bergé C, Bailo N, Doublet P, Bayliss R, Terradot L. 2015. The structure of *Legionella pneumophila* LegK4 type four secretion system (T4SS) effector reveals a novel dimeric eukaryotic-like kinase. *Sci Rep* 5:14602–14614. <https://doi.org/10.1038/srep14602>.
 90. Moss SM, Taylor IR, Ruggero D, Gestwicki JE, Shokat KM, Mukherjee S. 2019. A *Legionella pneumophila* kinase phosphorylates the Hsp70 chaperone family to inhibit eukaryotic protein synthesis. *Cell Host Microbe* 25:454–462.e6. <https://doi.org/10.1016/j.chom.2019.01.006>.
 91. Michard C, Sperandio D, Bailo N, Pizarro-Cerdá J, LeClaire L, Chadeau-Argaud E, Pombo-Grégoire I, Hervet E, Vianney A, Gilbert C, Faure M, Cossart P, Doublet P. 2015. The *Legionella* kinase LegK2 targets the ARP2/3 complex to inhibit actin nucleation on phagosomes and allow bacterial evasion of the late endocytic pathway. *mBio* 6:e00354-15. <https://doi.org/10.1128/mBio.00354-15>.
 92. Lee P-C, Machner MP. 2018. The *Legionella* effector kinase LegK7 hijacks the host Hippo pathway to promote infection. *Cell Host Microbe* 24:429–438.e6. <https://doi.org/10.1016/j.chom.2018.08.004>.
 93. Lee P-C, Beyrakhova K, Xu C, Boniecki MT, Lee MH, Onu CJ, Grishin AM, Machner MP, Cygler M. 2020. The *Legionella* kinase LegK7 exploits the Hippo pathway scaffold protein MOB1A for allostery and substrate phosphorylation. *Proc Natl Acad Sci U S A* 117:14433–14443. <https://doi.org/10.1073/pnas.2000497117>.
 94. Black MH, Osinski A, Gradowski M, Servage KA, Pawłowski K, Tomchick DR, Tagliabraci VS. 2019. Bacterial pseudokinase catalyzes protein polyglutamylation to inhibit the SidE-family ubiquitin ligases. *Science* 364:787–792. <https://doi.org/10.1126/science.aaw7446>.
 95. Sulpizio A, Minelli ME, Wan M, Burrows PD, Wu X, Sanford EJ, Shin J-H, Williams BC, Goldberg ML, Smolka MB, Mao Y. 2019. Protein polyglutamylation catalyzed by the bacterial calmodulin-dependent pseudokinase SidJ. *Elife* 8:601. <https://doi.org/10.7554/eLife.51162>.
 96. Gan N, Zhen X, Liu Y, Xu X, He C, Qiu J, Liu Y, Fujimoto GM, Nakayasu ES, Zhou B, Zhao L, Puvar K, Das C, Ouyang S, Luo Z-Q. 2019. Regulation of phosphoribosyl ubiquitination by a calmodulin-dependent glutamylase. *Nature* 572:387–391. <https://doi.org/10.1038/s41586-019-1439-1>.
 97. Bhogaraju S, Bonn F, Mukherjee R, Adams M, Pfeleiderer MM, Galej WP, Matkovic V, Lopez-Mosqueda J, Kalayil S, Shin D, Dikic I. 2019. Inhibition of bacterial ubiquitin ligases by SidJ-calmodulin catalysed glutamylation. *Nature* 572:382–386. <https://doi.org/10.1038/s41586-019-1440-8>.
 98. Sreelatha A, Nolan C, Park BC, Pawłowski K, Tomchick DR, Tagliabraci VS. 2020. A *Legionella* effector kinase is activated by host inositol hexakisphosphate. *J Biol Chem* 295:6214–6224. <https://doi.org/10.1074/jbc.RA120.013067>.
 99. Levanova N, Mattheis C, Carson D, To K-N, Jank T, Frankel G, Aktories K, Schroeder GN. 2019. The *Legionella* effector LtpM is a new type of phosphoinositide-activated glucosyltransferase. *J Biol Chem* 294:2862–2879. <https://doi.org/10.1074/jbc.RA118.005952>.
 100. Swart AL, Hilbi H. 2020. Phosphoinositides and the fate of *Legionella* in phagocytes. *Front Immunol* 11:25. <https://doi.org/10.3389/fimmu.2020.00025>.
 101. Quaille AT, Stogios PJ, Egorova O, Evdokimova E, Valteau D, Nocek B, Kompella PS, Peisajovich S, Yakunin AF, Ensminger AW, Savchenko A. 2018. The *Legionella pneumophila* effector Ceg4 is a phosphotyrosine phosphatase that attenuates activation of eukaryotic MAPK pathways. *J Biol Chem* 293:3307–3320. <https://doi.org/10.1074/jbc.M117.812727>.
 102. Beyrakhova K, Li L, Xu C, Gagarinova A, Cygler M. 2018. *Legionella pneumophila* effector Lem4 is a membrane-associated protein tyrosine phosphatase. *J Biol Chem* 293:13044–13058. <https://doi.org/10.1074/jbc.RA118.003845>.
 103. Wagner MJ, Stacey MM, Liu BA, Pawson T. 2013. Molecular mechanisms of SH2- and PTB-domain-containing proteins in receptor tyrosine kinase signaling. *Cold Spring Harb Perspect Biol* 5:a008987. <https://doi.org/10.1101/cshperspect.a008987>.
 104. Kaneko T, Stogios PJ, Ruan X, Voss C, Evdokimova E, Skarina T, Chung A, Liu X, Li L, Savchenko A, Ensminger AW, Li SS-C. 2018. Identification and characterization of a large family of superbinding bacterial SH2 domains. *Nat Commun* 9:4549. <https://doi.org/10.1038/s41467-018-06943-2>.
 105. Rolando M, Escoll P, Nora T, Botti J, Boitez V, Bedia C, Daniels C, Abraham G, Stogios PJ, Skarina T, Christophe C, Dervins-Ravault D, Cazalet C, Hilbi H, Rupasinghe TWT, Tull D, McConville MJ, Ong SY, Hartland EL, Codogno P, Levade T, Naderer T, Savchenko A, Buchrieser C. 2016. *Legionella pneumophila* S1P-lyase targets host sphingolipid metabolism and restrains autophagy. *Proc Natl Acad Sci U S A* 113:1901–1906. <https://doi.org/10.1073/pnas.1522067113>.
 106. Degtyar E, Zusman T, Ehrlich M, Segal G. 2009. A *Legionella* effector acquired from protozoa is involved in sphingolipids metabolism and is targeted to the host cell mitochondria. *Cell Microbiol* 11:1219–1235. <https://doi.org/10.1111/j.1462-5822.2009.01328.x>.
 107. Viner R, Chetrit D, Ehrlich M, Segal G. 2012. Identification of two *Legionella pneumophila* effectors that manipulate host phospholipids biosynthesis. *PLoS Pathog* 8:e1002988. <https://doi.org/10.1371/journal.ppat.1002988>.
 108. Schroeder GN, Aurass P, Oates CV, Tate EW, Hartland EL, Flieger A, Frankel G. 2015. *Legionella pneumophila* effector LpdA is a palmitoylated phospholipase D virulence factor. *Infect Immun* 83:3989–4002. <https://doi.org/10.1128/IAI.00785-15>.
 109. Dolezal P, Aili M, Tong J, Jiang J-H, Marobbio CMT, Marobbio CM, Lee SF, Schuelein R, Belluzzo S, Binova E, Mousnier A, Frankel G, Giannuzzi G, Palmieri F, Gabriel K, Naderer T, Hartland EL, Lithgow T. 2012. *Legionella pneumophila* secretes a mitochondrial carrier protein during infection. *PLoS Pathog* 8:e1002459. <https://doi.org/10.1371/journal.ppat.1002459>.
 110. Sansom FM, Riedmaier P, Newton HJ, Dunstone MA, Müller CE, Stephan H, Byres E, Beddoe T, Rossjohn J, Cowan PJ, d'Apice AJF, Robson SC, Hartland EL. 2008. Enzymatic properties of an ecto-nucleoside triphosphate diphosphohydrolase from *Legionella pneumophila*: substrate specificity and requirement for virulence. *J Biol Chem* 283:12909–12918. <https://doi.org/10.1074/jbc.M801006200>.
 111. Zimmermann H, Zebisch M, Sträter N. 2012. Cellular function and molecular structure of ecto-nucleotidases. *Purinergic Signal* 8:437–502. <https://doi.org/10.1007/s11302-012-9309-4>.
 112. Sansom FM, Newton HJ, Crikis S, Cianciotto NP, Cowan PJ, d'Apice AJF, Hartland EL. 2007. A bacterial ecto-triphosphate diphosphohydrolase similar to human CD39 is essential for intracellular multiplication of *Legionella pneumophila*. *Cell Microbiol* 9:1922–1935. <https://doi.org/10.1111/j.1462-5822.2007.00924.x>.
 113. Riedmaier P, Sansom FM, Sofian T, Beddoe T, Schuelein R, Newton HJ, Hartland EL. 2014. Multiple ecto-nucleoside triphosphate diphosphohydrolases facilitate intracellular replication of *Legionella pneumophila*. *Biochem J* 462:279–289. <https://doi.org/10.1042/BJ20130923>.
 114. Galka F, Wai SN, Kusch H, Engelmann S, Hecker M, Schmeck B, Hippenstiel S, Uhlin BE, Steinert M. 2008. Proteomic characterization of the whole secretome of *Legionella pneumophila* and functional analysis of outer membrane vesicles. *Infect Immun* 76:1825–1836. <https://doi.org/10.1128/IAI.01396-07>.
 115. Herrmann V, Eidner A, Rydzewski K, Blädel I, Jules M, Buchrieser C, Eisenreich W, Heuner K. 2011. GamA is a eukaryotic-like glucoamylase responsible for glycogen- and starch-degrading activity of *Legionella pneumophila*. *Int J Med Microbiol* 301:133–139. <https://doi.org/10.1016/j.ijmm.2010.08.016>.
 116. Best A, Price C, Ozanic M, Santic M, Jones S, Abu Kwaik Y. 2018. A *Legionella pneumophila* amylase is essential for intracellular replication in human macrophages and amoebae. *Sci Rep* 8:6340–6312. <https://doi.org/10.1038/s41598-018-24724-1>.
 117. Price C, Jones S, Mihelcic M, Santic M, Abu Kwaik Y. 2020. Paradoxical pro-inflammatory responses by human macrophages to an amoebae host-adapted *Legionella* effector. *Cell Host Microbe* 27:571–584.e7. <https://doi.org/10.1016/j.chom.2020.03.003>.
 118. Boamah DK, Zhou G, Ensminger AW, O'Connor TJ. 2017. From many hosts, one accidental pathogen: the diverse protozoan hosts of *Legionella*. *Front Cell Infect Microbiol* 7:477. <https://doi.org/10.3389/fcimb.2017.00477>.
 119. Moliner C, Fournier P-E, Raoult D. 2010. Genome analysis of microorganisms living in amoebae reveals a melting pot of evolution. *FEMS Microbiol Rev* 34:281–294. <https://doi.org/10.1111/j.1574-6976.2010.00209.x>.
 120. Park JM, Ghosh S, O'Connor TJ. 2020. Combinatorial selection in amoebal hosts drives the evolution of the human pathogen *Legionella pneumophila*. *Nat Microbiol* 5:599–609. <https://doi.org/10.1038/s41564-019-0663-7>.
 121. Gomez-Valero L, Rusniok C, Rolando M, Neou M, Dervins-Ravault D, Demirtas J, Rouy Z, Moore RJ, Chen H, Petty NK, Jarraud S, Etienne J, Steinert M, Heuner K, Gribaldo S, Médigue C, Glöckner G, Hartland EL,

- Buchrieser C. 2014. Comparative analyses of *Legionella* species identifies genetic features of strains causing Legionnaires' disease. *Genome Biol* 15:505. <https://doi.org/10.1186/PREACCEPT-1086350395137407>.
122. Gomez-Valero L, Buchrieser C. 2019. Intracellular parasitism, the driving force of evolution of *Legionella pneumophila* and the genus *Legionella*. *Microbes Infect* 21:230–236. <https://doi.org/10.1016/j.micinf.2019.06.012>.
 123. Gomez-Valero L, Buchrieser C. 2013. Genome dynamics in *Legionella*: the basis of versatility and adaptation to intracellular replication. *Cold Spring Harb Perspect Med* 3:a009993. <https://doi.org/10.1101/cshperspect.a009993>.
 124. Gimenez G, Bertelli C, Moliner C, Robert C, Raoult D, Fournier P-E, Greub G. 2011. Insight into cross-talk between intra-amoebal pathogens. *BMC Genomics* 12:542. <https://doi.org/10.1186/1471-2164-12-542>.
 125. Ogata H, La Scola B, Audic S, Renesto P, Blanc G, Robert C, Fournier P-E, Claverie J-M, Raoult D. 2006. Genome sequence of *Rickettsia bellii* illuminates the role of amoebae in gene exchanges between intracellular pathogens. *PLoS Genet* 2:e76. <https://doi.org/10.1371/journal.pgen.0020076>.
 126. Wang Z, Wu M. 2017. Comparative genomic analysis of *Acanthamoeba* endosymbionts highlights the role of amoebae as a “melting pot” shaping the *Rickettsiales* evolution. *Genome Biol Evol* 9:3214–3224. <https://doi.org/10.1093/gbe/evx246>.
 127. Schmitz-Esser S, Tischler P, Arnold R, Montanaro J, Wagner M, Rattei T, Horn M. 2010. The genome of the amoeba symbiont “*Candidatus Amoebophilus asiaticus*” reveals common mechanisms for host cell interaction among amoeba-associated bacteria. *J Bacteriol* 192: 1045–1057. <https://doi.org/10.1128/JB.01379-09>.
 128. Buchrieser C, Charpentier X. 2013. Induction of competence for natural transformation in *Legionella pneumophila* and exploitation for mutant construction. *Methods Mol Biol* 954:183–195. https://doi.org/10.1007/978-1-62703-161-5_9.
 129. Kim H, Kubori T, Yamazaki K, Kwak M-J, Park S-Y, Nagai H, Vogel JP, Oh B-H. 2020. Structural basis for effector protein recognition by the Dot/Icm type IVB coupling protein complex. *Nat Commun* 11: 2623–2611. <https://doi.org/10.1038/s41467-020-16397-0>.
 130. Rowbotham TJ. 1980. Preliminary report on the pathogenicity of *Legionella pneumophila* for freshwater and soil amoebae. *J Clin Pathol* 33:1179–1183. <https://doi.org/10.1136/jcp.33.12.1179>.
 131. Escoll P, Rolando M, Gomez-Valero L, Buchrieser C. 2013. From amoeba to macrophages: exploring the molecular mechanisms of *Legionella pneumophila* infection in both hosts. *Curr Top Microbiol Immunol* 376:1–34. https://doi.org/10.1007/82_2013_351.
 132. Falkow S. 2008. I never met a microbe I didn't like. *Nat Med* 14: 1053–1057. <https://doi.org/10.1038/nm1008-1053>.
 133. Balczun C, Scheid PL. 2017. Free-living amoebae as hosts for and vectors of intracellular microorganisms with public health significance. *Viruses* 9:65. <https://doi.org/10.3390/v9040065>.
 134. Barker J, Brown MR. 1994. Trojan horses of the microbial world: protozoa and the survival of bacterial pathogens in the environment. *Microbiology (Reading, Engl)* 140:1253–1259. <https://doi.org/10.1099/00221287-140-6-1253>.
 135. Molmeret M, Horn M, Wagner M, Santic M, Abu Kwaik Y. 2005. Amoebae as training grounds for intracellular bacterial pathogens. *Appl Environ Microbiol* 71:20–28. <https://doi.org/10.1128/AEM.71.1.20-28.2005>.
 136. Wiles TJ, Guillemin K. 2019. The other side of the coin: what beneficial microbes can teach us about pathogenic potential. *J Mol Biol* 431: 2946–2956. <https://doi.org/10.1016/j.jmb.2019.05.001>.
 137. Seshadri R, Reeve WG, Ardley JK, Tennessen K, Woyke T, Kyrpides NC, Ivanova NN. 2015. Discovery of novel plant interaction determinants from the genomes of 163 root nodule bacteria. *Sci Rep* 5:16825–16829. <https://doi.org/10.1038/srep16825>.
 138. Díez-Vives C, Moitinho-Silva L, Nielsen S, Reynolds D, Thomas T. 2017. Expression of eukaryotic-like protein in the microbiome of sponges. *Mol Ecol* 26:1432–1451. <https://doi.org/10.1111/mec.14003>.
 139. Nguyen MTHD, Liu M, Thomas T. 2014. Ankyrin-repeat proteins from sponge symbionts modulate amoebal phagocytosis. *Mol Ecol* 23: 1635–1645. <https://doi.org/10.1111/mec.12384>.
 140. Moreno-Pino M, Cristi A, Gillooly JF, Trefault N. 2020. Characterizing the microbiomes of Antarctic sponges: a functional metagenomic approach. *Sci Rep* 10:645–612. <https://doi.org/10.1038/s41598-020-57464-2>.

Annex B

Legionella longbeachae secretes a Rab GTPase protein to hijack NLRP3 during infection

Research article

In preparation

Sonia Mondino^{1,2}, Pedro Escoll^{*1,2}, Daniel Schator^{*1,2,3}, Silke Schmidt^{1,2,3}, Gustavo F S Quirino⁴, Monica Rolando^{1,2}, Laura Gomez-Valero^{1,2}, Lena Oesterlin^{5,6}, Bruno Goud^{5,6}, Dario Zamboni⁴ and Carmen Buchrieser^{1,2}

¹Institut Pasteur, Biologie des Bactéries Intracellulaires, Paris, France; ²CNRS UMR 3525, Paris, France; ³Sorbonne Université, Collège doctoral, Paris, France; ⁴Department of Cell Biology, Ribeirão Preto Medical School, University of São Paulo, Ribeirão Preto, São Paulo, Brazil; ⁵Institut Curie, Mécanismes moléculaires du transport intracellulaire, Paris, France ⁶CNRS UMR 144, Paris, France.

*These authors contributed equally to this study

For correspondence:

Carmen Buchrieser
Institut Pasteur
Biologie des Bactéries Intracellulaires
28 rue du Dr. Roux, 75724 Paris Cedex 15, France
Tel: +33 (0)1 45 68 83 72
E-mail: cbuch@pasteur.fr

Contributions:

For this study, led by Sonia Mondino, I was involved in isolation of human monocyte-derived macrophages, infections, ELISA measurements of human pro-inflammatory cytokines by SP-X array, as well as analysis and interpretation of the data.

Abstract

Legionella spp. are environmental bacteria and accidental human pathogens that can cause a severe pneumonia, termed Legionnaires' disease. These bacteria replicate intracellularly in free living amoebae and human alveolar macrophages within a distinct compartment known as the *Legionella*-containing vacuole (LCV). The LCV resembles an endoplasmic reticulum (ER) structure due to the recruitment of vesicles from the host secretory pathway, partly by targeting Rab GTPases. Despite *L. pneumophila* secretes several protein effectors that modulate Rab function during infection, most of them are not conserved in the *L. longbeachae* genome. Instead, this understudied species harbours a novel family of eukaryotic Rab GTPase-like effector proteins with unknown function. Here we show that one of these proteins, named RabL, is a T4SS-dependent effector with intrinsic GTPase activity. RabL localizes to the Golgi when ectopically expressed in mammalian cells, but it is not involved in Golgi disruption during *L. longbeachae* infection. Moreover, RabL was required for efficient replication in C57BL/6 murine lungs, highlighting an important virulence role for this effector. Determination of RabL *in vivo* interactome by tandem affinity purification allowed us to identify STARD3NL (STARD3 N-terminal-like protein) and NLRP3 (NACHT, LRR and PYD domains-containing protein 3) as RabL partners in macrophages. STARD3NL mediates ER-endosome contacts and consequently endosome dynamics in eukaryotic cells. However, no differences in ER-recruitment to LCV were observed in an *L. longbeachae* *rabL* mutant strain, suggesting that RabL-STARD3NL interaction modulates other trafficking pathways in infection. Conversely, we demonstrated that RabL is important for IL-1 β secretion in infected macrophages, suggesting a role of this protein in NLRP3-mediated inflammasome activation. Thus, RabL is a eukaryotic Rab-like virulence factor crucial for *L. longbeachae* infection *in vivo*.

Annex C

Reverting the mode of action of the mitochondrial F₀F₁-ATPase by *Legionella pneumophila* preserves its replication niche

Research article

Published in

eLife

Vol. 10:e71978. Published 09 December 2021.

DOI: <https://doi.org/10.7554/eLife.71978>

Pedro Escoll^{1*}, Lucien Platon^{1,2†‡}, Mariatou Dramé^{1,3†}, Tobias Sahr¹, Silke Schmidt^{1,4},
Christophe Rusniok¹, Carmen Buchrieser^{1*}

¹Institut Pasteur, Biologie des Bactéries Intracellulaires and CNRS UMR 3525, Paris, France; ²Faculté des Sciences, Université de Montpellier, Montpellier, France; ³Faculté des Sciences, Université de Paris, Paris, France; ⁴Sorbonne Université, Collège doctoral, Paris, France

†These authors contributed equally to this work, Present address: ‡Institut Pasteur, Génétique du Paludisme et Résistance, Paris, France

*For correspondence:

Pedro Escoll pescoll@pasteur.fr

Carmen Buchrieser cbuch@pasteur.fr

Contributions:

For this study, led by Pedro Escoll, I performed the isolation of monocytes from human peripheral blood and differentiation of human monocyte-derived macrophages. Further, I was involved in reading and editing the article.

Reverting the mode of action of the mitochondrial F_0F_1 -ATPase by *Legionella pneumophila* preserves its replication niche

Pedro Escoll^{1*}, Lucien Platon^{1,2†‡}, Mariatou Dramé^{1,3†}, Tobias Sahr¹, Silke Schmidt^{1,4}, Christophe Rusniok¹, Carmen Buchrieser^{1*}

¹Institut Pasteur, Biologie des Bactéries Intracellulaires and CNRS UMR 3525, Paris, France; ²Faculté des Sciences, Université de Montpellier, Montpellier, France; ³Faculté des Sciences, Université de Paris, Paris, France; ⁴Sorbonne Université, Collège doctoral, Paris, France

Abstract *Legionella pneumophila*, the causative agent of Legionnaires' disease, a severe pneumonia, injects via a type 4 secretion system (T4SS) more than 300 proteins into macrophages, its main host cell in humans. Certain of these proteins are implicated in reprogramming the metabolism of infected cells by reducing mitochondrial oxidative phosphorylation (OXPHOS) early after infection. Here, we show that despite reduced OXPHOS, the mitochondrial membrane potential ($\Delta\psi_m$) is maintained during infection of primary human monocyte-derived macrophages (hMDMs). We reveal that *L. pneumophila* reverses the ATP-synthase activity of the mitochondrial F_0F_1 -ATPase to ATP-hydrolase activity in a T4SS-dependent manner, which leads to a conservation of the $\Delta\psi_m$, preserves mitochondrial polarization, and prevents macrophage cell death. Analyses of T4SS effectors known to target mitochondrial functions revealed that LpSpl is partially involved in conserving the $\Delta\psi_m$, but not LncP and MitF. The inhibition of the *L. pneumophila*-induced 'reverse mode' of the F_0F_1 -ATPase collapsed the $\Delta\psi_m$ and caused cell death in infected cells. Single-cell analyses suggested that bacterial replication occurs preferentially in hMDMs that conserved the $\Delta\psi_m$ and showed delayed cell death. This direct manipulation of the mode of activity of the F_0F_1 -ATPase is a newly identified feature of *L. pneumophila* allowing to delay host cell death and thereby to preserve the bacterial replication niche during infection.

***For correspondence:**
 pescoll@pasteur.fr (PE);
 cbuch@pasteur.fr (CB)

†These authors contributed equally to this work

Present address: [†]Institut Pasteur, Génétique du Paludisme et Résistance, Paris, France

Competing interest: The authors declare that no competing interests exist.

Funding: See page 16

Received: 07 July 2021

Accepted: 06 December 2021

Published: 09 December 2021

Reviewing Editor: Melanie Blokesch, Ecole Polytechnique Fédérale de Lausanne, Switzerland

© Copyright Escoll et al. This article is distributed under the terms of the [Creative Commons Attribution License](https://creativecommons.org/licenses/by/4.0/), which permits unrestricted use and redistribution provided that the original author and source are credited.

Editor's evaluation

The pathogenic bacterium *Legionella pneumophila* (Lp) is known for its ability to translocate cocktails of effector proteins into its eukaryotic host. Yet, despite an overall reduction in mitochondrial oxidative phosphorylation following *Legionella* infection, host cell mitochondria maintain their normal membrane potential ($\Delta\psi_m$). In this study, the authors show that the translocated effector protein LpSpl forces the host cell's F_0F_1 -ATPase to function in 'reverse mode,' thereby maintaining $\Delta\psi_m$, which, ultimately, supports bacterial replication by delaying host death.

Introduction

Beyond their essential role in cellular bioenergetics, mitochondria are integrated into diverse signaling pathways in eukaryotic cells and perform various signaling functions, such as immune responses or cell death, as they play crucial roles in the regulation of apoptosis (**Bock and Tait, 2020**). Thus,

mitochondria are targeted by several intracellular bacteria during infection to modulate their functions to the bacterial advantage (Spier et al., 2019). One of these bacteria is *Legionella pneumophila*, the causative agent of Legionnaires' disease. We have shown previously that this pathogen targets mitochondrial dynamics during infection of primary human monocyte-derived macrophages (hMDMs) by injecting type 4 secretion system (T4SS) effectors such as MitF, leading to a fragmented mitochondrial network via the recruitment of the host fission protein DNM1L to the mitochondrial surface (Escoll et al., 2017b). Importantly, *Legionella* induced mitochondrial fragmentation at early time points such as 5 hr post-infection (hpi), when bacterial replication has not started yet, and in the absence of cell death signs. The fragmentation of mitochondrial networks provoked a T4SS-dependent reduction of mitochondrial respiration in *Legionella*-infected macrophages, evidencing a functional connection between mitochondrial dynamics and mitochondrial respiration (Escoll et al., 2017b).

Mitochondrial respiration results from coupling the activity of five complexes in the electron transport chain (ETC) at mitochondrial cristae. In this process, the reduced coenzymes NADH and FADH₂ generated at the mitochondrial matrix by the tricarboxylic acid (TCA) cycle are oxidized at complexes I and II where their electrons are extracted to energize the mitochondrial ETC (Nolfi-Donagan et al., 2020). The sequential transit of these electrons through complexes I, III, and IV allows to pump protons from the matrix to the intermembrane space (IMS) and at complex IV, diatomic oxygen O₂ serves as the terminal electron acceptor, and H₂O is formed. The increased concentration of protons [H⁺] at the IMS, compared to [H⁺] at the matrix, generates the mitochondrial membrane potential ($\Delta\psi_m$). This is necessary to produce ATP by fueling the rotation of complex V, the mitochondrial F₀F₁-ATPase, in a process termed oxidative phosphorylation (OXPHOS) (Nolfi-Donagan et al., 2020). Our previous studies determined that at 5 hpi *L. pneumophila*, by altering mitochondrial dynamics, reduced OXPHOS as well as the cellular ATP content in hMDMs in a T4SS-dependent manner (Escoll et al., 2017b).

Why *L. pneumophila* and other species of intracellular bacteria reduce mitochondrial OXPHOS during infection of host cells remains a matter of debate (Escoll and Buchrieser, 2018; Russell et al., 2019). As intracellular bacteria can obtain resources only from host cells, it has been suggested that halting mitochondrial OXPHOS during infection might benefit pathogenic bacteria by redirecting cellular resources, such as glycolytic or TCA intermediates, to biosynthetic pathways that might sustain intracellular bacterial replication instead of fueling mitochondria (Escoll and Buchrieser, 2018; Russell et al., 2019). For instance, it has been shown that *Mycobacterium tuberculosis* redirects pyruvate to fatty acid synthesis and *Chlamydia trachomatis* subverts the pentose phosphate pathway to increase the synthesis of nucleotides for its own intracellular growth (Siegl et al., 2014; Singh et al., 2012). On the other hand, upon sensing bacterial lipopolysaccharides, macrophages redirect mitochondrial TCA intermediates, such as citrate or succinate, to drive specific immune functions such as the production of cytokines or the generation of antimicrobial molecules (Escoll and Buchrieser, 2019; Russell et al., 2019; O'Neill and Pearce, 2016). Thus, while these metabolic shifts, which are redirecting resources from mitochondria to the cytoplasm, should be activated in macrophages to develop their antimicrobial functions, they could also benefit intracellular bacteria as more resources would be available in the cytoplasm for bacterial growth. Importantly, reduction of OXPHOS may lead to decreased $\Delta\psi_m$ and ATP production at mitochondria, which are events that trigger the activation of cell death programs. How intracellular bacteria withdraw OXPHOS, deal with the subsequent $\Delta\psi_m$ drop, and host cell death but manage to preserve their host cell to conserve their replication niche is a question that remains poorly understood.

To answer this question, we monitored the evolution of mitochondrial polarization during infection of hMDMs by *L. pneumophila* and showed that in the absence of OXPHOS *L. pneumophila* regulates the enzymatic activity of the mitochondrial F₀F₁-ATPase during infection. This allows maintaining the $\Delta\psi_m$ and delays cell death of infected hMDMs in a T4SS-dependent manner. Our results identified a new virulence mechanism of *L. pneumophila*, namely, the manipulation of the mitochondrial F₀F₁-ATPase to preserve the integrity of infected host cells and thereby the maintenance of the bacterial replication niches.

Results

Despite *L. pneumophila*-induced reduction of mitochondrial respiration, the mitochondrial membrane potential is maintained

We have previously shown that *L. pneumophila* strain Philadelphia JR32 impairs mitochondrial respiration during infection (Escoll et al., 2017b). Here, we analyzed *L. pneumophila* strain Paris (Lpp) to learn whether this is a general characteristic of *L. pneumophila* infection. We infected hMDMs with Lpp WT or a T4SS-deficient mutant ($\Delta dotA$) for 6 hr and analyzed their mitochondrial function compared to uninfected hMDMs by using a cellular respiratory control assay in living cells (Brand and Nicholls, 2011; Connolly et al., 2018). This assay determines oxygen consumption rate (OCR) in basal conditions and during the sequential addition of mitochondrial respiratory inhibitors. OCR variations observed indicate how mitochondrial respiration is functioning in a cell population (Figure 1A, Figure 1—figure supplement 1A). Our results showed that basal respiration is significantly reduced ($p < 0.0001$) in WT-infected hMDMs compared to $\Delta dotA$ - and noninfected hMDMs (Figure 1A and B). This indicates that O_2 consumption, which is predominantly driven by ATP turnover and the flow of H^+ to the matrix through the mitochondrial F_0F_1 -ATPase, is severely impaired in WT-infected hMDMs. Further analysis of OCR changes upon addition of oligomycin, an inhibitor of the mitochondrial F_0F_1 -ATPase, indicated that the rate of mitochondrial respiration coupled to ATP synthesis is highly reduced in WT-infected hMDMs compared to $\Delta dotA$ - or noninfected cells. Other respiratory parameters such as proton leak were also reduced in WT-infected macrophages (Figure 1A, Figure 1—figure supplement 1A and B). Subsequent addition of an uncoupler to create a H^+ short-circuit across the inner mitochondrial membrane (IMM), such as FCCP, allowed measuring the maximum respiration rate and the spare respiratory capacity, revealing that both were severely impaired in WT-infected cells compared to $\Delta dotA$ - and noninfected hMDMs (Figure 1A, Figure 1—figure supplement 1A and B). Finally, inhibition of the respiratory complexes I and III with rotenone and antimycin A, respectively, measured O_2 consumption driven by nonmitochondrial processes, such as cytoplasmic NAD(P)H oxidases, which showed similar levels of nonmitochondrial O_2 consumption in all infection conditions (Figure 1A, Figure 1—figure supplement 1A and B).

Taken together, our results indicated that several mitochondrial respiration parameters were severely altered during infection with Lpp-WT, including respiration coupled to ATP production. Importantly, some of the respiratory parameters measured that are oligomycin-sensitive were reduced in Lpp-WT-infected hMDMs but not in $\Delta dotA$ -infected cells, suggesting that the mitochondrial F_0F_1 -ATPase activity may be altered during *L. pneumophila* infection in a T4SS-dependent manner.

The transition of electrons across mitochondrial ETC complexes allows the extrusion of H^+ from the matrix to the IMS generating a H^+ circuit where the mitochondrial F_0F_1 -ATPase is the dominant H^+ re-entry site during active ATP synthesis by OXPHOS. In cellular steady-state conditions, extrusion and re-entry H^+ fluxes across mitochondrial membranes are balanced (Brand and Nicholls, 2011). Therefore, any exogenous alteration of ATP turnover and/or F_0F_1 -ATPase activity influences this H^+ circuit and might be reflected in $\Delta\psi_m$ levels. Thus, we decided to quantify the $\Delta\psi_m$ in infected cells. We developed a miniaturized high-content assay based on kinetic measurements of tetramethylrhodamine methyl ester (TMRM) fluorescence in nonquenching conditions (10 nM), where TMRM fluorescence in mitochondria is proportional to the $\Delta\psi_m$ (Connolly et al., 2018; Duchen et al., 2003). This assay allowed to measure changes in the $\Delta\psi_m$ at the single-cell level and in thousands of living cells during infection (Figure 1C). Image analysis showed that the $\Delta\psi_m$ slightly increased in Lpp-WT-, Lpp- $\Delta dotA$ -, and noninfected cell populations during the first hours of infection (1–3 hpi), and progressively decreased during the time course with no differences between the infection conditions (Figure 1D). Single-cell analyses (Figure 1E, Figure 1—figure supplement 1C) showed that Lpp-WT-, Lpp- $\Delta dotA$ -, and noninfected single hMDMs showed a wide range of $\Delta\psi_m$ values at any time point (Figure 1—figure supplement 1C) with no significant differences between Lpp-WT- and Lpp- $\Delta dotA$ -infected hMDMs at 6 hpi. Infected cells with both strains showed a significantly higher $\Delta\psi_m$ compared to noninfected cells ($p < 0.0001$, Figure 1E, Figure 1—figure supplement 1D). Thus, despite a significant reduction of OXPHOS in WT-infected cells, the $\Delta\psi_m$ was maintained. This suggests that *L. pneumophila* manipulates the mitochondrial ETC to conserve the $\Delta\psi_m$ of hMDMs in the absence of OXPHOS.

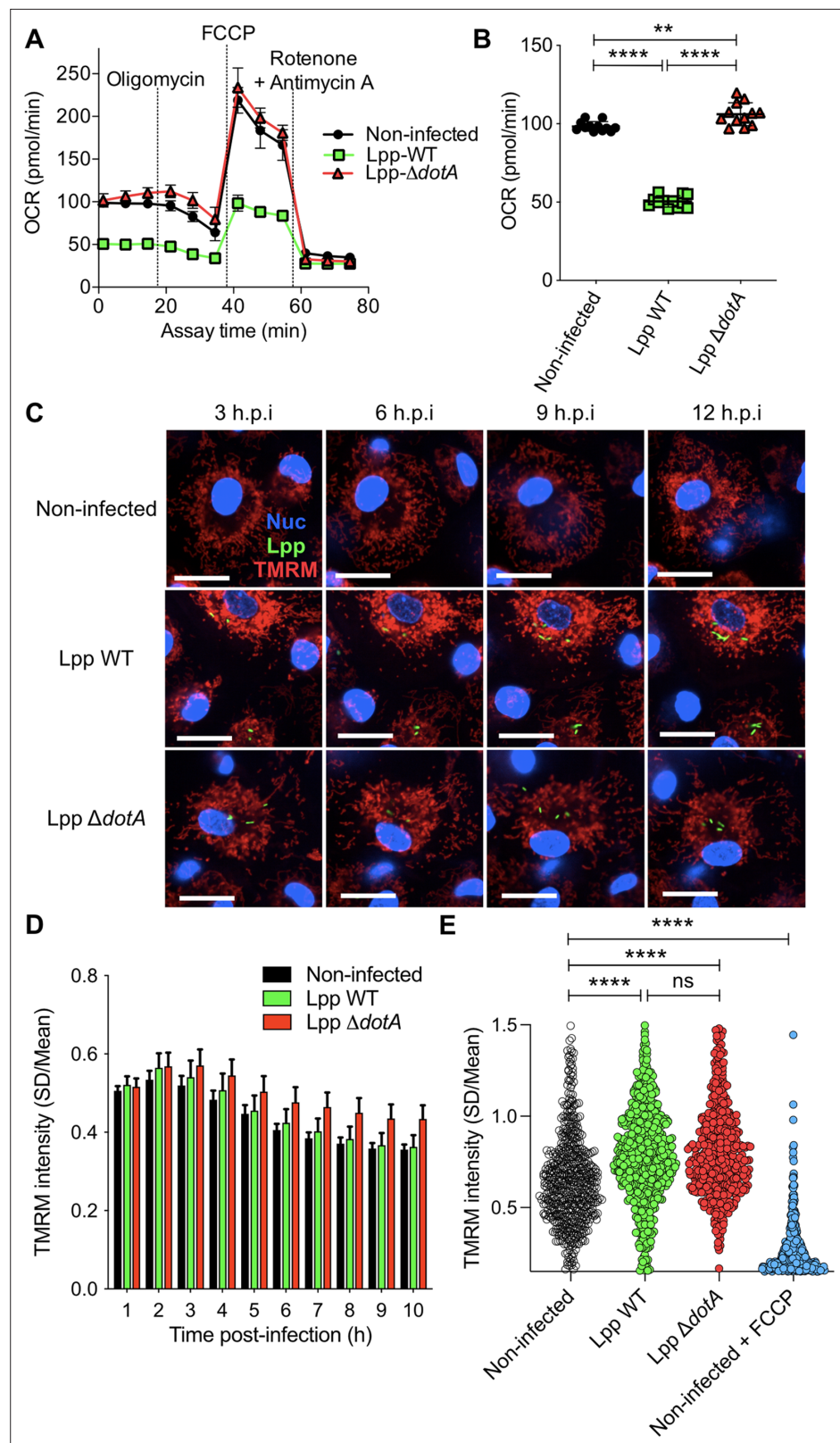


Figure 1. Despite a reduction of oxidative phosphorylation (OXPHOS), human monocyte-derived macrophages (hMDMs) maintain their $\Delta\psi_m$ during infection by *L. pneumophila*. **(A)** hMDMs were infected with *L. pneumophila* strain Paris (Lpp) wild-type (WT), a type 4 secretion system (T4SS)-deficient $\Delta dotA$ mutant, or left uninfected (noninfected). At 6 hr post-infection (hpi), a cellular respiratory control assay was performed by measuring

Figure 1 continued on next page

Figure 1 continued

oxygen consumption rate (OCR) during the sequential addition of mitochondrial respiratory inhibitors (see also **Figure 1—figure supplement S1A**). **(B)** Basal respiration of hMDMs in the same conditions as in **(A)**, at 6 hpi. **(C)** hMDMs were infected as in **(A)** with GFP-expressing bacteria (green), nuclei of host cells were stained with Hoechst (Nuc, blue), and $\Delta\psi_m$ was monitored from 1 to 12 hpi using tetramethylrhodamine methyl ester (TMRM) dye in nonquenching conditions (10 nM). Representative confocal microscope images of noninfected and infected cells at 3, 6, 9, and 12 hpi are shown. Intracellular bacterial replication can be observed in Lpp-WT infected hMDMs at 12 hpi. Bar: 20 μm . **(D)** Quantification of TMRM intensity at 1–10 hpi (expressed as SD/mean) in the assays described in **(C)**. Data from four independent experiments with a total of 10 replicates. Single-cell data from the entire time course are shown in **Figure 1—figure supplement S1C**. **(E)** hMDMs were infected with GFP-expressing bacteria or left uninfected (noninfected). At 6 hpi, nuclei of host cells were stained with Hoechst and $\Delta\psi_m$ was measured using TMRM dye in nonquenching conditions (10 nM), and FCCP (10 μM) was added or not to noninfected cells as a control to monitor complete mitochondrial depolarization. Single-cell analysis from assays performed in three donors is shown in **Figure 1—figure supplement S1D**. ** $p < 0.01$; **** $p < 0.00001$; ns, nonsignificant (Mann–Whitney U test).

The online version of this article includes the following figure supplement(s) for figure 1:

Figure supplement 1. Oxidative phosphorylation (OXPHOS) and $\Delta\psi_m$ during infection by *L. pneumophila*.

L. pneumophila infection induces the ‘reverse mode’ of the mitochondrial F_0F_1 -ATPase in a T4SS-dependent manner

The mitochondrial F_0F_1 -ATPase is a fascinating molecular machine that rotates clockwise when it works in the ‘forward mode,’ synthesizing ATP by using the $\Delta\psi_m$ generated by the H^+ circuit (**Figure 2A**, left). It can also rotate counterclockwise when it works in the ‘reverse mode’ (**Campanella et al., 2009**). In this case, it hydrolyzes ATP to maintain $\Delta\psi_m$ in the absence of OXPHOS (**Figure 2A**, right). As our results showed that *L. pneumophila* highly reduced OXPHOS, likely by an alteration of the F_0F_1 -ATPase activity, while the $\Delta\psi_m$ was conserved, we investigated in which activity mode the F_0F_1 -ATPase worked during *Legionella* infection. A widely used method to investigate the directionality of the F_0F_1 -ATPase in intact cells is to monitor changes in $\Delta\psi_m$ after the addition of F_0F_1 -ATPase inhibitors, such as oligomycin or dicyclohexylcarbodiimide (DCCD) (**Connolly et al., 2018; Gandhi et al., 2009**). These inhibitors block both modes of function; thus if the F_0F_1 -ATPase is working in the ‘forward mode’ the $\Delta\psi_m$ will increase after adding the inhibitor as the inhibition of the H^+ flux to the matrix through the ATPase leads to an accumulation of H^+ at the IMS (**Figure 2B**, left). If $\Delta\psi_m$ decreases after ATPase inhibition, the F_0F_1 -ATPase works in the ‘reverse mode’ since now H^+ cannot translocate to the IMS to maintain the $\Delta\psi_m$ (**Figure 2B**, right). Here, we used the aforementioned TMRM high-content assay to monitor the $\Delta\psi_m$ in living hMDMs at 6 hpi when OXPHOS is impaired and $\Delta\psi_m$ is maintained.

First, we recorded a baseline and then added medium as a control. As expected, this did not alter $\Delta\psi_m$ in any infection condition (**Figure 2C and D**). However, the addition of FCCP completely depolarized mitochondria, leading to an abrupt drop of $\Delta\psi_m$ in Lpp-WT-, Lpp- $\Delta dotA$ -, and noninfected hMDMs (**Figure 2C and E**), demonstrating that this assay can monitor changes in the $\Delta\psi_m$ simultaneously in hundreds of infected cells. To analyze whether the F_0F_1 -ATPase worked in the synthase (forward) or the hydrolase (reverse) mode, we added oligomycin (**Figure 2F**) or DCCD (**Figure 2G**) to the infected cells. The $\Delta\psi_m$ increased in noninfected or $\Delta dotA$ -infected hMDMs, which suggested that the ATPase worked in the ‘forward mode’ in these infection conditions. In contrast, the addition of oligomycin to Lpp-WT-infected hMDMs had no effect on the $\Delta\psi_m$ (**Figure 2F**), while addition of DCCD decreased the $\Delta\psi_m$ (**Figure 2G**). Thus, our results indicate that the F_0F_1 -ATPase worked in the ‘forward mode’ in noninfected or $\Delta dotA$ -infected macrophages, whereas the F_0F_1 -ATPase worked in the ‘reverse mode’ during infection of hMDMs with the WT strain. This suggests that the induction of the ‘reverse mode’ depends on the action of T4SS effector(s).

The T4SS effector LpSpl participates in the induction of the ‘reverse mode’ of the mitochondrial F_0F_1 -ATPase during infection

Among the more than 300 bacterial effectors that *L. pneumophila* injects into host cells through its T4SS (**Mondino et al., 2020**), 3 have been shown to target mitochondrial structures or functions. LncP is a T4SS effector targeted to mitochondria that assembles in the IMM and seems to transport ATP across mitochondrial membranes (**Dolezal et al., 2012**). The effector LpSpl (also known as LegS2) was

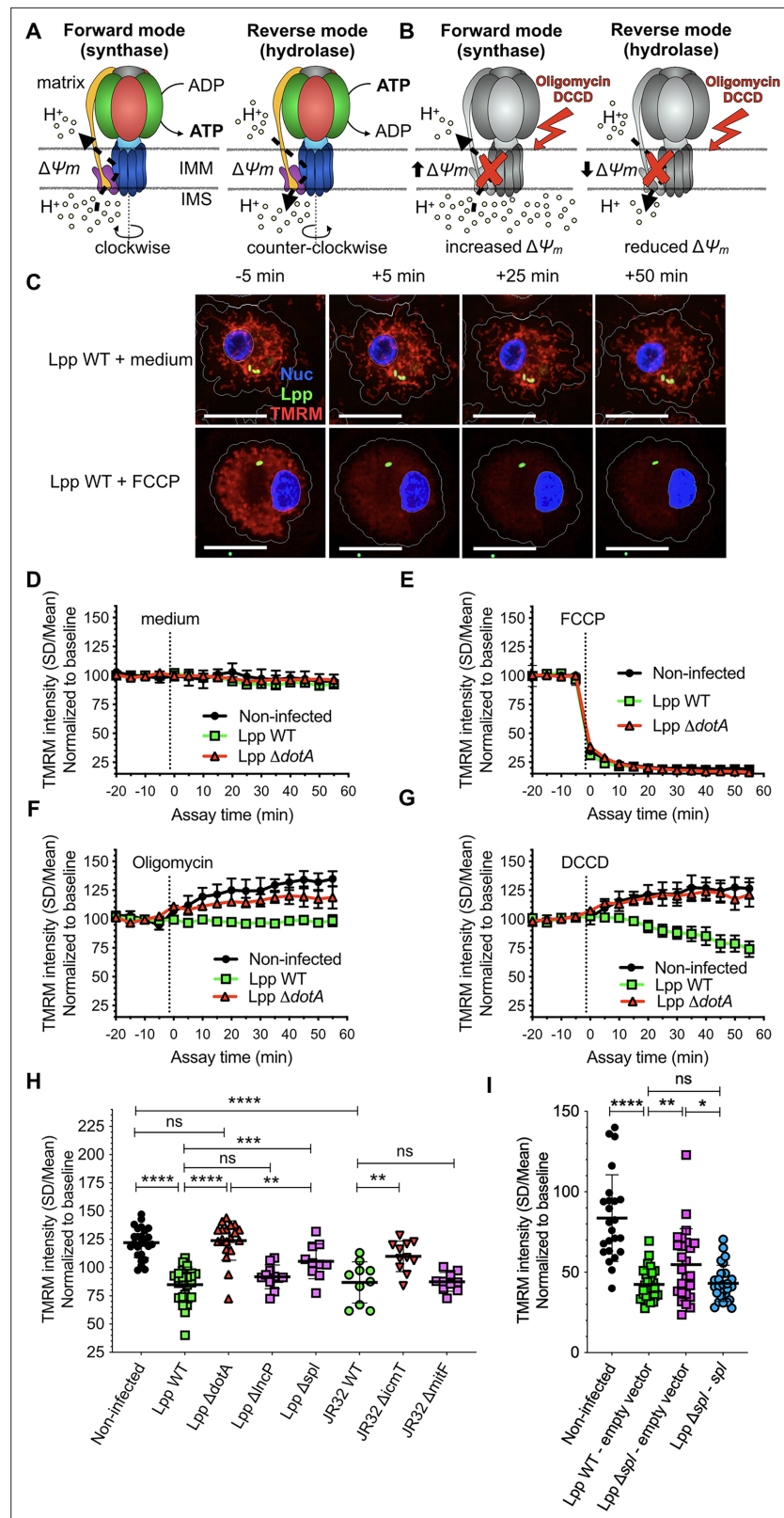


Figure 2. The mitochondrial F_0F_1 -ATPase works in the ‘reverse mode’ during infection of human monocyte-derived macrophages (hMDMs) by *L. pneumophila*. (A) In the ‘forward mode’ of the mitochondrial ATPase, the $\Delta\psi_m$ generated by the electron transport chain is used by the F_0F_1 -ATPase to synthesize ATP. The ‘reverse mode’ of the F_0F_1 -ATPase leads to ATP hydrolysis to pump H^+ to the intermembrane space (IMS). IMM, inner mitochondrial
 Figure 2 continued on next page

Figure 2 continued

membrane. (B) When the F_0F_1 -ATPase is inhibited by oligomycin or dicyclohexylcarbodiimide (DCCD), an increase in $\Delta\psi_m$ indicates that the ATPase was working in the 'forward mode' (H^+ accumulate in the IMS), while a decrease in $\Delta\psi_m$ indicates functioning in the 'reverse mode' (H^+ cannot be translocated to the IMS by the F_0F_1 -ATPase to sustain the $\Delta\psi_m$). (C) hMDMs were infected with GFP-expressing bacteria (green) or left uninfected (noninfected). At 5.5 hr post-infection (hpi), cells were labeled with Hoechst to identify the cell nucleus (Nuc, blue) and tetramethylrhodamine methyl ester (TMRM) (red) to quantify $\Delta\psi_m$. At 6 hpi, addition of medium (no changes) or FCCP (complete depolarization) was used as controls. Representative confocal images of Lpp-WT-infected hMDMs (6 hpi) at 5 min before the addition of medium (top) or FCCP (bottom), and at 5, 25, and 50 min after addition of medium or FCCP. Bar: 20 μ m. (D) Quantification of (C) before (baseline) and after the addition of medium. Each dot represents mean \pm SD of three independent experiments with a total of eight replicates. (E) Same as (D) but FCCP was added. (F) Same as (D) but oligomycin was added. (G) Same as (D) but DCCD was added. (H) Same as (C) but infection was performed with Lpp-WT, Lpp- $\Delta dotA$, Lpp- $\Delta lncP$, Lpp- Δspl , *L. pneumophila* strain Philadelphia JR32 (JR32-WT, JR32- $\Delta icmT$ or JR32- $\Delta mitF$). TMRM values (SD/mean) at 50 min after DCCD addition are shown. Data from a minimum of three experiments per strain with 10 or more replicates per strain. (I) hMDMs were infected with GFP-expressing bacteria or left uninfected (noninfected). At 5.5 hpi, cells were labeled with Hoechst to identify the cell nucleus and TMRM to quantify $\Delta\psi_m$. At 6 hpi, addition of DCCD revealed whether the F_0F_1 -ATPase works in the 'reverse mode.' Infection was performed with Lpp-WT expressing empty pBCKS vector (empty vector), Lpp- Δspl -expressing empty vector and Lpp- Δspl -expressing pBCKS-*spl* vector, which express *LpSpl* (complemented strain, Lpp- $\Delta spl::spl$). Data from three donors are shown. Each dot represents a replicate. * $p < 0.01$; ** $p < 0.001$; *** $p < 0.0001$; ns, nonsignificant (Mann-Whitney *U* test).

The online version of this article includes the following figure supplement(s) for figure 2:

Figure supplement 1. Basal respiration of human monocyte-derived macrophages (hMDMs) infected with *L. pneumophila* Δspl mutant and validation of the model in HEK-293 cells.

suggested to target mitochondria (Degtyar et al., 2009), the endoplasmic reticulum (ER) (Rolando et al., 2016), and mitochondrial-associated membranes (MAMs) (Escoll et al., 2017a). *LpSpl* encodes a sphingosine-1 phosphate (S1P) lyase that directly targets the host sphingolipid metabolism and restrains autophagy in infected cells. MitF (LegG1) activates the host small GTPase Ran to promote mitochondrial fragmentation during infection of human macrophages (Escoll et al., 2017b).

To learn if any of these effectors is involved in the T4SS-dependent induction of the 'reverse mode' of the F_0F_1 -ATPase, we infected hMDMs for 6 hr with Lpp-WT or its isogenic mutants lacking a functional T4SS (Lpp- $\Delta dotA$), lacking the effector LncP (Lpp- $\Delta lncP$), lacking the effector *LpSpl* (Lpp- Δspl), and *L. pneumophila* strain Philadelphia JR32 (JR32-WT) and its isogenic mutants lacking the T4SS (JR32- $\Delta icmT$) or the effector MitF (JR32- $\Delta mitF$). Using the TMRM high-content assay, we measured the $\Delta\psi_m$ after the inhibition of the F_0F_1 -ATPase by DCCD (Figure 2H). Our results indicated that, while the F_0F_1 -ATPase worked in the 'forward mode' in noninfected hMDMs and during infection with T4SS-deficient mutants (Lpp- $\Delta dotA$ and JR32- $\Delta icmT$), the F_0F_1 -ATPase worked in the 'reverse mode' during infection with the Lpp-WT and JR32-WT strains (Figure 2G and H). As infection of hMDMs by *L. pneumophila* strain Paris and *L. pneumophila* strain Philadelphia JR32 showed similar results, this suggests that inhibition of mitochondrial respiration and conservation of $\Delta\psi_m$ through the induction of the 'reverse mode' of the mitochondrial ATPase is a virulent strategy of *L. pneumophila*. Infection with Lpp- $\Delta lncP$ and JR32- $\Delta mitF$ was not significantly different compared to the WT strains, suggesting that these effectors are not involved in the induction of the 'reverse mode' of the mitochondrial ATPase. However, mitochondria of cells infected with Lpp- Δspl showed a significantly higher $\Delta\psi_m$ after DCCD treatment than mitochondria of cells infected with Lpp-WT ($p = 0.0006$), and a significantly lower $\Delta\psi_m$ after DCCD treatment than mitochondria of cells infected with the Lpp- $\Delta dotA$ strain ($p = 0.0034$). To confirm that *LpSpl* is indeed implicated in the induction of the 'reverse mode' of the F_0F_1 -ATPase, we complemented the Lpp- Δspl mutant strain with a plasmid expressing *LpSpl* (Lpp Δspl -*spl*) and infected hMDMs. Cells infected with the WT strain carrying the empty vector (Lpp WT-empty vector) showed a significantly lower $\Delta\psi_m$ after DCCD treatment than noninfected cells ($p < 0.0001$), and the Lpp Δspl mutant carrying the empty plasmid (Lpp Δspl -empty vector) showed a significantly higher $\Delta\psi_m$ after DCCD treatment compared to WT strain ($p = 0.0095$), as shown above. Complementation of Lpp Δspl recovered the WT phenotype as no significant differences in $\Delta\psi_m$ values after DCCD treatment compared to WT-infected cells were observed, but significant differences were still observed with the Lpp Δspl -empty vector ($p = 0.0216$) mutant strain, confirming a role of *LpSpl* in the induction

of the 'reverse mode' of the F_0F_1 -ATPase (**Figure 2I**). We also found a very small but significant difference in the oxygen consumption levels exhibited by Lpp-WT- and Lpp Δspl -infected hMDMs ($p=0.0148$, **Figure 2—figure supplement 1A**), suggesting that the role of LpSpl in the induction of the 'reverse mode' to maintain $\Delta\psi_m$ during infection might partially involve the modulation of the functioning of the OXPHOS machinery.

To further analyze our results obtained in hMDMs in an easy to transfect cell model, we used HEK-293 cells stably expressing the FcγRII receptor (**Arasaki and Roy, 2010**) as these cells allow efficient internalization of opsonized *L. pneumophila*. The bacteria were opsonized using a monoclonal antibody targeting *L. pneumophila* flagellin. First, the $\Delta\psi_m$ of noninfected cells was monitored upon addition or not of FCCP, showing that it decreased as expected compared to the addition of medium (**Figure 2—figure supplement 1B and C**). Then, we measured the direction of the F_0F_1 -ATPase during infection by treating cells with DCCD (like in hMDMs, **Figure 2G**). Our results showed that the $\Delta\psi_m$ decreased upon addition of DCCD in Lpp-WT-infected HEK-293 cells, confirming that the F_0F_1 -ATPase of WT-infected HEK-293 cells worked in the 'reverse mode' (**Figure 2—figure supplement 1D**). The results obtained for the mutant strains during infection of HEK-293 cells were equivalent to those shown in **Figure 2H** obtained in hMDMs. The change of the $\Delta\psi_m$ upon DCCD addition in $\Delta dotA$ -infected cells was similar to those in noninfected cells, while results obtained in Δspl -infected HEK-293 cells showed an intermediate phenotype between the WT and the $\Delta dotA$ mutant, but significantly different to both strains (**Figure 2—figure supplement 1E and F**).

Together, these data suggest that LpSpl is partially involved in the induction of the 'reverse mode' of the F_0F_1 -ATPase; however, other additional T4SS effector(s) seem to participate in the modulation of the F_0F_1 -ATPase activity mode.

Inhibition of *Legionella*-induced 'reverse mode' collapses the $\Delta\psi_m$ and ignites cell death of infected macrophages

To further analyze the importance of the activity mode of the F_0F_1 -ATPase during infection, we used BTB06584 (hereafter called BTB), a specific inhibitor of the 'reverse mode' of the mitochondrial F_0F_1 -ATPase (**Ivanov et al., 2014**). We used the TMRM high-content assay and added BTB to noninfected, Lpp-WT- or Lpp- $\Delta dotA$ -infected hMDMs at 6 hpi. As shown in **Figure 3A**, the $\Delta\psi_m$ collapsed specifically and significantly in WT-infected cells (**Figure 3B and C**) compared to noninfected ($p=0.0022$) and $\Delta dotA$ -infected cells ($p=0.0238$), further confirming that the F_0F_1 -ATPase works in the 'reverse mode' during WT infection. Indeed, the addition of BTB to Lpp-WT-infected hMDMs led to a significant reduction of the $\Delta\psi_m$ ($p<0.0001$) at every time point post-infection (1–10 hpi) and at the single-cell level compared to nontreated Lpp-WT-infected cells (**Figure 3D**), further confirming that conservation of $\Delta\psi_m$ during *L. pneumophila* infection is caused by induction of F_0F_1 -ATPase 'reverse mode.'

As OXPHOS cessation and $\Delta\psi_m$ collapse can trigger cell death, we reasoned that induction of the 'reverse mode' of mitochondrial ATPase by *L. pneumophila* to maintain $\Delta\psi_m$ in the absence of OXPHOS might delay cell death of infected cells. To test this hypothesis, we first measured the percentage of living cells after an FCCP treatment of 18 hr. An FCCP-induced collapse of the $\Delta\psi_m$ reduced the percentage of living cells by 32% compared to nontreated hMDMs ($p=0.0094$, **Figure 4—figure supplement 1A**). Then, we infected hMDMs with Lpp-WT and treated them with BTB or left them untreated, and then measured the percentage of living cells among infected cells (**Figure 4A**). Our results showed that the percentage of living, infected cells significantly decreased after 10 hpi in BTB-treated infected hMDMs compared to nontreated cells. As this reduction in the percentage of living, infected cells upon 'reverse mode' inhibition might be caused by increased cell death, we used our high-content assay to measure Annexin-V, a marker of early apoptosis, in a high number of living hMDMs during infection (**Figure 4B and C**). While addition of BTB for 24 hr did not increase the percentage of Annexin-V⁺ cells in noninfected cells or in Lpp- $\Delta dotA$ -infected cells (**Figure 4B, Figure 4—figure supplement 1B**), the addition of this 'reverse mode' inhibitor to Lpp-WT-infected hMDMs significantly increased the percentage of Annexin-V⁺ cells compared to nontreated cells ($p=0.0312$). Addition of BTB to Lpp- Δspl -infected cells significantly increased the percentage of Annexin-V⁺ cells compared to nontreated cells ($p=0.0375$, **Figure 4C**), but no significant difference was observed compared to WT-infected cells ($p=0.0571$, **Figure 4—figure supplement 1B**), suggesting that LpSpl is not the only effector playing a role. Thus, inhibition of the 'reverse mode' by BTB leads to a reduction in the percentage of living, infected cells, as increased cell death

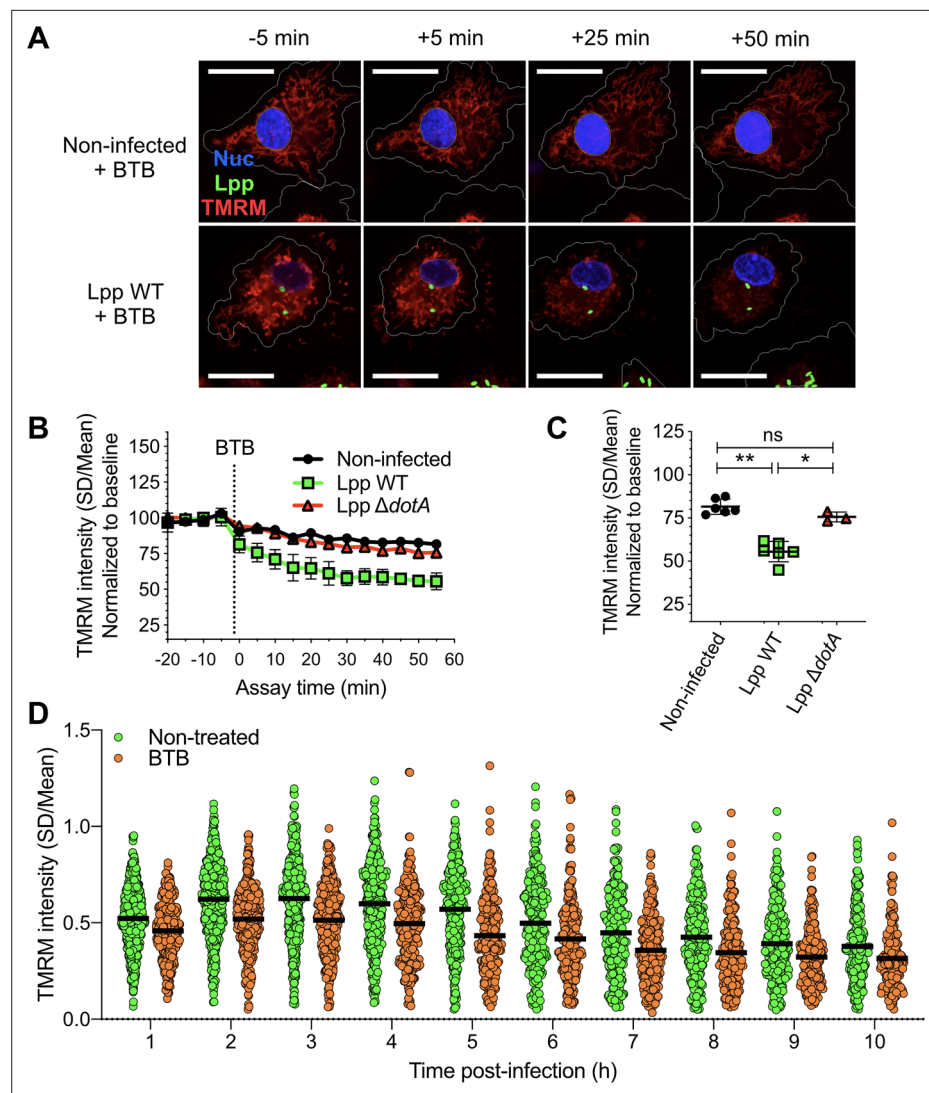


Figure 3. Inhibition of the ‘reverse mode’ of mitochondrial F_0F_1 ATPase reduces the $\Delta\psi_m$ of *L. pneumophila*-infected human monocyte-derived macrophages (hMDMs). **(A)** hMDMs were infected with GFP-expressing bacteria (green), Lpp-WT or Lpp- $\Delta dotA$, or left uninfected (noninfected). At 5.5 hr post-infection (hpi), cells were labeled with Hoechst to identify cell nucleus (Nuc, blue) and tetramethylrhodamine methyl ester (TMRM) (red) to quantify $\Delta\psi_m$. At 6 hpi, BTB06584 (BTB, 50 μ M), a specific inhibitor of the ‘reverse mode’ of the ATPase, was added and $\Delta\psi_m$ monitored. Representative confocal microscopy images of noninfected (top) and Lpp-WT-infected (bottom) hMDMs (6 hpi) at 5 min before the addition and at 5, 25, and 50 min after the addition of BTB. Bar: 20 μ m. **(B)** Quantification of **(A)** before (baseline) and after the addition of BTB. Each dot represents the mean \pm SD of three independent experiments with a total of six replicates. **(C)** Same infection conditions than **(A)** but TMRM values (SD/mean) at 50 min after BTB addition are shown. Data from three experiments with a total of six replicates (three replicates for Lpp- $\Delta dotA$). **(D)** Single-cell analysis of $\Delta\psi_m$ in Lpp-WT-infected hMDMs treated with BTB (50 μ M) or left untreated (nontreated). Single-cell data from one representative experiment * $p < 0.05$; ** $p < 0.01$; ns, nonsignificant (Mann–Whitney U test).

occurs specifically in infected cells. Single-cell analysis at 12 and 18 hpi (**Figure 4D**, **Figure 4—figure supplement 1C**) also showed higher levels of Annexin-V intensity in BTB-treated Lpp-WT-infected hMDMs compared to nontreated infected cells ($p < 0.0001$). BTB-treated infected cells also showed higher Hoechst nuclear levels compared to nontreated infected cells, a sign of nuclear condensation typical of apoptotic cells (**Figure 4—figure supplement 1D**), which further indicates that inhibition of the *Legionella*-induced ATPase ‘reverse mode’ ignites cell death of infected macrophages. Taken

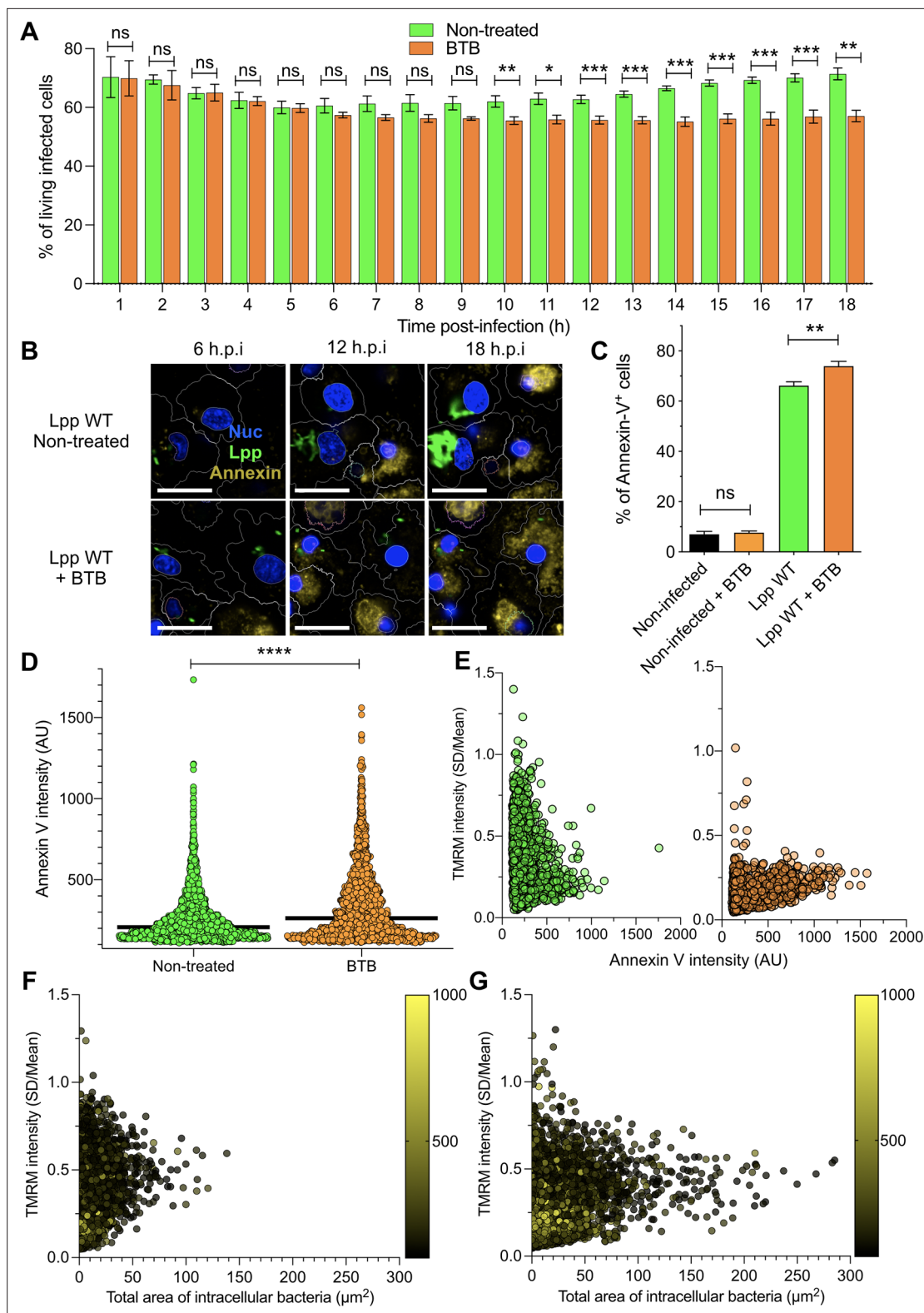


Figure 4. Inhibition of F_0-F_1 ATPase ‘reverse mode’ increases cell death in *L. pneumophila*-infected human monocyte-derived macrophages (hMDMs). (A) hMDMs were infected with Lpp-WT-GFP and were nontreated or treated with 50 μM BTB. The presence of GFP-expressing bacteria in each cell was monitored, and the number of living infected cells in the whole population was graphed as a percentage of living infected cells. Data from three independent experiments with a total of seven replicates per condition and time point. (B) hMDMs were infected with Lpp-WT-GFP (green), the nuclei of host cells were stained with Hoechst (Nuc, blue), and Annexin-V Alexa Fluor 647 was added to the cell culture to monitor early cell death (Annexin, Figure 4 continued on next page

Figure 4 continued

yellow) from 1 to 18 hr post-infection (hpi) in nontreated or BTB-treated hMDMs. Representative confocal images of nontreated and Lpp-WT-GFP-infected cells at 6, 12, and 18 hpi are shown. Intracellular bacterial replication can be observed in nontreated Lpp-WT-infected hMDMs at 12 and 18 hpi. Bar: 20 μm . (C) hMDMs stained as in (B) were infected with Lpp-WT-GFP or left uninfected (noninfected), and then were treated or not with BTB (50 μM). Percentage of Annexin-V⁺ cells at 24 hpi is shown. Data from three independent experiments with a total of seven replicates per condition (D) Single-cell analysis (12 hpi) of Annexin-V intensity of the assays described in (B). Single-cell data from one representative experiment (18 hpi shown in **Figure 2—figure supplement 1A**). (E) hMDMs were infected with Lpp-WT-GFP, nuclei of host cells were stained with Hoechst, and tetramethylrhodamine methyl ester (TMRM) and Annexin-V Alexa Fluor 647 were added to the cells to simultaneously monitor (1–18 hpi) $\Delta\psi_m$ and early cell death, respectively, in nontreated or BTB-treated hMDMs (representative multifield confocal images in **Figure 2—figure supplement 1C**). Single-cell analyses (12 hpi) of $\Delta\psi_m$ (TMRM SD/mean) and cell death (Annexin-V intensity) in more than 1600 cells per condition are shown. Single-cell data from one representative experiment. Green dots, nontreated Lpp-WT-infected single cells; orange dots, BTB-treated Lpp-WT-infected single cells. (F) Same infection conditions as in (E) but using nontreated cells. Bacterial replication was monitored in each single cell infected with Lpp-WT. Single-cell analyses (12 hpi) of $\Delta\psi_m$ (TMRM SD/mean), area of intracellular GFP-expressing bacteria (μm^2), a proxy for intracellular replication, and cell death (Annexin-V intensity) in more than 3800 cells are shown. Single-cell data from one representative experiment; color scale (yellow) represents Annexin-V intensity per cell (AU). (G) Same as in (F) at 18 hpi. * $p < 0.05$; ** $p < 0.01$; *** $p < 0.001$; **** $p < 0.00001$; ns, nonsignificant (Mann–Whitney U test).

The online version of this article includes the following figure supplement(s) for figure 4:

Figure supplement 1. Inhibition of F_0F_1 ATPase ‘reverse mode’ delays cell death in *L. pneumophila*-infected human monocyte-derived macrophages (hMDMs), while transfection of *LpSpl* into HEK-293 cells protected transfected cells from Staurosporine (STS)-induced cell death.

Figure supplement 2. BTB treatment, $\Delta\psi_m$ and cell death of *L. pneumophila*-infected human monocyte-derived macrophages (hMDMs).

together, our results suggest that the *Legionella*-induced ‘reverse mode’ of the mitochondrial F_0F_1 -ATPase aids to conserve $\Delta\psi_m$ during infection to delay cell death of infected macrophages.

If the induction of the ‘reverse mode’ in the mitochondrial F_0F_1 -ATPase prevents drops in $\Delta\psi_m$, and this delays cell death, transfection of *LpSpl* might protect cells from exogenously induced cell death. To test this hypothesis, we transfected HEK-293 cells with a plasmid expressing *LpSpl* or with a plasmid expressing a catalytically inactive *LpSpl* protein (*K366A) and analyzed their resistance to Staurosporine (STS)-induced cell death (**Figure 4—figure supplement 1E**). Our analyses showed that *LpSpl*-WT-transfected HEK-293 cells were significantly more resistant to STS-induced cell death compared to control plasmid-transfected cells ($p = 0.0008$), while cells transfected with catalytic inactive *LpSpl*-*K366A showed an intermediate phenotype but significantly different from *LpSpl*-WT- and control plasmid-transfected cells ($p = 0.0269$ and $p = 0.0380$, respectively). This suggests that although the K366 residue is important, it might not be the only residue in the protein involved in the enzymatic activity of *LpSpl* (**Figure 4—figure supplement 1F and G**). Thus, *LpSpl* induced ‘reverse mode’ of the mitochondrial F_0F_1 -ATPase might protect cells from infection-independent forms of cell death.

To understand at the single-cell level whether the *Legionella*-induced ‘reverse mode’ of the mitochondrial F_0F_1 -ATPase aids to conserve the $\Delta\psi_m$ during infection to delay cell death of infected macrophages, we simultaneously monitored $\Delta\psi_m$ and early cell death signs in the same infected cell by multiplexing Annexin-V and TMRM signals in our living cell assay (**Figure 4E, Figure 4—figure supplement 2A and B**). *L. pneumophila*-infected macrophages where the ‘reverse mode’ activity of the F_0F_1 -ATPase was inhibited by BTB suffered a collapsed $\Delta\psi_m$ and showed higher levels of Annexin-V at 12 and 18 hpi (**Figure 4E, Figure 4—figure supplement 2B**) compared to nontreated cells. Thus, both events, collapse of the $\Delta\psi_m$ and triggered cell death, occurred in the same infected cell when the *Legionella*-induced ‘reverse mode’ activity of the F_0F_1 -ATPase was inhibited. Furthermore, we correlated the area of GFP-expressing bacteria, a proxy for intracellular replication, with the $\Delta\psi_m$ and cell death at the single-cell level (12 and 18 hpi, **Figure 4F and G**, respectively). Indeed, an increased area of GFP fluorescence was observed at 18 hpi mainly in those infected macrophages with intermediate levels of TMRM (noncollapsed $\Delta\psi_m$) and low Annexin-V levels (yellow color scale, **Figure 4F and G**). This indicated that conservation of $\Delta\psi_m$ and delayed cell death are required for bacterial replication as they prolong macrophage survival.

Discussion

We show here that by inducing the ‘reverse mode’ of the mitochondrial F_0F_1 -ATPase *L. pneumophila* circumvents the collapse of $\Delta\psi_m$ and cell death caused by OXPHOS cessation in infected cells. This mechanism, which partially involves the T4SS effector *LpSpl*, maintains the $\Delta\psi_m$ and delays host cell death during infection, thus preserving bacterial replication niches in conditions where mitochondrial

respiration is abruptly reduced. Indeed, not only *L. pneumophila*, but also several other intracellular bacterial pathogens, such as *M. tuberculosis* or *Chlamydia pneumoniae*, reduce mitochondrial OXPHOS during infection (Siegl et al., 2014; Singh et al., 2012; Escoll and Buchrieser, 2019). OXPHOS reduction allows the pathogen to redirect cellular resources from mitochondria to the cytoplasm, which enhances glycolysis and biosynthetic pathways that can provide intracellular bacteria with resources needed for bacterial growth (Escoll and Buchrieser, 2018; Russell et al., 2019). In contrast, OXPHOS cessation in macrophages also enhances the biosynthetic pathways, leading to the synthesis of cytokines and antimicrobial compounds (O'Neill and Pearce, 2016; Russell et al., 2019). Furthermore, OXPHOS reduction may trigger profound consequences for host cells, such as the collapse of $\Delta\psi_m$ that may lead to subsequent cell death of infected cells. For macrophages, cell death is considered as a defense mechanism against infection (Chow et al., 2016). Indeed, pyroptosis of infected macrophages permits the spread of inflammatory mediators such as IL-1 β . Thus, for intracellular bacteria, many of which infect macrophages (Mitchell et al., 2016), the death of their host cell is an obstacle as their cellular replication niche is destroyed. Therefore, while bacterial-induced reduction of OXPHOS might be beneficial for intracellular bacteria to obtain host cell resources, they need to counterbalance the consequences of OXPHOS cessation, that is, the collapse of the mitochondrial $\Delta\psi_m$ and subsequent cell death, to preserve their replication niches.

We have previously shown that the *L. pneumophila* T4SS effector MitF is implicated in fragmenting the mitochondrial networks of infected macrophages. These changes in the mitochondrial dynamics have a profound impact on OXPHOS that was severely impaired and accompanied by increased glycolysis in *Legionella*-infected cells (Escoll et al., 2017b). Here, we show that, despite the impairment of mitochondrial respiration in infected cells, *L. pneumophila* conserves the $\Delta\psi_m$ of host cells by inducing the 'reverse mode' of the F_0F_1 -ATPase by a mechanism that is T4SS-dependent and partially mediated by the T4SS effector *LpSpl*. When translocated into human cells, the S1P-lyase activity of *L. pneumophila* *LpSpl* reduces S1P levels in infected cells and restrains autophagy, likely because S1P is involved in the initiation of autophagosome formation at MAMs (Rolando et al., 2016).

How *LpSpl* may regulate the activity of the F_0F_1 -ATPase is an interesting question. Our previous analyses of *LpSpl* function have shown that this protein encodes S1P lyase activity and alters the lipid profile of the host cell by decreasing sphingosine levels in infected THP-1 cells (Rolando et al., 2016). Indeed, phosphorylated lipids are critical regulators of mitochondrial functions and S1P is a potent lipid mediator that regulates various physiological processes as well as diverse mitochondrial functions such as mitochondrial respiration, ETC functioning, or mitochondrial-dependent cell death (Hernández-Corbacho et al., 2017; Nielson and Rutter, 2018). Furthermore, it was reported that S1P interaction with Prohibitin 2 (PHB2) regulates ETC functioning and mitochondrial respiration (Strub et al., 2011) and that a link between PHB2, ETC functioning and the activation of 'mitoflashes' (Jian et al., 2017) exists, which are dynamic and transient uncouplings of mitochondrial respiration from ATP production that are partially dependent on the 'reverse mode' of the F_0F_1 -ATPase (Wei-LaPierre and Dirksen, 2019). Thus, it is possible that *LpSpl* modulates mitochondrial S1P levels helping the induction of the 'reverse mode' of the mitochondrial F_0F_1 -ATPase by involving PHB2, ETC complex assembly, or the generation of mitoflashes, a fascinating possibility that we will further investigate.

The regulation of host cell death by intracellular bacteria is widely studied (Rudel et al., 2010). For *L. pneumophila*, T4SS effectors activating and inhibiting cell death of infected cells have been described (Speir et al., 2014), suggesting that a very delicate interplay of positive and negative signals governs the fate of infected macrophages. Here, we have shown that bacterial replication occurs preferentially in those infected macrophages that are able to conserve the $\Delta\psi_m$ and delay cell death, a condition that is difficult to achieve in the absence of mitochondrial respiration. Thus, the manipulation of the activity of the mitochondrial F_0F_1 -ATPase by *L. pneumophila*, which allows this pathogen to use the ATP hydrolase activity to pump H^+ to the IMS to maintain the $\Delta\psi_m$ in infected cells, is a novel virulence strategy that might contribute to the fine-tuning of the timing of host cell death during bacterial infection.

Materials and methods

Human primary cell cultures

Human blood was collected from healthy volunteers under the ethical rules established by the French National Blood Service (EFS). Peripheral blood mononuclear cells (PBMCs) were isolated by Ficoll-Hypaque density-gradient separation (Lympholyte-H; Cedarlane Laboratories) at room temperature. PBMCs were incubated with anti-human CD14 antibodies coupled to magnetic beads (Miltenyi Biotec) and subjected to magnetic separation using LS columns (Miltenyi Biotec). Positive selected CD14⁺ cells were counted, and CD14 expression was analyzed by flow cytometry, repeatedly showing a purity >90%. CD14 cells were plated in RPMI 1640 medium (Life Technologies) supplemented with 10% heat-inactivated fetal bovine serum (FBS, Biowest) in six-well multi-dish Nunc UpCell Surface cell culture plates or 10 cm Nunc UpCell Surface cell culture dishes (Thermo Fisher) and differentiated to hMDMs by incubation with 100 ng/ml of recombinant human macrophage colony-stimulating factor (rhM-CSF, Miltenyi Biotec) for 6 days at 37°C with 5% CO₂ in a humidified atmosphere. At day 3, additional rhM-CSF (50 ng/ml) was added. After 6 days differentiation, UpCell plates were placed at 20°C during 10 min and hMDMs were gently detached, counted, and plated in RPMI 1640 10% FBS in 384-well plates (Greiner Bio-One).

Bacterial strains, mutant construction, and complementation

L. pneumophila strain Paris or JR32 and their derivatives were grown for 3 days on N-(2-acetamido)-2-amino-ethanesulfonic acid (ACES)-buffered charcoal-yeast (BCYE) extract agar, at 37°C. For eGFP-expressing strains harboring pNT28 plasmid (Tiaden *et al.*, 2007), chloramphenicol (Cam; 5 µg/ml) was added. Knock-out mutant strains of *L. pneumophila* genes coding for the T4SS effectors *LpSpl* and *MitF/LegG1* were previously described (Escoll *et al.*, 2017b; Rolando *et al.*, 2016; Rothmeier *et al.*, 2013). Strains used for complementation experiments (Lpp-WT-expressing empty pBCKS vector, Lpp- Δspl -expressing pBCKS vector, and Lpp- Δspl -expressing pBCKS-*spl* vector, i.e., complemented strain) were previously described (Rolando *et al.*, 2016). The knock-out mutant strain of the *L. pneumophila* gene coding for the effector *LncP* was constructed as previously described (Brügge-mann *et al.*, 2006; Rolando *et al.*, 2016). In brief, the gene of interest was inactivated by introduction of an apramycin resistance (*apraR*) cassette into the chromosomal gene by three-step PCR. The g primers used for the *LncP* (*lpp2981*) knock-out mutant are as follows: *LncP_F*: ACCCTGGTTCATGGTAACAATGG; *LncP_Inv_R*: GAGCGGATCGGGGATTGTCTTATCAGGCGAATGGTGTGAAAGG; *LncP_Inv_F*: GCTGATGGAGCTGCACATGAAACGTCATGGTCGTGCTGGTTG; *LncP_R*: AATCAGATGGGTAAGCCGATTGG. To amplify the apramycin cassette, the primers *Apra_F*: TTCATGTGCAGCTCCATCAGC and *Apra_R*: AAGACAATCCCCGATCCGCTC were used.

Infection of hMDMs

hMDMs were infected with *L. pneumophila* grown for 3 days on BCYE agar plates. Bacteria were dissolved in 1× PBS (Life Technologies), the optical density (OD) was adjusted to OD₆₀₀ of 2.5 (2.2 × 10⁹ bacteria/ml), and the bacteria were then further diluted in serum-free XVIVO-15 medium (Lonza) prior to infection to obtain the respective multiplicity of infection (MOI). hMDMs were washed twice with serum-free XVIVO-15 medium and then infected (MOI = 10) with 25 µl of bacteria in 384-well plates (Greiner Bio-One). The infection was synchronized by centrifugation (200 × g for 5 min), and the infected cells were incubated at 37°C for 5 min in a water bath and then for 25 min at 37°C/5% CO₂. After three intensive washes with serum-free XVIVO-15 medium, the infection proceeded in serum-free XVIVO-15 medium for the respective time points.

Infection and transfection of HEK-293 cells

HEK-293 cells stably expressing the FcγRII receptor (gift of Prof. Craig Roy) (Arasaki and Roy, 2010) were maintained in DMEM +10% FBS. Before use, the cells were tested negative for *Mycoplasma* contamination. The HEK-293 cells stably expressing the FcγRII receptor were not authenticated. However, the only entry of misidentified HEK cells at the ICLAC database is ICLAC-00063, when HEK cells were misidentified in 1981 with HeLa cells. Therefore, our HEK cells were identified by morphology and attachment as HEK cells are morphologically different from HeLa cells and they attach very weakly to tissue culture-treated plastic, contrary to HeLa cells. Most importantly, the remote possibility of misidentification with HeLa cells would not change any consideration or conclusion in our study. For

infection, HEK-293 cells were plated in 384-well plates (Greiner Bio-One) and were infected with *L. pneumophila* grown for 3 days on BCYE agar plates following the same protocol used for hMDMs but using MOI = 20 without washing to avoid detaching of cells. The infection proceeded in serum-free XVIVO-15 medium for the respective time points. For transfection, HEK-293 cells were plated in 384-well plates (Greiner Bio-One) and FuGENE (Promega) and Opti MEM medium (Thermo Fisher) were used, following the manufacturer's recommendations. We used 1 µg DNA + 3 µl FuGENE + 500 µl Opti MEM, and then added 2.5 µl per well. Plasmid DNA was transfected during 24 hr. Transfected plasmids expressed *LpSpl* WT (harboring an Xpress tag) or a catalytically inactive *LpSpl* protein (*K366A, also harboring an Xpress tag), previously described (Rolando et al., 2016). The pGFPmax plasmid (Lonza) was used as a control (as cells transfected with a plasmid only expressing the small epitope Xpress, without any other protein, gave extremely low-intensity values during immunofluorescence experiments and could not be used as a control).

Automatic confocal imaging

Cell imaging was performed in 384-well plates. For living cells, 30 min prior imaging, 25 µl of culture medium were removed and replaced by 25 µl of 2× mix of dyes, to a final concentration of 200 ng/ml of Hoechst H33342 (nuclear staining; Life Technologies), 10 nM of TMRM (mitochondrial membrane potential; Life Technologies), and/or 1/100 Annexin-V-Alexa Fluor 647 (early apoptosis; Life Technologies). If chemical inhibitors of the ETC were used in the experiments, they were added to hMDMs at the indicated times points at the following concentrations: 5 µM oligomycin (Enzo), 100 µM DCCD (Sigma), 10 µM FCCP (Tocris), and 50 µM BTB06584 (Sigma). Once the assay was performed, cells were fixed with 4% PFA, permeabilized with 0.1% Triton-X100, blocked with 1% BSA, and stained with primary mouse antibodies against Xpress tag (1:100, Invitrogen) and secondary anti-mouse Alexa Fluor 488 antibodies (1:1000, Invitrogen). Image acquisitions of multiple fields (9–25) per well were performed on an automated confocal microscope (Opera Phenix, PerkinElmer) using ×40 or ×60 objective, excitation lasers at 405, 488, 561, and 640 nm, and emission filters at 450, 540, 600, and 690 nm, respectively.

Metabolic extracellular flux analysis

hMDMs (50,000) were plated in XF-96-cell culture plates (Seahorse Bioscience). For OCR measurements, XF Assay Medium (Seahorse Bioscience) supplemented with 1 mM pyruvate and 10 mM glucose was used, and OCR was measured in a XF-96 Flux Analyzer (Seahorse Bioscience). For the mitochondrial respiratory control assay, hMDMs were infected at MOI = 10 and at 6 hpi. Different drugs were injected (Mitostress kit, Seahorse Bioscience) while OCR was monitored. Specifically, oligomycin was injected through port A, then FCCP was injected through port B, and finally rotenone + antimycin A were injected through port C, to reach each of the drugs a final concentration in the well of 0.5 µM. Coupling efficiency (%) was calculated using the following formula: (ATP production rate)/(basal respiration rate) × 100. In this formula, ATP production rate was calculated as: (last rate measurement before oligomycin injection) – (minimum rate measurement after oligomycin injection), while basal respiration rate was calculated as: (last rate measurement before first injection) – (non-mitochondrial respiration rate).

Automatic high-content analyses (HCA)

All analyses were performed with Harmony software v.4.9 (PerkinElmer) using in-house scripts developed in Harmony running Acapella Assay Language version 5.0.1.124082 (available at https://github.com/bbi-ip/Legionella_and_mitochondrial_ATPase.git; Rusniok, 2021; copy archived at [swh:1:rev:657b662b912e3b3c630619f648489cc28652dcd9](https://www.swh.io/rev/657b662b912e3b3c630619f648489cc28652dcd9)). For the HCA of the mitochondrial membrane potential ($\Delta\psi_m$), the Hoechst signal was used to segment nuclei in the 405/450 channel (excitation/emission), Hoechst background signal in the cytoplasm was used to segment the cytoplasm region in the 405/450 channel, *L. pneumophila* was identified by measuring the GFP signal in the 488/540 channel, and TMRM (10 nM) signal in the 561/600 channel was used to measure $\Delta\psi_m$ by calculating SD/mean TMRM intensity values in each infected and noninfected cell. For the HCA of cell death, the Hoechst signal was used to segment nuclei in the 405/450 channel, Hoechst background signal in the cytoplasm was used to segment the cytoplasm region, and the identification of *L. pneumophila* was performed using the GFP signal in the 488/540 channel. Then, Annexin-V-Alexa Fluor

647 signal was measured in the 640/690 channel and the Hoechst signal intensity was measured in the 405/450 channel for each infected or noninfected cell. For the HCA combining $\Delta\psi_m$ and cell death, both the aforementioned HCA strategies were merged using high Hoechst signal in the 405/450 channel to segment nuclei, low Hoechst signal in the 405/450 channel to segment cytoplasm, GFP signal in the 488/540 channel to identify bacteria, TMRM signal in the 561/600 channel to measure $\Delta\psi_m$ (SD/mean), and Annexin-V-Alexa Fluor 647 signal in the 640/690 channel to measure cell death. For the HCA of transfected cells, GFP/Xpress-488 signal in the 488/540 channel was used to identify transfected cells and Annexin-V-Alexa Fluor 647 signal in the 640/690 channel to measure cell death.

Whole-genome sequencing for mutant validation

Chromosomal DNA was extracted from BCYE-grown *L. pneumophila* using the DNeasy Blood and Tissue Kit (QIAGEN). The Illumina NGS libraries were prepared using the Nextera DNA Flex Library Prep following the manufacturer's instructions (Illumina Inc). High-throughput sequencing was performed with a MiSeq Illumina sequencer (2 × 300 bp, Illumina Inc) by the Biomix Pole (Institut Pasteur). For the analysis, we first removed adapters from Illumina sequencing reads using Cutadapt software version 1.15 (Martin, 2011) and then used Sickle (<https://github.com/najoshi/sickle>, Buffalo, 2021) with a quality threshold of 20 (Phred score) to trim bad quality extremities. Reads were assembled using Spades (Nurk et al., 2013) and different K-mer values. The region corresponding to the gene of interest was identified by blastn, extracted, and compared to the homologous region in the *L. pneumophila* strain Paris WT genome and to the antibiotic cassette sequence using blastn. The results were visually inspected with Artemis Comparison Tool (ATC) (Carver et al., 2005). In addition, we searched the entire genome whether off-target mutations had occurred using Bowtie 2 (Langmead and Salzberg, 2012) to perform a mapping against the genome sequence of *L. pneumophila* strain Paris (NC_006368.1). SNPs and small indels were searched for with freebayes SNP caller (Garrison and Marth, 2012), and mutations and small indels were visualized in the Artemis genome viewer (Carver et al., 2005) to analyze them (new amino acid, synonymous mutation, frameshifts, etc.). We used Samtools to find regions with no coverage (or close to zero) (Li et al., 2009). Regions or positions with such anomalies were visualized and compared with the corresponding region of the assembly. This confirmed that no off-target mutations impacting the phenotype of the mutant had occurred.

Statistical analyses

The two-sample Student's *t*-test (Mann–Whitney *U* test, nonassumption of Gaussian distributions) was used in all data sets unless stated otherwise. Data analysis was performed using Prism v9 (GraphPad Software).

Acknowledgements

We acknowledge CB's, P Glaser's lab members, and F Stavru at Institut Pasteur for fruitful discussions. We specially thank Daniel Schator for help and discussions regarding HEK-293 infection and transfection. We thank N Aulner, A Danckaert, Photonic Biolmaging (PBI) UTechS and M Hassan, Center for Translational Science (CRT) at Institut Pasteur, for support. This research was funded by the Institut Pasteur, DARRI-Institut Carnot-*Microbe et santé* (grant number INNOV-SP10-19) to PE; the Agence National de Recherche (grant number ANR-10-LABX-62-IBEID to CB and ANR-21-CE15-0038-01 to PE), the Fondation de la Recherche Médicale (FRM) (grant number EQU201903007847) to CB, and the Région Ile-de-France (program DIM1Health) to PBI (part of FranceBiolmaging, ANR-10-INSB-04-01). MD was supported by the Ecole Doctorale FIRE – 'Programme Bettencourt.' SS was supported by the Pasteur Paris-University (PPU) International PhD Program.

Additional information

Funding

Funder	Grant reference number	Author
Agence Nationale de la Recherche	ANR-10-LABX-62-IBEID	Carmen Buchrieser
Fondation pour la Recherche Médicale	EQU201903007847	Carmen Buchrieser
Association Instituts Carnot	INNOV-SP10-19	Pedro Escoll
French National Research Agency	ANR- 21- CE15- 0038- 01	Pedro Escoll

The funders had no role in study design, data collection and interpretation, or the decision to submit the work for publication.

Author contributions

Pedro Escoll, Conceptualization, Formal analysis, Investigation, Supervision, Writing - original draft; Lucien Platon, Formal analysis, Investigation, Methodology; Mariatou Dramé, Silke Schmidt, Formal analysis, Investigation; Tobias Sahr, Investigation, Methodology; Christophe Rusniok, Data curation, Formal analysis; Carmen Buchrieser, Funding acquisition, Project administration, Supervision, Writing - review and editing

Author ORCIDs

Pedro Escoll  <http://orcid.org/0000-0002-5933-094X>

Lucien Platon  <http://orcid.org/0000-0001-7894-5977>

Carmen Buchrieser  <http://orcid.org/0000-0003-3477-9190>

Decision letter and Author response

Decision letter <https://doi.org/10.7554/eLife.71978.sa1>

Author response <https://doi.org/10.7554/eLife.71978.sa2>

Additional files

Supplementary files

- Transparent reporting form

Data availability

All data generated or analysed during this study are included in the manuscript. Source data files are uploaded to Github: https://github.com/bbi-ip/Legionella_and_mitochondrial_ATPase.git (copy archived at <https://archive.softwareheritage.org/swh:1:rev:657b662b912e3b3c630619f648489cc28652dcd9>).

References

- Arasaki K, Roy CR. 2010. Legionella pneumophila promotes functional interactions between plasma membrane syntaxins and Sec22b. *Traffic* **11**:587–600. DOI: <https://doi.org/10.1111/j.1600-0854.2010.01050.x>, PMID: 20163564
- Bock FJ, Tait SWG. 2020. Mitochondria as multifaceted regulators of cell death. *Nature Reviews. Molecular Cell Biology* **21**:85–100. DOI: <https://doi.org/10.1038/s41580-019-0173-8>, PMID: 31636403
- Brand MD, Nicholls DG. 2011. Assessing mitochondrial dysfunction in cells. *The Biochemical Journal* **435**:297–312. DOI: <https://doi.org/10.1042/BJ20110162>, PMID: 21726199
- Brüggemann H, Hagman A, Jules M, Sismeiro O, Dillies MA, Gouyette C, Kunst F, Steinert M, Heuner K, Coppée JY, Buchrieser C. 2006. Virulence strategies for infecting phagocytes deduced from the in vivo transcriptional program of Legionella pneumophila. *Cellular Microbiology* **8**:1228–1240. DOI: <https://doi.org/10.1111/j.1462-5822.2006.00703.x>, PMID: 16882028
- Buffalo V. 2021. sickle - A windowed adaptive trimming tool for FASTQ files using quality. v1.33. GitHub. <https://github.com/najoshi/sickle>

- Campanella M**, Parker N, Tan CH, Hall AM, Duchen MR. 2009. IF(1): setting the pace of the F(1)F(o)-ATP synthase. *Trends in Biochemical Sciences* **34**:343–350. DOI: <https://doi.org/10.1016/j.tibs.2009.03.006>, PMID: 19559621
- Carver TJ**, Rutherford KM, Berriman M, Rajandream MA, Barrell BG, Parkhill J. 2005. ACT: the Artemis Comparison Tool. *Bioinformatics* **21**:3422–3423. DOI: <https://doi.org/10.1093/bioinformatics/bti553>, PMID: 15976072
- Chow SH**, Deo P, Naderer T. 2016. Macrophage cell death in microbial infections. *Cellular Microbiology* **18**:466–474. DOI: <https://doi.org/10.1111/cmi.12573>, PMID: 26833712
- Connolly NMC**, Theurey P, Adam-Vizi V, Bazan NG, Bernardi P, Bolaños JP, Culmsee C, Dawson VL, Deshmukh M, Duchen MR, Düsselmann H, Fiskum G, Galindo MF, Hardingham GE, Hardwick JM, Jakobsons MB, Jonas EA, Jordán J, Lipton SA, Manfredi G, et al. 2018. Guidelines on experimental methods to assess mitochondrial dysfunction in cellular models of neurodegenerative diseases. *Cell Death and Differentiation* **25**:542–572. DOI: <https://doi.org/10.1038/s41418-017-0020-4>, PMID: 29229998
- Degtyar E**, Zusman T, Ehrlich M, Segal G. 2009. A Legionella effector acquired from protozoa is involved in sphingolipids metabolism and is targeted to the host cell mitochondria. *Cellular Microbiology* **11**:1219–1235. DOI: <https://doi.org/10.1111/j.1462-5822.2009.01328.x>, PMID: 19438520
- Dolezal P**, Aili M, Tong J, Jiang JH, Marobbio CMT, Marobbio CM, Lee SF, Schuelein R, Belluzzo S, Binova E, Mousnier A, Frankel G, Giannuzzi G, Palmieri F, Gabriel K, Naderer T, Hartland EL, Lithgow T. 2012. Legionella pneumophila secretes a mitochondrial carrier protein during infection. *PLOS Pathogens* **8**:e1002459. DOI: <https://doi.org/10.1371/journal.ppat.1002459>, PMID: 22241989
- Duchen MR**, Surin A, Jacobson J. 2003. 17] Imaging Mitochondrial Function in Intact Cells Methods in Enzymology, Biophotonics, Part B. Academic Press. DOI: [https://doi.org/10.1016/S0076-6879\(03\)61019-0](https://doi.org/10.1016/S0076-6879(03)61019-0)
- Escoll P**, Rolando M, Buchrieser C. 2017a. MAMs are attractive targets for bacterial repurposing of the host cell: MAM-functions might be key for undermining an infected cell. *BioEssays: News and Reviews in Molecular, Cellular and Developmental Biology* **39**:201600171. DOI: <https://doi.org/10.1002/bies.201600171>, PMID: 28026026
- Escoll P**, Song OR, Viana F, Steiner B, Lagache T, Olivo-Marin JC, Impens F, Brodin P, Hilbi H, Buchrieser C. 2017b. Legionella pneumophila Modulates Mitochondrial Dynamics to Trigger Metabolic Repurposing of Infected Macrophages. *Cell Host & Microbe* **22**:302–316. DOI: <https://doi.org/10.1016/j.chom.2017.07.020>, PMID: 28867389
- Escoll P**, Buchrieser C. 2018. Metabolic reprogramming of host cells upon bacterial infection: Why shift to a Warburg-like metabolism? *The FEBS Journal* **285**:2146–2160. DOI: <https://doi.org/10.1111/febs.14446>, PMID: 29603622
- Escoll P**, Buchrieser C. 2019. Metabolic reprogramming: an innate cellular defence mechanism against intracellular bacteria? *Current Opinion in Immunology* **60**:117–123. DOI: <https://doi.org/10.1016/j.coi.2019.05.009>, PMID: 31247377
- Gandhi S**, Wood-Kaczmar A, Yao Z, Plun-Favreau H, Deas E, Klupsch K, Downward J, Latchman DS, Tabrizi SJ, Wood NW, Duchen MR, Abramov AY. 2009. PINK1-associated Parkinson's disease is caused by neuronal vulnerability to calcium-induced cell death. *Molecular Cell* **33**:627–638. DOI: <https://doi.org/10.1016/j.molcel.2009.02.013>, PMID: 19285945
- Garrison E**, Marth G. 2012. Haplotype-Based Variant Detection from Short-Read Sequencing. *arXiv*. <https://arxiv.org/abs/1207.3907>
- Hernández-Corbacho MJ**, Salama MF, Canals D, Senkal CE, Obeid LM. 2017. Sphingolipids in mitochondria. *Biochimica et Biophysica Acta* **1862**:56–68. DOI: <https://doi.org/10.1016/j.bbali.2016.09.019>, PMID: 27697478
- Ivanov F**, Faccenda D, Gatliff J, Ahmed AA, Cocco S, Cheng CHK, Allan E, Russell C, Duchen MR, Campanella M. 2014. The compound BTB06584 is an IF1 -dependent selective inhibitor of the mitochondrial F1 Fo-ATPase. *British Journal of Pharmacology* **171**:4193–4206. DOI: <https://doi.org/10.1111/bph.12638>, PMID: 24641180
- Jian C**, Xu F, Hou T, Sun T, Li J, Cheng H, Wang X. 2017. Deficiency of PHB complex impairs respiratory supercomplex formation and activates mitochondrial flashes. *Journal of Cell Science* **130**:2620–2630. DOI: <https://doi.org/10.1242/jcs.198523>, PMID: 28630166
- Langmead B**, Salzberg SL. 2012. Fast gapped-read alignment with Bowtie 2. *Nature Methods* **9**:357–359. DOI: <https://doi.org/10.1038/nmeth.1923>, PMID: 22388286
- Li H**, Handsaker B, Wysoker A, Fennell T, Ruan J, Homer N, Marth G, Abecasis G, Durbin R. 2009. The Sequence Alignment/Map format and SAMtools. *Bioinformatics* **25**:2078–2079. DOI: <https://doi.org/10.1093/bioinformatics/btp352>
- Martin M**. 2011. Cutadapt removes adapter sequences from high-throughput sequencing reads. *EMBnet.Journal* **17**:10. DOI: <https://doi.org/10.14806/ej.17.1.200>
- Mitchell G**, Chen C, Portnoy DA. 2016. Strategies Used by Bacteria to Grow in Macrophages. *Microbiology Spectrum* **4**:2015. DOI: <https://doi.org/10.1128/microbiolspec.MCHD-0012-2015>, PMID: 27337444
- Mondino S**, Schmidt S, Rolando M, Escoll P, Gomez-Valero L, Buchrieser C. 2020. Legionnaires' Disease: State of the Art Knowledge of Pathogenesis Mechanisms of Legionella. *Annual Review of Pathology* **15**:439–466. DOI: <https://doi.org/10.1146/annurev-pathmechdis-012419-032742>, PMID: 31657966
- Nielson JR**, Rutter JP. 2018. Lipid-mediated signals that regulate mitochondrial biology. *The Journal of Biological Chemistry* **293**:7517–7521. DOI: <https://doi.org/10.1074/jbc.R117.001655>, PMID: 29348169

- Nolfi-Donagan D**, Braganza A, Shiva S. 2020. Mitochondrial electron transport chain: Oxidative phosphorylation, oxidant production, and methods of measurement. *Redox Biology* **37**:101674. DOI: <https://doi.org/10.1016/j.redox.2020.101674>, PMID: 32811789
- Nurk S**, Bankevich A, Antipov D, Gurevich AA, Korobeynikov A, Lapidus A, Prjibelski AD, Pyshkin A, Sirotkin A, Sirotkin Y, Stepanauskas R, Clingenpeel SR, Woyke T, McLean JS, Lasken R, Tesler G, Alekseyev MA, Pevzner PA. 2013. Assembling single-cell genomes and mini-metagenomes from chimeric MDA products. *Journal of Computational Biology* **20**:714–737. DOI: <https://doi.org/10.1089/cmb.2013.0084>, PMID: 24093227
- O'Neill LAJ**, Pearce EJ. 2016. Immunometabolism governs dendritic cell and macrophage function. *The Journal of Experimental Medicine* **213**:15–23. DOI: <https://doi.org/10.1084/jem.20151570>, PMID: 26694970
- Rolando M**, Escoll P, Nora T, Botti J, Boitez V, Bedia C, Daniels C, Abraham G, Stogios PJ, Skarina T, Christophe C, Dervins-Ravault D, Cazalet C, Hilbi H, Rupasinghe TWT, Tull D, McConville MJ, Ong SY, Hartland EL, Codogno P, et al. 2016. Legionella pneumophila S1P-lyase targets host sphingolipid metabolism and restrains autophagy. *PNAS* **113**:1901–1906. DOI: <https://doi.org/10.1073/pnas.1522067113>, PMID: 26831115
- Rothmeier E**, Pfaffinger G, Hoffmann C, Harrison CF, Grabmayr H, Repnik U, Hannemann M, Wölke S, Bausch A, Griffiths G, Müller-Taubenberger A, Itzen A, Hilbi H. 2013. Activation of Ran GTPase by a Legionella effector promotes microtubule polymerization, pathogen vacuole motility and infection. *PLOS Pathogens* **9**:e1003598. DOI: <https://doi.org/10.1371/journal.ppat.1003598>, PMID: 24068924
- Rudel T**, Kepp O, Kozjak-Pavlovic V. 2010. Interactions between bacterial pathogens and mitochondrial cell death pathways. *Nature Reviews. Microbiology* **8**:693–705. DOI: <https://doi.org/10.1038/nrmicro2421>, PMID: 20818415
- Rusniok C**. 2021. Legionella and mitochondrial_ATPase. 657b662. GitHub. https://github.com/bbi-ip/Legionella_and_mitochondrial_ATPase
- Russell DG**, Huang L, VanderVen BC. 2019. Immunometabolism at the interface between macrophages and pathogens. *Nature Reviews. Immunology* **19**:291–304. DOI: <https://doi.org/10.1038/s41577-019-0124-9>, PMID: 30679807
- Siegl C**, Prusty BK, Karunakaran K, Wischhusen J, Rudel T. 2014. Tumor suppressor p53 alters host cell metabolism to limit *Chlamydia trachomatis* infection. *Cell Reports* **9**:918–929. DOI: <https://doi.org/10.1016/j.celrep.2014.10.004>, PMID: 25437549
- Singh V**, Jamwal S, Jain R, Verma P, Gokhale R, Rao KVS. 2012. Mycobacterium tuberculosis-driven targeted recalibration of macrophage lipid homeostasis promotes the foamy phenotype. *Cell Host & Microbe* **12**:669–681. DOI: <https://doi.org/10.1016/j.chom.2012.09.012>, PMID: 23159056
- Speir M**, Vince JE, Naderer T. 2014. Programmed cell death in Legionella infection. *Future Microbiology* **9**:107–118. DOI: <https://doi.org/10.2217/fmb.13.139>, PMID: 24328384
- Spier A**, Stavru F, Cossart P. 2019. Interaction between Intracellular Bacterial Pathogens and Host Cell Mitochondria. *Microbiology Spectrum* **7**:2019. DOI: <https://doi.org/10.1128/microbiolspec.BAI-0016-2019>, PMID: 30848238
- Strub GM**, Paillard M, Liang J, Gomez L, Allegood JC, Hait NC, Maceyka M, Price MM, Chen Q, Simpson DC, Kordula T, Milstien S, Lesnefsky EJ, Spiegel S. 2011. Sphingosine-1-phosphate produced by sphingosine kinase 2 in mitochondria interacts with prohibitin 2 to regulate complex IV assembly and respiration. *FASEB Journal* **25**:600–612. DOI: <https://doi.org/10.1096/fj.10-167502>, PMID: 20959514
- Tiaden A**, Spirig T, Weber SS, Brüggemann H, Bosshard R, Buchrieser C, Hilbi H. 2007. The Legionella pneumophila response regulator LqsR promotes host cell interactions as an element of the virulence regulatory network controlled by RpoS and LetA. *Cellular Microbiology* **9**:2903–2920. DOI: <https://doi.org/10.1111/j.1462-5822.2007.01005.x>, PMID: 17614967
- Wei-LaPierre L**, Dirksen RT. 2019. Isolating a reverse-mode ATP synthase-dependent mechanism of mitoflash activation. *The Journal of General Physiology* **151**:708–713. DOI: <https://doi.org/10.1085/jgp.201912358>, PMID: 31010808

Analyses fonctionnelles de la capsule de *Legionella longbeachae* pour comprendre son rôle dans la détection immunitaire de l'hôte et la persistance environnementale

Résumé de thèse

Legionella longbeachae est une bactérie intracellulaire facultative qui peut provoquer une pneumonie grave chez l'Homme, la légionellose. *L. longbeachae* est la seule espèce du genre *Legionella* dont le génome code pour une capsule. En utilisant la microscopie électronique à transmission, j'ai montré que *L. longbeachae* exprime effectivement une capsule à sa surface. En utilisant un double rapporteur de fluorescence, j'ai pu montrer par microscopie confocale en direct que la capsule est transcrite intracellulairement lors de l'infection. La bactérie de type sauvage est très virulente dans un modèle d'infection chez la souris. En revanche, un mutant du transporteur de la capsule, qui n'est pas encapsulé, est complètement avirulent chez les souris. Le mutant de la capsule présente un grave défaut de réplication chez l'amibe, l'hôte environnemental de la bactérie. Cela indique que la capsule joue un rôle essentiel lors de l'infection par *L. longbeachae*. Les bactéries de type sauvage retardent la phagocytose dans les cellules hôtes, contrairement au mutant qui est facilement phagocyté. En outre, la présence de la capsule freine la sécrétion de cytokines pro-inflammatoires par les cellules immunitaires innées primaires par rapport au mutant de la capsule. La purification de la capsule et l'analyse par électrophorèse sur gel et HPLC montrent que *L. longbeachae* exprime un polysaccharide fortement anionique, absent chez le mutant. Les résultats obtenus au cours de ma thèse apportent la preuve d'un nouveau mécanisme de virulence de *L. longbeachae* et peuvent nous aider à comprendre comment ces bactéries peuvent provoquer des maladies chez l'Homme.

Mots clés: *Legionella longbeachae*, capsules bactériennes, virulence, évasion immunitaire

Functional analyses of the *Legionella longbeachae* capsule to understand its role in host immune sensing and environmental persistence

Summary of the thesis

Legionella longbeachae is a facultative intracellular bacterium that can cause a severe pneumonia in humans, known as Legionnaires' disease. *L. longbeachae* is the only species in the genus *Legionella* that encodes a capsule cluster in its genome. Using transmission electron microscopy, I could show that *L. longbeachae* indeed expresses a capsule on its surface. Furthermore, using a dual fluorescence reporter, I could show by live confocal microscopy that the capsule is transcribed intracellularly upon infection. The wild type bacteria are highly virulent in a mouse model of infection. In contrast, a mutant in the capsule transporter, which is non-encapsulated, is completely avirulent in mice. Additionally, the capsule mutant shows a severe replication defect in amoeba, the environmental host of the bacteria. This indicates that the capsule plays an essential role during infection of *L. longbeachae*. I could show that wild type bacteria delay phagocytosis into host cells, in contrast to the mutant that is readily phagocytosed by THP-1 cells. In addition, the presence of the capsule dampens the secretion of pro-inflammatory cytokines from primary innate immune cells as compared to the capsule mutant. Purification of the capsule and analysis by gel electrophoresis and HPLC show that *L. longbeachae* expresses a highly anionic polysaccharide, which is absent in the capsule mutant. The results obtained during my thesis provide evidence for a novel virulence mechanism of *L. longbeachae* and may inform our understanding of how these bacteria can cause disease in humans.

Key words: *Legionella longbeachae*, bacterial capsules, virulence, immune evasion